DISSECTION OF THE MOLECULAR BASIS OF FATTY ACID COMPOSITION IN OIL CROPS AND MOLECULAR BREEDING OF OIL CROPS WITH IMPROVED FATTY ACID COMPOSITION

EDITED BY: Yong Xiao, Jacqueline Batley, Hyun Uk Kim and Dongdong LI

PUBLISHED IN: Frontiers in Plant Science

frontiers Research Topics

frontiers

ISSN 1664-8714
ISBN 978-2-83250-694-3
DOI 10.3389/978-2-83250-694-3

About Frontiers

Frontiers is more than just an open-access publisher of scholarly articles: it is a pioneering approach to the world of academia, radically improving the way scholarly research is managed. The grand vision of Frontiers is a world where all people have an equal opportunity to seek, share and generate knowledge. Frontiers provides immediate and permanent online open access to all its publications, but this alone is not enough to realize our grand goals.

Frontiers Journal Series

The Frontiers Journal Series is a multi-tier and interdisciplinary set of open-access, online journals, promising a paradigm shift from the current review, selection and dissemination processes in academic publishing. All Frontiers journals are driven by researchers for researchers; therefore, they constitute a service to the scholarly community. At the same time, the Frontiers Journal Series operates on a revolutionary invention, the tiered publishing system, initially addressing specific communities of scholars, and gradually climbing up to broader public understanding, thus serving the interests of the lay society, too.

Dedication to Quality

Each Frontiers article is a landmark of the highest quality, thanks to genuinely collaborative interactions between authors and review editors, who include some of the world's best academicians. Research must be certified by peers before entering a stream of knowledge that may eventually reach the public - and shape society; therefore, Frontiers only applies the most rigorous and unbiased reviews.
Frontiers revolutionizes research publishing by freely delivering the most outstanding research, evaluated with no bias from both the academic and social point of view. By applying the most advanced information technologies, Frontiers is catapulting scholarly publishing into a new generation.

What are Frontiers Research Topics?

Frontiers Research Topics are very popular trademarks of the Frontiers Journals Series: they are collections of at least ten articles, all centered on a particular subject. With their unique mix of varied contributions from Original Research to Review Articles, Frontiers Research Topics unify the most influential researchers, the latest key findings and historical advances in a hot research area! Find out more on how to host your own Frontiers Research Topic or contribute to one as an author by contacting the Frontiers Editorial Office: frontiersin.org/about/contact

DISSECTION OF THE MOLECULAR BASIS OF FATTY ACID COMPOSITION IN OIL CROPS AND MOLECULAR BREEDING OF OIL CROPS WITH IMPROVED FATTY ACID COMPOSITION

Topic Editors:
Yong Xiao, Chinese Academy of Tropical Agricultural Sciences, China
Jacqueline Batley, University of Western Australia, Australia
Hyun Uk Kim, Sejong University, South Korea
Dongdong LI, Hainan University, China

Citation: Xiao, Y., Batley, J., Kim, H. U., LI, D., eds. (2022). Dissection of the Molecular Basis of Fatty Acid Composition in Oil Crops and Molecular Breeding of Oil Crops With Improved Fatty Acid Composition. Lausanne: Frontiers Media SA. doi: 10.3389/978-2-83250-694-3

Table of Contents

frontiers | Frontiers in Plant Science

TYPE Editorial
PUBLISHED 20 October 2022
DOI 10.3389/fpls.2022.1053735

OPEN ACCESS

EDITED AND REVIEWED BY
Rosario Paolo Mauro,
University of Catania, Italy

*CORRESPONDENCE
Hyun Uk Kim
hukim64@sejong.ac.kr

SPECIALTY SECTION
This article was submitted to Crop and Product Physiology, a section of the journal Frontiers in Plant Science

RECEIVED 26 September 2022
ACCEPTED 30 September 2022
PUBLISHED 20 October 2022

CITATION
Kim HU and Li D (2022) Editorial: Dissection of the molecular basis of fatty acid composition in oil crops and molecular breeding of oil crops with improved fatty acid composition. *Front. Plant Sci.* 13:1053735. doi: 10.3389/fpls.2022.1053735

Editorial: Dissection of the molecular basis of fatty acid composition in oil crops and molecular breeding of oil crops with improved fatty acid composition

Hyun Uk Kim[1]* and Dongdong Li[2]

[1]Department of Bioindustry and Bioresource Engineering, Plant Engineering Research Institute, Sejong University, Seoul, South Korea, [2]College of Tropical Crops, Hainan University, Haikou, China

KEYWORDS

arabidopsis*, *camellia*, fatty acid, oil palm, rapeseeds, rice, *physaria fendleri*, *torreya grandis

Editorial on the Research Topic

Dissection of the molecular basis of fatty acid composition in oil crops and molecular breeding of oil crops with improved fatty acid composition

Humans are using vegetable oil produced by various oilseed crops such as oil palm, rapeseed, and soybean for food and industry (Tokel and Erkencioglu, 2021). Vegetable oil produced from seeds and fruits of oilseed crops is in the form of triacylglycerol (TAG), and their fatty acid (FA) composition varies depending on the plant species. In the *Arabidopsis* model plant, the metabolism of FA and TAG biosynthesis has been well elucidated through genetics, molecular biochemistry, and genomics (Li-Beisson et al., 2013). However, studies on the metabolic mechanism of FA and TAG synthesis in various oilseed crops are scarce.

Given the need for research in oilseed crops, this special issue covers recent research on genetic and molecular mechanisms underlying oil-crop traits, specifically about FA. The first is the discovery of a novel transcription factor network that regulates FA synthesis and changes in FA composition by abscisic acid (ABA) treatment of oil palm. In addition, research in *Physaria fendleri* has been applied to enhance the production of industrially useful hydroxy FAs (HFAs), and transcriptomic analysis of gymnosperm *Torreya grandis* Fortune ex Lindl. kernels provided further clarity on FA metabolism. Next, important progress has been made in understanding available genetic resources

through studies that assembled the chloroplast genome of the tea-oil tree *Camellia*, comprehensively mapped quantitative trait loci (QTLs) related to oil production and disease resistance in rapeseed (*Brassica napus*), and explored disease-resistance mechanisms in the lipid metabolism of rice. Finally, a rapeseed cultivar without erucic acid production in seeds was developed through gene editing. These biotechnological advances benefit the production of vegetable oils optimized for food and industrial raw materials.

New molecular mechanisms of FA biosynthesis in oil palm, rice, and *Arabidopsis thaliana*

The world's largest oil-producing crop is the oil palm (*Elaeis guineensis*), which accumulates up to 90% of its oil in the mesocarp (Bhagya et al., 2020; Zhou et al., 2020). However, few reports are available on transcription factor (TF) networks

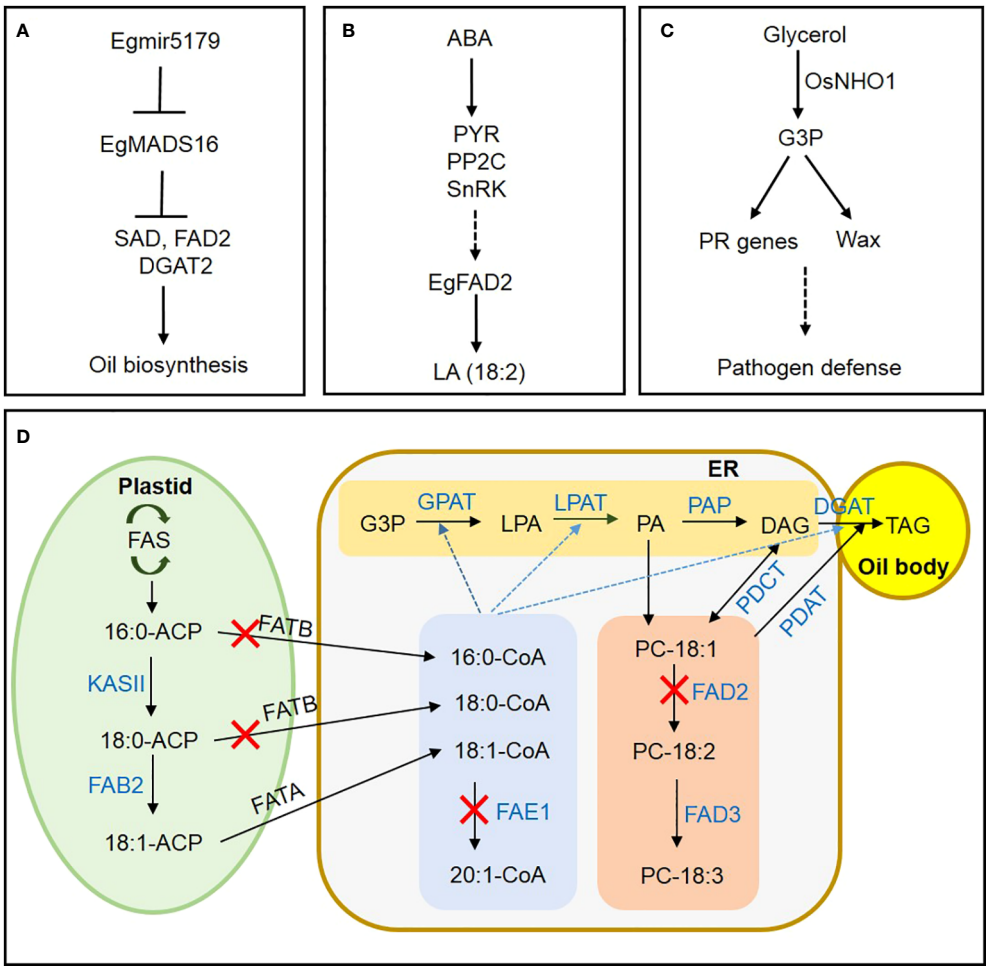

FIGURE 1
A novel mechanism for regulating lipid metabolism in oil crops and a metabolic pathway for FA and TAG synthesis in oilseeds. **(A)** In oil-palm mesocarp, mir5179 inhibits MADS16 expression and regulates the expression of oil synthesis genes *SAD*, *FAD2*, and *DGAT2*. **(B)** ABA induces linoleic acid synthesis through ABA signaling pathway in oil palm mesocarp. **(C)** Induction of disease resistance in rice through regulating PR gene expression and wax synthesis by glycerol kinase OsNHO1. **(D)** Suppression of *FAE1* expression for EA-free oil crop development. Suppressing *FATB* inhibits saturated-FA synthesis. Suppressing *FAD2* expression blocks polyunsaturated-FA synthesis, resulting in elevated production of oleic acid. Black arrows indicate the direction of FA biosynthesis and metabolism. Blue dotted arrows indicate acyl-CoA migration. Blue letters indicate enzymes involved in the metabolic pathways. Red Xs indicate enzyme inhibition. FAS, fatty acid synthase; ACP, acyl carrier protein; KAS, KASII, 3-ketoacyl-ACP synthase II; FAB2, fatty acid biosynthesis2; G3P, glycerol-3phosphate; LPA, lysophosphatidic acid; PA, phosphatidic acid; DAG, diacylglycerol; TAG, triacylglycerol; CoA, coenzyme A; GPAT, glycerol-3-phosphate acyltransferase; LPAT, lysophosphatidic acid acyltransferase; PAP, phosphatidate phosphatase; DGAT, diacylglycerol acyltransferases; PDAT, phospholipid diacylglycerol acyltransferase; PC, phosphatidylcholine; FAD2, fatty acid desaturase 2; FAD3, fatty acid desaturase 3; ER, endoplasmic reticulum; FAE1, fatty acid elongase 1; FATA, fatty acid thioesterase A; FATB, fatty acid thioesterase B; PDCT, phosphatidylcholine diacylglycerol choline phosphotransferase; PDAT, phosphatidylcholine diacylglycerol acyltransferase.

regulating lipid metabolism in oil palm (Yeap et al., 2017; Li et al., 2020). Wang et al. suggested that EgMADS16 negatively regulates *FAD2, SAD*, and *DGAT2* transcription during oil-palm mesocarp development, interacting with EgGLO1 to affect FA and triacylglycerol (TAG) biosynthesis. The authors also proposed a mechanism to explain the suppression of *EgMADS16* expression by its target *Egmir5179*, a small RNA involved in oil accumulation (Figure 1A). Next, a study by Shi et al. examined how ABA treatment increases the unsaturated FA linoleic acid in oil-palm mesocarp. Through transcriptome analysis, they hypothesized that exogenous ABA increases linoleic acid (18:2) accumulation *via* activating ABA signaling genes *PYR*, *PP2C*, and *SnRK*, as well as TFs such as ABI5, resulting in upregulation of *FAD2* expression (Figure 1B).

Glycerol kinase (GK) catalyzes the conversion of glycerol to glycerol-3-phosphate (G3P), but its physiological significance in rice defense against pathogens remains unclear. Xiao et al. confirmed that the GK gene *OsNHO1* was upregulated in *Xanthomonas oryzae* pv. *oryzae* (*Xoo*) strain PXO99. Additionally, in the transgenic rice line overexpressing *OsHNO1-OE*, GK content and *OsNHO1* transcription both increased, improving resistance to bacterial blight and blast diseases. In contrast, resistance was impaired in the OsNHO1-RNAi line. Similarly, wax content and wax-synthesis gene expression increased significantly in the overexpression line, while decreasing in the OsNHO1-RNAi line. Inhibiting OsNHO1 also led to decreased transcription of its interaction partners, OsSRC2 and OsPR. Xiao et al. concluded that OsNHO1 confers disease resistance through affecting wax content and regulating pathogenesis-related (PR) gene transcription (Figure 1C).

As a major seed energy source, TAG is stored in the form of fixed carbon (Baud and Lepiniec, 2009). Photosynthetic processes in chlorophyll-containing green seeds mainly involves FA synthesis by ATP and reducing agents (NADPH and NADH) produced in leaves and other green plant parts (Goffman et al., 2005; Hua et al., 2014; Zhang et al., 2016). However, the contribution of FA accumulation in non-green seeds remains uncertain. Nwafor et al. demonstrated that photosynthesis in *Arabidopsis* non-green seeds is responsible for 20% of FA synthesis, whereas photosynthesis in siliques and leaves/stems is responsible for 40%. The authors further suggested that the oxidized pentose phosphate pathway may be a source of the carbon, energy, and reducing agents required for FA synthesis during seed development.

Genome evaluation of various oil-crop resources

Considerable effort has been devoted to developing elite rapeseed cultivars with high oil content, high yield, and disease resistance (Bao et al., 2018; Chen et al., 2018). QTLs are particularly important for deciphering agronomic traits. A recent study aligned 4,555 QTLs (identified over 25 years across 12 countries) to construct a quantitative genomic map containing 128 traits from 79 populations (Raboanatahiry et al.). These results revealed 517 regions of overlapping QTLs that harbor 2,744 candidate genes simultaneously affecting multiple traits. This data can be used to develop new rapeseed varieties.

Torreya grandis Fortune ex Lindl. is a commercial species of gymnosperm that produces oil-rich nuts with high unsaturated FA content in mature kernels (Shi et al., 2018). Zhang et al. compared *de novo* transcriptome and FA accumulation during kernel development of two varieties: high-oil (52.9%) *T. grandis* 'Xifei' and medium-oil (41.6%) *T. grandis* 'Dielsii'. The authors inferred that differences in FA and TAG accumulation, along with related transcript expression, were the primary factors responsible for oil-content variation (oleic acid ratio, sciadonic acid ratio) between the two varieties.

Camellia is one of the four most commercially valued woody plants worldwide. *Camellia* oil is rich in polyphenols, saponins, and other nutritional components. Owing to its health benefits, camellia oil has strong economic competitiveness and broad market prospects (Zhu et al., 2010). Chen et al. identified an oil-tea *Camellia* species previously unknown in Hainan by comparing chloroplast genomic (cpDNA) sequences of 13 Chinese oil-tea *Camellia* samples. They concluded that cpDNA of oil-tea *Camellia* species exhibits a conserved tetrad structure with specific length polymorphisms. Additionally, simple sequence repeats (SSR) and other mutations led to an abundance of divergent hotspots in coding sequences (CDS) and intergenic space (IGS). The presence of these hotspots suggests that the entire cpDNA sequence can be used for species identification and phylogenetic analysis of *Camellia*.

Gene editing and biotechnology to improve FA composition for human consumption and industrial uses

Brassicaceae oilseeds produce a very long-chain monounsaturated FA called erucic acid (EA, C22:1), a compound extensively used in various chemical industries (Sakhno, 2010). However, EA is not easily digested and absorbed. Moreover, high-EA rapeseed (HEAR) oil often contains glucosinolates, which have been implicated in disease. Biotechnology research is thus necessary to produce low-EA rapeseed oil (LEAR) in addition to HEAR. In their review, Wang et al. examined the EA biosynthetic pathway and EA resources in various Brassicaceae crops. The available data led them to promote commercialization of genetically modified products that improved EA content in *Brassica* oilseeds. In the same vein, Liu et al. developed rapeseed lines with significantly lower EA content by

using CRISPR/Cas9 to knock out one or both *FAE1* copies in the amphidiploid plant. Knocking out *BnaC03.FAE1* decreased EA content by more than 10%, whereas knocking out both *BnaA08.FAE1* and *BnaC03.FAE1* almost completely abolished EA content. Instead, oleic acid content increased considerably. These experiments ultimately lowered seed oil content, without affecting other agricultural characteristics.

Physaria fendleri (Brassicaceae) accumulates the long-chain HFA lesquerolic acid (20:1OH) (Dierig et al., 2011), suggesting that this oilseed species can be an alternative crop to castors for producing industrially valuable HFAs. In support of this application, seed-specific RNAi knockdown of TAG lipase *SUGAR DEPENDENT 1* (*SDP1*) increased seed weight and total seed-oil content, without significantly affecting seedling establishment (Azeez et al.).

In their review of the biochemistry and molecular genetics underlying oil synthesis, Wallis et al. highlighted valuable tools for blocking relevant genes during seed development to lower polyunsaturated fatty acid (PUFA) content in oil. The authors introduced successful breeding programs that produced high-oleic, low-PUFA varieties of soybean, canola, and other oilseed crops. Finally, Park and Kim reviewed current case studies and future strategies for regulating FA and TAG metabolism using CRISPR/Cas9 (Figure 1D).

Outlook

Vegetable oils contribute significantly to calorie intake in the human diet, but their FA composition is not ideal for nutrition nor the needs of the food industry. Therefore, the mechanisms of FA and TAG synthesis in oil crops should be identified. Clearly, to meet the growing demand for vegetable oil, further biotechnology research and better breeding programs are necessary to improve crop oil content and FA composition.

Author contributions

All authors listed have made substantial, direct, and intellectual contributions to the work, and approved it for publication.

Funding

This work was supported by a grant from the New Breeding Technologies Development Program (Project No. PJ016533), Rural Development Administration, Republic of Korea.

Acknowledgments

We thank all authors, reviewers, and editorial staff who contributed to the finalization of this special issue.

Conflict of interest

The authors declare that the research was conducted in the absence of any commercial or financial relationships that could be construed as a potential conflict of interest.

Publisher's note

References

Bao, B., Chao, H., Wang, H., Zhao, W., Zhang, L., Raboanatahiry, N., et al. (2018). Stable, environmental specific and novel QTL identification as well as genetic dissection of fatty acid metabolism in *Brassica napus*. *Front. Plant Sci.* 9. doi: 10.3389/fpls.2018.01018

Baud, S., and Lepiniec, L. (2009). Regulation of *de novo* fatty acid synthesis in maturing oilseeds of *Arabidopsis*. *Plant Physiol. Biochem.* 47, 448–455. doi: 10.1016/j.plaphy.2008.12.006

Bhagya, H. P., Kalyana Babu, B., Gangadharappa, P. M., Naika, M. B. N., Satish, D., and Mathur, R. K. (2020). Identification of QTLs in oil palm (*Elaeis guineensis* jacq.) using SSR markers through association mapping *J. Genet.* 99, 19. doi: 10.1007/s12041-020-1180-4

Chen, F., Zhang, W., Yu, K., Sun, L., Gao, J., Zhou, X., et al. (2018). Unconditional and conditional QTL analyses of seed fatty acid composition in *Brassica napus* l. *BMC Plant Biol.* 18, 49. doi:10.1186/s12870–018-1268-7.

Dierig, D. A., Wang, G., Mccloskey, W. B., Thorp, K. R., Isbell, T. A., Ray, D. T., et al. (2011). *Lesquerella*: New crop development and commercialization in the US. *Ind. Crop Prod.* 34, 1381–1385. doi: 10.1016/j.indcrop.2010.12.023

Goffman, F. D., Alonso, A. P., Schwender, J., Shachar-Hill, Y., and Ohlrogge, J. B. (2005). Light enables a very high efficiency of carbon storage in developing embryos of rapeseed. *Plant Physiol.* 138, 2269–2279. doi: 10.1104/pp.105.063628

Hua, S., Chen, Z. H., Zhang, Y., Yu, H., Lin, B., and Zhang, D. (2014). Chlorophyll and carbohydrate metabolism in developing silique and seed are prerequisite to seed oil content of *Brassica napus* l. *Bot. Stud.* 55, 34. doi: 10.1186/1999-3110-55-34

Li-Beisson, Y., Shorrosh, B., Beisson, F., Andersson, M. X., Arondel, V., Bates, P. D., et al. (2013). Acyl-lipid metabolism. *Arabidopsis Book* 11, e0161. doi: 10.1199/tab.0161

Li, S. Y., Zhang, Q., Jin, Y. H., Zou, J. X., Zheng, Y. S., and Li, D. D. (2020). A MADS-box gene, EgMADS21, negatively regulates EgDGAT2 expression and decreases polyunsaturated fatty acid accumulation in oil palm (*Elaeis guineensis* jacq.). *Plant Cell Rep.* 39, 1505–1516. doi: 10.1007/s00299-020-02579-z

Sakhno, L. O. (2010). Variability in the fatty acid composition of rapeseed oil: classical breeding and biotechnology. *Cytol. Genet.* 44, 389–397. doi: 10.3103/S009545271006010

Shi, L. K., Mao, J. H., Zheng, L., Zhao, C. W., Jin, Q. Z., and Wang, X. G. (2018). Chemical characterization and free radical scavenging capacity of oils obtained from *Torreya grandis* fort. ex. lindl. and *torreya grandis* fort. var. *merrillii*: A comparative study using chemometrics. *Ind. Crops Prod.* 115, 250–260. doi: 10.1016/j.indcrop.2018.02.037

Tokel, D., and Erkencioglu, B. N. (2021). "Production and trade of oil crops, and their contribution to the world economy," in *Oil crop genomics*. Eds. H. Tombuloglu, T. Unver, G. Tombuloglu and K. R. Hakeem (Cham: Springer). doi: 10.1007/978-3-030-70420-9_20

Von Mark, V. C., and and Dierig, D. A. (2015). "Germplasm improvement to develop commercially viable lines of the new oilseed crop lesquerella," in *Industrial crops* (New York, USA: Springer), 315–334.

Yeap, W. C., Lee, F. C., Shabari Shan, D. K., Musa, H., Appleton, D. R., and Kulaveerasingam, H. (2017). WRI1-1, ABI5, NF-YA3 and NF-YC2 increase oil biosynthesis in coordination with hormonal signaling during fruit development in oil palm. *Plant J.* 91, 97–113. doi: 10.1111/tpj.13549

Zhang, Y., Mulpuri, S., and Liu, A. (2016). High light exposure on seed coat increases lipid accumulation in seeds of castor bean (*Ricinus communis* l.), a nongreen oilseed crop. *Photosynth. Res.* 128, 125–140. doi: 10.1007/s11120-015-0206-x

Zhou, Y., Zhao, W., Lai, Y., Zhang, B., and Zhang, D. (2020). Edible plant oil: Global status, health issues, and perspectives. *Front. Plant Sci.* 11. doi: 10.3389/fpls.2020.01315

Zhu, B., Zhong, H. Y., Cao, Q. M., and Long, Q. Z. (2010). Advance in research on bioactive compounds in camellia spp. *Nonw. For. Res.* 28, 140–145. doi: 10.14067/j.cnki.1003-8981.2010.03.026

frontiers in Plant Science

ORIGINAL RESEARCH
published: 26 July 2021
doi: 10.3389/fpls.2021.722596

EgmiR5179 Regulates Lipid Metabolism by Targeting EgMADS16 in the Mesocarp of Oil Palm (*Elaeis guineensis*)

Yifei Wang[1†], Jixin Zou[1,2†], Jin Zhao[1], Yusheng Zheng[1] and Dongdong Li[1*]*

[1]College of Tropical Crops, Hainan University, Haikou, China, [2]Rubber Research Institute of Chinese Academy of Tropical Agricultural Sciences (CATAS), Haikou, China

EgMADS16, one of the MADS-box transcription factors in oil palm, has a high expression level in the late fruit development of the oil palm fruit mesocarp. At the same time, it is also predicted to be the target gene of *EgmiR5179,* which has been identified in previous research. In this paper, we focused on the function and regulatory mechanism of the *EgMADS16* gene in oil palm lipid metabolism. The results indicated that the transcription level of *EgMADS16* was highest in the fourth stage, and a dual-luciferase reporter assay proved that the *EgMADS16* expression level was downregulated by *EgmiR5179*. In both the OX*EgMADS16 Arabidopsis* seeds and oil palm embryonic calli, the total lipid contents were significantly decreased, but the contents of C18:0 and C18:3 in OX*EgMADS16* lines were significantly increased. As expected, EgmiR5179 weakened the inhibitory effect of *EgMADS16* on the oil contents in transgenic *Arabidopsis* plants that coexpressed *EgmiR5179* and *EgMADS16* (OXEgmiR5179-*EgMADS16*). Moreover, yeast two-hybrid and BiFC analyses suggested that there was an interaction between the *EgMADS16* protein and EgGLO1 protein, which had been proven to be capable of regulating fatty acid synthesis in our previous research work. In summary, a model of the molecular mechanism by which miRNA5179 targets *EgMADS16* to regulate oil biosynthesis was hypothesized, and the research results provide new insight into lipid accumulation and molecular regulation in oil palm.

Keywords: oil palm, MADS-box gene, micorRNA5179, lipid content, fatty acid

OPEN ACCESS

Edited by:
María Serrano, Miguel Hernández University of Elche, Spain

Reviewed by:
Hadi Pirasteh-Anosheh, Agricultural Research Education and Extention Organization, Iran
Benjamin Lau, Malaysian Palm Oil Board, Malaysia

***Correspondence:**
Yusheng Zheng
yusheng.zheng@hainanu.edu.cn
Dongdong Li
lidd@hainanu.edu.cn

[†]These authors have contributed equally to this work

Specialty section:
This article was submitted to Crop and Product Physiology, a section of the journal Frontiers in Plant Science

Received: *09 June 2021*
Accepted: *07 July 2021*
Published: *26 July 2021*

Citation:
Wang Y, Zou J, Zhao J, Zheng Y and Li D (2021) EgmiR5179 Regulates Lipid Metabolism by Targeting EgMADS16 in the Mesocarp of Oil Palm (Elaeis guineensis). Front. Plant Sci. 12:722596. doi: 10.3389/fpls.2021.722596

INTRODUCTION

Oil palm (*Elaeis guineensis* Jacq.), which belongs to the Arecaceae family, is the most productive oil crop in the world and can accumulate up to 90% oil in the mesocarp (Bhagya et al., 2020). At present, the main oil crops that produce vegetable oils are oil palm, soybean, rape, and sunflower. They produce 79% of the total oil yields (Dyer et al., 2008). The palm oil produced by oil palm accounts for 36% of the total oil yields (Osorio-Guarin et al., 2019). Although much progress has been made on plant lipid metabolism and regulatory mechanisms *via* plant molecular biology research, it is still very difficult to obtain the ideal palm oil with the highest nutritional value or the largest yield. Presently, there are also few reports about

the genes involved in the regulation of oil metabolism and related transcription factor regulation networks in oil palm (Li et al., 2020).

In plant seeds, lipids are the main form of carbon storage, constituting up to 60% of the dry seed weight (Ohlroggeav and Browse, 1995). The biosynthesis of vegetable oil is affected by many factors, including transcription factors, microRNAs (miRNAs), plant hormones, signaling molecules, and environmental factors. Several transcription factors have been found to participate in the regulation of oil biosynthesis. For example, *ZmWRI1*, which belongs to the AP2/EREBP family, could regulate FA biosynthesis and increase seed oil by up to 46% in maize seeds overexpressing ZmWRI1 without affecting the germination, seedling growth, and grain yield (Shen et al., 2010). *GmMYB73*, which belongs to the MYB family, and *GmbZIP123*, which belongs to the bZIP family, could enhance lipid contents in both the seeds and leaves of transgenic *Arabidopsis* plants (Song et al., 2013; Liu et al., 2014). In oil palm, *EgMADS21* regulates *EgDGAT2* expression and ultimately affects fatty acid accumulation in the mesocarp (Li et al., 2020). In addition, *EgWRI1-1* participated in the regulation of oil biosynthesis by interacting directly with the EgNF-YA3 protein. *EgWRKY40* interacted with *EgWRKY2* to inhibit the transcription of oil biosynthesis-related genes (Yeap et al., 2017). However, little is known about the molecular mechanism of lipid accumulation in the mesocarp of oil palm.

In our previous research, overexpressing *EgmiR5179* significantly increased the oil yield in *Arabidopsis* seeds, and one MADS-box transcription factor (*EgMADS16*) was predicted to be the target gene of *EgmiR5179* (Gao et al., 2019). In this study, we cloned full-length *EgMADS16* from the mesocarp of oil palm. Transgenic *Arabidopsis* plants and oil palm embryoids overexpressing *EgMADS16* were obtained, and the contents of oil and fatty acids were tested. Finally, transgenic *Arabidopsis* overexpressing *EgmiR5179* and *EgMADS16* was obtained, and lipid and fatty acid contents were detected to confirm the relationship between *EgMADS16*, *EgmiR5179*, and oil biosynthesis. The results depicted one pathway by which miRNAs target transcription factors and ultimately regulate lipid metabolism, providing a new strategy for lipid metabolism research in oil palm.

MATERIALS AND METHODS

Plant Materials and Strains

Oil palm (*Elaeis guineensis* Jacq.) fruits were collected at the Chinese Academy of Tropical Agricultural Sciences in Hainan, PR China. These fruits were divided into phase 1 [30–60 days after pollination (DAP)], phase 2 (60–100 DAP), phase 3 (100–120 DAP), phase 4 (120–140 DAP), and phase 5 (140–160 DAP) according to the developmental stage (Tranbarger et al., 2011) and stored at −80°C until the next experiment. Three independent bunches were collected from three distinct individuals which at the similar stage. *Arabidopsis thaliana* plants were grown in a 23°C incubator with 16 h light/8 h dark cycles. In addition, oil palm embryoids were induced and cultured using the method in previous research (Zou et al., 2019). All strains, including *DH5α* (*E. coli*), Y187 and Y2HGold (yeast), and GV3101 (*Agrobacterium*), were maintained by our laboratory.

RNA Extraction and Real-Time PCR Analysis

Total RNA of oil palm fruit mesocarps (0.5 g), *Arabidopsis* leaves (0.1 g), and oil palm embryoids (0.2 g) was extracted by an RNAprep Pure Plant Kit (Polysaccharides and Polyphenolics-rich; Tiangen, Beijing, China). Protoplastic RNA was isolated using TRIzol Reagent (Invitrogen, United States). cDNA was synthesized using the FastQuant RT kit (with gDNase; Tiangen, Beijing, China), and quantitative real-time PCR (qPCR) was performed with TB GreenTM Premix Ex TaqTM II (Tli RNaseH Plus; TaKaRa, Japan) on a CFX96 Touch System (Bio-Rad, United States). Each sample was set to three replicates, and the internal control for the oil palm sample was β-Actine, while that for the *Arabidopsis* sample was Actin7. In addition, all experimental steps were provided by the manufacturer, and the related primers designed by Primer Premier 5 are shown in **Supplementary Table 1**.

Gene Cloning and Vector Construction

The vector pCAMBIA3301 was used for plant transformation. pGreen II 62-SK (SK) was used for protoplast transfection and the dual-luciferase reporter assay. pCAMBIA1300S containing the green fluorescent protein (GFP) gene was used for subcellular localization. The pHiS2.1, pGADT7, and pGBKT7 vectors were used for the yeast hybrid assay, and the pSPYNE and pSPYCE vectors were used for BiFC analysis. The CDS of *EgMADS16* was cloned using different primers and ligated into pGreen II 0800-miRNA (LUC), pGADT7, and pGBKT7 using a One Step Cloning Kit (Vazyme) according to the principle of homologous recombination. The CDS of *EgMADS16* without the final TGA was cloned into pCAMBIA1300S and pSPYNE. Likewise, the CDS of EgGLO1 without the final TGA was cloned into pSPYCE vectors. For the *EgMADS16*-p3301 vector, we ligated the CDS of *EgMADS16* into the pCAMBIA1300S vector, cut the 35S::*EgMADS16*::NOS terminator, and inserted the terminator into the multiple cloning site of the pCAMBIA3301 vector using a restriction enzyme. The plasmids about *EgmiR5179* were constructed and conserved in our laboratory (Gao et al., 2019). All the primers used for the vector construction are shown in **Supplementary Table 2.**

Abbreviations: AP2, APETALA2; AS, acetosyringone; BiFC, bimolecular fluorescence complementation; BR, biological reagent; CDSs, coding region sequences; CoA, coenzyme A; DAP, days after pollination; DAPI, 4', 6-diamidino-2-phenylindole; DGAT, diacylglycerol acyltransferase; FA, fatty acid; FAD, fatty acid dehydrogenase; FAME, fatty acid methyl ester; GC, gas chromatography; GFP, green fluorescent protein; LACS, long-chain acyl-CoA synthetase; MS medium, Murashige and Skoog medium; OD, optical density; OX, over-expressed; PEG, polyethylene glycol; qPCR, quantitative real-time PCR; SAD, stearoyl-ACP desaturase; YFP, yellow fluorescent protein.

Subcellular Localization in *Nicotiana benthamiana*

The subcellular localization of *EgMADS16* protein was performed in *Nicotiana benthamiana* leaves according to previous research (Jessen et al., 2015). *Agrobacterium tumefaciens* GV3101 strains harboring *EgMADS16*-p1300SGFP plasmids, which encode the MADS16-EGFP fusion protein, were incubated to an OD 600 of 0.6; after centrifugation (4,000 rpm, 10 min), they were resuspended in the equal volume buffer (0.01 M $MgCl_2$, 0.01 M MES, PH5.5, and 150 μm AS) and infiltrated into the leaves of *Nicotiana benthamiana*. After incubation for 36–72 h, the GFP signals in the lower epidermis of these leaves were observed using a fluorescence inverted microscope (Nikon, TS2-LS) with an excitation wavelength of 430–510 nm. At the same time, nuclei were stained with 4', 6-diamidino-2-phenylindole (Sigma-Aldrich, United States) and observed using excitation wavelengths of 330–380 nm.

Dual-Luciferase Reporter Assay

The 10 μg EgMADS16-LUC plasmids were transformed into 200 μl oil palm protoplasts (5×10^5/ml) with 10 μg EgmiR5179-SK or SK plasmids; each sample was set to three replicates. After incubating for 14–18 h, the firefly and Renilla luciferase activities were tested using a dual-luciferase reporter gene assay kit (Promega, United States). At the same time, *EgMADS16*-LUC was transformed into wild-type or OXEgmiR5179 *Arabidopsis* protoplasts, and the dual-luciferase activities were analyzed using the same method.

Protoplast Isolation and Transformation

The protoplast isolation and transfection of *Arabidopsis* leaves were performed as described in a previous study (Yoo et al., 2007). In addition, protoplasts of oil palm leaves were isolated according to the preparation of *Arabidopsis* leaf protoplasts, but the contents of Cellulase R10 (BR) and Macerozyme R10 (BR) were doubled. The plasmids were transferred into oil palm protoplasts using an equal volume 40% (w/v) polyethylene glycol/50 mm $MgCl_2$ solution, and heat shock treatment was performed as described in previous research (Masani et al., 2014).

Arabidopsis thaliana Transformation

A. thaliana was cultured in 16 h light/8 h dark at 23°C. *EgMADS16*-p3301 plasmids were transformed into GV3101 *Agrobacterium* and then introduced into *A. thaliana* using the floral dip method (Jin et al., 2017). Moreover, transformants were selected by 1/2 Murashige and Skoog medium containing 60 mg/L glufosinate ammonium.

Oil Palm Embryoids Culture and Transformation

Oil palm embryoids were cultured using woody plant medium in a 28°C incubator with 12 h light/12 h dark cycles according to previous research (Zou et al., 2019). *A. tumefaciens* GV3101, which contained *EgMADS16*-p3301 plasmids, was used to infect oil palm embryoids for 15 min with an OD_{600} of 0.5. Then, these embryoids were cultured on cocultivation medium (woody plant medium supplemented with 100 mg/L cysteine and 100 μm AS) at 19°C for 2 days and on screening medium (woody plant medium supplemented with 400 mg/L timentin and 60 mg/L glufosinate ammonium) at 28°C for 4 months, and the medium was regenerated every 20 days.

Total Lipid Extraction and Fatty Acid Analysis of the *Arabidopsis* Plants and Oil Palm Embryoids

Both the lipid and fatty acid analyses of *Arabidopsis* plants and oil palm embryoids were conducted according to previous studies (Yuan et al., 2017). In brief, 5 ml chloroform-methanol (volume ratio 2:1) was used to extract lipids, and then, lipids were dried by a Termovap sample concentrator. In addition, 10 μg C17:0 was added to the lipid samples as an internal standard. All samples were methylated by 3 ml concentrated sulfuric acid-methanol (volume ratio 1:40) at 80°C for 2 h. Then, 3 ml N-hexane and 2 ml 0.9% (W/V) sodium chloride solution were added. After centrifuging at 4,000 rpm for 5 min, the supernatant was transferred to a new tube and dried by a Termovap sample concentrator. The fatty acid methyl ester was finally dissolved in 1 ml n-hexane for GC analysis. The GC analysis was performed by the Analytical and Testing Center of Hainan University. Detailed operation parameters: the oven temperature was initially maintained at 150°C for 1 min, then increased at 8°C/min to 250°C, and then increased to 250°C and maintained for 5 min. The split ratio was 1:30, and the carrier gas was helium at a flow rate of 1.0 ml/min in constant flow mode. The injector was at 250°C, and the detector, at 230°C. And the lipid mass was calculated using the internal standard method.

Yeast Two-Hybrid Assays

Yeast two-hybrid assays were performed using Matchmaker™ Gold Yeast Two-Hybrid System (Clontech, United States). According to the user manual, EgMADS16-pGBKT7 plasmids were transfected into Y2H Gold yeast strains, and the autoactivation of EgMADS16 transcription factor was tested. Then, the EgMADS16-pGBKT7 Y2H Gold yeast strains and oil palm library strains which kept by our laboratory were combined. After incubation at 30°C for 20–24 h at 45 rpm, these strains were plated on SD/Try/Leu/-His/Ade/+X-α-Gal/+Aba mediums.

Bimolecular Fluorescence Complementation Analysis

EgMADS16-pSPYNE and EgGLO1-pSPYCE were transformed into Agrobacterium strains GV3101, respectively. And then these strains were coinfiltrated into the leaves of *N. benthamiana* using the same method as subcellular localization. Moreover, after incubation for 36–72 h, the yellow fluorescent protein (YFP) signal was observed using the excitation wavelength of 430–510 nm.

Bioinformational Analysis

Conserved domain was analyzed in the web site.[1] Multiple sequence alignment was carried out by Clustal Omega.[2] Small RNA target analysis was performed using the web site.[3] The phylogenetic tree of EgMADS16 and other MADS proteins from different species was constructed using the neighbor-joining method in MEGA6.

Statistical Analysis

The values are the means ± SD ($n \geqq 3$). Significant differences between groups were analyzed by SPSS software using Student's *t*-test. "*" represents a significant difference ($p < 0.05$), and "**" represents a highly significant difference ($p < 0.01$).

RESULTS

Cloning and Subcellular Localization of *EgMADS16*

The mRNA of *EgMADS16* (NM_001303583) is 951 bp in length and encodes a protein of 225 amino acids (NP_001290512.1). The CDS of *EgMADS16*, which is 678 bp, from oil palm mesocarp using primers is shown in **Supplementary Table 2**. qPCR indicated that the expression of *EgMADS16* fluctuated from phase 1 to phase 3 and then sharply increased and reached a peak in phase 4; however, there was a gradual decline from phase 4 to phase 5 (**Figure 1A**). Conserved domain analysis (see footnote 1) showed that there are MADS_MEF2_like and K-box domains in the *EgMADS16* amino acid sequence (**Figure 1B**). In addition, we constructed a phylogenetic tree of EgMADS16 and other MADS proteins from different species using the neighbor-joining method in MEGA6, including EgGLO1 (XP_010911271.1), EgGLO2 (AAQ03229.1), OsMADS2 (XP_015623988.1), OsMADS4 (XP_015640709.1), OsMADS6 (XP_015623947.1), OsMADS8 (XP_015610824.1), OsMADS16 (XP_015641661.1), AcMADS16 (XP_020082339.1), BnAGL11 (XP_013719732.1), BnTT16 (NP_001303188.1), CenDEF (ALB26780.1), CenDEF3 (AFH66787.1), OitaDEF1 (BAO00916.1), OitaDEF2 (BAO00917.1), OitaDEF3 (BAO00918.1), MaMADS16 (XP_009418316.1), and PdMADS16 (XP_008781489.1). As shown in **Figure 1C**, *EgMADS16* was closest to PdMADS16 (91.56% identity), AcMADS16 (87.56% identity), and MaMADS16 (84.89% identity).

Moreover, to identify whether *EgMADS16* localized to the nucleus, similar to other transcription factors, we conducted a subcellular localization test in tobacco leaf epidermal cells, and the results indicated that the *EgMADS16*-GFP fusion protein was localized in the nucleus (**Figure 2**).

Verification of the Target Relationship Between *EgmiR5179* and *EgMADS16*

According to previous research, *OitaDEF2* is the target of *OitamiR5179* in *Orchid orchis italics* (Aceto et al., 2014). Likewise, *CenDEF3* is the target of *CenmiR5179* in *Cymbidium ensifolium* (Li et al., 2015). Therefore, small RNA target analysis (see footnote 3) suggested that *EgMADS16* is targeted by *EgmiR5179*. To verify this target relationship, we performed a dual-luciferase reporter assay in *Arabidopsis* and oil palm protoplasts. The results indicated that the relative luciferase activity of *EgMADS16*-LUC-transfected protoplasts was decreased with the expression of *EgmiR5179* (**Figures 3A,B**). At the same time, we transformed either or both EgmiR5179-SK and *EgMADS16*-LUC into oil palm protoplasts, and then, the relative expression level of *EgMADS16* was detected by qPCR. The results were consistent with the results of the dual-luciferase reporter assay in which the *EgMADS16* expression level was downregulated by *EgmiR5179* (**Figure 3C**).

Effect of *EgMADS16* on Lipid Biosynthesis

To characterize the role of *EgMADS16* in lipid biosynthesis, we obtained *EgMADS16*-overexpressing *Arabidopsis* lines (OX*EgMADS16* Line A and Line B; **Figure 4A**) and oil palm embryonic callus lines (OX*EgMADS16* Line 1 and Line 2; **Figure 5A**). Compared with the wild type, all OX*EgMADS16* lines had higher *EgMADS16* expression. Meanwhile, the relative fatty acid contents of OX*EgMADS16 Arabidopsis* seeds and oil palm embryonic calli were tested by GC. The results showed that the C18:0 and C18:3 contents of the OX*EgMADS16* lines significantly increased, while the C18:1 content decreased compared with that of the wild type (**Figures 4D, 5D**). In addition, there were significant decreases in the lipid contents of both OX*EgMADS16 Arabidopsis* seeds and oil palm embryonic calli (**Figures 4C, 5C**).

Regulation of *EgMADS16* in Lipid Biosynthesis by *EgmiR5179*

Based on the predicted targeting regulatory relationship, *EgmiR5179* should regulate the expression of *EgMADS16* and thus play a role in lipid biosynthesis. To verify this hypothesis, we generated transgenic *Arabidopsis* plants that coexpressed *EgmiR5179* and *EgMADS16* (OXEgmiR5179-*EgMADS16*; **Figure 6A**) and analyzed the FA and oil contents. As expected, *EgmiR5179* weakened the inhibitory effect of *EgMADS16* on oil contents (**Figure 6B**). Additionally, the relative contents of C18:0 and C18:3 in OXEgmiR5179-*EgMADS16* seeds decreased compared with those of the OX*EgMADS16* seeds, while those in OX*EgMADS16* seeds rose compared with WT seeds. The C18:1 content of OXEgmiR5179-*EgMADS16* seeds increased compared with that of OX*EgMADS16* seeds, while that of OX*EgMADS16* seeds decreased compared with that of WT seeds (**Figure 6C**).

Identification of the Downstream Genes of *EgMADS16*

EgMADS16 belongs to MADS-box family. This means that it is likely to function as a transcription factor to regulate lipid biosynthesis by regulating lipid biosynthesis-related genes. Therefore, we selected seven related genes according to the

[1]https://www.ncbi.nlm.nih.gov/Structure/cdd/wrpsb.cgi
[2]http://www.ebi.ac.uk/Tools/msa/clustalo/
[3]http://plantgrn.noble.org/psRNATarget/analysis?function=3

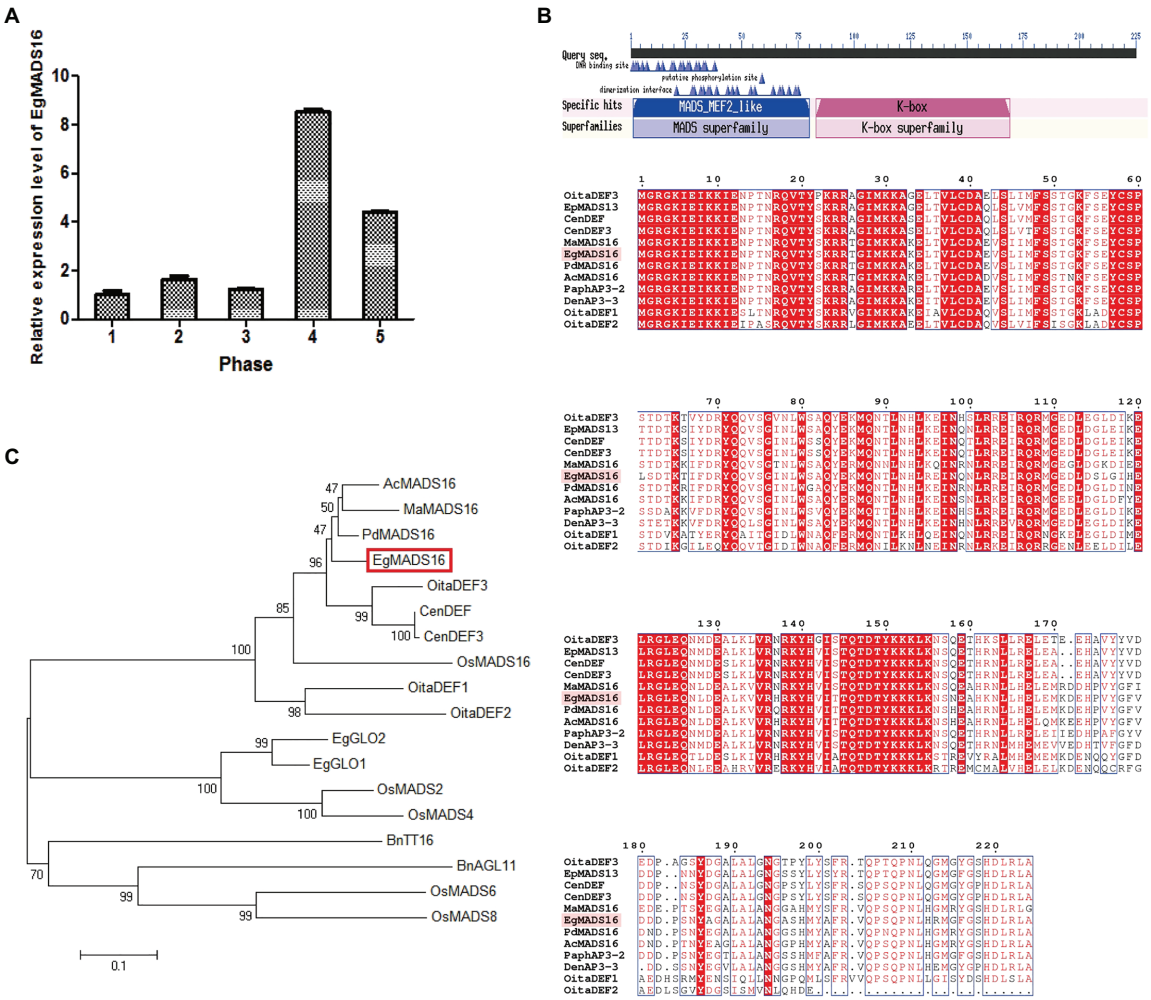

FIGURE 1 | The expression patterns and sequence analysis of *EgMADS16*. **(A)** The relative expression level of *EgMADS16* in different developmental stages of oil palm fruit mesocarp. Phase 1–5: fruits 30–60 days, 60–100 days, 100–120 days, 120–140 days, and 140–160 days after pollination. The values are the means±SD (n = 3). **(B)** Conserved domains analysis of EgMADS16 protein. **(C)** The phylogenetic tree of EgMADS16 and other MADS proteins, including EgGLO1 (XP_010911271.1), EgGLO2 (AAQ03229.1), OsMADS2 (XP_015623988.1), OsMADS4 (XP_015640709.1), OsMADS6 (XP_015623947.1), OsMADS8 (XP_015610824.1), OsMADS16 (XP_015641661.1), AcMADS16 (XP_020082339.1), BnAGL11 (XP_013719732.1), BnTT16 (NP_001303188.1), CenDEF (ALB26780.1), CenDEF3 (AFH66787.1), OitaDEF1 (BAO00916.1), OitaDEF2 (BAO00917.1), OitaDEF3 (BAO00918.1), MaMADS16 (XP_009418316.1), and PdMADS16 (XP_008781489.1).

results of fatty acid compositions and contents of OXEgMADS lines, and we examined the expression level of these genes in OXEgMADS oil palm embryonic callus by qPCR. As a result, the expression levels of *EgFAD2*, *EgDGAT2*, and *EgSAD* significantly declined, while those of *EgFAD7*, *EgFAD6*, *EgLACS9*, and *EgDGAT1* did not significantly change (**Figures 7A–G**).

To further investigate whether *EgMADS16* protein regulates the expression of *EgFAD2*, *EgDGAT2*, and *EgSAD* by binding to their promoters, we conducted yeast one-hybrid assays. However, interactions between *EgMADS16* and the promoters of *EgFAD2*, *EgDGAT2*, or *EgSAD* were not detected (**Supplementary Figure 1**), suggesting that *EgMADS16* downregulated these genes by interacting with other DNA-binding transcription factors rather than directly binding to their promoters.

EgMADS16 Binds to EgGLO1 Proteins

Next, we used yeast two-hybrid assays to identify the transcription factors that interact with *EgMADS16* proteins. Considering the activation domains of transcription factors, we tested the autoactivation of *EgMADS16* on yeast reporters. The results showed that *EgMADS16* proteins have an activation domain, but Aba can inhibit its autoactivation (**Supplementary Figure 2**). Therefore, we performed yeast two-hybrid assays and found that there was an interaction between *EgMADS16* and EgGLO1 (XP_010911271.1) proteins (**Figure 8A**). To further verify this interaction, BiFC was used. YFP protein fluorescence was observed only when *EgMADS16*-pSPYNE and EgGLO1-pSPYCE were coinfiltrated into the leaves of *N. benthamiana* (**Figure 8B**), suggesting that *EgMADS16* binds to the EgGLO1 proteins.

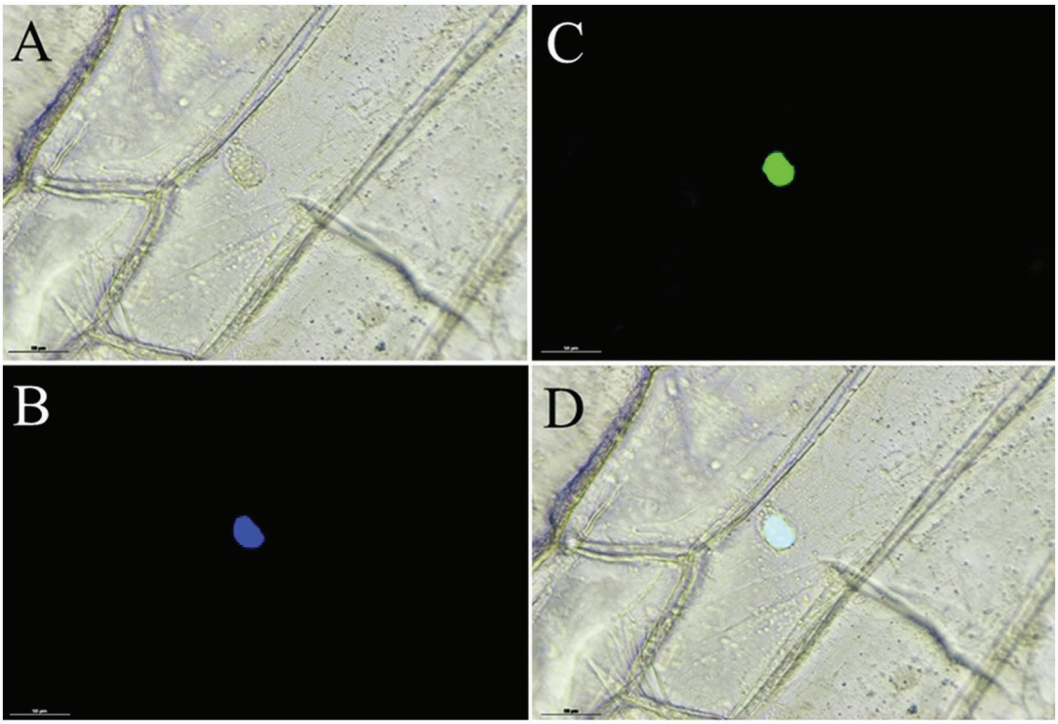

FIGURE 2 | Subcellular localization of EgMADS16 protein in onion epidermal cells. **(A)** Bright light. **(B)** DAPI. **(C)** EgMADS-GFP fluorescence. **(D)** Merged image. Scale bar, 50 μm.

DISCUSSION

In this paper, the role of the *EgMADS16* gene in oil biosynthesis was studied. Among the oil palm fruits at five different developmental stages, the *EgMADS16* gene had the highest transcription level in the fourth stage and decreased in the fifth stage. The phylogenetic tree analysis showed that PdMADS16 had the closest relationship with *EgMADS16*, followed by *AcMADS16* and *MaMADS16*, but their functions have not been reported. The subcellular localization results showed that *EgMADS16* protein was located in the nucleus, which is consistent with the localization of other transcription factors. Previous studies found that MADS-box genes were closely related to plant growth and development. In oil palm, it has been proven that the MADS-box gene *EgSQUA1* is related to the height of the plant and the length of pedicels and siliques; *EgGLO2* promotes a partial conversion of sepals to petals in whorl 1; and *EgAGL2-1* is involved in stamens and gynoecium development (Adam et al., 2007). However, the overexpression of *EgMADS16* (*EgDEF1*) did not change the phenotype of flowers (Adam et al., 2007) but participated in the biosynthesis of oil and fatty acids, which was demonstrated by the significant increases in C18:0 and C18:3 contents and the decreases in C18:1 content and total oil yield (**Figures 4, 5**).

As a transcription factor, *EgMADS16* likely participates in the regulation of oil biosynthesis in the same way. According to the fatty acid compositions and contents of OXEgMADS lines, *EgSAD*, *EgFAD2*, *EgFAD6*, *EgFAD7*, *EgLACS9*, *EgDGAT1*, and *EgDGAT2* were selected as candidate genes, and qRT-PCR was used to detect the expression levels of these seven oil biosynthesis-related genes in OX*EgMADS16* oil palm embryonic calli. As a result, the transcription levels of *EgSAD*, *EgFAD2*, and *EgDGAT2* were significantly suppressed (**Figures 7A–C**). This result indicates that *EgMADS16* regulates the contents of fatty acids and oil by inhibiting the expression of EgSAD, EgFAD2, and EgDGAT2. To determine whether the *EgMADS16* protein directly regulates the expression of these three genes by binding to their promoters, a yeast one-hybrid assay was conducted. However, the results showed that the *EgMADS16* protein cannot directly bind to the promoters of *EgSAD*, *EgFAD2*, and *EgDGAT2*. This means that *EgMADS16* protein likely inhibits the expression level of these three genes by interacting with an intermediate protein, which can directly bind to the promoters of *EgSAD*, *EgFAD2*, and EgDGAT2.

In addition, small RNA target analysis showed that *EgMADS16* is targeted by *EgmiR5179* (**Supplementary Figure 3**). Moreover, the dual-luciferase reporter assay and qRT-PCR in protoplasts further suggested this target relationship: *EgmiR5179* can inhibit the expression of *EgMADS16* (*EgDEF1*; **Figure 3**). The overexpression of *EgmiR5179* significantly increased the total oil content in seeds (Gao et al., 2019). In this study, the overexpression of *EgMADS16* significantly reduced the total oil content of *Arabidopsis* seeds and oil palm embryonic calli (**Figures 4, 5**), which is consistent with the role of *EgMADS16* as the target gene of *EgmiR5179*. In addition, compared with OXMADS16 transgenic *Arabidopsis* seeds, the total oil content

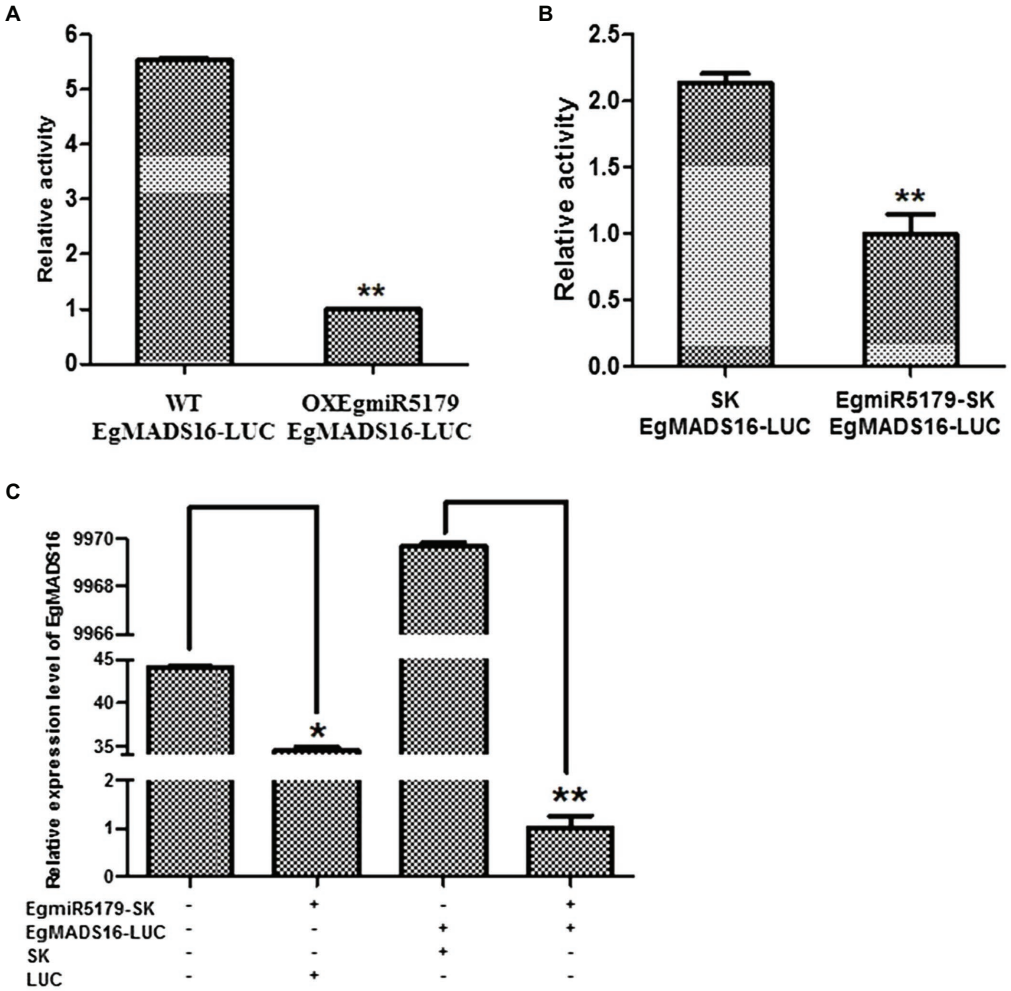

FIGURE 3 | *EgMADS16* is the target gene of *EgmiR5179*. **(A)** Dual-luciferase reporter assay in Arabidopsis protoplasts. EgMADS16-LUC was transformed into wild-type and OXEgmiR5179 Arabidopsis protoplasts, respectively. **(B)** Dual-luciferase reporter assay in oil palm protoplasts. EgMADS16-LUC and SK or EgmiR5179-SK were transformed into oil palm protoplasts, respectively. **(C)** The relative expression level of *EgMADS16* in oil palm protoplasts that transformed either or both of *EgmiR5179* and *EgMADS16*. The values are the means ± SD ($n = 3$), "*" represents a significant difference ($p < 0.05$), and "**" represents a highly significant difference ($p < 0.01$) using Student's *t*-test.

of OXEgmiR5179-*EgMADS16* seeds increased significantly, C18:0 and C18:3 decreased, and C18:1 increased. More interestingly, this trend of change was opposite to the trend of oil and fatty acid contents in the seeds of OXMADS16 plants relative to the wild type (**Figures 6B,C**). This implies that EgmiR5179 can inhibit the regulation of *EgMADS16* in the biosynthesis of oil and FAs and promote the accumulation of oil.

In previous studies, it has been proven that homologous complexes formed between MADS-box proteins to facilitate the binding of MADS-box proteins to DNA. For example, OsMADS16 protein interacts with OsMADS4, OsMADS6, and OsMADS8 proteins to regulate stamen development (Lee et al., 2003); GmMADS28 protein interacts with SOC1, AP1, and AGL8/FUL proteins to modulate floral organ number, petal identity, and sterility (Huang et al., 2014). Similarly, the results of yeast two-hybrid assays and BiFC suggested that there was an interaction between the *EgMADS16* protein and EgGLO1 protein (**Figure 8**). *EgMADS16* proteins regulate oil biosynthesis by interacting with the EgGLO1 proteins, which directly bind to the promoters of oil biosynthesis-related genes. However, there is no interaction between the OsMADS16 protein and OsMADS2 (Lee et al., 2003), which are homologs of *EgMADS16* and EgGLO1. In addition, this may be due to species differences.

In summary, we are hypothesizing a model of the molecular mechanism by which *EgMADS16* regulates oil biosynthesis (**Figure 9**). After *EgMADS16* is translated, the *EgMADS16* protein forms a complex with EgGLO1 or other proteins and binds to the promoter of *EgFAD2, EgSAD, EgDGAT2*, or other oil biosynthesis-related genes, inhibiting the transcription of these genes and affecting fatty acid components and oil accumulation. However, when *EgmiR5179* is overexpressed, the *EgmiR5179* mature sequence binds to *EgMADS16* mRNA and

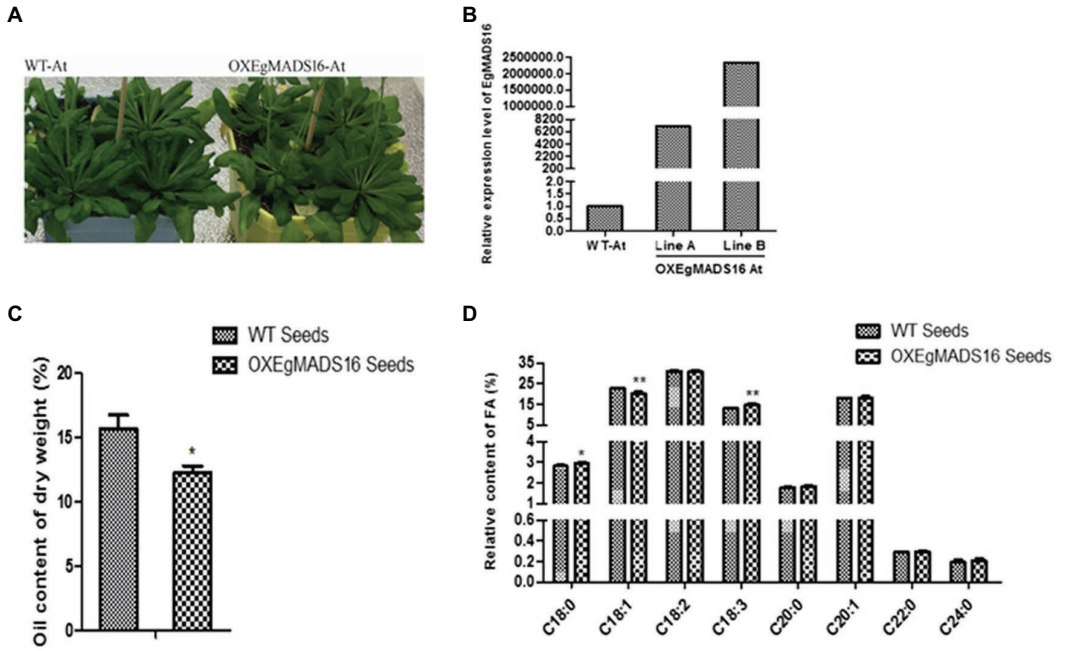

FIGURE 4 | Effect of EgMADS16 on lipid biosynthesis in oil palm embryonic callus. **(A)** Wild-type oil palm (WT-OP) embryonic callus and *EgMADS16* overexpression oil palm embryonic callus (OXEgMADS16 OP) on screening medium containing glufosinate ammonium. Scale bar, 3 mm. **(B)** The relative expression level of *EgMADS16* in WT-OP and OXEgMADS16 OP. **(C)** The oil content of WT and OXEgMADS16 oil palm embryonic callus. **(D)** The relative FA content of WT and OXEgMADS16 oil palm embryonic callus. The values are the means ± SD (n = 3), "*" represents a significant difference ($p < 0.05$), and "**" represents a highly significant difference ($p < 0.01$) using Student's t-test.

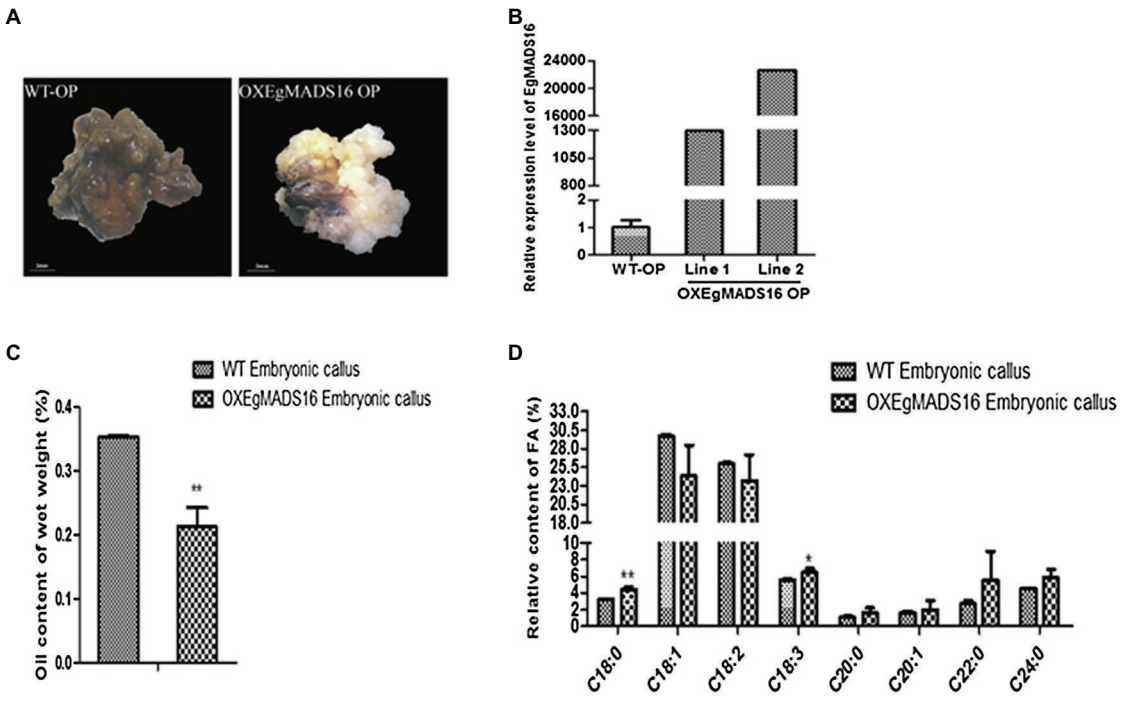

FIGURE 5 | Effect of EgMADS16 on lipid biosynthesis in *Arabidopsis*. **(A)** Wild-type Arabidopsis (WT-At) and *EgMADS16* overexpression Arabidopsis (OXEgMADS16 At). **(B)** The relative expression level of *EgMADS16* in WT-At and OXEgMADS16 At. **(C)** The oil content of WT and OXEgMADS16 Arabidopsis seeds. **(D)** The relative FA content of WT and OXEgMADS16 Arabidopsis seeds. The values are the means ± SD (n = 3), "*" represents a significant difference ($p < 0.05$), and "**" represents a highly significant difference ($p < 0.01$) using Student's t-test.

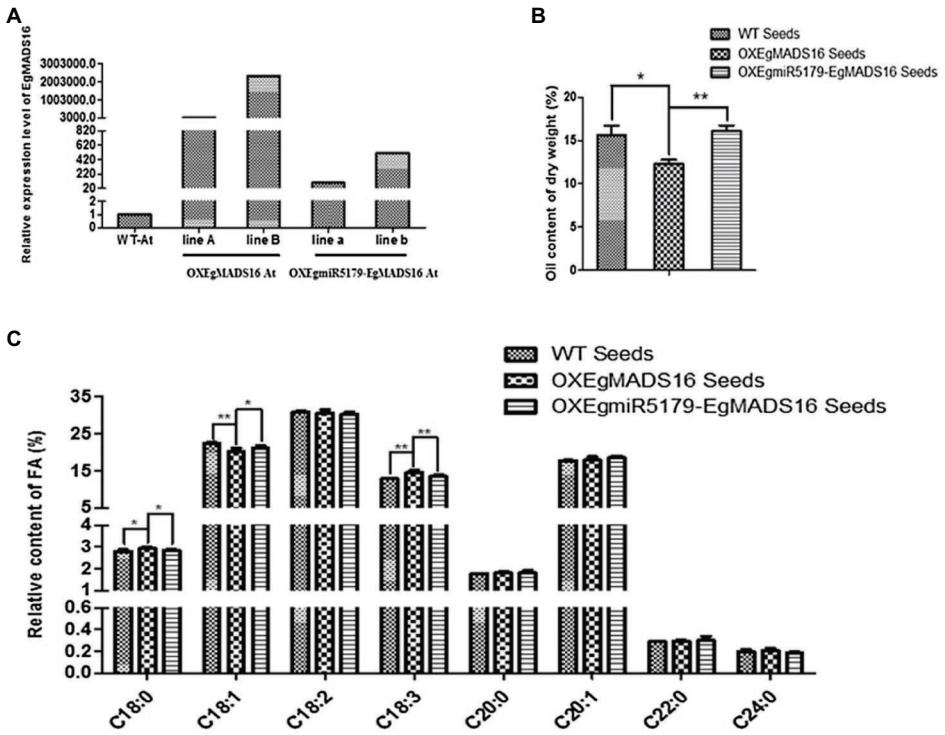

FIGURE 6 | The effect of *EgMADS16* on lipid biosynthesis is inhibited by *EgmiR5179* in Arabidopsis. **(A)** The relative expression level of *EgMADS16* in wild-type and transgenic Arabidopsis. **(B)** The oil content of wild-type and transgenic Arabidopsis seeds. **(C)** The relative FA content of wild-type and transgenic Arabidopsis seeds. The values are the means ± SD ($n = 3$), "*" represents a significant difference ($p < 0.05$), and "**" represents a highly significant difference ($p < 0.01$) using Student's *t*-test. OXEgmiR5179-EgMADS16 At: Arabidopsis coexpressed *EgmiR5179* and *EgMADS16*.

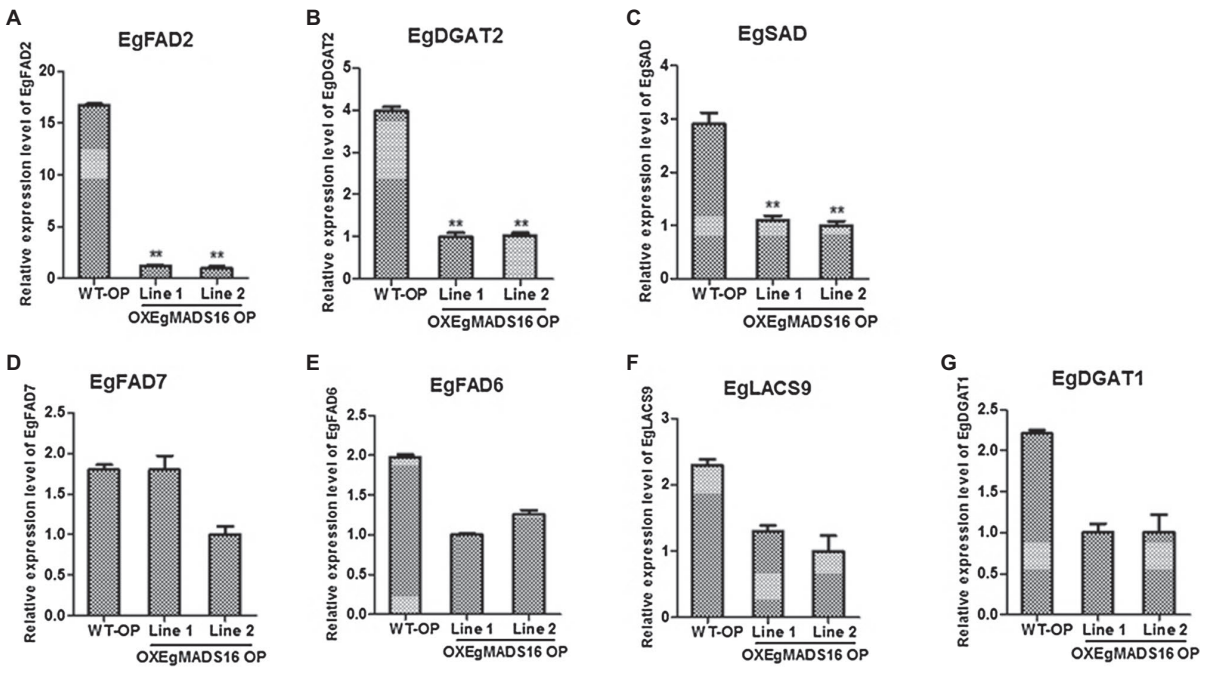

FIGURE 7 | Identification of downstream genes of EgMADS16 protein. **(A–G)** The relative expression level of *EgFAD2* **(A)**, *EgDGAT2* **(B)**, *EgSAD* **(C)**, *EgFAD7* **(D)**, *EgFAD6* **(E)**, *EgLACS9* **(F)**, and *EgDGAT1* **(G)** in WT and OXEgMADS16 oil palm embryonic callus. The values are the means ± SD ($n = 3$). "**" represents a highly significant difference ($p < 0.01$) using Student's *t*-test.

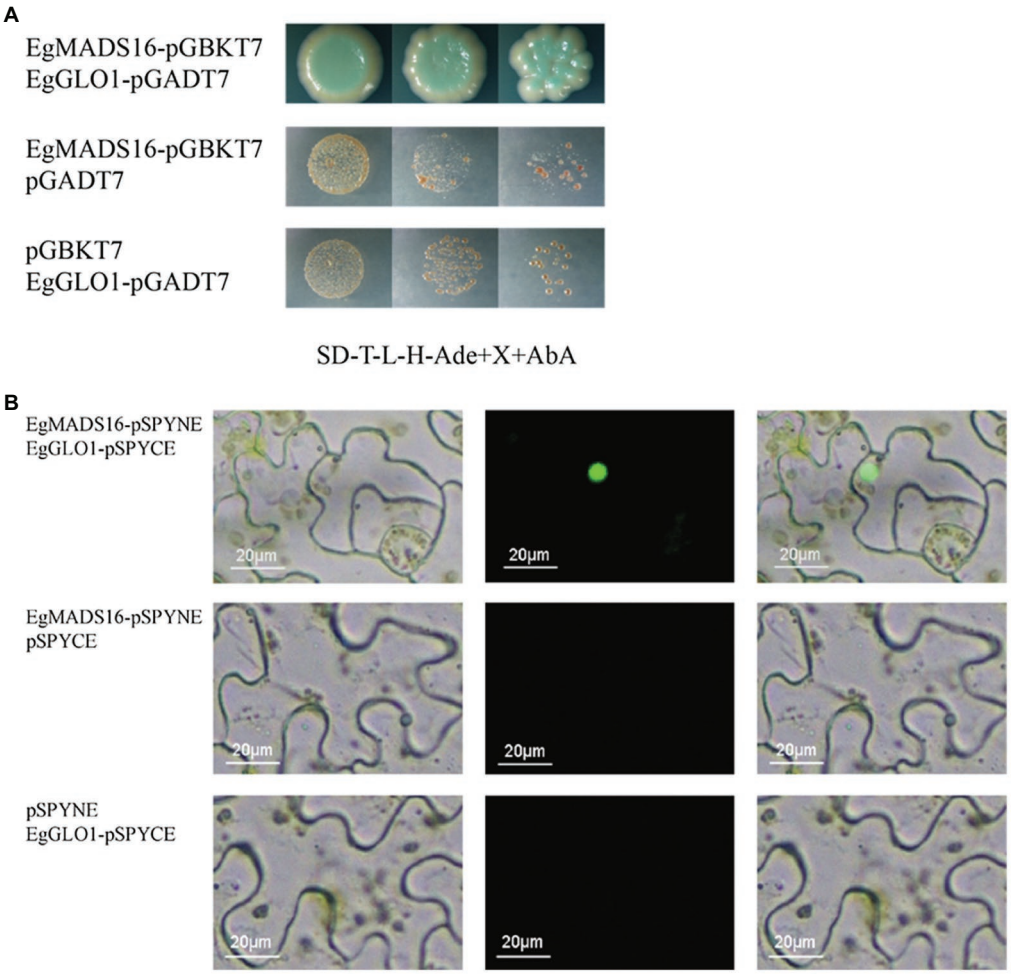

FIGURE 8 | EgMADS16 protein binds to EgGLO1 protein. **(A)** Yeast two-hybrid assay of EgMADS16 protein and EgGLO1 protein. **(B)** BiFC of EgMADS16 protein and EgGLO1 protein. Scale bar, 20 μm.

inhibits its expression so that the transcription of downstream oil biosynthesis-related genes cannot be inhibited by *EgMADS16* protein.

Nevertheless, the intermediate proteins regulated by *EgMADS16* proteins for the transcription of *EgSAD*, *EgFAD2*, and *EgDGAT2* have yet to be studied. It is unclear which oil biosynthesis-related genes, the *EgMADS16*/EgGLO1 complex, regulate. Nevertheless, the molecular mechanism presented in this paper provides a preliminary understanding of the regulation of oil biosynthesis by transcription factors in oil palm, which lays the foundation for further research and provides a strategy for obtaining a higher yield of oil palm in the future.

DATA AVAILABILITY STATEMENT

The datasets presented in this study can be found in online repositories. The names of the repository/repositories and accession number(s) can be found in the article/**Supplementary Material**.

AUTHOR CONTRIBUTIONS

DL and YZ designed the research. YW, JZo, and JZh performed the research. YZ and DL wrote the paper. All authors read and approved the final manuscript.

FUNDING

This research was supported by the Hainan Provincial Natural Science Foundation of China (No. 2019CXTD397), the National Natural Science Foundation of China (NSFC; No. 31660222), and the National Key R&D Program of China (2018YFD1000500).

SUPPLEMENTARY MATERIAL

The Supplementary Material for this article can be found online at: https://www.frontiersin.org/articles/10.3389/fpls.2021.722596/full#supplementary-material

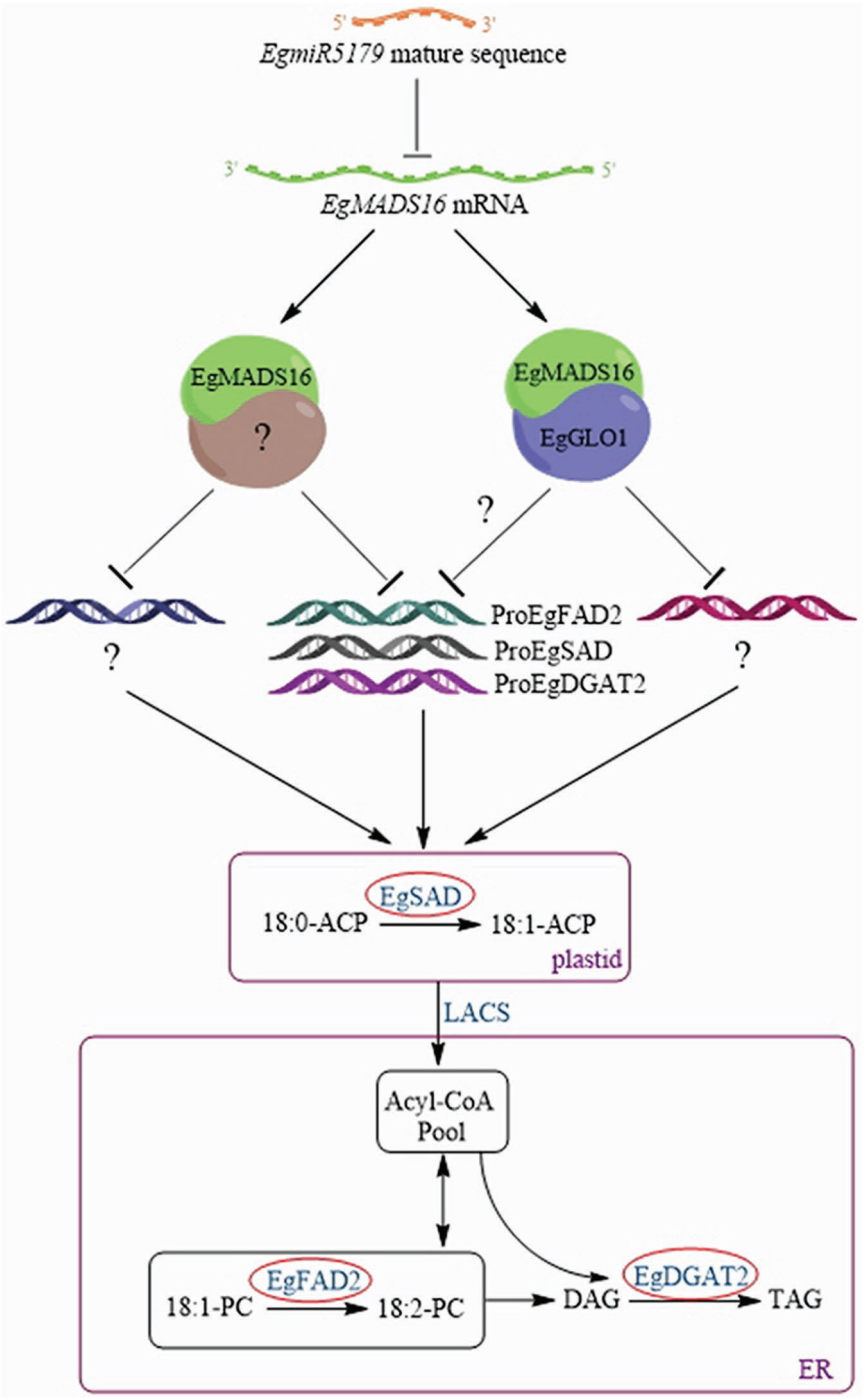

FIGURE 9 | A model about the molecular mechanism of *EgMADS16* regulating oil biosynthesis. EgMADS16 protein forms a complex with EgGLO1 or other proteins and binds to the promoter of *EgFAD2* or *EgSAD* or *EgDGAT2* or other oil biosynthesis-related genes, inhibiting the transcription of these genes and affecting fatty acid components and oil accumulation. However, *EgmiR5179* targets to *EgMADS16* mRNA and inhibits its expression, so that the oil accumulation is promoted.

REFERENCES

Aceto, S., Sica, M., De Paolo, S., D'argenio, V., Cantiello, P., Salvatore, F., et al. (2014). The analysis of the inflorescence miRNome of the orchid orchis italica reveals a DEF-like MADS-box gene as a new miRNA target. *PLoS One* 9:e97839. doi: 10.1371/journal.pone.0097839

Adam, H., Jouannic, S., Orieux, Y., Morcillo, F., Richaud, F., Duval, Y., et al. (2007). Functional characterization of MADS box genes involved in the determination of oil palm flower structure. *J. Exp. Bot.* 58, 1245–1259. doi: 10.1093/jxb/erl263

Bhagya, H. P., Kalyana Babu, B., Gangadharappa, P. M., Naika, M. B. N., Satish, D., and Mathur, R. K. (2020). Identification of QTLs in oil palm

(*Elaeis guineensis* Jacq.) using SSR markers through association mapping. *J. Genet.* 99:19. doi: 10.1007/s12041-020-1180-4

Dyer, J. M., Stymne, S., Green, A. G., and Carlsson, A. S. (2008). High-value oils from plants. *Plant J.* 54, 640–655. doi: 10.1111/j.1365-313X.2008.03430.x

Gao, L.-C., Wang, Y.-F., Zhu, Z., Chen, H., Sun, R.-H., Zheng, Y.-S., et al. (2019). EgmiR5179 from the mesocarp of oil palm (*Elaeis guineensis* Jacq.) regulates oil accumulation by targeting NAD transporter 1. *Ind. Crop. Prod.* 137, 126–136. doi: 10.1016/j.indcrop.2019.05.013

Huang, F., Xu, G., Chi, Y., Liu, H., Xue, Q., Zhao, T., et al. (2014). A soybean MADS-box protein modulates floral. *BMC Plant Biol.* 14, 1–4. doi: 10.1186/1471-2229-14-89

Jessen, D., Roth, C., Wiermer, M., and Fulda, M. (2015). Two activities of long-chain acyl-coenzyme a synthetase are involved in lipid trafficking between the endoplasmic reticulum and the plastid in Arabidopsis. *Plant Physiol.* 167, 351–366. doi: 10.1104/pp.114.250365

Jin, Y., Yuan, Y., Gao, L., Sun, R., Chen, L., Li, D., et al. (2017). Characterization and functional analysis of a type 2 diacylglycerol acyltransferase (DGAT2) gene from oil palm (*Elaeis guineensis* jacq.) mesocarp in saccharomyces cerevisiae and transgenic *Arabidopsis thaliana*. *Front. Plant Sci.* 8:1791. doi: 10.3389/fpls.2017.01791

Lee, S., Jeon, J.-S., An, K., Moon, Y.-H., Lee, S., Chung, Y.-Y., et al. (2003). Alteration of floral organ identity in rice through ectopic expression of OsMADS16. *Planta* 217, 904–911. doi: 10.1007/s00425-003-1066-8

Li, X., Jin, F., Jin, L., Jackson, A., Ma, X., Shu, X., et al. (2015). Characterization and comparative profiling of the small RNA transcriptomes in two phases of flowering in Cymbidium ensifolium. *BMC Genomics* 16:622. doi: 10.1186/s12864-015-1764-1

Li, S. Y., Zhang, Q., Jin, Y. H., Zou, J. X., Zheng, Y. S., and Li, D. D. (2020). A MADS-box gene, EgMADS21, negatively regulates EgDGAT2 expression and decreases polyunsaturated fatty acid accumulation in oil palm (*Elaeis guineensis* Jacq.). *Plant Cell Rep.* 39, 1505–1516. doi: 10.1007/s00299-020-02579-z

Liu, Y.-F., Li, Q.-T., Lu, X., Song, Q.-X., Lam, S.-M., Zhang, W.-K., et al. (2014). Soybean GmMYB73 promotes lipid accumulation in transgenic plants. *BMC Plant Biol.* 14:73. doi: 10.1186/1471-2229-14-73

Masani, M. Y., Noll, G. A., Parveez, G. K., Sambanthamurthi, R., and Prufer, D. (2014). Efficient transformation of oil palm protoplasts by PEG-mediated transfection and DNA microinjection. *PLoS One* 9:e96831. doi: 10.1371/journal.pone.0096831

Ohlroggeav, J., and Browse, J. (1995). Lipid biosynthesis. *Plant Cell* 7, 957–970. doi: 10.1105/2Ftpc.7.7.957

Osorio-Guarin, J. A., Garzon-Martinez, G. A., Delgadillo-Duran, P., Bastidas, S., Moreno, L. P., Enciso-Rodriguez, F. E., et al. (2019). Genome-wide association study (GWAS) for morphological and yield-related traits in an oil palm hybrid (*Elaeis oleifera* × *Elaeis guineensis*) population. *BMC Plant Biol.* 19:533. doi: 10.1186/s12870-019-2153-8

Shen, B., Allen, W. B., Zheng, P., Li, C., Glassman, K., Ranch, J., et al. (2010). Expression of ZmLEC1 and ZmWRI1 increases seed oil production in maize. *Plant Physiol.* 153, 980–987. doi: 10.1104/pp.110.157537

Song, Q.-X., Li, Q.-T., Liu, Y.-F., Zhang, F.-X., Ma, B., Zhang, W.-K., et al. (2013). Soybean GmbZIP123 gene enhances lipid content in the seeds of transgenic Arabidopsis plants. *J. Exp. Bot.* 64, 4329–4341. doi: 10.1093/jxb/ert238

Tranbarger, T. J., Dussert, S., Joet, T., Argout, X., Summo, M., Champion, A., et al. (2011). Regulatory mechanisms underlying oil palm fruit mesocarp maturation, ripening, and functional specialization in lipid and carotenoid metabolism. *Plant Physiol.* 156, 564–584. doi: 10.1104/pp.111.175141

Yeap, W. C., Lee, F. C., Shabari Shan, D. K., Musa, H., Appleton, D. R., and Kulaveerasingam, H. (2017). WRI1-1, ABI5, NF-YA3 and NF-YC2 increase oil biosynthesis in coordination with hormonal signaling during fruit development in oil palm. *Plant J.* 91, 97–113.

Yoo, S. D., Cho, Y. H., and Sheen, J. (2007). Arabidopsis mesophyll protoplasts: a versatile cell system for transient gene expression analysis. *Nat. Protoc.* 2, 1565–1572. doi: 10.1038/nprot.2007.199

Yuan, Y. J., Gao, L. C., Sun, R. H., Yu, T., Liang, Y. X., Li, D. D., et al. (2017). Seed-specific expression of an acyl-acyl carrier protein thioesterase CnFatB3 from coconut (*Cocos nucifera* L.) increases the accumulation of medium-chain fatty acids in transgenic Arabidopsis seeds. *Sci. Hortic.* 223, 5–9. doi: 10.1016/j.scienta.2017.05.029

Zou, J., Zhang, Q., Zhu, Z., Gao, L., Zheng, Y., and Li, D. (2019). Embryogenic callus induction and fatty acid composition analysis of oil palm (*Elaeis guineensis* cv. Tenera). *Sci. Hortic.* 245, 125–130. doi: 10.1016/j.scienta.2018.10.014

Conflict of Interest: The authors declare that the research was conducted in the absence of any commercial or financial relationships that could be construed as a potential conflict of interest.

Publisher's Note: All claims expressed in this article are solely those of the authors and do not necessarily represent those of their affiliated organizations, or those of the publisher, the editors and the reviewers. Any product that may be evaluated in this article, or claim that may be made by its manufacturer, is not guaranteed or endorsed by the publisher.

frontiers in Plant Science

ORIGINAL RESEARCH
published: 03 December 2021
doi: 10.3389/fpls.2021.748130

Abscisic Acid Improves Linoleic Acid Accumulation Possibly by Promoting Expression of *EgFAD2* and Other Fatty Acid Biosynthesis Genes in Oil Palm Mesocarp

Peng Shi[1,2,3], Wei Hua[1], Yin Min Htwe[2,3], Dapeng Zhang[2,3], Jun Li[1] and Yong Wang[2,3]**

[1] *Oil Crops Research Institute, Chinese Academy of Agricultural Sciences, Key Laboratory of Biology and Genetic Improvement of Oil Crops, Ministry of Agriculture and Rural Affairs, Wuhan, China,* [2] *Hainan Key Laboratory of Tropical Oil Crops Biology/Coconut Research Institute, Chinese Academy of Tropical Agricultural Sciences, Wenchang, China,* [3] *Hainan Key Laboratory for Biosafety Monitoring and Molecular Breeding in Off-Season Reproduction Regions/SanYa Research Institute, Chinese Academy of Tropical Agricultural Sciences, Sanya, China*

Abscisic acid plays an important role in fruit development. However, the effect of ABA on fatty acid biosynthesis in oil palm is still unknown. In this study, ABA treatments (CK, A1–A4) were applied to oil palm fruit at 16 WAP (weeks after pollination), and fatty acids in the mesocarp at 24 WAP were analyzed by GC-MS. Results showed that linoleic acid content under treatment A2 (20 μM ABA) was significantly higher (slightly increased by 8.33%) than the control. Therefore, mesocarp samples of A2, and the control at 16, 20, and 24 WAP was sampled for RNA-Seq. KEGG pathway enrichment analysis showed that 43 genes were differentially expressed in the fatty acid biosynthesis pathway, of which expression of *EgFAD2* (unigene 105050201) under 20 μM ABA treatment was 1.84-fold higher than in the control at 20 WAP. Further sequence analysis found that unigene 105050201 had more ABA-responsive elements (ABRE), complete conserved domains, and a C-terminal signaling motif among two *FAD2* copies. Furthermore, WGCNA and correlation analysis showed co-expression of *EgFAD2* (unigene 105050201) with transcription factors (TFs) (*WRI1*, *AP2-EREBP*, *bZIP*, *bHLH*, *C2C2-Dof*, *MYB*, *NAC*, and *WRKY*), ABA signaling genes (*PYR*, *PP2C*, *SnRK*, and *ABI5*), and other genes involved in fatty acid biosynthesis (*FATA*, *FATB*, *LACS*, *SAD*, *Oleosins*, and so on). These results indicated that ABA treatment promoted the expression of *FAD2* and other genes involved in fatty acid biosynthesis, which possibly resulted in the accumulation of linoleic acid. This study will be helpful for understanding the possible mechanisms through which ABA affects fatty acid biosynthesis and their accumulation in the mesocarp of oil palm.

Keywords: oil palm, linoleic acid, abscisic acid, *FAD2*, ABRE motif

OPEN ACCESS

Edited by:
Dongdong Li,
Hainan University, China

Reviewed by:
Enrique Martinez Force,
Instituto de la Grasa (IG), Spain
Zhou Kaibing,
Hainan University, China

****Correspondence:***
Jun Li
lijun@oilcrops.cn
Yong Wang
Elaeis@catas.cn

Specialty section:
This article was submitted to Crop and Product Physiology, a section of the journal Frontiers in Plant Science

Received: *27 July 2021*
Accepted: *29 October 2021*
Published: *03 December 2021*

Citation:
Shi P, Hua W, Htwe YM, Zhang D, Li J and Wang Y (2021) Abscisic Acid Improves Linoleic Acid Accumulation Possibly by Promoting Expression of EgFAD2 and Other Fatty Acid Biosynthesis Genes in Oil Palm Mesocarp. Front. Plant Sci. 12:748130. doi: 10.3389/fpls.2021.748130

INTRODUCTION

Oil palm (*Elaeis guineensis*) is a valuable tropical oil crop, providing approximately 36% of edible oils globally (Zhou et al., 2020). Its ability to produce high oil yields has led to its cultivation in tropical regions throughout the world. The fruit oil content of oil palm is high (about 50%), while unsaturated fatty acid content (about 50%) is lower than for other oil crops, such as rapeseed and

soybean. As unsaturated fatty acids have many health benefits, increasing the unsaturated fatty acid content of the mesocarp has important implications for improving palm oil quality.

The mesocarp is the most prolific oil production tissue in oil palm fruit; it mainly contains palmitic and oleic acids, and the fatty acid biosynthesis pathway and related genes have been already characterized (Dussert et al., 2013). Previous reports have shown that fatty acid biosynthesis is mainly involved in carbon chain extension and desaturation. Carbon chain extension takes place within plastids. In this process, fatty acids are synthesized from pyruvate, while pyruvate dehydrogenase complex (PDH), acetyl-CoA carboxylase (ACCase), malonyl-CoA (MAT), acyl carrier protein (ACP), ketoacyl-ACP synthase (KASI, KASII, and KASIII), ketoacyl-ACP reductase (KAR), hydroxyacyl-ACP dehydrase (HAD), enoyl-ACP reductase (EAR), stearate desaturase (SAD), and acyl-ACP thioesterase (FATA, FATB) participate in the process. Subsequently, 8:0–18:1 CoA are released to the endoplasmic reticulum by long-chain acyl-CoA synthetase (LACS). The 8:0–18:1 CoA is desaturated further by ω-6 desaturase (FAD2) and ω-3 desaturase FAD3 to concurrently synthesize triacylglycerol (TAG) with glycerol-3-phosphate (Glycerol-3-P). The enzymes glycerol-3-phosphate acyltransferase (GPAT), lysophosphatidic acid acyltransferase (LPAAT), phosphatidate phosphatase (PAP), diacylglycerol cholinephosphotransferase (CPT), phospholipid diacylglycerol acyltransferase (PDAT), 1-acylglycerol-3-phosphocholine acyltransferase (LPCAT), and diacylglycerol acyltransferase (DGAT) participate in this process. Finally, TAG accumulates in the cytoplasm with the oil formed by caleosin and oleosins proteins.

A few studies have investigated the effects of abscisic acid (ABA) on fatty acid biosynthesis in other organisms. Exogenous ABA increases levels of palmitic (C16:0) and stearic (C18:0) acids but decreases linoleic (C18:2) and α-linolenic (C18:3n3) acids in *Chlorella vulgaris* (Norlina et al., 2020). Exogenous ABA can enhance oleic (C18:1) and linoleic acid (C18:2) accumulation in developing Siberian apricot (*Prunus sibirica*) seeds, and *ABI3, SAD6, FAD2,* and *KCS1-like* showed upregulated expressions in ABA treatment compared with control (Huo et al., 2020); it can also enhance the linoleic acid and elaidic acid content in Cabernet Sauvignon (*Vitis vinifera* L.) grape berries (Ju et al., 2016). While studies on other plant species show that exogenous ABA influences linoleic acid biosynthesis, this process is still not well understood in oil palm. During mesocarp development, ABA remains at low levels at 12–14 weeks after pollination (WAP), while increasing sharply at 16–18 WAP and, thereafter, maintains a high level (Teh et al., 2014). Palmitic and oleic acid increased gradually from 10 to 23 WAP (weeks after pollination) in the mesocarp, while linoleic acid decreased gradually during these stages, with a sharp decline observed at 17 WAP. While ABA content increased, linoleic acid content declined simultaneously, suggesting that exogenous ABA plays an important role in fatty acid accumulation in oil palm mesocarp (Dussert et al., 2013). In order to confirm effects of exogenous ABA on fatty acid accumulation in oil palm mesocarp, we designed experiment of exogenous ABA treatment on oil palm fruit. Moreover, RNA-seq was also conducted to reveal a transcriptional mechanism that exogenous ABA regulated fatty acid accumulation.

MATERIALS AND METHODS

Field Conditions and Materials

Five fruit bunches (according to one control and four ABA treatments, respectively) aged 16 WAP from a 6-year-old oil palm tree (fruit form: Tenera) were selected from the oil palm germplasm nursery in the Coconut Research Institute, Chinese Academy of Tropical Agricultural Sciences, Wenchang, China (19°31′50″N, 110°45′58″E) during April 2020. Oil palms were spaced at 8 m × 8 m and drip irrigated. Four ABA [S-(+)-ABA, Yuanye Bio-Technology Co., Ltd, Shanghai, China] concentrations (10, 20, 50, and 200 μM) and a control (CK; with double-distilled water treatment) were prepared (**Table 1**). At 9:00 h with calm wind, at 26–33°C, ABA treatments were applied by spraying on the surface of fruits for 3 days in a row in the field. Mesocarps from three oil palm fruits were collected randomly at 1 day before treatment (CK_1, A1_1, A2_1, A3_1, and A4_1), 4 weeks later (CK_3, A1_3, A2_3, A3_3, and A4_3), and 8 weeks later (CK_5, A1_5, A2_5, A3_5, and A4_5). Each sample was collected in three biological replicates and immediately frozen in liquid nitrogen. Thereafter, they were kept in a freezer at −80°C for further analyses (**Table 1**).

Fatty Acid Analysis by GC-MS

Standard product configuration: 52 types of mixed standard solutions of fatty acid methyl ester were prepared with n-hexane to 0.5, 1, 5, 10, 25, 50, 100, 250, 500, 1,000, and 2,000 μg/ml concentration gradients. The concentration is the total concentration of each component.

Sample Pretreatment

Approximately 50 mg samples were mixed with 1 ml chloroform methanol (2:1) solution. The mixture was grounded in a high-throughput tissue grinder by shaking at 60 Hz for 1 min, and the process was repeated two times; subsequently, the mixture was subjected to ultrasound for 30 min at room temperature. Thereafter, the samples were centrifuged at 12,000 rpm at 4°C for 5 min. The supernatants were collected and mixed with 2 ml 1% sulfuric acid methanol, and vortexed for 1 min, and then followed by esterification in a water bath at 80°C for 30 min. After removal from the water bath, samples were allowed to cool and were then mixed thoroughly with 1 ml n-hexane and kept in room temperature for 5 min. To this mixture, 5 ml of ddH_2O (4°C) was added, and centrifugation took place at 12,000 rpm at 4°C for 10 min. The supernatant (700 μl) was collected and mixed thoroughly with 100 mg anhydrous sodium sulfate powder to remove excess water and centrifuged at 12,000 rpm for 5 min. Then, 10 μl of supernatant was collected and mixed with 490 μl n-hexane. Thereafter, 300 μl of diluent was collected. A total of 15 μl l,500 ppm methyl salicylate, which was used as an internal standard, was mixed with the collected diluents, and 250 μl of supernatant was collected for GC-MS analysis.

TABLE 1 | Treatment and sampling information.

Treatment	CK	A1	A2	A3	A4
ABA concentration	0 μM	10 μM	20 μM	50 μM	200 μM
Fatty acid composition measure	CK_5(24 WAP)	A1_5(24 WAP)	A2_5(24 WAP)	A3_5(24 WAP)	A4_5(24 WAP)
RNA-Seq	CK_1(16WAP), CK_3(20WAP), CK_5(24WAP)		A2_1(16WAP), A2_3(20WAP), A2_5(24WAP)		

GC-MS Analysis

GC-MS analysis was performed using a Thermo TG-FAME capillary column (50 m *0.25 mm ID *0.20 μm). The injection volume was 1 μl, and the split ratio was 8:1. The injection port temperature was 250°C, the ion source temperature was 230°C, the transmission line temperature was 250°C, and the quadrupole temperature was 150°C. The initial level of the programmed temperature was 80°C for 1 min; this subsequently rose to 160°C at 20°/min for 1.5 min; and 3°/min to 196° for 8.5 min. Finally, the temperature was raised to 250° at 20°/min for 3 min. Fatty acids were separated using helium as the carrier gas with a flow rate of 0.63 ml/min. The mass spectrometer was operated in the electron impact ionization (EI) mode at 70 eV.

RNA Extraction and Transcriptome Sequencing

Ethanol precipitation protocol and CTAB-pBIOZOL reagent were used for the purification of total RNA from the plant tissue according to the manual instructions. Grind about 80 mg samples into powder with liquid nitrogen and transfer the powder into 1.5 ml preheated 65°C CTAB-pBIOZOL reagents. The samples were incubated by a Thermo mixer for 15 min at 65°C to permit the complete dissociation of nucleoprotein complexes. After centrifuging at 12,000 × g for 5 min at 4°C, the supernatant was added 400 μl of chloroform per 1.5 ml of CTAB-pBIOZOL reagent and was centrifuged at 12,000 × g for 10 min at 4°C. The supernatant was transferred to a new 2 ml tube that added 700 μl acidic phenol and 200 μl chloroform, followed by centrifuging 12,000 × g for 10 min at 4°C. The aqueous phase was added equal volume of an aqueous phase of chloroform and centrifuged at 12,000 × g for 10 min at 4°C. The supernatant was added equal volume of supernatant of isopropyl alcohol and placed at −20°C for 2 h for precipitation. After that, the mix was centrifuged at 12,000 × g for 20 min at 4°C and then removed the supernatant. After washing with 1 ml of 75% ethanol, the RNA pellet was air-dried in the biosafety cabinet and was dissolved by adding 50 μl of DEPC-treated water. Subsequently, total RNA was qualified and quantified using a Nano Drop and Agilent 2100 bioanalyzer (Thermo Fisher Scientific, MA, United States).

Oligo (dT)-attached magnetic beads were used to purified mRNA. Purified mRNA was fragmented into small pieces with a fragment buffer at appropriate temperature. Then, first-strand cDNA was generated using random hexamer-primed reverse transcription, followed by a second-strand cDNA synthesis. Afterward, A-Tailing Mix and RNA Index Adapters were added by incubating to end repair. The cDNA fragments obtained from a previous step were amplified by PCR, and products were purified by Ampure XP Beads, and then dissolved in EB solution. The products were validated on the Agilent Technologies 2100 bioanalyzer for quality control. The double-stranded PCR products from a previous step were heated, denatured, and circularized by the splint oligo sequence to get the final library. The single-strand circle DNA (ssCir DNA) was formatted as the final library. The final library was amplified with phi29 to make DNA nanoball (DNB), which had more than 300 copies of one molecular, DNBs were loaded into the patterned nanoarray, and single-end 50 bases reads were generated on a MGISEQ500 platform (BGI-Shenzhen, China).

Transcriptome Data Processing, Reference Genome Selection, Differential Expression, and Functional Enrichment Analysis

The sequencing data were filtered with SOAPnuke v.1.4.0 and Trimmomatic v.0.36 (Li et al., 2008) by (1) removing reads containing a sequencing adapter; (2) removing reads whose the low-quality base ratio (base quality≤5) was>20%; (3) removing reads whose the unknown base ("N" base) ratio was>5%; afterward, clean reads were obtained and stored in a FASTQ format. The clean reads were mapped to the African oil palm genome[1] using HISAT2 v.2.1.0 (Kim et al., 2015). Bowtie2 v.2.2.5 (Langmead and Salzberg, 2012) was used to align the clean reads with the reference-coding gene set, and then the expression levels of genes were calculated using RSEM v.1.2.8 (Li and Dewey, 2011). The heatmap was drawn using the "pheatmap" tool of the R package according to gene expression in different samples. Essentially, differential expression analysis was performed using the DESeq2 v.1.4.5 (Love et al., 2014) with $Q \leq 0.05$. GO, and KEGG enrichment analysis of annotated differentially expressed genes was performed using the R function "Phyper" based on the hypergeometric test. The significant levels of terms and pathways were corrected using *Q*-value with a rigorous threshold ($Q \leq 0.05$) according to Bonferroni.

Statistical Analysis and Heatmap Drawing

Statistical analysis was performed to identify fatty acid compositions that were significant between treatments, using Fisher LSD in one-way ANOVA, at $p < 0.05$ or < 0.01. Correlation analysis was conducted using Origin 9.1. R package "pheatmap" was used for heatmap drawing.

[1]https://www.ncbi.nlm.nih.gov/assembly/GCF_000442705.1

Network Construction and Performance

R package "WGCNA" was used to construct a WGCNA network, correlation coefficients were calculated using Origin 9.1, and Cytoscape 3.8 was used to perform networking using WGCNA and the correlation network file.

Cis-Acting Element Prediction, Phylogenetic Tree Construction, and Protein Sequence Analysis

Promoter sequences used for *cis*-acting element prediction were downloaded from NCBI,[2] and then the FASTA format of promoter sequences was submitted to the PlantCARE website[3] for *cis*-acting element prediction. A phylogenetic tree was conducted in MEGA X using a maximum likelihood tree (Kumar et al., 2018). An alignment view of protein sequences was performed using GeneDoc software.

RESULTS

Effects of Exogenous Abscisic Acid on Fatty Acid Composition in the Mesocarps of Oil Palm

To determine fatty acid content and composition, mesocarps of the five treatments at 24 WAP were measured by GC-MS (**Table 1**). No significant differences were observed on oil content between ABA-treated samples (A2 and A4) and the control (**Figure 1** and **Supplementary Table 1**). The content of myristic acid, stearic acid, 10-transnonadecenoate, linoleic acid, arachidonic acid, behenic acid, and lignoceric acid increased significantly in A2 compared to CK, while content of main fatty acids components, such as palmitic acid and oleic acid, had no significant changes (**Figure 1** and **Supplementary Table 1**). Among those fatty acids, linoleic acid increased by 8.33% in A2 compared to CK. Although the standard deviation of linoleic acid in CK_5 was big, linoleic acid was selected for the object of in-depth analysis because its content was highest in those fatty acids, and it could possess higher application value.

Transcriptome Sequencing

Linoleic acid is reported to be an important unsaturated fatty acid in the oil palm mesocarp (Dussert et al., 2013). Therefore, A2 and CK samples at 16, 20, and 24 WAP were collected for RNA-seq analysis (**Table 1**). A total of 18 libraries were generated from the mesocarp of CK and A2 samples at 16, 20, and 24 WAP, with three biological replicates and produced 47.33–50.83 million raw reads (**Table 2**). After removing reads-containing adapters or poly-N and low-quality reads, the total number of clean reads per library was in the range of 41.95–43.48 million. Hierarchical indexing for spliced alignment of transcripts (HISAT) was used to compare clean reads to the reference genome[4] using Bowite2. Among the short clean reads, 80.34–83.31% were aligned against the reference genome.

Principal Component Analysis (PCA) showed that three biological replicates of each sample were well clustered. Two groups (CK_1 and A2_1) were clustered together, while the other four groups (CK_3, CK_5, A2_3, and A2_5) were distinguished from each other; in particular, A2_5 was found to be clearly distinguished from the remaining five groups (**Figure 2A**). To analyze the correlation of the samples, Pearson's correlation coefficient was calculated based on gene expression levels. Results showed that CK_1 was highly correlated with A2_1, and CK_3 was highly correlated with A2_3. Meanwhile A2_5 was clearly separated from other samples (**Figure 2B**), which was consistent with the PCA analysis.

The distribution of gene expression levels in each sample was then performed, and the degree of dispersion of the data distribution was observed (**Figure 2C**). The median values of genes expression under A2_5 were significantly lower ($p < 0.01$) than A2_1 and A2_3, and the same to CK_5 ($p < 0.01$).

Analysis of Differentially Expressed Genes

A total of 193 DEGs were detected in CK_1 vs. A2_1, of which 98 DEGs were upregulated and 95 DEGs were downregulated. In total, 5,807 DEGs were identified in CK_3 vs. A2-3, of which 2,930 DEGs were upregulated and 2,877 DEGs were downregulated. In CK_5 vs. A2_5, a total of 9,699 genes were identified as DEGs, of which 4,898 DEGs were upregulated and 4,801 DEGs were downregulated. A total of 118 DEGs overlapped among the groups (**Figures 3A,B**). The lowest number of DEGs (193) was identified in CK_1 vs. A2_1, which was sampled before ABA treatment, while the number of DEGs identified in CK_3 vs. A2_3 and CK_5 vs. A2_5 was sharply increased. These results indicated that ABA treatment had a great impact on transcriptional changes in oil palm mesocarps.

DEGs were subjected to Gene Ontology (GO) analysis to further understand their functions. Among 5,807 DEGs in CK_3 vs. A2_3, 4,361 were classified into three main GO categories: biological process, cellular component, and molecular function. The main biological processes represented were cellular process (1,309), metabolic process (1,144), and biological regulation (415). Major cellular component included membrane (1,386), cell (1,332), and membrane part (1,322). The main molecular functions were binding (2,246), catalytic activity (2,133), and transporter activity (260) (**Supplementary Figure 1A** and **Supplementary Table 2**). The top 20 GO enrichments were further analyzed, and results showed that the fatty acid biosynthetic process under the biological process was observed in these GO terms (**Supplementary Figure 1B** and **Supplementary Table 3**).

To identify significantly enriched pathways in CK_3 vs. A2_3, pathway annotation was conducted *via* the Kyoto Encyclopedia of Genes and Genomes (KEGG). In total, 2,763 DEGs were annotated in KEGG pathways; of which, 303, 263, and 271 DEGs were enriched in signal transduction, transcription, and lipid metabolism, respectively (**Supplementary Figure 1C** and

[2]https://www.ncbi.nlm.nih.gov/

[3]http://bioinformatics.psb.ugent.be/webtools/plantcare/html/

[4]https://www.ncbi.nlm.nih.gov/genome/2669

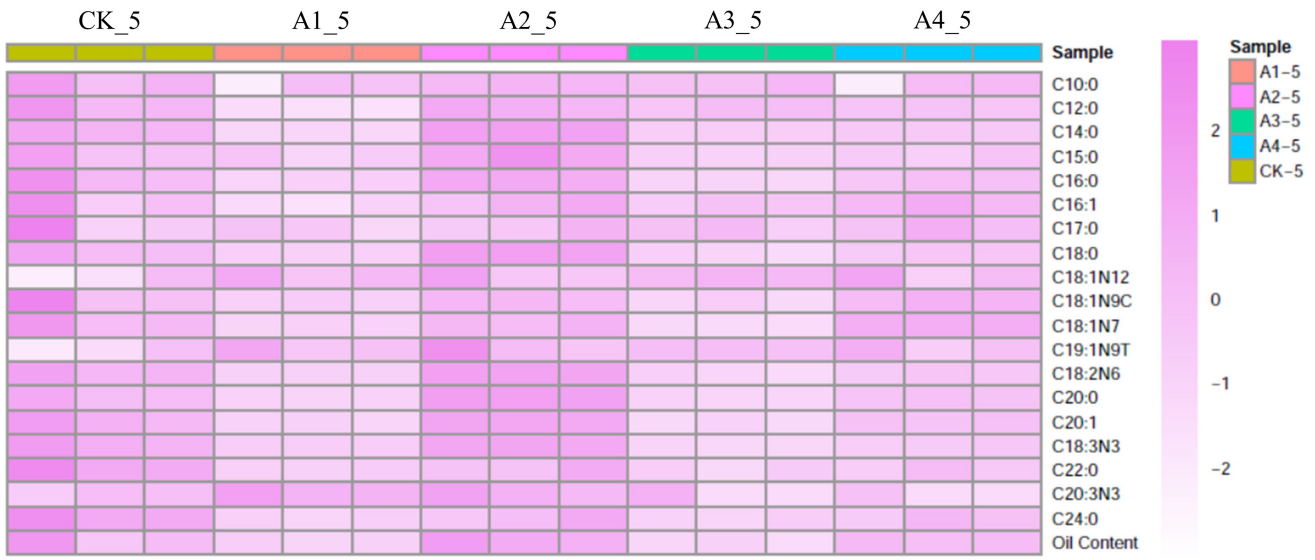

FIGURE 1 | Heat map of fatty acid composition content after different exogenous ABA treatments. CK, treatment with 0 μM ABA; A1, treatment with 10 μM ABA; A2, treatment with 20 μM ABA; A3, treatment with 50 μM ABA; A4, treatment with 200 μM ABA. Each colored cell on the map corresponds to a concentration value.

TABLE 2 | Categorization and a summary of abundance of RNA-seq reads and genes in 18 libraries.

Sample	Total raw reads (M)	Total clean reads (M)	Total clean bases (Gb)	Clean reads Q20 (%)	Clean reads Q30 (%)	Clean reads ratio (%)	Total genome mapping (%)	Uniquely genome mapping (%)	Total gene mapping (%)	Uniquely gene mapping (%)
A2_1A	49.08	43.45	6.52	94.47	88.22	88.52	82.62	38.42	75.73	60.63
A2_1B	49.08	43.30	6.50	94.34	87.94	88.23	82.40	37.87	76.05	61.10
A2_1C	49.08	43.45	6.52	94.43	88.13	88.52	82.22	37.81	75.28	60.33
A2_3A	47.33	42.04	6.31	94.41	88.09	88.83	82.80	38.64	78.98	63.14
A2_3B	49.08	43.48	6.52	94.26	87.77	88.60	82.60	37.36	79.62	63.84
A2_3C	47.33	42.01	6.30	94.34	87.96	88.77	82.60	37.74	79.13	63.27
A2_5A	50.83	43.42	6.51	94.26	87.89	85.42	80.34	36.93	75.98	59.67
A2_5B	49.08	43.35	6.50	94.31	87.91	88.33	81.78	36.95	77.74	60.71
A2_5C	49.08	43.28	6.49	94.38	88.03	88.19	81.61	37.35	77.11	60.09
CK_1A	49.08	43.45	6.52	94.71	88.72	88.53	82.95	39.24	76.00	60.57
CK_1B	49.08	43.10	6.46	94.27	87.81	87.82	81.83	37.03	75.42	60.23
CK_1C	47.33	41.95	6.29	94.26	87.75	88.63	81.76	37.03	74.42	59.49
CK_3A	47.33	42.10	6.32	94.61	88.51	88.96	82.96	39.55	77.84	61.73
CK_3B	49.08	43.36	6.50	94.27	87.75	88.35	82.43	37.47	77.87	62.04
CK_3C	42.16	37.59	5.64	94.37	87.97	89.15	82.50	37.84	77.60	61.71
CK_5A	49.08	43.45	6.52	94.53	88.36	88.53	83.31	39.30	78.12	63.06
CK_5B	47.33	42.22	6.33	94.30	87.83	89.22	83.31	38.06	78.47	63.47
CK_5C	47.33	42.05	6.31	94.40	88.05	88.85	82.91	38.39	77.31	62.28

Supplementary Table 4). We further analyzed the top 20 enriched pathways and observed that fatty acid biosynthesis and fatty acid metabolism were represented (**Supplementary Figure 1D** and **Supplementary Table 4**). Several pathways related to fatty acids were annotated: pyruvate metabolism (75), fatty acid metabolism (55), and fatty acid biosynthesis (43).

In CK_5 vs. A2_5, 7,227 of 9,699 DEGs were annotated in GO categories (**Supplementary Figure 2A** and **Supplementary Table 5**): Cellular process (2,122), metabolic process (1,842), and biological regulation (673) were represented as major categories under the biological process. Under the cellular component, membrane (2,354), membrane part (2,239), and cell (2,161) were the most highly represented categories. Major categories in molecular function were catalytic activity (3,536), binding (3,529), and transporter activity (432). When the top 20 GO categories were further analyzed, it was observed that cytoplasm (1,097), cytoplasmic part (882), and small molecule metabolic process (488) were the most highly represented categories (**Supplementary Figure 2B** and **Supplementary Table 6**). Significantly enriched KEGG pathways in CK_5

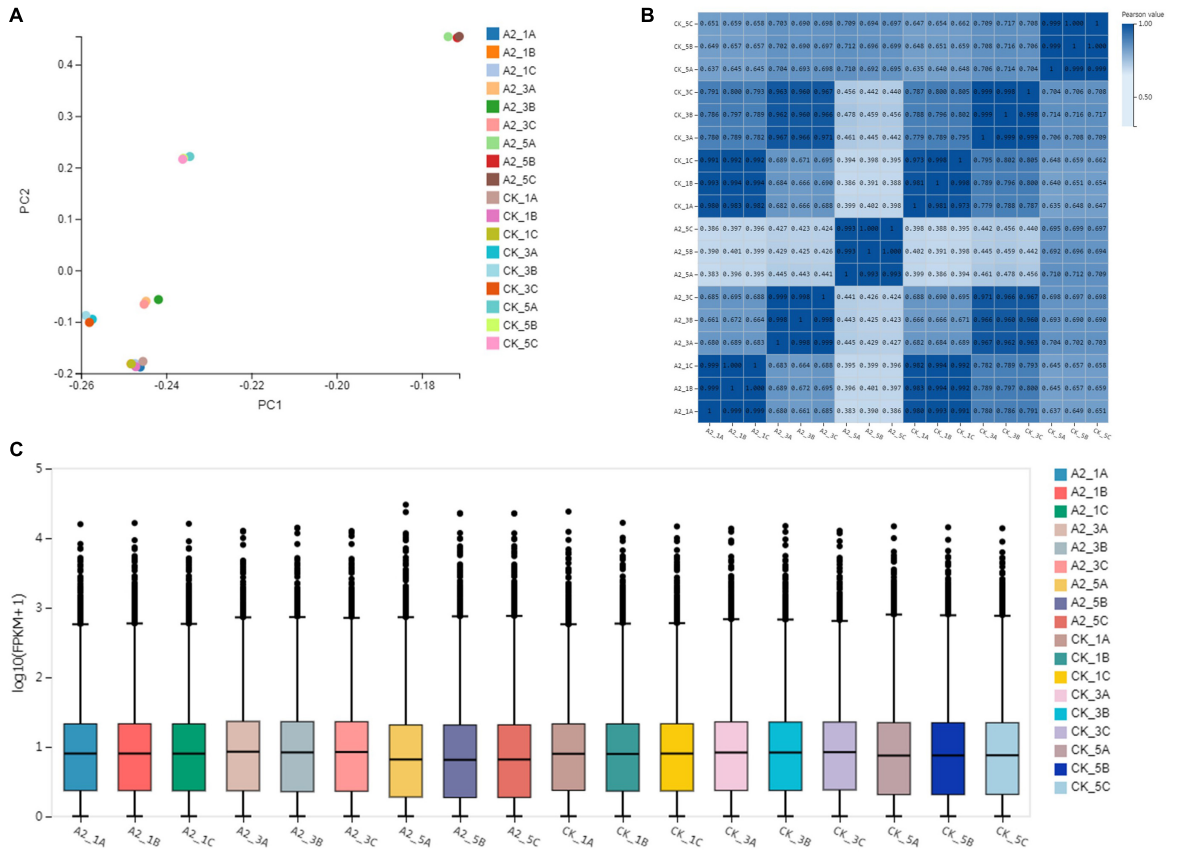

FIGURE 2 | Transcriptome at 0, 4, and 8 weeks after treatment with 0 and 20 μM ABA. **(A)** Principal component analysis of six samples. **(B)** Pearson correlation coefficient of gene expression levels between samples. **(C)** Distribution of gene expression levels in each sample. The *x*-axis shows the sample name, and the *y*-axis shows log10 [FPKM (fragments per kilobase of exon model per million mapped reads) + 1]. The box plot for each region corresponds to five statistics (upper to lower, upper quartile, median, and lower quartile, lower limit, where the upper and lower limits do not take outliers into account).

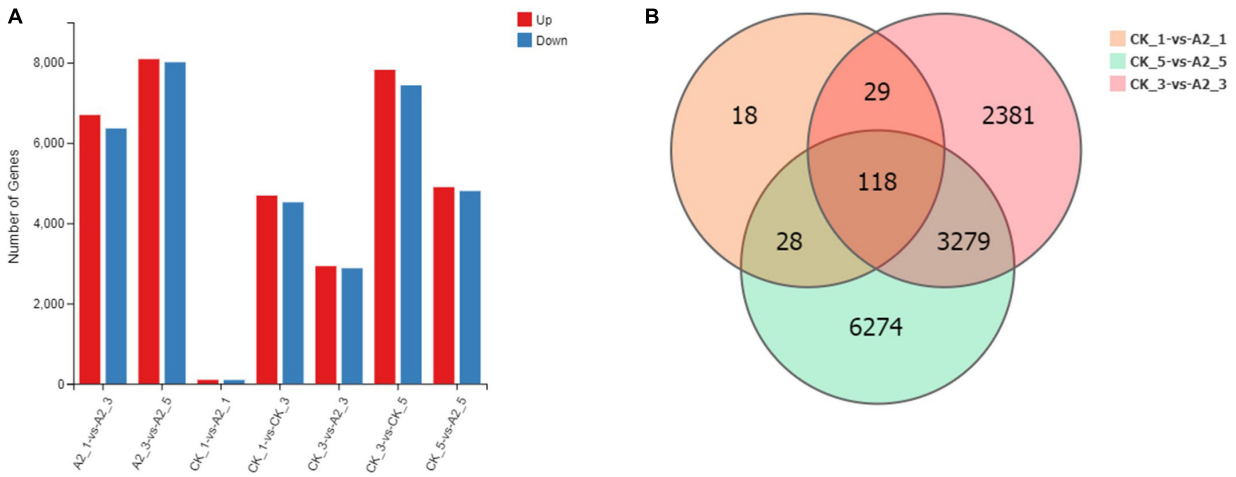

FIGURE 3 | A summary of DEGs between CK and A2. **(A)** Number of DEGs. **(B)** The Venn diagram of DEGs between CK and A2.

vs. A2_5 were further analyzed. In total, 4,453 DEGs were enriched in KEGG pathways (**Supplementary Figure 2C** and **Supplementary Table 7**). Similar to CK_3 vs. A2_3, fatty acid metabolism (73) and fatty acid biosynthesis (50) were represented as the top 20 KEGG pathways (**Supplementary Figure 2D** and **Supplementary Table 7**).

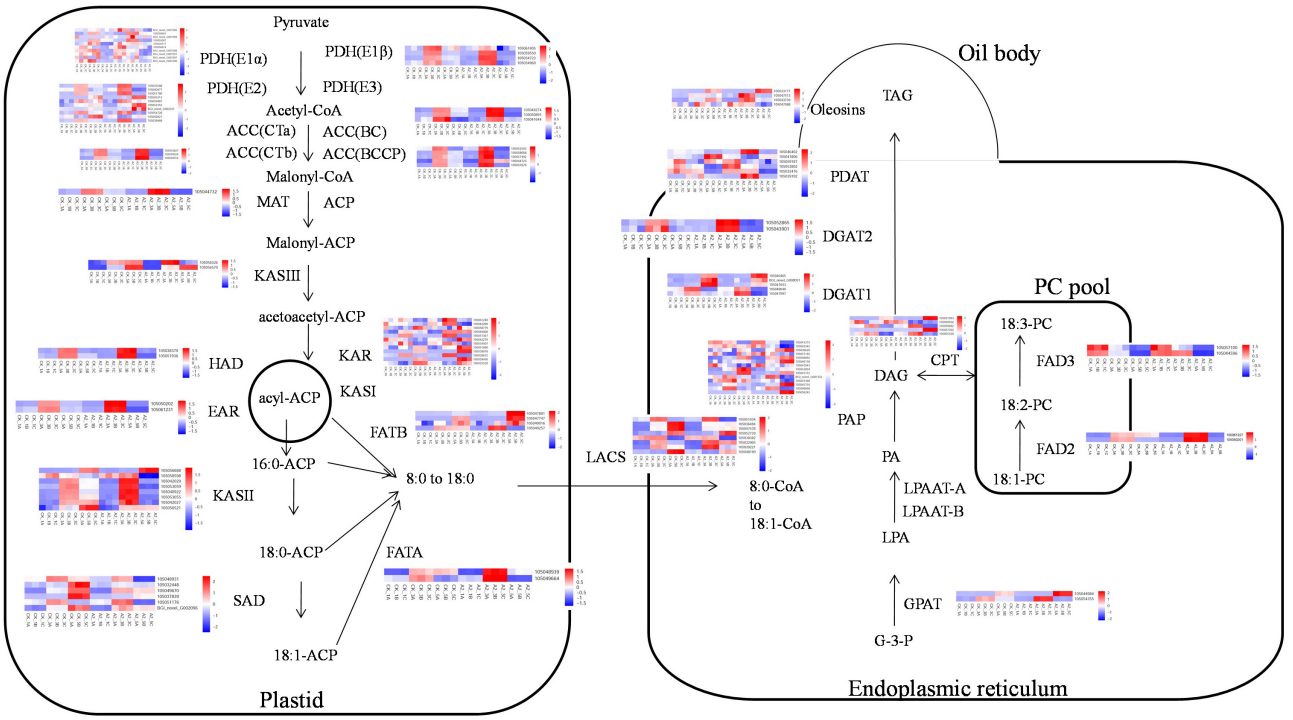

FIGURE 4 | The transcriptional model of fatty acid biosynthesis in developing oil palm mesocarp. The 18 squares in each horizontal row correspond to three replicates of three stages (16 WAP, 20 WAP, and 24 WAP) in CK and A2. G-3-P, glycerol-3-phosphate; LPA, 1-acylglycerol-3P; PA, phosphatidic acid; DAG, 1,2-diacylglycerol; and TAG, triacylglycerol.

EgFAD2 Upregulation Possibly Results in Increase of Linoleic Acid Biosynthesis

As exogenous ABA has a distinct impact on fatty acid accumulation, we further focused on the genes involved in lipid biosynthesis and ABA signaling pathways to identify possible mechanisms. A total of 14, 31, 520, 190 unigenes were, respectively, identified as ABA biosynthesis and metabolism, ABA signal transduction, TFs that could be related with ABA and fatty acid biosynthesis, and fatty acid biosynthesis in these transcriptome data (**Supplementary Table 10**). Among these unigenes, genes, such as *KAR*, *FAD2*, and *SAD*, were highly expressed with > 1,000 FPKM value, suggesting that these genes may play an important role in fatty acid synthesis. Most upregulated genes in the fatty acid biosynthesis pathway were expressed in A2_3 compared with CK_3, such as *PDH(E1α)*, *PDH(E1β)*, *PDH(E2)*, *ACC(CTb)*, *ACC(BC)*, *ACC(BCCP)*, *MAT*, *KASIII*, *HAD*, *EAR*, *KAR*, *KASII*, *FATA*, *FATB*, *LACS*, *GPAT*, *FAD2*, *FAD3*, *DGAT2*, *PDAT*, and *Oleosins* (**Figure 4**). Meanwhile some genes were upregulated in A2_5 compared with CK_5, such as *PDH(E2)*, *KASIII*, *KAR*, *KASII*, *FATB*, *GPAT*, *PAP*, *CPT*, *DGAT1*, and *Oleosins* (**Figure 4**). In addition, several genes involved in ABA signal transduction and TFs were also differentially expressed in A2_3_vs. CK_3 and A2_5_vs. CK_5, such as *PYR*, *PP2C*, *SnRK*, *ABI5*, *AP2-EREBP*, *bZIP*, *C2C2-Dof*, and *MYB* (**Supplementary Table 8**). In addition, exogenous ABA also affected the expression level of genes involved in ABA biosynthesis and metabolism (**Supplementary Table 8**). The expression level of some genes involved in ABA biosynthesis reduced after exogenous ABA treatment, such as *DXS*, *DXR*, and *ZEP*, while *PSY*, *PDS*, and *NCED* rose. Especially, the expression level of gene (*CYP707A*) involved in ABA metabolism was significantly (p-value < 0.01) higher in A2_5 than CK_5.

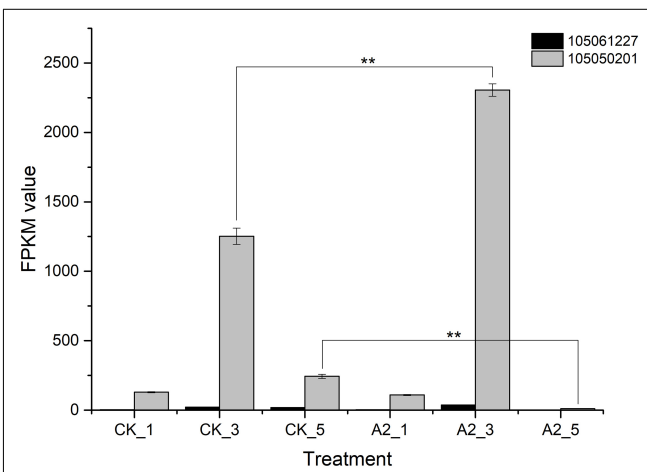

FIGURE 5 | *FAD2* expression in CK and A2. **Represents significance at $p < 0.01$. CK_1: 16 WAP with 0 μM ABA; CK_3: 20 WAP with 0 μM ABA; CK_5: 24 WAP with 0 μM ABA; A2_1: 16 WAP with 20 μM ABA; A2_3: 20 WAP with 20 μM ABA; A2_5: 24 WAP with 20 μM ABA.

TABLE 3 | ABRE cis-acting element prediction of *FAD2*.

Gene ID	Sequence	Position	Matrix Score	Strand	Organism
LOC105050201	GCAACGTGTC	755	9	+	*Hordeum vulgare*
	CACGTG	757	6	+	*Arabidopsis thaliana*
	ACGTG	758	5	+	*Arabidopsis thaliana*
	CACGTG	807	6	+	*Arabidopsis thaliana*
	ACGTG	808	5	+	*Arabidopsis thaliana*
	ACGTG	1,699	5	+	*Arabidopsis thaliana*
LOC105061227	CACGTG	183	6	+	*Arabidopsis thaliana*
	ACGTG	184	5	+	*Arabidopsis thaliana*
	GCAACGTGTC	376	9	+	*Hordeum vulgare*
	AACCCGG	705	7	-	*Arabidopsis thaliana*
	CACGTG	1,776	6	-	*Arabidopsis thaliana*
	ACGTG	1,777	5	+	*Arabidopsis thaliana*
	CACGTG	2,767	6	-	*Arabidopsis thaliana*
	ACGTG	2,768	5	+	*Arabidopsis thaliana*

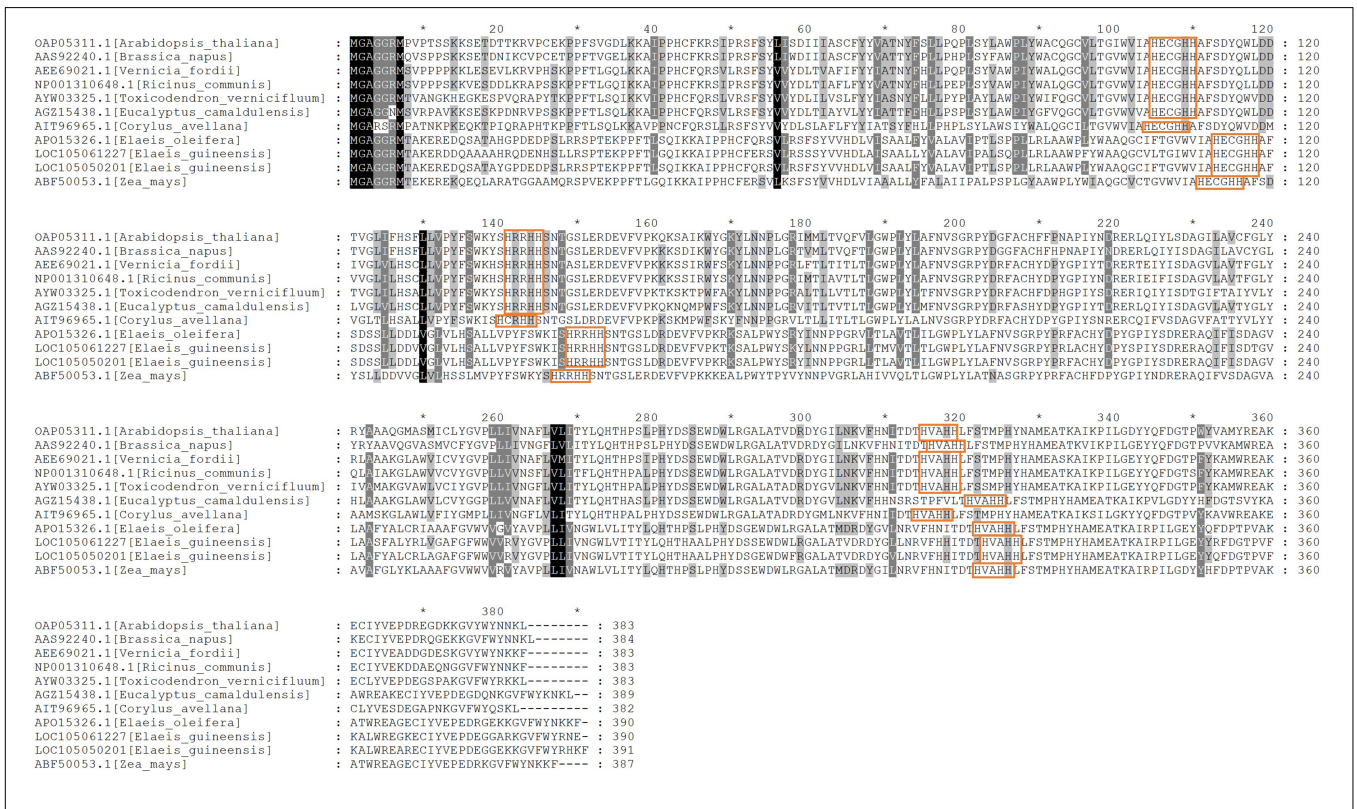

FIGURE 6 | An alignment view of two FAD2 copies. Red blocks represent histidine-rich domains.

Moreover, the content of other major fatty acid components did not increase significantly instead of linoleic acid, so we focused on linoleic acid (**Supplementary Table 1**). In the fatty acid biosynthesis pathway (**Figure 4**), *FAD2* is the key gene-catalyzing oleic acid (C18:1) to linoleic acid (C18:2) (Dussert et al., 2013). In this study, two genes encoding *FAD2* (gene ID:105061227, 105050201) were differentially expressed, of which the expression level of unigene 105050201 under A2_3 was significantly higher than for CK_3, the same to A2_5 vs. CK_5 (**Figure 5**), suggesting that exogenous ABA treatment can lead to the increased expression of *FAD2*. This result indicated the *FAD2* expression level was raised by exogenous ABA.

In order to investigate whether *FAD2* could respond to an ABA signal, the abscisic acid responsiveness element (ABRE) was predicted using a promoter and the PlantCARE online tool. Results showed that the promoter of *FAD2* had an ABRE *cis*-acting element. Unigene 105050201 had the highest expression level and had six ABRE motifs of the type "ACGTG" (**Table 3**). Similarly, unigene 105061227 had eight ABRE motifs.

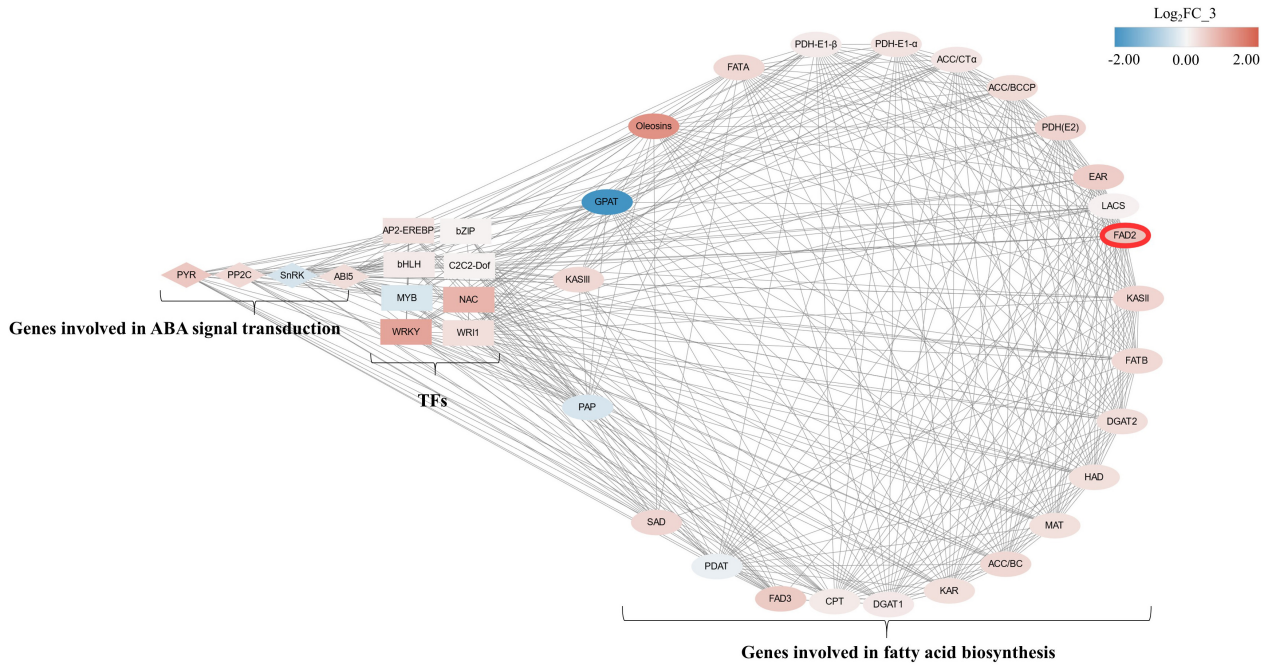

FIGURE 7 | Correlation network of genes involving fatty acid biosynthesis, ABA-signaling transduction, and transcriptional factors between CK and A2 during mesocarp development. Ellipses, diamonds, and rectangles, respectively, represent genes involving fatty acid biosynthesis, ABA-signaling transduction, and transcriptional factors. Node fill color is according to $\log_2$FC of FPKM value in CK_3 vs. A2_3 from blue to red; TFs, transcriptional factors; PYR, pyrabactin resistance; PP2C, type 2C protein phosphatases; SnRK, Snf1-related protein kinase; ABI5, ABA insensitive 5; AP2-EREBP, APETALA2-ethylene responsive element-binding protein; bZIP, basic leucine zipper; bHLH, basic helix loop helix; C2C2-Dof, downstream of FGFR; MYB, myeloblastosis; NAC, nascent polypeptide-associated complex; WRKY, WRKY transcriptional factor; WRI1, WRINKLED1; KASIII, 3-ketoacyl-ACP synthase III; GPAT, glycerol-3-phosphate acyltransferase; FATA, fatty acid acyl-ACP thioesterase A; PDH-E1-β, subunit b of E1 component of PDH complex; PDH-E1-α, subunit α of E1 component of PDH complex; ACC/CTα, carboxyltransferase a-subunit of heteromeric ACCase; ACC/BCCP, biotin carboxyl-carrier protein of heteromeric ACCase; PDH(E2), E2 component of PDH complex; EAR, enoyl-ACP reductase; LACS, long-chain acyl-CoA synthetase; FAD2, ω-6 desaturase; KASII, 3-ketoacyl-ACP synthase II; FATB, fatty acid acyl-ACP thioesterase B; DGAT2, diacylglycerol acyltransferase 2, HAD, 3-hydroxyacyl-ACP dehydratase; MAT, malonyl-CoA: ACP transacylase; ACC/BC, biotin carboxylase subunit of heteromeric acetyl-CoA carboxylase; KAR, 3-ketoacyl-ACP reductase; DGAT1, diacylglycerol acyltransferase 1; CPT, CDP-choline: DAG cholinephosphotransferase; FAD3, ω-3 desaturase; PDAT, phospholipid: diacylglycerol acyltransferase; SAD, stearoyl-ACP desaturase; PAP, phosphatic acid phosphohydrolase.

The sequence alignment analysis showed that AtFAD2 had 383 amino acid residues, and unigenes 105050201 and 105061227 had 390 and 391 residues, respectively (**Figure 6**). Three highly conserved histidine-rich motifs at EgFAD2 were included (HECGHH, HRRHH, and HVAHH). Meanwhile, unigenes 105050201 and 105061227 had complete histidine-rich motifs, and the lengths of protein sequences were similar to those of other species. The AtFAD2 protein can bind to endoplasmic reticulum because of the C-terminal signaling motif (YNNKL). Results showed that the C-terminal of unigene 105050201 was "YRHKF," and, for unigene 105061227, it was "YRNE," indicating that unigene 105050201 may also bind to endoplasmic reticulum.

In addition, the phylogenetic tree showed that unigenes 105061227 and 105050201 clustered together with American oil palm and maize FAD2. Results indicated that unigenes 105061227 and 105050201 had similar protein sequences (**Supplementary Figure 3**).

In conclusion, the promoter of unigene 105061227 had many ABRE motifs, and the protein sequence contained a complete histidine-rich domain, but the C-terminal lacked one resident compared to other organisms. A large number of ABRE motifs were found in the promoter region of unigene 105050201, and protein sequences contained complete histidine-rich domains, suggesting that expression of unigene 105050201 was upregulated in response to the ABA signal and thereby promoted linoleic acid synthesis.

Correlation Analysis Among *FAD2*, Transcription Factors, and Genes Involved in Fatty Acid Biosynthesis

To obtain a comprehensive understanding of genes that possibly play an important role in linoleic acid biosynthesis in oil palm during ABA treatments, weighted gene co-expression network analysis (WGCNA) was performed. After filtering the genes with a low expression (FPKM < 0.05), 1,348 genes were selected for WGCNA. Co-expression networks were constructed based on pairwise correlations of gene expression across all samples.

This analysis identified 11 distinct modules (**Supplementary Figure 4A**). The 11 modules were correlated with distinct samples according to sample-specific expression profiles. A total of 28 genes involved in fatty acid biosynthesis and ABA

signal transduction were found in the WGCNA network (**Supplementary Figure 4B**). A total of 47 genes, including TFs, such as *MYB*, *bZIP*, and *bHLH*, were significantly correlated with *PYR* (**Supplementary Figure 4C** and **Supplementary Table 9**). These TFs were reported to play a role in response to ABA signaling (Cutler et al., 2010). *WRI1* and *FAD2* were in a small network (**Supplementary Figure 4D**). Moreover, promoters of *PYR*, *PP2C*, *SnRK*, *ABI5*, *WRI1*, AP2-EREBP, *bZIP*, *C2C2-Dof*, *MYB*, and *NAC* were also found to possess ABRE motifs (**Supplementary File 1** and **Supplementary Table 10**).

In order to clarify the relationship between FAD2 and genes involved in fatty acid biosynthesis, ABA signaling transduction, and TFs, a total of 29 genes involved in fatty acid biosynthesis, ABA signaling transduction, and eight TFs were selected according to FPKM value > 10 for correlation analysis. The pairs significantly correlated ($p < 0.05$) were included in the network. *FAD2* (unigene 105050201) was found to be significantly correlated with *SnRK*, *ABI5*, *C2C2-Dof*, and *WRI1*; and 19 genes were involved in fatty acid biosynthesis (**Figure 7**).

DISCUSSION

Polyunsaturated fatty acids are essential for human health but cannot be synthesized by the human body; however, they can be supplied *via* edible vegetable oils. Palm oil plants produce the largest supply of edible vegetable oil in the world. It would, therefore, be of great benefit to improve the unsaturated fatty acid content in oil palm mesocarps, which composes around 50%. Research shows that palmitic acid content is around 44% in the mesocarp, with oleic acid at 40% and linoleic acid at 10% (Barcelos et al., 2015). So, there is a large potential for increasing linoleic acid levels. While previous studies on other plant species show that ABA could enhance the accumulation of linoleic acid (Ju et al., 2016; Huo et al., 2020; Norlina et al., 2020), the effect of ABA on oil palm mesocarp is still unknown. Results in this study showed 20 μM ABA was found to significantly promote linoleic acid content in mesocarp compared to an untreated control. A similar effect was also observed in Cabernet Sauvignon (*Vitis vinifera* L.) grape skins when 200 and 600 mg·L^{-1} ABA was applied to the surface of grape berries (Ju et al., 2016). In order to investigate transcriptional changes between control and ABA-treated samples, RNA-Seq analysis was conducted.

Compared with CK_1 vs. A2_1, abundant DEGs were, respectively, identified in CK_3 vs. A2_3 and CK_5 vs. A2_5. Results indicated that the spraying of ABA altered the transcriptional levels of a large number of genes in oil palm mesocarps. Moreover, DEGs analysis showed that many genes involved in ABA signal transduction, TFs, and fatty acid biosynthesis were differentially expressed in CK_3 vs. A2_3 and CK_5 vs. A2_5, such as *PYR*, *PP2C*, *SnRK*, *ABI5*, *AP2-EREBP*, *bZIP*, *C2C2-Dof*, *MYB*, *WRI1*, *FATA*, *FATB*, *LACS*, *GPAT*, *FAD2*, *DGAT2*, *PDAT*, and *Oleosins*. At the same time, the expression level of genes involved in ABA biosynthesis and metabolism was also affected by exogenous ABA. The expression level of some genes involved in ABA biosynthesis was up and down, but the expression level of gene involved in ABA metabolism was up. It indicated that exogenous ABA could affect ABA biosynthesis and promote endogenous ABA metabolism in mesocarp. There was no obvious change pattern for genes involved in ABA biosynthesis, possibly because of a large number of endogenous ABA synthesis during development and ripening of fruits (Teh et al., 2014).

The content of linoleic acid increased significantly after exogenous ABA treatment, while other major fatty acid components almost unchanged. It indicated that linoleic acid biosynthesis was affected by exogenous ABA, so genes involved in linoleic acid biosynthesis were emphatically analyzed. FAD2 is reported as a key enzyme-controlling linoleic acid biosynthesis (Dussert et al., 2013; He et al., 2020; Wang et al., 2021); thus, two unigenes annotated as *FAD2* were analyzed further. Of these two unigenes, expression levels of unigene 105050201 under A2_3 and A2_5 were significantly higher than CK_3 and CK_5, respectively, while unigene 105061227 still kept a low expression level. These results indicated that unigene 105050201 could respond to exogenous ABA. ABRE is an important element response to the ABA signal; ABA-responsive elements motif "ACGTC" was detected in the *FAD2* promoter region, and *FAD2* expression is known to be regulated by ABA (Kim et al., 2006; Xiao et al., 2014; Dar et al., 2017). Genes encoding the FAD2 enzyme contain eight conserved histidine residues in three clusters (HXXXH, HXXHH, and HXXHH) (Okuley et al., 1994). In the current study, similar ABRE motifs and histidine-rich motifs were found in unigene 105050201. Moreover, only unigene 105050201 had similar residents in the C-terminal as found in other organisms (Dehghan and Yarizade, 2014), indicating that unigene 105050201 may play a major role in promoting linoleic acid accumulation *via* response to the ABA signal.

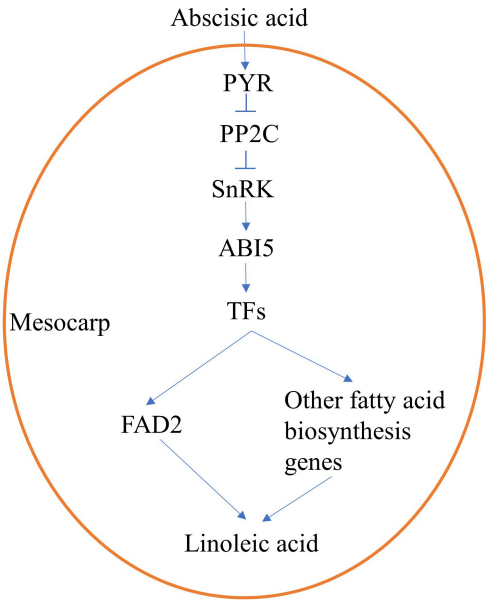

FIGURE 8 | An speculative regulation mechanism of ABA-promoting linoleic acid biosynthesis in oil palm mesocarp.

In order to understand the possible mechanism of ABA-regulating linoleic acid biosynthesis, genes involved in ABA signal transduction and related TFs were further analyzed. Previous study found that ABA-signaling genes, such as *PYR*, *PP2C*, *SnRK*, and ABI5, could activate some TFs (*bZIP*, *MYB*, *MYC*, *AP2*, *NAC*, *WRKY*, and *bHLH*); these TFs subsequently activate the expression of downstream protein-coding genes (Kim et al., 2007; Cutler et al., 2010; Aleman et al., 2016). Our results showed many genes included in fatty acid biosynthesis and ABA signaling, such as *PYR*, *ABI5*, and *WRI1* were increased significantly after ABA treatment, indicating their response to ABA (**Supplementary Table 10**).

A previous study shows that fatty acid biosynthesis is subjected to phytohormones, such as ABA, auxin, and jasmonic acid (JA) (Shahid et al., 2019). Linoleic acid, one of the most common unsaturated fatty acids, acts as a precursor of jasmonates and a regulator of stress signaling (He and Ding, 2020). Moreover, jasmonic acid also crosstalks with the ABA signaling pathway (Aleman et al., 2016; Yu et al., 2021). Previous research found that TFs play an important role in regulating fatty acid biosynthesis. For example, *NF-YA3*, *NF-YC2*, and *ABI5* directly activate *WRI1* and regulate fatty acid biosynthesis (Yeap et al., 2017). Furthermore, *ABI5* is a *bZIP* type of TF involved in ABA signal transduction. As a member of *AP2-EREBP*, *WRI1* also plays a key regulatory role in fatty acid biosynthesis within the oil palm mesocarp. In the current study, *ABI5* and *WRI1* were upregulated after ABA treatment. Moreover, ABRE motifs were detected in promoters of *ABI5*, *WRI1*, and *FAD2*, suggesting that these genes could respond to the ABA signal.

FAD2 expression has a high correlation with transcriptional factors, such as *WRI1*, *Dof*, and *ABI5* (Deng et al., 2019; He and Ding, 2020). WGCNA is an effective tool for exploring relationships across genes involved in fatty acid biosynthesis (Niu et al., 2020; Ma et al., 2021). Correlation analysis also showed that *EgFAD2* is co-expressed with these TFs, with several genes being involved in ABA signal transduction and fatty acid biosynthesis. These results suggested that the expression of *EgFAD2* was upregulated as a response to ABA signaling, possibly resulting in increased accumulation of linoleic acid.

Under exogenous ABA treatment, content of linoleic acid increased and expression of ABA-signaling genes, TFs, and fatty acids biosynthesis genes upregulated. Therefore, we speculated that ABA activated TFs through ABA signal transduction (*PYR*, *PP2C*, *SnRK*, and *ABI5*), and then promoted expression levels of *FAD2* or/and other fatty acids biosynthesis genes, resulting in increased accumulation of linoleic acid (**Figure 8**). Needless to say, further research is still required regarding the molecular mechanism by which ABA regulates linoleic acid biosynthesis; this can be extended from the current findings. Further experiments should be conducted to identify the upstream regulation factors of *FAD2* or other fatty acids biosynthesis genes, such as electrophoretic mobility shift assays, yeast one-hybrid and yeast two-hybrid assays, and ChIP-seq.

DATA AVAILABILITY STATEMENT

The datasets presented in this study can be found in online repositories. The names of the repository/repositories and accession number(s) can be found at: https://www.ncbi.nlm.nih.gov/, PRJNA719677.

AUTHOR CONTRIBUTIONS

PS and WH directed the project and wrote the manuscript. DZ and YH performed data analysis and revised the manuscript. YW and JL supervised this work and revised the manuscript. All authors read and approved the final manuscript.

FUNDING

This work was supported by the Open Project of Key Laboratory of Biology and Genetic Improvement of Oil Crops, Ministry of Agriculture and Rural Affairs, P.R. China (KF2019007), the Natural Science Foundation Project of Hainan Province (319QN323), and the Central Public-interest Scientific Institution Basal Research Fund for Chinese Academy of Tropical Agricultural Sciences (17CXTD-13).

ACKNOWLEDGMENTS

We are most grateful to the Germplasm Nursery for Tropical palms and the Scientific Observation and Experiment Station of Tropical oil crops of the Ministry of Agriculture and Rural affairs of China for providing oil palm materials.

SUPPLEMENTARY MATERIAL

The Supplementary Material for this article can be found online at: https://www.frontiersin.org/articles/10.3389/fpls.2021.748130/full#supplementary-material

REFERENCES

Aleman, F., Yazaki, J., Lee, M., Takahashi, Y., Kim, A. Y., Li, Z., et al. (2016). An ABA-increased interaction of the PYL6 ABA receptor with MYC2 Transcription Factor: a putative link of ABA and JA signaling. *Sci. Rep.* 6:28941. doi: 10.1038/srep28941

Barcelos, E., Rios, S. A., Cunha, R. N., Lopes, R., Motoike, S. Y., Babiychuk, E., et al. (2015). Oil palm natural diversity and the potential for yield improvement. *Front. Plant. Sci.* 6:190. doi: 10.3389/fpls.2015.00190

Cutler, S. R., Rodriguez, P. L., Finkelstein, R. R., and Abrams, S. R. (2010). Abscisic acid: emergence of a core signaling network. *Annu. Rev. Plant Biol.* 61, 651–679. doi: 10.1146/annurev-arplant-042809-112122

Dar, A. A., Choudhury, A. R., Kancharla, P. K., and Arumugam, N. (2017). The FAD2 gene in plants: occurrence, regulation, and role. *Front. Plant Sci.* 8:1789. doi: 10.3389/fpls.2017.01789

Dehghan, N. F., and Yarizade, K. (2014). Bioinformatics study of delta-12 fatty acid desaturase 2 (FAD2) gene in oilseeds. *Mol. Biol. Rep.* 41, 5077–5087. doi: 10.1007/s11033-014-3373-5

Deng, S., Mai, Y., Shui, L., and Niu, J. (2019). WRINKLED1 transcription factor orchestrates the regulation of carbon partitioning for C18:1 (oleic acid) accumulation in Siberian apricot kernel. *Sci. Rep.* 9:2693. doi: 10.1038/s41598-019-39236-9

Dussert, S., Guerin, C., Andersson, M., Joët, T., Tranbarger, T. J., Pizot, M., et al. (2013). Comparative transcriptome analysis of three oil palm fruit and seed tissues that differ in oil content and fatty acid composition. *Plant Physiol.* 162, 1337–1358. doi: 10.1104/pp.113.220525

He, M., and Ding, N. Z. (2020). Plant unsaturated fatty acids: multiple roles in stress response. *Front. Plant Sci.* 11:562785. doi: 10.3389/fpls.2020.562785

He, M., Qin, C. X., Wang, X., and Ding, N. Z. (2020). Plant unsaturated fatty acids: biosynthesis and regulation. *Front. Plant Sci.* 11:390. doi: 10.3389/fpls.2020.00390

Huo, K., Shui, L., Mai, Y., Zhou, N., Liu, Y., Zhang, C., et al. (2020). Effects of exogenous abscisic acid on oil content, fatty acid composition, biodiesel properties and lipid components in developing Siberian apricot (*Prunus sibirica*) seeds. *Plant Physiol. Biochem.* 154, 260–267. doi: 10.1016/j.plaphy.2020.06.020

Ju, Y. L., Liu, M., Zhao, H., Meng, J. F., and Fang, Y. L. (2016). Effect of exogenous abscisic acid and methyl jasmonate on anthocyanin composition, fatty acids, and volatile compounds of cabernet sauvignon (*Vitis vinifera* L.) grape berries. *Molecules* 21:1354. doi: 10.3390/molecules21101354

Kim, D., Langmead, B., and Salzberg, S. L. (2015). HISAT: a fast spliced aligner with low memory requirements. *Nat. Methods* 12, 357–360. doi: 10.1038/nmeth.3317

Kim, M. J., Kim, H., Shin, J. S., Chung, C. H., Ohlrogge, J. B., and Suh, M. C. (2006). Seed-specific expression of sesame microsomal oleic acid desaturase is controlled by combinatorial properties between negative cis-regulatory elements in the *SeFAD2* promoter and enhancers in the 5'-UTR intron. *Mol. Genet. Genomics* 276, 351–368. doi: 10.1007/s00438-006-0148-2

Kim, M. J., Kim, J. K., Shin, J. S., and Suh, M. C. (2007). The SebHLH transcription factor mediates trans-activation of the SeFAD2 gene promoter through binding to E- and G-box elements. *Plant Mol. Biol.* 64, 453–466. doi: 10.1007/s11103-007-9165-8

Kumar, S., Stecher, G., Li, M., Knyaz, C., and Tamura, K. (2018). MEGA X: molecular evolutionary genetics analysis across computing platforms. *Mol. Biol. Evol.* 35, 1547–1549. doi: 10.1093/molbev/msy096

Langmead, B., and Salzberg, S. L. (2012). Fast gapped-read alignment with Bowtie 2. *Nat. Methods* 9, 357–359. doi: 10.1038/nmeth.1923

Li, B., and Dewey, C. N. (2011). RSEM: accurate transcript quantification from RNA-Seq data with or without a reference genome. *BMC Bioinform.* 12:323. doi: 10.1186/1471-2105-12-323

Li, R., Li, Y., Kristiansen, K., and Wang, J. (2008). SOAP: short oligonucleotide alignment program. *Bioinformatics* 24, 713–714. doi: 10.1093/bioinformatics/btn025

Love, M. I., Huber, W., and Anders, S. (2014). Moderated estimation of fold change and dispersion for RNA-seq data with DESeq2. *Genome Biol.* 15:550. doi: 10.1186/s13059-014-0550-8

Ma, L., Cheng, X., Wang, C., Zhang, X., Xue, F., Li, Y., et al. (2021). Explore the gene network regulating the composition of fatty acids in cottonseed. *BMC Plant Biol.* 21:177. doi: 10.1186/s12870-021-02952-4

Niu, Y., Wu, L., Li, Y., Huang, H., Qian, M., Sun, W., et al. (2020). Deciphering the transcriptional regulatory networks that control size, color, and oil content in *Brassica* rapaseeds. Biotechnol. *Biofuels* 13:90. doi: 10.1186/s13068-020-01728-6

Norlina, R., Norashikin, M. N., Loh, S. H., Aziz, A., and Cha, T. S. (2020). Exogenous abscisic acid supplementation at early stationary growth phase triggers changes in the regulation of fatty acid biosynthesis in *Chlorella vulgaris* UMT-M1. *Appl. Biochem. Biotechnol.* 191, 1653–1669. doi: 10.1007/s12010-020-03312-y

Okuley, J., Lightner, J., Feldmann, K., Yadav, N., Lark, E., and Browse, J. (1994). *Arabidopsis* FAD2 gene encodes the enzyme that is essential for polyunsaturated lipid synthesis. *Plant Cell* 6, 147–158. doi: 10.1105/tpc.6.1.147

Shahid, M., Cai, G., Zu, F., Zhao, Q., Qasim, M. U., Hong, Y., et al. (2019). Comparative transcriptome analysis of developing seeds and silique wall reveals dynamic transcription networks for effective oil production in *Brassica napus* L. *Int. J. Mol. Sci.* 20:1982. doi: 10.3390/ijms20081982

Teh, H. F., Neoh, B. K., Wong, Y. C., Kwong, Q. B., Ooi, T. E., Ng, T. L., et al. (2014). Hormones, polyamines, and cell wall metabolism during oil palm fruit mesocarp development and ripening. *J. Agric. Food Chem.* 62, 8143–8152. doi: 10.1021/jf500975h

Wang, J. J., Liu, Z. J., Liu, H., Peng, D. S., Zhang, J. P., and Chen, M. X. (2021). *Linum usitatissimum* FAD2A and FAD3A enhance seed polyunsaturated fatty acid accumulation and seedling cold tolerance in *Arabidopsis thaliana*. *Plant Sci.* 311:111014. doi: 10.1016/j.plantsci.2021.111014

Xiao, G., Zhang, Z. Q., Yin, C. F., Liu, R. Y., Wu, X. M., Tan, T. L., et al. (2014). Characterization of the promoter and 5'-UTR intron of oleic acid desaturase (FAD2) gene in *Brassica napus*. *Gene* 545, 45–55. doi: 10.1016/j.gene.2014.05.008

Yeap, W. C., Lee, F. C., Shabari, S. D. K., Musa, H., Appleton, D. R., and Kulaveerasingam, H. (2017). WRI1-1, ABI5, NF-YA3 and NF-YC2 increase oil biosynthesis in coordination with hormonal signaling during fruit development in oil palm. *Plant J.* 91, 97–113. doi: 10.1111/tpj.13549

Yu, Q., Hua, X. Y., Yao, H., Zhang, Q., He, J., Peng, L., et al. (2021). Abscisic acid receptors are involves in the Jasmonate signaling in *Arabidopsis*. *Plant Signal. Behav.* 16:1948243. doi: 10.1080/15592324.2021.1948243

Zhou, Y., Zhao, W., Lai, Y., Zhang, B., and Zhang, D. (2020). Edible plant oil: global status, health issues, and perspectives. *Front. Plant Sci.* 11:1315. doi: 10.3389/fpls.2020.01315

Conflict of Interest: The authors declare that the research was conducted in the absence of any commercial or financial relationships that could be construed as a potential conflict of interest.

Publisher's Note: All claims expressed in this article are solely those of the authors and do not necessarily represent those of their affiliated organizations, or those of the publisher, the editors and the reviewers. Any product that may be evaluated in this article, or claim that may be made by its manufacturer, is not guaranteed or endorsed by the publisher.

frontiers in Plant Science

ORIGINAL RESEARCH
published: 20 January 2022
doi: 10.3389/fpls.2021.800625

A Novel Glycerol Kinase Gene *OsNHO1* Regulates Resistance to Bacterial Blight and Blast Diseases in Rice

Xiaorong Xiao [1,2,3†], Rui Wang [1†], Shahneela Khaskhali [1†], Zhiliang Gao [1], Wenya Guo [1,2], Honggang Wang [1], Xiaolei Niu [1], Chaoze He [1], Xiaohui Yu [1] and Yinhua Chen [1,2*]*

[1] Hainan Key Laboratory for Sustainable Utilization of Tropical Bioresources, College of Tropical Crops, Hainan University, Haikou, China, [2] School of Life Science, Hainan University, Haikou, China, [3] Cereal Crops Institute, Hainan Academy of Agricultural Sciences/Sanya Institute, Hainan Academy of Agricultural Sciences, Sanya, China

OPEN ACCESS

Edited by:
Yong Xiao, Chinese Academy of Tropical Agricultural Sciences, China

Reviewed by:
Huanbin Zhou, Institute of Plant Protection, Chinese Academy of Agricultural Sciences (CAAS), China
Maoteng Li, Huazhong University of Science and Technology, China

***Correspondence:**
Xiaohui Yu
xiaohuiyu@hainanu.edu.cn
Yinhua Chen
yhchen@hainanu.edu.cn

† These authors have contributed equally to this work

Specialty section:
This article was submitted to Crop and Product Physiology, a section of the journal Frontiers in Plant Science

Received: *23 October 2021*
Accepted: *26 November 2021*
Published: *20 January 2022*

Citation:
Xiao X, Wang R, Khaskhali S, Gao Z, Guo W, Wang H, Niu X, He C, Yu X and Chen Y (2022) A Novel Glycerol Kinase Gene OsNHO1 Regulates Resistance to Bacterial Blight and Blast Diseases in Rice. Front. Plant Sci. 12:800625. doi: 10.3389/fpls.2021.800625

Glycerol-induced resistance to various pathogens has been reported in different plants. Glycerol kinase (GK), a vital rate-limiting enzyme that catalyzes glycerol conversion to glycerol-3-phosphate (G3P), participates in responses to both abiotic and biotic stresses. However, its physiological importance in rice defenses against pathogens remains unclear. In this research, quantification analysis revealed that GK levels were significantly induced in rice leaves infected by *Xanthomonas oryzae* pv. *oryzae (Xoo)* strain PXO99. A typical GK-encoding gene *OsNHO1* was cloned in rice. The transcriptional levels of *OsNHO1* were significantly induced by salicylic acid, jasmonic acid, and *Xoo*-PXO99. Ectopic expression of *OsNHO1* partially rescued the resistance to *P. s. pv. phaseolicola* in the *Arabidopsis nho1* mutant. In the overexpressing transgenic rice lines (*OsNHO1*-OE), the content of GK and the transcriptional level of *OsNHO1* were increased and the resistance to bacterial blight and blast was improved, while reduced *OsNHO1* expression impaired the resistance in *OsNHO1*-RNAi lines. The wax contents and expression of the wax synthesis regulatory genes were significantly increased in the overexpression lines but decreased in the *OsNHO1*-RNAi lines. We then confirmed the interaction partner of OsNHO1 using yeast two-hybrid and bimolecular fluorescence complementation assays. The transcription of the interaction partner-encoding genes *OsSRC2* and *OsPRs* in *OsNHO1*-RNAi lines was downregulated but upregulated in *OsNHO1*-OE lines. Thus, we concluded that *OsNHO1* provided disease resistance by affecting the wax content and modulating the transcription levels of *PR* genes.

Keywords: rice, glycerol kinase, non-host resistance, bacterial blight, pathogen, wax

INTRODUCTION

Plants are threatened by many pathogens through environmental exposure. However, they have evolved a series of complex defense mechanisms. Constitutive resistance and inducible resistance are two typical defense mechanisms by which plants deal with pathogen invasion (Mysore and Ryu, 2004; Ellis, 2006). The constitutive defenses are provided by plant cell walls, cytoskeleton, obstacles, and a variety of secondary metabolites (Yun et al., 2003). Induced defenses include

the accumulation of active antimicrobial substances, the activation of plant defense signal transduction pathways, calcium influx, the accumulation of reactive oxygen species (ROS), the production of nitric oxide, the occurrence of hypersensitivity reactions, the expression of defense-related genes, etc. (Lipka, 2005; Lee et al., 2017). In recent decades, significant progress has been made in understanding inducible defense mechanisms, ranging from the pathogen-associated molecular pattern (PAMP)-induced basal resistance to effector-induced cultivar-specific resistance (Jones and Dangl, 2006; Delventhal et al., 2017).

Recent evidence has suggested that primary metabolic pathways and metabolic signaling in both plants and pathogens can interface with disease-related signaling (Rolland and Sheen, 2002). The components of primary metabolism can act as signals regulating plant defense (Schaaf and Hess, 1995; Chandra-Shekara et al., 2007). Both the fatty acid and carbohydrate metabolism play important roles in plant defense and are involved in cross-talk with various phytohormones, namely, salicylic acid (SA), jasmonic acid (JA), and abscisic acid (ABA) (Scheideler et al., 2002; Kachroo et al., 2003, 2004, 2005). Vitamin B1 and sucrose also induce resistance to pathogens in *Arabidopsis* and rice (*Oryza sativa*), respectively (Ahn et al., 2005; Gómez-Ariza et al., 2007).

Glycerol is a common cellular metabolite present in a wide range of organisms. Glycerol metabolism is initiated upon its conversion to glycerol-3-phosphate (G3P), which can be derived *via* glycerol kinase (GK)-mediated phosphorylation of glycerol or G3P dehydrogenase (G3Pdh)-mediated reduction of dihydroxyacetone phosphate (DHAP) (Chanda et al., 2008). The participation of glycerol and its metabolites in host defense has been reported in *Arabidopsis*, wheat, pepper, and soybean (Kachroo et al., 2004, 2005, 2008; Chandra-Shekara et al., 2007). *AtNHO1*, which encodes flagellin-induced GK in *Arabidopsis*, is an essential factor in gene-for-gene resistance against *Pst* DC3000 and basal resistance against *Colletotrichum higginsianum* (Kang et al., 2003; Chanda et al., 2008). G3P levels in *Arabidopsis* are associated with defense against the hemibiotrophic fungal pathogen *Colletotrichum higginsianum*. Transgenic plants that are impaired in the utilization of plastidial G3P, accumulate elevated levels of pathogen-induced G3P and display enhanced resistance. *TaGLI1*, which encodes GK, contributes to systemic acquired resistance against *Puccinia striiformis f. sp. Tritici* in wheat (Yang et al., 2013). All these previous findings suggested that regulating glycerol metabolism could enhance the immune response in plants.

Glycerol-3-phosphate can be transported between the cytosol and the plastidial stroma. In the plastids, G3P is acylated with oleic acid (18:1) by the ACT1-encoded G3P acyltransferase. This ACT1-utilized 18:1 is derived from stearoyl-acyl carrier protein (ACP)-desaturase (SSI2)-catalyzed desaturation of stearic acid (18:0). The 18:1-ACP generated by ACT1 either enters the prokaryotic lipid biosynthetic pathway through acylation of G3P or is exported from the plastids as a CoA-thioester to enter the eukaryotic lipid biosynthetic pathway (Brisson et al., 2001). C16 and C18 chain fatty acids are important precursors for wax synthesis in the endoplasmic reticulum (Wang et al., 2018). As a type of secondary metabolite, wax is widely involved in many physiological resistance processes, namely, stress defenses and resistance to pests and diseases. Wax and cutin, the main components of the cuticle, form the first line of defense against pathogen infection in plants and they play a critical role in physical resistance (physical barrier) and chemical resistance (bacteriostasis) as constitutive defense components (Ye et al., 2009). The inducible wax component can also act as a signal molecule or inducer to activate downstream resistance reactions and exert its chemical resistance function (He et al., 2018).

As a model monocot plant, rice (*Oryza sativa*) is one of the staple crops in many countries and has significant economic significance. However, the yield is adversely impacted by bacterial blight and rice blast caused by *Xanthomonas oryzae* pv. *oryzae* (*Xoo*) and *Magnaporthe oryzae* (*M. oryzae*), respectively. There is an urgent need to identify broad-spectrum resistance genes to the diseases. In this study, we isolated a rice GK gene *OsNHO1* and found that *OsNHO1* can contribute to the non-host resistance in *Arabidopsis*. Moreover, it acts as a positive regulator in resistance to *Xoo*-PXO99 and *M. oryzae* Y34. Overexpression of the *OsNHO1* gene significantly increased the wax content of transgenic plants and regulated the expression of the downstream *PR* genes. In this study, we provided evidence that modifying glycerol metabolism may also regulate the resistance of rice by affecting wax synthesis.

MATERIALS AND METHODS

Bacterial Strains and Plants

Bacterial strains *Xanthomonas oryzae* pv. *oryzae (Xoo)*-PXO99, *M. oryzae* Y34, *P. s. phaseolicola*, *E. coli* DH5α, and *A. tumefaciens* were preserved and routinely cultured in our laboratory.

Arabidopsis ecotype Columbia [Col-0, wild type (WT)], *nho1* mutant (Col-0 background), and rice (*Oryza sativa L.*) var. *Nippobare*, DJ, and TP309 were provided by the Institute of Microbiology, the Chinese Academy of Sciences. All the *Arabidopsis* plants were grown in growth chambers at 20°C at night and 22°C during the day with a 10-h/day photoperiod. Rice plants were grown at 30°C/28°C with a 14 h/10 h day/night cycle.

Isolation, Sequencing, and Phylogenetic Analysis of *OsNHO1*

The cDNA sequence of *OsNHO1* (LOC_Os04g55410) was obtained from the Rice Annotation Project Database (http://rice.plantbiology.msu.edu/) by BLAST with the amino acid sequence of *AtNHO1* gene (accession number: AT1G80460). We designed specific primers tailed with *Bam*H I and *Sac* I (*OsNHO1*-F/R, **Supplementary Table S1**) to amplify the full-length *OsNHO1*. The identification of the amplified *OsNHO1* was verified by sequencing. Multiple sequence alignment of OsNHO1 with other GK proteins was conducted using DNAMAN Version 6.0 (Lynnon Corporation, Canada). A phylogenetic tree including the OsNHO1 and other GK proteins was constructed using the MEGA7 (Tamura, Stecher, and Kumar 2016) program. The accession numbers of proteins used in multiple sequence alignment and phylogenetic analysis are listed in **Supplementary Table S2**.

Cloning and Analysis of *OsNHO1* Promoter

We designed specific primers (Ppronho1-62F/R, **Supplementary Table S1**) to clone the promoter sequence of *OsNHO1* by chromosome walking. The fragment was sequenced, and the promoter sequence was analyzed with the PlantCARE online website (http://bioinformatics.psb.ugent.be/webtools/plantcare/html/) and visualized by TBtools software (Chen et al., 2020) (**Supplementary Figure S1**).

Expression Profile Analysis of *OsNHO1*

Germinant WT (TP309) rice seedlings were grown in pots at 30°C/28°C with a 14 h/10 h day/night cycle. For hormone treatments, rice plants with 4 leaves were sprayed with 1 mmol/l SA and 0.1 mmol/l methyl jasmonate (MeJA), and the control plants were sprayed with deionized water. Leaves were sampled at 0, 1, 4, 8, 12, and 24 h after treatment. For pathogen infection, rice leaves were detached from plants and infected with *Xoo*-PXO99 (OD 0.4–0.6), and the control was infected with water. The leaves were sampled at 0, 1, 4, 8, 12, and 24 h. All the samples were immediately frozen in liquid nitrogen and stored at −80°C.

The roots, stems, and leaves of TP309 rice plants were sampled and ground in liquid nitrogen. Total RNA was extracted using the TRIzol method. DNase I (Invitrogen) was employed to digest the genomic DNA. Total RNA (1 μg) was subsequently used for first-strand cDNA synthesis catalyzed by M-MLV reverse transcriptase with Oligo d_T18 primer. cDNA was stored at −20°C. Quantitative real-time PCR (qRT-PCR) was performed using the SYBR Green Mix PCR Kit, with *GAPDH* as an internal reference gene (**Supplementary Table S1**). The gene-specific primers used for qPCR analysis are given in **Supplementary Table S1**.

Acquisition and Identification of Transgenic Rice Plants

The *OsNHO1* full-length fragment was digested with *Bam*H I and *Sac* I, and then inserted into the binary vector pTCK303 (Wang et al., 2004). The fragment for RNAi vector construction was amplified using specific primers (*OsNHO1*i-F/R, **Supplementary Table S1**) with *Spe* I/*Bam*H I and *Sac* I/*Kpn* I restriction enzyme sites. The purified fragments of approximately 600 bp were digested with *Spe* I and *Sac* I, inserted into pTCK303 in the sense orientation and then digested with *Bam*H I and *Kpn* I in the antisense orientation. The recombinant plasmids pTCK303-*NHO1* full and pTCK303-*NHO1i* were transferred into the *Agrobacterium* LBA4404 strain. Then, the two positive strains were preserved and used for rice plant transformation.

Transgenic rice plants were acquired *via* the *Agrobacterium*-mediated transformation method (Wang et al., 2004). Homozygous transgenic rice offspring were obtained after three generations of self-crossing, as detected by qRT-PCR and Western blotting.

Pathogen Infection Experiment

Xoo-PXO99 was cultivated on a solid pressure-sensitive adhesive (PSA) medium at 28°C and then a single colony was grown in a liquid PSA medium at 180 revolutions per minute (rpm) for 24 h. Subsequently, the bacteria were cultivated on solid PSA medium again at 28°C in the dark for 2 d. Then, the bacterial culture was suspended in sterile water, and the solution was adjusted to OD600 = 0.5. Then, rice leaves were treated with the bacteria. Ten to twenty rice plants for each line at the four-leaf stage were included in the experiment. Three fully expanded leaves of each plant were cut for further observation and analysis. The lengths of disease speckles and diseased leaves were surveyed after 14 days.

M. oryzae isolate Y34 was cultivated on oatmeal agar containing 30 g/l oatmeal and 15 g/l agar. After 15 min of sterilization at 115°C, 100 μg/ml carbenicillin, 50 μg/ml kanamycin, and 50 μg/ml streptomycin were added. Rice leaves at the four-leaf stage were cut into fragments of approximately 6 cm and washed with sterile water. The leaves were placed on filter paper wetted with 100 mg/l 6-benzylaminopurine (6-BA). The two ends of each leaf were fixed with cotton to ensure that the leaf remained close to the filter paper. Bacterial colonies of the same size were selected and inoculated into each leaf using a 0.5-cm diameter perforator. The bacterial incidence in the leaves was surveyed 1 week later.

GK and Wax Content Quantification

The content of GK in the offspring of transgenic rice was determined by the double-antibody sandwich method of ELISA, and the specific operation was carried out according to the instructions of the kit (Shanghai Jining, China, Cat.no.JN19516).

For wax quantification, we measured the wax content by the hot chloroform extraction method (Zhou et al., 2013). Leaves of WT and transgenic rice were cut into pieces and dipped into 60°C chloroform. The leaves were removed immediately after 30 s of oscillation. After the extraction volatilized at room temperature, the wax was weighed.

Yeast Two-Hybrid Assays

To identify proteins interacting with OsNHO1, yeast transformation, and library screening were performed using the Match-Maker™ GAL4 Two Hybrid System 3 (Clontech, Mountain View, California, USA). A cDNA library was generated from rice samples subjected to abiotic stress and biotic stress and cloned into pGADT7, which was used as a prey protein. The coding region of *OsNHO1* was cloned into pGBKT7 as a bait protein. The resultant vectors were used to transform yeast strain AH109. Positive clones were selected on a medium lacking leucine, threonine, and histidine, and positivity was ensured by culturing a medium lacking leucine, threonine, histidine, and adenine but containing X-α-Gal. Then, the samples were sequenced and verified using phytozome and rice annotation databases.

Bimolecular Fluorescence Complementation Assay

For the bimolecular fluorescence complementation (BiFC) assay, the full-length coding sequences of *OsNHO1* and OsSRC2 were cloned into the binary BiFC vectors pSPYNE-35S and pSPYCE-35S using a gateway system (Walter et al., 2004). The combination vectors OsNHO1-YFPC and OsSRC2-YFPN were

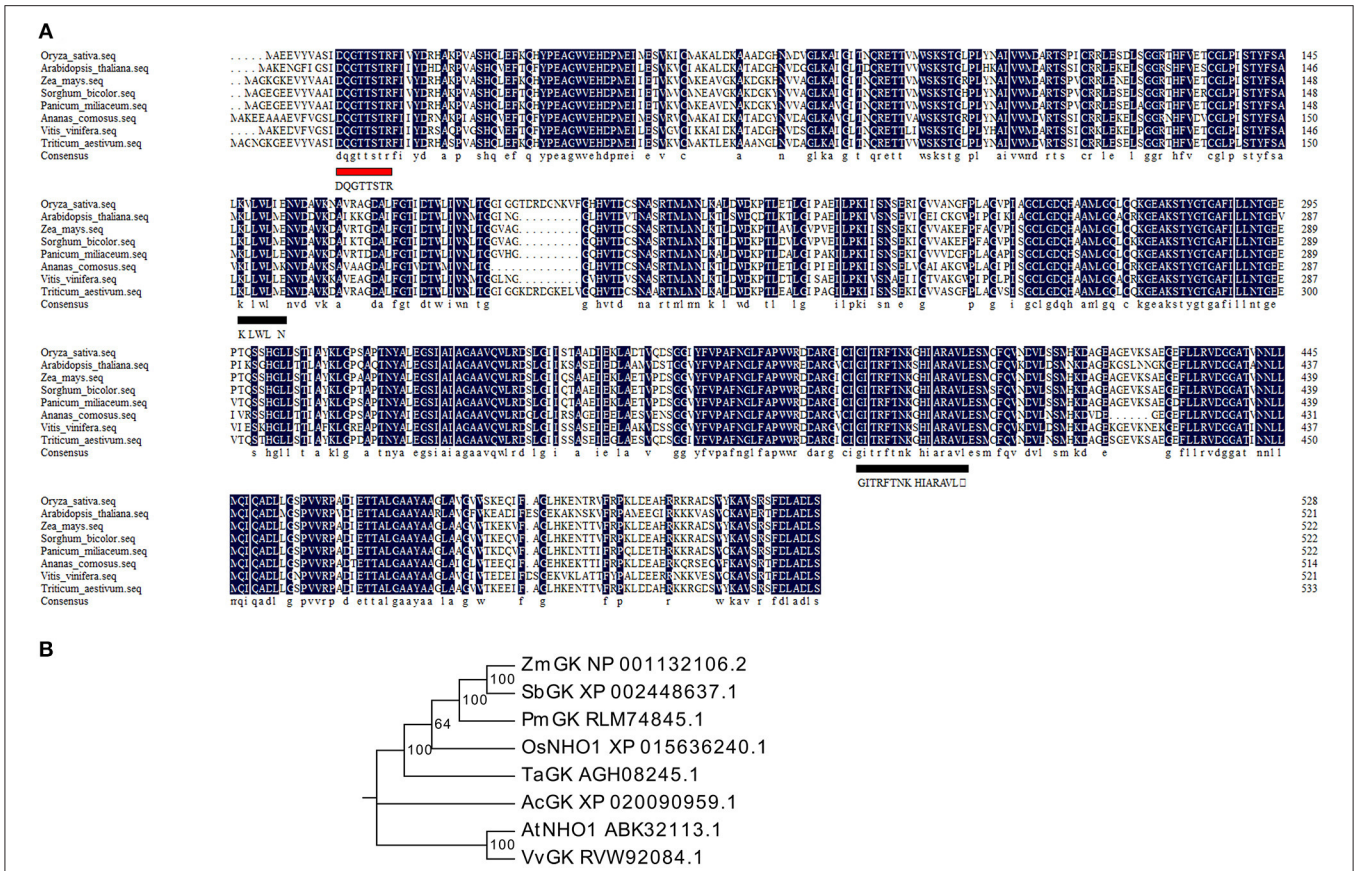

FIGURE 1 | Sequence and phylogenetic analysis of OsNHO1 and GK proteins from other species. **(A)** Protein sequence alignment using DNAMAN software. The ATP-binding motif is underlined with a red solid line. The FGGY signature motives are underlined with a black solid line. **(B)** Phylogenetic analysis of GK proteins constructed using Mega6 based on the neighbor-joining method. *Oryza sativa* (accession number: XP_015636240.1), *Arabidopsis thaliana* (accession number: ABK32113.1), *Triticum aestivum* (accession number: AGH08245.1), *Zea mays* (accession number: NP_001132106.2), *Sorghum bicolor* (accession number: XP_002448637.1), *Panicum miliaceum* (accession number: RLM74845.1), *Ananas comosus* (accession number: XP_020090959.1), and *Vitis vinifera* (accession number: RVW92084.1). GK, glycerol kinase.

coinfiltrated into *Nicotiana benthamiana via* an *Agrobacterium*-mediated method. Yellow fluorescent protein (YFP) signals were detected with a confocal microscope.

Statistical Analysis

Data are presented as the mean ± SD. Significant differences between transgenic lines and WT plants were analyzed using a *t*-test ($p < 0.05$). The displayed measured values are the means of three biological replicates.

RESULTS

OsNHO1 Encodes a Glycerol Kinase Which Can Be Induced by *Xoo*

Glycerol kinase (GK) is the critical enzyme in the production of glycerol metabolites and belongs to the FGGY superfamily. A BLASTp search showed that only one gene locus (LOC_Os04g55410) in rice shared high homology with GKs from monocot and dicot plants. The coding sequence of this locus was cloned from rice and named the *OsNHO1* gene. Multiple sequence alignment analysis showed that OsNHO1 contained one conserved ATP-binding motif (DQGTTSTR) and two FGGY signature motifs (**Figure 1A**). The phylogenetic tree of GK proteins from several species showed that OsNHO1 had a close relationship with GKs from the grass family (**Figure 1B**). The evolutionary relationships were consistent with the relatedness of the species.

To determine whether GK is involved in the resistance of rice against *Xoo*, we inoculated the leaves with *Xoo*-PXO99, and compared the GK content in the leaves at different time points. The GK content was strongly increased at 12 h postinoculation (hpi) compared with the control (**Figure 2A**). The results indicated that GK is involved in response to *Xoo*.

The expression profile of *OsNHO1* was analyzed by qPCR in rice cultivar TP309 seedlings treated with *Xoo*-PXO99, JA, and SA (**Figure 2B**). In the presence of JA, the relative expression of *OsNHO1* slowly increased before peaking at 12 h, with a 10-fold increase compared with that of the control. *OsNHO1* was also induced by SA. The relative expression level of *OsNHO1* increased nearly 4-fold compared with the control at 8 h and then

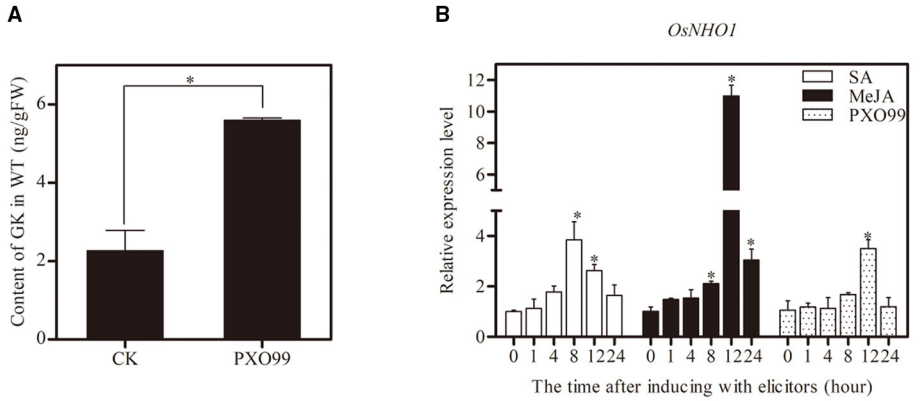

FIGURE 2 | Determination of GK content and expression profiles of *OsNHO1* treated with *Xoo*-PXO99. **(A)** The GK level was increased by *Xoo* infection in rice leaves after inoculation with the *Xoo*-PXO99. **(B)** Transcriptional levels of *OsNHO1* in plants treated with JA, SA, and *Xoo*-PXO99. Each value represents the mean ± SE of three biological replicates. GK, glycerol kinase; JA, jasmonic acid; SA, salicylic acid. * indicates a significant difference at the 0.05 level.

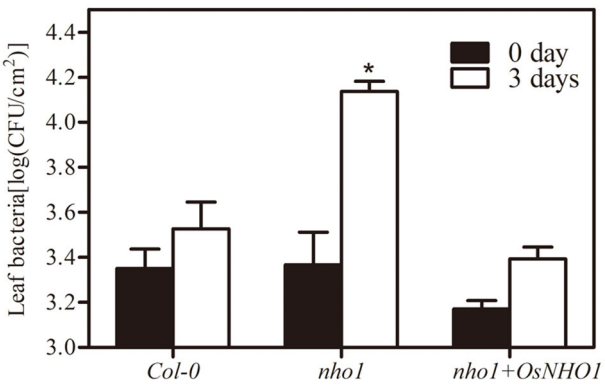

FIGURE 3 | Bacterial growth of *P. s. phaseolicola* in Col-0, *nho1* mutant, and *nho1* + *OsNHO1* lines was measured at 0 and 3 days after inoculation. Asterisks indicate significant differences compared with the other two varieties at 3 days ($p < 0.05$) by one-way ANOVA followed by the Tukey's highest significant difference (HSD) analysis. The error bars indicate the SEs. Three independent experiments were performed with similar results.

gradually declined. When inoculated with *Xoo*-PXO99, *OsNHO1* was significantly induced only at 12 h. These results showed that *OsNHO1* could be induced by JA, SA, and *Xoo*-PXO99.

OsNHO1 Partially Rescued the Functional Defect of the *Arabidopsis nho1* Mutant

AtNHO1 is required for both the general and specific resistance against bacteria and fungi and is involved in flagellin-induced non-host resistance to *Pseudomonas* in *Arabidopsis*. To explore whether *OsNHO1* functions in a similar way to the homologous gene *AtNHO1* in *Arabidopsis*, we obtained *Arabidopsis nho1* mutant plants with *OsNHO1* ectopic expressed. The transgenic progeny was inoculated with the pathogen *P. s. pv. phaseolicola* and the bacterial counts were conducted at 0 d and 3 days. The bacterial number in Col-0 at 3 days was 1.6 times that at 0 day and in the *nho1* mutant, it was 5.5 times that at 0 day (**Figure 3**). However, in the presence of *OsNHO1*, the bacterial number at 3 days decreased to 1.8 times higher than that at 0 day. In addition, bacterial fecundity in Col-0 and *nho1* + *OsNHO1* was significantly lower than that in the *nho1* mutant (**Figure 3**), indicating that *OsNHO1* functions similarly to *AtNHO1* in resisting *P. s. pv. phaseolicola.*

Regulation of *OsNHO1* Expression Could Change Defenses Against Pathogens in Transgenic Rice

The *AtNHO1* was required for defense against *Pseudomonas* bacteria in *Arabidopsis* (Lu et al., 2001). To test the function of the *OsNHO1* gene in rice defense, we obtained *OsNHO1* overexpression (OE) and knockdown transgenic plants using the *Agrobacterium*-mediated genetic transformation method. After four generations of screening, homozygous transgenic lines (T4), namely, two *OsNHO1*-OE lines and two *OsNHO1*-RNAi lines, were used for subsequent research. The relative expression level of *OsNHO1* in the knockdown transgenic lines RNAi 72 and RNAi 85 was reduced by 50%, while it was increased approximately 3-fold in the OE lines *OsNHO1*-OE1 and *OsNHO1*-OE2 (**Figure 4A**). Western blotting results also showed that *OsNHO1* was expressed in the *OsNHO1*-OE lines (**Figure 4B**).

To confirm whether *OsNHO1* could affect GK accumulation, we quantified the GK contents in different transgenic plants. The content of GK in *OsNHO1*-OE plants was significantly higher than that in WT plants but was only marginally reduced in *OsNHO1*-RNAi plants compared with WT plants (**Figure 4C**). Meanwhile, to further verify that GK is involved in rice responses to pathogens, we measured the changes in GK contents in different materials after pathogen treatments. We found that the GK level was strongly increased in both the *OsNHO1*-OE and *OsNHO1*-RNAi lines after inoculation with *Xoo*-PXO99 at 12 hpi compared with 0 hpi (**Figure 4C**).

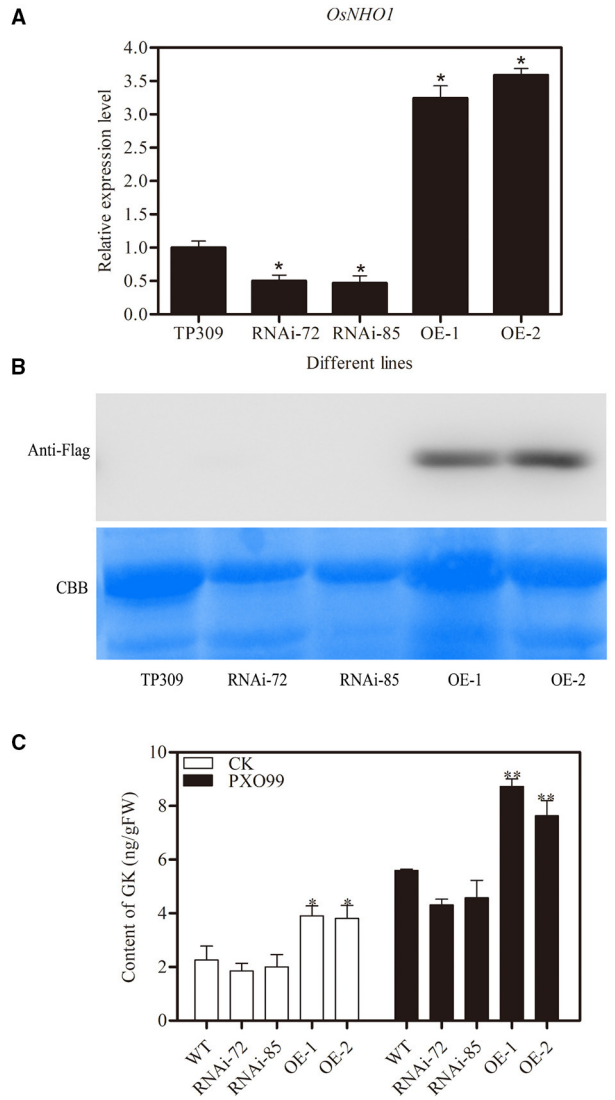

FIGURE 4 | Identification of transgenic materials. **(A)** *OsNHO1* transcript levels in RNAi, OE, and WT (TP309) plants by qPCR. **(B)** Protein-level determination in different plants. **(C)** Content of GK in different transgenic plants. GK, glycerol kinase; OE, overexpression; WT, wild type. * indicates a significant difference at the 0.05 level; ** indicates a significant difference at the 0.01 level.

The obtained transgenic plants were used for *Xoo* and blast resistance test. We infected rice leaves with *Xoo*-PXO99 and measured the lesion length produced by *Xoo*-PXO99 after 13–15 days (**Figures 5A,B**), and the lesion area produced by Y34 was measured after 7–8 days (**Figures 5C,D**). We observed that the lesion length in the WT line was approximately 8.5 cm, while it was 11 cm in the *OsNHO1*-RNAi lines and 6 cm in the *OsNHO1*-OE lines. In addition, the lesion areas in the two overexpression lines were significantly less than those in the WT line, while the lesion areas in the two *OsNHO1*-RNAi lines were increased approximately 2-fold compared with those in the WT line.

These results showed that the defects in *OsNHO1* led to increased susceptibility to *Xoo*-PXO99 and *M. oryzae* Y34 while overexpressing *OsNHO1* inhibited the spread of bacterial blight and blast. Thus, we concluded that *OsNHO1* positively regulates rice immunity against pathogens.

OsNHO1 Influences the Contents of Wax

Glycerol metabolism is initiated upon its conversion to G3P *via* the GK-mediated phosphorylation of glycerol. G3P is involved in the synthesizing of C16 and C18 chain fatty acids, which are essential precursors for wax synthesis. To analyze whether GK is related to wax synthesis, we measured the wax contents in different *OsNHO1* transgenic lines. The wax content in the *OsNHO1*-RNAi lines was reduced in comparison with that in TP309. However, the wax content in the *OsNHO1*-OE lines was higher than that in the WT (**Figure 6A**).

Rice wax synthesis regulatory genes (*OsWRs*) modulate wax synthesis by the alteration of long-chain fatty acids and alkanes (Wang et al., 2012; Zhou et al., 2013). In this study, we analyzed the relative transcript levels of *OsWR1*, *OsKCS1*, *OsCUT1*, and *OsERF104* in the transgenic lines (**Figure 6B**). These four genes were upregulated in *OsNHO1*-OE lines and showed no significant difference in the *OsNHO1*-RNAi lines compared with the WT. These results implied that overexpression of the *OsNHO1* gene increased the content of wax.

OsNHO1 Regulates the Expression of *OsPR5* and *OsAOS1* in Transgenic Rice Lines

Glycerol-induced resistance was reported in non-host resistance with upregulation of several *PR* genes (Jiang et al., 2009; Zhang et al., 2015). Pathogenesis-related proteins (PRs) are important components in plant responses to biotic and abiotic stresses. In this study, we analyzed the relative transcript levels of *OsPRs* in the transgenic lines (**Figure 7**). We found that the expression of *OsPR10*, *OsNH1*, and *OsICS1* genes was no significant difference, while *OsPR5*, *OsAOS1,* and *OsWRKY6* showed different transcription levels in different materials. Silencing of *OsNHO1* decreased the relative expression of *OsPR5* by 85%, while overexpression of *OsNHO1* increased the expression of *OsPR5*.

OsSRC2 Is the Interaction Partner of *OsNHO1*

To identify the components in the *OsNHO1*-mediated signaling pathway, we screened the interaction partners of OsNHO1 by the yeast two-hybrid method using a rice cDNA library prepared from rice leaf tissue treated with biotic stresses. We obtained 13 potential candidate proteins (**Table 1**). Among these candidate proteins, the protein LOC_Os01g70790 contains a C2 domain (calcium-dependent lipid-binding domain, CaLB) and exhibits highly homologous with the protein SRC2 in soybeans, which is induced by cold stress. *In vivo* interaction between OsNHO1 and OsSRC2 indicated by BiFC analysis showed that these two proteins colocalized in the nucleus (**Figure 8**).

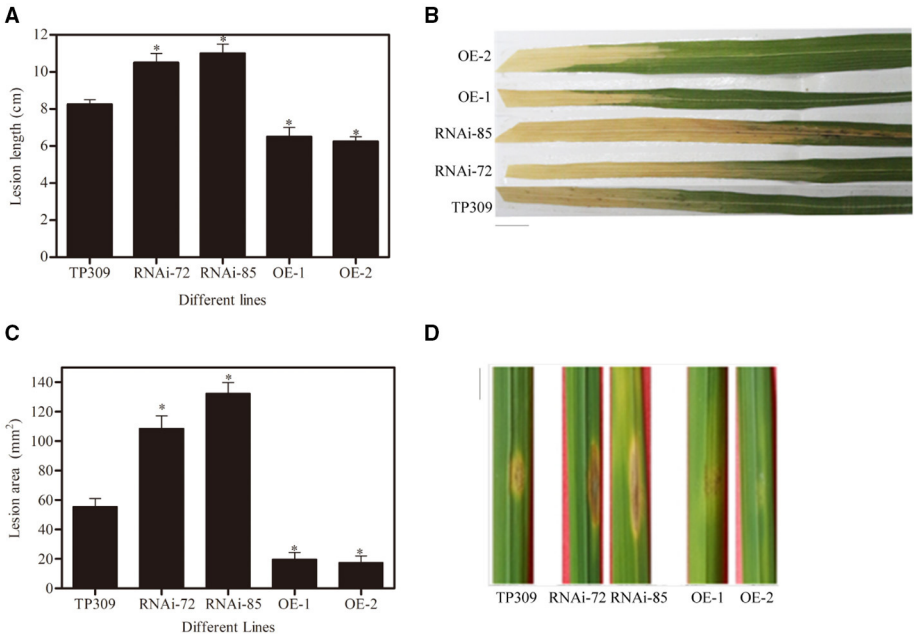

FIGURE 5 | Disease resistance identification of transgenic materials. **(A)** Lesion lengths in transgenic plants were measured at 14 days postinoculation with *Xoo*-PXO99. **(B)** A photograph depicting disease symptom development in leaves 14 d postinfection with *Xoo*-PXO99. Scale bars = 1 cm. **(C)** Lesion areas of transgenic plants were measured using ImageJ software at 7 days postinoculation with Y34. **(D)** A photograph depicting disease symptom development in leaves 7 d postinfection with Y34. Scale bars = 1 cm. TP309: wild-type; RNAi-72 and RNAi-85: two RNAi-*OsNHO1* lines; OE1 and OE2, two *OsNHO1* overexpression lines. Asterisks indicate significant differences compared to TP309 ($p < 0.05$) by one-way ANOVA followed by Tukey's HSD analysis. Error bars indicate SEs. Three independent experiments were performed with similar results.

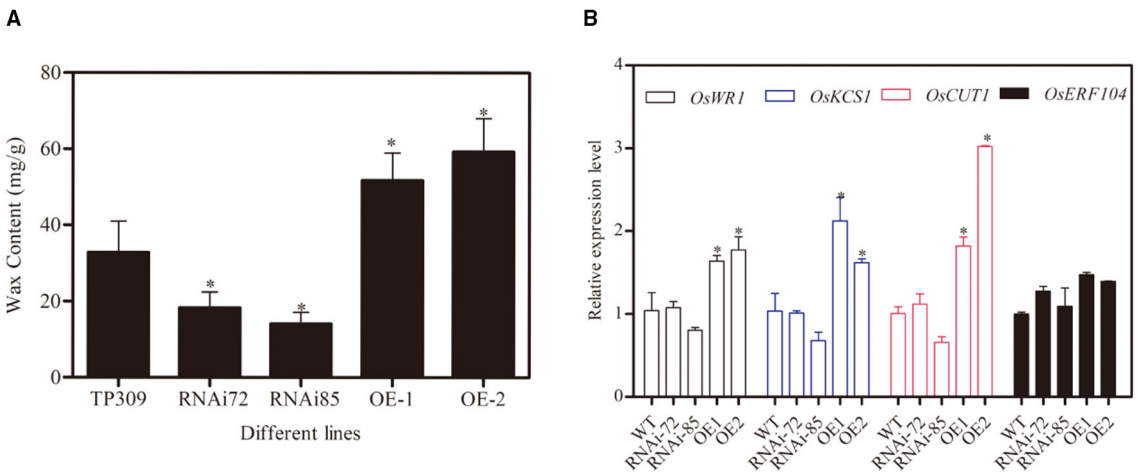

FIGURE 6 | Contents of wax and relative expression of *OsWRs* genes in the WT (TP309), *OsNHO1*-RNAi, and *OsNHO1*-OE lines. **(A)** Contents of wax were measured by the hot chloroform extraction method. **(B)** Relative expression of *OsWRs* genes. Each value represents the mean ± SE of three biological replicates. Asterisks indicate significant differences compared to TP309 ($p < 0.05$) by one-way ANOVA followed by the Tukey's HSD analysis. OE, overexpression; WT, wild type.

C2 domain-containing proteins play important roles in plant immunity, and the OsSRC2 protein contains a C2 domain. Previous results show that OsSRC2 functions as the interacting partner of OsNHO1. To analyze whether SRC2 is regulated by NHO1, we detected the transcription levels of *OsSRC2* in different *OsNHO1* transgenic lines by qPCR (**Supplementary Figure S2**). *OsSRC2* was upregulated in the *OsNHO1*-OE lines but downregulated in the *OsNHO1*-RNAi lines. These results implied that OsNHO1 may interact with the OsSRC2 protein to modulate responses to pathogens.

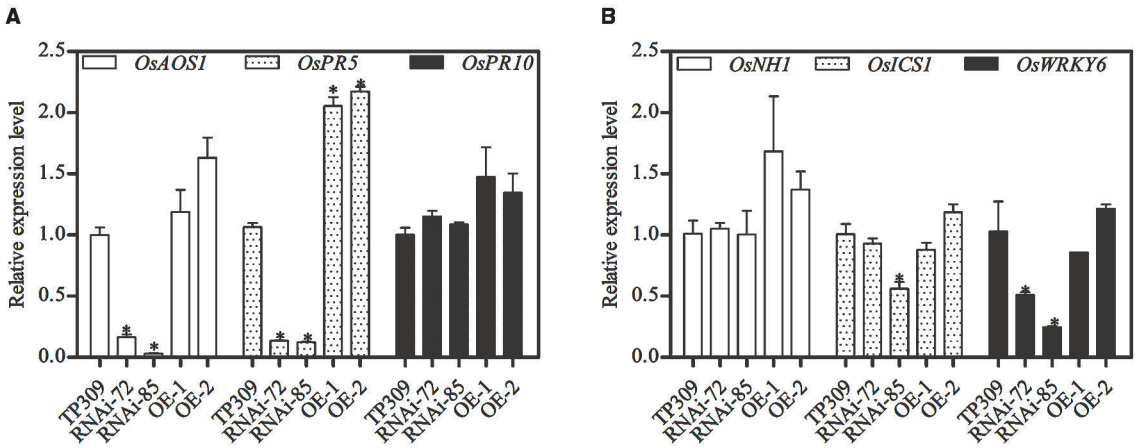

FIGURE 7 | Relative expression of *OsPRs* in transgenic lines determined by qPCR with an SYBR® Premix Ex Taq TM II Kit. The transcript levels of *PR* genes in WT were considered 100%. Expression levels of the target gene were normalized to the *ACTIN* reference gene. **(A)** Relative expression of *OsAOS1*, *OsPR5*, and *OsPR10*. **(B)** Relative expression of *OsNH1*, *OsICS1*, and *OsWRKY6*. Each value represents the mean ± SE of three biological replicates. Asterisks indicate significant differences compared to TP309 ($P < 0.05$) by one-way ANOVA followed by Tukey's HSD analysis. The error bars indicate the standard errors. Three independent experiments were performed with similar results. qPCR, quantitative PCR; WT, wild type.

TABLE 1 | Partner proteins of NHO1 selected in the process of yeast two-hybrid (Y2H) screening.

Partner protein	Protein ID
OsSRC2	LOC_Os01g70790
DnaK family protein	LOC_Os01g62290
RNA recognition motif family protein	LOC_Os02g07070
PCNA-Putative DNA replicative polymerase clamp	LOC_Os02g56130
Calcium/calmodulin depedent protein kinase	LOC_Os03g17980
DnaK family protein	LOC_Os03g60620
Expressed protein	LOC_Os05g14270
MTA/SAH nucleosidase	LOC_Os06g02220
Glycosyl hydrolase, family 31	LOC_Os07g23944
Ubiquinol-cytochrome C chaperone family protein	LOC_Os07g30790
PAP fibrillin family domain containing protein	LOC_Os09g04790
C-5 cytosine-specific DNA methylase	LOC_Os10g01570
DnaK family protein	LOC_Os11g47760

DISCUSSION

OsNHO1 Plays an Important Role in Resisting Bacterial and Fungal Pathogens

Glycerol can be utilized as a sole carbon and energy source for both bacteria and fungi (Wei et al., 2004). This study found that glycerol may work as a significant transferred metabolite from plant to pathogen. The way to assimilate glycerol is the phosphorylative catabolic pathway, the key enzyme of glycerol metabolism is GK. Early study found that glycerol-insensitive mutants *gli1* seedings lacking glycerol kinase are more resistant to abiotic stress (Eastmond, 2004), but *NHO1* is needed for resistance to the fungal pathogen *Botrytis cinerea* and to the bacterial resistance. Consistent with results in *Arabidopsis*, we found that *OsNHO1* was significantly induced by *Xoo*-PXO99 (**Figure 2**). Moreover, *OsNHO1*-OE plants showed increased resistance to *Xoo*-PXO99 and Y34, and *OsNHO1*-RNAi plants were more susceptible to pathogens (**Figure 5**). The correlation of *OsNHO1* transcriptional levels with different reactions implies an essential role of these biochemical processes in disease resistance. A possible explanation might be that GK can alter plant glycerol pools then affect nutrient availability for pathogens.

OsNHO1 May Influence the Interactions Between Plants and Biotic Agents by Upregulating the Wax-Related Genes

Cutin is an extracellular lipid polymer that contributes to protective cuticle barrier functions against biotic and abiotic stresses in land plants. The cuticle wax is chemically composed of lipids. GK deficiency alters the expression of genes involved in lipid and carbohydrate metabolism (Rahib et al., 2007). In contrast, the wax biosynthetic genes *OWR1*, *OsKCS1*, and *OsCUT1* in *OsNHO1*-OE plants are upregulated (**Figure 6B**). Corresponding to waxy gene expression, the wax content in *OsNHO1*-OE materials increases accordingly (**Figure 5**).

In addition, cuticle wax in plants is considered to contribute to drought, insect (Lee et al., 2014), and pathogen resistance (Jenks et al., 1994; Özer et al., 2017). Studies have shown that the content of wax in plants may also be correlated with disease resistance. For example, the wax contents of maize disease-resistant varieties were significantly higher than those of susceptible varieties (Russin et al., 1997), and the wax contents of leaves of resistant cassava varieties were higher than those of susceptible varieties (Zinsou et al., 2006). Similarly, in this study, we found that the wax content in the *OsNHO1*-OE plants, which showed increased resistance to *Xoo*-PXO99 and Y34, was far greater than that in

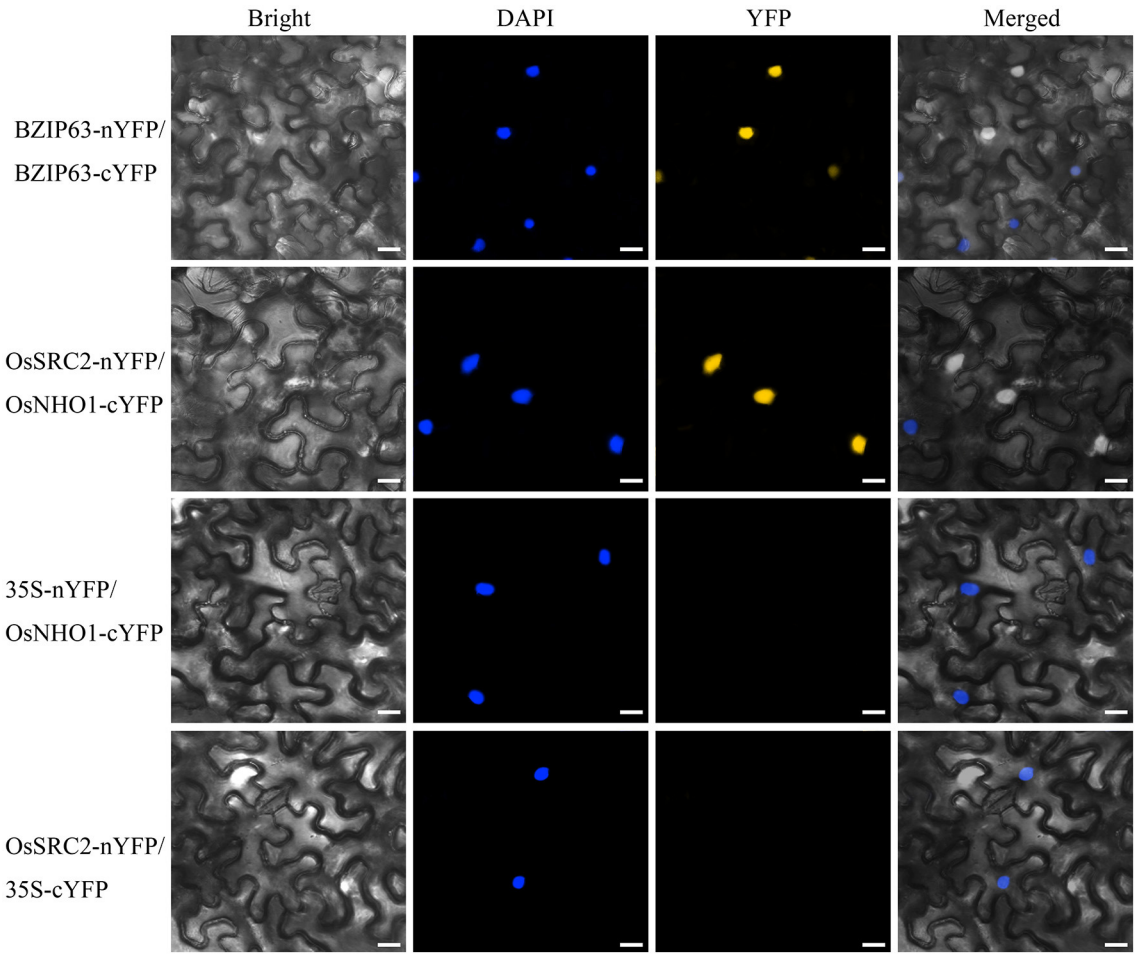

FIGURE 8 | *In vivo* interaction between *OsNHO1* and OsSRC2 by BiFC analysis. *N. benthamiana* leaves were co-infiltrated with *Agrobacterium* carrying 35S::OsSRC2-nYFP and 35S::OsNHO1-cYFP. BZIP63 was used as a positive control. 35S-nYFP/OsNHO1-cYFP and OsSRC2-nYFP/35S-cYFP were used as negative controls. Fluorescence [yellow fluorescent protein (YFP)] and bright and merged field confocal images were acquired at 72 h. DAPI was used for nuclear staining. Scale bars = 20 μm.

OsNHO1-RNAi plants (**Figure 5**). This indicated that abnormal *OsNHO1* expression may disturb rice pathogen resistance by altering the wax content.

Plant hormones can work as signal molecules and then affect plant responses to stress by mediating the deposition of cuticle wax. Ethylene (ETH) could increase the content and change the structure of wax to protect citrus plants from *Penicillium digitatum* invasion (Cajuste et al., 2010). Under water stress, ABA promoted the expression of several wax-synthesis genes in *Arabidopsis* by upregulating the expression of the transcription factor *MYB96* and eventually promoted the accumulation of wax (Seo et al., 2011). Exogenous SA, MeJA, and 1-aminocyclopropane-1-carboxylate (ACC) could induce the deposition of cuticle wax in *Brassica napus*. SA is essential for sugars and glycerol-mediated disease resistance (Qian et al., 2015). Glycerol-induced resistance was reported in non-host resistance with upregulation of several *PR* genes and ROS accumulation. *OsPR5* and *OsICS1* are the key genes of the SA signaling pathway. JA and cutin wax belong to the fatty acid metabolism pathway and have a common synthetic precursor (Zhang et al., 2020). *OsAOS1* is involved in the JA signal pathway. The expression of *PR* genes was significantly reduced in *Arabidopsis* waxy epidermis mutants *cer6* and *cer2* (Garbay et al., 2007), suggesting that the transcription level of *PR* genes is closely related to waxy components. Remarkably, the transcriptional level of the *OsPR5* gene in *OsNHO1*-OE plants was higher than those in WT and *OsNHO1*-RNAi plants (**Figure 7A**), indicating that *OsNHO1* have an additive influence on cuticular wax biosynthesis that is SA-dependent.

OsNHO1 Participated in a Novel Pathway Regulating Plant Defense

Glycerol metabolism is initiated upon its conversion to G3P *via* the GK-mediated phosphorylation of glycerol. G3P is involved in the synthesis of C16 and C18 chain fatty acids,

which are important precursors for wax synthesis. In addition, cuticle wax in plants is considered to contribute to drought, insect (Lee et al., 2014), and pathogen resistance (Jenks et al., 1994; Özer et al., 2017). Studies have shown that the content of wax in plants may also be correlated with disease resistance. For example, the wax contents of maize disease-resistant varieties were significantly higher than those of susceptible varieties (Russin et al., 1997), and the wax contents of leaves of resistant cassava varieties were higher than those of susceptible varieties (Zinsou et al., 2006). Similarly, in our research, we found that the wax content in the *OsNHO1*-OE plants, which showed increased resistance to *Xoo*-PXO99 and Y34, was far greater than that in *OsNHO1*-RNAi plants (**Figure 7**). This indicated that abnormal *OsNHO1* expression may disturb rice pathogen resistance by altering the wax content.

The cuticle wax is chemically composed of lipids. In mice, SRC2 and SRC3 regulate epidermis-specific sphingolipid production (Oda et al., 2009). In plants, SRC2 is a C2 domain-containing protein or calcium-dependent lipid-binding protein. C2 domains are found in over 100 different proteins with functions ranging from signal transduction to vesicular trafficking. The C2 domain of CaSRC2-1 is crucial for plasma membrane targeting, and the PcINF1-SRC2-1 complex is required in PcINF1-induced pepper immunity (Liu et al., 2015). In addition, the transcript level of *OsSRC2* was upregulated by *M. oryzae* according to the Rice MetaSysB database (Sureshkumar et al., 2019). Other C2 domain-containing proteins, such as SS52 in pepper (Kim et al., 2008; Sakamoto et al., 2009); OsERG1, OsERG3, and GTPase-activating protein (GAP) in rice (Kim et al., 2003; Cheung et al., 2008); and BON1/CPN1, BAP1, and BAP2 in *Arabidopsis* (Liu et al., 2005; Yang et al., 2006, 2007), play important roles in plant immunity. Here, we found that the OsSCR2 protein, which is one of the interaction partners of OsNHO1 (**Table 1**), contains a C2 domain. BiFC results showed that these two proteins co-localized in the nucleus (**Figure 7**). Our results showed that the transcriptional levels of the *OsSRC2* gene in *OsNHO1*-OE plants were higher than those in WT and *OsNHO1*-RNAi plants (**Supplementary Figure S2**).

Thus, we concluded that *OsNHO1* participates in a novel pathway regulating plant defense. *OsNHO1* significantly contributed to pathogen resistance to bacterial blight and rice blast by interacting with OsSRC2 protein upon pathogen infection, affecting the content of wax and modulating the expression of *PR* genes. *OsNHO1* was a potential candidate gene for disease resistance engineering. Accordingly, further investigations may focus on the following important areas.

The regulation between OsNHO1 and its partner OsSRC2 should be further investigated. The roles of OsSRC2 in innate immunity and their relationships with wax generation and PR gene activation will be of great interest in future explorations.

DATA AVAILABILITY STATEMENT

The original contributions presented in the study are included in the article/**Supplementary Material**, further inquiries can be directed to the corresponding author/s.

AUTHOR CONTRIBUTIONS

YC, XY, XN, and CH designed the research. HW, WG, and ZG performed the research. XX, RW, and SK wrote the paper. All authors read and approved the final manuscript.

ACKNOWLEDGMENTS

We thank the National Key Research and Development Program of China (2018YFD1000500), the Key R&D Program of Hainan Province (ZDYF2019063), and PHD CJ for providing TBtools software. We are particularly grateful to Xiaofei Zhang from Alliance of Bioversity International and CIAT for his revised recomendation.

SUPPLEMENTARY MATERIAL

The Supplementary Material for this article can be found online at: https://www.frontiersin.org/articles/10.3389/fpls.2021.800625/full#supplementary-material

REFERENCES

Ahn, I. P., Kim, S., and Lee, Y. H. (2005). Vitamin B1 functions as an activator of plant disease resistance. *Plant Physiol.* 138, 1505–1515. doi: 10.1104/pp.104.058693

Brisson, D., Vohl, M. C., St-Pierre, J., Hudson, T., and Gaudet, D. (2001). Glycerol: a neglected variable in metabolic processes? *Bioessays* 23, 534–542 doi: 10.1002/bies.1073

Cajuste, J. F., González-Candelas, L., Veyrat, A., García-Breijo, F. J., and Reig-Armiñana, J. (2010). Epicuticular wax content and morphology as related to ethylene and storage performance of 'Navelate' orange fruit. *Postharvest Biol. Technol.* 1, 29–35. doi: 10.1016/j.postharvbio.2009.07.005

Chanda, B., Venugopal, S. C., Kulshrestha, S., Navarre, D. A., Downie, B., Vaillancourt, L., et al. (2008). Glycerol-3-phosphate levels are associated with basal resistance to the hemibiotrophic fungus colletotrichum higginsianum in Arabidopsis. *Plant Physiol.* 147, 2017–2029. doi: 10.1104/pp.108.121335

Chandra-Shekara, A.C., Venugopal, S.C., Barman, S.R., Kachroo, A., and Kachroo, P. (2007). Plastidial fatty acid levels regulate resistance gene-dependent defense signaling in Arabidopsis. In: *Proceedings of the National Academy of Sciences of the United States of America*. doi: 10.1073/pnas.0609259104

Chen, C., Chen, H., Zhang, Y., Thomas, H. R., Frank, M. H., He, Y., et al. (2020). Tbtools: an integrative toolkit developed for interactive analyses of big biological data. *Mol. Plant.* 13, 1194–1202. doi: 10.1016/j.molp.2020.06.009

Cheung, M. Y., Zeng, N. Y., Tong, S. W., Li, W. F., Xue, Y., Zhao, K. J., et al. (2008). Constitutive expression of a rice GTPase-activating protein induces defense responses. *New Phytol.* 179, 530–545. doi: 10.1111/j.1469-8137.2008.02473.x

Delventhal, R., Rajaraman, J., Stefanato, F. L., Rehman, S., Aghnoum, R., Mcgrann, G., et al. (2017). A comparative analysis of nonhost resistance across the two Triticeae crop species wheat and barley. *BMC Plant Biol.* 17, 1–17. doi: 10.1186/s12870-017-1178-0

Eastmond, P. J. (2004). Glycerol-insensitive Arabidopsis mutants: *gli1*seedlings lack glycerol kinase, accumulate glycerol and are more resistant to abiotic stress. *Plant J.* 37, 617–625. doi: 10.1111/j.1365-313X.2003.01989.x

Ellis, J. (2006). Insights into nonhost disease resistance: can they assist disease control in agriculture? *Plant Cell.* 18, 523–528. doi: 10.1105/tpc.105.040584

Garbay, B., Tautu, M. T., and Costaglioli, P. (2007). Low level of pathogenesis-related protein 1 mRNA expression in 15-day-old Arabidopsis cer6-2 and cer2 eceriferum mutants. *Plant Sci.* 2, 299–305.

Gómez-Ariza, J., Campo, S., Rufat, M., Estopà M., Messeguer, J., Segundo, B. S., et al. (2007). Sucrose-mediated priming of plant defense responses and broad-spectrum disease resistance by overexpression of the maize pathogenesis-related PRs protein in rice plants. *Mol. Plant Microbe. Interact.* 20, 832–842. doi: 10.1094/MPMI-20-7-0832

He, Y., Han, J., Liu, R., Ding, Y., Wang, J., Sun, L., et al. (2018). Integrated transcriptomic and metabolomic analyses of a wax deficient citrus mutant exhibiting jasmonic acid-mediated defense against fungal pathogens. *Hortic. Res.* 5, 43. doi: 10.1038/s41438-018-0051-0

Jenks, M. A., Joly, R. J., Peters, P. J., Rich, P. J., Axtell, J. D., Ashworth, E. N. (1994). Chemically Induced Cuticle Mutation Affecting Epidermal Conductance to Water Vapor and Disease Susceptibility in Sorghum bicolor (L.) Moench. *Plant Physiol.* 105, 1239–1245. doi: 10.1104/pp.105.4.1239

Jiang, C., Hasegawa, M., Shimono, M., Sugano, S., Maeda, S., Inoue, H., et al. (2009). Suppression of the rice fatty-acid desaturase gene OsSSI2 enhances resistance to blast and leaf blight diseases in rice. *Molec. Plant-Microbe Interac.* 22:820–829. doi: 10.1094/MPMI-22-7-0820

Jones, J., and Dangl, J. (2006). The plant immune system. *Nature* 444, p. 323–329. doi: 10.1038/nature05286

Kachroo, A., Fu, D. Q., Havens, W., Navarre, D. R., Kachroo, P., and Ghabrial, S. A. (2008). An oleic acid–mediated pathway induces constitutive defense signaling and enhanced resistance to multiple pathogens in soybean. *Mol. Plant Microbe. Interact.* 21, 564–575. doi: 10.1094/MPMI-21-5-0564

Kachroo, A., Lapchyk, L., Fukushige, H., Hildebrand, D., Klessig, D., and Kachroo, P. (2003). Plastidial fatty acid signaling modulates salicylic acid- and jasmonic acid-mediated defense pathways in the Arabidopsis ssi2 mutant. *Plant Cell.* 15, 2952–2965. doi: 10.1105/tpc.017301

Kachroo, A., Venugopal, S. C., Lapchyk, L., Falcone, D., and Hildebrand, D., Kachroo (2004). Oleic acid levels regulated by glycerolipid metabolism modulate defense gene expression in Arabidopsis. *Proc. Nat. Acad. Sci. US Am.* 101, 5152–5157. doi: 10.1073/pnas.0401315101

Kachroo, P., Venugopal, S. C., Navarre, D. A., Lapchyk, L., and Kachroo, A. (2005). Role of salicylic acid and fatty acid desaturation pathways in ssi2-mediated signaling. *Plant Physiol.* 139, 1717–1735. doi: 10.1104/pp.105.071662

Kang, L., Li, J., Zhao, T., Xiao, F., Tang, X., Thilmony, R., et al. (2003). Interplay of the Arabidopsis nonhost resistance gene NHO1 with bacterial virulence. *Proc. Nat. Acad. Sci.* 100, 3519–3524. doi: 10.1073/pnas.0637377100

Kim, C., Koo, Y., Jin, J., and Moon, B. (2003). Rice C2 domain proteins are induced and translocated to the plasma membrane in response to a fungal elicitor. *Biochemistry*. 42, 11625–11631. doi: 10.1021/bi034576n

Kim, Y.-C., Kim, S.-Y., Choi, D., Ryu, C.-M., and Park, J. M. (2008). Molecular characterization of a pepper C2 domain-containing SRC2 protein implicated in resistance against host and non-host pathogens and abiotic stresses. *Planta* 227, 1169–1179. doi: 10.1007/s00425-007-0680-2

Lee, H.-A., Lee, H.-Y., Seo, E., Lee, J., Kim, S.-B., Oh, S., et al. (2017). Current understandings of plant nonhost resistance. *Molec. Plant-Microbe Interac.* 30, 5–15. doi: 10.1094/MPMI-10-16-0213-CR

Lee, S. B., Kim, H., Kim, R. J., and Suh, M. C. (2014). Overexpre Arabidopsis MYB96 confers drought resistance in Camelina sativa via cuticular wax accumulation. *Plant cell Rep.* 33, 1535–1546. doi: 10.1007/s00299-014-1636-1

Lipka, V. (2005). Pre- and postinvasion defenses both contribute to nonhost resistance in Arabidopsis. *Science.* 310, 1180–1183. doi: 10.1126/science.1119409

Liu, J., Jambunathan, N., and McNellis, T. W. (2005). Transgenic expression of the von Willebrand A domain of the BONZAI 1/COPINE 1 protein triggers a lesion-mimic phenotype in Arabidopsis. *Planta.* 221, 85–94. doi: 10.1007/s00425-004-1413-4

Liu, Z., Qiu, A., Shi, L., Cai, J., Huang, X., Yang, S., et al. (2015). SRC2-1 is required in PcINF1-induced pepper immunity by acting as an interacting partner of PcINF1. *J. Exp.Bot.* 13, 3683–3698. doi: 10.1093/jxb/erv161

Lu, M., Tang, X., and Zhou, J. M. (2001). Arabidopsis NHO1 is required for general resistance against pseudomonas bacteria. *Plant Cell.* 13, 437–447. doi: 10.2307/3871287

Mysore, K. S., and Ryu, C. M. (2004). Nonhost resistance: how much do we know? *Trends Plant Sci.* 9, 97–104. doi: 10.1016/j.tplants.2003.12.005

Oda, Y., Uchida, Y., Moradian, S., Crumrine, D., Elias, P. M., and Bikle, D. D. (2009). Vitamin D receptor and coactivators SRC2 and 3 regulate epidermis-specific sphingolipid production and permeability barrier formation. *J. Invest. Dermatol.* 129, 1367–1378. doi: 10.1038/jid.2008.380

Özer, N., Şabudak, T., Özer, C., Gindro, K., Schnee, S., and Solak, E. (2017). Investigations on the role of cuticular wax in resistance to powdery mildew in grapevine. *J. Gen Plant Pathol.* 5, 316–328. doi: 10.1007/s10327-017-0728-5

Qian, Y., Tan, D. X., Reiter, R. J., and Shi, H. (2015). Comparative metabolomic analysis highlights the involvement of sugars and glycerol in melatonin-mediated innate immunity against bacterial pathogen in Arabidopsis. *Sci. Rep.* 5, 15815. doi: 10.1038/srep15815

Rahib, L., MacLennan, N. K., Horvath, S., Liao, J. C., and Dipple, K. M. (2007). Glycerol kinase deficiency alters expression of genes involved in lipid metabolism, carbohydrate metabolism, and insulin signaling. *Eur. J. Hum. Genet.* 15, 646–657. doi: 10.1038/sj.ejhg.5201801

Rolland, F., and Sheen, M. J. (2002). Supplement: signal transduction || sugar sensing and signaling in plants. *Plant Cell.* 14, S185–S205. doi: 10.1105/tpc.010455

Russin, J. S., Guo, B. Z., Tubajika, K. M., Brown, R. L., Cleveland, T. E., and Widstrom, N. W. (1997). Comparison of Kernel Wax from corn genotypes resistant or susceptible to aspergillus flavus. *Phytopathology* 87, 529–533. doi: 10.1094/PHYTO.1997.87.5.529

Sakamoto, M., Tomita, R., and Kobayashi, K. (2009). A protein containing an XYPPX repeat and a C2 domain is associated with virally induced hypersensitive cell death in plants. *FEBS Lett.* 583, 2552–2556. doi: 10.1016/j.febslet.2009.07.020

Schaaf, J., and Hess, W. D. (1995). Primary metabolism in plant defense. *Plant Physiol.* 108, 949–960. doi: 10.1104/pp.108.3.949

Scheideler, M., Schlaich, N. L., Fellenberg, K., Beissbarth, T., Hauser, N. C., Vingron, M., et al. (2002). Monitoring the switch from housekeeping to pathogen defense metabolism in Arabidopsis thaliana using cDNA arrays. *J. Biol. Chem.* 277, 10556–10561. doi: 10.1074/jbc.M104863200

Seo, P. J., Lee, S. B., Suh, M. C., Park, M. J., Go, Y. S., and Park, C. M. (2011). The MYB96 transcription factor regulates cuticular wax biosynthesis under drought conditions in Arabidopsis. *Plant cell* 23, 1138–1152 doi: 10.1105/tpc.111.083485

Sureshkumar, V., Dutta, B., Kumar, V., Prakash, G., Mishra, D. C., and Chathurvedi, K. K., et al. (2019). RiceMetaSysB: a database of blast and bacterial blight responsive genes in rice and its utilization in identifying key blast-resistant WRKY genes. *J. Biol. Databaaases* 2019. doi: 10.1093/database/baz015

Walter, M., Chaban, C., Schütze, K., Batistic, O., Weckermann, K., Näke, C., et al. (2004). Visualization of protein interactions in living plant cells using bimolecular fluorescence complementation. *Plant J.* 40, 428–438. doi: 10.1111/j.1365-313X.2004.02219.x

Wang, T., Xing, J., Liu, X., Yao, Y., Hu, Z., Peng, H., et al. (2018). GCN5 contributes to stem cuticular wax biosynthesis by histone acetylation of CER3 in Arabidopsis. *J. Exper. Botany.* 69, 2911–2922. doi: 10.1093/jxb/ery077

Wang, Y., Wan, L., Zhang, L., Zhang, Z., Zhang, H., Quan, R., et al. (2012). An ethylene response factor OsWR1 responsive to drought stress transcriptionally activates wax synthesis related genes and increases wax production in rice. *Plant Mol. Biol.* 78, 275–288. doi: 10.1007/s11103-011-9861-2

Wang, Z., Chen, C., Xu, Y., Jiang, R., and Xu, Z. (2004). A practical vector for efficient knockdown of gene expression in rice (Oryza sativa L.). *Plant Mol. Biol. Rep.* 22, 409–417. doi: 10.1007/BF02772683

Wei, Y., Shen, W., Dauk, M., Wang, F., Selvaraj, G., and Zou, J. (2004). Targeted gene disruption of glycerol-3-phosphate dehydrogenase in Colletotrichum gloeosporioides reveals evidence that glycerol is a significant transferred nutrient from host plant to fungal pathogen. *J. Biol. Chem.* 1, 429–435. doi: 10.1074/jbc.M308363200

Yang, H., Li, Y., and Hua, J. (2006). The C2 domain protein BAP1 negatively regulates defense responses in Arabidopsis. *Plant J.* 48, 238–248. doi: 10.1111/j.1365-313X.2006.02869.x

Yang, H., Yang, S., Li, Y., and Hua, J. (2007). The Arabidopsis BAP1 and BAP2 genes are general inhibitors of programmed cell death. *Plant Physiol.* 145, 135–146. doi: 10.1104/pp.107.100800

Yang, Y., Jing, Z., Peng, L., Xing, H., Li, C., Wei, G., et al. (2013). Glycerol-3-phosphate metabolism in wheat contributes to systemic acquired

resistance against puccinia striiformis f. sp. tritici. *PLoS ONE.* 8, e81756. doi: 10.1371/journal.pone.0081756

Ye, X., Gao, Q. M., Yu, K., Lapchyk, L., and Kachroo, P. (2009). An intact cuticle in distal tissues is essential for the induction of systemic acquired resistance in plants. *Cell Host and Microbe.* 5, 151–165. doi: 10.1016/j.chom.2009.01.001

Yun, B. W., Atkinson, H. A., Gaborit, C., Greenland, A., Read, N. D., Pallas, J. A., et al. (2003). Loss of actin cytoskeletal function and EDS1 activity, in combination, severely compromises non-host resistance in Arabidopsis against wheat powdery mildew. *Plant J.* 34, 768–777. doi: 10.1046/j.1365-313X.2003.01773.x

Zhang, Q., Li, X., Long, X., Hu, B., Xiao, X., Zhang, X., et al. (2020). Metabolism of the cutin and wax of plants and their disease resistance mechanisms (in Chinese). *J. Zhejiang AandF Univ.* 37, 1207–1215. doi: 10.11833/j.issn.2095-0756.20190745

Zhang, Y., Smith, P., Maximova, S. N., and Guiltinan, M. J. (2015). Application of glycerol as a foliar spray activates the defence response and enhances disease resistance of Theobroma cacao. *Mol. Plant Pathol.* 16, 27–37. doi: 10.1111/mpp.12158

Zhou, X., Jenks, M. A., Liu, J., Liu, A., Zhang, X., Xiang, J., et al. (2013). Overexpression of transcription factor OsWR2 regulates wax and cutin biosynthesis in rice and enhances its tolerance to water deficit. *Plant Molec. Biol. Repor.* 32, 719–731. doi: 10.1007/s11105-013-0687-8

Zinsou, V., Wydra, K., Ahohuendo, B., and Schreiber, L. (2006). Leaf waxes of cassava (manihot esculenta crantz) in relation to ecozone and resistance to xanthomonas blight. *Euphytica.* 149, 189–198. doi: 10.1007/s10681-005-9066-3

Conflict of Interest: The authors declare that the research was conducted in the absence of any commercial or financial relationships that could be construed as a potential conflict of interest.

Publisher's Note: All claims expressed in this article are solely those of the authors and do not necessarily represent those of their affiliated organizations, or those of the publisher, the editors and the reviewers. Any product that may be evaluated in this article, or claim that may be made by its manufacturer, is not guaranteed or endorsed by the publisher.

frontiers in Plant Science

ORIGINAL RESEARCH
published: 07 February 2022
doi: 10.3389/fpls.2021.798581

Comparison of the Chloroplast Genome Sequences of 13 Oil-Tea Camellia Samples and Identification of an Undetermined Oil-Tea Camellia Species From Hainan Province

Jing Chen[1,2], *Yujian Guo*[1,2], *Xinwen Hu*[1,2]* *and Kaibing Zhou*[1,2]*

[1] *Engineering Research Center for Breeding of New Varieties of Tropical Crops, Ministry of Education, Haikou, China,*
[2] *College of Horticulture, Hainan University, Haikou, China*

OPEN ACCESS

Edited by:
Jacqueline Batley,
University of Western Australia, Australia

Reviewed by:
Jun Rong,
Nanchang University, China
Yuanwen Teng,
Zhejiang University, China

***Correspondence:**
Xinwen Hu
1263714995@qq.com
Kaibing Zhou
zkb@hainanu.edu.cn

Specialty section:
This article was submitted to Crop and Product Physiology, a section of the journal Frontiers in Plant Science

Received: *20 October 2021*
Accepted: *17 December 2021*
Published: *07 February 2022*

Citation:
Chen J, Guo Y, Hu X and Zhou K (2022) Comparison of the Chloroplast Genome Sequences of 13 Oil-Tea Camellia Samples and Identification of an Undetermined Oil-Tea Camellia Species From Hainan Province. Front. Plant Sci. 12:798581. doi: 10.3389/fpls.2021.798581

The comparison of chloroplast genome (cpDNA) sequences among different plant species is an important source of plant molecular phylogenetic data. In this paper, the cpDNA sequences of 13 different oil-tea camellia samples were compared to identify an undetermined oil-tea camellia species from Hainan Province. The cpDNA of the samples was sequenced and resequenced, and divergence hotspots and simple sequence repeat (SSR) variations were analyzed. Bayesian inference (BI) and maximum-likelihood (ML) phylogenetic trees were constructed based on the full cpDNA sequences. The cpDNA sequences were 156512∼157089 bp in length and had the circular tetrad structure typical of angiosperms. The inverted repeats (IRs) of different species included varying contractions and expansions. The cpDNA sequences of the samples of the undetermined species of oil-tea camellia from Hainan Province and *Camellia gauchowensis* from Xuwen County were identical. In total, 136 genes were annotated, including 91 protein-coding genes (PCGs), 37 tRNA genes and 8 rRNA genes. The GC content of the cpDNA was 37.3%. The small single-copy (SSC)/IR boundary was rich in variation. Divergence hotspots were mainly located in the intergenic space (IGS) and coding sequences (CDSs), and there were obvious differences in divergence hotspots among species. The same divergence hotspots were found in *Camellia vietnamensis*, *Camellia gauchowensis* and the undetermined species of oil-tea camellia from Hainan Province. A total of 191∼198 SSR loci were detected. Most of the SSRs included A or T, and the distribution of SSRs in the cpDNA was uneven. Different species shared common SSRs and exhibited unique SSRs. Based on the full cpDNA sequences, the evolutionary relationships of different species of *Camellia* were well identified. The thirteen samples were classified into 2 clades and 6 subclades, and the different sections of *Camellia* clustered on the same branch in 2 clades and 2 subclades. *Camellia vietnamensis* was more closely related to the undetermined species of oil-tea camellia from Hainan Province and the sample of *Camellia gauchowensis* from Xuwen County than to the sample of *Camellia gauchowensis* from Luchuan County. *Camellia*

osmantha was closely related to *Camellia gauchowensis* and *Camellia vietnamensis*. In conclusion, the cpDNA of different oil-tea camellia species has a conserved tetrad structure with certain length polymorphisms. SSRs are expected to be developed as "barcodes" or "identity cards" for species identification. SSR variations and other factors result in abundant divergence hotspots in the CDSs and IGS (one non-CDS region), indicating that full cpDNA sequences can be used for the species identification and phylogenetic analysis of *Camellia*. Accordingly, the undetermined species of oil-tea camellia from Hainan Province is likely *Camellia vietnamensis*, *Camellia vietnamensis* and *Camellia gauchowensis* may be the same species, and additional genetic evidence is needed to determine whether *Camellia osmantha* is a new independent species. The previous division of related sections of *Camellia* may need readjustment based on full cpDNA sequences.

Keywords: oil-tea camellia, cpDNA, divergence hotspots, SSRs, phylogenetic tree

INTRODUCTION

Oil-tea camellia trees, as one of the four largest woody oil plants in the world, are endemic in China and have a long history of cultivation. The group consists of nearly 20 species of *Camellia*, such as *Camellia oleifera*, *Camellia meiocarpa,* and *Camellia vietnamensis*, and approximately 30 common subspecific taxa. Camellia oil is rich in tea polyphenols, tea saponins and other health components and free of cholesterol, erucic acid and other harmful components. The oil has extremely high nutritional and health-beneficial value and thus has strong market competitiveness and wide market prospects (Zhu et al., 2010). Oil-tea camellia trees, with the characteristics of strong resistance, wide adaptability and good tolerance of typhoons (Chen et al., 2012), are suitable for afforestation in low-yielding or desolated woodlands and can be expected to provide immense ecological benefits.

Oil-tea camellia trees have been planted in Hainan Province for approximately 2000 years. Four 600-year-old trees were discovered as the most ancient individuals, and the area of oil-tea camellia afforestation reached approximately 6,000 hectares in the 1950s to 1960s. As people in Hainan Province have always had a special preference for camellia oil, regarding it as "magic oil," camellia oil has always been in short supply; thus, the selection and breeding of afforestation varieties is urgently needed to promote the rapid development of the Hainan oil-tea camellia industry (Dai and Zhong, 2017). Since 2007, *C. oleifera* cultivars from outside Hainan Island have been introduced to Wuzhishan city in Hainan Province for afforestation, as local oil-tea camellia tree seedlings planted for afforestation show weak growth, low survival rates and poor economic performance. New cultivars bred from native germplasm resources have been increasingly realized as crucial to the development of the oil-tea camellia industry in Hainan Province. Furthermore, the lack of afforestation cultivars of local species of oil-tea camellia trees is the primary bottleneck in the development of the oil-tea camellia industry in Hainan Province (Chen et al., 2017).

The oil-tea camellia trees in Hainan Province have been identified as *Camellia oleifera* (Yuan et al., 2014; Ye et al., 2015), and the features of native oil-tea camellia trees, such as large fruits with thick pericarps and the unique oil scent, are different from those of *C. oleifera* grown outside Hainan Island, which is attributed to the influence of the tropical environment (Zheng D. J. et al. , 2016; Zheng W. W. et al., 2016). However, *C. oleifera* cultivars introduced from outside Hainan Island presented poor growth, harvest properties and survival rates (Chen et al., 2017). Overall, the above results indicate that native oil-tea camellia trees from Hainan Province might not belong to *C. oleifera*.

Traditional plant identification methods based on morphological characteristics have difficulties eliminating interference factors such as environmental factors and tree ages, and DNA barcoding does not differentiate closely related species because of resolution limitations (Hebert et al., 2003; Zhang et al., 2015). The chloroplast genome (cpDNA), which has uniparental maternal inheritance, is small, and its variations provide much more information than that obtained from a single DNA barcode without recombination. cpDNA can be used to identify different species and even different populations of the same species; therefore, it is called a "super barcode" (Li et al., 2015). The coding sequences (CDSs) and non-coding sequences (non-CDSs) of cpDNA differ greatly in evolutionary rates and have low sequencing costs and small splicing errors. cpDNA has the advantages of convenience, accuracy and low cost for exploring the systematic evolution, classification and identification of plant species (Semerikova and Semerikov, 2014). Therefore, in the past 30 years, researchers have increasingly preferred to use cpDNA comparisons for the identification, classification and evolutionary relationship determination of plant species (Leigh et al., 2013). *Camellia* plants easily hybridize and cross-pollinate and may also have intraspecific polyploids, making identification at the species level difficult (Liu et al., 2012). Therefore, identification studies need to be carried out from multiple perspectives, among which cpDNA comparative analysis is important for studying species identification and evolutionary relationships. At the time of writing this paper, the NCBI genome database[1] contained 7556 complete cpDNA sequences, 45 of

[1]https://www.ncbi.nlm.nih.gov/genome/organelle/

which were from *Camellia* (10 cpDNA sequences assembled by this research group have not yet been published), providing a foundation for discussing the evolutionary relationships and species identification of *Camellia* and other plants.

In brief, to breed appropriate afforestation cultivars and guide the introduction and collection of suitable germplasm resources, it is necessary to compare the cpDNA sequences of different oil-tea camellia samples and identify the undetermined oil-tea camellia species from Hainan Province. Furthermore, the results of cpDNA analyses also have important significance in brand creation and cultural value development of camellia oil.

MATERIALS AND METHODS

Plant Materials

Information on the leaf sampling of forestland and the location, species, age and number of each plant sampled is shown in **Table 1**. From October 15 to November 5, 2017, 30 leaves were collected from each plant, immediately frozen in liquid nitrogen in the field, and brought back to the laboratory for storage in an ultralow-temperature (−80°C) freezer.

Chloroplast Genome Extraction, Sequencing and Genome Library Construction

Whole-genome DNA was extracted from 10 g samples of fresh leaves using an E.Z.N.A.® XXX DNA Kit. An Illumina TruSeq™ Nano DNA Sample Prep Kit was used to construct a PE library, and an 8-cycle enriched library was amplified by PCR. The target band was recovered in 2% Certified Low Range Ultra Agarose. PicoGreen nucleic acid dye was quantitatively detected with a TBS380 microfluorometer and mixed in proportion to the obtained data. A TruSeq PE Cluster Kit V3-BOT-HS was used to amplify and generate DNA clusters by bridging PCR with the cBot System. Finally, the DNA clusters were sequenced on the Illumina HiSeq 4000-PE150 sequencing platform to produce the original sequences (raw read length of 150 bp). The original sequences were subjected to quality control, whereby adapter sequences and bases containing non-AGCT at the 5′ end were removed, reads with sequencing quality values less than Q20 were trimmed, reads with N proportions more than or equal to 10% were removed, and joint sequences and small segments with lengths less than 75 bp were discarded after pruning. As a result, high-quality read sequences (clean reads) were obtained. The NT library was randomly selected to detect whether the sequencing results were contaminated.

Chloroplast Genome Splicing, Annotation, and Submission of *Camellia oleifera*

SOAPdenovo (version: 2.04) short-sequence assembly software was used to assemble the clean data from *Camellia oleifera*. The optimal assembly results were obtained after the parameters were adjusted several times. Then, the following two methods were used to screen cpDNA contigs: a homologous sequence searching method based on the cpDNA sequences of related species and a screening method based on cpDNA characteristics such as larger copy numbers, lower GC contents and unique kmer frequencies. Then, the reads were mapped to the assembled contigs, and local assembly and the optimization of the assembly results were performed according to paired ends and read overlaps. GapCloser (version 1.12) software was used to repair inner gaps in the assembly results, and redundant sequences were removed to obtain the final assembly results. Homologous alignment prediction and *de novo* prediction were combined to predict the genome of *Camellia oleifera*. Homologous alignment prediction was performed using the protein-coding genes (PCGs) of reference genomes. The PCGs were rapidly aligned to the sample genome sequence, poor alignment results were filtered to remove redundancy, and then GeneWise was used to produce exact alignment. AUGUSTUS software was used to predict *de novo* genes in plant mitochondrial/chloroplast genomes. Finally, EVidenceModeler V1.1.1 software was used to integrate the gene set and obtain the *Camellia oleifera* coding genes. DOGMA, RNAmmer-1.2 and TRNAscan-SE V1.3.1 were used to predict ncRNA in the genome. After the amino acid sequences of *Camellia oleifera* were predicted based on the identified genes, they were compared with the known protein database, and the *Camellia oleifera* genes were annotated with corresponding functional information. The optimal comparison result of each gene was retained as the annotation result. The amino acid sequences of the samples were compared with the non-redundant protein (NR), Swiss-Prot, eggNOG, Kyoto Encyclopedia of Genes and Genomes (KEGG) and Gene Ontology (GO) databases to obtain the functional annotation information of the PCGs of *Camellia oleifera*. After sequence annotation, the genome sequence was edited by Sequin and submitted to GenBank under accession number MN078090.

Chloroplast Genome Splicing, Annotation and Submission of the Other 12 Oil-Tea Camellia Trees

First, SPAdes software was used to preliminarily splice the clean data. Based on the above cpDNA data from *Camellia oleifera* and PCG sequences, blastn and Exonerate comparisons were performed (the criteria were an e-value of 1e-10 and a protein similarity threshold of 70%). The scaffold that matched each gene was selected, and splicing coverage was determined to remove fragments that were obviously not part of the target genome. PRICE and MITObim were used to carry out extended merging and splicing of the collected fragmented target sequence, and this process was iterated 50 times. With the results of iteration splicing, Bowtie2 was used to examine the original sequencing reads, paired reads were selected, and SPAdes was used for resplicing. The path was examined, and an obvious ring graph was selected. Otherwise, the iterative stitching and comparison steps were repeated until the ring graph was assembled successfully. The comparison of the obtained cpDNA of all oil-tea camellia species with the PCGs of *Camellia oleifera* described above was performed by blastn, and

TABLE 1 | Basic information about the different oil-tea species.

Forestland	Sample tree site	Species		Tree age/a	Sample symbol
		Common name	Latin name		
Wangsha village, Changpo town Gaozhou city, Guangdong Province	N22°0′40.87″ E111°6′25.49″	Gaozhou population of Gaozhou oil-tea camellia	*Camellia gauchowensis* Chang	> 40	HD01
Guanshan village, Shahu town, Luchuan County, Guangxi Zhuang Autonomous Region	N22°21′48.27″ E110°12′20.55″	Luchuan population of Gaozhou oil-tea camellia	*Camellia gauchowensis* Chang	> 40	HD02
Youbang village, Nalin town, Bobai city, Guangxi Zhuang Autonomous Region	N22°14′7.45″ E109°43′53.85″	Bobai large-fruit oil-tea camellia	*Camellia gigantocarpa* Hu et T. C. Huang	> 40	HD03
Guangxi Research Institute of Forestry	N22°55′13.45″ E108°21′3.85″	Wantian red-flower oil-tea camellia	*Camellia polyodonta* How.ex Hu	13	HD04
Guangxi Research Institute of Forestry	N22°55′13.45″ E108°21′3.85″	Small-fruit oil-tea camellia	*Camellia meiocarpa* Hu*	> 40	HD05
Guangxi Research Institute of Forestry	N22°55′13.45″ E108°21′3.85″	Guangning red-flower oil-tea camellia	*Camellia semiserrata* Chi.	16	HD06
Guangxi Research Institute of Forestry	N22°55′13.45″ E108°21′3.85″	Common oil-tea camellia	*Camellia oleifela* Abel.	> 40	HD07
Guangxi Research Institute of Forestry	N22°55′13.45″ E108°21′3.85″	Xianghua oil-tea camellia	*Camellia osmantha* Ye CX, Ma JL et Ye H*	13	HD08
Guangxi Research Institute of Forestry	N22°55′13.45″ E108°21′3.85″	Vietnam oil-tea camellia	*Camellia vietnamensis* T. C. Huang ex Hu		HD09
Zhongjiu village, Huishan town, Qionghai city, Hainan Province	N19°5′18.30″ E110°18′18.29″	Hainan oil-tea camellia	Undetermined species	> 600	HD10
Xingwen village, Wangwu town, Danzhou city, Hainan Province	N19°40′22.66″ E109°20′48.84″	Hainan oil-tea camellia	Undetermined species	> 195	HD11
Zaha village, Changhao region, Wuzhishan city, Hainan Province	N18°40′31″ E109°27′56″	Hainan oil-tea camellia	Undetermined species	> 40	HD12
Andong village, Longtang town, Xuwen County, Guangdong province	N20°18′32.66″ E110°20′44.86″	Xuwen population of Gaozhou oil-tea camellia	*Camellia gauchowensis* Chang	> 40	HD13

** Latin names do not exist in The Flora of China and were obtained from other references (Chen, 2008; Wang et al., 2014; State Forestry Administration state-owned forest farm and tree seed and seedling work station, 2016; Liang et al., 2017).*

comparisons between PCGs and nucleic acids were performed to confirm the existence and boundaries of genes. If the predicted amino acid sequence was too long or too short, the starting codon was adjusted, other variable codons were used, or the gene was checked for introns. Exonerate software was used to compare the amino acid sequences of *Camellia oleifera* genes to determine intron boundaries and lengths. Chloroplast tRNA annotations were submitted to tRNAscan-SE online for annotation. For rRNA annotation, the sequences were submitted to the RNAmmer 1.2 server for prediction and supplemented by homologous sequence alignment to correct the boundary ranges. The tRNA annotation and ribonuclease rnpB were submitted to ARAGORN and Bcheck, respectively, for annotation. After sequence annotation of the HD01∼HD06 and HD08∼HD13 samples, the sequences were edited by Sequin and submitted to GenBank under accession numbers MN078084∼MN078089 and MN078091∼MN078093 (the sequences of the HD10∼HD13 samples were the same), respectively.

Characterization of Chloroplast Genome

Bitmap Graph Creation

The physical map of cpDNA was drafted by submitting the edited GenBank annotation file to OGDRAW. According to the assembled results of the 13 samples, non-CDSs were extracted by scripts, and the distribution regions [large single-copy (LSC), small single-copy (SSC), and inverted repeat (IR)] and sizes were determined.

Expansion and Contraction Analysis of Inverted Repeat Boundaries

First, a script was used to identify IR region A (IRA) and IR region B (IRB) sequences to determine the boundary positions of IRs. Then, according to the genome annotation results, the genes that crossed or were closest to the IR boundaries were located. Finally, the distances from the gene boundaries to the IR boundaries were extracted, and the results were plotted using AI.

Analysis of the Divergence Hotspots of Genomic Systems

Based on the literature (Yang et al., 2013), mVISTA software was used to analyze the evolutionary divergence hotspots of the genomic system, with the cpDNA of *Panax ginseng* C. A. Mey used as a reference. MAFFT software was used for multisequence alignment, and then a script was used to obtain the input file required by mVISTA. mVISTA was used to obtain the original output results. After overlapping gene names were adjusted and intron annotations were added, a divergence hotspot diagram was obtained.

Simple Sequence Repeat Analysis

According to the method reported in the literature (Zheng W. W. et al., 2016), the SSR sequences were analyzed with MISA software, with the parameters set as follows: 1-8, 2-4, 3-4, 4-3, 5-3 and 6-3.

Construction of a Chloroplast Genome Phylogenetic Tree

The complete cpDNAs of all *Camellia* plants were downloaded from the NCBI database, and 64 sequences were obtained. *Hartia laotica* (LAOstipa camellia) (NC_041509.1) was chosen as an outgroup species. The above 65 sequences were combined with 10 sample sequences (the HD10∼HD13 sequences were identical, and HD10 was used to represent these 4 samples) for phylogenetic analysis. The LSC, SSC and IR regions of 75 sequences were extracted, and LSC + IR + SSC data was used for analysis. The data was examined using MAFFT software (default parameters), sequence pruning was performed using Gblocks (parameters: -t, D, -b5, h), and a phylogenetic tree was constructed using MrBayes and IQ-TREE software.

Bayesian Inference

The outgroup was again set as *Hartia laotica* (NC_041509.1). The model parameters were LSET NST = 6 and rates = invgamma, which denoted a nucleic acid molecule replacement model of GTR. The rate variation across sites followed an inverse gamma model. The prior probability model parameters were set to the default values. The parameters of Markov chain Monte Carlo (MCMC) sampling were *N*runs = 2, *N*chain = 4, *N*gen = 1000000, Samplefreq = 500 and Temp = 0.05, indicating that two groups of analyses were run simultaneously. One cold chain and three hot chains were set in each group to run 1000000 generations, and the Markov chain was sampled once every 500 generations. When the original tree results were obtained from MrBayes software, branches unrelated to the sample were cut off to obtain the final phylogenetic tree.

Maximum Likelihood

For model checking, the optimal model was selected via the IQ-TREE model finder. The optimal model of the full sequence was K3Pu + F + R2.

To build the Maximum likelihood (ML) tree, the outgroup was set as *Hartia laotica* (NC_041509.1), and the parameters were set as -BB 1000 and -ALRT 1000. When the original tree results were obtained, branches unrelated to the sample were cut off to obtain the final phylogenetic tree.

RESULTS AND ANALYSIS

Sequencing and Assembly of Chloroplast Genome

In the cpDNA sequencing of HD07 (*Camellia oleifera*), the raw data totaled 3235 MB, and the clean data totaled 2875 MB after quality control processing. The GC content of the clean data was 40.67%, the Q20-value was 97.95%, and the Q30 value was 94.02%. The cpDNA map is shown in **Figure 1**. The GC content of the genome was 37.29%, there were no unknown bases in the assembly sequence, and the sequencing coverage rate reached 100%. These results indicated that the quality of the cpDNA sequencing and assembly results was very high. cDNA resequencing of the other 12 samples was performed, and the cpDNA map of *Camellia oleifera* was used as a reference. The statistical results of the sequencing data are shown in **Table 2**. The numbers of reads ranged from 161988448 to 28787468, the base numbers ranged from 2361193019 to 4242730440, the Q20 value was above 98.24%, the Q30 value was above 95.19%, the sequencing coverage rate reached 100%, and the average sequencing depth ranged from 76.019 to 458.4672 times, all indicating that the sequencing results were relatively reliable. The clean reads of these samples were mapped to create **Figure 1**, and then the cpDNA map of each sample was assembled.

Organization of Camellia Chloroplast Genome

The cpDNA structures and sequence variations of 13 different oil-tea camellia samples were compared. The cpDNA of oil-tea camellia samples was highly conserved, and no inversion or translocation variations were observed. The full-length cpDNA sequences of all samples were 156512∼157089 bp, with a circular tetrad structure containing LSC, SSC, IRA, and IRB regions (**Figure 1**).

The structural information of each part of the cpDNA tetrad of the 13 samples is shown in **Table 3**. The total lengths of the cpDNA sequences ranged from 156512 bp in HD05 (*C. meiocarpa*) to 157089 bp in HD02 (*C. gauchowensis* from Luchuan County). The IR lengths ranged from 25943 bp in HD05 (*C. meiocarpa*) to 26165 bp in HD02 (*C. gauchowensis* from Luchuan County). The LSC lengths ranged from 86224 bp in HD05 (*C. meiocarpa*) to 86657 bp in HD04 (*C. polyodonta*) and HD09 (*C. vietnamensis*), and the SSC lengths ranged from 18132 bp in HD02 (*C. gauchowensis* from Luchuan County) to 18902 bp in HD05 (*C. meiocarpa*). The variation in SSC length was the main factor affecting the cpDNA length, while the length variations in the two IRs were less important. The GC content of the cpDNA of the 13 samples was 37.29% and very stable. These results indicated that the cpDNA of the different known species had significant polymorphisms in total length and tetrad region length. The cpDNA sequences of HD10∼HD12 (the undetermined species of oil-tea camellia from Hainan Province) and HD13 (*C. gauchowensis* from Xuwen County) were identical, indicating that HD10∼HD12 (the undetermined species of oil-tea camellia from Hainan Province) and HD13 (*C. gauchowensis* from Xuwen County) were closely related. The cpDNA of HD10, which represented the undetermined species (HD10-HD12), HD13 (*C. gauchowensis* from Xuwen County) and the other 9 samples was analyzed as reported below.

As shown in **Figure 1** and **Table 4**, the cpDNA of all samples contained 136 genes, including 84 genes in the LSC region, 12 genes in the SSC region, and 20 genes each in the IRA and IRB regions. The gene sequences, gene contents, and length ratios of CDSs and non-CDSs of genes were consistent, reflecting good collinearity of the gene distribution. Thus, a circle diagram was

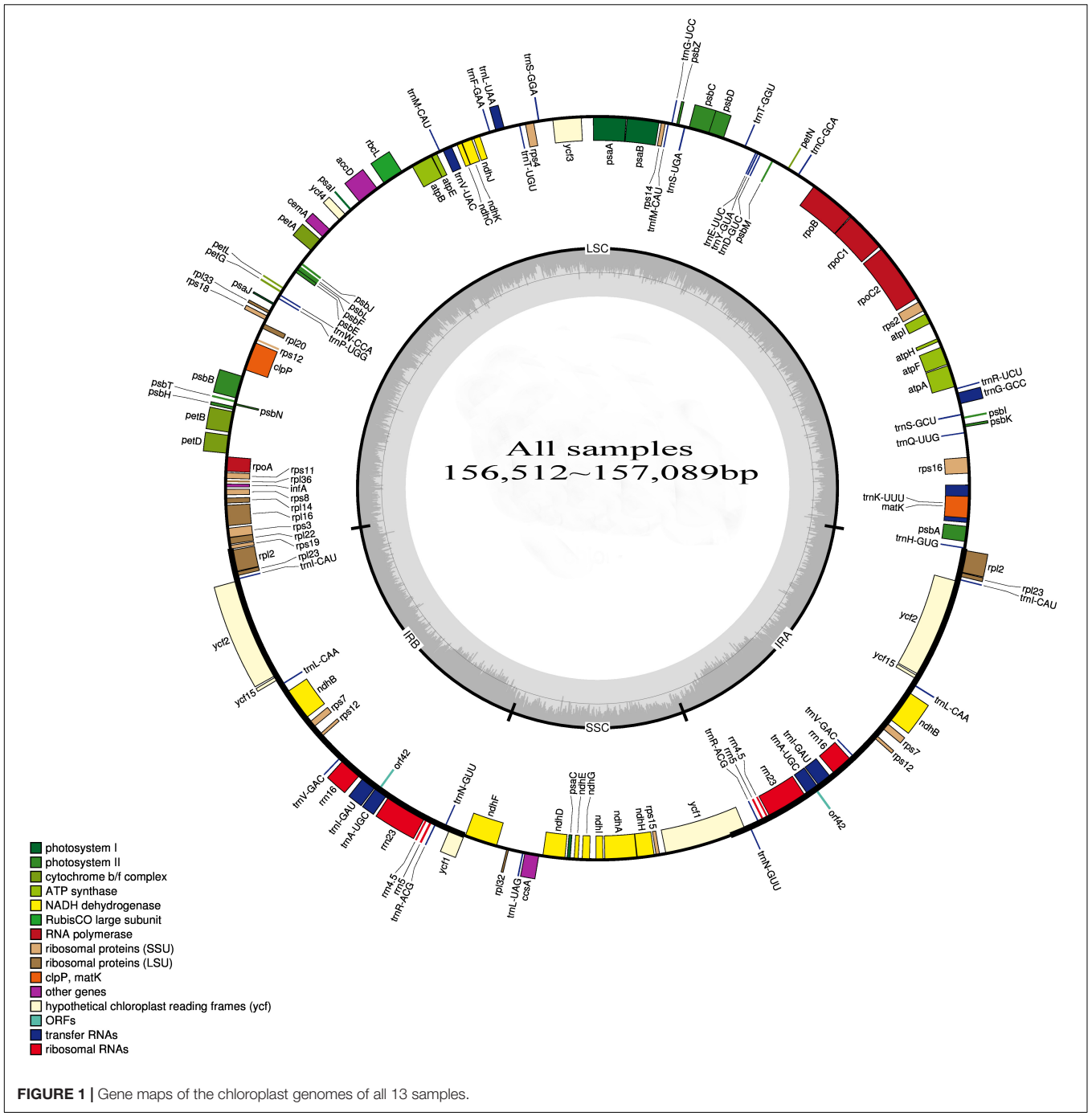

FIGURE 1 | Gene maps of the chloroplast genomes of all 13 samples.

used to annotate the cpDNA of the 13 samples (**Figure 1**). According to the statistics of translation products, 90 PCGs, 8 rRNA genes and 37 tRNA genes were detected.

The list of genes classified according to function is shown in **Table 4**. All genes were divided into 4 categories and 19 groups, including genes for photosynthesis (7 groups), self-replication genes (5 groups), other genes (5 groups) and unknown-protein function genes (2 groups). Further analysis of **Figure 1** and **Tables 3**, **4** shows that all genes in the cpDNA tetrad were not evenly distributed in each region. PCGs were distributed in all regions of the tetrad, including 60 genes in the LSC region, 18 genes in the IR regions and 12 genes in the SSC region. All 8 rRNA genes were distributed in the IR regions. Twenty-two tRNA genes were located in the LSC region, 14 were distributed in the IR regions, and 1 was located in the SSC region. There were 19 genes with 2 copies, all of which were in the IRA and IRB regions, including 4 PCGs (*ndhB*, *rps7*, *rpl2*, and *rpl23*), all 4 rRNA genes (*rrn4.5*, *rrn5*, *rrn16*, and *rrn23*), 7 tRNA genes (*trnA-UGC*, *trnI-CAU*, *trnI-GAU*, *trnL-CAA*, *trnN-GUU*, *trnR-ACG* and *trnV-GAC*) and 4 genes of unknown function (*ycf1*, *ycf2*, *ycf15*,

TABLE 2 | Statistical analysis of the clean data from 12 samples.

Samples	Reads	Bases	Q20 (%)	Q30 (%)	Coverage rate (%)	Average depth
HD01	20004566	2939694796	98.43	95.24	100	250.4872
HD02	24591370	3625835612	98.52	95.57	100	298.8911
HD03	28787468	4242730440	98.47	95.39	100	458.4672
HD04	20434016	3013499362	98.49	95.35	100	293.3693
HD05	22032226	3236303925	98.43	95.27	100	160.4196
HD06	16198848	2361193019	98.24	95.84	100	122.353
HD08	21757040	3199535730	98.43	95.28	100	132.5983
HD09	17784594	2614477674	98.42	95.24	100	158.2691
HD10	19311150	2841574064	98.46	95.35	100	85.9634
HD11	22204902	3271245689	98.49	95.40	100	187.113
HD12	20475900	3010885178	98.40	95.19	100	76.019
HD13	19796336	2916824139	98.48	95.52	100	148.721

and *orf42*). The *rps12* gene had 3 copies, one of which was located in the LSC region, while the others were located in the IRA and IRB regions, and this gene was the only trans-splicing gene. There were 5 genes with one intron, including the genes *atpF*, *ndhA*, *ndhB*, *rpl2* and *rpoC1*, and 2 genes with 2 introns, including the genes *ycf3* and *clpP*.

Inverted Repeat Contraction and Expansion

Inverted repeat expansion and contraction analysis of the cpDNA of the 13 samples was performed to investigate the gene variation in the boundaries of IRs, LSCs and SSCs, as shown in **Figure 2**. The cpDNA of the 13 samples was highly conserved at the boundaries on both sides of the LSC region, the *rpl2* gene was 106 bp from the boundary of the IRA region, and the *trnH-GUG* gene was 2 bp from the boundary of the LSC region. The *rps19* gene straddled the boundary of the LSC and IRB regions, and it contained 46 bp of the IRB. The *ycf1* gene crossed the boundary between the SSC and IRA regions, and it extended 963 bp∼1209 bp into the SSC region. That is, in the 8 samples, including HD01 (*C. gauchowensis* from Gaozhou city), HD06 (*C. semiserrrata*), HD08 (*C. osmantha*), HD09 (*C. vietnamensis*), HD10 (the undetermined species of oil-tea camellia from Hainan Province) and HD13 (*C. gauchowensis* from Xuwen County), the gene was located at 1069 bp. In HD02 (*C. gauchowensis* from Luchuan County), the gene was located at 1209 bp. In HD03 (*C. gigantocarpa*), the gene was is located at 967 bp, and in HD04 (*C. polyodonta*), HD05 (*C. meiocarpa*) and HD07 (*C. oleifera*), it was located at 963 bp. The genes *ycf1* and *ndhF* were located on both sides of the SSC and IRB boundary of HD04 (*C. polyodonta*), HD05 (*C. meiocarpa*) and HD07 (*C. oleifera*) and at 140 bp and 34 bp, respectively, on both sides of the SSC and IRB boundary in the population of HD02 (*C. gauchowensis* from Luchuan County). The genes were located at 106 bp and 57 bp on both sides of the SSC and IRB boundary in the 7 samples of HD06 (*C. semiserrrata*), HD08 (*C. osmantha*), HD09 (*C. vietnamensis*), HD10-HD12 (the undetermined species of oil-tea camellia from Hainan Province) and HD13 (*C. gauchowensis* from Xuwen County), respectively. The *ycf1* gene extended into the IRB region by 2 bp and 26 bp at the SSC and IRB boundary in the samples of HD01 (*C. gauchowensis* from Gaozhou city) and HD03 (*C. gigantocarpa*), respectively. The *ndhF* gene was located on the SSC side of the boundary between the SSC and IRB regions in the populations of HD01 (*C. gauchowensis* from Gaozhou city) and HD03 (*C. gigantocarpa*). In conclusion, the IRs of different oil-tea camellia species contracted and expanded differently, resulting in variations in the relative lengths of tetrads and the full length of cpDNA.

Synteny Analysis and Divergence Hotspots

The results of the phylogenetic divergence hotspot analysis of cpDNA from the 13 samples are shown in **Figure 3**. The depressed gaps in the figure are the divergence hotspots. Based on the pairwise genomic synteny of the cpDNA, the distribution characteristics of the divergence hotspots are shown in **Table 5**. There were 42 divergence hotspots in the intergenic space (IGS), accounting for 60% of the total. There were 23 divergence hotspots in exons (CDSs), accounting for 32.86% of the total. Only 5 divergence hotspots were located in introns, accounting for 7.14% of the total. There were 44 divergence hotspots in the LSC region, accounting for 62.86% of the total. Only 6

TABLE 3 | Comparison of chloroplast genome organization among 13 samples.

Samples	Size (bp)	LSC (bp)	SSC (bp)	IR (bp)	Total genes	Protein-coding genes	tRNA genes	rRNA genes	GC content (%)
HD01	157003	86656	18297	26025	135	90(18)	37(14)	8(8)	37.29
HD02	157089	86627	18132	26165	135	90(18)	37(14)	8(8)	37.29
HD03	156953	86631	18402	25960	135	90(18)	37(14)	8(8)	37.29
HD04	156983	86657	18414	25956	135	90(18)	37(14)	8(8)	37.29
HD05	156512	86224	18902	25943	135	90(18)	37(14)	8(8)	37.29
HD06	157018	86652	18282	26042	135	90(18)	37(14)	8(8)	37.29
HD07	156939	86644	18407	25944	135	90(18)	37(14)	8(8)	37.29
HD08	156981	86647	18284	26025	135	90(18)	37(14)	8(8)	37.29
HD09	157004	86657	18284	26025	135	90(18)	37(14)	8(8)	37.29
HD10	156999	86652	18297	26025	135	90(18)	37(14)	8(8)	37.29
HD11	156999	86652	18297	26025	135	90(18)	37(14)	8(8)	37.29
HD12	156999	86652	18297	26025	135	90(18)	37(14)	8(8)	37.29
HD13	156999	86652	18297	26025	135	90(18)	37(14)	8(8)	37.29

TABLE 4 | List of genes found in 13 chloroplast genome samples.

Category of genes	Group of genes	Gene names
Genes for photosynthesis	ATP synthase	*atp*A, *atp*B, *atp*E, *atp*F*, *atp*H, *atp*I
	Cytochrome b/f complex	*pet*A, *pet*B, *pet*D, *pet*G, *pet*L, *pet*N
	NADH dehydrogenase	*ndh*A*, *ndh*B*[1], *ndh*C, *ndh*D, *ndh*E, *ndh*F, *ndh*G, *ndh*H, *ndh*I, *ndh*J, *ndh*K
	Photosystem I	*psa*A, *psa*B, *psa*C, *psa*I, *psa*J
	Photosystem II	*psb*A, *psb*B, *psb*C, *psb*D, *psb*E, *psb*F, *psb*H, *psb*I, *psb*J, *psb*K, *psb*L, *psb*M, *psb*N, *psb*T, *psb*Z
	Rubisco CO large subunit	*rbc*L
	ATP-dependent protease subunit p gene	*clp*P**
Self-replication	Ribosomal proteins (SSU)	*rps*2, *rps*3, *rps*4, *rps*7[1], *rps*8, *rps*11, *rps*12[#]·*rps*12[#1], *rps*14, *rps*15, *rps*16, *rps*18, *rps*19
	Ribosomal proteins (LSU)	*rpl*2*[1], *rpl*14, *rpl*16, *rpl*20, *rpl*22, *rpl*23[1], *rpl*32, *rpl*33, *rpl*36
	Ribosomal RNAs	*rrn*4.5[1], *rrn*5[1], *rrn*16[1], *rrn*23[1]
	Transfer RNAs	*trnA*[1]*-UGC*, *trnC-GCA*, *trnD-GUC*, *trnE-UUC*, *trnF-GAA*, *trnfM-CAU*, *trnG-GCC*, *trnG-UCC*, *trnH-GUG*, *trnI*[1]*-CAU*, *trnI*[1]*-GAU*, *trnK-UUU*, *trnL*[1]*-CAA*, *trnL-UAA*, *trnL-UAG*, *trnM-CAU*, *trnN*[1]*-GUU*, *trnP-UGG*, *trnQ-UUG*, *trnR*[1]*-ACG*, *trnR-UCU*, *trnS-GCU*, *trnS-GGA*, *trnS-UGA*, *trnT-GGU*, *trnT-UGU*, *trnV*[1]*-GAC*, *trnV-UAC*, *trnW-CCA*, *trnY-GUA*
	RNA polymerase	*rpo*A, *rpo*B, *rpo*C1*, *rpo*C2
Other genes	Subunit of acetyl-CoA-carboxylase	*acc*D
	c-type cytochrome synthesis ccsA gene	*ccs*A
	Translation initiation factor IF-1	*inf*A
	Maturase	*mat*K
	Envelop membrane protein	*cem*A
Proteins of unknown function	Hypothetical chloroplast reading frames	*ycf*1[1], *ycf*2[1], *ycf*3**, *ycf*4, ycf15[1]
	ORFs	*Orf*42[1]

*The symbols * and ** represent one intron and two introns in protein-coding genes, respectively. The symbol # indicates trans-splicing genes. The number 1 indicates two copies of genes in the IR region.*

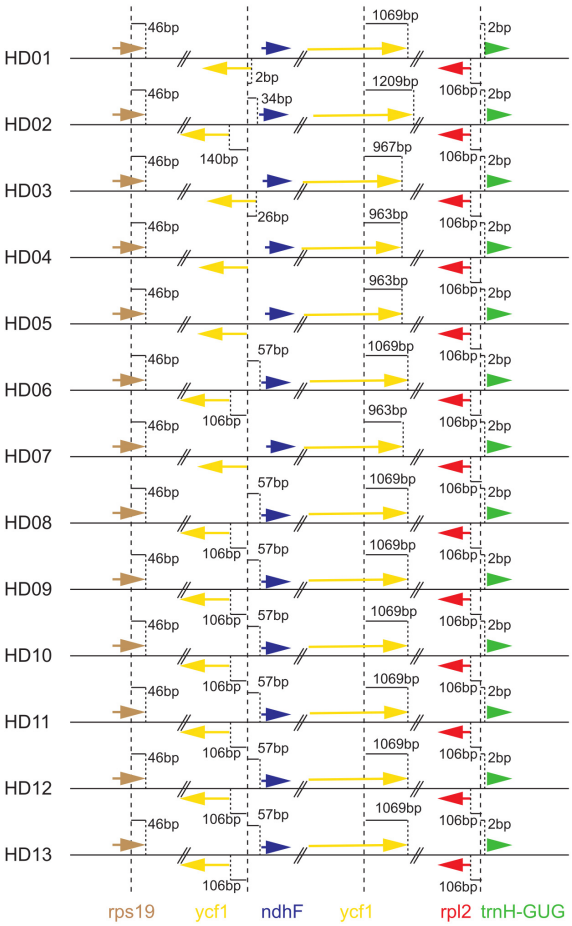

FIGURE 2 | Comparison of the border positions of large single-copy (LSC), inverted repeat (IR) and small single-copy (SSC) among the thirteen chloroplast genome samples.

divergence hotspots were located in the SSC region, accounting for 8.57% of the total. The frequency of divergence hotspots in the IRs was intermediate but asymmetrical between the IRA and IRB regions, accounting for 12.86% and 15.71% of the total, respectively. The LSC and IGS regions were the main regions containing variations in the latent sequence. Among the 23 PCGs, the exons of *trnH-GUC*, *atpA*, *ndhK*, *trnfM-CAU*, *petD*, *ndhB*, *ycf1,* and *ndhF* were very important divergence hotspots. Among the 42 IGSs, *rps19*∼*trnH-GUC*, ycf2∼*TrnL-CAA*, *rps12*∼*TrnV-GAC*, *rrn5*∼*trnR-ACG*, *TrnR-ACG*∼*trnN-GUU*, *rpl32*∼*ndhF*, *trnG-UCC*∼*trnS-GCU, trnQ-UUG*∼*rps16* and *rps16*∼trnKUUU were especially rich in divergence hotspots. The introns of the *rps16* and *trnK-UUU* genes also contained important divergence hotspots. The IGS and a few exons were the main divergence hotspots, and the introns contained few divergence hotspots. As shown in **Figure 3**, the divergence hotspots of HD01 (*C. gauchowensis* from Gaozhou city), HD02 (*C. gauchowensis* from Luchuan County), HD09 (*C. vietnamensis*), HD10-HD12 (the undetermined species of oil-tea camellia from Hainan Province), and HD13 (*C. gauchowensis* from Xuwen County) were identical, indicating that the undetermined species of oil-tea camellia from Hainan Province was closely related to *C. gauchowensis* and *C. vietnamensis*.

Simple Sequence Repeats of Chloroplast Genome

The characteristics of SSR polymorphisms and distributions in different samples are shown in **Table 6**. The total numbers of SSRs in different samples ranged from 191 to 198, and the numbers

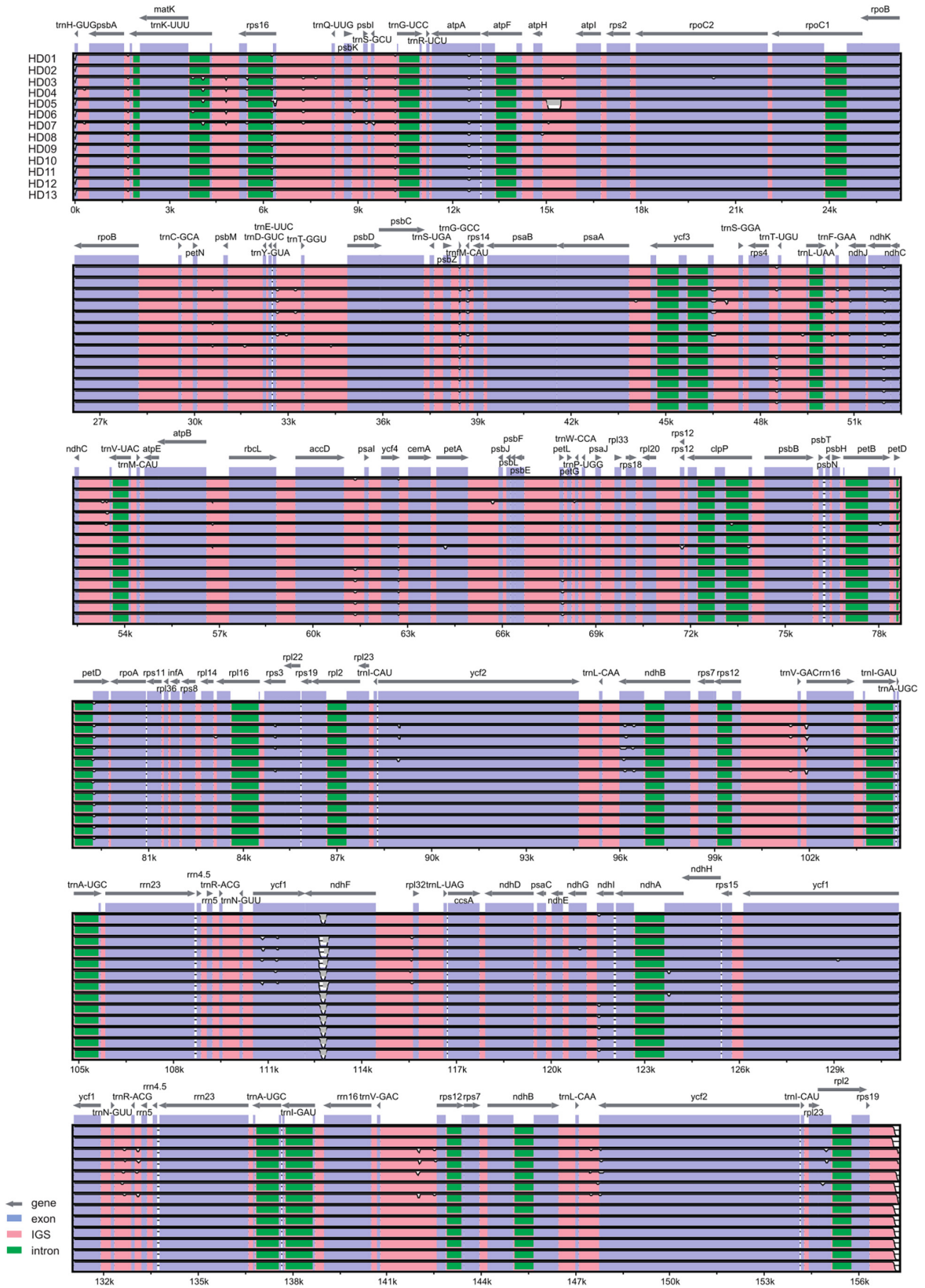

FIGURE 3 | Analysis of hotspots of evolutionary branches of the genomic system.

TABLE 5 | Characteristics of the divergence hotspot distribution.

	LSC	SSC	IRA	IRB	Total	Rate (%)
IGS	30	2	1	9	42	60.00
Intron	5	0	0	0	5	7.14
Exon	9	4	8	2	23	32.86
Total	44	6	9	11	70	100.00
Rate (%)	62.86	8.57	12.86	15.71	100	

of monobase to hexabase SSRs were 138 to 147, 38 to 41, 1, 12 to 13, 0 to 1, and 0 to 2, respectively; thus, polymorphisms were found in the number of SSRs and the sequence of repeat units. Tribase SSRs were located in the IGS of the LSC region. Tetrabase SSRs were mainly distributed in the IGS of the LSC region, and the numbers of SSRs differed by 1 at most, while the numbers of SSRs in the SSC, IRA and IRB regions were stable at 3, 2 and 2, respectively. There were only 2 dibase SSRs in the SSC regions of different samples, and a number of polymorphisms were found in the IGS and exons of other regions, which were mainly distributed in the IGS and exons of the LSC region, accounting for more than half of the total. There were a number of monobase SSR polymorphisms in all regions of the tetrad. The number of monobase SSRs was the highest in the LSC and IGS regions, and the number of single-base SSRs was the highest in exons. None of the samples except HD04 (*C. polyodonta*) contained pentabase SSRs. Hexabase SSRs were found in the IGS of the IRs of HD03 (*C. gigantocarpa*), HD04 (*C. polyodonta*) and HD07 (*C. oleifera*), and one was found in the IGS of the LSC region of HD08 (*C. osmantha*). The distributions of SSRs in the IGS, exons and introns of the tetrad of cpDNA were uneven, and the numbers of mono- and dibase SSR polymorphisms varied among species or samples. Tetrabase SSRs were represented by the most types of repeated-unit sequences, at up to 12 types, although this group of SSRs was not the largest. Among the 12 kinds of tetrabase SSRs, 11 were present in the same number in different samples. The loci of the LSC regions of HD04 (*C. polyodonta*) and HD08 (*C. osmantha*) were identified by a pentabase SSR and a hexabase SSR, which might be useful as identification markers for the respective species.

The SSRs of different samples were classified according to sequence differences in repeat units and could be divided into SSRs with the same repeat unit in all samples (**Table 7**) and SSRs with specific repeat units in different samples (**Table 8**). As shown in the two tables, the majority of SSR repeat units were mainly composed of A and T, and SSRs containing C or G were rarely observed, indicating that the SSRs of different samples had an obvious bias in the base types of repeat units. Comprehensive analysis of the two tables shows that few SSRs of specific repeat units were found in different oil-tea camellia species, and most of those identified were the same. As shown in **Table 8**, the only tribase SSR was TTC, and tetrabase SSRs included AAAT, AATA, AGAT, ATAG, CCCT, GAGG, GACT, TCTA, TCTT and TTTC. These tribase and tetrabase SSRs in different samples not only contained the same repeat units but were also present in the same number. The numbers of monobases A, C, and T and dibases AT, CT, GA, and TC were inconsistent among samples, indicating polymorphisms of the same mono- and dibase SSRs.

As shown in **Tables 6**, **8**, HD04 (*C. polyodonta*) uniquely contained one pentabase SSR, AATAG, in the IGS of the SSC region, and HD08 (*C. osmantha*) uniquely contained one TAAGAT hexabase SSR in the IGS of the LSC region. One AAAAAG SSR and one CTTTTT SSR were found in the IRs of HD03 (*C. gigantocarpa*), HD04 (*C. polyodonta*) and HD07 (*C. oleifera*), but the other samples did not contain these hexabase SSRs. HD04 (*C. polyodonta*), HD05 (*C. meiocarpa*) and HD07 (*C. oleifera*) all contained the tetrabase SSR AAAG in the IGS of the LSC region, but the other samples did not. The SSRs of HD09 (*C. vietnamensis*), HD01 (*C. gauchowensis* from Gaozhou city), HD02 (*C. gauchowensis* from Luchuan County), HD13 (*C. gauchowensis* from Xuwen County) and HD10∼HD12 (the undetermined species of oil-tea camellia from Hainan Province) contained the same repeat units and differed from those of other oil-tea camellia species. Therefore, these SSR combinations may be used for species identification, and HD04 (*C. polyodonta*) and HD08 (*C. osmantha*) also have unique SSR markers. The undetermined species of oil-tea camellia from Hainan Province may be closely related to *C. vietnamensis* and *C. gauchowensis*.

In addition, according to the sequencing results, the SSRs of different samples also contained 27-30 interval SSRs, in which the TTC tribase SSR was distributed. All types, intermediate sequence lengths, compositions of base pairs and lengths of SSRs in the samples showed polymorphism. The maximum interval SSR was 484 bp in length, containing three copies each of T(9) and T(8) and one copy each of T(12) and A(12). HD04 (*C. polyodonta*) had a specific SSR complex, namely, A(10)(AAAG)3*, wherein (AAAG)3* was AAAGAAAGA. Therefore, the intermediate sequence and the SSR complex can be used to infer genetic diversity, and A(10)(AAAG)3* may be a unique marker of HD04 (*C. polyodonta*).

Phylogenetic Inference

Hartia laotica was taken as the outgroup, and Bayesian inference (BI) and ML phylogenetic analyses of the whole cp-DNA of HD01-HD10 and 7 other *Camellia* species were performed. The results are shown in **Figures 4**, **5**.

The samples belonged to the same two clades. HD03 (*C. gigantocarpa*), HD04 (*C. polyodonta*), HD05 (*C. meiocarpa*) and HD07 (*C. oleifera*) belonged to one major clade. Four samples belonging to four different subclades, namely, HD07 (*C. oleifera*), were identified as *C. oleifera*. HD03 (*C. gigantocarpa*) was associated with *C. crapaelliana*, HD04 (*C. polyodonta*) was associated with *C. chekiangoleosa* and *C. japonica*, and HD05 (*C. meiocarpa*) and *C. sasanque* belonged to different subclades. The rest of the samples belonged to another major clade, and HD06 (*C. semiserrrata*) and *C. aztea* were clustered into one subclade. The samples of HD01 (*C. gauchowensis* from Gaozhou city), HD02 (*C. gauchowensis* from Luchuan County), HD09 (*C. vietnamensis*), HD10 (the undetermined species of oil-tea camellia from Hainan Province), HD08 (*C. osmantha*) and *C. granthamiana* belonged to another subclade. HD01 (*C. gauchowensis* from Gaozhou city), HD02 (*C. gauchowensis* from Luchuan County), HD10 (the undetermined species of oil-tea camellia from Hainan Province), HD09 (*C. vietnamensis*) and HD08 (*C. osmantha*) were clustered on the same branch of

TABLE 6 | Simple sequence repeats (SSRs) in chloroplast genome (cpDNA).

Sample	Category	Number	Intergenic spacer	Coding sequence	Intron	LSC	SSC	IRA	IRB
HD01	Mono-nucleotide	144	81	37	26	97	31	8	8
	Dinucleotide	38	14	15	9	22	2	7	7
	Trinucleotide	1	1	0	0	1	0	0	0
	Tetranucleotide	12	6	4	2	5	3	2	2
	Pentanucleotide	0	0	0	0	0	0	0	0
	Hexanucleotide	0	0	0	0	0	0	0	0
	Subtotal	195	102	56	37	125	36	17	17
HD02	Mononucleotide	147	85	36	26	99	30	9	9
	Dinucleotide	38	14	15	9	22	2	7	7
	Trinucleotide	1	1	0	0	1	0	0	0
	Tetranucleotide	11	5	4	2	4	3	2	2
	Pentanucleotide	0	0	0	0	0	0	0	0
	Hexanucleotide	0	0	0	0	0	0	0	0
	Subtotal	197	105	55	37	126	35	18	18
HD03	Mononucleotide	143	83	34	26	96	31	8	8
	Dinucleotide	40	13	17	10	22	2	8	8
	Trinucleotide	1	1	0	0	1	0	0	0
	Tetranucleotide	12	6	4	2	5	3	2	2
	Pentanucleotide	0	0	0	0	0	0	0	0
	Hexanucleotide	2	2	0	0	0	0	1	1
	Subtotal	198	105	55	38	124	36	19	19
HD04	Mononucleotide	140	80	34	26	94	30	8	8
	Dinucleotide	41	14	17	10	23	2	8	8
	Trinucleotide	1	1	0	0	1	0	0	0
	Tetranucleotide	13	7	4	2	6	3	2	2
	Pentanucleotide	1	1	0	0	0	1	0	0
	Hexanucleotide	2	2	0	0	0	0	1	1
	Subtotal	198	105	55	38	124	36	19	19
HD05	Mononucleotide	138	78	34	26	92	30	8	8
	Dinucleotide	39	14	16	9	23	2	7	7
	Trinucleotide	1	1	0	0	1	0	0	0
	Tetranucleotide	13	7	4	2	6	3	2	2
	Pentanucleotide	0	0	0	0	0	0	0	0
	Hexanucleotide	0	0	0	0	0	0	0	0
	Subtotal	191	100	54	37	122	35	17	17
HD06	Mononucleotide	142	81	35	26	95	31	8	8
	Dinucleotide	41	14	17	10	23	2	8	8
	Trinucleotide	1	1	0	0	1	0	0	0
	Tetranucleotide	12	6	4	2	5	3	2	2
	Pentanucleotide	0	0	0	0	0	0	0	0
	Hexanucleotide	0	0	0	0	0	0	0	0
	Subtotal	196	102	56	38	124	36	18	18
HD07	Mononucleotide	141	81	34	26	95	30	8	8
	Dinucleotide	40	15	16	9	24	2	7	7
	Trinucleotide	1	1	0	0	1	0	0	0
	Tetranucleotide	13	7	4	2	6	3	2	2
	Pentanucleotide	0	0	0	0	0	0	0	0
	Hexanucleotide	2	2	0	0	0	0	1	1
	Subtotal	197	106	54	37	126	35	18	18
HD08	Mononucleotide	146	83	36	27	98	32	8	8
	Dinucleotide	38	14	15	9	22	2	7	7
	Trinucleotide	1	1	0	0	1	0	0	0
	Tetranucleotide	12	6	4	2	5	3	2	2
	Pentanucleotide	0	0	0	0	0	0	0	0
	Hexanucleotide	1	1	0	0	1	0	0	0
	Subtotal	197	104	55	38	126	37	17	17
HD09	Mononucleotide	145	83	36	26	98	31	8	8
	Dinucleotide	38	14	15	9	22	2	7	7
	Trinucleotide	1	1	0	0	1	0	0	0
	Tetranucleotide	12	6	4	2	5	3	2	2
	Pentanucleotide	0	0	0	0	0	0	0	0
	Hexanucleotide	0	0	0	0	0	0	0	0
	Subtotal	196	104	55	37	126	36	17	17

(Continued)

TABLE 6 | (Continued)

Sample	Category	Number	Intergenic spacer	Coding sequence	Intron	LSC	SSC	IRA	IRB
HD10	Mononucleotide	145	83	36	26	98	31	8	8
	Dinucleotide	38	14	15	9	22	2	7	7
	Trinucleotide	1	1	0	0	1	0	0	0
	Tetranucleotide	12	6	4	2	5	3	2	2
	Pentanucleotide	0	0	0	0	0	0	0	0
	Hexanucleotide	0	0	0	0	0	0	0	0
	Subtotal	196	104	55	37	126	36	17	17
Total		2549	1349	715	485	1627	466	228	228

this subclade. In other words, two samples (HD11∼HD12) of oil-tea camellia from Hainan Province and HD13 (*C. gauchowensis* from Xuwen County) were also located on this branch. Therefore, the 13 samples were clustered into 6 subclades, namely, the first major clade of 4 subclades, including the *C. oleifera* subclade, *C. chekiangoleosa* and *C. japonica* subclade, *C. sasanque* subclade, and *C. crapaelliana* subclade. The second major clade of the two subclades included the *C. aztea* subclade and the *C. granthamiana* subclade.

TABLE 7 | Common Simple sequence repeats (SSRs) in the chloroplast genome (cpDNA) of different samples.

SSRs	HD01	HD02	HD03	HD04	HD05	HD06	HD07	HD08	HD09	HD10
A	61	61	63	62	61	61	62	61	61	61
AAAT	2	2	2	2	2	2	2	2	2	2
AATA	1	1	1	1	1	1	1	1	1	1
AG	3	3	3	3	3	3	3	3	3	3
AGAT	1	1	1	1	1	1	1	1	1	1
AT	15	15	15	15	15	15	16	15	15	15
ATAG	1	1	1	1	1	1	1	1	1	1
C	2	3	3	2	2	3	3	3	3	3
CCCT	1	1	1	1	1	1	1	1	1	1
CT	2	2	3	3	3	3	3	2	2	2
G	2	2	2	2	2	2	2	2	2	2
GA	4	4	5	5	4	5	4	4	4	4
GAAA	1	1	1	1	1	1	1	1	1	1
GAGG	1	1	1	1	1	1	1	1	1	1
GTCT	1	1	1	1	1	1	1	1	1	1
T	90	92	87	86	84	88	86	91	90	90
TA	10	10	10	10	10	10	10	10	10	10
TC	4	4	5	5	4	5	4	4	4	4
TCTA	1	1	1	1	1	1	1	1	1	1
TCTT	1	1	1	1	1	1	1	1	1	1
TTC	1	1	1	1	1	1	1	1	1	1
TTTC	1	1	1	1	1	1	1	1	1	1

TABLE 8 | Unique Simple sequence repeats (SSRs) in the chloroplast genome (cpDNA) of different samples.

SSR	HD01	HD02	HD03	HD04	HD05	HD06	HD07	HD08	HD09	HD10
AAAAAG	0	0	1	1	0	0	1	0	0	0
AAAG	0	0	0	1	1	0	1	0	0	0
AATAG	0	0	0	1	0	0	0	0	0	0
CTTTTT	0	0	1	1	0	0	1	0	0	0
TAAGAT	0	0	0	0	0	0	0	1	0	0

Genes drawn outside of the circle are transcribed counterclockwise, while genes shown inside of the circle are transcribed clockwise. Genes belonging to different functional groups are color-coded. Darker gray in the inner circle indicates GC content, while lighter gray corresponds to AT content.

Although the topological maps constructed by the two methods were different in terms of the end nodes of the subclades, such as *C. chekiangoleosa* and *C. japonica*, *C. sasanque* and *C. granthamiana*, and the genetic distances among the different samples within each subclade were inconsistent, the results of clustering analysis of the 13 samples, including the major clades and subclades, were not affected.

In conclusion, HD01 (*C. gauchowensis* from Gaozhou city), HD02 (*C. gauchowensis* from Luchuan County), HD09 (*C. vietnamensis*), HD10-HD12 (the undetermined species of oil-tea camellia from Hainan Province) and HD13 (*C. gauchowensis* from Xuwen County) may be different ecotypes of *C. vietnamensis* or *C. gauchowensis*. HD08 (*C. osmantha*) was closely related to *C. vietnamensis* and *C. gauchowensis*. Therefore, the phylogenetic relationships of different species and populations of *Camellia* could be well identified based on whole cpDNA sequences.

The branch nodes of HD09 (*C. vietnamensis*) and HD01 (*C. gaochowensis* from Gaozhou city) were the outermost nodes, and the branch node of HD10 (the undetermined species of oil-tea camellia from Hainan Province) was one level inward. The phylogenetic relationship between HD10-HD12 (the undetermined species of oil-tea camellia from Hainan Province) and HD01 (*C. gaochowensis* from Gaozhou city) or HD09 (*C. vietnamensis*) was closer than that between HD02 (*C. gauchowensis* from Luchuan County) and HD01 (*C. gaochowensis* from Gaozhou city) or HD09 (*C. vietnamensis*). These results indicate that the three samples of undetermined species of oil-tea camellia from Hainan Province and *C. gaochowensis* from Xuwen County were closely related to *C. gaochowensis* from Gaozhou city and *C. vietnamensis*. The results also illustrate that the undetermined species of oil-tea camellia from Hainan Province may be *C. vietnamensis*, and *C. gaochowensis*u may be merged with *C. vietnamensis*.

DISCUSSION

Chloroplast Genome Variation and Evolution

The total length of plant cpDNA is generally between 107 and 218 kb and consists of LSC and SSC regions and two IRs in a tetrad structure (Henry et al., 2016). Changes in the total length are mainly caused by the boundary contraction and expansion of IRs (Wang et al., 2008). The cpDNA of the 13 samples also showed a tetrad structure, and the maximum differences in total,

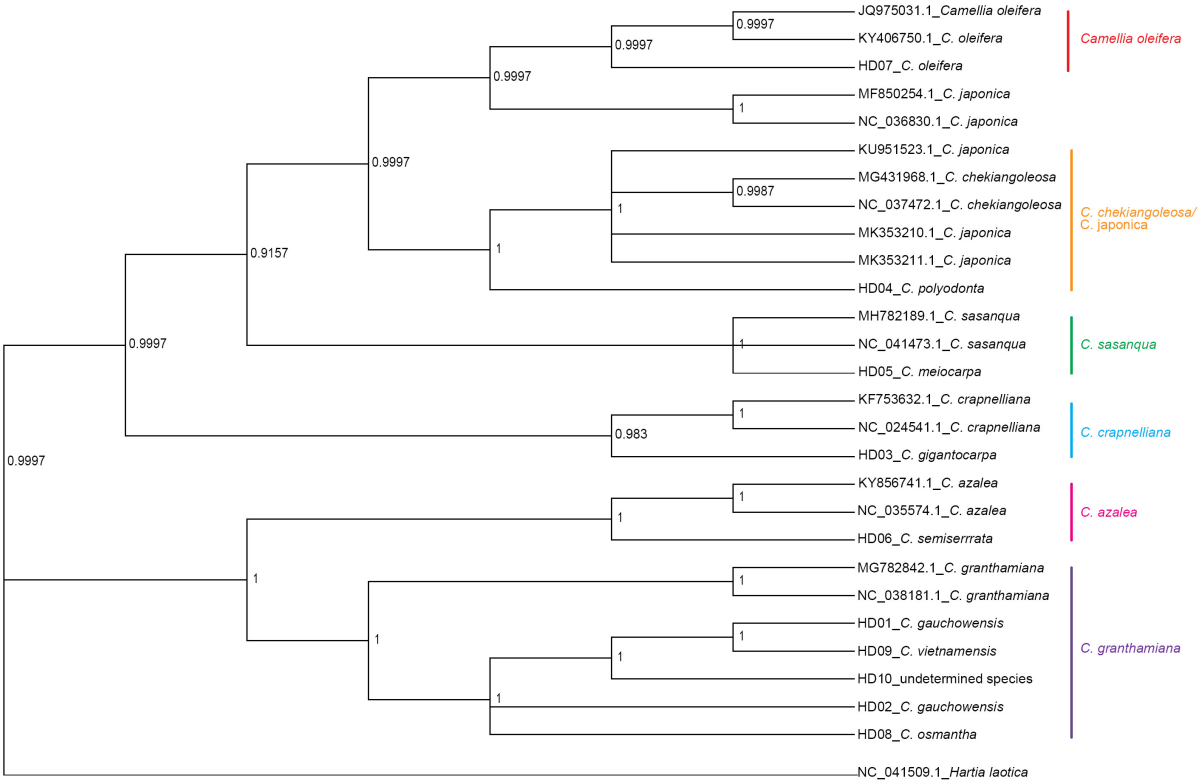

FIGURE 4 | Phylogenetic tree of 13 samples based on chloroplast genome (cpDNA) constructed using the Bayes inference method (BI).

IR, LSC and SSC lengths were 577 kb, 222 kb, 433 kb, and 770 kb, respectively. The results also showed that the IRs of different samples exhibited different boundary contractions and expansion phenomena on the SSC sides, which resulted in great differences in the SSC and IR sequences among different samples. Therefore, the results in this paper are basically consistent with previous reports of plants of *Camellia* with cpDNA lengths below 600 kb, and the different cpDNA samples had a consistent type, quantity, and order (Wang et al., 2008), showing that the *Camellia* cpDNA structure is highly conserved and confirming the conservatism of the plant cpDNA structure. The results in this paper also confirmed that the boundary contraction and expansion of IRs are the main reasons for differences in the size of cpDNA and indicated that IRs play an important role in stabilizing the structure of cpDNA (Chen et al., 2014). The results in this paper showed a large number of different SSR variants in the cpDNA of different samples, which also led to changes in cpDNA size. Therefore, SSR variants in *Camellia* may be another important reason for small variations in cpDNA size.

Application Prospect of Simple Sequence Repeats in Chloroplast Genome

Simple Sequence Repeats have the advantages of high polymorphism, codominance, and a wide distribution, and SSRs of cpDNA share these advantages as well as the characteristics of conserved sequences, a simple structure, and uniparental inheritance (Palmer and Thompson, 1982). Therefore, SSRs have been widely applied in studies on species evolution (Kaundun and Matsumoto, 2011) and genetic diversity analyses (Flannery et al., 2006; Allender et al., 2007). They are often developed as "barcodes" or "identity cards" for plant species identification. The results in this paper show that the SRs of oil-tea camellia are SSRs with a preference for A/T, and they have polymorphisms in composition, number and length, which is consistent with previous sequencing results in tea plants (Wang et al., 2008). The results also show that *C. ploydonta* contains a unique SSR (AATAG) in the IGS of the SSC region, and *C. gigantocapa*, *C. polyodonta* and *C. oleifera* each contain 3 SSRs (AAAAAG and CTTTTT, respectively) in the IGS of IRs. The existence of pentabase SSRs was not previously reported in cpDNA sequences of *Camellia* plants (Wang et al., 2008), making this the first discovery of such SSRs in *Camellia* plants. These specific SSRs may have important application significance in the species identification of *C. gigantocapa*, *C. polyodonta,* and *C. oleifera*. In this paper, 13 samples of 7 oil-tea camellia species were examined. The abundant cpSSR variation could be divided into two categories: SSRs shared among all samples and SSRs with inconsistencies in different samples. Pairs of species always showed differences in SSRs. The former category may reflect the specificity of kinship above the genus level, while the latter may reflect differences in species within *Camellia*. In short, if various codes are established for SSRs with differences in grading

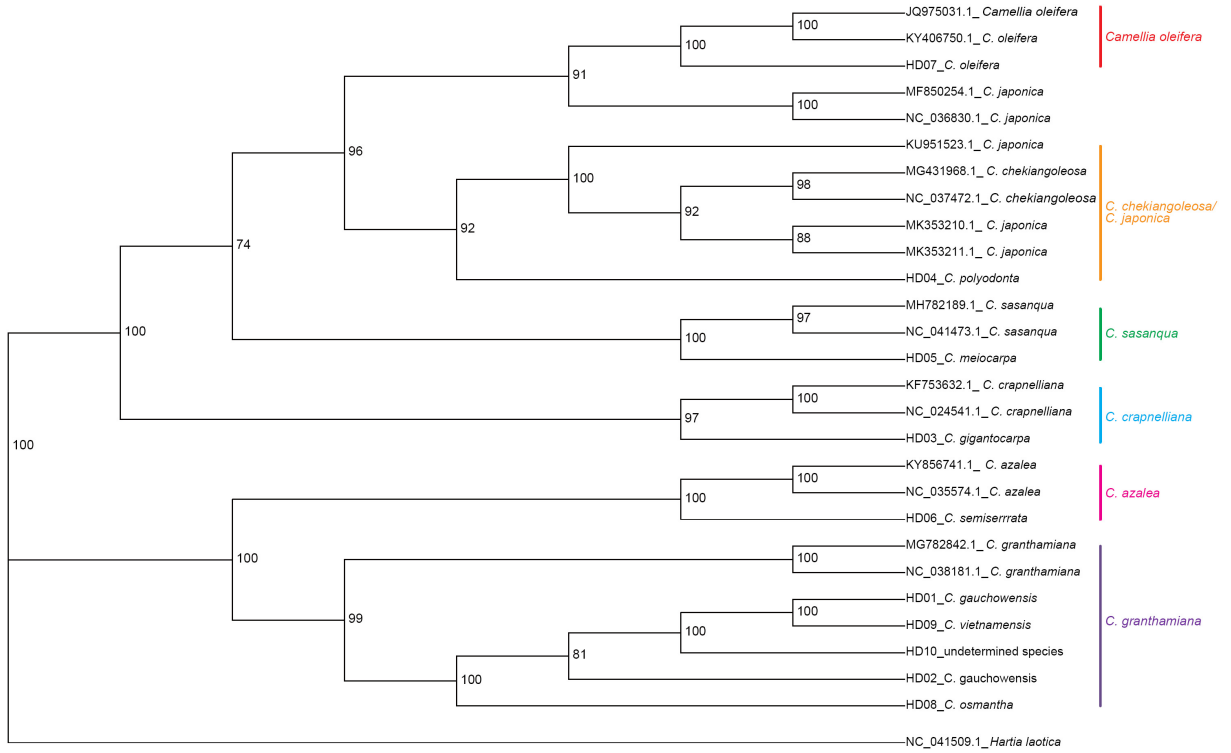

FIGURE 5 | Phylogenetic tree of 13 samples based on chloroplast genome (cpDNA) constructed using the maximum likelihood method (ML).

units, each oil-tea camellia species will differ from others in its code combination. The similarity of different codes also directly indicates the kinship and phylogenetic relatedness among species. Consistent with previous predictions for oil-tea camellia (Leigh et al., 2013), with the accumulation of cpSSR sequence information from different oil-tea camellia species, it is entirely possible to successfully establish "barcodes" or "identity cards" for individual oil-tea camellia species.

Genetic Relationships Between Different Species of *Camellia* and Identification of the Undetermined Species of Oil-Tea Camellia From Hainan Province

The phylogenetic trees of 7 ornamental species of *Camellia* were constructed by ML and BI methods based on cpDNA, LSC, SSC, CDS, intron, IGS and IR sequences. The topological structures of different sequence data were highly similar. The analysis method had no effects on the topological maps; specifically, the same topological maps were obtained based on the cpDNA, IGS, SSC and IR sequences (Leigh et al., 2013). With the development of high-throughput sequencing technology, it is becoming increasingly common to construct phylogenetic trees based on full cpDNA sequences (Nie et al., 2012; Chen et al., 2014; Huang et al., 2014; Song et al., 2017; Yang et al., 2019). The results in this paper showed that divergence hotspots and SSR variants were distributed mostly in the IGS (one kind of non-CDS), somewhat distributed in CDSs, and less common in introns (another kind of non-CDS). Therefore, in this paper, based on full chloroplast genome sequences, phylogenetic trees were constructed to explore the evolutionary relationships between different oil-tea camellia species. *C. oleifera*, *C. meiocarpa*, *C. vietnamensis*, *C. gigantocarpa*, *C semiserrrata,* and *C. polyodonta* were located on different branches, and a consensus regarding these species divisions in terms of taxonomy of oil-tea camellia has gradually been reached (Chen, 2008; State Forestry Administration state-owned forest farm and tree seed and seedling work station, 2016). Furthermore, it is feasible to identify different species of *Camellia* plants based on the clustering analysis results in this paper.

HD10∼HD12 (the undetermined species of oil-tea camellia from Hainan Province) and HD13 (*C. gauchowensis* from Xuwen County) were clustered on the same branch as HD09 (*C. vietnamensis*), and their genetic relationship with HD09 (*C. vietnamensis*) was closer than that with HD02 (*C. gauchowensis* from Luchuan County), which indicated that the undetermined species of oil-tea camellia from Hainan Province may be *C. vietnamensis*. Based on these results combined, *C. vietnamensis*, *C. gauchowensis* and the undetermined species of oil-tea camellia from Hainan Province had the same divergence hotspots, while the sample of *C. gauchowensis* from Xuwen County (located at the southernmost tip of Leizhou Peninsula and on the northern Qiongzhou Strait) had the same cpDNA sequence as the undetermined species of oil-tea camellia from Hainan Province, indicating that *C. gaochowensis* and *C. vietnamensis* may be merged into the same species.

Although previous studies have attempted to prove that *C. osmantha* is a new oil-tea camellia species based on agronomic and economic traits, inter SSR (ISSR) molecular markers of nuclear DNA, and other evidence (Wang et al., 2014; Liang et al., 2017), the results in this paper show that HD08 (*C. osmantha*) is closely related to *C. gauchowensis* and *C. vietnamensis*. Therefore, additional genetic evidence needs to be collected to resolve the controversial issue of whether *C. osmantha* is a new species of *Camellia*.

Phylogenetic trees were constructed in this paper, and 3 species of Section Heterogenea Sealy (*C. gigantocarpa*, *C. granthamiana*, and *C. crapnelliana*), 5 species of Section Camellia (*C. semiserrrata*, *C. polyodonta*, *C. japonica*, *C. azalea*, and *C. chekiangoleosa*) and 5 species of Section Oleifera H.T. Chang (*C. oleifera*, *C. meiocarpa*, *C. vietnamensis*, *C. gauchowensis*, *C. sasanqua*, and *C. osmantha*, which is a new species undergoing confirmation but not included in this citation) were used (Zhang and Min, 1999). Based on the topological structures of the phylogenetic trees obtained with different sequence regions and different methods, the species of Section Heterogenea Sealy, Section Camellia and Section Oleifera H.T. Chang belong to two clades. In addition, one subclade contained the species from the different sections of *Camellia* in each of the two clades, and one subclade contained *C. granthamiana* (Section Heterogenea Sealy) as well as *C. vietnamensis* and *C. gauchowensis* (Section Oleifera H.T. Chang). Another subclade included *C. oleifera* (Section Oleifera H.T. Chang) and *C. japonica* (Section Camellia), and the other 4 subclades contained the species from the same section. The results show that the previous classification of *Camellia* plant sections may not be accurate enough. Section division is based on the morphological characteristics of different species, which are affected by environmental conditions, tree ages and other factors, producing a risk of unreasonable division (Luo et al., 1999). In this paper, cpDNA sequence differences were used to distinguish and cluster species, as such differences are not affected by the environment and may be more suitable for classification (Zhang and Min, 1999; Leigh et al., 2013). It is possible that the results in this paper can provide important information on the classification of sections of *Camellia* and how to adjust them.

CONCLUSION

Based on whole-genome high-throughput sequencing, the full cpDNA of seven *Camellia* species was successfully assembled. The tetrad structure was conserved with good collinearity, but certain polymorphisms in length were found due to the contraction and expansion of IRs, SSRs and other variations. The largest numbers of divergence hotspots and SSR variants were observed in the IGS and CDSs, respectively. Different species showed specific SSRs, and these SSRs can be developed as "barcodes" or "ID cards" for species identification. Therefore, full cpDNA sequences can be used for the identification and phylogenetic analysis of *Camellia* plants. The phylogenetic trees based on full cpDNA sequences showed that HD10∼HD12 (the undetermined species of oil-tea camellia from Hainan Province) probably belonged to *Camellia vietnamensis*, while *Camellia vietnamensis* and *Camellia gauchowensis* may be merged into the same species. *Camellia osmantha* is closely related to *Camellia gauchowensis* and *Camellia vietnamensis*, and additional genetic evidence is needed to determine whether it is an independent new species. The current section-level division of *Camellia* plants based on morphology may need to be adjusted based on cpDNA sequence differences.

DATA AVAILABILITY STATEMENT

The datasets presented in this study can be found in online repositories. The names of the repository/repositories and accession number(s) can be found below: https://www.ncbi.nlm.nih.gov/genbank/, MN078084; https://www.ncbi.nlm.nih.gov/genbank/, MN078085; https://www.ncbi.nlm.nih.gov/genbank/, MN078086; https://www.ncbi.nlm.nih.gov/genbank/, MN078087; https://www.ncbi.nlm.nih.gov/genbank/, MN078088; https://www.ncbi.nlm.nih.gov/genbank/, MN078089; https://www.ncbi.nlm.nih.gov/genbank/, MN078090; https://www.ncbi.nlm.nih.gov/genbank/, MN078091; https://www.ncbi.nlm.nih.gov/genbank/, MN078092; https://www.ncbi.nlm.nih.gov/genbank/, MN078093.

AUTHOR CONTRIBUTIONS

JC was the lead author, and she completed the main research work of this manuscript. YG was the second author, and she assisted the lead author in the experiment. KZ was the assistant supervisor of JC, a Ph.D. student, and he is responsible for specific guidance work. XH was the supervisor of JC, a Ph.D. student. All authors contributed to the article and approved the submitted version.

REFERENCES

Allender, C. J., Allainguillaume, J., Lynn, J., and King, G. J. (2007). Simple sequence repeats reveal uneven distribution of genetic diversity in chloroplast genomes of *Brassica oleracea* L. and (n=9) wild relatives. *Theor. Appl. Genet.* 114, 609–618. doi: 10.1007/s00122-006-0461-5

Chen, C. M., Ma, C. L., Ma, J. Q., Liu, S. C., and Chen, L. (2014). Sequencing of Chloroplast Genome of Camellia sinensis and Genetic Relationship for Camellia Plants Based on Chloroplast DNA Sequences. *J. Tea Sci.* 34, 371–380.

Chen, L. Q., Yang, W. B., Li, Y., Wang, Y., Fu, D. Q., Niu, X. Q., et al. (2012). The development course and prospect of camellia oil industry in Hainan Island. *Mod. Agricult. Sci. Technol.* 1:374.

Chen, Y. Z. (2008). *Excellent germplasm resources of oil-tea camellia*. Beijing: China Forestry Press, 159.

Chen, Y. Z., Chen, L. S., Li, R. F., and Ma, L. (2017). Survey and the industry development proposals of Camellia sp. Resources in Haina n. *Trop. Forest.* 45, 49–52.

Dai, J., and Zhong, S. J. (2017). Development Status of Camellia Oil Industry in Hainan and Suggestions. *Trop. Agricult. Eng.* 41, 61–64.

Flannery, M. L., Mitchel, F. J. G., Coyne, S., Kavanagh, T. A., Burke, J. I., Salamin, N., et al. (2006). Plastid genome characterisation in *Brassica* and *Brassicaceae* using a new set of nine SSRs [J]. *Theor. Appl. Genet.* 113, 1221–1231. doi: 10.1007/s00122-006-0377-0

Hebert, P. D. N., Cywinska, A., Ball, S. L., and Dewaard, J. R. (2003). Biological identifications through DNA barcodes[J]. *Proc. R. Soc. B-Biol. Sci.* 270, 313–321. doi: 10.1098/rspb.2002.2218

Henry, D., Lin, C. S., Yu, M., and Chang, W. J. (2016). Chloroplast genomes: diversity, evolution, and applications in genetic engineering. *Genom. Biol.* 17, 134–163. doi: 10.1186/s13059-016-1004-2

Huang, H., Shi, C., Liu, Y., Mao, S. Y., and Gao, L. Z. (2014). Thirteen Camellia chloroplast genome sequences determined by high-throughput sequencing:genome structure and phylogenetic relationships. *BMC Evol. Biol.* 14:151. doi: 10.1186/1471-2148-14-151

Kaundun, S. S., and Matsumoto, S. (2011). Molecular evidence for maternal inheritance of the chloroplast genome in tea,*Camellia sinensis* (L.) O. Kuntze. *J. Sci. Food Agricult.* 91, 2660–2663. doi: 10.1002/jsfa.4508

Leigh, F. J., Mackay, I., Oliveira, H. R., Nicholas, E., Richard, G. A., Huw, H. J., et al. (2013). Using diversity of the chloroplast genome to examine evolutionary history of wheat species. *Genet. Resour. Crop Evol.* 60, 1831–1842. doi: 10.1007/s10722-013-9957-4

Li, X., Yang, Y., Henry, R. J., Rossetto, M., Wang, Y. T., and Chen, S. (2015). Plant DNA barcoding:from genes to genome. *Biol. Rev.* 90, 157–166. doi: 10.1111/brv.12104

Liang, G. X., Liu, K., Ma, J. L., Chen, G. C., Ye, H., and Jiang, Z. P. (2017). Molecular taxonomy and identifi cation of *Camellia osmantha*. *Nonwood Forest Res.* 35, 26–29.

Liu, Y., Yang, S. X., Ji, P. Z., and Gao, L. Z. (2012). Phylogeography of *Camellia taliensis* (Theaceae) inferred from chloroplast and nuclear DNA: insights into evolutionary history and conservation[J]. *BMC Evol. Biol.* 12:92. doi: 10.1186/1471-2148-12-92

Luo, C. Q., Tan, X. F., and Qi, L. L. (1999). A classification summary on plant of Genus Camellia. *J. Cent. South Forest. Coll.* 19, 78–81.

Nie, X. J., Lu, S. Z., Zhang, Y. X., Du, X. H., Wang, L., Biradar, S. S., et al. (2012). Complete chloroplast genome sequence of a major invasive species, Crofton Weed (*Ageratina adenophora*). *PLoS One* 7:e36869. doi: 10.1371/journal.pone.0036869

Palmer, J. D., and Thompson, W. F. (1982). Chloroplast DNA rearrangements are more frequent when a large inverted repeat sequence is lost. *Cell* 29, 537–550. doi: 10.1016/0092-8674(82)90170-2

Semerikova, S. A., and Semerikov, V. L. (2014). Molecular phylogenetic analysis of the genus Abies (*Pinaceae*) based on the nucleotide sequence of chloroplast DNA. *Russ J. Genet.* 50, 7–19. doi: 10.1134/S1022795414010104

Song, J., Long, Y. H., Lin, L. M., Yin, F., and Xing, C. B. (2017). Analysis on structure and phylogeny of chloroplast genomes in Araliaceae species. *Chin. Trad. Herb. Drugs* 48, 5070–5075.

State Forestry Administration state-owned forest farm and tree seed and seedling work station (2016). *Chinese oil tea cultivars*. Beijing: China Forestry Press, 11–15.

Wang, D. X., Ye, H., Ma, J. L., and Zhou, Z. D. (2014). Evaluation and selection of *Camellia osmantha* germplasm resources. *Nonwood Forest Res.* 32, 159–162.

Wang, R. J., Cheng, C. L., Chang, C. C., Wu, C. L., Su, T. M., and Chaw, S. M. (2008). Dynamics and evolution of the inverted repeat-large single copy junctions in the chloroplast genomes of monocots[J]. *BMC Evol. Biol.* 8, 36–51. doi: 10.1186/1471-2148-8-36

Yang, J. B., Yang, S. X., Li, H. T., Yang, J., and Li, D. Z. (2013). Comparative Chloroplast Genomes of *Camellia* Species[J]. *PLoS One* 8, 1–12. doi: 10.1371/journal.pone.0073053

Yang, Z., Wang, G. X., Ma, Q. H., Ma, W. X., Liang, L. S., and Zhao, T. T. (2019). The complete chloroplast genomes of three Betulaceae species: implications for molecular phylogeny and historical biogeography. *PeerJ.* 7, 1–25. doi: 10.7717/peerj.6320

Ye, Z. C., Wu, Y. G., Dai, J., Zhou, K. B., and Hu, X. W. (2015). Distribution of Duckweed Community and the Environmental Factors that Affect the Community Structure. *J. Trop. Biol.* 2015, 310–314.

Yuan, J., Han, Z. Q., He, S. Y., Huang, L. Y., and Zhou, N. F. (2014). Investigation and Cluster Analysis of Main Morphological and Economical Characters for Oiltea Resource in Hainan Province. *J. Plant Genet. Resour.* 15, 1380–1384.

Zhang, J., Chen, M., Dong, X., Lin, R. Z., Fan, J. H., and Chen, Z. D. (2015). Evaluation of fpur commonly used DNA barcoding loci for Chinese medicinal plants of the family Schisandraceae[J]. *PLoS One* 10:e0125574. doi: 10.1371/journal.pone.0125574

Zhang, W. J., and Min, T. L. (1999). A Cytogeological Study of Genus Camellia[J]. *Acta Bot. Yunnan.* 21, 184–196.

Zheng, D. J., Pan, X. Z., Zhang, D. M., Xie, L. S., Zeng, J. H., Zhang, Z. L. et al. (2016). Survey and analysis on Oli-tea camellia resource in Hainan. *J. Northw. Forest. Univ.* 31, 130–135.

Zheng, W. W., Chen, J. H., Hao, Z. D., and Shi, J. S. (2016). Comparative Analysis of the Chloroplast Genomic Information of *Cunninghamia lanceolata* (Lamb.) Hook with Sibling Species from the *Genera Cryptomeria* D. Don, *Taiwania* Hayata, and *Calocedrus* Kurz. *Internat. J. Mole. Sci.* 17, 1–16. doi: 10.3390/ijms17071084

Zhu, B., Zhong, H. Y., Cao, Q. M., and Long, Q. Z. (2010). Advance in research on biaoactive compounds in Camellia spp. *Nonw. For. Res.* 28, 140–145.

Conflict of Interest: The authors declare that the research was conducted in the absence of any commercial or financial relationships that could be construed as a potential conflict of interest.

Publisher's Note: All claims expressed in this article are solely those of the authors and do not necessarily represent those of their affiliated organizations, or those of the publisher, the editors and the reviewers. Any product that may be evaluated in this article, or claim that may be made by its manufacturer, is not guaranteed or endorsed by the publisher.

frontiers in Plant Science

ORIGINAL RESEARCH
published: 10 February 2022
doi: 10.3389/fpls.2022.848723

CRISPR/Cas9-Targeted Mutagenesis of *BnaFAE1* Genes Confers Low-Erucic Acid in *Brassica napus*

Yunhao Liu[1,2†], Zhuolin Du[1,2†], Shengli Lin[1,2], Haoming Li[1,2], Shaoping Lu[1,2], Liang Guo[1,2] and Shan Tang[1,2*]*

[1] National Key Laboratory of Crop Genetic Improvement, Huazhong Agricultural University, Wuhan, China, [2] Hubei Hongshan Laboratory, Wuhan, China

Rapeseed (*Brassica napus*) is an important oilseed crop widely planted in the world, providing substantial edible oil and other nutrients for mankind. The composition of fatty acids affects the edible and processing quality of vegetable oils, among which erucic acid (EA) is potentially to cause health problems. Therefore, low erucic acid (LEA) has always been a breeding trait of *B. napus*. *Fatty acid elongase 1* (*FAE1*) plays a decisive role in the synthesis of EA. There are two functional homologous copies of *FAE1* on the A08 and C03 chromosomes in *B. napus*. In this study, we used CRISPR/Cas9 technology to create targeted mutations on these two homologous copies of *BnaFAE1* in three *B. napus* germplasms with high EA (>30%) and high oil (>50%). Our results show that the EA content was significantly reduced by more than 10 percentage points in the mutant of *BnaC03.FAE1* (*c03*), while the double mutation of *BnaA08.FAE1* and *BnaC03.FAE1* (*a08c03*) resulted in nearly zero EA in three *BnaFAE1*-edited germplasms, and the oleic acid content was increased in different degrees. In addition, knockout of *BnaA08.FAE1* or/and *BnaC03.FAE1* mildly decreased seed oil content, but had no significant effect on other agronomic traits. In general, we successfully created low EA germplasms of *B. napus*, which provides a feasible way for future low EA breeding.

Keywords: *Brassica napus*, CRISPR/Cas9, *FAE1*, erucic acid, seed oil content

OPEN ACCESS

Edited by:
Hyun Uk Kim,
Sejong University, South Korea

Reviewed by:
Kyeong-Ryeol Lee,
Rural Development Administration, South Korea
John Harwood,
Cardiff University, United Kingdom

***Correspondence:**
Liang Guo
guoliang@mail.hzau.edu.cn
Shan Tang
tangshan@mail.hzau.edu.cn

† These authors have contributed equally to this work

Specialty section:
This article was submitted to Crop and Product Physiology, a section of the journal Frontiers in Plant Science

Received: *05 January 2022*
Accepted: *20 January 2022*
Published: *10 February 2022*

Citation:
Liu Y, Du Z, Lin S, Li H, Lu S, Guo L and Tang S (2022) CRISPR/Cas9-Targeted Mutagenesis of BnaFAE1 Genes Confers Low-Erucic Acid in Brassica napus. Front. Plant Sci. 13:848723. doi: 10.3389/fpls.2022.848723

INTRODUCTION

In oilseeds, the *de novo* synthesis of fatty acids occurs in plastids with acetyl-coenzyme A (CoA) as substrates. Acetyl-CoA carboxylase (ACC) catalyzes the condensation of acetyl-CoA and CO_2 to form malonyl-CoA, then the malonyl group of malonyl-CoA is transferred from CoA to acyl carrier protein (ACP) under the catalysis of malonyl-CoA:acyl carrier protein malonyltransferase (MCMT). Acetyl-CoA and malonyl-ACP, respectively, enter the fatty acid synthesis complex (FAS) and undergo a series of reactions including condensation, reduction, dehydration, and re-reduction to form C4:0-ACP. Going through the same cycle reaction, C4:0-ACP reacts with acetyl-CoA, adding two carbons every cycle, to produce C16:0-ACP eventually. In the first cycle, the condensation reaction is catalyzed by ketoacyl-ACP synthase III (KAS III) and the condensation reactions in the next six turns of the cycles are then catalyzed by ketoacyl-ACP synthase I (KAS I). Each cycle uses malonyl-ACP as a source of 2C units (Ohlrogge and Browse, 1995;

Li-Beisson et al., 2013). The synthesized C16:0-ACP is extended to C18:0-ACP under the action of 3-ketoacyl-ACP synthases II (KAS II), then C18:0-ACP is desaturated to form C18:1-ACP by stearoyl-ACP desaturase (SAD). The synthesized C16- or C18-ACP are released from FAS to form free fatty acids by acyl-ACP thioeserase (FAT), and the fatty acids are catalyzed to acyl-CoA by long-chain acyl-CoA synthase (LACS) (Chapman and Ohlrogge, 2012; Li-Beisson et al., 2013). These acyl-CoA are transported to the endoplasmic reticulum, and then the fatty acid chain is desaturated and extended. Oleic acid (C18:1) is desaturated to form linoleic acid (C18:2) and linolenic acid (C18:3) under the catalysis of fatty acid desaturase 2 (FAD2) and fatty acid desaturase 3 (FAD3), or is extended to C20-C24 very long-chain fatty acids (VLCFAs) by the fatty acid elongase 1 (*FAE1*) (Browse and Somerville, 1991; Li-Beisson et al., 2013).

Emergence of CRISPR-Cas9 provides researchers and breeders a powerful tool to study gene function and obtain desired traits by precise and efficient mutagenesis of specific genes (Razzaq et al., 2019; Li et al., 2021; Zhang et al., 2021). In recent years, gene editing technology has been widely used in fatty acid improvement. CRISPR-Cas9 mediated genome editing of *FAD2* could produce high oleic acid/low linoleic acid seeds in *Camelina sativa* (Jiang et al., 2017; Morineau et al., 2017), rice (Abe et al., 2018; Bahariah et al., 2021), rapeseed (Okuzaki et al., 2018; Huang et al., 2020), peanut (Yuan et al., 2019), soybean (Pham et al., 2012; Al Amin et al., 2019; Wu et al., 2020), which provides a new idea for the breeding of oil crops with high oleic acid. In addition, knocking out *FAE1* by CRISPR technology could significantly reduce VLCFAs from 22 to <2% in *C. sativa* (Ozseyhan et al., 2018).

Rapeseed is one of the most important oil crops and produces ˜13% of edible oil globally (Tang et al., 2021). Erucic acid (EA, *cis*-D13 C22:1 fatty acid, hereafter abbreviated as C22:1) is found in many vegetable oils. It has been publicly recognized that EA is one of the major factors that restrain the utilization of rapeseed oil containing high EA for edible oil (Knutsen et al., 2016). In the history of rapeseed genetic improvement, low erucic acid (LEA) revolution made great contributions to the popularization of rapeseed oil. In 1960s, a natural LEA mutant was identified in a feed rapeseed "Liho" (Stefansson et al., 1961). F1 seeds from cross between this mutant and a high EA variety displayed intermediate EAC between those of its parents, suggesting the genetic regulators of EAC act in an additive manner. The segregation ratios of EACs in F2 and F3 seeds were in good agreement with the theoretical ratios under regulation of two genes (Harvey and Downey, 1964). These two genes were identified to be *BnaFAE1* in rapeseed and two *BnaFAE1* genes on chromosome A08 and C03 play major roles in the synthesis of EA (Gupta et al., 2004; Qu et al., 2017).

At present, breeders own multiple *Brassica napus* germplasms with high seed oil content (SOC), but they cannot be well utilized in breeding because many high SOC germplasms contain high EAC. In order to improve the EAC of three germplasms and evaluate the impact of *BnaFAE1* on the agronomic traits of *B. napus*, we used gene editing technology to knock out the *BnaFAE1* genes, and finally obtained *BnaFAE1* knockout mutants with reduced EAC. The EAC of *BnaA08.FAE1* and *BnaC03.FAE1* double mutants were almost reduced to zero, while the content of C18:1 was greatly increased to more than 66%. This study provides new LEA germplasm resources for the breeding of *B. napus*.

MATERIALS AND METHODS

Plant Materials

The germplasms used in this study were three high SOC and high EA *B. napus* inbred lines WH3411, WH3417, and GY284, which were obtained from the National Engineering Research Center of Rapeseed, Wuhan, China.

Sequence Alignment and Gene Expression Analysis

Amino acid sequences in this research were found from the Tair[1] and *B. napus* transcriptome information resource (BnTIR)[2] (Liu et al., 2021). Amino acid sequence alignment was performed by MEGA7 and gene expression data of *FAE1*s in *B. napus* were obtained from BnTIR (Liu et al., 2021).

Construction of CRISPR/Cas9 Vector

To generate *BnaFAE1* mutants, two sgRNAs simultaneously targeting at *BnaA08.FAE1* and *BnaC03.FAE1* were designed by CRISPR-P[3] (Lei et al., 2014) and putative off-target sites were manually eliminated. U6-26 and U6-29 promoters from Arabidopsis were employed to separately drive these two sgRNA cassettes, which were fused in T-DNA region of pKSE410 vector carrying a Kanamycin selection marker (Xing et al., 2014). Primers used in the construction of the CRISPR/Cas9 vector were listed in **Supplementary Table 1**.

Agrobacterium-Mediated Transformation of *Brassica napus*

Agrobacterium tumefaciens (GV3101 strain) cells were transfected with the BnaFAE1-CRISPR-Cas9 recombinant plasmid by electroporation method. *A. tumefaciens*-mediated hypocotyl transformation in *B. napus* were conducted as previously described (Dai et al., 2020).

Identification of *BnaFAE1* Mutants

T0 plants were obtained by kanamycin screening (25 mg/L), and the Cas9 protein was identified by primer pairs Cas9F/R. Then the positive plants with Cas9 were selected to amplify *BnaA08.FAE1* and *BnaC03.FAE1*, respectively, and the amplified fragments were sequenced and analyzed to identify edited T0 mutants. To obtain homozygous mutants, the T0 mutants were self-crossed for T1 and T2 generations and confirmed by sequencing. Primers used in the identification were listed in **Supplementary Table 1**.

[1]https://www.arabidopsis.org/

[2]http://yanglab.hzau.edu.cn/BnTIR

[3]http://crispr.hzau.edu.cn/CRISPR/

Field Experiments and Investigation of Agronomic Traits

T0 and T1 mutant plants and WT plants were grown in a greenhouse (16/8 h of light/dark at 22°C) in 2018 and 2019, respectively. The confirmed homozygous T2 mutant lines without Cas9 were grown in the winter-type growing season (2020–2021) in the experimental farm of Huazhong Agricultural University, Wuhan, China. The field experiment followed a randomized complete block with three replications. Each line was planted in one row with 8–10 plants, with a distance of 21 cm between plants within each row and 30 cm between rows. The field management was performed in line with standard breeding practice. Yield-related traits including plant height, branch height, branch number, silique length, number of siliques per plant, 1000-seed weight, and yield per plant were measured as described previously (Cai et al., 2016).

Analysis of Seed Quality-Related Traits

Mature seeds were harvested and dried for the measurement of seed quality-related traits, including fatty acids composition and SOC. Fatty acids were extracted using the gas chromatograph (GC) fatty acid methyl ester method as described previously (Lu et al., 2016). A total of nine fatty acid species were measured with an Agilent 6890 GC. SOC is scanned by near infrared spectroscopy using 2000–3000 seeds per scan (Gan et al., 2003).

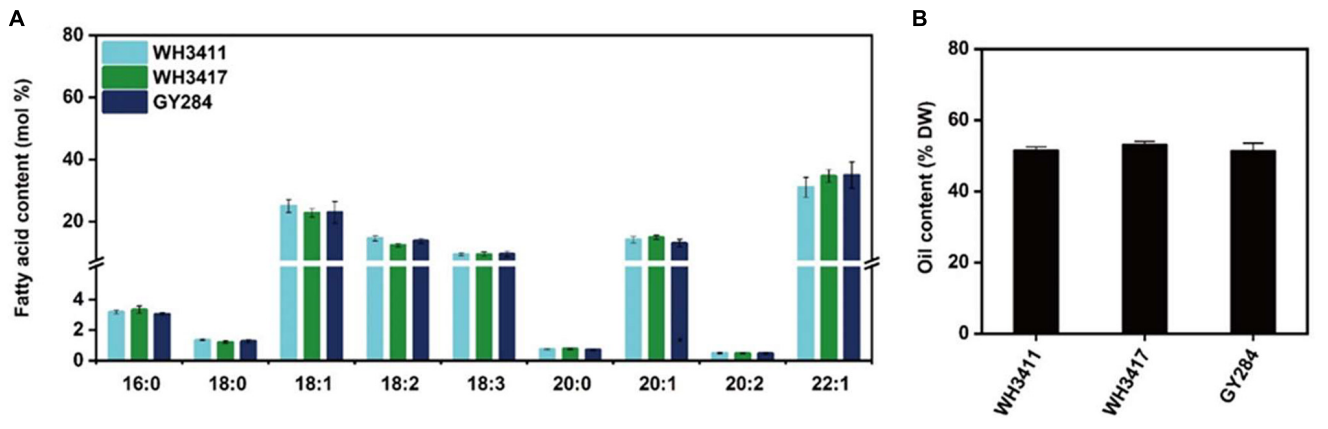

FIGURE 1 | Fatty acid composition and oil content of three germplasms (WH3411, WH3417, GY284). **(A)** Fatty acids were extracted from mature seeds and analyzed using the gas chromatograph method. Values are means ± SD (n = 3∼5). **(B)** Seed oil content is determined by near infrared spectroscopy. Values are means ± SD (n = 12∼20).

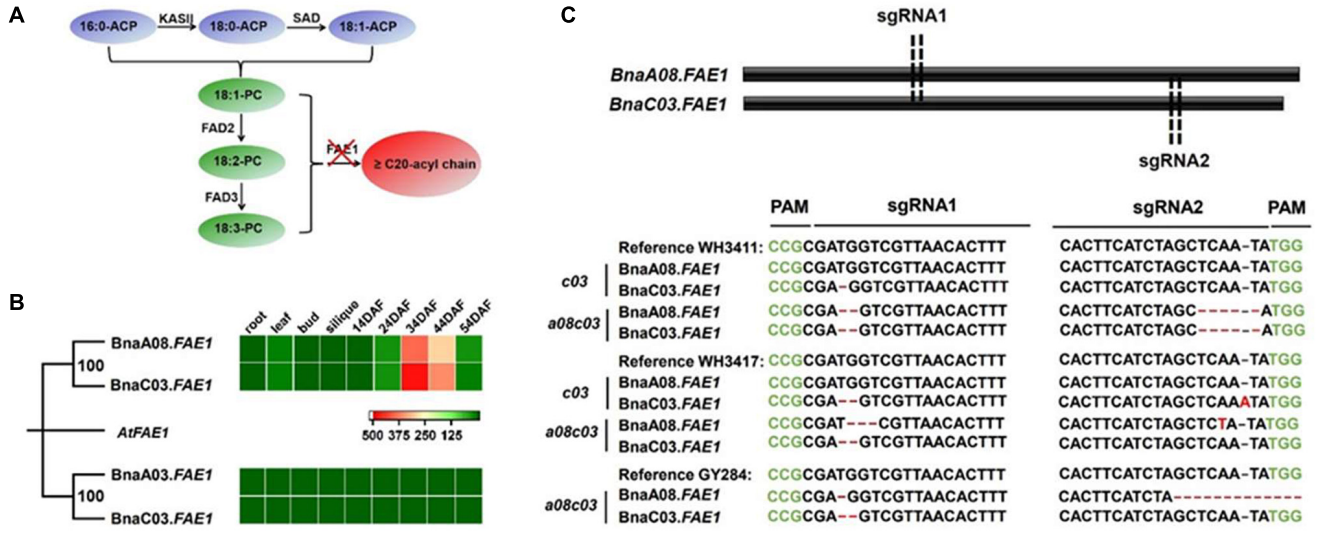

FIGURE 2 | *BnaFAE1* gene analysis and mutant generation. **(A)** Illustration of desaturation and elongation of fatty acids. Red cross indicates mutation of *FAE1* genes to block the synthesis of EA. **(B)** Expression pattern of *BnaFAE1s* in different tissues. **(C)** Location of CRISPR/Cas9 sgRNA-1 and sgRNA-2 targeting *BnaFAE1* genes and sequencing identification of T2 homozygous mutants. PAM is indicated in green. Red "-" means deletions. Red font indicates nucleotide insertions and substitutions.

RESULTS

Selection and Identification of Three High Erucic Acid and High Seed Oil Content *Brassica napus* Seeds

Three natural *B. napus* germplasms WH3411, WH3417, and GY284 were selected and their fatty acid composition characters were measured. Fatty acids were determined by GC analysis, and the results show that EA of these three germplasms were between 31.05 and 34.95 mol% (**Figure 1A**). SOC was measured by near infrared spectroscopy, and the SOC of three germplasms ranged from 51.28 to 53.08% (**Figure 1B**). The results show that WH3411, WH3417, and GY284 have high EAC and high SOC.

Creation of *BnaFAE1* Mutants by CRISPR/Cas9

In order to reduce EA in above three germplasms, CRISPR/Cas9 technology was employed to knock out *BnaFAE1s* (**Figure 2A**). There are four homologous copies of *BnaFAE1* in *B. napus* and the expression data in different tissues showed that *BnaA03.FAE1* and *BnaC03.FAE1-2* were barely expressed in different tissues, while *BnaA08.FAE1* and *BnaC03.FAE1* were mainly expressed in the developing seeds, especially in the middle and late periods of seed development (**Figure 2B**). Based on the expression levels, *BnaA08.FAE1* and *BnaC03.FAE1* were selected to design target mutation sites. Both *BnaA08.FAE1* and *BnaC03.FAE1* were about 1500 bp in size and only consisted of one exon. We designed target sites at ˜600 and 1300 bp, respectively. As a result, homozygous *BnaC03.FAE1* mutations (*c03*) of WH3411, WH3417, and GY284, and homozygous *BnaA08.FAE1* and *BnaC03.FAE1* double mutations (*a08c03*) of WH3411 and WH3417 were identified by sequencing in T2 generation (**Figure 2C** and **Supplementary Figure 1**). All of them cause early termination of translation except $a08c03^{WH3417}$ has one amino acid deletion and one amino acid mutations in the *BnaA08.FAE1* (**Supplementary Figure 2**).

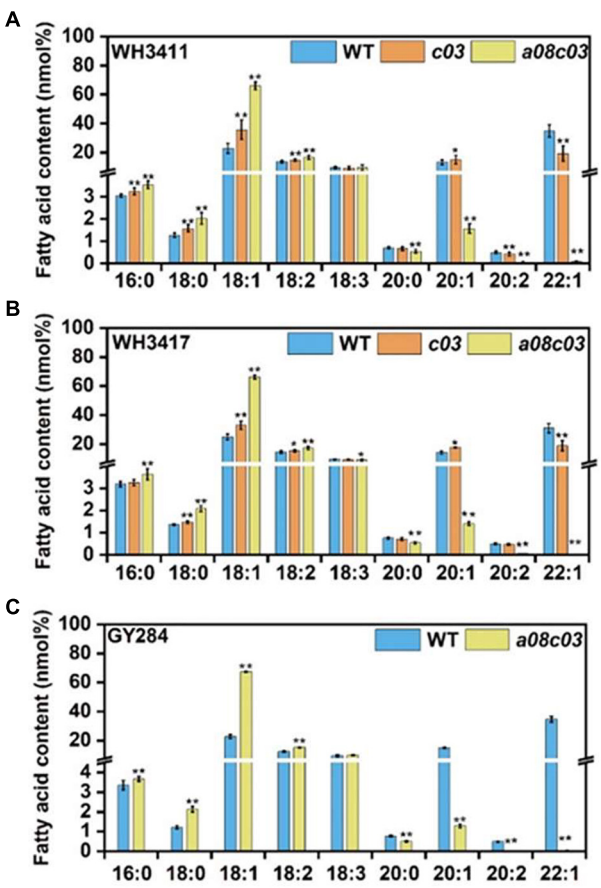

FIGURE 3 | The fatty acid composition phenotype of T2 mutants. Phenotype of fatty acid composition in WH3411 **(A)**, WH3417 **(B)**, and GY284 **(C)** backgrounds. *c03* represents *BnaC03.FAE1* homozygous mutant. *a08c03* represents *BnaC03.FAE1* and *BnaA08.FAE1* homozygous double mutant. Values are means ± SD (n = 3∼5). $^{*}P \leq 0.05$; $^{**}P \leq 0.01$.

CRISPR/Cas9-Induced Mutations in *BnaFAE1s* Greatly Reduce Erucic Acid Content in *Brassica napus* Seed

We analyzed the fatty acids of mature seeds of T2 generation by GC method, and the results showed that the C22:1 of *c03* and *a08c03* was decreased from 34.9 to 19.3 and 0.07% when WH3411 was used as receptor. In addition, the composition of oleic acid (C18:1) in *c03* and *a08c03* was increased from 22.9 to 35.6 and

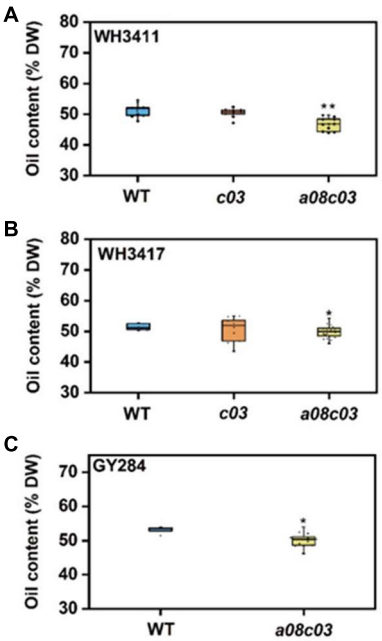

FIGURE 4 | Seed oil content of *BnaFAE1* mutants. Seed oil content of WH3411 **(A)**, WH3417 **(B)**, and GY284 **(C)** and their Bna*FAE1* mutants was determined by near infrared spectroscopy. *c03* represents *BnaC03.FAE1* homozygous mutant. *a08c03* represents *BnaC03.FAE1* and *BnaA08.FAE1* homozygous double mutant. Values are means ± SD (n = 6∼20). $^{*}P \leq 0.05$; $^{**}P \leq 0.01$.

66.0%, respectively. Moreover, the composition of linoleic acid (C18:2) was increased to varied degrees (**Figure 3A**). In WH3417, the C22:1 of *c03* and *a08c03* was decreased from 31.0 to 18.8 and 0.03%, respectively. Meanwhile, C18:1 was increased from 25.0 to 32.9 and 66.2% in *c03* and *a08c03*, respectively (**Figure 3B**). Only homozygous *a08c03* double mutant was obtained in GY284 background. The composition of C22:1 was reduced from 34.6 to 0.02%. C18:1 was increased from 22.8 to 67.3% and C18:2 was increased from 12.4 to 15.2% (**Figure 3C**). These results suggest that knocking out of *BnaFAE1s* can greatly reduce EAC and increase the content of oleic acid and linoleic acid in *B. napus*.

Mutation of *BnaFAE1* Results in Mild Decrease of Seed Oil Content

To determine whether the mutation of *BnaFAE1* affects the SOC, SOC of these mutant lines was analyzed by near infrared spectroscopy. The results indicate that the SOC of *BnaC03.FAE1* mutant (*c03*) was not significantly altered in WH3411 and WH3417 background (**Figures 4A,B**). The SOC of *BnaA08.FAE1* and *BnaC03.FAE1* double mutants (*a08c03*) was significantly reduced from 51.28, 51.49, and 53.08% to 46.69, 49.96, and 50.17%, respectively, in WH3411, WH3417, and GY284 background (**Figures 4A–C**). The results indicate that knocking out of *BnaA08.FAE1* and *BnaC03.FAE1* simultaneously could slightly reduce seed oil accumulation in *B. napus*.

Investigation of Agronomic Trait in Field

To evaluate the impact of knockout of *BnaFAE1s* on the agronomic traits, mutant lines were sown in field under the natural environment. During the whole growth period, the mutants did not show obvious visible difference in growth. At mature stage, these mutants did not exhibit obvious morphological changes compared with WT (**Figures 5A–C**). Meantime, we investigated the agronomic traits including plant height, branch number, branch length, silique number, silique length, thousand seed weight, and yield. The results show that these agronomic traits were not significantly altered in these mutants (**Figure 5D**), indicating that knockout of *BnaA08.FAE1* or/and *BnaC03.FAE1* had no significant effect on plant growth and yield.

DISCUSSION

The synthetic pathway of EA involves a variety of enzymes, including 3-ketoacyl-CoA synthase (KCS), 3-ketoacyl-CoA reductase (KCR), 3-hydroxyacyl-CoA dehydratase (HCD), and *trans*-2,3-enoyl-CoA reductase (ECR) (Yu et al., 2011). Among these, the KCS encoded by *FAE1* was the most critical one (Millar and Kunst, 1997). Therefore, finding or creating *BnaFAE1* mutants has become an important way to cultivate LEA *B. napus* varieties. Until now, there are two main methods to acquire LEA mutants. One is to screen from natural or EMS mutagenic mutants (Harvey and Downey, 1964; Wang et al., 2008), and the other is to inhibit *BnaFAE1* expression by RNAi (Js et al., 2017). In this study, new LEA mutants were created using CRISPR/Cas9-driven knockout of *BnaFAE1* using three high SOC and high EAC germplasms, which broadens the breeding resources of *B. napus* with LEA.

D

	Material	Plant height (cm)	Number of effective branches	Inflorescence length (cm)	Silique number of main Inflorescence	Silique number per plant	Silique length (cm)	Thousand seed weight (g)	Yield per plant (g)
WH3411	WT	141.1±6.3	4.6±1.0	55.7±6.5	60.1±5.3	237.9±54.9	5.0±0.3	3.7±0.3	9.8±1.6
	c03	143.7±6.7	4.7±0.5	55.8±6.6	64.8±4.8	217.0±32.1	4.5±0.3	3.6±0.2	8.2±2.4
	a08c03	140.3±8.8	4.8±1.2	54.6 ±5.8	62.4±6.4	198.9±44.0	4.7±0.7	3.6±0.7	7.8±2.9
WH3417	WT	132.8±8.1	4.9±0.6	52.6±8.9	59.5±6.1	236.9±55.9	5.9±0.3	3.5±0.2	12.8±4.5
	c03	130.9±7.8	5.0±0.8	48.6±7.8	58.1±11.3	198.3±53.6	5.7±0.3	3.3±0.2	10.9±3.6
	a08c03	133.4±8.7	5.1±1.1	52.9±7.0	53.6±9.8	203.6±54.2	6.4±1.3	3.3±0.2	12.5±5.1
GY284	WT	147.4±12.5	8.6±2.7	45.6±7.5	33.0±12.6	194.8±29.6	8.1±0.6	4.4±0.5	7.2±4.4
	a08c03	142.0±11.6	7.0±2.2	45.8±10.4	31.2±9.6	177.0±78.7	8.7±0.5	4.0±0.3	6.1±3.4

FIGURE 5 | Agronomic traits investigation. **(A–C)** Morphology of WH3411, WH3417, GY284, and their Bna*FAE1* mutants. **(D)** Comparison of agronomic traits of WH3411, WH3417, GY284 with their *FAE1* mutants. Values are means ± SD (n = 6~8).

In addition, this study shows that CRISPR/Cas9 induced mutation of the *BnaFAE1* genes significantly changed the fatty acid profiles in seeds, resulting in significantly decreased EA. The reduction of EA in the double mutant (*a08c03*) is much stronger than that in the single mutant (*c03*), which indicates that *BnaA08.FAE1* and *BnaC03.FAE1* have a dose effect on EA level, and *BnaA08.FAE1* and *BnaC03.FAE1* have certain functional redundancy. This is also consistent with previous results (Stefansson and Hougen, 1964). Previous studies have reported that the content of VLCFAs in the *FAE1* mutants of *Arabidopsis* was greatly reduced, while the content of oleic acid was significantly increased (Lemieux et al., 1990). In this study, we also observed similar results, especially in the *BnaA08.FAE1* and *BnaC03.FAE1* double mutants (*a08c03*), and the oleic acid content significantly increased (over 66%), accompanying with the increase of linoleic acid (**Figure 3**). Taken together, our results demonstrate that knockout of the *BnaFAE1s* substantially improves the nutritional quality of *B. napus* seed oil.

Owing to the significance of high SOC and LEA in production, understanding of fatty acid metabolism and seed oil accumulation has obvious practical application value in oil crop breeding. Previous studies showed that *BnaFAE1* was significantly associated with SOC (Li et al., 2014). Ecke et al. (1995) used the double haploid (DH) population to locate three SOC QTLs in the rape genome, and found that two of them were highly correlated with *BnaA08.FAE1* and *BnaC03.FAE1*, and each additional high EA allele increased the SOC by 1 percentage point. Our results show that when *BnaC03.FAE1* was knocked out, the SOC was not significantly decreased, and when both *BnaA08.FAE1* and *BnaC03.FAE1* were knocked out, the SOC was decreased by 1.53–4.59%. This is consistent with previous findings that inhibition of *BnaFAE1* expression significantly reduces the SOC (Js et al., 2017). In order to make up this penalty on oil content, favorable genes/alleles such as DAGT may be introduced into the mutant (*a08c03*) to promote seed oil accumulation (Taylor et al., 2009). Both *BnaA08.FAE1* and *BnaC03.FAE1* are highly expressed in developing seeds while have low expression in other tissues. It is not surprising that knockout of *BnaA08.FAE1* or/and *BnaC03.FAE1* had no obvious effect on agronomic traits and plant architecture of *B. napus*. Above results suggest that it is feasible to breed LEA *B. napus* using high EA germplasms by direct genome editing of *BnaA08.FAE1* and *BnaC03.FAE1*.

CONCLUSION

In brief, this is the first report using CRISPR/Cas9 to create LEA germplasms of *B. napus* by mutating *BnaFAE1s* in three germplasms with consistent results. The EAC was significantly reduced when *BnaA08.FAE1* or/and *BnaC03.FAE1* were mutated in different germplasms. The EA content was reduced to nearly zero when *BnaA08.FAE1* and *BnaC03.FAE1* were both knocked out. Our findings reveal that knockout of *BnaA08.FAE1* or/and *BnaC03.FAE1* had no remarkable effects on agronomic traits except mildly decreased SOC. Our work successfully generated new LEA germplasms for breeding LEA *B. napus*.

DATA AVAILABILITY STATEMENT

The original contributions presented in the study are included in the article/**Supplementary Material**, further inquiries can be directed to the corresponding authors.

AUTHOR CONTRIBUTIONS

LG and ST designed this study. ZD, YL, SLi, and HL performed the experiments. YL and ST analyzed the data and wrote the manuscript. LG, ST, and SLu revised the manuscript. All authors contributed to the article and approved the submitted version.

FUNDING

The work was supported by grants from Hubei Hongshan Laboratory (2021HSZD004) and Higher Education Discipline Innovation Project (B20051).

SUPPLEMENTARY MATERIAL

The Supplementary Material for this article can be found online at: https://www.frontiersin.org/articles/10.3389/fpls.2022.848723/full#supplementary-material

REFERENCES

Abe, K., Araki, E., Suzuki, Y., Toki, S., and Saika, H. (2018). Production of high oleic/low linoleic rice by genome editing. *Plant Physiol. Biochem.* 131, 58–62. doi: 10.1016/j.plaphy.2018.04.033

Al Amin, N., Ahmad, N., Wu, N., Pu, X., Ma, T., Du, Y., et al. (2019). CRISPR-Cas9 mediated targeted disruption of FAD2-2 microsomal omega-6 desaturase in soybean (*Glycine max*. L). *BMC Biotechnol.* 19:9. doi: 10.1186/s12896-019-0501-2

Bahariah, B., Masani, M. Y. A., Rasid, O. A., and Parveez, G. K. A. (2021). Multiplex CRISPR/Cas9-mediated genome editing of the FAD2 gene in rice: a model genome editing system for oil palm. *J. Genet. Eng. Biotechnol.* 19:86. doi: 10.1186/s43141-021-00185-4

Browse, J., and Somerville, C. (1991). Glycerolipid synthesis: biochemistry and regulation. *Annu. Rev. Plant Physiol. Plant Mol. Biol.* 42, 467–506. doi: 10.1146/annurev.pp.42.060191.002343

Cai, G., Yang, Q., Chen, H., Yang, Q., Zhang, C., Fan, C., et al. (2016). Genetic dissection of plant architecture and yield-related traits in *Brassica napus*. *Sci. Rep.* 6:21625.

Chapman, K. D., and Ohlrogge, J. B. (2012). Compartmentation of triacylglycerol accumulation in plants. *J. Biol. Chem.* 287, 2288–2294. doi: 10.1074/jbc.R111.290072

Dai, C., Li, Y., Li, L., Du, Z., and Lu, S. (2020). An efficient Agrobacterium-mediated transformation method using hypocotyl as explants for *Brassica napus*. *Mol. Breed.* 40:96. doi: 10.1007/s11032-020-01174-0

Ecke, W., Uzunova, M., and Weileder, K. (1995). Mapping the genome of rapeseed (*Brassica napus* L.). II. Localization of genes controlling erucic acid synthesis and seed oil content. *Theor. Appl. Genet.* 91, 972–977. doi: 10.1007/BF00223908

Gan, L., Sun, X. L., Jin, L., Wang, G., Xiu, J., Wei, Z., et al. (2003). Establishment of math models of NIRS analysis for oil and protein contents in seed of *Brassica napus*. *Sci. Agric. Sin.* 36, 1609–1613.

Gupta, V., Mukhopadhyay, A., Arumugam, N., Sodhi, Y. S., Pental, D., and Pradhan, A. K. (2004). Molecular tagging of erucic acid trait in oilseed mustard (*Brassica juncea*) by QTL mapping and single nucleotide polymorphisms in FAE1 gene. *Theor. Appl. Genet.* 108, 743–749. doi: 10.1007/s00122-003-1481-z

Harvey, B. L., and Downey, R. K. (1964). The inheritance of erucic acid content in rapeseed (*Brassica napus*). *Can. J. Plant Sci.* 44, 104–111. doi: 10.4141/cjps64-019

Huang, H., Cui, T., Zhang, L., Yang, Q., Yang, Y., Xie, K., et al. (2020). Modifications of fatty acid profile through targeted mutation at BnaFAD2 gene with CRISPR/Cas9-mediated gene editing in *Brassica napus*. *Theor. Appl. Genet.* 133, 2401–2411. doi: 10.1007/s00122-020-03607-y

Jiang, W. Z., Henry, I. M., Lynagh, P. G., Comai, L., Cahoon, E. B., and Weeks, D. P. (2017). Significant enhancement of fatty acid composition in seeds of the allohexaploid, *Camelina sativa*, using CRISPR/Cas9 gene editing. *Plant Biotechnol. J.* 15, 648–657. doi: 10.1111/pbi.12663

Js, A., Cl, A., Fw, A., Xw, A., Rl, A., Tao, Z. A., et al. (2017). Depressed expression of FAE1 and FAD2 genes modifies fatty acid profiles and storage compounds accumulation in *Brassica napus* seeds. *Plant Sci.* 263, 177–182. doi: 10.1016/j.plantsci.2017.07.014

Knutsen, H. K., Alexander, J., Barregård, L., Bignami, M., Brüschweiler, B., Ceccatelli, S., et al. (2016). Erucic acid in feed and food. *EFSA J.* 14:e04593. doi: 10.2903/j.efsa.2016.4593

Lei, Y., Lu, L., Liu, H. Y., Li, S., Xing, F., and Chen, L. L. (2014). CRISPR-P: a web tool for synthetic single-guide RNA design of CRISPR-system in plants. *Mol. Plant* 7, 1494–1496. doi: 10.1093/mp/ssu044

Lemieux, B. M. M., Miquel, M., Somerville, C. R., and Browse, J. (1990). Mutants of Arabidopsis with alterations in seed lipid fatty-acid composition. *Theor. Appl. Genet.* 80, 234–240. doi: 10.1007/BF00224392

Li, C., Brant, E., Budak, H., and Zhang, B. (2021). CRISPR/Cas: a Nobel Prize award-winning precise genome editing technology for gene therapy and crop improvement. *J. Zhejiang Univ. Sci. B.* 22, 253–284. doi: 10.1631/jzus.B2100009

Li, F., Chen, B., Xu, K., Wu, J., Song, W., Ian, B., et al. (2014). Genome-wide association study dissects the genetic architecture of seed weight and seed quality in rapeseed (*Brassica napus* L.). *DNA Res.* 21, 355–367. doi: 10.1093/dnares/dsu002

Li-Beisson, Y., Shorrosh, B., Beisson, F., Andersson, M. X., Arondel, V., Bates, P. D., et al. (2013). Acyl-lipid metabolism. *Arabidopsis Book* 11:e0161. doi: 10.1199/tab.0133

Liu, D., Yu, L., Wei, L., Yu, P., Wang, J., Zhao, H., et al. (2021). BnTIR: an online transcriptome platform for exploring RNA-seq libraries for oil crop *Brassica napus*. *Plant Biotechnol. J.* 19, 1895–1897. doi: 10.1111/pbi.13665

Lu, S., Yao, S., Wang, G., Guo, L., Zhou, Y., Hong, Y., et al. (2016). Phospholipase Dε enhances *Brassica napus* growth and seed production in response to nitrogen availability. *Plant Biotechnol. J.* 14, 926–937. doi: 10.1111/pbi.12446

Millar, A. A., and Kunst, L. (1997). Very-long-chain fatty acid biosynthesis is controlled through the expression and specificity of the condensing enzyme. *Plant J.* 12, 121–131. doi: 10.1046/j.1365-313X.1997.12010121.x

Morineau, C., Bellec, Y., Tellier, F., Gissot, L., Kelemen, Z., Nogue, F., et al. (2017). Selective gene dosage by CRISPR-Cas9 genome editing in hexaploid *Camelina sativa*. *Plant Biotechnol. J.* 15, 729–739. doi: 10.1111/pbi.12671

Ohlrogge, J., and Browse, J. (1995). Lipid biosynthesis. *Plant Cell* 7, 957–970. doi: 10.2307/3870050

Okuzaki, A., Ogawa, T., Koizuka, C., Kaneko, K., Inaba, M., Imamura, J., et al. (2018). CRISPR/Cas9-mediated genome editing of the fatty acid desaturase 2 gene in *Brassica napus*. *Plant Physiol. Biochem.* 131, 63–69. doi: 10.1016/j.plaphy.2018.04.025

Ozseyhan, M. E., Kang, J., Mu, X., and Lu, C. (2018). Mutagenesis of the FAE1 genes significantly changes fatty acid composition in seeds of *Camelina sativa*. *Plant Physiol. Biochem.* 123, 1–7. doi: 10.1016/j.plaphy.2017.11.021

Pham, A. T., Shannon, J. G., and Bilyeu, K. D. (2012). Combinations of mutant FAD2 and FAD3 genes to produce high oleic acid and low linolenic acid soybean oil. *Theor. Appl. Genet.* 125, 503–515. doi: 10.1007/s00122-012-1849-z

Qu, C., Jia, L., Fu, F., Zhao, H., Lu, K., Wei, L., et al. (2017). Genome-wide association mapping and Identification of candidate genes for fatty acid composition in *Brassica napus* L. using SNP markers. *BMC Genomics* 18:232. doi: 10.1186/s12864-017-3607-8

Razzaq, A., Saleem, F., Kanwal, M., Mustafa, G., Yousaf, S., Imran Arshad, H. M., et al. (2019). Modern trends in plant genome editing: an inclusive review of the CRISPR/Cas9 toolbox. *Int. J. Mol. Sci.* 20:4045. doi: 10.3390/ijms20164045

Stefansson, B. R., and Hougen, F. W. (1964). Selection of rape plants (*Brassica napus*) with seed oil practically free from erucic acid. *Can. J. Plant Sci.* 44, 359–364. doi: 10.4141/cjps64-069

Stefansson, B. R., Hougen, F. W., and Downey, R. K. (1961). Note on the isolation of rape plants with seed oil free from erucic acid. *Can. J. Plant Sci.* 41, 218–219. doi: 10.4141/cjps61-028

Tang, S., Zhao, H., Lu, S., Yu, L., Zhang, G., Zhang, Y., et al. (2021). Genome- and transcriptome-wide association studies provide insights into the genetic basis of natural variation of seed oil content in *Brassica napus*. *Mol. Plant* 14, 470–487. doi: 10.1016/j.molp.2020.12.003

Taylor, D. C., Zhang, Y., Kumar, A., Francis, T., Giblin, E. M., Barton, D. L., et al. (2009). Molecular modification of triacylglycerol accumulation by over-expression of DGAT1 to produce canola with increased seed oil content under field conditions. *Botany* 87, 533–543. doi: 10.1139/B08-101

Wang, N., Wang, Y., Tian, F., King, G. J., Zhang, C., Long, Y., et al. (2008). A functional genomics resource for *Brassica napus*: development of an EMS mutagenized population and discovery of FAE1 point mutations by TILLING. *New Phytol.* 180, 751–765. doi: 10.1111/j.1469-8137.2008.02619.x

Wu, N., Lu, Q., Wang, P., Zhang, Q., Zhang, J., Qu, J., et al. (2020). Construction and analysis of GmFAD2-1A and GmFAD2-2A soybean fatty acid desaturase mutants based on CRISPR/Cas9 technology. *Int. J. Mol. Sci.* 21:1104. doi: 10.3390/ijms21031104

Xing, H. L., Dong, L., Wang, Z. P., Zhang, H. Y., Han, C. Y., Liu, B., et al. (2014). A CRISPR/Cas9 toolkit for multiplex genome editing in plants. *BMC Plant Biol.* 14:327. doi: 10.1186/s12870-014-0327-y

Yu, N. I., Zhang, F. C., Wang, Y. C., Fei, P. U., and Jia-Na, L. I. (2011). Cloning and functional analysis of enoyl-CoA reductase gene BnECR from oilseed rape (*Brassica napus* L.). *Acta Agron. Sin.* 37, 424–432. doi: 10.1016/S1875-2780(11)60012-6

Yuan, M., Zhu, J., Gong, L., He, L., Lee, C., Han, S., et al. (2019). Mutagenesis of FAD2 genes in peanut with CRISPR/Cas9 based gene editing. *BMC Biotechnol.* 19:24. doi: 10.1186/s12896-019-0516-8

Zhang, D., Zhang, Z., Unver, T., and Zhang, B. (2021). CRISPR/Cas: a powerful tool for gene function study and crop improvement. *J. Adv. Res.* 29, 207–221. doi: 10.1016/j.jare.2020.10.003

Conflict of Interest: The authors declare that the research was conducted in the absence of any commercial or financial relationships that could be construed as a potential conflict of interest.

Publisher's Note: All claims expressed in this article are solely those of the authors and do not necessarily represent those of their affiliated organizations, or those of the publisher, the editors and the reviewers. Any product that may be evaluated in this article, or claim that may be made by its manufacturer, is not guaranteed or endorsed by the publisher.

frontiers in Plant Science

ORIGINAL RESEARCH
published: 11 March 2022
doi: 10.3389/fpls.2022.862363

Construction of a Quantitative Genomic Map, Identification and Expression Analysis of Candidate Genes for Agronomic and Disease-Related Traits in *Brassica napus*

*Nadia Raboanatahiry[1], Hongbo Chao[1,2], Jianjie He[1], Huaixin Li[1], Yongtai Yin[1] and Maoteng Li[1]**

[1] Department of Biotechnology, College of Life Science and Technology, Huazhong University of Science and Technology, Wuhan, China, [2] School of Agricultural Sciences, Zhengzhou University, Zhengzhou, China

OPEN ACCESS

Edited by:
Yong Xiao,
Chinese Academy of Tropical Agricultural Sciences, China

Reviewed by:
Zaiyun Li,
Huazhong Agricultural University, China
Nian Wang,
Huazhong Agricultural University, China

***Correspondence:**
Maoteng Li
limaoteng426@hust.edu.cn

Specialty section:
This article was submitted to Crop and Product Physiology, a section of the journal Frontiers in Plant Science

Received: *25 January 2022*
Accepted: *15 February 2022*
Published: *11 March 2022*

Citation:
Raboanatahiry N, Chao H, He J, Li H, Yin Y and Li M (2022) Construction of a Quantitative Genomic Map, Identification and Expression Analysis of Candidate Genes for Agronomic and Disease-Related Traits in Brassica napus. Front. Plant Sci. 13:862363. doi: 10.3389/fpls.2022.862363

Rapeseed is the second most important oil crop in the world. Improving seed yield and seed oil content are the two main highlights of the research. Unfortunately, rapeseed development is frequently affected by different diseases. Extensive research has been made through many years to develop elite cultivars with high oil, high yield, and/or disease resistance. Quantitative trait locus (QTL) analysis has been one of the most important strategies in the genetic deciphering of agronomic characteristics. To comprehend the distribution of these QTLs and to uncover the key regions that could simultaneously control multiple traits, 4,555 QTLs that have been identified during the last 25 years were aligned in one unique map, and a quantitative genomic map which involved 128 traits from 79 populations developed in 12 countries was constructed. The present study revealed 517 regions of overlapping QTLs which harbored 2,744 candidate genes and might affect multiple traits, simultaneously. They could be selected to customize super-rapeseed cultivars. The gene ontology and the interaction network of those candidates revealed genes that highly interacted with the other genes and might have a strong influence on them. The expression and structure of these candidate genes were compared in eight rapeseed accessions and revealed genes of similar structures which were expressed differently. The present study enriches our knowledge of rapeseed genome characteristics and diversity, and it also provided indications for rapeseed molecular breeding improvement in the future.

Keywords: ***Brassica napus*, quantitative genomic map, oil content, seed yield, disease, candidate genes, gene expression, structural variation**

INTRODUCTION

Rapeseed (*Brassica napus*, AACC = 38) is a tetraploid species derived from the natural hybridization between turnip rape (*B. rapa*, AA = 20) and cabbage (*B. oleracea*, CC = 18) (Nagaharu, 1935; Al-Shehbaz et al., 2006; Chalhoub et al., 2014). Both *Brassica* species and the model plant *Arabidopsis thaliana* belong to the *Brassicaceae* family; their separation took place about 14–20 million years ago (Yang et al., 1999; Beilstein et al., 2006). Rapeseed is the second most important oil crop in the world, which could supply 13% of the world's vegetable oil (Hajduch et al., 2006; Amar et al., 2009).

Rapeseed utilization is not limited to oil sources, it also can be used for food and energy production, remediation, and as sightseeing attraction (Raboanatahiry et al., 2021). To fulfill the global high demand for oil, the main objectives of researchers are to discover ways to increase the oil content and to develop high-yielding varieties, to succeed in sustainable manufacture in the future. Unfortunately, abiotic and biotic factors frequently weaken the rapeseed development, such as the invasion of *Sclerotinia sclerotiorum* (steam rot) and *Plasmodiophora brassicae* (blackleg disease), which resulted in yield losses of 10–80% (Wang Z. et al., 2014) and 20–30% (Wang et al., 2011), respectively, in China. Besides, drought is one of the most devastating abiotic stresses for seed yield, which affects 40% of the worldwide land area (Zhang et al., 2014).

It would be of great interest to find the genetic loci that could control the traits associated with seed yield and quality, and disease traits, simultaneously, for artificial selection breeding. Rapeseed has experienced selection which contributed to the diversification of winter and spring types. The selection also caused region restructuring where genes controlling agronomically important traits are located. Thus, intensive breeding allowed to optimize those important traits such as oil content, flowering time, and pathogen resistance (Chalhoub et al., 2014). Diversity in the same species is because every individual has their uniqueness starting from their genome and it is reflected into their trait characteristics. Diversity among different species could be understood by analyzing their genomes. Variations within the genome are a reflection of breeding events. Genome diversity might be exploited to detect beneficial phenotypes associated with specific loci on the genome and linked to environmental conditions.

Quantitative trait loci (QTLs) are correlated with variations of phenotype and are extensively used for agronomic trait analysis and in plant breeding. Lots of phenotypic traits are usually responsible for the improvement of most crops, they are quantitative in nature, and are influenced both by many genes and environmental conditions (Zhu and Zhao, 2007). QTL mapping could be used to decipher regulatory loci and genetic mechanism of traits (Paran and Zamir, 2003) to identify the genomic regions which are responsible for trait variation, and to establish a link between phenotype and polymorphic markers in random biparental populations (Cao et al., 2010; Jiang et al., 2014). Several research works have revealed that the phenotypic effect of QTLs for one character in one genetic background might produce a different phenotypic effect in another genetic background. For example, *KN* (*KenC-8* × *N53-2*) and *TN* (*Tapidor* × *Ningyou7*) are two populations that were both cultivated in China, the oil content (OC) and detected QTLs were not similar: 41 QTLs for OC were found with a maximum OC of 50.9% in the 202 *TN-DH* lines (Jiang et al., 2014), whereas in the 348 *KN-DH* lines, 63 OC-QTLs were found with maximum OC of 54.8% (Wang et al., 2013), and in 300 *KN-DH* lines, 67 QTLs were detected with a maximum OC of 57.17% (Chao et al., 2017). To uncover the similarities and differences between the discovered QTLs, a consensus map that displays multiple QTLs from different genetic and environmental backgrounds is indispensable.

Earlier, building a consensus map was possible, but it was limited by the difference of markers that were used in different studies (Raman et al., 2013). Now, it can be overcome with a QTL alignment map which has been used for seed oil content and seed yield QTLs by using *B. napus Darmor-bzh* as the reference genome (Liu S. et al., 2016; Chao et al., 2017; Raboanatahiry et al., 2017, 2018). The advantage of QTL alignment is to allow the easy comparison between QTLs and the regions of overlapping QTLs and can be used to uncover the "stable" or "specified" regions for a trait or an environment, but also to detect the pleiotropic loci, i.e., regions that control multiple traits, simultaneously. In our previous studies, regions of overlapping QTLs were displayed: on one hand, the regions involved QTLs of the same traits but originated from different populations (e.g., OC-QTL from *KN* and *TN* which were both cultivated in China and overlapped in the same region), these regions can be qualified as "stable" for Chinese environment, despite the change in populations, or if the QTLs were from two populations which were developed in two different environments (e.g., *KN* in China, and *PT* in Canada), these regions were "stable" for the studied trait (e.g., oil content). On another hand, QTLs of different traits which overlapped in the same region were also found, and they might have a pleiotropic effect for those multiple traits (Raboanatahiry et al., 2017, 2018).

Quantitative trait loci (QTLs) investigation and the discovery of related candidate genes can be done together, this strategy helps to comprehend the authority of these genes over traits (Remington and Purugganan, 2003; Zhu and Zhao, 2007). The identification of candidate genes implies the detection of important genes for agricultural and economic quantitative traits. Candidate genes are present within the QTL regions and are responsible for phenotype variation (Tabor et al., 2002). The effect of these genes on the variation of phenotype could be elucidated *via* investigation on the gene arrangement and the interaction of loci affecting this variation (Zhu and Zhao, 2007). This technique has already been used to identify potential candidate genes in *B. napus Darmor-bzh*, for instance, Chao et al. (2017) used this technique to identify potential candidate genes for seed oil content traits, and found 448 genes underlying 41 oil content QTLs. Moreover, 76 candidate genes were found for 57 QTLs for oil content and fatty acids (Raboanatahiry et al., 2017), and 147 candidate genes were discovered inside a region where 131 yield QTLs were overlapping (Raboanatahiry et al., 2018). Candidate genes can be manipulated to get the most beneficial gene combination to get the maximum profit, especially those genes which were found in the region of overlapping QTLs

involving many traits. For instance, LPAT2 and LPAT5 were identified as candidate genes in the QTL interval for oil content in the *KN* population of *B. napus* (Wang et al., 2013; Chao et al., 2017), and the seeds of the mutants *lpat2* and *lpat5* lines displayed a decrease in oil content (Zhang K. et al., 2019).

Additionally, the release of various *B. napus* genome sequences: *Darmor-bzh* (Chalhoub et al., 2014), *Tapidor* (Bayer et al., 2017), *Zhongshuang11—ZS11* (Sun et al., 2017), *Gangan, Shengli, Zheyou7, Quinta, No2127, Westar,* and 1689 other accessions (Song et al., 2021), has represented a precious resource, which will have a tremendous impact on understanding rapeseed accessions diversity, notably the structural variation of regions which are associated with agronomic traits.

In our previous study, regions of overlapping QTLs for a single trait were detected (e.g., oil content or seed yield). In this study, the purpose was to construct a quantitative genomic map and to detect genomic regions that might control multiple traits associated with seed, yield, hormones level, and diseases, simultaneously, and the related candidate genes were also identified. Moreover, the structural variation and gene expression levels of those candidate genes were studied in eight different accessions. Consequently, the ultimate objectives were: (1) to build a quantitative genomic map of QTLs associated with agronomic and disease-related traits to display overlapping regions with multiple traits; (2) to reveal the candidate genes within those regions of overlapping QTLs, to find genes that might have pleiotropic effects on seed composition, seed yield, hormones, and disease, and to analyze their interaction; (3) to identify the homologous of these candidate genes in eight rapeseed accessions and to analyze the genes expression and the structural variation. The present study would enhance the knowledge of rapeseed genome characteristics and diversity, the findings can be used to develop molecular markers associated with the studied traits, and also can provide some guidance for molecular design for breeding. Identified candidate genes might be used to target genomics-based improvement and better seed yield, seed composition, and disease resistance in the future.

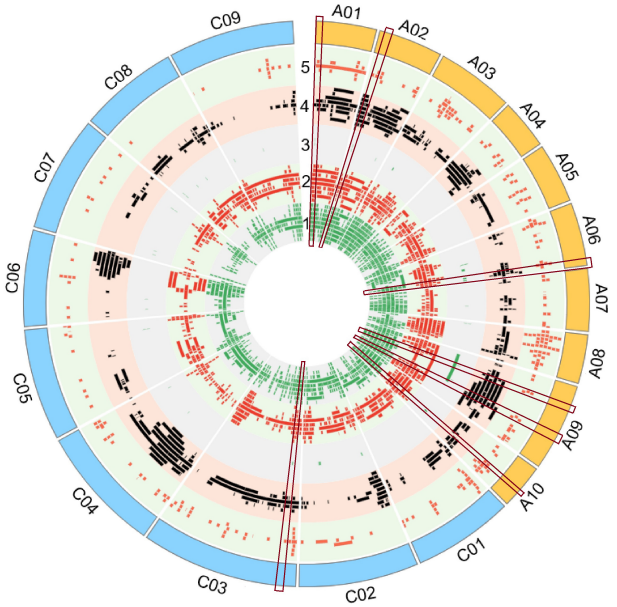

FIGURE 1 | Quantitative trait loci (QTLs) alignment of agronomic and disease-related traits on the physical map of *Darmor-bzh*. QTLs were arranged in each track, from inner to outer circle according to their apparition on the physical map of *Darmor-bzh*. Track 1: Yield-related traits, track 2: Seed composition, track 3: hormone level, track 4: biotic factor, track 5: abiotic factor. The region of overlapping QTLs with five categories of traits is shown inside the red rectangular label. The map was built using Circos software.

RESULTS

A Quantitative Genomic Map of Quantitative Trait Locus Controlling Seed Yield, Seed Components, Hormone Level, and Disease-Related Traits

A total of 4,555 QTLs of 128 agronomic and disease-related traits, developed from 79 different populations of three different ecotypes and grown in 12 different countries (**Supplementary Table 1**), were gathered and combined in one unique map (**Figure 1**). A total distance of 978.4 Mb on the physical map of *Darmor-bzh* was covered (**Figure 2A**, **Supplementary Figure 1**, and **Supplementary Table 2**). Further observation revealed that 2,695 and 1,860 QTLs were located on A and C genomes, respectively. A3 and C3 chromosomes contained the highest number of QTLs, with 430 and 399 QTLs, respectively. A9, A3, and C3 chromosomes contained the highest number of traits (80, 71, and 69 traits, respectively) (**Figure 2A**). Most QTLs for seed components, seed yield, hormones level, and disease-related traits were found in the A genome rather than in the C genome.

It is crucial to locate regions of the genome where multiple traits overlapped the most. Thereby, the above-mentioned 128 traits were subdivided into five categories: 10 abiotic factor traits (A), nine biotic factor traits (B), four hormones related traits (H), 26 seed components traits (S), and 79 yield-related traits (Y). The total number of QTLs in each category were 349 (A), 334 (B), 42 (H), 1392 (S), and 2,438 (Y). Each region on *Darmor-bzh* genome was carefully observed to detect the regions where QTLs of more than one category of trait could overlap, i.e., regions with two, three, four, or five categories of traits, which were present in one region, simultaneously. A total of 517 regions that hosted overlapping QTLs were observed (**Figure 2B** and **Supplementary Figure 1**). The region of overlapping QTLs on each chromosome, the number of QTLs, and the categories of traits are summarized in **Supplementary Table 3**. First, eight regions were found to harbor all the five categories of studied traits (A, B, H, S, and Y) (**Supplementary Table 4**). Those eight regions were located on six chromosomes: one region was found on each of A1 (1.71–1.71 Mb, with 40 QTLs), A2 (2.31–2.31 Mb, with 20 QTLs), A10 (11.78–11.87 Mb, with 14 QTLs), and C3 (5.09–5.33 Mb, with 11 QTLs), and two regions were found on A6 (21.68–21.95 Mb with 15 QTLs and 22–22.30 Mb with 13 QTLs), and A9 (8.12–9.87 and 20.76–22.51 Mb, with 34 QTLs on each of them). Second, 107 regions that contained four categories of traits were found in all

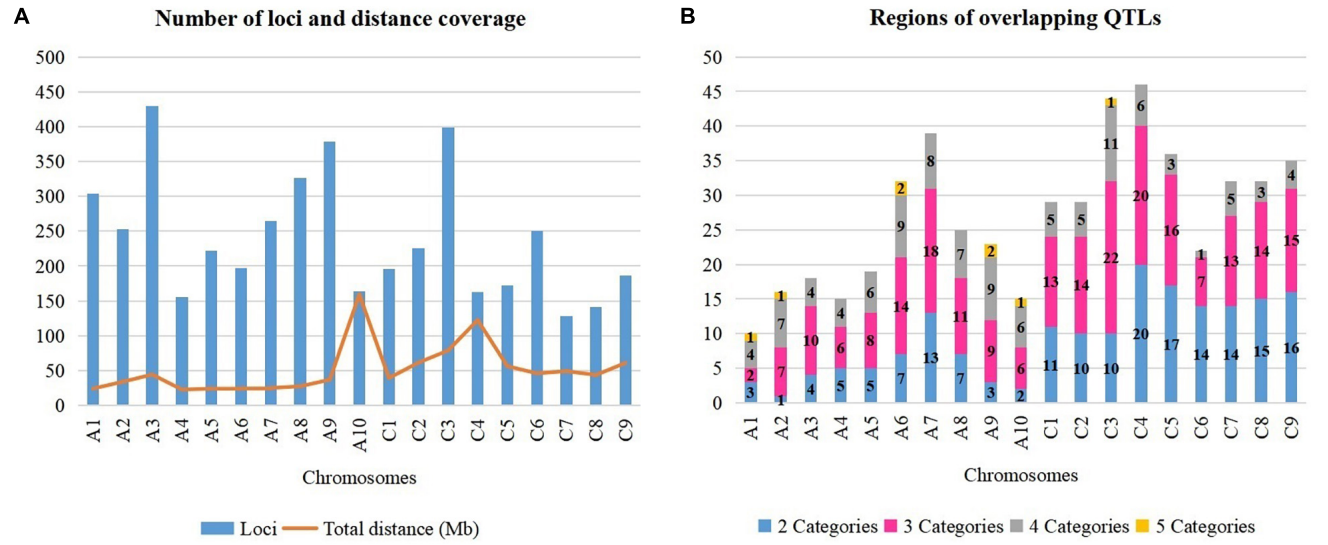

FIGURE 2 | Dissection of rapeseed genome. **(A)** Number of loci and total distance. **(B)** Regions on chromosomes with overlapping QTLs.

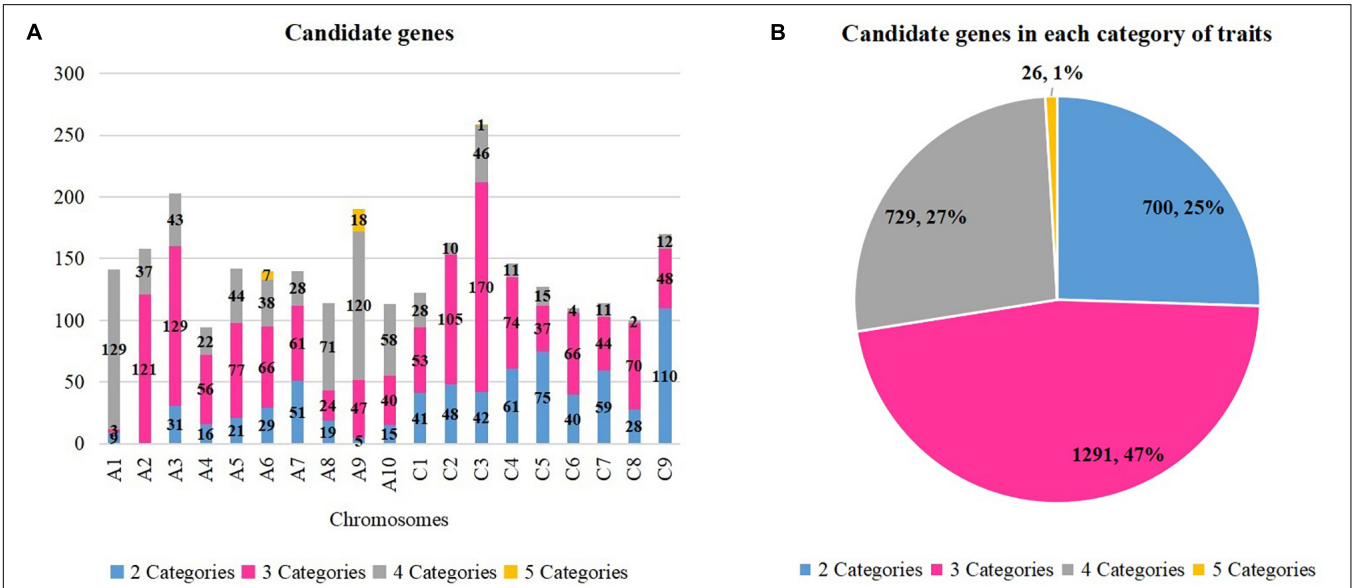

FIGURE 3 | Candidate genes in each category of traits. **(A)** Candidate genes in each chromosome. **(B)** Candidate genes in each category of traits. The number and percentage of genes in each category are displayed. Different colors correspond to different categories.

19 chromosomes. The number of regions in each chromosome was, respectively, 11 on C3, nine on each of A6 and A9, eight on A7, seven on each of A2 and A8, six on each of A6, A10, and C4, five on C1 and C2, four on each of A1, A3, A4, and C9, three on each of C5 and C8, and one on C6. For example, 28 QTLs of four categories of traits (1A, 12B, 5S, 10Y) overlapped on A2 (1.49–2.31 Mb). Note that the region on A2 (1.71–22.04 Mb) included 288 overlapping QTLs (12A, 22B, 63S, and 191Y), which was the richest region of overlapping QTLs in *B. napus* genome. Third, 225 regions on all 19 chromosomes were found to have overlapping QTLs involving three categories of traits: 22 on C3, 20 on C4, 18 on A7, 16 on C5, 15 on C9, 14 on each of A6, C2, and C8, 13 on each of C1 and C7, 11 on A8, 10 on A3, nine on A9, eight on A5, seven on each of A2 and C6, six on each of A4 and A10, and two on A1. For instance, on a region of A5 (3.49–5.29 Mb), 40 QTLs of three categories of traits (5B, 12S, 23Y) overlapped. Fourth, 177 regions were found to contain overlapping QTLs which involved two categories of traits: 20 on C4, 17 on C5, 16 on C9, 15 on C8, 14 on each of C6 and C7, 13 on A7, 11 on C1, 10 on each of C2 and C3, seven on each of A6 and A8, five on each of A4 and A5, four on A3, three on A1 and A9, two on A10, and one on A2. As an example,

13 QTLs of two categories of traits (10B, 3Y) overlapped on C4 (20.66–20.70 Mb).

Note that some QTLs might overlap multiple times with other QTLs in different regions because of their extended length, for example, a QTL for C16:0 was located on A1 (2.25–19.86 Mb) and it could overlap two times with QTLs in the region which involved five and four categories (1.71–1.71 and 1.71–22.04 Mb, respectively). Then, the most abundant and the most overlapping categories of traits were S and Y categories, they were found in 403 among the 517 regions of overlapping QTLs detected in this study. OC and seed yield (SY) are the two most important traits in rapeseed, and the seed yield is determined by the number of seeds per siliques (SNP), the number of siliques per plant, the seed weight (Qzer et al., 1999; Quarrie et al., 2006; Chen et al., 2007), and the overlapping QTLs for OC and SY traits were observed in 82 regions (**Supplementary Table 5**), where the chromosome A9 had the richest regions with 11 regions of overlapping QTLs for OC and SY. The H category of the trait was found rarely in the overlapping region since the identified QTLs in early published papers were few (42 QTLs), so far, this H category was found in 39 among the 517 regions of the overlapping QTLs of this study. Otherwise, the regions of overlapping QTLs which involved one environment or one population were observed. No specified region was found exclusively for one population. Also, only specified regions of overlapping QTLs, which involved some populations developed exclusively in China, were found in 11 areas of the genome: four areas on C3 (36.94–37.27, 37.27–38.94, 39.94–40.21, and 41.40–46.52 Mb), two areas on A8 (16.87–17.37 and 17.37–18.00 Mb), and one area on each of A7 (17.48–18.48 Mb), A10 (0.14–1.64 Mb), C4 (42.73–44.22 Mb), C6 (8.43–9.43 Mb), and C7 (24.87–25.45 Mb) (**Supplementary Table 3**). For instance, the region on A8 (16.87–17.37 Mb) had four QTLs (3S, 1Y), which were all found with the Chinese experimental field. Besides, "hot QTL regions" had been detected in four locations on the rapeseed genome. Those regions were enriched with more than 100 QTLs which were aligned: on chromosome A1 (1.71–22.04 Mb), a total of 228 QTLs of four categories of traits (A, B, S, Y) was found. Chromosome A3 (0.63–6.75 Mb) had 139 QTLs of three categories of traits (B, S, Y), and A8 (9.63–11.12 Mb) contained 111 QTLs of four categories of traits (A, B, S, Y). Then, chromosome C6 (29.29–36.52 Mb) was enriched with 144 QTLs of three categories of traits (B, S, Y). Ultimately, the rapeseed genome had been finely dissected to unveil regions that harbored multiple traits, simultaneously. It would be crucial to couple those findings with the identification of genes that were located within those regions to understand the influence of those genes over those traits.

Candidate Genes Identified Within Regions of Overlapping Quantitative Trait Locus, and Their Interaction Network

Previous studies identified 439 genes that were related to oil formation (Raboanatahiry et al., 2017), 1,398 genes that were related to yield traits (Raboanatahiry et al., 2018), and 1,344 genes which were resistance genes (Dolatabadian et al., 2017). Thus, a total of 3,181 genes were selected because they correlated with the studied traits, and they were aligned to the physical map of *Darmor-bzh* to detect the candidate genes. A total of 2,744 candidate genes were found within overlapping QTLs of two to five categories of traits (**Figure 3A** and **Supplementary Table 6**). A total number of genes of 26 (1%), 729 (47%), 1,291 (27%), and 700 (25%) were found for five, four, three, and two categories of traits, respectively (**Figure 3B**).

Eight regions of the overlapping QTLs of five categories of traits (A, B, H, S, and Y) were found in six chromosomes (A1, A2, A6, A9, A10, and C3). A total of 26 candidate genes were found on three among those six chromosomes: seven genes on A6 (four on 21.68–21.95 Mb and three on 22–22.30 Mb), 18 genes on A9 (six on 8.12–9.87 Mb and 12 on 20.76–22.51 Mb), and one gene on C3 (5.09–5.33 Mb). For example, three candidates were found on A6 (22–22.30 Mb) which were a *DHLAT* gene (BnaA06g33300D), an *RLK* gene (BnaA06g33320D), and an *AAPPT* gene (BnaA06g33540D). Meanwhile, 729 candidate genes were found within overlapping QTLs of four categories of traits in all 19 chromosomes, and they were, respectively, of 129 (A1), 120 (A9), 71 (A8), 58 (A10), 46 (C3), 44 (A5), 43 (A3), 38 (A6), 37 (A2), 28 (A7 and C1, each), 22 (A4), 15 (C5), 12 (C9), 11 (C4 and C7, each), 10 (C2), four (C6), and two (C8). For example, three candidate genes (*CCT* BnaA03g14860D, *RLK* BnaA03g15210D, and *KAT2* BnaA03g15290D) on A3 (6.84–7.12 Mb) were found within 19 overlapping QTLs (2B, 1H, 5S, 11Y). Moreover, 1,289 candidate genes were located within overlapping QTLs of three categories of traits, and they were found on all 19 chromosomes: 169 (C3), 129 (A3), 121 (A2), 104 (C2), 77 (A5), 74 (C4), 70 (C8), 66 (A6 and C6), 61 (A7), 56 (A4), 53 (C1), 48 (C9), 47 (A9), 44 (C7), 40 (A10), 37 (C5), 24 (A8), and three (A1). For instance, two candidate genes (*ADC2* BnaC01g03710D, and *FAE* BnaC01g04130D) were found on C1 (1.93–2.16 Mb) involving 13 overlapping QTLs (4B, 1S, 8Y). At last, overlapping QTLs of 2 categories of traits contained 700 candidate genes in 18 chromosomes (excluding A2): 110 (C9), 75 (C5), 61 (C4), 59 (C7), 51 (A7), 48 (C2), 42 (C3), 41 (C1), 40 (C6), 31 (A3), 29 (A6), 28 (C8), 21 (A5), 19 (A8), 16 (A4), 15 (A10), 9 (A1), and 5 (A9). For example, two candidate genes (*RLK* BnaC07g13860D and *RN* BnaC07g14020D) were found on C7 (19.60–19.79 Mb) involving two overlapping QTLs (1 A and 1 B). In assumption from those findings, important genes which were located within regions of overlapping QTL with multiple traits were identified. They might influence more than one category of traits, and they could be selected according to the desired improvement of two or multiple traits.

The interaction network analysis of the 2,744 candidate genes was made with their 1,555 orthologous genes in *A. thaliana* because *B. napus* are not available on the String database. Gene ontology (GO) analysis indicated that the 1,555 genes could be classified into 16 categories, according to Panther GO-slim biological process's classification (**Supplementary Table 7**): it included the cellular process, biological phase, reproductive process, multi-organism process, localization, interspecies interaction between organisms, reproduction, biological regulation, response to stimulus, signaling, developmental process, rhythmic process, multicellular organismal process, metabolic process, growth, immune system process. Other

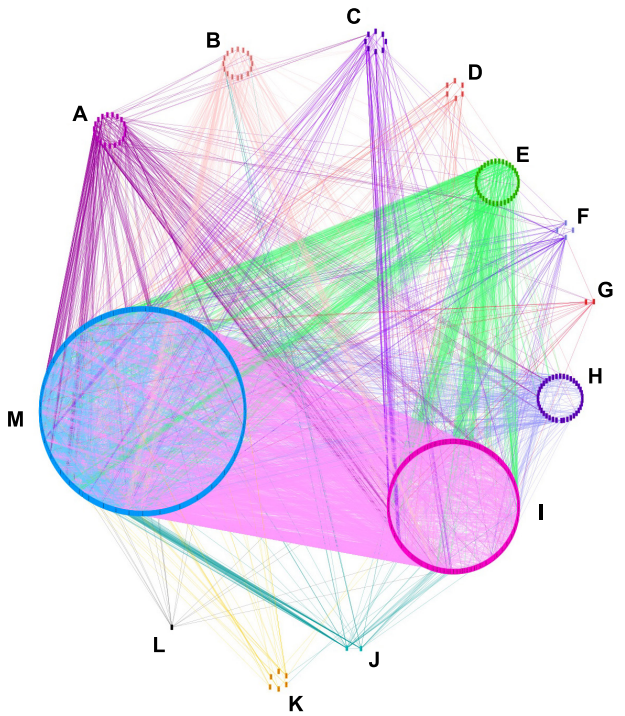

FIGURE 4 | Candidate genes interaction network. The interaction analysis was made with orthologous *A. thaliana* genes by using STRING (http://string-db.org/) and visualized with Cytoscape_V3.8.2. 1271 nodes and 10101 edges are shown. Eleven categories of genes are displayed according to their GO term enrichment. **(A)** Signaling, **(B)** multicellular organism, **(C)** growth, **(D)** biological regulation, **(E)** cellular process, **(F)** developmental process, **(G)** immune system process, **(H)** localization, **(I)** metabolic process, **(J)** rythmic process, **(K)** response to stimulus, **(L)** reproduction, **(M)** others.

genes which could not fit into those categories were classified as "Others."

The interaction network was visualized with Cytoscape and 1,271 nodes and 10,101 edges were displayed (**Figure 4**). In this network, 34 genes might be more influential over other genes (degree layout, DL≧60) (**Supplementary Table 8**). Those genes belonged to the GO categories of the cellular process, metabolic process, multicellular organismal process, rhythmic process, and "others" category. *ACP, DGAT, KASI, KASII, KASIII, LPAAT,* and *MCMT* had functions related to oil biosynthesis (Li-Beisson et al., 2013), *AGL20, AP2, AUX1, CO, COP1, EMB, FLC, FLD, FRI, FT, FVE, GI, LPAAT, PHYA, PHYB, RGA, SVP, TFL1*, and *TFL2* were related to yield traits, while A*P40, ARP, ERD, GMP synthase, HEME, SH3,* and *WUS* were involved in plant resistance to disease (Poole, 2007). The 26 candidate genes detected in the region of overlapping QTLs involving five categories of traits had less influence over the other genes DL < 46 (**Supplementary Table 9**), in comparison to the 11 above-mentioned genes. The most influential genes had different functions and were involved in different metabolism pathways, yet they might have a higher effect over other genes, this might indicate that the simultaneous control of multiple categories of traits might be affected at different paths of metabolisms.

Gene Expression and Structural Variation of Candidate Genes in Eight Rapeseed Accessions

The 34 most influential genes of the interaction network in *B. napus* were selected for the current gene expression analysis. Additionally, the 26 candidate genes which were found within QTLs of five categories (A, B, H, S, and Y) were also added to the analysis (**Supplementary Table 10**). Two groups of genes could be observed, the first group was the genes that were mainly expressed in the seeds and siliques, including *FUS3, PRP4 KINASE B, KR, RCN1, KASI, KASIII, MCAT, FLC, FVE,* and *EMB* (**Figure 5A** and **Supplementary table 11**), with higher expression in the seeds rather than in the siliques, except for the *EMB* gene. The second group had the genes expressed in different tissues and the genes with very low expression levels (**Figure 5B** and **Supplementary Table 11**).

A quantitative PCR (qPCR) was performed using the complementary DNA (cDNA) from the seeds and siliques of *KenC-8*. It was observed that the genes had higher expression in the seeds than in the siliques, except for the *PRP4 KINASE B* gene which had higher expression in the siliques than in the seeds. Moreover, the *EMB* gene which had a higher expression in the siliques than in the seeds of *ZS11*, had a higher expression in the seeds than in the siliques of *KenC-8* (**Figure 6**).

Besides, the gene expression and the structural variation of the above-mentioned 10 genes were analyzed in eight rapeseed varieties, including two winter-types (*Quinta* and *Tapidor*), two spring-types (*Westar* and *No2127*), and four semi-winter types (*ZS11, Zheyou7, Shengli* and *Gangan*). The synteny of the genes in the nine rapeseed varieties is shown in **Figure 7**. The genes were located in five chromosomes in *Darmor-bzh*, and in eight chromosomes in the other eight rapeseed varieties. The length of the genes was almost similar in the eight varieties but they were much longer in size in *Darmor-bzh* (**Supplementary Table 12**). The expression of those 10 genes was compared in the eight rapeseed varieties (**Supplementary Figure 2**). The nucleotide sequence identity was analyzed (**Supplementary Table 13**). Genes with a higher rate of sequences identity had similar gene expressions. It was the case of the *KASIII* genes in *Zheyou* and *ZS11*. However, genes that displayed 100% of sequence identity could also have different expression profiles, such as the *KR* genes of the eight varieties that shared 100% of sequence identity but displayed a different expression level. More, some other genes with different sequences identity showed similar expression profiles, like the case of *FLC* genes in *Gangan* and *No2127*.

DISCUSSION

The current study aimed to combine QTLs for seed component, seed yield, hormones, and disease-related traits, which were detected in previous studies, in one physical map in rapeseed, to identify the related candidate genes and to analyze their expression and structural variation in different rapeseed accessions. The same strategy was used to find the regions

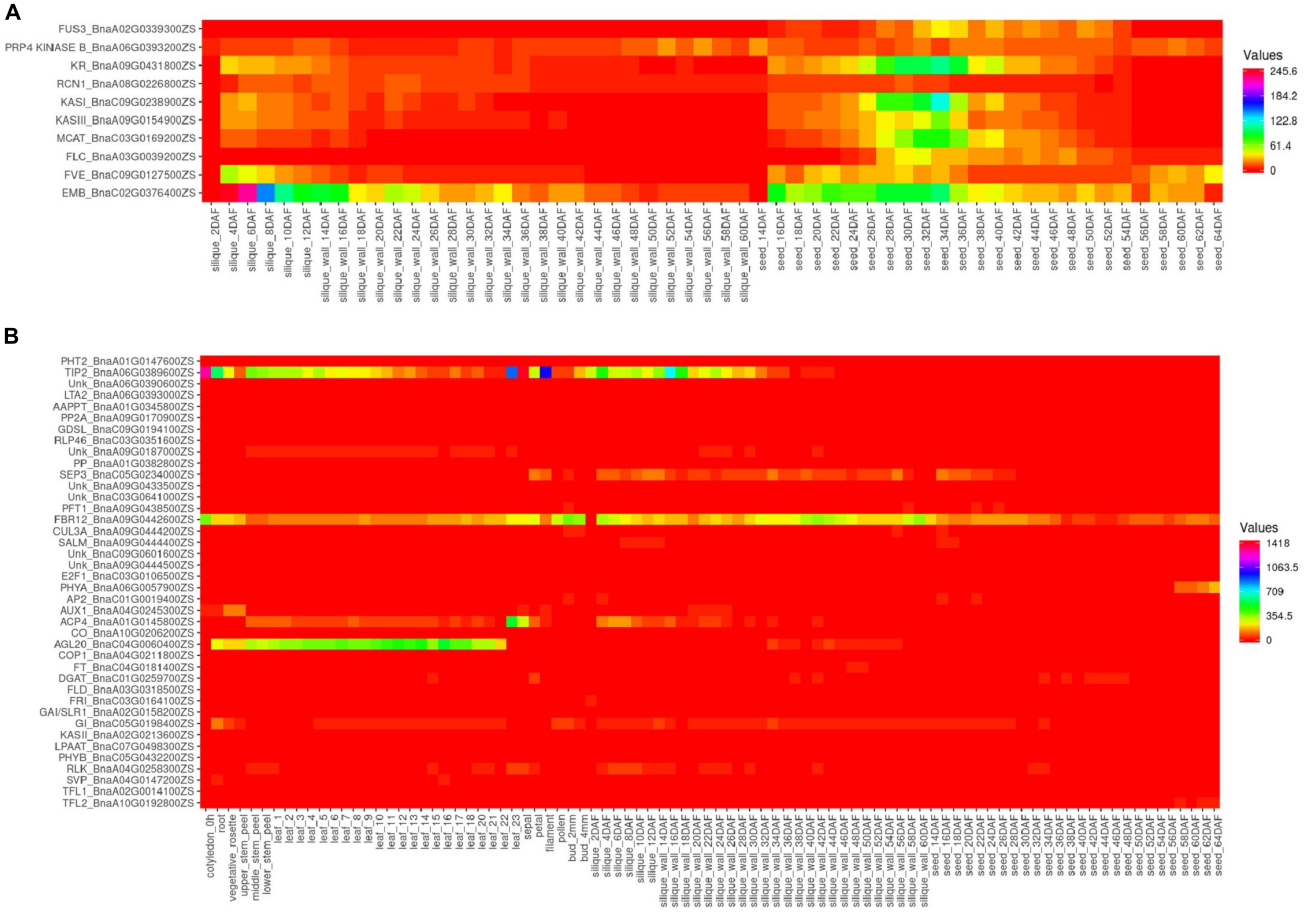

FIGURE 5 | Expression level of the candidate genes in *ZS11*. **(A)** Ten genes exclusively with higher expression in the siliques and seeds. **(B)** Expression of other genes in different tissues. The heatmap was built using Heatmapper (http://www2.heatmapper.ca/).

that might control multiple traits of one category, i.e., seed oil (Raboanatahiry et al., 2017) and seed yield (Raboanatahiry et al., 2018). In those two studies, some regions were suggested to possibly contribute to the improvement of one trait or multiple traits of one category, and some regions were supposed to be stable for one given environment. For example, a region on A1 (2.50–2.99 Mb) had overlapping QTLs for plant height, which was from two populations developed in China (*Tapidor* × *Ningyou7* and *Express617* × *V8*), so this region might affect the plant height and it is a stable region for the Chinese environment (Raboanatahiry et al., 2018). More, QTLs for C16:0, C18:0, C18:1, C18:2, C20:0, and C22:1 were overlapping on C3 (53.75–58.29 Mb), thus, this region might control those six traits, simultaneously (Raboanatahiry et al., 2017). The current study was made at a higher level because it was not limited to one category of trait as in the previous studies, but five categories which involved almost all the studied traits in rapeseed.

Increasing seed oil and seed yield is among the main focus of researchers on rapeseed, to cater to the increasing demand for

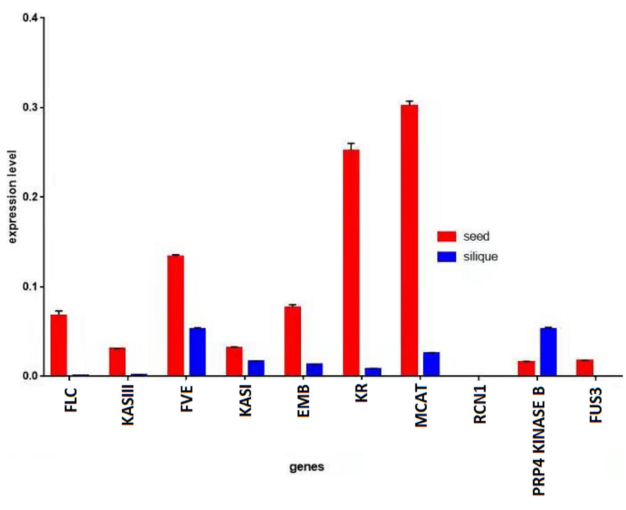

FIGURE 6 | Expression level of genes in seeds vs. siliques of *KenC-8*. *Actin* was used as reference gene.

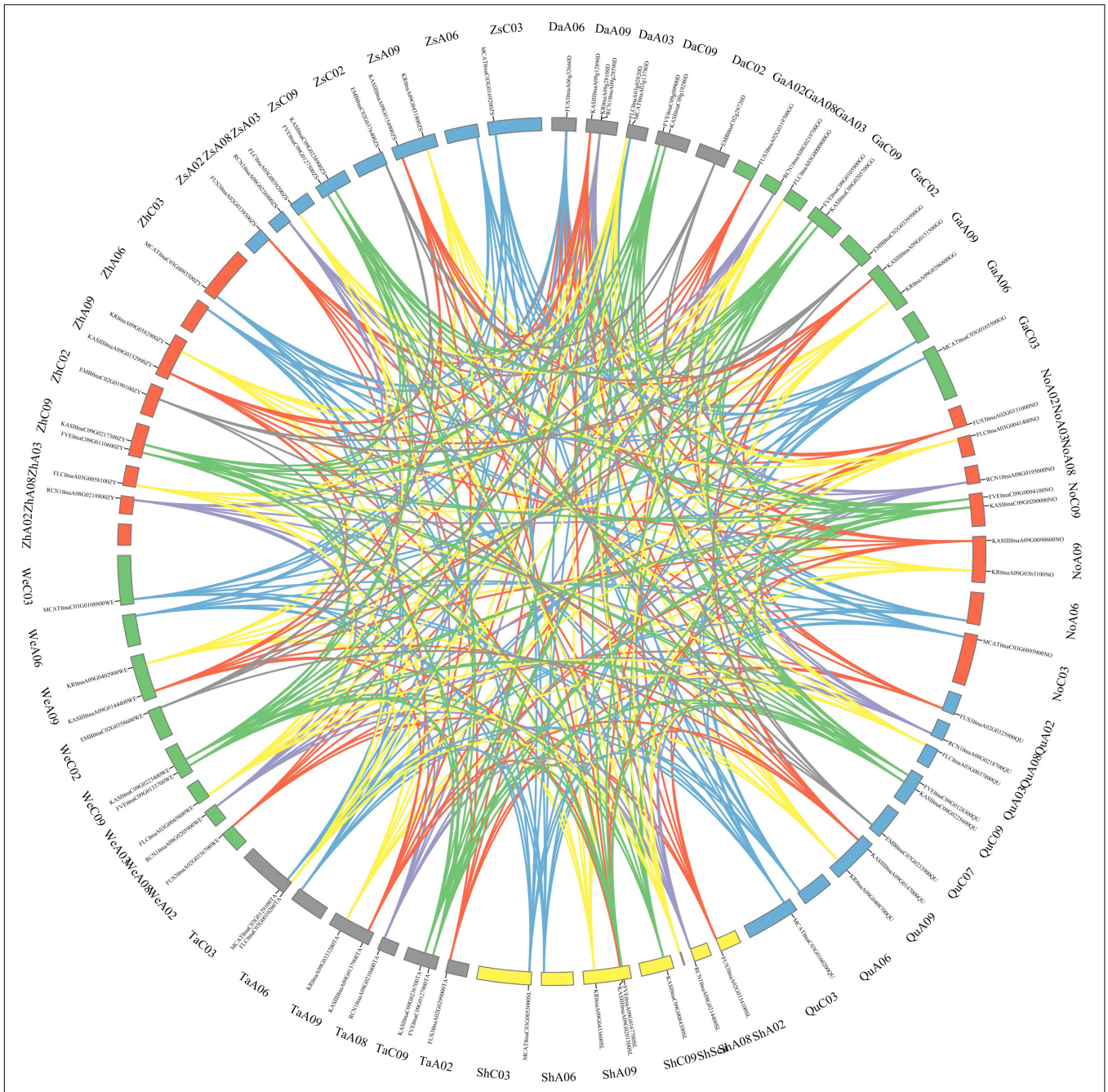

FIGURE 7 | Synteny of the ten genes in nine rapeseed varieties. The map was built with TBtools software, with *Darmor-bzh (Da), Gangan (Ga), No2127 (No), Quinta (Qu), Shengli (Sh), Tapidor (Ta), Westar (We), Zheyou (Zh), Zhongshuang 11 (Zs).* Chromosome location is displayed near the genome name.

oil. However, the usage of rapeseed is not limited to biomass for oil, but also multiple purposes, such as protein, carbohydrate, vitamins sources, and many more (Raboanatahiry et al., 2021). Despite the effort in improving seed components and seed yield, rapeseed crops are under attack from various diseases that resulted in huge crop loss. For example, *Leptosphaeria maculans* causes blackleg disease (West et al., 2001), which has created an economic loss of $900 million per growing season globally (Fitt et al., 2008). Although resistant cultivars have been developed and cultivated since the 1990s in Canada (Kutcher et al., 2010), which has decreased the yield loss by 1% (Gugel and Petrie, 1992), abiotic stresses have also caused about 50% yield reduction in major crops (Bray et al., 2000). Extensive research is still undertaken to take total control of those biotic and abiotic diseases, *via* selective breeding. Otherwise, phytohormones play important roles in plant growth

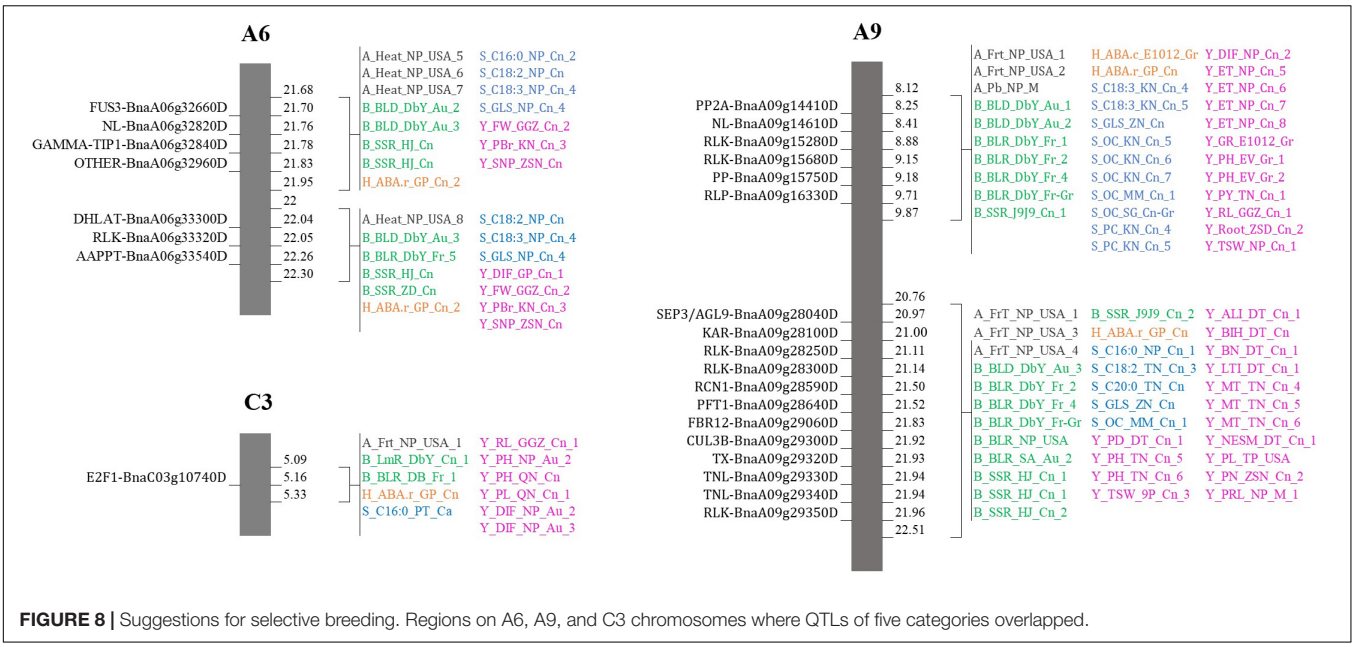

FIGURE 8 | Suggestions for selective breeding. Regions on A6, A9, and C3 chromosomes where QTLs of five categories overlapped.

and development, such as IAA (Grossmann, 2010), but also on plant adaptation to assure survival to face the environmental fluctuation. Abscisic acid (ABA) responds to both biotic and abiotic stresses (Cao et al., 2011), which have an influence on one another (Fujita et al., 2006). Those phytohormones support agronomic trait improvement and response to disease. Therefore, all the five categories of traits analyzed in the current study are correlated and are pivotal for rapeseed crop improvement.

Dissection of Rapeseed Genome Revealed Regions Controlling Multiple Traits

The current study is the first study to gather all the QTLs of important agronomic and disease-related traits discovered in *B. napus* over 25 years, to construct a quantitative genomic map, which is crucial to uncover similarities and differences in QTLs detected from different populations and environments, but also to reveal the regions that might control multiple beneficial traits, simultaneously.

It was obvious that most of the QTLs were found on the A rather than C genome (2,695 vs. 1,860 QTLs, respectively). Selection has played important role in improving *B. napus*. It was reported that the C genome rather than the A genome, contained extended breeding regions (51.15 Mb on C vs. 16.80 Mb on A) which might contribute more to alleles producing elite traits (Wang Z. et al., 2014). However, a recent investigation on the origin of *B. napus* and the genetic loci that contributed to its improvement had revealed that the parallel selection of the A and C genomes had led to seed quality improvement in *B. napus* (Lu et al., 2019). "A" genome-specific selection greatly enhanced disease resistance, oil accumulation, and environment adaptation of *B. napus* during its first stage of improvement, while the C genome had improved developmental traits. This might explain the fact that most of the QTLs of studied traits in the current study could be found on the A genome. Particularly, for Asian *B. napus* varieties, it was reported that they have experienced strong artificial selection from the A genome which contributed to their adaptation following their introduction from Europe (Zou et al., 2019).

Apart from that, 517 regions were found with overlapping QTLs involving at least two categories of traits. Those regions might be suitable for selection to improve two or more desired traits, simultaneously, for example, to improve both abiotic stress response, seed component, and seed yield (A4:3.07–4.11 Mb). Several studies have already investigated on the co-location of QTLs from a different category of traits (Shi et al., 2012; Zhao J. et al., 2012; Ding et al., 2014; Bouchet et al., 2016; Körber et al., 2016; Stein et al., 2017; Wan et al., 2017; Rahaman et al., 2018; Jan et al., 2019; Wrucke et al., 2019; Wu et al., 2019; Zhang K. et al., 2019). Those studies demonstrated the importance of analyzing multiple traits, at the same time, to target the loci for breeding cultivars with the most advantageous profile. For example, a study that focused on flowering time (FT) and *Sclerotinia* stem rot resistance (SSR) reported that early FT might increase susceptibility to *S. sclerotiorum*, and regions of co-location of FT and SSR resistance traits were found which were crucial for breeding early maturing and SSR resistance cultivars. Moreover, four co-localized QTL hotspots of SSR resistance and FT on A2 (0–7.7 Mb), A3 (0.8–7.5 Mb), C2 (–15.2 Mb), C6 (20.2–36.6 Mb), which were consensual with previous studies (Wu et al., 2019). In the current study, the QTL of SSR and DIF (FT) were also co-localized in those regions.

Particularly, seed components and seed yield traits often overlapped in this study. In earlier studies, yield traits such as the flowering time, the morphology of the root, and the plant growth environment could affect seed quality traits such as erucic acid, oil, protein, and glucosinolate contents (Paran and Zamir, 2003; Si et al., 2003; Quijada et al., 2006;

Shi et al., 2013; Wang X. et al., 2017). In oil crops, QTLs that could influence both seed quality and yield traits had already been discovered in several studies, positively or negatively. For instance, oil and protein contents were positively correlated with seed weight in 11 *B. carinata* lines developed in Canada (Getinet et al., 1996). Zhao et al. (2006) found evidence of a positive correlation between oil content and seeds per silique while evaluating 282 *DH* lines from a cross between *Sollux* and *Gaoyou* (*B. napus*), and developed in Germany and China. In a study performed by Chen et al. (2010) in a *DH* population derived from a cross between high and low oil content *B. napus* and developed in Canada, oil content and flowering time were negatively correlated. In that study, QTLs for oil content, flowering time, and seed yield were co-localized on a small region of LG7 where alleles of low oil content, early flowering time, and higher seed yield were found together. However, QTLs for high oil content and early flowering time were found in the co-location on LG2. Otherwise, since oil content and seed yield are the most important trait in rapeseed, 82 QTL regions were discovered, where QTLs for these two traits overlapped. They could be selected to improve the two traits, simultaneously.

Overlapping QTLs of multiple traits might happen when gene alteration frequencies at nearly linked loci occur, but also, it might be caused by the pleiotropic effect when an appropriate substitution of genes occurs (Smith and Haigh, 1974). Also, pleiotropy or/and linked genes might have caused this phenomenon. Hot QTLs regions were also discovered with more than 100 aligned QTLs, which is interesting for rapeseed molecular breeding, because the region with the QTLs of diverse traits could be targeted to improve multiple traits, simultaneously, and the more the number of QTLs increased in that region, the more the locus was stable because, despite the diversity in population and environment background, it did not alter the location of the QTL on the genome.

The region on the chromosome which was exclusively for QTLs from one population was not found, and those exclusively for one environment were for China only (fixed environment for China). This indicated that those QTLs remained unchanged, despite the variation of population and environment.

Identified Candidates Genes Might Be Pleiotropic or Linked Genes?

In previous studies, 110 genes in *Arabidopsis* were identified to be involved in oil formation (Li-Beisson et al., 2013) and 439 homologous genes were found in *B. napus* (Raboanatahiry et al., 2017). Moreover, 425 yield genes which were related to branch number, flowering time, maturity time, plant height, pod number, seed number, seed weight, and seed yield in *Arabidopsis* were identified (Shi et al., 2009) and 1,398 homologous genes were detected in *B. napus* (Raboanatahiry et al., 2018). Dolatabadian et al. (2017) found 1,344 resistance genes in *B. napus*. Those genes had a relationship with the currently studied traits, thus, they were selected to uncover the candidate genes.

The function of those selected genes correlated with the studied traits. Since many genes could be found within a region of a genome, a preselection is necessary, so that the candidates have a close connection to the studied traits, and have a functional outcome on the process (Zhu and Zhao, 2007). A total of 2,744 genes related to oil, yield, and resistance were found within overlapping QTLs involving two to five categories of traits. As mentioned above, overlapping QTLs might be caused by pleiotropy or linked genes. Pleiotropy is when one gene can control multiple unrelated phenotypic traits (Stearns, 2010; Conner et al., 2011; Wagner and Zhang, 2011; Solovieff et al., 2013). Pleiotropy is largely distributed due to biochemical and developmental systems and it affects development and evolution and creates correlations between genes and phenotype, and it affects selection and imposes the accessibility of the evolution extent (Gromko, 1987; Lynch and Walsh, 1998). The pleiotropic organization of traits (dominant or epistatic) can be modified by selection and inbreeding (Goodnight, 1988; Cheverud and Routman, 1996; Hansen and Wagner, 2001). Linked genes are genes located close to each other on the same chromosome and are inherited together during meiosis. Genes might separately control different phenotypes but are found closely located on the same region of a chromosome.

Candidates found within the region of overlapping QTLs with five categories of traits attracted more attention since they might be more influential than the others over multiple traits. A total of 26 candidates were found on five regions distributed on A6, A9, and C3 chromosomes, and they would be the most recommended in this study, for genomic selection to target multiple traits simultaneously (**Figure 8**). They belonged to different families and might have different distinct roles, but the way they act to influence each other or to affect the studied traits still needs a deep investigation. Functional investigation of each gene over the studied traits would be indispensable to comprehend their influence on the traits and would reveal whether they were pleiotropic genes or linked genes.

Gene interaction network revealed that 34 genes might have more influence over the other genes. Genes are responsible for the genetic variation of traits (Tabor et al., 2002), and the structure and dynamism of the genetic regulatory network have an impact on quantitative traits (Frank, 2003). In this study, *KAS, ACP, AUX1, CO, FT, PHYA, and AGL20* were also identified as the most influential genes in our previous studies (Raboanatahiry et al., 2017, 2018). Despite the number of genes identified in this study being far larger than those of the previous study, and the gene function were also broader, those seven genes of different functions still had higher influence over the other genes, indicating that simultaneous control of multiple traits might be affected at different metabolism pathways.

The expression analysis of the candidate genes revealed an exclusive increase for 10 genes (*FUS3, PRP4 KINASE B, KR, RCN1, KASI, KASIII, MCAT, FLC, FVE,* and *EMB)* in the seeds and siliques of *ZS11,* with higher expression in the seeds than in the siliques, except for *EMB.* Reversely, the *PRP4 KINASE B* of *KenC-8* had increased expression in the siliques in comparison

to the seeds. Previous studies reported the function of those 10 genes: *MCAT, KASI,* and *KASIII* (β-*ketoacyl-ACP synthase I* and *III*), and *KR (*β-*ketoacyl- ACP reductase)* are enzymes of fatty acid biosynthesis. *MCAT (Malonyl-CoA:ACP transacylase)* was suggested to be essential for a high oil content *B. napus*, and might be used to improve the seed oil contents (Qu et al., 2014). Plastidial *KASIII* genes could alter the fatty acid profile of *B. napus* seeds, by increasing the C18:2 and C18:3 contents at the expense of C18:1 (Verwoert et al., 1995). *KASI* played a positive role in *Arabidopsis* morphology and fertility, and in polar lipid composition. Moreover, *KASI* disruption affected embryo development and decreased the fatty acid contents (Wu and Xue, 2010). *FUS3 (FUSCA3)* is a regulator of seed development and seed oil content. It induces the genes of fatty acid biosynthesis during development in *Arabidopsis* (Wang et al., 2007). Likewise, the oil production decreased in *fus3* of *B. napus* (Elahi et al., 2015). In Arabidopsis, *RCN1 (roots curl in naphthylphthalamic acid1)* encodes a regulatory α-subunit of protein phosphatase 2A. *RCN1* modulates auxin responses in roots (Garbers et al., 1996), and defection resulted in increased basipetal auxin transport and a significant delay in gravitropism (Rashotte et al., 2001). Moreover, *rcn1* roots had a reduced elongation in seedlings and hypocotyl elongation (Muday et al., 2006). *FLC (FLOWERING LOCUS C)* is a vernalization regulator with a high expression level in winter-type rapeseeds (Schiessl et al., 2019). It induces a delayed flowering time in *Arabidopsis* and *Brassica rapa* (Kim et al., 2007), but also in *B. napus* (Tadege et al., 2001). However, *FLC* could be repressed by *FVE* genes which act on the regulation of flowering time (Baek et al., 2008; Yu et al., 2016). *EMB (EMBRYO DEFECTIVE) is* required for growth and development in *Arabidopsis* (Devic, 2008; Meinke, 2020). In the current study, the particular presence of those genes in the seeds indicated their importance at an early stage of plant formation.

The expression and structural variation analysis of the genes in eight rapeseed varieties showed that some genes which had 100% sequence identity displayed different expression profiles, and some other genes with different sequences identity showed similar expression profiles. Note that Vector NTI software (Invitrogen) was used to calculate the sequence identity, and it was observed that even with a large structural variation, the software still displayed a 100% of sequence identity between the genes, which was unexpected. However, genes with several SNPs had less than 100% of sequence identity. Several SNPs (case of *KASI*) and a large structure variation (case of *MCAT* genes) in the candidate genes were observed, which might explain the difference in expression. This probably implied that trait variations possibly occur because of the structure and expression variation of the candidate genes, which can be verified in future studies.

Epigenetics is one of the factors which might cause an alteration in gene expression while preserving the primary DNA sequence or genotype (Bird, 2002; Tchurikov, 2005). Epigenetic mechanisms include DNA methylation which commonly induces gene silencing by blocking the transcription binding sites, histone modification which alters chromatin structure and accessibility of genes for transcription, and non-coding RNA-associated gene silencing which targets mRNA transcripts for destruction induce and preserve epigenetic change (Egger et al., 2004; Tirado, 2014). Even if an epigenetic change is natural and regular, it can also be influenced by environmental factors (Aguilera et al., 2010; Feil and Fraga, 2012). In the case of our study, further analysis is needed to conclude about epigenetic *via* comparison of promoter sequence between genes. Because the full genomic sequences are absent in Brassica napus pan-genome information resource (BnPIR), the analysis could not be done in the current study. Also, the eight accessions were produced with different genetic and environmental backgrounds, and the age of plant materials also plays a role in gene expression. Thus, the difference in the gene expression even with a similar sequence was expected.

Breeding a Super-Rapeseed Cultivar That Meets Expectations

The current study uncovered regions, with two, three, four, or five categories of traits that can be chosen and used for marker-assisted selection, to produce a customized rapeseed cultivar with desired traits. For instance, stresses imposed by heat are detrimental to seed yield and quality (reviewed by Sehgal et al., 2018). To control these traits at once, the region on A3 (11.40–12.47 Mb) could be selected for fine-mapping, since it contained overlapping QTLs for heat, seed yield, and seed composition. Candidate genes included in this region could be cloned and validated through functional analysis, to understand the related molecular mechanism.

Another innovation of the current study is the usage of the rapeseed pan-genome of BnPIR to compare the gene expression and gene structure of candidate genes. This strategy aimed to comprehend how the same genes of different accessions would be expressed, and how their structures are different. This might serve later to explain their functions. Since numerous rapeseed accessions have been sequenced, performing the same study as our current study is now feasible in those other accessions. It would enhance our understanding of rapeseed genome variation. In the future, it would be interesting to know whether the QTLs of multiple traits could also be found overlapping in the same region of the other rapeseed varieties, as found in *Darmor-bzh* of this study. It is important to discover if the regions were maintained in all the varieties of rapeseed. The characterization of haplotypes is also needed to understand if those regions could be inherited together.

Besides, compared to rice, the rapeseed breeding program needs more effort and innovation. Until now, rapeseed research focused on QTLs and the studied traits were repetitive. However, the rice breeding program already focuses on QTG (quantitative trait gene) and QTN (quantitative trait nucleotide) for the improvement of this crop (Wei et al., 2021). This effort was made to further close the gap between genomic studies and practical breeding, and to facilitate the localization of causative variants of all known traits. A collection of rice varieties with those variations was made and a genome navigation system was established for

breeding. Thus, research on rapeseed should switch progressively into those QTG and QTN analyses. Multiple rapeseed accessions are also available and a collection of variations should be implanted for breeding.

Finally, the current study has enhanced our knowledge of rapeseed genome characteristics and diversity. Co-localized QTLs might have an ally or antagonistic effect. For the usage in practical breeding, identification of the most favorable alleles combinations which will produce maximum profits is still crucial.

MATERIALS AND METHODS

Alignment of Quantitative Trait Locus on the Physical Map of *Darmor-bzh*

Extensive literature inquiry allowed us to identify more than 350 papers that reported on genome-wide association studies (GWAS) and QTLs analyses in *B. napus* over the last 25 years (1995–2020). They were manually sorted according to data availability. Research articles with missing information were removed (absence of flanking markers, marker sequence, or physical position of QTLs on *Darmor-bzh*). QTLs/GWAS with just one flanking marker were kept and given an area of 1 cm from the unique marker as loci. A total of 4,555 QTLs for seed, yield, hormones, and disease-related traits were collected from 145 research articles, involving 79 different populations of three different ecotypes and grown in 12 different countries (**Supplementary Table 1**). They were aligned in the physical map of *Darmor-bzh*. The location of QTLs flanking markers on the physical map was detected via e-PCR (Schuler, 1997; Rotmistrovsky et al., 2004), and the method of alignment was as similar as our previous studies (Raboanatahiry et al., 2017, 2018). The map was built using Circos software (Krzywinski et al., 2009).

Identification of Candidate Genes

Genes in *B. napus* which were reported in three different pieces of literature were selected as a basis for the identification of candidate genes in the current study: 439 genes were related to oil formation (Raboanatahiry et al., 2017), 1,398 genes were related to yield traits (Raboanatahiry et al., 2018), and 1,344 genes were resistance genes (Dolatabadian et al., 2017). They were aligned into the physical map of *Darmor-bzh*, and the genes located within overlapping QTLs were identified as candidates for the traits.

Construction of Gene Interaction Network

The gene interaction network was predicted using STRING (Szklarczyk et al., 2015).[1] Orthologous genes in *A. thaliana* were used to perform the analysis (Chao et al., 2017; Raboanatahiry et al., 2017, 2018). The genes were clustered using Panther GO-slim biological process (Mi et al., 2021),[2] and the interaction was visualized with Cytoscape_V3.6.0 (Shannon et al., 2003).

Gene Expression and Structural Variation Analyses of Candidate Genes

The gene expression was obtained from BnTIR (Liu et al., 2021), because *ZS11* is the only rapeseed variety available in the BnTIR database, it was used as a reference for this analysis. *ZS11* genes were acquired from the BnPIR database (Song et al., 2021) and the genes expression analysis was obtained from the BnTIR database (Liu et al., 2021). The heatmap was built using Heatmapper (Babicki et al., 2016).[3] The developing siliques and the seeds of *KenC-8* were collected 30 days after flowering for the q-PCR analysis, and *Actin7* was used as an internal control.

The identification of homologous candidate genes in *Gangan, No2127, Quinta, Shengli, Tapidor, Westar, Zheyou7,* and *ZS11* was made with a blast tool in the BnPIR database (Song et al., 2021),[4] using *Darmor-bzh* gene sequences as a query sequence. *In silico* gene expression analysis was made using the "gene expression" tool of BnPIR. The identity percentage between CDS sequences was calculated using Vector NTI Advance 11.5.1.

DATA AVAILABILITY STATEMENT

The original contributions presented in the study are included in the article/**Supplementary Material**, further inquiries can be directed to the corresponding author/s.

AUTHOR CONTRIBUTIONS

NR wrote the manuscript. NR and HC performed the analysis of the QTL alignment map and candidate genes identification. NR and JH made the synteny analysis and the gene interaction network. NR, HL, and YY analyzed the gene expression. ML supervised the work and revised the manuscript. All authors contributed to the article and approved the submitted version.

FUNDING

This work was funded by the National Natural Science Foundation of China (31871656, 32072098, 31701456, and 32172087) and the China Postdoctoral Science Foundation (2016M602309).

SUPPLEMENTARY MATERIAL

The Supplementary Material for this article can be found online at: https://www.frontiersin.org/articles/10.3389/fpls.2022.862363/full#supplementary-material

[1] http://string-db.org/

[2] http://pantherdb.org/

[3] http://www2.heatmapper.ca/

[4] http://cbi.hzau.edu.cn/bnapus/

REFERENCES

Aguilera, O., Fernández, A. F., Muñoz, A., and Fraga, M. F. (2010). Epigenetics and environment: a complex relationship. *J. Appl. Physiol.* 109, 243–251. doi: 10.1152/japplphysiol.00068.2010

Al-Shehbaz, P. I. A., Beilstein, M. A., and Kellogg, E. (2006). Systematics and phylogeny of the *Brassicaceae (Cruciferae)*: an overview. *Plant Systemat. Evolut.* 259, 89–120. doi: 10.1007/s00606-006-0415-z

Amar, S., Becker, H. C., and Möllers, C. (2009). Genetic variation in phytosterol content of winter rapeseed (*Brassica napus L.*) and development of NIRS calibration equations. *Plant Breed.* 128, 78–83. doi: 10.1111/j.1439-0523.2008.01531

Arifuzzaman, M., Mamidi, S., McClean, P., and Rahman, M. (2016). QTL mapping for root vigor and days to flowering in *Brassica napus L. Can. J. Plant Sci.* 97, 99–109. doi: 10.1139/cjps-2016-0048

Asghari, A., Asghar Fathi, A., Mohammadi, S. A., and Mohammaddust, H. (2009). QTL analysis for diamondback moth resistance in canola (*Brassica napus L.*). *Int. J. Plant Product.* 3, 29–34. doi: 10.22069/IJPP.2012.649

Babicki, S., Arndt, D., Marcu, A., Liang, Y., Grant, J. R., Maciejewski, A., et al. (2016). Heatmapper: web-enabled heat mapping for all. *Nucleic Acids Res.* 44, W147–W153. doi: 10.1093/nar/gkw419

Baek, I. S., Park, H. Y., You, M. K., Lee, J. H., and Kim, J. K. (2008). Functional conservation and divergence of *FVE* genes that control flowering time and cold response in rice and Arabidopsis. *Mol. Cells* 26, 368–372.

Bao, B., Chao, H., Wang, H., Zhao, W., Zhang, L., Raboanatahiry, N., et al. (2018). Stable, environmental specific and novel QTL identification as well as genetic dissection of fatty acid metabolism in *Brassica napus*. *Front. Plant Sci.* 9:1018. doi: 10.3389/fpls.2018.01018

Basnet, R. K., Duwal, A., Tiwari, D. N., Xiao, D., Monakhos, S., Bucher, J., et al. (2015). Quantitative Trait Locus Analysis of Seed Germination and Seedling Vigor in *Brassica rapa* Reveals QTL Hotspots and Epistatic Interactions. *Front. Plant Sci.* 6:1032. doi: 10.3389/fpls.2015.01032

Basunanda, P., Radoev, M., Ecke, W., Friedt, W., Becker, H. C., and Snowdon, R. J. (2010). Comparative mapping of quantitative trait loci involved in heterosis for seedling and yield traits in oilseed rape (*Brassica napus L.*). *Theoret. Appl. Genet.* 120:271. doi: 10.1007/s00122-009-1133-z

Basunanda, P., Spiller, T. H., Hasan, M., Gehringer, A., Schondelmaier, J., Lühs, W., et al. (2007). Marker-assisted increase of genetic diversity in a double-low seed quality winter oilseed rape genetic background. *Plant Breed.* 126, 581–587. doi: 10.1111/j.1439-0523.2007.01404.x

Bayer, P. E., Hurgobin, B., Golicz, A. A., Chan, C. K., Yuan, Y., Lee, H., et al. (2017). Assembly and comparison of two closely related *Brassica napus* genomes. *Plant Biotechnol. J.* 15, 1602–1610. doi: 10.1111/pbi.12742

Behnke, N., Suprianto, E., and Mollers, C. (2018). A major QTL on chromosome C05 significantly reduces acid detergent lignin (ADL) content and increases seed oil and protein content in oilseed rape (*Brassica napus L.*). *Theoret. Appl. Genet* 131, 2477–2492. doi: 10.1007/s00122-018-3167-6

Beilstein, M. A., Al-Shehbaz, I. A., and Kellogg, E. A. (2006). *Brassicaceae* phylogeny and trichome evolution. *Am. J. Bot.* 93, 607–619. doi: 10.3732/ajb.93.4.607

Bird, A. (2002). DNA methylation patterns and epigenetic memory. *Genes Devel.* 16, 6–21. doi: 10.1101/gad.947102

Bouchet, A. S., Laperche, A., Bissuel-Belaygue, C., Baron, C., Morice, J., Rousseau-Gueutin, M., et al. (2016). Genetic basis of nitrogen use efficiency and yield stability across environments in winter rapeseed. *BMC Genetics* 17:131. doi: 10.1186/s12863-016-0432-z

Bray, E. A., Bailey-Serres, J., and Weretilnyk, E. (2000). "Responses to abiotic stress," in *Biochemistry and Molecular Biology of Plants*, eds W. Gruissem and R. Jones (Rockville: American Society of Plant Physiologists), 1158–1203.

Butruille, D. V., Guries, R. P., and Osborn, T. C. (1999). Linkage analysis of molecular markers and quantitative trait loci in populations of inbred backcross lines of *Brassica napus L. Genetics* 153, 949–964. doi: 10.1093/genetics/153.2.949

Cao, F. Y., Yoshioka, K., and Desveaux, D. (2011). The roles of ABA in plant–pathogen interactions. *J. Plant Res.* 124, 489–499. doi: 10.1007/s10265-011-0409-y

Cao, Z., Tian, F., Wang, N., Jiang, C., Lin, B., Xia, W., et al. (2010). Analysis of QTLs for erucic acid and oil content in seeds on A8 chromosome and the linkage drag between the alleles for the two traits in *Brassica napus*. *J. Genet. Genom.* 37, 231–240. doi: 10.1016/S1673-8527(09)60041-2

Chalhoub, B., Denoeud, F., Liu, S., Parkin, I. A., Tang, H., Wang, X., et al. (2014). Early allopolyploid evolution in the post-Neolithic *Brassica napus* oilseed genome. *Science* 345, 950–953. doi: 10.1126/science.1253435

Chao, H., Raboanatahiry, N., Wang, X., Zhao, W., Chen, L., Guo, L., et al. (2019). Genetic dissection of harvest index and related traits through genome-wide quantitative trait locus mapping in *Brassica napus L. Breed. Sci.* 69, 104–116. doi: 10.1270/jsbbs.18115

Chao, H., Wang, H., Wang, X., Guo, L., Gu, J., Zhao, W., et al. (2017). Genetic dissection of seed oil and protein content and identification of network associated with oil content in *Brassica napus*. *Scient. Rep.* 7:46295. doi: 10.1038/srep46295

Chen, F., Zhang, W., Yu, K., Sun, L., Gao, J., Zhou, X., et al. (2018). Unconditional and conditional QTL analyses of seed fatty acid composition in *Brassica napus L. BMC Plant Biol.* 18:49. doi: 10.1186/s12870-018-1268-7

Chen, G., Geng, J., Rahman, M., Liu, X., Tu, J., Fu, T., et al. (2010). Identification of QTL for oil content, seed yield, and flowering time in oilseed rape (*Brassica napus*). *Euphytica* 175, 161–174. doi: 10.1007/s10681-010-0144-9

Chen, W., Zhang, Y., Liu, X., Chen, B., Tu, J., and Tingdong, F. (2007). Detection of QTL for six yield-related traits in oilseed rape (*Brassica napus*) using DH and immortalized F2 populations. *Theoret. Appl. Genet.* 115, 849–858. doi: 10.1007/s00122-007-0613-2

Chen, Y., Qi, L., Zhang, X., Huang, J., Wang, J., Chen, H., et al. (2013). Characterization of the quantitative trait locus OilA1 for oil content in *Brassica napus*. *Theoret. Appl. Genet.* 126, 2499–2509. doi: 10.1007/s00122-013-2150-5

Cheng, X., Xia, S., Zeng, X., Gu, J., Yang, Y., Xu, J., et al. (2016). Identification of quantitative trait loci associated with oil content and development of near isogenic lines for stable *qOC-A10* in *Brassica napus L. Can. J. Plant Sci.* 96, 423–432. doi: 10.1139/cjps-2014-0442

Cheverud, J. M., and Routman, E. J. (1996). Epistasis as a source of increased additive genetic variance at population bottlenecks. *Evolution* 50, 1042–1051. doi: 10.1111/j.1558-5646.1996.tb02345.x

Conner, J. K., Karoly, K., Stewart, C., Koelling, V. A., Sahli, H. F., and Shaw, F. H. (2011). Rapid independent trait evolution despite a strong pleiotropic genetic correlation. *Am. Natural.* 178, 429–441. doi: 10.1086/661907

Delourme, R., Falentin, C., Huteau, V., Clouet, V., Horvais, R., Gandon, B., et al. (2006). Genetic control of oil content in oilseed rape (*Brassica napus L.*). *Theoret. Appl. Genet.* 113, 1331–1345. doi: 10.1007/s00122-006-0386-z

Delourme, R., Piel, N., Horvais, R., Pouilly, N., Domin, C., Vallée, P., et al. (2008). Molecular and phenotypic characterization of near isogenic lines at QTL for quantitative resistance to *Leptosphaeria maculans* in oilseed rape (*Brassica napus L.*). *Theory Appl. Genet.* 117, 1055–1067. doi: 10.1007/s00122-008-0844-x

Devic, M. (2008). The importance of being essential: EMBRYO-DEFECTIVE genes in Arabidopsis. *Compt. Rendus Biol.* 331, 726–736. doi: 10.1016/j.crvi.2008.07.014

Di, F., Wang, T., Ding, Y., Chen, X., Wang, H., Li, J., et al. (2020). Genetic mapping combined with a transcriptome analysis to screen for candidate genes responsive to abscisic acid treatment in *Brassica napus* embryos during seed germination. *DNA Cell Biol.* 39, 533–547. doi: 10.1089/dna.2019.5169

Ding, G. D., Zhao, Z. K., Wang, L., Zhang, D., Shi, L., and Xu, F. (2014). Identification and multiple comparisons of QTL and epistatic interaction conferring high yield under boron and phosphorus deprivation in *Brassica napus*. *Euphytica* 198, 337–351. doi: 10.1007/s10681-014-1110-8

Ding, X. Y., Xu, J. S., Huang, H., Ding, X., Xu, J., Huang, H., et al. (2020). Unraveling waterlogging tolerance-related traits with QTL analysis in reciprocal intervarietal introgression lines using genotyping by sequencing in rapeseed (*Brassica napus L.*). *J. Integr. Agricult.* 19, 1974–1983. doi: 10.1016/S2095-3119(19)62783-8

Dolatabadian, A., Patel, D. A., Edwards, D., and Batley, J. (2017). Copy number variation and disease resistance in plants. *Theor. Appl. Genet.* 130, 2479–2490. doi: 10.1007/s00122-017-2993-2

Duan, X., Wang, X., Jin, K., Wang, W., Liu, H., Liu, L., et al. (2019). Genetic dissection of root architectural traits by QTL and genome-wide association mapping in rapeseed (*Brassica napus*). *Plant Breed.* 138, 184–192. doi: 10.1111/pbr.12665

Egger, G., Liang, G., Aparicio, A., and Jones, P. A. (2004). Epigenetics in human disease and prospects for epigenetic therapy. *Nature* 429, 457–463. doi: 10.1038/nature02625

Elahi, N., Duncan, R. W., and Stasolla, C. (2015). Decreased seed oil production in *FUSCA3* Brassica napus mutant plants. *Plant Physiol. Biochem.* 96, 222–230. doi: 10.1016/j.plaphy.2015.08.002

Fan, C., Cai, G., Qin, J., Li, Q., Yang, M., Wu, J., et al. (2010). Mapping of quantitative trait loci and development of allele-specific markers for seed weight in *Brassica napus*. *Theoret. Appl. Genet.* 121, 1289–1301. doi: 10.1007/s00122-010-1388-4

Feil, R., and Fraga, M. (2012). Epigenetics and the environment: emerging patterns and implications. *Nat. Rev. Genet.* 13, 97–109. doi: 10.1038/nrg3142

Fitt, B. D. L., Hu, B. C., Li, Z. Q., Liu, S. Y., Lange, R. M., Kharbanda, P. D., et al. (2008). Strategies to prevent spread of *Leptosphaeria maculans* (phoma stem canker) onto oilseed rape crops in China, costs and benefits. *Plant Pathol.* 57, 652–664. doi: 10.1111/j.1365-3059.2008.01841.x

Frank, S. A. (2003). Genetic variation of polygenic characters and the evolution of genetic degeneracy. *J. Evolut. Biol.* 16, 138–142. doi: 10.1046/j.1420-9101.2003.00485.x

Fu, Y., Wei, D., Dong, H., He, Y., Cui, Y., Mei, J., et al. (2015). Comparative quantitative trait loci for silique length and seed weight in *Brassica napus*. *Scient. Rep.* 5:14407. doi: 10.1038/srep14407

Fu, Y., Zhang, D. Q., Gleeson, M., Zhang, Y., Lin, B., Hua, S., et al. (2017). Analysis of QTL for seed oil content in *Brassica napus* by association mapping and QTL mapping. *Euphytica* 17:123. doi: 10.1007/s10681-016-1817-9

Fujita, M., Fujita, Y., Noutoshi, Y., Takahashi, F., Narusaka, Y., Yamaguchi-Shinozaki, K., et al. (2006). Crosstalk between abiotic and biotic stress responses: a current view from the points of convergence in the stress signaling networks. *Curr. Opin. Plant Biol.* 9, 436–442. doi: 10.1016/j.pbi.2006.05.014

Gabur, I., Chawla, H. S., Lopisso, D. T., von Tiedemann, A., Snowdon, R. J., and Obermeier, C. (2020). Gene presence-absence variation associates with quantitative *Verticillium longisporum* disease resistance in *Brassica napus*. *Scient. Rep.* 10:4131. doi: 10.1038/s41598-020-61228-3

Gan, L., Zhang, C. Y., Wang, X. D., Wang, H., Long, Y., Yin, Y. T., et al. (2013). Proteomic and comparative genomic analysis of two *Brassica napus* lines differing in oil content. *J. Proteom. Res.* 12, 4965–4978. doi: 10.1021/pr4005635

Garbers, C., DeLong, A., Deruére, J., Bernasconi, P., and Söll, D. (1996). A mutation in protein phosphatase 2A regulatory subunit A affects auxin transport in *Arabidopsis*. *EMBO J.* 15, 2115–2124. doi: 10.1002/j.1460-2075.1996.tb00565.x

Getinet, A., Rakow, G., and Downey, R. K. (1996). Agronomic performance and seed quality of Ethiopian mustard in Saskatchewan. *Can. J. Plant Sci.* 76, 387–392. doi: 10.4141/cjps96-069

Goodnight, C. J. (1988). Epistasis and the effect of founder events on the additive genetic variance. *Evolution* 42, 441–454. doi: 10.1111/j.1558-5646.1988.tb04151.x

Gromko, M. H. (1987). Genetic constraint on the evolution of courtship behavior in *Drosophila melanogaster*. *Heredity* 3:58. doi: 10.1038/hdy.1987.72

Grossmann, K. (2010). Auxin herbicides: current status of mechanism and mode of action. *Pest Manage Sci.* 66, 113–120. doi: 10.1002/ps.1860

Guan, M., Huang, X., Xiao, Z., Jia, L., Wang, S., Zhu, M., et al. (2019). Association mapping analysis of fatty acid content in different ecotypic rapeseed using mrMLM. *Front. Plant Sci.* 9:1872. doi: 10.3389/fpls.2018.01872

Gugel, P. K., and Petrie, G. A. (1992). History, occurrence, impact and control of blackleg of rapeseed. *Can. J. Plant Pathol.* 14, 36–45. doi: 10.1080/07060669209500904

Gyawali, S., Harrington, M., Durkin, J., Horner, K., Parkin, I. A., Hegedus, D. D., et al. (2016). Microsatellite markers used for genome-wide association mapping of partial resistance to *Sclerotinia sclerotiorum* in a world collection of *Brassica napus*. *Mol. Breed.* 36:72. doi: 10.1007/s11032-016-0496-5

Hackenberg, D., Asare-Bediako, E., Baker, A., Walley, P., Jenner, C., Greer, S., et al. (2020). Identification and QTL mapping of resistance to Turnip yellows virus (TuYV) in oilseed rape *Brassica napus*. *Theory Appl. Genet.* 133, 383–393. doi: 10.1007/s00122-019-03469-z

Hajduch, M., Casteel, J. E., Hurrelmeyer, K. E., Song, Z., Agrawal, G. K., and Thelen, J. J. (2006). Proteomic analysis of seed filling in *Brassica napus*. *Plant Physiol.* 141, 32–46. doi: 10.1104/pp.105.075390

Hansen, T. F., and Wagner, G. P. (2001). Modeling genetic architecture: a multilinear theory of gene interaction. *Theoret. Populat. Biol.* 59, 61–86. doi: 10.1006/tpbi.2000.1508

He, Y., Wu, D., Wei, D., Fu, Y., Cui, Y., Dong, H., et al. (2017). GWAS, QTL mapping and gene expression analyses in *Brassica napus* reveal genetic control of branching morphogenesis. *Scient. Rep.* 7:15971. doi: 10.1038/s41598-017-15976-4

Hua, Y., Zhang, D., Zhou, T., He, M., Ding, G., Shi, L., et al. (2016a). Transcriptomics-assisted quantitative trait locus fine mapping for the rapid identification of a nodulin 26-like intrinsic protein gene regulating boron efficiency in allotetraploid rapeseed. *Plant Cell Environ.* 39, 1601–1618. doi: 10.1111/pce.12731

Hua, Y., Zhou, T., Ding, G., Yang, Q., Shi, L., and Xu, F. (2016b). Physiological, genomic and transcriptional diversity in responses to boron deficiency in rapeseed genotypes. *J. Exp. Bot.* 67, 5769–5784. doi: 10.1093/jxb/erw342

Huang, C., Yang, M., Shao, D., Wang, Y., Wan, S., He, J., et al. (2020). Fine mapping of the BnUC2 locus related to leaf up-curling and plant semi-dwarfing in *Brassica napus*. *BMC Genomics* 21:530. doi: 10.1186/s12864-020-06947-7

Huang, J., Chen, F., Zhang, H., Ni, X., Wang, Y., Liu, H., et al. (2017). Dissection of additive, epistatic and QTL × environment effects involved in oil content variations in rapeseed. *Plant Breed.* 136, 728–737. doi: 10.1111/pbr.12522

Huang, Y. J., Jestin, C., Welham, S. J., King, G. J., Manzanares-Dauleux, M. J., Fitt, B. D., et al. (2016). Identification of environmentally stable QTL for resistance against *Leptosphaeria maculans* in oilseed rape *(Brassica napus)*. *Theory Appl. Genet.* 129, 169–180. doi: 10.1007/s00122-015-2620-z

Huang, Y. J., Paillard, S., Kumar, V., King, G. J., Fitt, B. D. L., and Delourme, R. (2019). Oilseed rape *(Brassica napus*) resistance to growth of Leptosphaeria maculans in leaves of young plants contributes to quantitative resistance in stems of adult plants. *PLoS One* 14:e0222540. doi: 10.1371/journal.pone.0222540

Jan, H. U., Guan, M., Yao, M., Liu, W., Wei, D., Abbadi, A., et al. (2019). Genome-wide haplotype analysis improves trait predictions in *Brassica napus* hybrids. *Plant Sci.* 283, 157–164. doi: 10.1016/j.plantsci.2019.02.007

Javed, N., Geng, J., Tahir, M., McVetty, P. B. E., Li, G., and Duncan, R. W. (2016). Identification of QTL influencing seed oil content, fatty acid profile and days to flowering in *Brassica napus L. Euphytica* 191:207. doi: 10.1007/s10681-015-1565-2

Jian, H., Zhang, A., Ma, J., Wang, T., Yang, B., Shuang, L. S., et al. (2019). Joint QTL mapping and transcriptome sequencing analysis reveal candidate flowering time genes in *Brassica napus L. BMC Genomics* 20:21. doi: 10.1186/s12864-018-5356-8

Jiang, C., Shi, J., Li, R., Long, Y., Wang, H., Li, D., et al. (2014). Quantitative trait loci that control the oil content variation of rapeseed (*Brassica napus L.*). *Theoret. Appl. Genet.* 127, 957–968. doi: 10.1007/s00122-014-2271-5

Kaur, S., Cogan, N. O., Ye, G., Baillie, R. C., Hand, M. L., Ling, A. E., et al. (2009). Genetic map construction and QTL mapping of resistance to blackleg (*Leptosphaeria maculans*) disease in Australian canola (*Brassica napus L.*) cultivars. *Theory Appl. Genet.* 120, 71–83. doi: 10.1007/s00122-009-1160-9

Kebede, B., and Rahman, H. (2019). QTL mapping of root and aboveground biomass in the Brassica C genome using a *B. napus* population carrying genome content introgressed from *B. oleracea*. *Mol. Breed.* 39:169. doi: 10.1007/s11032-019-1064-6

Khan, S. U., Jiao, Y. M., Liu, S., Zhang, K., Khan, M. H. U., Zhai, Y., et al. (2019). Genome-wide association studies in the genetic dissection of ovule number, seed number, and seed weight in *Brassica napus L. Industr. Crops Products* 142:111877. doi: 10.1016/j.indcrop.2019.111877

Khanzada, H., Wassan, G. M., He, H., Mason, A. S., Keerio, A. A., Khanzada, S., et al. (2020). Differentially evolved drought stress indices determine the genetic variation of *Brassica napus* at seedling traits by genome-wide association mapping. *J. Adv. Res.* 24, 447–461. doi: 10.1016/j.jare.2020.05.019

Kim, S. Y., Park, B. S., Kwon, S. J., Kim, J., Lim, M. H., Park, Y. D., et al. (2007). Delayed flowering time in Arabidopsis and Brassica rapa by the overexpression of FLOWERING LOCUS C (FLC) homologs isolated from Chinese cabbage (*Brassica rapa L.: ssp Pekinensis*). *Plant Cell Rep.* 26, 327–336. doi: 10.1007/s00299-006-0243-1

Knoch, D., Abbadi, A., Grandke, F., Meyer, R. C., Samans, B., Werner, C. R., et al. (2020). Strong temporal dynamics of QTL action on plant growth progression

revealed through high-throughput phenotyping in canola. *Plant Biotechnol. J.* 18, 68–82. doi: 10.1111/pbi.13171

Körber, N., Bus, A., Li, J., Parkin, I. A., Wittkop, B., Snowdon, R. J., et al. (2016). Agronomic and seed quality traits dissected by genome-wide association mapping in *Brassica napus*. *Front. Plant Sci.* 7:386. doi: 10.3389/fpls.2016.00386

Krzywinski, M., Schein, J., Birol, I., Connors, J., Gascoyne, R., Horsman, D., et al. (2009). Circos: An information aesthetic for comparative genomics. *Genome Res. Adv.* 19, 1639–1645. doi: 10.1101/gr.092759.109

Kumar, V., Paillard, S., Fopa-Fomeju, B., Falentin, C., Deniot, G., Baron, C., et al. (2018). Multi-year linkage and association mapping confirm the high number of genomic regions involved in oilseed rape quantitative resistance to blackleg. *Theory Appl. Genet.* 131, 1627–1643. doi: 10.1007/s00122-018-3103-9

Kutcher, H. R., Yu, F., and Brun, H. (2010). Improving blackleg disease management of *Brassica napus* from knowledge of genetic interactions with *Leptosphaeria maculans*. *Can. J. Plant Pathol.* 32, 29–34. doi: 10.1080/07060661003620961

Larkan, N. J., Raman, H., Lydiate, D. J., Robinson, S. J., Yu, F., Barbulescu, D. M., et al. (2016). Multi-environment QTL studies suggest a role for cysteine-rich protein kinase genes in quantitative resistance to blackleg disease in *Brassica napus*. *BMC Plant Biol.* 16:183. doi: 10.1186/s12870-016-0877-2

Li, B., Gao, J., Chen, J., Wang, Z., Shen, W., Yi, B., et al. (2020). Identification and fine mapping of a major locus controlling branching in *Brassica napus*. *Theory Appl. Genet.* 133, 771–783. doi: 10.1007/s00122-019-03506-x

Li, B., Zhao, W., Li, D., Chao, H., Zhao, X., Ta, N., et al. (2018). Genetic dissection of the mechanism of flowering time based on an environmentally stable and specific QTL in *Brassica napus*. *Plant Sci.* 277, 296–310. doi: 10.1016/j.plantsci.2018.10.005

Li, F., Chen, B., Xu, K., Gao, G., Yan, G., Qiao, J., et al. (2016b). A genome-wide association study of plant height and primary branch number in rapeseed (*Brassica napus*). *Plant Sci.* 242, 169–177. doi: 10.1016/j.plantsci.2015.05.012

Li, J. Q., Zhao, Z. K., Hayward, A., Cheng, H., and Fu, D. (2015). Integration analysis of quantitative trait loci for resistance to *Sclerotinia sclerotiorum* in *Brassica napus*. *Euphytica* 205, 483–489. doi: 10.1007/s10681-015-1417-0

Li, L., Luo, Y., Chen, B., Xu, K., Zhang, F., Li, H., et al. (2016a). A Genome-Wide Association Study Reveals New Loci for Resistance to Clubroot Disease in *Brassica napus*. *Front. Plant Sci.* 7:1483. doi: 10.3389/fpls.2016.01483

Li-Beisson, Y., Shorrosh, B., Beisson, F., Andersson, M. X., Arondel, V., Bates, P. D., et al. (2013). Acyl-lipid metabolism. *Arabidopsis Book* 11:e0161. doi: 10.1199/tab.0161

Liu, D., Yu, L., Wei, L., Yu, P., Wang, J., Zhao, H., et al. (2021). BnTIR: an online transcriptome platform for exploring RNA-seq libraries for oil crop *Brassica napus*. *Plant Biotechnol. J.* 19, 1895–1897. doi: 10.1111/pbi.13665

Liu, J., Wang, J., Wang, H., Wang, W., Zhou, R., Mei, D., et al. (2016). Multigenic control of pod shattering resistance in Chinese rapeseed germplasm revealed by genome-wide association and linkage analyses. *Front. Plant Sci.* 7:1058. doi: 10.3389/fpls.2016.01058

Liu, J., Wang, W., Mei, D., Wang, H., Fu, L., Liu, D., et al. (2016). Characterizing variation of branch angle and genome-wide association mapping in rapeseed (*Brassica napus L.*). *Front. Plant Sci.* 7:21. doi: 10.3389/fpls.2016.00021

Liu, S., Fan, C., Li, J., Cai, G., Yang, Q., Wu, J., et al. (2016). A genome wide association study reveals novel elite allelic variations in seed oil content of *Brassica napus*. *Theoret. Appl. Genet.* 129, 1203–1215. doi: 10.1007/s00122-016-2697-z

Liu, Y., Zhou, X., Yan, M., Wang, P., Wang, H., Xin, Q., et al. (2020). Fine mapping and candidate gene analysis of a seed glucosinolate content QTL, *qGSL-C2*, in rapeseed (*Brassica napus L.*). *Theory Appl. Genet.* 133, 479–490. doi: 10.1007/s00122-019-03479-x

Lu, K., Peng, L., Zhang, C., Lu, J., Yang, B., Xiao, Z., et al. (2017). Genome-wide association and transcriptome analyses reveal candidate genes underlying yield-determining traits in *Brassica napus*. *Front. Plant Sci.* 8:206. doi: 10.3389/fpls.2017.00206

Lu, K., Wei, L., Li, X., Wang, Y., Wu, J., Liu, M., et al. (2019). Whole-genome resequencing reveals *Brassica napus* origin and genetic loci involved in its improvement. *Nat. Commun.* 10:1154. doi: 10.1038/s41467-019-09134-9

Luo, Z., Wang, M., Long, Y., Huang, Y., Shi, L., Zhang, C., et al. (2017). Incorporating pleiotropic quantitative trait loci in dissection of complex traits: seed yield in rapeseed as an example. *Theoret. Appl. Genet.* 130, 1569–1585. doi: 10.1007/s00122-017-2911-7

Lynch, M., and Walsh, B. (1998). *Genetics and Analysis of Quantitative Traits*. Sunderland, MA: Sinauer Associates, .

Meinke, D. W. (2020). Genome-wide identification of EMBRYO-DEFECTIVE (EMB) genes required for growth and development in *Arabidopsis*. *New Phytol.* 226, 306–325. doi: 10.1111/nph.16071

Mi, H., Ebert, D., Muruganujan, A., Mills, C., Albou, L. P., Mushayamaha, T., et al. (2021). PANTHER version 16: a revised family classification, tree-based classification tool, enhancer regions and extensive API. *Nucleic Acids Res.* 49, D394–D403. doi: 10.1093/nar/gkaa1106

Muday, G. K., Brady, S. R., Argueso, C., Deruère, J., Kieber, J. J., and DeLong, A. (2006). RCN1-regulated phosphatase activity and EIN2 modulate hypocotyl gravitropism by a mechanism that does not require ethylene signaling. *Plant Physiol.* 141, 1617–1629. doi: 10.1104/pp.106.083212

Nguyen, T. C. T., Abrams, S. R., Friedt, W., and Snowdon, R. J. (2018). Quantitative trait locus analysis of seed germination, seedling vigour and seedling-regulated hormones in *Brassica napus*. *Plant Breed.* 137, 388–401. doi: 10.1111/pbr.12576

Paran, I., and Zamir, D. (2003). Quantitative traits in plants: beyond the QTL. *Trends Genet.* 19, 303–306. doi: 10.1016/S0168-9525(03)00117-3

Poole, R. L. (2007). The TAIR database. *Methods Mol. Biol.* 406, 179–212. doi: 10.1007/978-1-59745-535-0_8

Qasim, M. U., Zhao, Q., Shahid, M., Samad, R. A., Ahmar, S., Wu, J., et al. (2020). Identification of QTLs Containing resistance genes for Sclerotinia stem rot in *Brassica napus* using comparative transcriptomic studies. *Front. Plant Sci.* 11:776. doi: 10.3389/fpls.2020.00776

Qi, L., Mao, L., Sun, C., Pu, Y., Fu, T., Ma, C., et al. (2014). Interpreting the genetic basis of silique traits in *Brassica napus* using a joint QTL network. *Plant Breed.* 133, 52–60. doi: 10.1111/pbr.12131

Qian, L., Qian, W., and Snowdon, R. J. (2014). Sub-genomic selection patterns as a signature of breeding in the allopolyploid *Brassica napus* genome. *BMC Genomics* 15:1170. doi: 10.1186/1471-2164-15-1170

Qu, C., Jiang, H., and Zhang, L. (2014). Cloning and Enzymatic Activity Analysis of the Malonyl-CoA:acyl Carrier Protein Transacylase in *Brassica napus* Cultivars with Different Oil Content. *Am. J. Plant Sci.* 5, 2599–2610. doi: 10.4236/ajps.2014.518274

Qu, C., Jia, L., Fu, F., Zhao, H., Lu, K., Wei, L., et al. (2017). Genome-wide association mapping and Identification of candidate genes for fatty acid composition in *Brassica napus L.* using SNP markers. *BMC Genomics* 18:232. doi: 10.1186/s12864-017-3607-8

Quarrie, S. A., Pekic Quarrie, S., Radosevic, R., Rancic, D., Kaminska, A., Barnes, J. D., et al. (2006). Dissecting a wheat QTL for yield present in a range of environments: from the QTL to candidate genes. *J. Exp. Bot.* 57, 2627–2637. doi: 10.1093/jxb/erl026

Quijada, P. A., Udall, J. A., Lambert, B., and Osborn, T. C. (2006). Quantitative trait analysis of seed yield and other complex traits in hybrid spring rapeseed (*Brassica napus L.*): 1. *Theoret. Appl. Genet.* 113, 549–561. doi: 10.1007/s00122-006-0323-1

Qzer, H., Oral, E., and Dogru, U. (1999). Relationships between yield and yield components on currently improved spring rapeseed cultivars. Turkish. *J. Agricult. Forest.* 53, 603–607.

Raboanatahiry, N., Chao, H., Dalin, H., Pu, S., Yan, W., Yu, L., et al. (2018). QTL alignment for seed yield and yield related traits in *Brassica napus*. *Front. Plant Sci.* 9:1127. doi: 10.3389/fpls.2018.01127

Raboanatahiry, N., Chao, H., Guo, L., Gan, J., Xiang, J., Yan, M., et al. (2017). Synteny analysis of genes and distribution of loci controlling oil content and fatty acid profile based on QTL alignment map in *Brassica napus*. *BMC Genomics* 18:776. doi: 10.1186/s12864-017-4176-6

Raboanatahiry, N., Li, H., Yu, L., and Li, M. (2021). Rapeseed (*Brassica napus*): Processing Utilization, and Genetic Improvement. *Agronomy* 11:1776. doi: 10.3390/agronomy11091776

Radoev, M., Becker, H. C., and Ecke, W. (2008). Genetic analysis of heterosis for yield and yield components in rapeseed (*Brassica napus L.*) by quantitative trait locus mapping. *Genetics* 179, 1547–1558. doi: 10.1534/genetics.108.089680

Rahaman, M., Mamidi, S., and Rahman, M. (2018). Genome-wide association study of heat stresstolerance traits in spring-type *Brassica napus L.* under controlled conditions. *Crop J.* 6, 115–125. doi: 10.1016/j.cj.2017.08.003

Rahman, M., Mamidi, S., del Rio, L., Ross, A., Kadir, M. M., Rahaman, M. M., et al. (2016). Association mapping in *Brassica napus (L.)* accessions identifies a major

QTL for blackleg disease resistance on chromosome A01. *Mol. Breed.* 36:90. doi: 10.1007/s11032-016-0513-8

Raman, H., Raman, R., Diffey, S., Qiu, Y., McVittie, B., Barbulescu, D. M., et al. (2018). Stable Quantitative Resistance Loci to Blackleg Disease in Canola *(Brassica napus L.)* Over Continents. *Front. Plant Sci.* 9:1622. doi: 10.3389/fpls.2018.01622

Raman, H., Raman, R., Kilian, A., Detering, F., Long, Y., Edwards, D., et al. (2013). A consensus map of rapeseed (*Brassica napus L.*) based on diversity array technology markers: applications in genetic dissection of qualitative and quantitative traits. *BMC Genomics* 14:277. doi: 10.1186/1471-2164-14-277

Raman, H., Raman, R., McVittie, B., Orchard, B., Qiu, Y., and Delourme, R. (2017). A Major Locus for Manganese Tolerance Maps on Chromosome A09 in a Doubled Haploid Population of *Brassica napus L. Front. Plant Sci.* 8:1952. doi: 10.3389/fpls.2017.01952

Raman, H., Raman, R., Qiu, Y., Yadav, A. S., Sureshkumar, S., Borg, L., et al. (2019). GWAS hints at pleiotropic roles for FLOWERING LOCUS T in flowering time and yield-related traits in canola. *BMC Genomics* 20:636. doi: 10.1186/s12864-019-5964-y

Raman, R., Diffey, S., Barbulescu, D. M., Coombes, N., Luckett, D., Salisbury, P., et al. (2020). Genetic and physical mapping of loci for resistance to blackleg disease in canola *(Brassica napus L.)*. *Scientific Rep.* 10:4416. doi: 10.1038/s41598-020-61211-y

Raman, R., Diffey, S., Barbulescu, D. M., Coombes, N., Luckett, D., Salisbury, P., et al. (2012). Molecular mapping of qualitative and quantitative loci for resistance to *Leptosphaeria maculans* causing blackleg disease in canola (*Brassica napus L.*). *Theory Appl. Genet.* 125, 405–418. doi: 10.1007/s00122-012-1842-6

Rashotte, A. M., DeLong, A., and Muday, G. K. (2001). Genetic and chemical reductions in protein phosphatase activity alter auxin transport, gravity response, and lateral root growth. *Plant Cell* 13, 1683–1697. doi: 10.1105/tpc.010158

Remington, D. L., and Purugganan, M. D. (2003). Candidate gene, quantitative loci, and functional trait evolution in plants. *Int. J. Plant Sci.* 164, S7–S20. doi: 10.1086/367812

Rotmistrovsky, K., Jang, W., and Schuler, G. D. (2004). A web server for performing electronic PCR. *Nucleic Acids Res.* 32, W108–W112. doi: 10.1093/nar/gkh450

Schiessl, S. V., Quezada-Martinez, D., Tebartz, E., Snowdon, R. J., and Qian, L. (2019). The ernalization regulator FLOWERING LOCUS C is differentially expressed in biennial and annual *Brassica napus*. *Scient. Rep.* 9:14911. doi: 10.1038/s41598-019-51212-x

Schuler, G. D. (1997). Sequence mapping by electronic PCR. *Genome Res.* 7, 541–550. doi: 10.1101/gr.7.5.541

Sehgal, A., Sita, K., Siddique, K. H. M., Kumar, R., Bhogireddy, S., Varshney, R. K., et al. (2018). Drought or/and heat-stress effects on seed filling in food crops: impacts on functional biochemistry, seed yields, and nutritional quality. *Front. Plant Sci.* 9:1705. doi: 10.3389/fpls.2018.01705

Shannon, P., Markiel, A., Ozier, O., Baliga, N. S., Wang, J. T., Ramage, D., et al. (2003). Cytoscape: A software environment for integrated models of biomolecular interaction networks. *Genome Res.* 13, 2498–2504. doi: 10.1101/gr.1239303

Shen, W., Qin, P., Yan, M., Li, B., Wu, Z., Wen, J., et al. (2019). Fine mapping of a silique length and seed weight-related gene in *Brassica napus*. *Theory Appl. Genet.* 132, 2985–2996. doi: 10.1007/s00122-019-03400-6

Shen, Y., Yang, Y., Xu, E., Ge, X., Xiang, Y., and Li, Z. (2018). Novel and major QTL for branch angle detected by using DH population from an exotic introgression in rapeseed (*Brassica napus L.*). *Theory Appl. Genet.* 131, 67–78. doi: 10.1007/s00122-017-2986-1

Shi, J., Li, R., Qiu, D., Jiang, C., Long, Y., Morgan, C., et al. (2009). Unraveling the complex trait of crop yield with quantitative trait loci mapping in *Brassica napus*. *Genetics* 182, 851–861. doi: 10.1534/genetics.109.101642

Shi, J., Li, R., Zou, J., Long, Y., and Meng, J. (2011). A dynamic and complex network regulates the heterosis of yield-correlated traits in rapeseed *(Brassica napus L.)*. *PLoS One* 6:e21645. doi: 10.1371/journal.pone.0021645

Shi, J., Zhan, J., Yang, Y., Ye, J., Huang, S., Li, R., et al. (2015). Linkage and regional association analysis reveal two new tightly-linked major-QTLs for pod number and seed number per pod in rapeseed (*Brassica napus L.*). *Scient. Rep.* 5:14481. doi: 10.1038/srep14481

Shi, L., Shi, T., Broadley, M. R., White, P. J., Long, Y., Meng, J., et al. (2013). High-throughput root phenotyping screens identify genetic loci associated with root architectural traits in *Brassica napus* under contrasting phosphate availabilities. *Anna. Bot.* 112, 381–389. doi: 10.1093/aob/mcs245

Shi, L., Yang, J. P., Liu, J., Li, R., Long, Y., Xu, F., et al. (2012). Identification of quantitative trait loci associated with low boron stress that regulate root and shoot growth in *Brassica napus* seedlings. *Mol. Breed.* 30, 393–406. doi: 10.1007/s11032-011-9629-z

Si, P., Mailer, R. J., Galwey, N., and Turner, D. (2003). Influence of genotype and environment on oil and protein concentrations of canola (*Brassica napus L.*) grown across southern Australia. *Austral. J. Agricult. Res.* 54, 397–407. doi: 10.1071/AR01203

Smith, J. M., and Haigh, J. (1974). The hitch-hiking effect of a favourable gene. *Genet. Res.* 23, 23–35. doi: 10.1017/s0016672300014634

Solovieff, N., Cotsapas, C., Lee, P. H., Purcell, S. M., and Smoller, J. W. (2013). Pleiotropy in complex traits: challenges and strategies. *Nat. Rev. Genet.* 14, 483–495. doi: 10.1038/nrg3461

Song, J. M., Liu, D. X., Xie, W. Z., Yang, Z., Guo, L., Liu, K., et al. (2021). BnPIR: *Brassica napus* pan-genome information resource for 1689 accessions. *Plant Biotechnol. J.* 19, 412–414. doi: 10.1111/pbi.13491

Stearns, F. W. (2010). One hundred years of pleiotropy: a retrospective. *Genetics* 186, 767–773. doi: 10.1534/genetics.110.122549

Stein, A., Coriton, O., Rousseau-Gueutin, M., Samans, B., Schiessl, S. V., Obermeier, C., et al. (2017). Mapping of homoeologous chromosome exchanges influencing quantitative trait variation in *Brassica napus*. *Plant Biotechnol.* 15, 1478–1489. doi: 10.1111/pbi.12732

Sun, F., Fan, G., Hu, Q., Zhou, Y., Guan, M., Tong, C., et al. (2017). The high-quality genome of *Brassica napus* cultivar *'ZS11'* reveals the introgression history in semi-winter morphotype. *Plant J.* 92, 452–468. doi: 10.1111/tpj.13669

Sun, F., Liu, J., Hua, W., Sun, X., Wang, X., and Wang, H. (2016). Identification of stable QTLs for seed oil content by combined linkage and association mapping in *Brassica napus*. *Plant Sci.* 252, 388–399. doi: 10.1016/j.plantsci.2016.09.001

Sun, M., Hua, W., Liu, J., Huang, S., Wang, X., Liu, G., et al. (2012). Design of new genome- and gene-sourced primers and identification of QTL for seed oil content in a specially high-oil *Brassica napus* cultivar. *PLoS One* 7:e47037. doi: 10.1371/journal.pone.0047037

Szklarczyk, D., Franceschini, A., Wyder, S., Forslund, K., Heller, D., Huerta-Cepas, J., et al. (2015). STRING v10: protein-protein interaction networks, integrated over the tree of life. *Nucleic Acids Res.* 43, D447–D452. doi: 10.1093/nar/gku1003

Tabor, H. K., Risch, N. J., and Myers, R. M. (2002). Candidate-gene approaches for studying complex genetic traits: practical considerations. *Nat. Rev. Genet.* 3, 391–397. doi: 10.1038/nrg796

Tadege, M., Sheldon, C. C., Helliwell, C. A., Stoutjesdijk, P., Dennis, E. S., and Peacock, W. J. (2001). Control of flowering time by FLC orthologues in *Brassica napus*. *Plant J.* 28, 545–553. doi: 10.1046/j.1365-313x.2001.01182.x

Tchurikov, N. A. (2005). Molecular mechanisms of epigenetics. *Biochem. Moscow* 70, 406–423. doi: 10.1007/s10541-005-0131-2

Had, L., and Möllers, C. (2016). Genetic variation and inheritance of phytosterol and oil content in a doubled haploid population derived from the winter oilseed rape *Sansibar* × *Oase* cross. *Theoret. Appl. Genet.* 129, 181–199. doi: 10.1007/s00122-015-2621-y

Tirado, C. A. (2014). *In book: Pathobiology of Human Disease Chapter: Epigenetics*. Netherland: Elsevier doi: 10.1016/B978-0-12-386456-7.06601-6

Tudor, E. H., Jones, D. M., He, Z., Bancroft, I., Trick, M., Wells, R., et al. (2020). QTL-seq identifies *BnaFT.A02* and *BnaFLC.A02* as candidates for variation in vernalization requirement and response in winter oilseed rape (*Brassica napus*). *Plant Biotechnol. J.* 18, 2466–2481. doi: 10.1111/pbi.13421

Nagaharu, U. (1935). Genome analysis in *Brassica* with special reference to the experimental formation of *B. napus* and peculiar mode of fertilization. *Jap. J. Bot.* 7, 389–452.

Udall, J. A., Quijada, P. A., Lambert, B., and Osborn, T. C. (2006). Quantitative trait analysis of seed yield and other complex traits in hybrid spring rapeseed (*Brassica napus L.*): 2. *Theoret. Appl. Genet.* 113, 597–609. doi: 10.1007/s00122-006-0324-0

Verwoert, I. I., van der Linden, K. H., Walsh, M. C., Nijkamp, H. J., and Stuitje, A. R. (1995). Modification of *Brassica napus* seed oil by expression of the

Escherichia coli fabH gene, encoding 3-ketoacyl-acyl carrier protein synthase III. *Plant Mol. Biol.* 27, 875–886. doi: 10.1007/BF00037016

Wagner, G. P., and Zhang, J. (2011). The pleiotropic structure of the genotype-phenotype map: the evolvability of complex organisms. *Nat. Rev. Genet.* 12, 204–213. doi: 10.1038/nrg2949

Wan, H., Chen, L., Guo, J., Li, Q., Wen, J., Yi, B., et al. (2017). Genome-wide association study reveals the genetic architecture underlying salt tolerance-related traits in rapeseed (*Brassica napus L.*). *Front. Plant Sci.* 8:593. doi: 10.3389/fpls.2017.00593

Wan, H., Wei, Y., Qian, J., Gao, Y., Wen, J., Yi, B., et al. (2018). Association mapping of salt tolerance traits at germination stage of rapeseed (*Brassica napus L.*). *Euphytica* 214:190. doi: 10.1007/s10681-018-2272-6

Wang, X., Zhang, C., Li, L., Fritsche, S., Endrigkeit, J., Zhang, W., et al. (2012). Unraveling the genetic basis of seed tocopherol content and composition in rapeseed *(Brassica napus L.). PLoS One* 7:e50038. doi: 10.1371/journal.pone.0050038

Wang, B., Wu, Z., Li, Z., Zhang, Q., Hu, J., Xiao, Y., et al. (2018). Dissection of the genetic architecture of three seed-quality traits and consequences for breeding in *Brassica napus*. *Plant Biotechnol. J.* 16, 1336–1348. doi: 10.1111/pbi.12873

Wang, F., and Guan, C. Y. (2010). Molecular mapping and identification of quantitative trait loci for yield components in rapeseed (*Brasscia napus L.*). *Yi Chuan* 32, 271–277. (In Chinese). doi: 10.3724/sp.j.1005.2010.00271

Wang, H., Cheng, H., Wang, W., Liu, J., Hao, M., Mei, D., et al. (2016a). Identification of *BnaYUCCA6* as a candidate gene for branch angle in *Brassica napus* by QTL-seq. *Scient. Rep.* 6:38493. doi: 10.1038/srep38493

Wang, H., Guo, J., Lambert, K. N., and Lin, Y. (2007). Developmental control of *Arabidopsis* seed oil biosynthesis. *Planta* 226, 773–783. doi: 10.1007/s00425-007-0524-0

Wang, H., Zaman, Q. U., Huang, W., Mei, D., Liu, J., Wang, W., et al. (2019). QTL and Candidate Gene Identification for Silique Length Based on High-Dense Genetic Map in *Brassica napus L. Front. Plant Sci.* 10:1579. doi: 10.3389/fpls.2019.01579

Wang, J., Huang, Y., Zhang, Y., and Yao, J. (2011). Control of rapeseed clubroot by screened antagonistic microorganisms against *Plasmodiophora brassicae*. *Chin. J. Oil Crop Sci.* 33, 169–174.

Wang, J., Jian, H., Wei, L., Qu, C., Xu, X., Lu, K., et al. (2015). Genome-Wide Analysis of Seed Acid Detergent Lignin (ADL) and Hull Content in Rapeseed (*Brassica napus L.*). *PLoS One* 10:e0145045. doi: 10.1371/journal.pone.0145045

Wang, J., Kuang, L., Wang, X., Liu, G., Dun, X., and Wang, H. (2019). Temporal genetic patterns of root growth in *Brassica napus L.* revealed by a low-cost, high-efficiency hydroponic system. *Theory Appl. Genet.* 132, 2309–2323. doi: 10.1007/s00122-019-03356-7

Wang, J., Xian, X., Xu, X., Qu, C., Lu, K., Li, J., et al. (2017). Genome-wide association mapping of seed coat color in *Brassica napus*. *J. Agricult. Food Chem.* 65, 5229–5237. doi: 10.1021/acs.jafc.7b01226

Wang, N., Chen, B., Xu, K., Gao, G., Li, F., Qiao, J., et al. (2016). Association mapping of flowering time QTLs and insight into their contributions to rapeseed growth habits. *Front. Plant Sci.* 7:338. doi: 10.3389/fpls.2016.00338

Wang, N., Li, F., Chen, B., Xu, K., Yan, G., Qiao, J., et al. (2014). Genome-wide investigation of genetic changes during modern breeding of *Brassica napus*. *Theoret. Appl. Genet.* 127, 1817–1829. doi: 10.1007/s00122-014-2343-6

Wang, T., Wei, L., Wang, J., Xie, L., Li, Y. Y., Ran, S., et al. (2020). Integrating GWAS, linkage mapping and gene expression analyses reveals the genetic control of growth period traits in rapeseed (*Brassica napus L.*). *Biotechnol. Biofuels* 13:134. doi: 10.1186/s13068-020-01774-0

Wang, W., Zhang, Y., Ding, G. D., White, P. J., Broadley, M. R., Hammond, J. P., et al. (2019). Identification of QTLs for relative root traits associated with phosphorus efficiency in two culture systems in *Brassica napus*. *Euphytica* 215:192. doi: 10.1007/s10681-019-2512-4

Wang, X., Chen, L., Wang, A., Wang, H., Tian, J., Zhao, X., et al. (2016). Quantitative trait loci analysis and genome-wide comparison for silique related traits in *Brassica napus*. *BMC Plant Biol.* 16:71. doi: 10.1186/s12870-016-0759-7

Wang, X., Chen, Y., Thomas, C. L., Ding, G., Xu, P., Shi, D., et al. (2017). Genetic variants associated with the root system architecture of oilseed rape (*Brassica napus L.*) under contrasting phosphate supply. *DNA Res.* 24, 407–417. doi: 10.1093/dnares/dsx013

Wang, X., Long, Y., Yin, Y., Zhang, C., Gan, L., Liu, L., et al. (2015). New insights into the genetic networks affecting seed fatty acid concentrations in *Brassica napus*. *BMC Plant Biol.* 15:91. doi: 10.1186/s12870-015-0475-8

Wang, X., Wang, H., Long, Y., Li, D., Yin, Y., Tian, J., et al. (2013). Identification of QTLs associated with oil content in a high-oil *Brassica napus* cultivar and construction of a high-density consensus map for QTLs comparison in *B. napus*. *PLoS One* 8:e80569. doi: 10.1371/journal.pone.0080569

Wang, Y., Chen, W., Chu, P., Wan, S., Yang, M., Wang, M., et al. (2016). Mapping a major QTL responsible for dwarf architecture in *Brassica napus* using a single-nucleotide polymorphism marker approach. *BMC Plant Biol.* 16:178. doi: 10.1186/s12870-016-0865-6

Wang, Z., Fang, H., Chen, Y., Chen, K., Li, G., Gu, S., et al. (2014). Overexpression of *BnWRKY33* in oilseed rape enhances resistance to *Sclerotinia sclerotiorum*. *Mol. Plant Pathol.* 15, 677–689. doi: 10.1111/mpp.12123

Wei, D. Y., Mei, J. Q., Fu, Y., Disi, J. O., Li, J., and Qian, W. (2014). Quantitative trait loci analyses for resistance to *Sclerotinia sclerotiorum* and flowering time in *Brassica napus*. *Mol. Breed.* 34, 1797–1804. doi: 10.1007/s11032-014-0139-7

Wei, L., Jian, H., Lu, K., Filardo, F., Yin, N., Liu, L., et al. (2016). Genome-wide association analysis and differential expression analysis of resistance to *Sclerotinia* stem rot in B*rassica napus*. *Plant Biotechnol. J.* 14, 1368–1380. doi: 10.1111/pbi.12501

Wei, X., Qiu, J., Yong, K., Fan, J., Zhang, Q., Hua, H., et al. (2021). A quantitative genomics map of rice provides genetic insights and guides breeding. *Nat. Genet.* 53, 243–253. doi: 10.1038/s41588-020-00769-9

West, J. S., Kharbanda, P. D., Barbetti, M. J., and Fitt, B. D. L. (2001). Epidemiology and management of *Leptosphaeria maculans* (phoma stem canker) on oilseed rape in Australia Canada and Europe. *Plant Pathol.* 50, 10–27. doi: 10.1046/j.1365-3059.2001.00546.x

Wrucke, D. F., Mamidi, S., and Rahman, M. (2018). Genome-wide association study for frost tolerance in canola (*Brassica napus L.*) under field conditions. *J. Plant Biochem. Biotechnol.* 28, 211–222. doi: 10.1007/s13562-018-0472-8

Wrucke, D. F., Talukder, Z. I., and Rahman, M. (2019). Genome-wide association study for frost tolerance in rapeseed/canola (*Brassica napus*) under simulating freezing conditions. *Plant Breed.* 139, 356–367. doi: 10.1111/pbr.12771

Wu, G. Z., and Xue, H. W. (2010). *Arabidopsis* β-ketoacyl-[acyl carrier protein] synthase I is crucial for fatty acid synthesis and plays a role in chloroplast division and embryo development. *Plant Cell* 22, 3726–3744. doi: 10.1105/tpc.110.075564

Wu, J., Cai, G., Tu, J., Li, L., Liu, S., Luo, X., et al. (2013). Identification of QTLs for resistance to Sclerotinia stem rot and BnaC.IGMT5.a as a candidate gene of the major resistant QTL SRC6 in *Brassica napus*. *PLoS One* 8:e67740. doi: 10.1371/journal.pone.0067740

Wu, J., Chen, P., Zhao, Q., Cai, G., Hu, Y., Xiang, Y., et al. (2019). Co-location of QTL for *Sclerotinia* stem rot resistance and flowering time in *Brassica napus*. *Crop J.* 7, 227–237. doi: 10.1016/j.cj.2018.12.007

Wu, J., Zhao, Q., Liu, S., Shahid, M., Lan, L., Cai, G., et al. (2016). Genome-wide association study identifies new loci for resistance to *Sclerotinia* stem rot in *Brassica napus*. *Front. Plant Sci.* 7:1418. doi: 10.3389/fpls.2016.01418

Xu, L., Hu, K., Zhang, Z., Guan, C., Chen, S., Hua, W., et al. (2016). Genome-wide association study reveals the genetic architecture of flowering time in rapeseed (*Brassica napus L.*). *DNA Res.* 23, 43–52. doi: 10.1093/dnares/dsv035

Yan, X. Y., Li, J. N., Fu, F. Y., Jin, M. Y., Chen, L., and Liu, L. Z. (2009). Co-location of seed oil content, seed hull content and seed coat color QTL in three different environments in *Brassica napus L. Euphytica* 170, 355–364. doi: 10.1007/s10681-009-0006-5

Yang, P., Shu, C., Chen, L., Xu, J., Wu, J., and Liu, K. (2012). Identification of a major QTL for silique length and seed weight in oilseed rape (*Brassica napus L.*). *Theoret. Appl. Genet.* 125, 285–296. doi: 10.1007/s00122-012-1833-7

Yang, S., Zhang, B., Liu, G., Hong, B., Xu, J., Chen, X., et al. (2018). A comprehensive and precise set of intervarietal substitution lines to identify candidate genes and quantitative trait loci in oilseed rape (*Brassica napus L.*). *Theory Appl. Genet.* 13, 2117–2129. doi: 10.1007/s00122-018-3140-4

Yang, Y., Shi, J., Wang, X., Liu, G., and Wang, H. (2016). Genetic architecture and mechanism of seed number per pod in rapeseed: elucidated through linkage and near-isogenic line analysis. *Scient. Rep.* 6:24124. doi: 10.1038/srep24124

Yang, Y. W., Lai, K. N., Tai, P. Y., and Li, W. H. (1999). Rates of nucleotide substitution in angiosperm mitochondrial DNA sequences and dates of

divergence between *Brassica* and other angiosperm lineages. *J. Mol. Evolut.* 48, 597–604. doi: 10.1007/PL00006502

Ye, J., Yang, Y., Chen, B., Shi, J., Luo, M., Zhan, J., et al. (2017). An integrated analysis of QTL mapping and RNA sequencing provides further insights and promising candidates for pod number variation in rapeseed (*Brassica napus L.*). *BMC Genomics* 18:71. doi: 10.1186/s12864-016-3402-y

Yu, C. W., Chang, K. Y., and Wu, K. (2016). Genome-Wide Analysis of Gene Regulatory Networks of the FhadHDA6-FLD Complex in Arabidopsis. *Front. Plant Sci.* 7:555. doi: 10.3389/fpls.2016.00555

Yu, K. J., Wang, X. D., Li, W. J., Sun, L., Peng, Q., Chen, F., et al. (2019). Identification and physical mapping of QTLs associated with flowering time in *Brassica napus L. Euphytica* 215:152. doi: 10.1007/s10681-019-2480-8

Zhang, F., Huang, J., Tang, M., Cheng, X., Liu, Y., Tong, C., et al. (2019). Syntenic quantitative trait loci and genomic divergence for *Sclerotinia* resistance and flowering time in *Brassica napus*. *J. Integr. Plant Biol.* 61, 75–88. doi: 10.1111/jipb.12754

Zhang, F., Xiao, X., Xu, K., Cheng, X., Xie, T., Hu, J., et al. (2020). Genome-wide association study (GWAS) reveals genetic loci of lead (Pb) tolerance during seedling establishment in rapeseed *(Brassica napus L.). BMC Genomics* 21:139. doi: 10.1186/s12864-020-6558-4

Zhang, F. G., Xiao, X., Yan, G. X., Hu, J., Cheng, X., Li, L., et al. (2018). Association mapping of cadmium-tolerant QTLs in *Brassica napus L.* and insight into their contributions to phytoremediation. *Environ. Exp. Bot.* 155, 420–428. doi: 10.1016/j.envexpbot.2018.07.014

Zhang, K., Nie, L., Cheng, Q., Yin, Y., Chen, K., Qi, F., et al. (2019). Effective editing for lysophosphatidic acid acyltransferase 2/5 in allotetraploid rapeseed (*Brassica napus L.*) using CRISPR-Cas9 system. *Biotechnol. Biofuels* 12:225. doi: 10.1186/s13068-019-1567-8

Zhang, L., Li, S., Chen, L., and Yang, G. (2012). Identification and mapping of a major dominant quantitative trait locus controlling seeds per silique as a single Mendelian factor in *Brassica napus L. Theoret. Appl. Genet.* 125:695. doi: 10.1007/s00122-012-1861-3

Zhang, L., Yang, G., Liu, P., Hong, D., Li, S., and He, Q. (2011). Genetic and correlation analysis of silique-traits in *Brassica napus L.* by quantitative trait locus mapping. *Theoret. Appl. Genet.* 122, 21–31. doi: 10.1007/s00122-010-1419-1

Zhang, X., Lu, G., Long, W., Zou, X., Li, F., and Nishio, T. (2014). Recent progress in drought and salt tolerance studies in *Brassica* crops. *Breed. Sci.* 64, 60–73. doi: 10.1270/jsbbs.64.60

Zhang, Y., Li, X., Chen, W., Wen, J., Shen, J., Ma, C., et al. (2011). Identification of two major QTL for yellow seed color in two crosses of resynthesized *Brassica napus* line *No. 2127-17*. *Mol. Breed.* 28, 335–342. doi: 10.1007/s11032-010-9486-1

Zhao, J., Huang, J., Chen, F., Xu, F., Ni, X., Xu, H., et al. (2012). Molecular mapping of *Arabidopsis thaliana* lipid-related orthologous genes in *Brassica napus*. *Theoret. Appl. Genet.* 124, 407–421. doi: 10.1007/s00122-011-1716-3

Zhao, J., Udall, J. A., Quijada, P. A., Grau, C. R., Meng, J., and Osborn, T. C. (2006). Quantitative trait loci for resistance to *Sclerotinia sclerotiorum* and its association with a homeologous non-reciprocal transposition in *Brassica napus L. Theory Appl. Genet.* 112, 509–516. doi: 10.1007/s00122-005-0154-5

Zhao, J. Y., Becker, H. C., Ding, H. D., Zhang, Y. F., Zhang, D. Q., and Ecke, W. (2005). QTL of three agronomically important traits and their interactions with environment in a European x Chinese rapeseed population. *Yi Chuan Xue Bao* 32, 969–978.

Zhao, Q., Wu, J., Cai, G., Yang, Q., Shahid, M., Fan, C., et al. (2019). A novel quantitative trait locus on chromosome A9 controlling oleic acid content in *Brassica napus*. *Plant Biotechnol. J.* 17, 2313–2324. doi: 10.1111/pbi.13142

Zhao, W., Wang, X., Wang, H., Tian, J., Li, B., Chen, L., et al. (2016). Genome-wide identification of QTL for seed yield and yield-related traits and construction of a high-density consensus map for QTL comparison in *Brassica napus*. *Front. Plant Sci.* 7:17. doi: 10.3389/fpls.2016.00017

Zhao, W., Zhang, L., Chao, H., Wang, H., Ta, N., Li, H., et al. (2019). Genome-wide identification of silique-related traits based on high-density genetic linkage map in *Brassica napus*. *Mol. Breed.* 39:86. doi: 10.1007/s11032-019-0988-1

Zhao, Z., Wu, L., Nian, F., Ding, G., Shi, T., Zhang, D., et al. (2012). Dissecting quantitative trait loci for boron efficiency across multiple environments in *Brassica napus*. *PLoS One* 7:e45215. doi: 10.1371/journal.pone.0045215

Zhao, Z., Wu, L., Nian, F., Ding, G., Shi, T., Zhang, D., et al. (2019). QTL analysis of four yield-related traits for *Brassica napus L.* in multiple environments. *Mol. Breed.* 39:166. doi: 10.1007/s11032-019-1067-3

Zhou, Q., Han, D., Mason, A. S., Zhou, C., Zheng, W., Li, Y., et al. (2018). Earliness traits in rapeseed (*Brassica napus*): SNP loci and candidate genes identified by genome-wide association analysis. *DNA Res.* 25, 229–244. doi: 10.1093/dnares/dsx052

Zhu, M., and Zhao, S. (2007). Candidate gene identification approach: progress and challenges. *Int. J. Biol. Sci.* 3, 420–427. doi: 10.7150/ijbs.3.420

Zhu, Q., King, G. J., Liu, X., Shan, N., Borpatragohain, P., Baten, A., et al. (2019). Identification of SNP loci and candidate genes related to four important fatty acid composition in *Brassica napus* using genome wide association study. *PLoS One* 14:e0221578. doi: 10.1371/journal.pone.0221578

Zhu, Y., Ye, J., Zhan, J., Zheng, X., Zhang, J., Shi, J., et al. (2020). Validation and characterization of a seed number per silique quantitative trait locus *qSN.A7* in rapeseed *(Brassica napus L.). Front. Plant Sci.* 11:68. doi: 10.3389/fpls.2020.00068

Zou, J., Mao, L., Qiu, J., Wang, M., Jia, L., Wu, D., et al. (2019). Genome-wide selection footprints and deleterious variations in young Asian allotetraploid rapeseed. *Plant Biotechnol. J.* 17, 1998–2010. doi: 10.1111/pbi.13115

Zou, J., Zhao, Y., Liu, P., Shi, L., Wang, X., Wang, M., et al. (2016). Seed quality traits can be predicted with high accuracy in *Brassica napus* using genomic data. *PLoS One* 11:e0166624. doi: 10.1371/journal.pone.0166624

Conflict of Interest: The authors declare that the research was conducted in the absence of any commercial or financial relationships that could be construed as a potential conflict of interest.

Publisher's Note: All claims expressed in this article are solely those of the authors and do not necessarily represent those of their affiliated organizations, or those of the publisher, the editors and the reviewers. Any product that may be evaluated in this article, or claim that may be made by its manufacturer, is not guaranteed or endorsed by the publisher.

frontiers | Frontiers in Plant Science

REVIEW
published: 11 May 2022
doi: 10.3389/fpls.2022.899076

A Review of Erucic Acid Production in Brassicaceae Oilseeds: Progress and Prospects for the Genetic Engineering of High and Low-Erucic Acid Rapeseeds (*Brassica napus*)

Pandi Wang[1], Xiaojuan Xiong[1], Xiaobo Zhang[2], Gang Wu[1] and Fang Liu[1]**

[1] Key Laboratory of Biology and Genetics Improvement of Oil Crops, Ministry of Agriculture and Rural Affairs, Oil Crops Research Institute, Chinese Academy of Agricultural Sciences, Wuhan, China, [2] State Key Laboratory of Crop Breeding Technology Innovation and Integration, Life Science and Technology Center, China National Seed Group Co., Ltd., Wuhan, China

OPEN ACCESS

Edited by:
Dongdong Li,
Hainan University, China

Reviewed by:
Enrique Martinez Force,
Institute for Fats (CSIC), Spain
Liang Guo,
Huazhong Agricultural University, China

***Correspondence:**
Gang Wu
wugang@caas.cn
Fang Liu
liufang03@caas.cn

Specialty section:
This article was submitted to Crop and Product Physiology, a section of the journal Frontiers in Plant Science

Received: *18 March 2022*
Accepted: *21 April 2022*
Published: *11 May 2022*

Citation:
Wang P, Xiong X, Zhang X, Wu G and Liu F (2022) A Review of Erucic Acid Production in Brassicaceae Oilseeds: Progress and Prospects for the Genetic Engineering of High and Low-Erucic Acid Rapeseeds (Brassica napus). Front. Plant Sci. 13:899076. doi: 10.3389/fpls.2022.899076

Erucic acid (C22:1, ω-9, EA) is a very-long-chain monounsaturated fatty acid (FA) that is an important oleochemical product with a wide range of uses in metallurgy, machinery, rubber, the chemical industry, and other fields because of its hydrophobicity and water resistance. EA is not easily digested and absorbed in the human body, and high-EA rapeseed (HEAR) oil often contains glucosinolates. Both glucosinolates and EA are detrimental to health and can lead to disease, which has resulted in strict guidelines by regulatory bodies on maximum EA contents in oils. Increasingly, researchers have attempted to enhance the EA content in Brassicaceae oilseeds to serve industrial applications while conversely reducing the EA content to ensure food safety. For the production of both LEAR and HEAR, biotechnology is likely to play a fundamental role. Elucidating the metabolic pathways of EA can help inform the improvement of Brassicaceae oilseeds through transgenic technology. In this paper, we introduce the industrial applications of HEAR oil and health benefits of low-EA rapeseed (LEAR) oil first, following which we review the biosynthetic pathways of EA, introduce the EA resources from plants, and focus on research related to the genetic engineering of EA in Brassicaceae oilseeds. In addition, the effects of the environment on EA production are addressed, and the safe cultivation of HEAR and LEAR is discussed. This paper supports further research into improving FAs in Brassicaceae oilseeds through transgenic technologies and molecular breeding techniques, thereby advancing the commercialization of transgenic products for better application in various fields.

Keywords: erucic acid, plant resources, genetic engineering, industrial applications, FAE (fatty acid elongase), LPAT/LPAAT (lysophosphatidic acid acyltransferase), FAD (fatty acid desaturase)

HIGHLIGHTS

- This review presents a comprehensive and systematic evaluation of erucic acid production in Brassicaceae oilseeds, highlighting the factors that influence erucic acid production in genetically engineered *Brassica napus*.

INTRODUCTION

Erucic acid (EA; C22:1 ω-9; C22:1 Δ13C; *cis*-13-docosenoic acid) is a very-long-chain monounsaturated fatty acid (FA) that uses sucrose, a photosynthetic product, as the main carbon source, and is formed through carbon chain lengthening and desaturation (Sakhno, 2010; **Figure 1**). EA is mainly present in the form of triglycerides in the fat of plant seeds. Due to its hydrophobicity and excellent lubrication properties, EA is an important oleochemical product that is widely used in various industries, and its primary use is mainly as an intermediate of fine chemicals: (1) EA can be obtained as a saturated straight-linked FA, namely behenic acid (Bährle-Rapp, 2007a), after hydrogenation reaction, and behenic acid and its derivatives can be used as plasticizers, lubricants, and stabilizers, which are widely used in the plastic industry, pharmaceutical industry, and food industry; (2) EA can be oxidized to obtain tridecanedioic acid and nonanoic acid, which are the main raw materials for synthesizing nylon-13 and nylon-1313, and can also be made into fragrance, musk, and low temperature- and light-resistant plasticizers; (3) EA derivatives also have many industrial uses, for instance, EA amide can be used as a plasticizer, anti-adhesive agent, waterproofing agent, and lubricant (Wu et al., 2007; Taylor et al., 2011); and (4) rapeseed oil with a high EA content can be used as diesel engine fuel by alkali-catalyzed transesterification and is also being used as a chemical raw material (Qi and Wang, 2009; Mcvetty and Duncan, 2015). However, in recent years, due to the promotion of double-low rapeseed (low EA and low glucosinolate), the supply of high-EA rapeseeds (HEARs) has become increasingly scarce. EA is mainly extracted from HEARs, and therefore increasing numbers of countries are focusing on HEARs and cultivating them in large quantities to meet industrial demands (Piazza and Foglia, 2001; Wu et al., 2007). Moreover, increasing the EA content in HEARs can help reduce the cost of EA production and increase its market prospects. Therefore, due to the substantial commercial value of high-EA oil in the market, further research should focus on rapeseed resources.

Both HEARs and low-EA rapeseeds (LEARs) exist, with the former being important for industry and the latter being important for health safety reasons. Before LEARs were developed, the EA content of rapeseed oil generally ranged from 45 to 50%. However, numerous zoological experiments have demonstrated that the long-term intake of large amounts of rapeseed oil with a high EA content can lead to myocardial fibrosis, cardiomyopathy, fatty deposits in the heart muscle and kidneys, stunting and retarded weight gain in animals, and can even affect male reproductive function. This is mainly attributed to the incomplete metabolism of EA in the body, resulting in the accumulation of triacylglycerols (Vles et al., 1978; Bremer and Norum, 1982; Flatmark et al., 1983; Kramer et al., 1992; Reyes et al., 2010), while heart lesions seem to be fully reversible by the avoidance of EA intake (Wallace et al., 2016). China's national standard GB/T1536-2004 stipulates that oilseed rape with an EA content of less than 3% is considered a LEAR. In 2019, the European Commission (EU) issued regulation 2019/1870, which stipulates that the maximum content of EA in vegetable oils and fats provided to the final consumer should be no higher than 2% along with a tolerable daily intake (TDI) of 7.5 mg/kg body weight EA. Furthermore, the content of EA in camelina oil, mustard oil, and borage oil should contain no more than 5% EA, and mustard oil should contain no more than 3.5% EA (Russo et al., 2021).

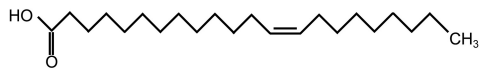

Name: Erucic Acid (EA);
C22:1 ω-9;
C22:1 Δ^{13C};
cis-13-docosenoic acid;

Molecular formula: $C_{22}H_{42}O_2$;
$C_9H_{18}=C_{13}H_{24}O_2$;
$CH_3(CH_2)_7CH=CH(CH_2)_{11}COOH$

Molecular weight: 338.57

Characteristics: ω-9 very long chain monounsaturated fatty acid;
colorless needle-like crystals;
very soluble in ether;
soluble in ethanol and methanol;
insoluble in water

FIGURE 1 | Chemical structure and other basic information of erucic acid.

Increasing numbers of studies aim to increase the EA content in Brassicaceae oilseeds to serve industrial applications. Though conventional breeding techniques to breed high-EA Brassicaceae oilseeds have increased the EA content, the maximum theoretical content of 66% has not been surpassed using conventional breeding methods (Rui et al., 2014). On the contrary, studies have also focused on reducing the EA content in Brassicaceae oilseeds to ensure food safety. Although LEAR varieties have been produced through conventional cross breeding, thereby promoting the use of many new double-low varieties (low EA and low glucosinolate), the EA content of many commercial double-low rapeseed varieties at present is generally higher than the current low-EA standard, mainly due to the mixed cultivation of rape varieties and varieties scale is more difficult to unify (Warner and Lewis, 2019).

Transgenic technology is likely to play an important role in addressing this practical issue and obtaining double-low varieties. Genetic engineering has been widely used to improve existing plant resources or produce new cultivars with desirable characteristics, thus representing a promising avenue for the breeding of HEAR and LEAR varieties (Nath et al., 2009; Huai et al., 2015; Shi et al., 2017; Qi et al., 2018; Liu et al., 2022).

In recent decades, biotechnology has developed rapidly through cutting-edge technologies such as gene editing (Zhang et al., 2020), synthetic biology (French, 2019), gene drive (Siddiqui et al., 2021), and others, resulting in many major breakthroughs and providing further technical means for genetic engineering and the realization of single-gene and multi-gene editing (Sakurai and Shindo, 2021; Nadakuduti and Enciso-Rodríguez, 2021). Further understanding the metabolic pathways of EA can provide a foundation for the quality improvement and breeding of Brassicaceae oilseeds through biotechnology.

Numerous transgenic experiments have significantly increased or decreased the EA content in recent years and these recent advances in transgenic technology are getting very close to realizing the optimal production of LEARs and HEARs. However, the available information on the engineering of EA content in Brassicaceae oilseeds is derived from isolated studies, and therefore a thorough summary and discussion of all relevant studies and reviews is required to present a comprehensive and systematic evaluation.

In this paper, we review the biosynthetic pathways of EA, introduce EA resources from plants, and summarize the available information related to the genetic engineering of EA biosynthesis in Brassicaceae oilseeds. In addition, factors affecting EA production in the genetic engineering of oilseed crops are discussed in detail, as well as the influence of the environment on EA production and the safe cultivation of HEARs and LEARs. This paper supports further work to improve the FA content of oilseed crops through transgenic technology and molecular breeding techniques, thus advancing the commercialization of transgenic products for better application in various fields.

ERUCIC ACID BIOSYNTHESIS AND ASSEMBLY

In oilseeds, FAs are *de novo* synthesized in the plastids with acetyl-coenzyme A (CoA) as the substrate, and EA is no exception. The elongation of EA starts from oleic acid (C18:1) using four core enzymes located at the endoplasmic reticulum (ER) membrane in the cytoplasm (Ohlrogge et al., 1979; Taylor et al., 2011; Li-Beisson et al., 2013; **Figure 2**). Finally, EA is assembled and stored as triacylglycerols (TAGs) *via* the *Kennedy* pathway (Li-Beisson et al., 2013; Chen et al., 2017; **Figure 2**).

Sucrose is the main carbon source for the synthesis of EA. During plant development, sucrose is converted to pyruvic acid through the Calvin cycle and further synthesized into acetyl-CoA by the pyruvate dehydrogenase complex (PDH); a precursor of FAs (Gooch, 2001). This is followed by the synthesis of malonyl-CoA catalyzed by acetyl-CoA carboxylase (ACCase), after which the malonyl group of malonyl-CoA is transferred from CoA to acyl carrier protein (ACP). Acetyl-CoA and malonyl-ACP enter the fatty acid synthesis complex (FAS) separately and undergo a sequential reaction including condensation, reduction, dehydration, and re-reduction to form C4:0-ACP, which is catalyzed by 3-ketoacyl-ACP synthase III (KAS III). Going through the same cycle reaction, the synthesis of C16:0-ACP is then catalyzed by 3-ketoacyl-ACP synthase I (KAS I) with a frequency of two carbon additions per cycle (Harwood, 2005; Li-Beisson et al., 2013). The synthesized C16:0-ACP is extended to C18:0-ACP and catalyzed by 3-ketoacyl-ACP synthase II (KAS II), following which C18:0-ACP is desaturated to form C18:1-ACP, which is catalyzed by stearoyl-ACP desaturase. C18:1-ACP is hydrolyzed and released from FAS to form free FAs by acyl-ACP thioesterases (Fat A/B). The free FAs are ultimately activated to acyl-CoA by a long-chain acyl-CoA synthetase (LACS), and then the acyl-CoA is transported to the ER and the FA chain is desaturated and extended (Salas and Ohlrogge, 2002; Bonaventure et al., 2003; Li-Beisson et al., 2013; Tjellström et al., 2013; **Figure 2**).

Oleic acid (C18:1) is converted to linoleic acid (C18:2) and linolenic acid (C18:3) catalyzed by fatty acid desaturase 2 (FAD2) and fatty acid desaturase 3 (FAD3), or extended to C20–C26 (including EA) very long-chain fatty acids (VLCFAs) by the FA elongation enzyme complex located at the ER membrane. The complex sequentially adds two carbon units to a growing acyl chain using four core enzymes, namely 3-ketoacyl-CoA synthase (KCS), 3-ketoacyl-CoA reductase (KCR), 3-hydroxyacyl-CoA dehydratase (HCD), and *trans*-2,3-enoyl-CoA reductase (ECR). Each elongation cycle involves four successive reactions. Malonyl-CoA and a long-chain acyl-CoA are condensed by KCS, which is then reduced by KCR to 3-hydroxyacyl-CoA, and then 3-hydroxyacyl-CoA is dehydrated by HCD and subsequently reduced to form elongated acyl-CoA catalyzed by ECR (Harwood, 2005; Haslam and Kunst, 2013; Li-Beisson et al., 2013; Huai et al., 2015; Fan et al., 2018; **Figure 2**).

KCS is encoded by the *FAE1* (*Fatty acid elongase 1*) gene and is a rate-limiting enzyme in the first step of the FA elongation reaction (Katavic et al., 2000); therefore, KCS is an important regulatory target for altering the EA content through genetic engineering (James et al., 1995; Qi et al., 1998; Domergue et al., 2000; Mietkiewska et al., 2004, 2007; Wang et al., 2008; Nath et al., 2009; Taylor et al., 2009; Tian et al., 2011; Shi et al., 2015, 2017; Saini et al., 2019).

After synthesis, EA is assembled and stored as TAGs, and the pathway consists of the sequential acylation and dephosphorylation of glycerol-3-phosphate (G3P). G3P is catalyzed by glycerol-3-phosphate acyltransferase (GPAT) to produce lysophospholipids (LPAs); LPA is catalyzed by lysophosphatidic acid acyltransferase (LPAT/LPAAT) to produce phosphatidic acid (PA); PA is catalyzed by phosphatidic acid phosphorylase (PAP) to produce diacylglycerol (DAG); and DAG is catalyzed by diacylglycerol acyltransferase (DGAT) to produce TAG (Stumpf and Pollard, 1983; Bates et al., 2009; Li-Beisson et al., 2013; Fan et al., 2018; **Figure 2**). GPAT, LPAAT, and DGAT are the three main enzymes of the *Kennedy* pathway and play very important regulatory roles in the biosynthesis of lipids and phospholipids. GPAT catalyzes the attachment of FAs on acyl-CoA to the sn-1 position of G3P, which is also the first reaction step. LPAAT catalyzes the attachment of acyl groups from acyl donors to the sn-2 position of LPA. DGAT catalyzes the formation of TAG from DAG at the sn-3 position (Taylor et al., 2011; **Figure 2**).

A reciprocal transformation exists between phospholipids and TAGs, which is another important pathway for TAG

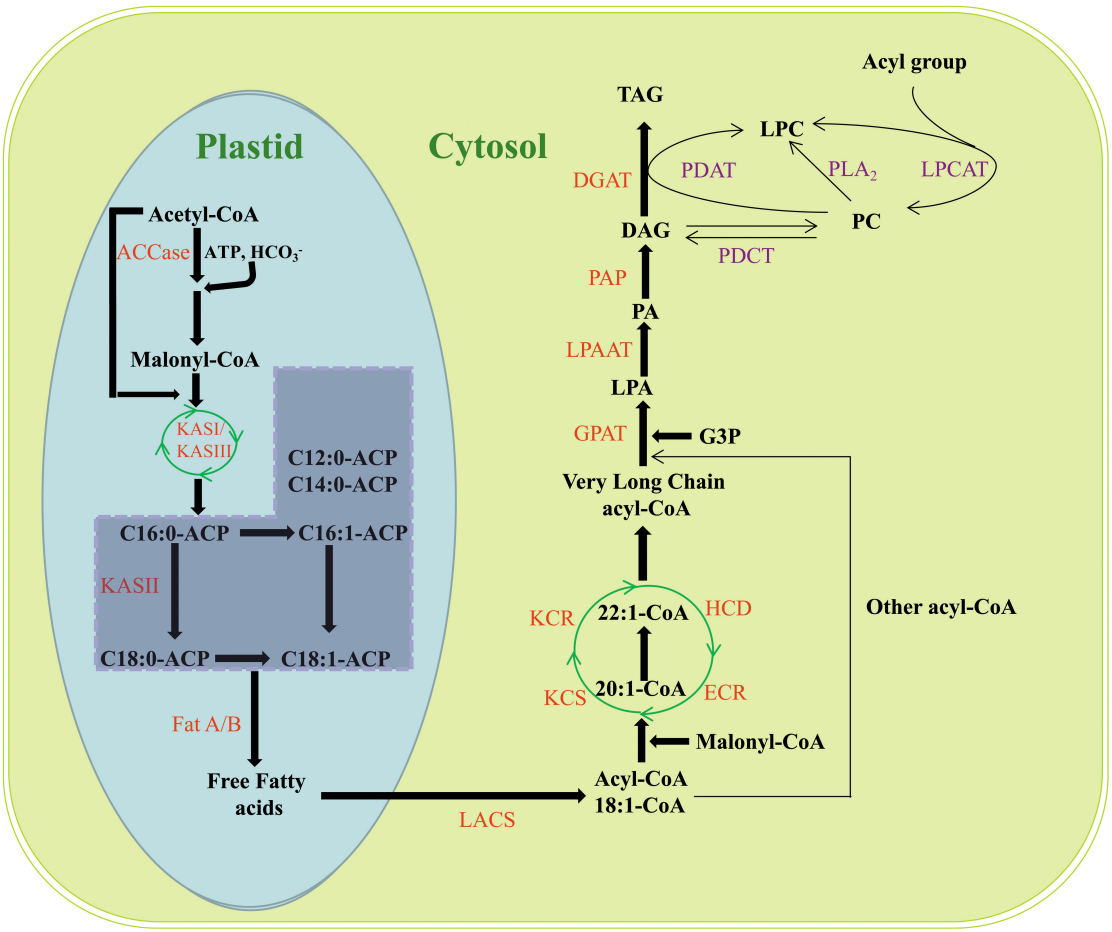

FIGURE 2 | Biosynthesis and accumulation of EA in plants. ACCase, acetyl-CoA carboxylase; KAS, 3-ketoacyl-ACP synthase; LACS, long-chain acyl-CoA synthase; FAD2, fatty acid desaturase 2; FAD3, fatty acid desaturase 3; LA, linoleic acid; ALA, linolenic acid; KCS, 3-ketoacyl-CoA synthase; KCR, 3-ketoacyl-CoA reductase; HCD, 3-hydroxyacyl-CoA dehydratase; ECR, *trans*-2,3-enoyl-CoA reductase; G3P, glycerol-3-phosphate; GPAT, glycerol-3-phosphate acyltransferase; LPA, lysophospholipids; LPAAT, lysophosphatidic acid acyltransferase; PA, phosphatidic acid; PAP, phosphatidic acid phosphorylase; DAG, diacylglycerol; DGAT, diacylglycerol acyltransferase; TAG, triacylglycerol; PDAT, phospholipid diacylglycerol acyltransferase; PC, phosphatidylcholine; LPC, lysophosphatidylcholine; PDCT, phosphatidylcholine diacylglycerol cholinephosphotransferase; LPCAT, Lysophosphatidylcholine acyltransferase.

synthesis in plants. Phospholipid diacylglycerol acyltransferase (PDAT) allows the transfer of FAs from the sn-2 position of phosphatidylcholine (PC) to the sn-3 position of DAG, producing TAG and lysophosphatidylcholine (LPC) products (Bates et al., 2009; Lu et al., 2009; Taylor et al., 2011; Fan et al., 2018; **Figure 2**). PDCT mediates a symmetrical interconversion between phosphatidylcholine (PC) and DAG by catalyzing the shuffling of acyl groups between them. Through the reactions of PDCT, the acyl groups on DAG enter PC and then return to DAG after they are desaturated or otherwise modified on PC, so as to enrich PC-modified FAs in the DAG pool prior to forming TAG (Taylor et al., 2011; Hu et al., 2012; **Figure 2**). Lysophosphatidylcholine acyltransferase (LPCAT) catalyzes the acyl exchange at the sn-2 position of PC with the acyl-CoA pool, resulting in an enrichment of PUFA-CoAs in the acyl-CoA pool, which affords new opportunities to introduce PUFAs or other modified FAs into TAGs (Taylor et al., 2011; **Figure 2**).

ERUCIC ACID RESOURCES

Erucic acid is a naturally occurring long-chain FA that is found in nature mainly in the seeds of plants of the Brassicaceae and Tropaeolaceae families, but also in deep-sea fish such as trout, salmon, and cod (Ackman, 2008), which contain mainly docosenoic acid (also known as cetolic acid) accompanied by a small proportion of EA. Currently, industrial EA is mainly extracted from rapeseed oil and fish oil. Although it is possible to increase the EA content in fish liver by increasing feed intake (Lundebye et al., 2017), it is not an effective feeding strategy. For example, the feed for salmon in Norway is mainly one-third fish oil and two-thirds LEAR oil (Ytrestøyl et al., 2015), mainly because HEAR oil is often accompanied by high levels of thioglycosides, the degradation products of which are toxic and harmful. In addition, with increasing marine pollution and a growing human population, relying on aquaculture to provide EA is not a sustainable strategy (Tocher et al., 2019).

Among plants, EA is mainly found in the seeds of Brassicaceae, such as rapeseed, mustard, *Thlaspi arvense*, *Crambe abyssinica*, radish, *Lunaria annua*, *Tropaeolum majus,* and *Limnanthes alba.* Rapeseed is mainly grown in India, Canada, and Australia, and in China, it is mainly distributed in the Yangtze River Basin and southwest and northwest China. According to the agronomic traits and morphological characteristics, rapeseed can be divided into three main species (**Table 1**): *Brassica napus*, *B. juncea,* and *B. campestris.* Although the EA content in *B. napus* is lower than *B. juncea*, *B. napus* has strong disease resistance and high yield, while *B. juncea* is grown in drought regions and rainless mountainous areas in northwest and southwest China. *Brassica campestris* is relatively short, its seeds fall easily, and it has weak resistance to diseases and insects and poor yield stability (Mcvetty and Duncan, 2015; Panel et al., 2016). Mustard comprises about 40 species and is one of the oldest recorded spices; it spread over thousands of years to Asia, North Africa, and Europe. Three varieties of mustard are widely used: *Brassica nigra* (black), *B. juncea* (brown), and *Sinapis alba* (white or yellow) (Vetter et al., 2020; **Table 1**). *Brassica carinata*, which is a hybrid of *B. nigra* and *B. oleracea*, has been planted for 6000 years mainly in western Canada and has an EA content of about 41%. However, it is characterized by a low yield, poor nutritional quality (low oleic acid, high EA, high sulfur glycosides) and long growth period (it matures 2–3 weeks later than *B. napus*) (Getinet et al., 1996; Jiang et al., 2010; Taylor et al., 2010). *Thlaspi arvense* is an annual weed in the mustard family; it has an EA content of 30–55% and prefers poor soils with some moisture in full sun, though it is tolerant of various conditions. Its seedpods shatter readily when mature (Claver et al., 2020). *Crambe abyssinica* is currently cultivated in the United States, Germany, Canada, and many other countries and has high yield potential, a short reproductive period, and a high fat and protein content. However, its cultivation area is small and thus difficult to scale, and as the seed sulfur glycoside content is high, the cake meal remaining after oil extraction cannot be used as feed (Saghai-Maroof et al., 1984; Qi et al., 2018). Radish (*Raphanus sativus*) seeds contain about 15–35% EA, and broccoli (*Brassica oleracea*) seeds contain about 50% EA. However, it is the roots or flower buds of these plants that are mainly consumed, and EA is not present in the roots or flower

TABLE 1 | Summary of the information including seed oil content, EA content and EA production limitations on the main plant seeds rich in EA.

Species	Oil content (%)	EA content (%)	Origin	Problems	References
Brassica napus	35–50	43–53	Europe	high EA content, contains glucosinolates	Mcvetty and Duncan, 2015; Panel et al., 2016
Brassica campestris	38–45	38–45	Asia	poor disease resistance, low yield	Mcvetty and Duncan, 2015; Panel et al., 2016
Brassica juncea	30–40	20–50	Europe	suitable in mountainous areas with drought and less rain	Mcvetty and Duncan, 2015; Panel et al., 2016
Brassica nigra	2.5–12.5	30–40	Europe	seeds are very small and mainly suitable to tropical areas	Vetter et al., 2020
Sinapis alba	2.5–12.5	30–40	the Mediterranean region and the Crimea	suitable in temperate climates with some humidity	Vetter et al., 2020
Brassica carinata	low content	30.9–45.7	Sudan in northeastern Africa and Ethiopia	low yield, poor nutritional quality, and long growth period	Getinet et al., 1996; Jiang et al., 2010; Taylor et al., 2010
Thlaspi arvense	28–34	30–55	Eurasia	preference for poor soils with some moisture	Claver et al., 2020
Crambe abyssinica	30–45	59–65	Mediterranean region	difficult to grow on a large scale, and seeds are high in sulfur glycosides	Saghai-Maroof et al., 1984; Qi et al., 2018
Raphanus sativus	32–52	15–35	Europe and Asia	the seeds are not consumed, only the root	Vetter et al., 2020
Brassica oleracea	26.3	50	southern Italy	oil has a pungent odor and the seeds are not consumed, only the flower buds	Vetter et al., 2020
Eruca sativa	30	44–46	South Europe and central Asia	contains a high level of thio-functionalised glucosinolates	Lazzeri et al., 2004
Lunaria annua	25–35	43–50	from Europe to western Asia	low yield and fragile seeds	Taylor et al., 2009; Dodos et al., 2015
Tropaeolum majus	6–10	75–80	South America in the Andes from Peru, Bolivia north to Colombia	difficult to obtain seeds and propagate	Taylor et al., 2009; Zasada et al., 2012
Limnanthes alba	20–30	12–15	Northern California, southern Oregon, and western Canada	low yields and require insect pollination to set seed	Bährle-Rapp, 2007b

buds (Vetter et al., 2020). *Eruca sativa* is an annual herb with EA content of 44–46% and high level of glucosinolates; Seeds can be extracted for oil, and stems and leaves can be used as vegetables (Lazzeri et al., 2004). *Lunaria annua* is a biennial herb that grows from Europe to western Asia but is characterized by low EA yields and fragile seeds (Taylor et al., 2009; Dodos et al., 2015).

In addition to Brassicaceae species, *Tropaeolum majus*, which belongs to Tropaeolaceae, is the only plant with more than 66% EA content found to date. It was introduced into Europe in the sixteenth century and elsewhere subsequently. It has an EA content of 75–80% but a low oil content of 6–10%, and seed collection and propagation are difficult (Taylor et al., 2009; Zasada et al., 2012). *Limnanthes alba* (*L. alba*), which belongs to Limnanthaceae, has a short growth habit and is adapted to growing in marshes and a cool climate. Although the seed oil EA content of *L. alba* is not high, it contains more than 95% unsaturated long-chain FAs longer than C-20, and has unsaturated bonds mainly at the Δ5 position, and therefore it has substantial antioxidant capacity. Therefore, *L. alba* seed oil is widely used in skin care and cosmetics products (Bährle-Rapp, 2007b). Through genetic manipulation techniques, it is theoretically possible to improve the EA content of *L. alba* seed oil to more than 90%.

Although there are some natural plant resources that are rich in EA, *B. napus* is the most desirable germplasm resource for meeting the industrial production of EA. The protein products from rapeseed are important sources of feed and food proteins (Nosenko et al., 2014). *B. napus* not only has strong self-compatibility and high self-fruitfulness (generally above 70–80%), as well as strong resistance to disease and leaf fall, it also has high seedling transplanting yield. It is a winter oil crop, which can be staggered with other oil crops, such as peanut and soybean. Therefore, *B. napus* has great commercial industrial value.

In addition, rapeseed oil is regarded as a nutritionally valuable edible oil on the market (Kruse et al., 2015) and has been granted Substances Generally Recognized as Safe (GRAS) status in the United States. LEAR oil occupies an important position in the food industry (Altinoz et al., 2021). LEAR oil contains a large amount of unsaturated FAs (90%), which are beneficial to human health, as well as other nutrients such as natural vitamin E. It is also stable at high temperatures, and the absorption rate of LEAR oil by the human body is up to 99%. LEAR oil is also recommended in infant formula and homemade foods for children in moderate amounts (Stimming et al., 2015; Russo et al., 2021).

More research is focusing on how to increase the EA content of *B. napus* for industrial use as well as reducing the EA content of *B. napus* for dietary use.

GENETIC ENGINEERING OF ERUCIC ACID BOISYNTHESIS IN BRASSICACEAE OILSEEDS

Erucic acid is determined by the embryo genotype and is influenced by the cytoplasm (Li-Beisson et al., 2013; Liu et al., 2022). Numerous studies have shown that the inheritance of EA content is controlled by two pairs of master genes and multiple genes in cooperation with each other (Anand and Downed, 1981; Jourdren et al., 1996; Alemayehu et al., 2001), and the additive effect is significantly greater than the dominant effect. Moreover, several studies have shown that EA in rapeseeds is not only controlled by the master gene for inheritance but is also influenced by other modifier genes and the environment (Bechyne and Kondra, 1970; Wilmer et al., 1997).

Erucic acid in rapeseeds exists in the form of TAG, which can only bind to the sn-1 and sn-3 positions at the ends of the glycerol backbone and usually cannot get to the sn-2 position. Therefore, the maximum theoretical EA content is 66% (Rui et al., 2014). It is difficult to exceed this limit through conventional breeding. Therefore, the use of genetic engineering techniques to alter EA content is a pertinent research topic (Nath, 2008).

Increasing the Extension Efficiency to Increase Erucic Acid Content

Currently, the *FAE1* gene has been cloned from *Crambe abyssinica*, *Tropaeolum majus*, *B. napus,* and *Arabidopsis thaliana* (Rossak et al., 2001; Wang et al., 2008). By cloning this gene and overexpressing it in plants, the EA content in transgenic crops can be increased to varying degrees (**Table 2**). The *FAE1* gene has seed-specific expression properties. In HEARs, there are two functional copies of *FAE1*, located on chromosomes A8 and C3, with more than 98% sequence similarity. The FA elongase complex is present in HEARs, whereas the activity of this complex is not detectable in LEARs, which is mainly associated with the absence of KCS enzyme activity (Roscoe et al., 2001; Puyaubert et al., 2005).

Studies have shown that different species have different types and numbers of *KCS* genes encoding different KCSs with different substrate specificities, and therefore, the EA content in different crops varies greatly (**Table 2**). Transfer of the *FAE1* gene from *C. abyssinica* into a zero-EA *A. thaliana* mutant increased the EA content from 0 to 12.8%. Transfer of the *FAE1* gene from *C. abyssinica* into *B. carinata* increased the EA content from 35.5 to 51.9%, while the transfer of this gene from *Tropaeolum majus* to a zero-EA *A. thaliana* mutant increased the EA content from 2.1 to 9.6%, leading to a fivefold increase.

The current selection for LEARs is based on loss-of-function mutations in *FAE1* and *FAE2* (Das et al., 2002; Wu et al., 2008; **Table 3**). The world's first zero-EA rapeseed "Oro" was derived from a dramatic decrease in EA content after targeted mutation of the 845th base of *FAE1*. Insertion of the endogenous long-terminal repeat (LTR) retrotransposon BRACOPIA into the 5' coding region of *FAE1* also led to the discovery of the world's first low-EA *B. rapa* (Fukai et al., 2019). The EA content of *B. napus* can be reduced from 40% to less than 3% by inhibiting *FAE1* gene expression by RNA interference (RNAi). Similarly, the EA content of *B. napus* can be reduced from 40 to 0.36% by inhibiting *FAE1* gene expression by intron-spliced hairpin RNA (ihpRNA), while the EA content of *B. napus* can be reduced from 42.25 to 2.02% in HEAR and from 0.87% to undetectable levels in LEAR by inhibiting *BnaFAE1* and *BnaFAD2* (*Brassica napus fatty acid Δ12-desaturase 2*) expression

TABLE 2 | Comparison of research on improving EA content by means of genetic engineering in Brassicaceae oilseeds.

Gene	Donor species	EA content of donor species/%	Receptor species	Expression	EA content of the control (%)	EA content of transgenic receptor species (%)	Fold-change	References
FAE	*Tropaeolum majus*	70–75	*Arabidopsis thaliana*	35s:*FAE*	2.1	3.2–4.0	1.7-fold increase	Mietkiewska, 2004
			Arabidopsis thaliana	Napin:*FAE*	2.1	9.6	4.5-fold increase	
			Arabidopsis thaliana		1.8 ± 0.1	11.3 ± 2.6	Sevenfold increase	
FAE	*Crambe abyssinica*	55–60	*Arabidopsis thaliana* (a *fae1* mutant line)	Napin:*CrFAE*	0.0 ± 0.0	10.1 ± 2.7	12-fold increase	Mietkiewska et al., 2007
			Brassica carinata		35.5	47.4	1.3-fold increase	
FAE1	*Thlaspi arvense*	38–40	*Arabidopsis thaliana*	OLE2:*TaFAE1*	< 2.5	7.43–8.56	3∼4-fold increase	Claver et al., 2020
LPAAT	*Limnanthes alba*	12–15	*Brassica napus*	Napin:*LPAAT*	37.7–39	37.5–41	No change	Lassner et al., 1995
FAE	*Arabidopsis*	1.8	*Brassica napus*	*FAE1* + *LPAAT*	43	48–53	low increase	Katavic et al., 2001
LPAAT	yeast	0						
FAE1	HEAR	52	HEAR	*BnFAE1* + *LdLPAAT*	54	63	1.2-fold increase	Nath et al., 2009
LPAAT	*Limnanthes douglasii*	12–15						
FAE	*Crambe abyssinica*	55–60	*Brassica carinata*	*CrFAE* + *FAD2*-ihpRNA	40	66.5	1.7-fold increase	Mietkiewska et al., 2008
FAD2	*Brassica carinata*	40						
FAE1	*Brassica napus*	40	*Crambe abyssinica*	*BnFAE1* + *LdLPAAT* + *CaFAD2*-RNAi	60	72.9–76.9	1.2∼1.3-fold increase	Li et al., 2012
LPAAT	*Limnanthes douglasii*	0						
FAD2	*Crambe abyssinica*	60						
FAD2	*Brassica carinata*	12	*Brassica carinata*	*FAD2*-co-supression	12	27	2.25-fold increase	Jadhav et al., 2005
	Brassica carinata	5	*Brassica carinata*	*FAD2*-antisense	5	19	3.8-fold increase	
FAD2	*Brassica napus*	42.25	*Brassica napus*	*BnFAD2*-RNAi	42.25	45.62	1.1-fold increase	Shi et al., 2017
FAD2	HEAR	47.26	HEAR	*BnFAD2*-amiRNA	47.26	50.37–52.38	1.1–1.8	Wang et al., 2019
FAD2	LEAR	0.53	LEAR		0.53	0.69–0.98	1.3∼1.8-fold increase	
FAD2	*Thlaspi arvense*	35	*Thlaspi arvense*	*TaFAD2*-CRISPR/Cas9	35	40	1.1-fold increase	Jarvis et al., 2021
FAE	*Brassica napus*	40	*Crambe abyssinica*	*CaLPAT2*-RNAi	62.5	63.1–66.3	1.0∼1.1-fold increase	Qi et al., 2018
LPAT	*Limnanthes douglasii*	52		*BnFAE* + *LdLPAT*		< 66.4	1.1-fold increase	
FAD2	*Crambe abyssinica*	62.5		*BnFAE* + *LdLPAT* + *CaFAD2*-RNAi		≤ 79.2	1.3-fold increase	
LPAT2				*BnFAE* + *LdLPAT* + *CaFAD2*-RNAi + *CaLPAT2*-RNAi		≤ 71.6	1.1-fold increase	

by RNAi. In addition, the EA content was reduced to nearly zero in *B. napus* when CRISPR/Cas9 technology was used to create targeted mutations on *BnaFAE1* (*BnaA08.FAE1* and *BnaC03.FAE1*) (Liu et al., 2022; **Table 3**). Therefore, inhibiting the expression of *FAE* to significantly reduce the amount of EA constitutes an effective strategy.

TABLE 3 | Comparison of research on decreasing EA content by means of genetic engineering in Brassicaceae oilseeds.

Gene	Species	EA content of species (%)	Expression	EA content of transgenic receptor species (%)	References
FAE1.1	*Brassica napus*	40	*BnFAE1.1*-ihpRNA	0.36	Tian et al., 2011
FAE1	*Brassica napus*	40	*BnFAE1*-RNAi	< 3	Shi et al., 2015
FAE1	*Brassica napus*	42.25	*BnFAE1*-RNAi	1.1	Shi et al., 2017
FAD2			*BnFAD2*-RNAi + *BnFAE1*-RNAi	2.02	
FAE1	*Thlaspi arvense*	35	*TaFAE1*-CRISPR/Cas9 + *TaFAD2*-CRISPR/Cas9	nearly zero	Jarvis et al., 2021
FAD2					
FAE1	*Brassica napus*	31.05–34.95	*BnaA08.FAE1*-CRISPR/Cas9 + *BnaC03.FAE1*-CRISPR/Cas9	zero	Liu et al., 2022

KCS activity was restored and EA content was greatly increased after transfer of the *FAE* gene into *B. napus* (Lassner and Lardizabal, 1996). Since KCS has different substrate specificities, to increase EA content, genes with high KCS activity should be selected.

Although the EA content of rapeseed could be increased to a certain extent using this approach, the limit of 66% cannot be exceeded because the sn-2 position of TAG cannot not bind EA.

Increasing Assembly Efficiency to Increase Erucic Acid Content

The pathway to exceed the EA content limit of 66% is the entry of EA into the sn-2 position of TAG. LPAAT has a strong ability to transfer EA to the sn-2 position of TAG (Nath et al., 2009; Li-Beisson et al., 2013). When the *LaLPAAT* and *LdLPAAT* genes, which were cloned in *Limnanthes* spp., were transferred into rapeseed, the EA content increased at the sn-2 position and formed triglycerides, but the total EA content did not increase (Lassner et al., 1995; **Table 2**). This indicates that the increase of EA at sn-2 position is compensated by the decrease of EA content at the sn-1 and sn-3 positions. This result suggests that, in the absence of an increase in EA synthesis, the introduction of the *LPAAT* gene only caused a redistribution of EA at the three hydroxyl positions of glycerol (Lassner et al., 1995; Brough et al., 1996).

When *FAE* and *LPAAT* were simultaneously introduced into *B. napus*, overexpression of *FAE* and *LPAAT* ensured the insertion of EA at the sn-2 position of the glycerol backbone, resulting in only a small and non-significant increase in EA content (Katavic et al., 2001; Nath et al., 2009; **Table 2**). This result may be due to the presence of competitive desaturation and irreversible binding to the storage lipids, or a lack of available fatty acyl groups during FA chain extension. When *FAE* and *LPAAT* were simultaneously introduced into *B. napus* with a high EA content, the EA content increased significantly from 54 to 63%, and the recombinant F2 plants exhibited an EA content of up to 72% (Nath et al., 2009; **Table 2**).

Although the EA content of rapeseed can be increased and exceed the limit of 66% using this approach, industrial applications would require increases of at least 80% and above in order for EA production to be financially viable, as EA contents above 90% would greatly reduce the cost of purification (Li et al., 2012).

Inhibiting Competing Substrates to Increase Erucic Acid Content

The overexpression of *KCS* and *LPAAT* did not significantly increase the EA content in some transgenic receptors (**Table 2**), likely because of the competition between FA elongation and the desaturation reaction of the same substrate, namely oleic acid. One of the metabolic pathways of oleic acid is the synthesis of EA by carbon chain lengthening under the action of the FAE1 enzyme, and the other is the synthesis of polyunsaturated fatty acids (PUFAs) such as C18:2 and C18:3 by desaturation under the action of the FAD2 enzyme, which is the first and key step in the synthesis of PUFAs. Therefore, inhibiting the expression of the *FAD2* gene is also an important way in which the EA content can be increased. Inhibition of the *FAD2* gene increases the content of oleic acid, which in turn provides sufficient substrate for EA synthesis and increases EA content in small amounts (1.1∼3.8-fold increase) (**Table 2**). In *B. carinata,* following the expression of the co-suppressed *FAD2* gene, the EA content was significantly increased from 12 to 27%; after antisense *FAD2* gene expression, the EA content was also significantly increased from 5 to 19% (Jadhav et al., 2005; **Table 2**). The EA content increased from 47.26 to 52.38% after the silencing of the *FAD2* gene by artificial miRNA in *B. napus* with a high EA content, and the EA content was increased from 0.53 to 0.98% after the silencing of the *FAD2* gene by artificial miRNA in *B. napus* with a low EA content (Wang et al., 2019; **Table 2**). In *B. napus,* inhibition of the *FAD2* gene by RNAi resulted in EA content increases of 42.25–45.62% (Shi et al., 2017; **Table 2**). In addition, the EA content increased from 35 to 40% in *Thlaspi arvense* when CRISPR/Cas9 technology was used to create targeted mutations on *TaFAD2* (Jarvis et al., 2021; **Table 2**).

Erucic acid is not only genetically controlled by the master gene, but is also influenced by other modifier genes. Infiltration of the multigene expression vector: *BnFAE* (*Brassica napus FAE*) + LdLPAAT (*Limnanthes douglasii LdLPAAT*) + *CaFAD2*-RNAi (*Crambe abyssinica FAD2*) into *C. abyssinica* increased the EA content to 73% in the transgenic progeny, and the individual EA content was found to be as high as 76.9% after single-seed

analysis (Li et al., 2012). Therefore, genetic engineering by overexpressing *FAE* and *LPAAT*, along with the inhibition of *FAD2* gene expression, can effectively increase EA content.

Suppressing the Expression of Endogenous *LPAT* to Increase Erucic Acid Content

The LPAT2 enzyme in Brassicaceae cannot use EA as a substrate to catalyze the incorporation of FA into triglycerides on the sn-2 position (Kuo and Gardner, 2002). To maximize the EA content of high-EA Brassicaceae oilseeds, genetic modification strategies have been developed by incorporating EA on the sn-2 position by introducing *LdLPAT* (*Limnanthes douglasii LPAT*), which can use EA as a substrate (Lassner et al., 1995). The transfer of endogenous *CaLPAT2* in *C. abyssinica* allowed an increased carbon flux to EA and less to PUFA (Qi et al., 2018). Compared with the wild-type, the EA content of the *CaLPAT2*-RNAi transgenic T1 seed oil was higher by 64.5% on average and ranged from 63.1 to 66.3% (**Table 2**). The infiltration of the multigene expression vectors *BnFAE* + *LdLPAT* + *CaFAD2*-RNAi and *BnFAE* + *LdLPAT* + *CaFAD2*-RNAi + *CaLPAT2*-RNAi into *C. abyssinica* resulted in EA contents of as much as 79.2 and 71.6%, respectively, in the transgenic progeny. The four-gene transformants of *BnFAE* + *LdLPAT* + *CaFAD2*-RNAi + *CaLPAT2*-RNAi presented greater carbon resource deposition into the C22:1 and C18:1 moieties and lower PUFAs when compared to the wild-type and the transformants of other vectors. This demonstrates that the suppression of endogenous *LPAT2* is a new and promising strategy for altering the EA content of Brassicaceae oilseeds (**Table 2**).

Increasing Assembly Efficiency to Increase Erucic Acid Content

The expression of *DGAT* also plays an important role in the accumulation of FAs (Maisonneuve et al., 2010; Maraschin et al., 2018). DGAT, as a rate-limiting enzyme, is the catalyst of the final step of TAG biosynthesis and exclusively uses acetyl-CoA as the acyl donor. DGAT1 and DGAT2 are the main contributors to the acylation of diacylglycerols and are present in oil crops. Four isomers of each type exist, and it is therefore important to select the appropriate DGAT isomer that can contribute to the FA composition of the enzyme and enhance specific FAs. The overexpression of ricinoleic acid hydroxylase in *A. thaliana* resulted in a decrease in ricinoleic acid and oil content, whereas the coexpression of DGAT2 of ricin restored the oil content close to the wild-type levels (Burgal et al., 2008). Overexpression of *AtDGAT1* in *Jatropha* resulted in a significant increase in oil in the seeds and leaves (Maravi et al., 2016). During seed development in LEARs and HEARs, BnDGAT2 isomers were found to exhibit significant differences toward 22:1-CoA, being more active in HEARs, and BnDGAT2 produced 6–14 times more TAG using 22:1-CoA than in LEARs (Kamil et al., 2019). Most likely, these shifts are due to the selection pressure for increased oil content within breeding programs. Therefore, to increase the EA content or oil content, it is essential that DGAT specificities are optimized.

Selection of Unique Promoters to Increase Erucic Acid Content

In addition to using the above genes to alter the EA content, the EA content can also be increased through the use of unique promoters. It is well known that the transcription level of genes is influenced not only by the gene characteristics, but may also be restricted by the promoter (Saini et al., 2019). In transgenic Brassicaceae oilseeds, the overexpression of *FAE* using powerful seed-specific promoters significantly increased the EA content in the seeds and reduced the potential risk of constitutive expression of the *FAE* gene. For example, the EA content increased from 2.1 to 9.6% when *FAE* was expressed by napin promoters in *A. thaliana*, while the EA content increased from 2.1% to 3.2%–4.0% when *FAE* was expressed by the 35S promoter in *A. thaliana* (**Table 2**).

EFFECTS OF THE ENVIRONMENT ON ERUCIC ACID PRODUCTION

In addition to genetic control, EA production is also influenced by environmental factors (Shi et al., 2003). The sowing time, climate of the planting site, lodging angle, planting density, and fertilizer all affect EA production (Yaniv et al., 1994; Uğur et al., 2010; Sanyal and Linder, 2013; Liu et al., 2015; Khan et al., 2018; Davoudi et al., 2019). The EA content of *Eruca sativa* with autumn sowing was 54.79%, while spring sowing decreased the content to 46.64% (Uğur et al., 2010). The EA content of the winter rapeseed cultivar Huayouza 62 increased from 1.13 to 1.49% when the plant lodging angle was manually increased from 0° (vertical) to 90° (horizontal) (Khan et al., 2018). The EA content was reduced from 1.46 to 1.05% when the planting density increased from 15 plants m^{-2} to 45 plants m^{-2} (Khan et al., 2018). However, the EA content did not vary significantly with different nitrogen rates (180 kg N ha^{-1} and 360 kg N ha^{-1}) (Khan et al., 2018) and nitrogen forms {manure; nitrate [Ca(NO3)2, 15.5% N]; ammonium [(NH4)2SO4, 21% N]} (Uğur et al., 2010). The EA content of a LEAR differed significantly when irrigation was conducted at three levels, including routine irrigation (control), irrigation interruption at the pod formation stage, and irrigation interruption at the flowering stage. Under the three levels of irrigation, the EA contents of the Dalgan cultivar were 0.17, 0.27, and 0.41%, respectively, and the EA contents of the Hyola 401 cultivar were 0.22, 0.29, and 0.35%, respectively (Farda et al., 2018). In addition, selenium also has an effect on EA content, and after spraying rapeseed leaves with sodium selenate, the EA content of a LEAR was significantly reduced from 0.32 to 0.29% (Davoudi et al., 2019).

SAFE CULTIVATION OF HIGH-EA RAPESEEDs AND LOW-EA RAPESEEDs

In recent decades, oil crops and transgenic oil crops have been promoted and planted on a large scale due to improved breeding, market incentives, and interest in improving the nutritional quality of oil crops (Kramer et al., 1983;

Abbadi and Leckband, 2011). Genetically modified organisms (GMOs) have been a major concern for the public and regulatory agencies. Although some opponents fear that GMOs pose risks to the ecosystem, scientists generally agree that genetically modified foods do not pose a particular risk to human consumption, and even if certain risks exist, such as allergenicity and toxicity, they have long been documented and measures have been taken to avoid such risks (Chen and Gao, 2014).

Although the price of HEARs has increased, producers are concerned that if HEARs are planted in large quantities, they will contaminate the LEARs and make it impossible to maintain low EA levels (Warner and Lewis, 2019). There are two main causes of contamination; one is the contamination of autochthonous seedlings due to crop rotation, and the other is increased EA contents through accidental pollination when HEARs are planted nearby. Unacceptable EA levels have some health and industrial impacts when transmitted through the food chain. Therefore, to avoid contamination, it is firstly very important to choose a crop rotation duration of at least 3 years, because simulations have found that it takes 16 years after harvest of a GM crop to reduce viable seeds to less than 1%. Secondly, it is important to maintain a safe distance between crops or establish strict isolation zones to minimize the effects of cross-pollination. In addition, measures are needed to manage weeds such as wild mustard (*Brassica kaber*, 31.5% EA) and wild radish (*Raphanus raphanistrum* subsp. *raphanistrum*, 26.7% EA) (Leaper and Melloul, 2011).

CONCLUSION AND PERSPECTIVES

Brassicaceae oilseeds not only provide common edible oils for human consumption, but also play an important role in human nutrition, alternative energy sources, and industry. Improving the nutritional value of crop products through plant genetic engineering has shown great potential and has created enormous economic and social benefits (Huai et al., 2015; Liu et al., 2021). The genetic regulation of EA content is of great importance in obtaining HEARs and LEARs. Thus far, transgenic HEARs with EA contents up to 72% are presently available and can be further developed *via* transgenic engineering to obtain higher EA content cultivars (Nath et al., 2009). LEAR oil contains a large amount of unsaturated FAs (90%), which are beneficial to human health, and thus LEAR oil is one of the most common vegetable edible oils on the market and is also recommended for infant and child nutrition due to its good FA composition (Hilbig et al., 2012; Stimming et al., 2015). Biotechnology can be used to more precisely regulate the EA synthesis pathway so as to obtain varieties with the target EA contents. This will also be of great significance to the oil crop industry and oil processing industry.

AUTHOR CONTRIBUTIONS

PW and FL designed and structured the review, collected the information, organized the tables, and wrote and revised the manuscript. XX prepared the figures. FL, GW, and XZ commented on the manuscript. All authors read and approved the final manuscript.

FUNDING

This work was supported by the Oil Crops Research Institute, Chinese Academy of Agricultural Sciences, the key task of emerging discipline construction of synthetic biology special (CAAS-OCRI-XKPY-202106); the Agricultural Science and Technology Innovation Program of Chinese Academy of Agricultural Sciences, China.

ACKNOWLEDGMENTS

We thank LetPub (www.letpub.com) for its linguistic assistance and scientific consultation during the preparation of this manuscript.

REFERENCES

Abbadi, A., and Leckband, G. (2011). Rapeseed breeding for oil content, quality, and sustainability. *Eur. J. Lipid Sci. Technol.* 113, 1198–1206. doi: 10.1002/ejlt.201100063

Ackman, R. G. (2008). "Fatty acids in fish and shellfifish," in *Fatty Acids in Foods and Their Health Implications*, ed. C. K. Chow (London: Tylor & Francis Group), doi: 10.1201/9781420006902.ch8

Alemayehu, N., Becker, H. C., and Heiko, C. (2001). Variation and inheritance of erucic acid content in *Brassica carinata* germplasm collections from Ethiopia. *Plant Breed.* 120, 331–335. doi: 10.1046/j.1439-0523.2001.00623.x

Altinoz, M. A., Elmaci, I., Hacimuftuoglu, A., Ozpinar, A., Hacker, E., and Ozpinar, A. (2021). PPARδ and its ligand erucic acid may act anti-tumoral, neuroprotective, and myelin protective in neuroblastoma, glioblastoma, and Parkinson's disease. *Mol. Aspects Med.* 78:100871. doi: 10.1016/j.mam.2020.100871

Anand, I. J., and Downed, R. K. (1981). A study of erucic acid alleles in digenomic rapeseed (*B. napus L.*). *Can. J. Plant Sci.* 61, 199–203. doi: 10.4141/cjps81-030

Bährle-Rapp, M. (2007a). "Behenic acid," in *Springer Lexikon Kosmetik und Körperpflege*, in Springer Lexikon Kosmetik und Körperpflege, ed. M. Bährle-Rapp (Berlin: Springer). doi: 10.1007/978-3-540-71095-0_1046.

Bährle-Rapp, M. (2007b). "*Limnanthes alba* seed oil," in *Springer Lexikon Kosmetik und Körperpflege*, ed. M. Bährle-Rapp (Berlin: Springer). doi: 10.1007/978-3-540-71095-0_6014

Bates, P. D., Durrett, T. P., Ohlrogge, J. B., and Pollard, M. (2009). Analysis of acyl fluxes through multiple pathways of triacylglycerol synthesis in developing soybean embryos. *Plant Physiol.* 150, 55–72. doi: 10.1104/pp.109.137737

Bechyne, M., and Kondra, Z. P. (1970). Effect of seed pod location on the fatty acid composition of seed oil from rapeseed (*Brassica napus* and *B. campestris*). *Can. J. Plant Sci.* 50, 151–154. doi: 10.4141/cjps70-028

Bonaventure, G., Salas, J. J., Pollard, M. R., and Ohlrogge, J. B. (2003). Disruption of the FATB gene in *Arabidopsis* demonstrates an essential role of saturated fatty acids in plant growth. *Plant Cell* 15, 1020–1033. doi: 10.1105/tpc.008946

Bremer, J., and Norum, K. R. (1982). Metabolism of very long-chain monounsaturated fatty acids (22:1) and the adaptation to their presence in the diet. *J. Lipid Res.* 23, 243–256. doi: 10.1089/jir.1982.2.593

Brough, C. L., Coventry, J. M., Christie, W. W., Kroon, J. T. M., Brown, A. P., Barsby, T. L., et al. (1996). Towards the genetic engineering of triacylglycerols of de- fined fatty acid composition: major changes in erucic acid content at the sn-2 position affected by the intro- duction of a 1-acyl-sn-glycerol-3-phosphate acyltransferase from *Limnanthes douglasii* into oil seed rape. *Mol. Breed.* 2, 133–142. doi: 10.1007/BF00441428

Burgal, J., Shockey, J., Lu, C., Dyer, J., Larson, T., Graham, I., et al. (2008). Metabolic engineering of hydroxy fatty acid production in plants: RcDGAT2 drives dramatic increases in ricinoleate levels in seed oil. *Plant Biotechnol. J.* 6, 819–831. doi: 10.1111/j.1467-7652.2008.00361.x

Chen, J. M., Qi, W. C., Wang, S. Y., Guan, R. Z., and Zhang, H. S. (2017). Correlation of Kennedy pathway efficiency with seed oil content of canola (*Brassica napus L.*) lines. *Can. J. Plant Sci.* 91, 251–259. doi: 10.4141/CJPS09178

Chen, K., and Gao, C. (2014). Targeted genome modification technologies and their applications in crop improvements. *Plant Cell Rep.* 33, 575–583. doi: 10.1007/s00299-013-1539-6

Claver, A., de la Vega, M., Rey-Giménez, R., Luján, M. Á, Picorel, R., López, M. V., et al. (2020). Functional analysis of β-ketoacyl-CoA synthase from biofuel feedstock *Thlaspi arvense* reveals differences in the triacylglycerol biosynthetic pathway among Brassicaceae. *Plant Mol. Biol.* 104, 283–296. doi: 10.1007/s11103-020-01042-7

Das, S., Roscoe, T. J., Delseny, M., Srivastava, P. S., and Lakshmikumaran, M. (2002). Cloning and molecular characterization of the Fatty Acid Elongase 1 (FAE 1) gene from high and low erucic acid lines of *Brassica campestris* and *Brassica oleracea*. *Plant Sci.* 162, 245–250. doi: 10.1016/S0168-9452(01)00556-8

Davoudi, A., Mirshekari, B., Shirani-Rad, A., Farahvash, F., and Rashidi, V. (2019). Effect of selenium foliar application on oil yield, fatty acid composition and glucosinolate content of rapeseed cultivars under late-season thermal stress. *OCL* 26:43. doi: 10.1051/ocl/2019027

Dodos, G. S., Karonis, D., Zannikos, F., and Lois, E. (2015). Renewable fuels and lubricants from *Lunaria annua L. Ind. Crops Prod.* 75, 43–50. doi: 10.1016/j.indcrop.2015.05.046

Domergue, F., Chevalier, S., Créach, A., Cassagne, C., and Lessire, R. (2000). Purification of the acyl-CoA elongase complex from developing rapeseed and characterization of the 3-ketoacyl-CoA synthase and the 3-hydroxyacyl-CoA dehydratase. *Lipids* 35, 487–494. doi: 10.1007/s11745-000-548-4

Fan, Y., Meng, H. M., Hu, G. R., and Li, F. L. (2018). Biosynthesis of nervonic acid and perspectives for its production by microalgae and other microorganisms. *Appl. Microbiol. Biot.* 102, 3027–3035. doi: 10.1007/s00253-018-8859-y

Farda, N. S., Abada, H. H. S., Rad, A. H. S., Heravan, A. E. M., and Daneshian, B. J. (2018). Effect of drought stress on qualitative characteristics of canola cultivars in winter cultivation. *Ind. Crops Prod.* 114, 87–92. doi: 10.1016/j.indcrop.2018.01.082

Flatmark, T., Christiansen, E. N., and Kryvi, H. (1983). Evidence for a negative modulating effect of erucic acid on the peroxisomal beta-oxidation enzyme system and biogenesis in rat liver. *Biochim. Biophys. Acta* 753, 460–466. doi: 10.1016/0005-2760(83)90071-1

French, K. E. (2019). Harnessing synthetic biology for sustainable development. *Nature* 2, 250–252. doi: 10.1038/s41893-019-0270-x

Fukai, E., Karim, M. M., Shea, D. J., Tonu, N. N., Falk, K. C., Funaki, T., et al. (2019). An LTR retrotransposon insertion was the cause of world's first low erucic acid *Brassica rapa* oilseed cultivar. *Mol. Breed.* 39:15. doi: 10.1007/s11032-018-0916-9

Getinet, A., Rakow, G., Downey, R. K., Getinet, A., Rakow, G., Downey, R. K., et al. (1996). Agronomic performance and seed qualily of ethiopian mustard in saskatchewanl. *Can. J. Plant Sci.* 76, 387–392. doi: 10.4141/cjps96-069

Gooch, J. W. (2001). "Calvin cycle," in *Encyclopedic Dictionary of Polymers*, ed. J. W. Gooch (New York, NY: Springer), 666–758. doi: 10.1007/978-1-4419-6247-8_13302

Harwood, J. L. (2005). "Fatty acid biosynthesis," in *Plant Lipids: Biology, Utilization and Manipulation*, ed. D. J. Murphy (Oxford: Blackwell), 27–66. doi: 10.1201/9780367813123-2

Haslam, T. M., and Kunst, L. (2013). Extending the story of very-long-chain fatty acid elongation. *Plant Sci.* 210, 93–107. doi: 10.1016/j.plantsci.2013.05.008

Hilbig, A., Lentze, M. J., and Kersting, M. (2012). Einführung und Zusammensetzung der Beikost. *Monatsschr. Kinderheilkund.* 160, 1089–1095. doi: 10.1007/s00112-012-2638-0

Hu, Z., Ren, Z., and Lu, C. (2012). The phosphatidylcholine diacylglycerol cholinephosphotransferase is required for efficient hydroxy fatty acid accumulation in transgenic Arabidopsis. *Plant Physiol.* 158, 1944–1954. doi: 10.1104/pp.111.192153

Huai, D., Zhang, Y., Zhang, C., Cahoon, E. B., and Zhou, Y. (2015). Combinatorial effects of fatty acid elongase enzymes on nervonic acid production in *Camelina sativa*. *PLoS One* 10:e0131755. doi: 10.1371/journal.pone.0131755

Jadhav, A., Katavic, V., Marillia, E. F., Michael Giblin, E., Barton, D. L., and Kumar, A. (2005). Increased levels of erucic acid in *Brassica carinata* by co-suppression and antisense repression of the endogenous FAD2 gene. *Metab. Eng.* 7, 215–220. doi: 10.1016/j.ymben.2005.02.003

James, D. W., Lim, E., Keller, J., Plooy, I., Ralston, E., and Dooner, H. K. (1995). Directed tagging of the *Arabidopsis* Fatty Acid Elongation1 (FAE1) gene with the maize transposon activator. *Plant Cell* 7, 309–319. doi: 10.1105/tpc.7.3.309

Jarvis, B. A., Romsdahl, T. B., Mcginn, M. G., Nazarenus, T. J., Cahoon, E. B., Chapman, K. D., et al. (2021). Crispr/cas9-induced fad2 and rod1 mutations stacked with fae1 confer high oleic acid seed oil in pennycress (*Thlaspi arvense L.*). *Front. Plant Sci.* 12:652319. doi: 10.3389/fpls.2021.652319

Jiang, Y., Tian, E., Li, R., Chen, L., and Meng, J. (2010). Genetic diversity of *Brassica carinata* with emphasis on the interspecific crossability with *B. rapa*. *Plant Breed.* 126, 487–491. doi: 10.1111/j.1439-0523.2007.01393.x

Jourdren, C., Barret, P., Horvais, R., Foisset, N., Delourme, R., and Renard, M. (1996). Identification of RAPD markers linked to the loci controlling erucic acid level in rapeseed. *Mol. Breed.* 2, 61–71. doi: 10.1007/BF00171352

Kamil, D., Simon, J., Ida, L., Agnieszka, M., Katarzyna, J. G., Magorzata, W., et al. (2019). Isoforms of acyl-coa:diacylglycerol acyltransferase2 differ substantially in their specificities toward erucic acid. *Plant Physiol.* 181, 1468–1479. doi: 10.1104/pp.19.01129

Katavic, V., Friesen, W., Barton, D. L., Gossen, K. K., Giblin, E. M., and Luciw, T. (2001). Improving erucic acid content in rapeseed through biotechnology: what can the *Arabidopsis* FAE1 and the yeast SLC1-1 genes contribute? *Crop Sci.* 41, 739–747. doi: 10.2135/cropsci2001.413739x

Katavic, V., Friesen, W., Barton, D. L., Gossen, K. K., Giblin, E. M., Luciw, T., et al. (2000). Utility of the *Arabidopsis* FAE1 and yeast SLC1-1 genes for improvements in erucic acid and oil content in rapeseed. *Biochem. Soc. Trans.* 28, 935–937. doi: 10.1042/BST0280935

Khan, S., Anwar, S., Kuai, J., Noman, A., Shahid, M., Din, M., et al. (2018). Alteration in yield and oil quality traits of winter rapeseed by lodging at different planting density and nitrogen rates. *Sci. Rep.* 8:634. doi: 10.1038/s41598-017-18734-8

Kramer, J. K., Sauer, F. D., and Pigden, W. J. (1983). *High and Low Erucic Acid in Rapeseed Oils*. London: Academic Press Ltd, doi: 10.1016/C2012-0-01579-7

Kramer, J., Sauer, F. D., Wolynetz, M. S., Farnworth, E. R., and Johnston, K. M. (1992). Effects of dietary saturated fat on erucic acid induced myocardial lipidosis in rats. *Lipids* 27, 619–623. doi: 10.1007/BF02536120

Kruse, M., von Loeffelholz, C., Hoffmann, D., Pohlmann, A., Seltmann, A. C., Osterhoff, M., et al. (2015). Dietary rapeseed/canola-oil supplementation reduces serum lipids and liver enzymes and alters postprandial inflammatory responses in adipose tissue compared to olive-oil supplementation in obese men. *Mol. Nutr. Food Res.* 59, 507–519. doi: 10.1002/mnfr.201400446

Kuo, T. M., and Gardner, H. W. (2002). *Lipid Biotechnology*. Basel, NY: Marcel Dekker, Inc, doi: 10.1201/9780203908198

Lassner, M. W., and Lardizabal, K. (1996). A jojoba β-ketoacyl-CoA synthase cDNA complements the canola fatty acid elongation mutation in transgenic plants. *Plant Cell* 8, 281–292. doi: 10.1105/tpc.8.2.281

Lassner, M. W., Levering, C. K., Davies, H. M., and Knutzon, D. S. (1995). Lysophosphatidic acid acyltransferase from meadowfoam mediates insertion of erucic acid at the sn-2 position of triacylglycerol in transgenic rapeseed oil. *Plant Physiol.* 109, 1389–1394. doi: 10.1104/pp.109.4.1389

Lazzeri, L., Errani, M., Leoni, O., and Venturi, G. (2004). *Eruca sativa spp. oleifera*: a new non-food crop. *Ind. Crops Prod.* 20, 67–73. doi: 10.1016/j.indcrop.2002.06.001

Leaper, D. J., and Melloul, S. (2011). *The Impact of Clearfield® Production System on the Quality of Oilseed Rape*. Available online at: https://www.gcirc.org/fileadmin/documents/Proceedings/IRCPrague2011vol1/crop%20management/372-375.pdf (accessed January 6, 2022).

Li, X., van Loo, E. N., Gruber, J., Fan, J., Guan, R., Frentzen, M., et al. (2012). Development of ultra-high erucic acid oil in the industrial oil crop Crambe abyssinica. *Plant Biotechnol. J.* 10, 862–870. doi: 10.1111/j.1467-7652.2012.00709.x

Li-Beisson, Y., Shorrosh, B., Beisson, F., Andersson, M. X., Arondel, V., Bates, P. D., et al. (2013). Acyl-lipid metabolism. *Arabidopsis Book* 11:e0161. doi: 10.1199/tab.0133

Liu, F., Wang, P., Xiong, X., Zeng, X., Zhao, X., and Wu, G. (2021). A review of nervonic acid production in plants: prospects for the genetic engineering of

high nervonic acid cultivars plants. *Front. Plant Sci.* 12:626625. doi: 10.3389/fpls.2021.626625

Liu, N., Tang, T., Fan, Q., Meng, D., Li, Z., Chen, J., et al. (2015). Effects of site, sowing date and nitrogen application amount on economical characters, quality traits of high erucic acid rapeseed. *J. Gansu Agric. Univ.* 3, 68–72. doi: 10.13432/j.cnki.jgsau.2015.03.008

Liu, Y., Du, Z., Lin, S., Li, H., Lu, S., Guo, L., et al. (2022). CRISPR/Cas9-Targeted Mutagenesis of BnaFAE1 Genes Confers Low-Erucic Acid in *Brassica napus*. *Front. Plant Sci.* 13:848723. doi: 10.3389/fpls.2022.848723

Lu, C., Xin, Z., Ren, Z., Miquel, M., and Browse, J. (2009). An enzyme regulating triacylglycerol composition is encoded by the ROD1 gene of *Arabidopsis*. *Proc. Natl. Acad. Sci. U.S.A.* 106, 18837–18842. doi: 10.1073/pnas.0908848106

Lundebye, A. K., Lock, E. J., Rasinger, J. D., Nøstbakken, O. J., Hannisdal, R., Karlsbakk, E., et al. (2017). Lower levels of Persistent Organic Pollutants, metals and the marine omega 3-fatty acid DHA in farmed compared to wild Atlantic salmon (*Salmo salar*). *Environ. Res.* 155, 49–59. doi: 10.1016/j.envres.2017.01.026

Maisonneuve, S., Bessoule, J. J., Lessire, R., Delseny, M., and Roscoe, T. J. (2010). Expression of rapeseed microsomal lysophosphatidic acid acyltransferase isozymes enhances seed oil content in *Arabidopsis*. *Plant Physiol.* 152, 670–684. doi: 10.4161/psb.5.7.12101

Maraschin, F. D. S., Kulcheski, F. R., Segatto, A. L. A., Trenz, T. S., Barrientos-Diaz, O., Margis-Pinheiro, M., et al. (2018). Enzymes of glycerol-3-phosphate pathway in triacylglycerol synthesis in plants: function, biotechnological application and evolution. *Prog. Lipid Res.* 73, 46–64. doi: 10.1016/j.plipres.2018.12.001

Maravi, D. K., Kumar, S., Sharma, P. K., Kobayashi, Y., Goud, V. V., Sakurai, N., et al. (2016). Ectopic expression of AtDGAT1, encoding diacylglycerol O-acyltransferase exclusively committed to TAG biosynthesis, enhances oil accumulation in seeds and leaves of Jatropha. *Biotechnol. Biofuels* 9:226. doi: 10.1186/s13068-016-0642-7

Mcvetty, P. B. E., and Duncan, R. W. (2015). "Canola, rapeseed, and mustard: for biofuels and bioproducts," in *Industrial Crops, Handbook of Plant Breeding 9*, V. Von Mark. A Cruz and David (New York, NY: Springer), doi: 10.1007/978-1-4939-1447-0_7

Mietkiewska, E. (2004). Seed-Specific heterologous expression of a Nasturtium FAE Gene in *Arabidopsis* results in a dramatic increase in the proportion of erucic acid. *Plant Physiol.* 136, 2665–2675. doi: 10.1104/pp.104.046839

Mietkiewska, E., Brost, J. M., Giblin, E. M., Barton, D. L., and Taylor, D. C. (2007). Cloning and functional characterization of the fatty acid elongase 1 (FAE1) gene from high erucic *Crambe abyssinica cv. Prophet*. *Plant Biotechnol.* 5, 636–645. doi: 10.1111/j.1467-7652.2007.00268.x

Mietkiewska, E., Giblin, E. M., Wang, S., Barton, D. L., Dirpaul, J., Brost, J. M., et al. (2004). Seed-specific heterologous expression of a nasturtium FAE gene in *Arabidopsis* results in a dramatic increase in the proportion of erucic acid. *Plant Physiol.* 136, 2665–2675.

Mietkiewska, E., Hoffman, T. L., Brost, J. M., Giblin, E. M., Barton, D. L., Francis, T., et al. (2008). Hairpin-RNA mediated silencing of endogenous FAD2 gene combined with heterologous expression of *Crambe abyssinica* FAE gene causes an increase in the level of erucic acid in transgenic *Brassica carinata* seeds. *Mol. Breed.* 22, 619–627. doi: 10.1007/s11032-008-9204-4

Nath, U. K. (2008). *Increasing Erucic Acid Content in the Seed Oil Of Rapeseed (Brassica napus L.) by Combining Selection for Natural Variation and Transgenic Approaches*. PhD thesis. Germany: Georg-August-University Göttingen, doi: 10.53846/goediss-3388.

Nath, U. K., Wilmer, J. A., Wallington, E. J., Becker, H. C., and Möllers, C. (2009). Increasing erucic acid content through combination of endogenous low polyunsaturated fatty acids alleles with Ld-LPAAT + Bn-fae1 transgenes in rapeseed (*Brassica napus L.*). *Theor. Appl. Genet.* 118, 765–773. doi: 10.1007/s00122-008-0936-7

Nosenko, T., Kot, T., and Kichshenko, V. (2014). Rape Seeds as a Source of Feed and Food Proteins. *Pol. J. Food Nutr. Sci.* 64, 109–114. doi: 10.2478/pjfns-2013-0007

Ohlrogge, J. B., Kuhn, D. N., and Stumpf, D. (1979). Subcellular localization of acyl carrier protein in leaf protoplasts of *Spinacia oleracea*. *Proc. Natl. Acad. Sci. U.S.A.* 76, 1194–1198. doi: 10.1073/pnas.76.3.1194

Panel, E. C., Knutsen, H. K., Alexander, J., Barregard, L., Bignami, M., Br€uschweiler, B., et al. (2016). Scientific Opinion Erucic acid in feed and food EFSA Panel on Contaminants in the Food Chain (CONTAM). *EFSA J.* 14, 1–173. doi: 10.2903/j.efsa.2016.4593

Piazza, G. J., and Foglia, T. A. (2001). Rapeseed oil for oleochemical usage. *Eur. J. Lipid Sci. Technol.* 103, 450–454. doi: 10.1016/j.biochi.2009.03.021

Puyaubert, J., Garcia, C., Chevalier, S., and Lessire, R. (2005). Acyl-CoA elongase, a key enzyme in the development of high-erucic acid rapeseed? *Eur. J. Lipid Sci. Technol.* 107, 263–267. doi: 10.1002/ejlt.200590024

Qi, P. P., and Wang, F. (2009). Investigation on preparation and properties of biodiesel from rapeseed oil with high content of erucic acids. *J. Nanjing For. Univ.* 33, 87–91. doi: 10.1360/972009-1551

Qi, Q., Rose, P. A., Abrams, G. D., Taylor, D. C., Abrams, S. R., and Cutler, A. J. (1998). (+)-Abscisic acid metabolism, 3-ketoacyl-coenzyme A synthase gene expression, and very-long-chain monounsaturated fatty acid biosynthesis in *Brassica napus* embryos. *Plant Physiol.* 117, 979–987. doi: 10.1104/pp.117.3.979

Qi, W. C., Tinnenbroek-Capel, I. E. M., Salentijn, E. M. J., Zhang, Z., Huang, B. Q., Chen, J. H., et al. (2018). Genetically engineering *Crambe abyssinica* - A potentially high-value oil crop for salt land improvement. *Land. Degrad. Dev.* 29, 1096–1106. doi: 10.1002/ldr.2847

Reyes, H., Ribalta, J., Hernández, I., Arrese, M., Pak, N., Wells, M., et al. (2010). Is dietary erucic acid hepatotoxic in pregnancy? An experimental study in rats and hamsters. *Hepatology* 21, 1373–1379. doi: 10.1002/hep.1840210522

Roscoe, T. J., Lessire, R., Puyaubert, J., Renard, M., and Delseny, M. (2001). Mutations in the fatty acid elongation 1 gene are associated with a loss of beta-ketoacyl-CoA synthase activity in low erucic acid rapeseed. *FEBS Lett.* 492, 107–111. doi: 10.1016/s0014-5793(01)02243-8

Rossak, M., Smith, M., and Kunst, L. (2001). Expression of the FAE1 gene and FAE1 promoter activity in developing seeds of *Arabidopsis thaliana*. *Plant Mol. Biol.* 46, 717–725. doi: 10.1023/A:1011603923889

Rui, G., Lager, I., Li, X., Stymne, S., and Zhu, L. H. (2014). Bottlenecks in erucic acid accumulation in genetically engineered ultrahigh erucic acid *Crambe abyssinica*. *Plant Biotechnol.* 12, 193–203. doi: 10.1111/pbi.12128

Russo, M., Yan, F., Stier, A., Klasen, L., and Honermeier, B. (2021). Erucic acid concentration of rapeseed (*Brassica napus L.*) oils on the German food retail market. *Food Sci. Nutr.* 9, 3664–3672. doi: 10.1002/fsn3.2327

Saghai-Maroof, M. A., Soliman, K. M., Jorgensen, R. A., and Allard, R. W. (1984). Ribosomal DNA spacer-length polymorphisms in barley: mendelian inheritance, chromosomal location, and population dynamics. *Proc. Natl. Acad. Sci. U.S.A.* 81, 8014–8018. doi: 10.1073/pnas.81.24.8014

Saini, N., Yashpal, Koramutla, M. K., Singh, N., and Yadava, D. K. (2019). Promoter polymorphism in FAE1.1 and FAE1.2 genes associated with erucic acid content in *Brassica juncea*. *Mol. Breed.* 39:75. doi: 10.1007/s11032-019-0971-x

Sakhno, L. O. (2010). Variability in the fatty acid composition of rapeseed oil: classical breeding and biotechnology. *Cytol. Genet.* 44, 389–397. doi: 10.3103/S0095452710060101

Sakurai, T., and Shindo, T. (2021). Production of single- and multiple-gene-modified mice via maternal SpCas9-based gene editing. *STAR Protoc.* 2:100509. doi: 10.1016/j.xpro.2021.100509

Salas, J. J., and Ohlrogge, J. B. (2002). Characterization of substrate specificity of plant FatA and FatB acyl-ACP thioesterases. *Arch. Biochem. Biophys.* 403, 25–34. doi: 10.1016/S0003-9861(02)00017-6

Sanyal, A., and Linder, C. R. (2013). Plasticity and constraints on fatty acid composition in the phospholipids and triacylglycerols of *Arabidopsis* accessions grown at different temperatures. *BMC Plant Biol.* 13:63. doi: 10.1186/1471-2229-13-63

Shi, C., Zhang, H., Wu, J., Li, C., and Ren, Y. (2003). Genetic and genotype×environment interaction effects analysis for erucic acid content in rapeseed (*Brassica napus L.*). *Euphytica* 130, 249–254. doi: 10.1023/A:1022867100199

Shi, J. H., Lang, C. X., Wu, X. L., Liu, R. H., Zheng, T., Zhang, D. Q., et al. (2015). RNAi knockdown of fatty acid elongase1 alters fatty acid composition in *Brassica napus*. *Biochem. Biophys. Res. Commun.* 466, 518–522. doi: 10.1016/j.bbrc.2015.09.062

Shi, J., Lang, C., Wang, F., Wu, X., Liu, R., Zheng, T., et al. (2017). Depressed expression of FAE1 and FAD2 genes modifies fatty acid profiles and storage

compounds accumulation in *Brassica napus* seeds. *Plant Sci.* 263, 177–182. doi: 10.1016/j.plantsci.2017.07.014

Siddiqui, H. A., Harvey-Samuel, T., and Mansoor, S. (2021). Gene drive: a faster route to plant improvement. *Trends Plant Sci.* 26, 1204–1206.

Nadakuduti, S. S., and Enciso-Rodríguez, F. (2021). Advances in genome editing with CRISPR systems and transformation technologies for plant DNA manipulation. *Front. Plant Sci.* 11:637159. doi: 10.3389/fpls.2020.637159

Stimming, M., Mesch, C. M., Kersting, M., and Libuda, L. (2015). Fish and rapeseed oil consumption in infants and mothers: dietary habits and determinants in a nationwide sample in Germany. *Eur. J. Nutr.* 54, 1069–1080. doi: 10.1007/s00394-014-0784-y

Stumpf, P. K., and Pollard, M. R. (1983). "Pathways of fatty acid biosynthesis in higher plants with particular reference to developing rapeseed," in *High Low Erucic Acid Rapeseed Oils*, eds J. K. Kramer, F. Sauer, and W. J. Pigden (Cambridge, MA: Academic Press), 131–141. doi: 10.1016/B978-0-12-425080-2.50010-4

Taylor, D. C., Falk, K. C., Palmer, C. D., Hammerlindl, J., Babic, V., Mietkiewska, E., et al. (2010). *Brassica carinata*–a new molecular farming platform for delivering bio-industrial oil feedstocks: case studies of genetic modifications to improve very long-chain fatty acid and oil content in seeds. *Biofuels Bioprod. Biorefin.* 4, 538–561. doi: 10.1002/bbb.231

Taylor, D. C., Francis, T., Guo, Y., Brost, J. M., Katavic, V., Mietkiewska, E., et al. (2009). Molecular cloning and characterization of a KCS gene from Cardamine graeca and its heterologous expression in Brassica oilseeds to engineer high nervonic acid oils for potential medical and industrial use. *Plant Biotechnol. J.* 7, 925–938. doi: 10.1111/j.1467-7652.2009.00454.x

Taylor, D. C., Smith, M. A., Fobert, P., Mietkiewaska, E., and Weselake, R. J. (2011). Metabolic engineering of higher plants to produce bio-industrial oils. *Compr. Biotechnol.* 4, 67–85. doi: 10.1016/b978-0-08-088504-9.00256-7

Tian, B., Wei, F., Shu, H., Zhang, Q., and Lian, Y. (2011). Decreasing erucic acid level by RNAi-mediated silencing of fatty acid elongase 1 (BnFAE1.1) in rapeseeds (*Brassica napus L.*). *Afr. J. Biotechnol.* 10, 13194–13201. doi: 10.5897/AJB11.1465

Tjellström, H., Strawsine, M., Silva, J., Cahoon, E. B., and Ohlrogge, J. B. (2013). Disruption of plastid acyl:acyl carrier protein synthetases increases medium chain fatty acid accumulation in seeds of transgenic *Arabidopsis*. *FEBS Lett.* 587, 936–942. doi: 10.1016/j.febslet.2013.02.021

Tocher, D. R., Betancor, M. B., Sprague, M., and Olsen, R. E. (2019). Omega-3 long-chain polyunsaturated fatty acids, EPA and DHA: bridging the gap between supply and demand. *Nutrients* 11:89. doi: 10.3390/nu11010089

Uğur, A., Süntar, I., Sinem Aslan, S., Orhan, E., Kartal, M., Şekeroğlu, N., et al. (2010). Variations in fatty acid compositions of the seed oil of *eruca sativa mill.* caused by different sowing periods and nitrogen forms. *Phcog. Mag.* 6, 305–308. doi: 10.4103/0973-1296.71801

Vetter, W., Darwisch, V., and Lehnert, K. (2020). Erucic acid in Brassicaceae and salmon-An evaluation of the new proposed limits of erucic acid in food. *NFS J.* 19, 9–15. doi: 10.1016/j.nfs.2020.03.002

Vles, R. O., Bijster, G. M., Kleinekoort, J. S. W., Timmer, W. G., and Zaalberg, J. (1978). Nutritional Status of Low-Erucic-Acid Rapeseed Oils. *Eur. J. Lipid Sci. Technol.* 78, 128–131. doi: 10.1002/lipi.19760780307

Wallace, H., Knutsen, H. K., Alexander, J., Barregaard, L., Bignami, M., Brüschweiler, B., et al. (2016). Erucic acid in feed and food. *EFSA J.* 14:4593.

Wang, N., Wang, Y., Tian, F., King, G. J., Zhang, C., Long, Y., et al. (2008). A functional genomics resource for *Brassica napus*: development of an EMS mutagenized population and discovery of FAE1 point mutations by TILLING. *New Phytol.* 180, 751–765. doi: 10.1111/j.1469-8137.2008.02619.x

Wang, Z. W., Zhang, Z. Y., Lin, L. T., Zhang, J. W., Liu, M. J., and Qiao, Y. (2019). Artificial miRNA regulation of erucic acid in *Brassica napus*. *J. Nucl. Agric.* 33, 0024–0030. doi: 10.11869/j.issn.100-8551.2019.01.0024

Warner, D. J., and Lewis, K. A. (2019). Evaluation of the risks of contaminating low erucic acid rapeseed with high erucic rapeseed and identification of mitigation strategies. *Agriculture* 9:190. doi: 10.3390/agriculture9090190

Wilmer, J. A., Helsper, J., and Plas, L. (1997). Effects of abscisic acid and temperature on erucic acid accumulation in oilseed rape (*Brassica napus L.*). *J. Plant Physiol.* 150, 414–419. doi: 10.1016/S0176-1617(97)80091-0

Wu, G. T., Lang, C. X., and Chen, J. Q. (2007). Breeding and application of high erucic acid oleaginous rape for industrial use. *J. Nucl. Agric.* 21, 374–377. doi: 10.3969/j.issn.1000-8551.2007.04.013

Wu, G., Wu, Y., Xiao, L., Li, X., and Lu, C. (2008). Zero erucic acid trait of rapeseed (*Brassica napus L.*) results from a deletion of four base pairs in the fatty acid elongase 1 gene. *Theor. Appl. Genet.* 116, 491–499. doi: 10.1007/s00122-007-0685-z

Yaniv, Z., Schafferman, D., and Zur, M. (1994). The effect of temperature on oil quality and yield parameters of high- and low-erucic acid Cruciferae seeds (rape and mustard). *Ind. Crops Prod.* 3, 247–251. doi: 10.1016/0926-6690(94)00041-V

Ytrestøyl, T., AaS, T. S., and Åsgård, T. (2015). Utilisation of feed resources in production of Atlantic salmon (*Salmo salar*) in Norway. *Aquaculture* 448, 365–374. doi: 10.1016/j.aquaculture.2015.06.023

Zasada, I. A., Weiland, J. E., Reed, R. L., and Stevens, J. F. (2012). Activity of meadowfoam (*Limnanthes alba*) seed meal glucolimnanthin degradation products against soilborne pathogens. *J. Agric. Food Chem.* 60, 339–345. doi: 10.1021/jf203913p

Zhang, D. Q., Zhang, Z. Y., Unver, T., and Zhang, B. (2020). CRISPR/Cas: a powerful tool for gene function study and crop improvement. *J. Adv. Res.* 29, 207–221. doi: 10.1016/j.jare.2020.10.003

Conflict of Interest: XZ was employed by China National Seed Group Co., Ltd.

The remaining authors declare that the research was conducted in the absence of any commercial or financial relationships that could be construed as a potential conflict of interest.

Publisher's Note: All claims expressed in this article are solely those of the authors and do not necessarily represent those of their affiliated organizations, or those of the publisher, the editors and the reviewers. Any product that may be evaluated in this article, or claim that may be made by its manufacturer, is not guaranteed or endorsed by the publisher.

frontiers | Frontiers in Plant Science

REVIEW
published: 02 June 2022
doi: 10.3389/fpls.2022.908608

Molecular Approaches Reduce Saturates and Eliminate *trans* Fats in Food Oils

*James G. Wallis, Jesse D. Bengtsson and John Browse**

Institute of Biological Chemistry, Washington State University, Pullman, WA, United States

Vegetable oils composed of triacylglycerols (TAG) are a major source of calories in human diets. However, the fatty acid compositions of these oils are not ideal for human nutrition and the needs of the food industry. Saturated fatty acids contribute to health problems, while polyunsaturated fatty acids (PUFA) can become rancid upon storage or processing. In this review, we first summarize the pathways of fatty acid metabolism and TAG synthesis and detail the problems with the oil compositions of major crops. Then we describe how transgenic expression of desaturases and downregulation of the plastid *FatB* thioesterase have provided the means to lower oil saturates. The traditional solution to PUFA rancidity uses industrial chemistry to reduce PUFA content by partial hydrogenation, but this results in the production of *trans* fats that are even more unhealthy than saturated fats. We detail the discoveries in the biochemistry and molecular genetics of oil synthesis that provided the knowledge and tools to lower oil PUFA content by blocking their synthesis during seed development. Finally, we describe the successes in breeding and biotechnology that are giving us new, high-oleic, low PUFA varieties of soybean, canola and other oilseed crops.

Keywords: biotechnology, high-oleic, polyunsaturated fatty acid, oilseed, saturated fatty acid, *trans* fat, triacylglycerol, vegetable oil

OPEN ACCESS

Edited by:
Jacqueline Batley, University of Western Australia, Australia

Reviewed by:
Xue-Rong Zhou, Commonwealth Scientific and Industrial Research Organisation (CSIRO), Australia
Qing Liu, Commonwealth Scientific and Industrial Research Organisation (CSIRO), Australia

***Correspondence:**
John Browse
jab@wsu.edu

Specialty section:
This article was submitted to Crop and Product Physiology, a section of the journal Frontiers in Plant Science

Received: *30 March 2022*
Accepted: *02 May 2022*
Published: *02 June 2022*

Citation:
Wallis JG, Bengtsson JD and Browse J (2022) Molecular Approaches Reduce Saturates and Eliminate trans Fats in Food Oils. Front. Plant Sci. 13:908608. doi: 10.3389/fpls.2022.908608

INTRODUCTION

Vegetable oils constitute one of the world's most important plant commodities, with current annual production in excess of 605 million metric tons (USDA FAS, 2022) with a total value of $US244 billion (Kamble and Roshan, 2022). Consumption has increased steadily since 1970 at an average annual rate of 4%—about twice the rate of growth in world population. The major use of plant oils is in human and animal diets; in western diets plant oils and other fats contribute ~35% of calorie intake [CDC (US Centers for Disease Control), 2021]. Seed oils are composed almost entirely of triacylglycerols (TAG) in which fatty acids are esterified to each of the three hydroxyl groups of glycerol. The use of TAG as a seed reserve maximizes the quantity of stored energy for seedling germination and establishment, because the fatty acids are a highly reduced form of carbon (Graham, 2008; Baud and Lepiniec, 2010). A large variety of different fatty acid structures are found in nature (Hilditch and Williams, 1964; Gunstone, 1998), but just five account for >90% of the food oils produced: palmitic (16:0), stearic (18:0), oleic (18:1), linoleic (18:2), and α-linolenic (18:3) acids. These fatty acids are

the ones also found most commonly in membrane lipids of plant cells (Ohlrogge and Browse, 1995). Monographs (Hilditch and Williams, 1964; Weiss, 1983) and searchable databases (Plantfadb.org; Ohlrogge et al., 2018) provide detailed information on oil compositions of many plant species. In **Figure 1**, we have summarized data from relevant oil crops to show the proportions of monounsaturated (mainly 18:1), polyunsaturated (PUFA; 18:2 plus 18:3) and saturated (16:0 and 18:0) fatty acids.

To a large extent the increases in oil production over the last 50 years have been fueled by the release of improved varieties and efficiencies of cultivation for a relatively few species—soybean (*Glycine max*), oil palm (*Elaeis guineensis*), canola (*Brassica napus*), and sunflower (*Helianthus annuus*). As a result, expansion of oil production has continued even though these major vegetable oils exhibit fatty acid compositions that make them less than ideal for human nutrition and the requirements of the food industry. For example, as shown in **Figure 1**, both traditional soybean and canola oils contain PUFA levels that threaten the shelf life of products made from them (Weiss, 1983; Gurr, 1992). Tropical oils, including palm and coconut, contain high levels of saturated fat, which are undesirable because they contribute to the development of atherosclerosis (Hooper et al., 2020). By contrast, monounsaturated oleic (18:1) and palmitoleic (16:1) acids protect against heart disease and metabolic syndrome (Gillingham et al., 2011). Modifying the fatty acid compositions of food oil crops is therefore an attractive goal that will permit diversification of agricultural production into a new generation of custom-designed crops (Msanne et al., 2020). As a result, there is unprecedented interest among plant biotechnology companies in modifying oil composition by changing the expression of endogenous genes, and by the use of cloned genes, to alter the products of seed lipid metabolism (Napier and Graham, 2010; Lu et al., 2011; Chen and Lin, 2013).

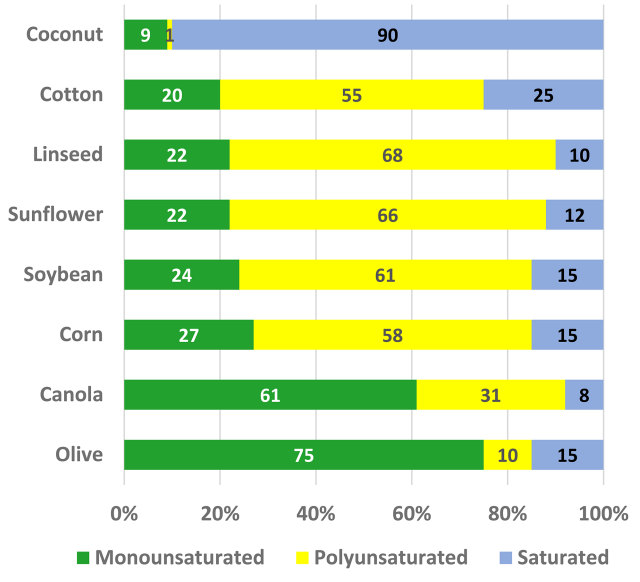

FIGURE 1 | The oil compositions of some major crops. The percentages of monounsaturated (mainly 18:1), polyunsaturated (18:2 + 18:3), and saturated (16:0 + 18:0) fatty acids are shown.

In this review, we shall first present the issues and challenges related to the fatty acid compositions of seed oils. Then we will describe how discoveries in the biochemistry, genetics, genomics and molecular biology of lipid metabolism have provided the tools and insight needed to engineer desirable changes in the fatty acid compositions of soybean, canola and other oilseed crops. These achievements have already led to the production of improved oilseed varieties.

THE NETWORK OF PATHWAYS FOR TAG SYNTHESIS IN OILSEEDS

Most of the major oilseed crops (including soybean, canola, and sunflower) are characterized by oils containing predominantly 18-carbon unsaturated fatty acids plus lower proportions of saturated 16:0 and 18:0 that are also the major fatty acids of plant membrane lipids. The synthesis and accumulation of TAG in oilseeds occurs through a complex network of pathways located in the plastid, cytosol, endoplasmic reticulum, and lipid droplets. The pathways are summarized in **Figure 2**. Insights into the pathways and enzymes in this scheme have come from biochemical studies in many oilseeds (Voelker and Kinney, 2001; Bates et al., 2013) as well as genetic studies in the model oilseed Arabidopsis (Miquel and Browse, 1992; Browse et al., 1993; Lu et al., 2009; Wallis and Browse, 2010). The present formulation of the pathways shown in **Figure 2** has benefited greatly from characterization of mutants (Lemieux et al., 1990; Miquel and Browse, 1992; Lu et al., 2009). Cloning of genes encoding several of the enzymes also depended on mutant analysis (Arondel et al., 1992; Okuley et al., 1994; Lu et al., 2009).

In plants, fatty acid synthase (FAS) is a multi-component (Type II) enzyme located in the plastid (Ohlrogge and Browse, 1995). The first committed step of fatty acid synthesis is the conversion of acetyl-CoA to malonyl-CoA by acetyl-CoA carboxylase (ACCase; Konishi and Sasaki, 1994). In dicots the ACCase is a multicomponent enzyme that is subject to feedback regulation by the actions of biotin attachment domain-containing (BADC) proteins (Salie et al., 2016; Keereetaweep et al., 2018). Following synthesis, the malonyl group of malonyl-CoA, is transferred to acyl carrier protein (ACP) by malonyl-CoA:ACP malonyltransferase (Lessire and Stumpe, 1983). The fatty acid synthase utilizes acetyl-CoA as the starting unit for condensation reactions, with malonyl-ACP providing two-carbon units in seven cycles of condensation and reduction to yield 16:0-ACP. Some 16:0 is released by thioesterases of the FATB family (Jones et al., 1995), but most is elongated through one more cycle of fatty acid synthesis to 18:0-ACP and efficiently desaturated by a stromal Δ9 stearoyl-ACP desaturase (Lindqvist et al., 1996) before being released by a FATA thioesterase. Thus, 16:0, 18:0 and 18:1 are the products exported from the plastid, after conversion to CoA thioesters by long-chain acyl-CoA synthetase (LACS) enzymes in the plastid envelope (Schnurr et al., 2002;

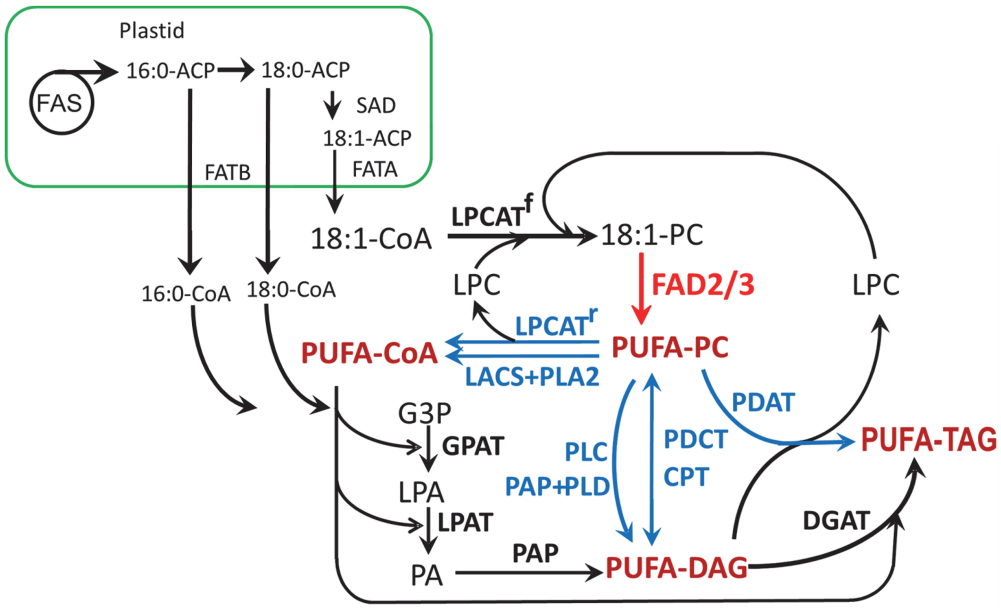

ACP	Acyl Carrier Protein	LPAT	acyl-CoA:LPA acyltransferase
FAS	Fatty Acid Synthetase	LPCAT	acyl-CoA:lysoPC acyltransferase
FAD2	Δ12 18:1 Desaturase	PAP	phosphatidic acid phosphatase
FatA	Oleoyl-ACP thioesterase	PDAT	PC:DAG acyltransferase
FatB	Palmitoyl-ACP thioesterase	PDCT	PC:DAG cholinephosphotransferase
CPT	CDP-choline:DAG cholinephosphotranferase	PLA	Phospholipase A
DGAT	acyl-CoA:DAG acyltransferase	PLC	Phospholipase C
GPAT	acyl-CoA:G3P acyltransferase	PLD	Phospholipase D
LACS	longchain acyl-CoA synthetase	SAD	Δ9 Stearoyl-ACP desaturase

FIGURE 2 | A simplified metabolic scheme for the synthesis of fatty acids and TAG in oilseeds. Following synthesis in the plastid, 16:0, 18:0, and 18:1 are exported to the cytoplasm and edoplasmic reticulum as acyl-CoAs. Saturated 16:0 and 18:0 are mainly incorporated through GPAT of the Kennedy pathway. Monounsaturated 18:1 may also enter the Kennedy pathway, but most is incorporated directly into PC by LPCAT. PUFA are synthesized from 18:1 on PC by the FAD2 desaturase, with some being further desaturated by FAD3 (red arrow). The three pathways that can mobilize PUFA from PC for TAG synthesis, shown in blue, are: (1) removal of PUFA from PC to the acyl-CoA pool by reverse LPCAT or combined PLA2 and LACS; (2) removal of the PC phosphocholine head group to produce PUFA-DAG by PDCT, reverse CPT, PLC, or PLD/PAP; (3) direct transfer to DAG by PDAT. Substrate abbreviations are as follows: DAG, diacylglycerol; G3P, glycerol-3-phosphate; LPA, lyso-phosphatidic acid; LPC, lyso-phosphatidylcholine; PA, phosphatidic acid; PC, phosphatidylcholine; TAG, triacylglycerol.

Shockey et al., 2002), to become the primary substrates for glycerolipid synthesis in the endoplasmic reticulum.

The most direct route for TAG synthesis, sometimes called the Kennedy Pathway, could use only the 16:0-, 18:0- and 18:1-CoAs produced by the plastid to sequentially acylate glycerol-3-phosphate. The initial step in this pathway (**Figure 2**) is the transfer of an acyl group from acyl-CoA to the *sn*-1 position of glycerol-3-phosphate by acyl-CoA:glycerol-3-phosphate acyltransferase 9 (GPAT9) that generates lysophosphatidic acid (Shockey et al., 2016; Singer et al., 2016). Next, acyl-CoA:lysophosphatidic acid acyltransferase 2 (LPAT) forms phosphatidic acid (PA) by transferring an acyl group from the acyl-CoA to the *sn*-2 position of lysophosphatidic acid (Kim et al., 2005). Then, a phosphatidic acid phosphatase (PAP) enzyme removes the phosphate group at the *sn*-3 position to form diacylglycerol (DAG) before acyl-CoA:diacylglycerol acyltransferase (DGAT) adds a third acyl group to produce TAG. In this simple scenario TAG would contain only 16:0, 18:0, and 18:1 fatty acids, but seed oils also contain varying proportions of PUFA (**Figure 1**). In oilseeds conversion of 18:1 to 18:2 and 18:3 occurs on phosphatidylcholine (PC), the main structural lipid of the endoplasmic reticulum (Ohlrogge and Browse, 1995). In seeds, and also in other tissues, 18:1-PC is converted to 18:2-PC by fatty acid desaturase2 (FAD2), with some further desaturation to 18:3-PC by FAD3 (**Figure 2**, red arrow; Arondel et al., 1992; Okuley et al., 1994).

The transfer of 18:1 into PC for desaturation occurs by two main routes. The first and major route, acyl-editing (Bates et al., 2012), involves the transfer of 18:1 from 18:1-CoA to the *sn*-2 position of lyso-PC by acyl-CoA:lysoPC acyltransferase (LPCAT; Ståhl et al., 2004, 2008; Wang et al., 2012) and possibly other enzymes (Lager et al., 2015). The second is the conversion of 18:1-DAG to PC by either CDP-choline:DAG cholinephosphotransferase (CPT; Liu et al., 2015) or PC:DAG cholinephosphotransferase (PDCT; Lu et al., 2009; **Figure 2**).

Following the synthesis of PUFA on PC, there are three routes and at least seven possible mechanisms for the transfer of PUFA back into the pathways of TAG synthesis (**Figure 2**, blue). The LPCAT reaction is reversible, so that PUFA may enter the acyl-CoA pool and be used by the acyltransferases of the Kennedy pathway, and PUFA-CoA may also be formed by the combined actions of phospholipase A2 (PLA2) and LACS. The CPT reaction is also reversible, while the PDCT reaction is symmetrical, so that a new DAG molecule is generated each time 18:1-DAG is converted to PC. In principle, PUFA-PC may also be converted to PUFA-DAG by phospholipase C (PLC), or by phospholipase D (PLD) combined with PAP. Finally, direct transfer of the *sn*-2 fatty acid of PC to the *sn*-3 of DAG occurs by the action of phospholipid:DAG acyltransferase (PDAT; Dahlqvist et al., 2000; Mhaske et al., 2005). Lyso-PC is a co-product of the PDAT reaction and this can be reincorporated into the acyl editing cycle to channel 18:1 into PC for desaturation.

Metabolic labeling studies in various plant species has shown that the pathways and reactions within the network shown in **Figure 2** contribute to TAG synthesis differently between species. In Arabidopsis, the DAG substrate for TAG formation comes mainly from PC (Bates and Browse, 2012), while acyl flux occurs primarily through the Kennedy pathway in other species. Once formed, nascent TAG accumulates between the leaflets of the endoplasmic reticulum bilayer membrane, which stimulates lipid droplet formation for sequestration in the maturing seed. New evidence indicates that, in some species, TAG molecules may be remodeled after synthesis by acyl-exchange reactions (Bhandari and Bates, 2021).

In the following sections, we will review the ways in which studies of lipid metabolism in Arabidopsis have resulted in new discoveries and a better understanding of the reactions, pathways and control of oil synthesis and accumulation in seeds, as well as new molecular tools that have allowed successful production of more-healthy oils.

IN VEGETABLE OILS BOTH SATURATES AND PUFA PRESENT CHALLENGES

Saturated Fats Are Unhealthy

Diets high in saturated fats are a known risk factor for heart attack, stroke and other diseases (Wang et al., 2016a,c). The reasons for this connection to health problems lie in the biophysical properties of saturated fatty acids. Animal fats (TAG), such as lard, beef tallow, and butter, contain 40%–70% saturates (Soyeurt et al., 2006), and are solid at room temperature because weak Van der Waals forces along the hydrocarbon chains of adjacent fatty acids favor the solid state (Kučerka et al., 2015). This property also encourages deposition of saturated TAG and fatty acid in atherosclerotic plaques in blood vessels, raising the risk for heart attack and stroke. The presence of a single, *cis* double bond produces a bend in the fatty acid chain that prevents extensive Van der Waals interactions (**Figure 3**). As a result, the melting temperature of lipids containing monounsaturated fatty acids are close to 0°C compared with ~50°C for saturated lipids (Dratz and Deese, 1986; Niebylski and Salem, 1994; Stillwell and Wassall, 2003; Lin et al., 2017).

Although the biophysical issues are more complicated in biological membranes, the same properties of saturated fatty acid also make them unsuitable, by themselves, as components of the glycerolipids that make up the bilayer of these membranes. The membranes of essentially all cellular organisms require the majority of fatty acid in their glycerolipids to be *cis*-unsaturated to provide the fluidity and function to support cell processes (Pilch et al., 1980; McConn and Browse, 1998; Ballweg and Ernst, 2017).

Polyunsaturated Fatty Acids Become Rancid by Oxidation

In plants, the predominant PUFA are 18:2 and 18:3, which are major components of many seed oils (**Figure 1**). These same PUFA perform essential functions as constituents of plant membranes and as substrates for plant hormone synthesis. As constituents of membrane lipids, PUFA are vital to a wide range of membrane functions, conferring fluidity, flexibility, and selective permeability to membranes (Los et al., 2013), while also supporting efficient photosynthesis (Allakhverdiev et al., 2009). These PUFA affect many other metabolic and physiological processes, including cold adaptation and survival (Liu et al., 2013; Hou et al., 2016), heat adaptation (Falcone et al., 2004), modulation of ion channels (Gutla et al., 2012; Elinder and Liin, 2017), as well as endocytosis/exocytosis (Murphy et al., 2005; König et al., 2008; Doherty and McMahon, 2009). PUFA have roles in optimizing the activities of membrane-associated enzymes that are sensitive to biophysical properties of lipid membranes (Upchurch, 2008). The oxylipin jasmonic acid is derived from 18:3 and, as the hormone jasmonyl-isoleucine, helps regulate insect and pathogen defense, reproductive development, and other key processes (Browse, 2009; Chung et al., 2009; Browse and Wallis, 2019).

PUFA play similarly important structural and signaling roles in animals, but mammals have no orthologue of the plant FAD2 desaturase (**Figure 2**), and thus are unable to synthesize PUFA *de novo* (Wallis et al., 2002), so suitable fatty acids must be acquired in the diet. Mammals require both 18:2 and 18:3 as essential fatty acids, and these are used as substrates to synthesize longer chain fatty acids, 20:4 n-6 (arachidonic acid), 20:5 n-3 (eicosapentaenoic acid) and 22:6 n-3 (docosahexaenoic acid). These very-long-chain PUFA are vital membrane components, especially in the brain and nerve tissues (Kaur et al., 2014). They are also substrates for cyclooxygenase enzymes in pathways that lead to the synthesis of the n-3 and n-6 families of eicosanoids, including prostaglandins, leukotrienes, and thromboxanes, that bind to specific G-protein-coupled receptors and signal cellular responses that mediate fever, inflammation, vasodilation, blood pressure, and pain (Saini and Keum, 2018).

Meat is a relatively poor source of essential fatty acids (Saini and Keum, 2018). Vegetable oils are the major source 18:2 and 18:3 in human diets; however, it has been calculated that the minimum required intake of these PUFA is typically met

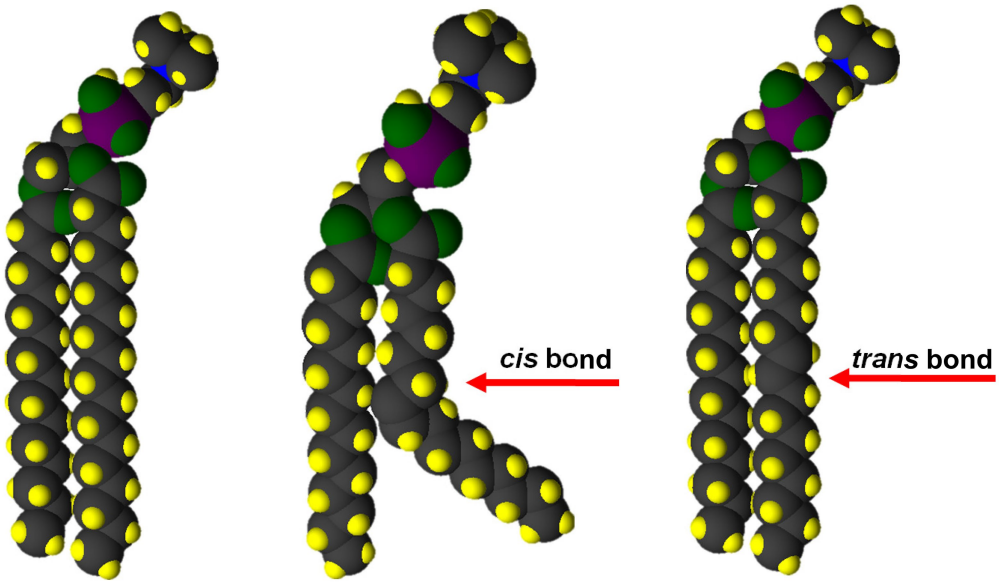

FIGURE 3 | Only *cis* double bonds provide the membrane fluidity and functionality required for life. The bend in the fatty acid chain caused by a C=C *cis* double bond (center) disrupts Van der Waals interactions. Both saturated (left) and *trans* unsaturated (right) fatty acids provide for maximum Van der Waals interaction and a rigid structure.

from other plant sources, such as green leafy vegetables (Johnson et al., 2018). Furthermore, because of the inefficiencies of human PUFA metabolism it is actually preferable to obtain very-long-chain PUFA directly from eating fish and other marine animals (Mori, 2014). Extracted fish oils are also widely used as dietary supplements. The origin of very-long-chain PUFA, 20:4 n-6, 20:5 n-3, and 22:6 n-3, found in fish is microalgae (phytoplankton); the PUFA synthesized in algae are concentrated by the food chain into fish tissues (Ryckebosch et al., 2012). Several microalgae have also been grown in culture as sources of PUFA (Vrenna et al., 2021). For these reasons, the PUFA components of plant oils are not required for optimum nutrition in humans and other mammals. The fact that PUFA are inessential components of plant oils is fortunate because, as described below, their presence has been a challenge to food processing for more than a century—and for storage of oils for millennia.

The dietary requirement for PUFA is complicated by differences in human metabolism that result from consuming n-3 and n-6 fatty acids. Both n-3 and n-6 very-long-chain PUFA are metabolized to produce eicosanoid regulatory molecules, but the derivatives of the n-3 fatty acids, 20:5 and 22:6 quell excitation of the inflammatory response in tissues, while an excess of 20:4 n-6 derivatives have the opposite effect, elevating inflammation in a variety of tissues (Serhan and Savill, 2005). Persistent inappropriate stimulation of the inflammatory response is linked to development of cardiovascular disease (Harris et al., 2007) and cancer (Kwon, 2016). Human health is damaged when intake of n-6 fatty acids greatly exceeds that of n-3 fatty acids. In contrast, consumption of high levels of n-3 fatty acids are correlated with reductions in diabetes, obesity, osteoporosis, and some forms of neurological degeneration (Natto et al., 2019). The key to health is in the balance of n-3 and n-6 fatty acids (Simopoulos, 2003). The high levels of the n-6 PUFA, 18:2, from vegetable oils in the diets of many countries has led to efforts to enrich diets for n-3 fatty acids by promoting changes in diet to fish oils or designing food-stuffs that are n-3 enriched. In this respect, green leafy vegetables, which contain a high ratio of 18:3 n-3 to 18:2 n-6, are a good source of these essential fatty acids. Some seed and nut oils also offer naturally high levels of n-3 fatty acids (Kuhnt et al., 2012). Successful transgenic modification of commercial oil crops to produce very-long-chain PUFA have recently obtained regulatory approval in some countries, and may become important sources of these fatty acids, particularly by providing plant-based feed stocks for aquaculture (Napier et al., 2019; Han et al., 2020).

A pervasive risk from PUFA chemistry is the propensity of these fatty acids to undergo oxidation. The susceptibility to oxidation increases considerably with each additional double bond in the carbon chain. In both plants and animals, membrane integrity and function are threatened by oxidation initiated by reactive oxygen species generated during photosynthesis, respiration and other processes (Foyer and Shigeoka, 2011; Smirnoff and Arnaud, 2019). Living cells employ a range of metabolic defenses to limit and repair this damage (Gill and Tuteja, 2010; Das and Roychoudhury, 2014; Zandalinas et al., 2020). For vegetable oils—and fish oils—PUFA oxidation during storage and food manufacture are a particular challenge, especially during high-temperature applications. Free radical formation by abstraction of a hydrogen atom and addition of molecular oxygen to the *cis*, *cis*-1,4-pentadiene structures of PUFA leads to the production of aldehydes, alcohols, and fatty acid peroxides (**Figure 4**; Schneider, 2009). Isoprostanes are also formed and

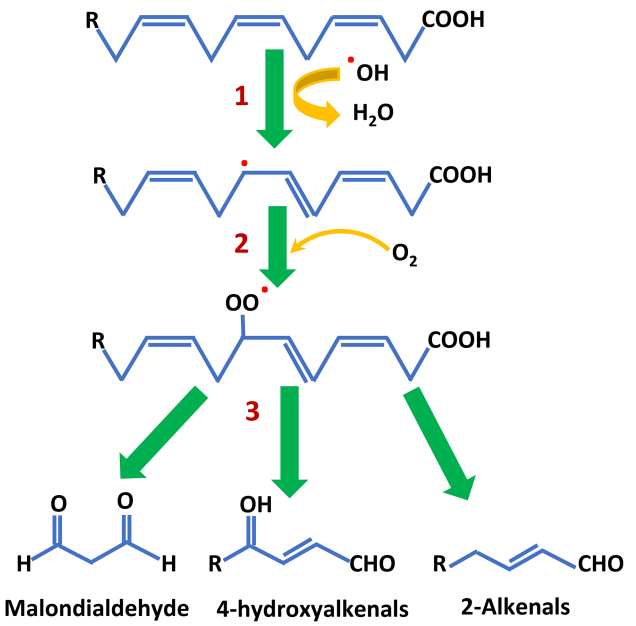

FIGURE 4 | An abbreviated scheme of PUFA oxidation that results in rancidity. 1. Reaction of the *cis*, *cis*-1,4-pentadiene structure with reactive oxygen species (shown here as the hydroxyl radical) produces a PUFA free radical. 2. Addition of molecular oxygen produces a peroxy radical. 3. Intramolecular rearrangements and further oxidation leads to chain cleavage and the production of a number of low molecular weight products. Note that the peroxy radical can abstract a proton from another PUFA molecule to propagate and accelerate PUFA breakdown.

these are a health concern because they can mimic prostaglandins (Roberts and Milne, 2009). The rancid smell of oxidized oils during storage, or in baked goods and other food products, comes from release of these compounds as PUFA break down. The process is greatly accelerated when oils containing PUFA are heated, for example in frying. The addition of antioxidants and oil blending can ameliorate the effects of oxidation to some extent (Mishra et al., 2021) but, as described below, conversion of PUFA by partial hydrogenation has previously been widely used to stabilize oil and produce margarine and other solid fats.

STRATEGIES TO LOWER SATURATE CONTENT OF VEGETABLE OILS

Desaturase Genes

Some plant TAGs contain high proportions of saturated fatty acids that are comparable to levels in animal fats. For example, cocoa butter (*Theobroma cocao*) contains 60% 16:0 + 18:0 (Lipp et al., 2001; Gilabert-Escrivá et al., 2002), while palm oil has 50% saturates (Mukherjee and Mitra, 2009). The same health issues are a concern with these in food products. Even though most food oils have much lower proportions of saturates (**Figure 1**), it is nevertheless desirable to reduce the levels further. One strategy that has been investigated for this purpose is to desaturate 16:0, which is the major saturated fatty acid in most plant oils.

Macadamia nuts (*Macadamia integrifolia*) and seeds of the subtropical cat's claw vine (*Doxantha unguis-cati*) have variant acyl-ACP desaturases (Cahoon et al., 1998) that convert a major proportion of 16:0 to 16:1 Δ9 (palmitoleate). To investigate whether the cat's claw enzyme could reduce the level of saturates in plant oils, Bondaruk et al. (2007) cloned a cDNA encoding this enzyme and expressed it in developing seeds of Arabidopsis and canola. Although the transgenic desaturase catalyzed synthesis of 16:1 (some of which was elongated to longer-chain monounsaturates), the proportion of 16:0 in the seed oil was reduced only slightly—14% in Arabidopsis and less than 5% in canola (Bondaruk et al., 2007). In another study, site-directed mutagenesis of the castor (*Ricinus communis*) 18:0-ACP desaturase based on analysis of the crystal structure of the protein (Lindqvist et al., 1996) produced a modified enzyme (COM25) with high activity and specificity towards 16:0 (Whittle and Shanklin, 2001). Seed from transgenic plants expressing this engineered desaturase contained large increases in 16:1 and its elongation products, but no significant decrease in 16:0, or in total saturates in the oil (Cahoon and Shanklin, 2000; Nguyen et al., 2010). Expression of the COM25 desaturase in mutants of lipid metabolism, such as *fab1* (16:0-ACP elongase, KASII), or *fae1* (acyl-CoA elongase), resulted in larger increases in 16:1, but also increased 16:0—to 19%–22% compared to 10% in the non-transgenic controls (Nguyen et al., 2010). These results indicate that targeting 16:0-ACP for desaturation immediately following its synthesis on the plastid fatty acid synthase is not a successful strategy for reducing saturate content of seed oils.

More fruitful oilseed engineering efforts have focused on desaturating fatty acids following export from the plastid. Several of these experiments used animal acyl-CoA desaturases expressed in seed tissue. A stearoyl-CoA desaturase from rat was expressed in soybean seeds with a seed-specific promoter. This enzyme acts on fatty acids as acyl-CoAs, rather than acting on acyl-ACPs. Compared to controls, transgenic lines with the rat desaturase expressing seeds had 0.6% less 16:0, and <0.1% less 18:0 (Moon et al., 2000). A more successful experiment used a *Caenorhabditis elegans* acyl-CoA desaturase specific to 16:0 (Watts and Browse, 2000). This desaturase, FAT5, when expressed in Arabidopsis seeds, reduced saturated fatty acid content by 65%, from 8.6% to 3.0% of total fatty acids in the oil (Fahy et al., 2013). In vegetative tissues, 16:0 is essential for proper growth and development, and large reductions in 16:0 content resulted in poor germination, establishment, and defective growth (Bonaventure et al., 2003). However, seed-specific FAT5 expression did not result in compromised seed characteristics, or plant development (Fahy et al., 2013).

Other strategies to reduce saturated fatty acid content in seed oil have used cyanobacterial glycolipid desaturase. Cyanobacteria desaturases use ferredoxin as an electron carrier rather than cytochrome b5 used in eukaryotic desaturases. A desaturase from *Synechococcus elongatus* has activity when targeted to the leaf chloroplasts (Ishizaki-Nishizawa et al., 1996), but its utility in oil seed engineering seemed limited (Bai et al., 2016). However, by adding an endoplasmic reticulum targeting sequence, and subjecting the gene to random mutagenesis in the desaturase deficient yeast (*ole1Δ*), variants with high levels

of activity in eukaryotic systems were identified, and when these variants were expressed in Arabidopsis seed, initial transformants had reduced 16:0 levels, comparable to the best homozygous FAT5 lines, but also had reductions in 18:0, unlike the 16-carbon specific FAT5 (Bai et al., 2016).

Blocking 16:0 Export From the Plastid

Expression of desaturases in the endoplasmic reticulum has been successful in reducing saturates by 65% in Arabidopsis seed oil. Strategies targeting the enzyme that allows for export of saturated fatty acids from the chloroplast, fatty acid thioesterase B (FatB) have also yielded seeds with low saturated fatty acid content. Analysis of *fatb* mutants in Arabidopsis showed that knockout of the gene results in 3.6% 16:0 in seed oil compared to 8.6% in controls. However, the *fatb* knockout mutation severely compromised growth, with deleterious alterations throughout lipid metabolism, including defective sphingolipid and chloroplast lipid biosynthesis (Bonaventure et al., 2003). These results indicate that molecular techniques, such as CRISPR/Cas9, that produce constitutive knock out of the *FATB* gene are not viable as a means to reducing saturates in seed oils. For this reason, a number of engineered oilseeds with low saturated and high monounsaturated fatty acids content are based on seed-specific reductions in *FATB* expression (Ozseyhan et al., 2018; Wood et al., 2018). As described later, the Vistive Gold soybean produced by Monsanto (now Bayer), harbors a seed-specific RNAi construct that reduces *FATB* expression.

INDUSTRIAL CHEMISTRY IS THE WRONG SOLUTION TO THE PUFA PROBLEM

Beginning early in the twentieth century, food processors addressed the problem of PUFA oxidation and rancidity by subjecting vegetable oils to a process of partial hydrogenation (Korver and Katan, 2006). The process of hydrogenation involves heating the oil in a closed (oxygen free) reaction vessel in the presence of hydrogen gas and a nickel-based catalyst. Under these conditions, hydrogen is added across the double bonds to generate saturated C-C single bonds. The reaction may be continued to completion to generate a product with fully-saturated, solid TAG; however, in most applications, the process is stopped in order to yield products that range from lightly hydrogenated oils used for cooking or as salad oils, to more highly hydrogenated semi-solid fats such as margarine. These partially hydrogenated fats have been used in baked goods, commercial food preparation and in margarines for many years. However, during partial hydrogenation, many of the *cis* double bonds present in the original oil are converted to *trans* isomers. As indicated earlier, *cis*-unsaturated fatty acids are essential for life on earth, because the presence of *cis* double bonds in a fatty acid esterified to glycerolipids produces a bend in the fatty acid chain that reduces van der Waals interactions and provides the molecular mobility and fluidity required to maintain the structure and biological function of membranes of living cells. All-*trans* fatty acids behave biophysically, and thus physiologically, like saturated fatty acids (**Figure 3**). Furthermore, *trans* fatty acids are poorly metabolized by humans, leading to their accumulation, along with cholesterol, in tissues and blood vessels (Mozaffarian et al., 2006; Micha and Mozaffarian, 2008, 2009; Wang et al., 2016c).

Only very low amounts of *trans* fatty acids appear naturally in foods. Industrial production of *trans*-enriched oils greatly increased the consumption of these formerly rare fatty acids. Industrial production of *trans* fats developed rapidly from its inception early in the last century (Korver and Katan, 2006) and they were widely used to replace saturated fats, such as butter and lard, that were known to be unhealthy. Typically, in foods containing partially hydrogenated oils, *trans* fats made up 10%–30% of the total fat content (Satchithanandam et al., 2004). However, health concerns about *trans* fats themselves were raised when research revealed that their consumption increased blood cholesterol levels (Mensink and Katan, 1990; Troisi et al., 1992). By the mid-1990's alarms were sounded about the connections between *trans* fatty acids and risk factors for coronary heart disease, including atherosclerosis, inflammation and calcification of arteries (Willett et al., 1993; Willett and Ascherio, 1994; Ascherio et al., 1999; Mozaffarian et al., 2006), as well inhibition of prostacyclin synthesis required for blood flow regulation (Kummerow et al., 2013). In some countries, *trans* fat consumption exceeded 7% of total fat consumed beginning in the mid-1970s; consumption in North America was particularly high (Craig-Schmidt, 2006; Micha et al., 2014). Consumption of *trans* fats was shown to have additional unforeseen negative effects on human health, including increased risk of diabetes, cancer, and inflammatory diseases (Kiage et al., 2013; De Souza et al., 2015; Dawczynski and Lorkowski, 2016; Kwon, 2016).

The dangers of foods containing *trans* fats were well established by 1998, but objections and prevarication from industry interests, as well as lethargic responses from some regulatory agencies delayed elimination of *trans* fats from foods for 20 years. Worldwide, more than half a million deaths per year have been attributed to high levels of *trans* fat consumption (Wang et al., 2016a), suggesting a 20-year global death toll of 10 million people. In the U.S., the 20,000 excess deaths in 2010 conservatively estimated by the Centers for Disease Control as being due to *trans* fats is equivalent to deaths from opioid overdoses in that year [NIDA (National Institute on Drug Abuse), 2020].

FAD2 IS THE GATEWAY TO PUFA SYNTHESIS

Synthesis of the PUFA 18:2 from 18:1 is catalyzed by a desaturase (FAD2) that acts on 18:1 esterified to PC, the major structural glycerolipid of the endoplasmic reticulum (**Figure 2**). Analysis of the FAD2 amino-acid sequence identified four hydrophobic, α-helical segments predicted to span the bilayer membrane and three conserved histidine boxes that coordinate the oxo-bridged diiron complex at the active site (Okuley et al., 1994). The Alpha-fold model of the Arabidopsis FAD2 protein

(**Figure 5**) shows how the four hydrophobic α-helical segments are predicted to anchor the protein into the endoplasmic reticulum, while an additional amphipathic α-helix is shown at the membrane-cytoplasm interface (Goddard et al., 2018; Jumper et al., 2021; Pettersen et al., 2021; Varadi et al., 2021). In the folded protein, the three histidine-boxes are brought together to form the active site within the protein domain that sits outside the plane of the membrane.

Following identification of the plant 18:1-PC desaturase (Stymne and Appelqvist, 1978), biochemical and genetic analyses of Arabidopsis *fad2* mutants (Miquel and Browse, 1992, 1994; Miquel et al., 1993) provided a detailed understanding of the biochemical role of the 18:1-PC desaturase in membrane biology and seed-oil synthesis. The FAD2 enzyme is responsible for ~95% of PUFA synthesis in Arabidopsis and other oilseeds (Voelker and Kinney, 2001; Bates et al., 2013). In the null *fad2-2* mutant of Arabidopsis, PUFA are reduced to 3% of seed fatty acids. The remaining fraction is produced by the plastid FAD6 enzyme (Browse et al., 1989). For this reason, reducing or eliminating FAD2 expression is an attractive strategy for greatly lowering the PUFA content of soybean, canola, and other plant oils. In principle, blocking transfer of 18:1 into PC (**Figure 2**) would also reduce PUFA synthesis; however, combining mutations in *ROD1* (PDCT), *LPCAT1* and *LPCAT2* in Arabidopsis reduced PUFA by only 65% (Bates et al., 2012)

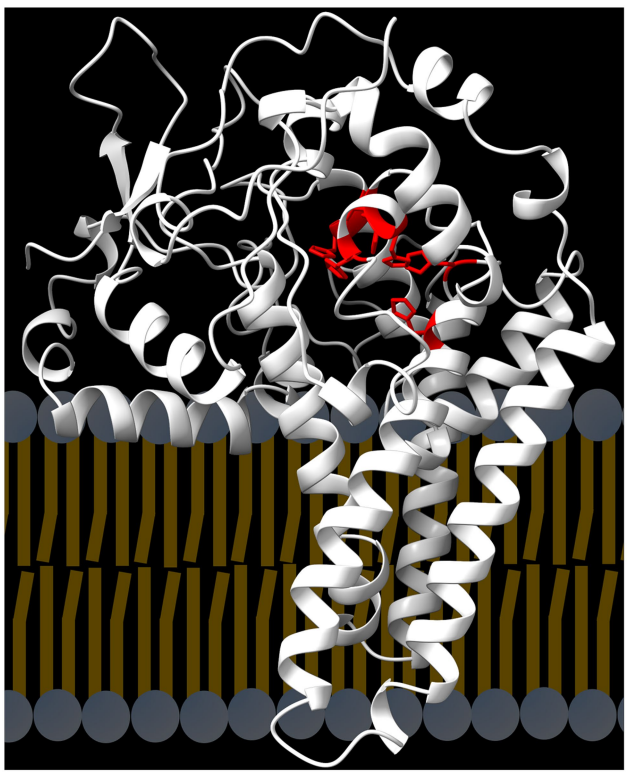

FIGURE 5 | Structure of the FAD2 desaturase. The protein contains four hydrophobic, α–helices that span the enodplasmic reticulum bilayer. In the folded protein the three conserved histidine boxes (red) are brought together to coordinate the diiron-oxo complex at the active site.

because the essential CPT activity catalyzes *de novo* synthesis of PC (**Figure 2**). The cloning of the Arabidopsis *FAD2* gene (At3g12120) by T-DNA tagging (Okuley et al., 1994) allowed the identification and cloning of *FAD2* genes from many plant species, including soybean and canola.

Arabidopsis contains a single *FAD2* gene that is responsible for 18:1 desaturation in all tissues. Plants containing the null *fad2-2* mutation are damaged and killed by low temperatures (Miquel et al., 1993) and *fad2-2* seeds are compromised in development and germination (Miquel and Browse, 1994). These results indicated that strategies to reduce FAD2 activity and PUFA content of oilseeds need to be carefully designed and investigated. Early success in reducing PUFA in soybean was possible because cloning experiments using Arabidopsis *FAD2* as a probe identified two classes of *FAD2* genes. *GmFAD2-2* encodes a constitutive enzyme, while two *GmFAD2-1* genes (*GmFAD2-1A and FAD2-1B*) are expressed only in developing seeds (Heppard et al., 1996; Kinney, 1996). By using a transgene construct to suppress expression of the two seed specific genes, scientists at Dupont Co. successfully produced lines whose seed oil contained <10% PUFA. These lines were available by the mid-1990s, and could have been used to replace partially hydrogenated soybean oil, thereby reducing dietary intake of *trans* fats, providing an attendant reduction in the burden on human health and wellbeing. Unfortunately, the agricultural and food industries were not interested in considering the new oils because partial hydrogenation of conventional soybean oil was cheap, and because the new cultivars were based on transgenic technology. High-oleic varieties of canola and sunflower were also available in the 1990s (Schuppert et al., 2006; Tarrago-Trani et al., 2006), but these were limited to specialty markets because the food industry, especially in the United States, remained wedded to hydrogenation as a means to stabilize vegetable oils and to produce spreads and shortenings.

COMMITTING TO ELIMINATING *TRANS* FATS

The accumulating evidence, for example from the Nurses' Health Study at Harvard, documenting the detrimental effects of *trans* fats on human health (Oh et al., 2005; Ardisson Korat et al., 2014) led to calls from health advocates in the US and other countries to restrict *trans* fats in food. The rate of reduction and elimination of *trans* fats from food has varied greatly from country to country. As early as 1995 industry in the Netherlands and other European countries began voluntary reductions of levels by reformulation of margarines (Katan, 2006). In 2003 voluntary labeling began in Denmark (Leth et al., 2006). In these and other European countries, this early appreciation of dangers of *trans* fats in food led to reformulation of many food products to reduce *trans* fats (List, 2014; Wang et al., 2016b). One method to achieve this was to carry out hydrogenation to completion to provide a fully saturated TAG, then mixing this with untreated oil and using lipase enzymes to bring about interesterification of the TAG fractions to achieve a desired semi-soft or hard product (Sivakanthan and Madhujith,

2020). As a result, *trans*-fat intake in Western Europe in the years 1990–2010 was 60% less than that in North America (1.1% vs. 2.9% of energy; Micha et al., 2014), even though U.S. margarine producers made some efforts to reformulate their products during this period (Tarrago-Trani et al., 2006).

The Canadian government required mandatory labeling of *trans* fat content on foods beginning in the 2005. Concerns expressed to the United States Food and Drug Administration (FDA), beginning in 2000 took some time to persuade regulators. The FDA eventually ruled that after 1 January 2006 the level of *trans* fat must be specified on all food products. The inclusion of this new line item in Nutrition Facts labels greatly boosted public awareness of the dangers of *trans* fats and was followed in the same year by New York City limiting the use of *trans* fats in restaurants (L'abbé et al., 2009). Publicity about these efforts drove consumer opposition to partially hydrogenated oils and resulted in rapid declines in *trans*-fat consumption. This led to reduced demand for soybean oil in favor of canola oil and other alternatives (Goldsmith, 2008). The result was a 32% drop in market share for soybean oil between 2006 and 2014 (United Soybean Board, 2013). Finally, prompted in part by a petition and subsequent litigation (Amico et al., 2021), the FDA agreed in 2015 to ban *trans* fats from foods with final implementation in 2018.

Elsewhere in the world, labeling, limits on *trans*-fat content, and some outright bans on *trans* fats in food were instituted in many countries (Restrepo and Rieger, 2016; Downs et al., 2017). These actions produced rapid declines in global *trans*-fat consumption, although several countries still use more than the World Health Organization (WHO) benchmark for safe consumption (Wanders et al., 2017). The WHO has an active program to convince countries to lower *trans* fatty use [WHO (World Health Organization), 2019].

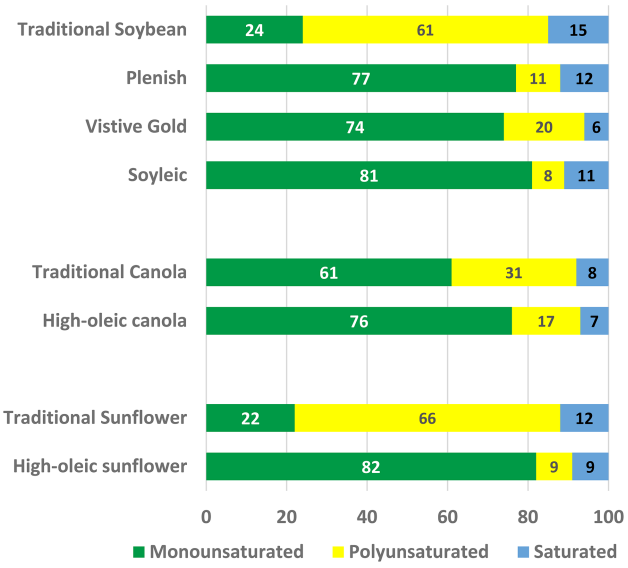

FIGURE 6 | The oil compositions of high-oleic varieties of soybean, canola, and sunflower. The percentages of monounsaturated (mainly 18:1), polyunsaturated (18:2 + 18:3), and saturated (16:0 + 18:0) fatty acids are shown.

IMPROVED OILS BY DESIGN

The cloning and characterization of the Arabidopsis *FAD2* gene was the key to understanding the genetics of high-oleic oilseed varieties in crops species such as canola and sunflower (Dar et al., 2017), and to the development of strategies that quickly led to the production of high-oleic soybean through gene silencing of the two seed-specific *FAD2* homologues, *GmFAD2-1A* and *GmFAD2-1B* (Heppard et al., 1996). As discussed earlier the resulting varieties were not initially accepted by the wider food industry. The high-oleic line developed by DuPont Co. (now Corteva Inc.), Plenish, has a doubly attractive fatty acid profile because the down regulation of *FAD2* genes not only reduces PUFA in favor of monounsaturated 18:1, but also leads to a reduction in 16:0 content to 12%, compared to 15% in regular soybean oil (**Figure 6**; Heppard et al., 1996). The approach taken by Monsanto (now Bayer) scientists, in addition to targeting the *FAD2-1* genes, included the seed-specific suppression of the *GmFatB* gene. This additional gene knockdown results in a substantial additional decline in 16:0 to 6%, thereby further improving the fatty acid profile of this soybean oil marketed as Vistive Gold (**Figure 6**). For soybean and other crops with seeds-specific *FAD2* genes other genomic techniques of gene silencing, such as TALENs and CRISPR/Cas9 are also appropriate and have been used to reduce soybean oil PUFA content (Haun et al., 2014; Demorest et al., 2016).

The fact that the *GmFAD2-1* genes show seed-specific expression indicates that traditional mutation breeding should provide comparable changes in oil composition without requiring transgenic approaches. Indeed, the identification of mutations in both *GmFAD2-1A* and *GmFAD2-1B* genes and their combination produced a soybean line with 18:1 and PUFA levels (**Figure 6**) comparable to those in Plenish soybean oil (Pham et al., 2010, 2011; Shi et al., 2015), and derived varieties are now marketed by the Missouri Soybean Merchandising Council as traditionally bred, high-oleic soybeans. Although marketing of the genetically modified Plenish and Vistive Gold oils faced regulatory challenges in Europe and China, these were cleared in 2017 to permit global sales of these oils.

A challenge for these technologies, as with all novel crop traits, is the need to breed them into the many genetic backgrounds that have been optimized for production in the different climate zones and soil types in which soybeans are grown. With consumer opinion and now FDA regulation targeting partial hydrogenation as a means to reduce PUFA content of oils, this breeding bottleneck was (and still is) an ongoing barrier to efforts for recovering market share for soybeans in the U.S. and elsewhere. This barrier was recognized by the United Soybean Board (USB) in 2012 when they decided to provide funding to Dupont-Pioneer and Monsanto to accelerate the breeding of high-oleic cultivars to cover up to 80% of U.S. soybean acres by 2020, as well as funds for an advertising campaign to encourage farmers to begin growing the high-oleic varieties (United Soybean Board, 2012). Without this

injection of funds (a planned total of $60 million over 3 years), industry projections predicted only 5%–10% coverage by 2020, at a cost to farmers of over $1 billion in lost crop sales (Wilson, 2012; United Soybean Board, 2013).

In many oilseed crop species, the FAD2 desaturases that produces PUFA in seeds are encoded by genes that are expressed throught the plant. For example, canola is an allotetraploid and contains four *FAD2* isogenes, designated *FAD2.A1, FAD2.A5, FAD2.C1,* and *FAD2.C5* (where the nomenclature indicates the subgenome (A or C) and the chromosome location of the gene). The *FAD2.A1* isoform contains deletion and insertion events that preclude it from encoding an active enzyme. The *FAD2.A5*, *FAD2.C5,* and *FAD2.C1* isoforms encode closely related proteins (>90% sequence identity) and mutations in these genes demonstrate that they each contribute to PUFA synthesis in all tissues of the plant. In the 1990s, several breeding programs produced lines with 70%–85% 18:1 (and 20% to 8% PUFA), presumeably by combining mutations at the three remaining loci. Most lines grew well in greenhouses, but when planted in field plots lines with the highest 18:1 levels failed to thrive. Arabidopsis *fad2-2* plants are damaged and killed by low temperatures (Miquel et al., 1993), suggesting that the canola lines with the lowest FAD2 expression are also susceptible to the low temperatures that are typical in the field during planting and early growth. To better understand these results, Bai et al. (2019) identified a series of hypomorphic and null mutations in the FAD2.A5 isoform and then combined four of these with null mutations in the other two isozymes, FAD2.C5 and FAD2.C1. The resulting mutant lines contained 71%–87% 18:1 in their seed oil (21% to 4% PUFA), compared with 62% in wild-type controls. All the mutant lines grew well in a greenhouse, but in field experiments a clear demarcation in plant performance was observed. Mutant lines containing less than 80% 18:1 in the seed oil were indistinguishable from wild-type controls in growth parameters and seed oil content. By contrast, lines with more than 80% 18:1 in the seed oil had significantly lower seedling establishment and vigor, delayed flowering and reduced plant height at maturity. These lines also had 7%–11% reductions in seed oil content. These results define the practical limit to increasing oil 18:1 content in canola (**Figure 6**), and by extension other crop species that rely on constitutively expressed *FAD2* genes for seed PUFA synthesis.

One strategy to lower oil PUFA while maintaining required PUFA synthesis in other tissues of the plant is to use seed-specific RNA-interference or artificial microRNA approaches. These have been applied to canola (Peng et al., 2010; Lee et al., 2016) and a number of other species, including cotton (*Gossypium hirsutum*; Liu et al., 2002), camelina (*Camelina sativa*; Nguyen et al., 2013), linseed (*Linum usitatissimum*; Chen et al., 2015), and safflower (*Carthamus tinctorius*; Wood et al., 2018). A caveat to these approaches is that investigations of the Arabidopsis *fad2-2* mutant indicate that normal seed development and germination both require some minimal content of PUFA, particularly at low temperatures (Miquel and Browse, 1994). Very strong knockdown of seed *FAD2* expression in oilseed species may likewise compromise seed physiology and crop viability.

CONCLUSION

Vegetable oils make a large contribution to calorie intake in human diets, but the fatty acid compositions of oils from most oilseed crops are not ideal for human nutrition and the needs of the food industry. On one hand, saturated fatty acids are a known risk factor for coronary heart disease, obesity, and other diseases common in developed countries. On the other hand, polyunsaturated fatty acids can become rancid during storage and processing. Discoveries in lipid biochemistry and biotechnology over the last 30 years have provided the means to ameliorate both of these challenges. Genetic engineering of oilseeds has successfully reduced saturate content of oils, both by transgenic expression of fatty acid desaturases and by down-regulation of the acyl-ACP thioesterase responsible for 16:0 unloading from the plastid fatty acid synthase. The original, industrial-chemistry solution to the PUFA problem, initiated in the early 20th century, was to process oils by partial hydrogenation. This process leads to the production of *trans* fatty acids that are actually more damaging to human health than saturated fatty acids, with epidemiological estimates blaming them for half a million excess deaths worldwide each year during much of the 20th century. The dangers of foods containing *trans* fats were well established by 1998, but it has taken more than two decades for legislation in many countries to ban them from food. Indeed, more work is needed to stop production and consumption of *trans* fats in countries around the world. Ironically, identification and cloning of the *FAD2* gene that encodes the gateway enzyme of PUFA synthesis in 1994 provided the tools and understanding to engineer high-oleic, low PUFA lines of many oilseed crops, meaning that the solution to the *trans*-fat problem has been available for over 25 years.

AUTHOR CONTRIBUTIONS

All authors listed have made a substantial, direct, and intellectual contribution to the work and approved it for publication.

FUNDING

Research on lipid metabolism in our laboratory has been funded by grants from the US National Science Foundation (grants MCB-0420199 and IOS-1339385), the USDA National Institute of Food and Agriculture (grants 2010-65115-20393 and 2018-67013-27459), BASF Innovation Center Gent, and the Agricultural Research Center at Washington State University.

ACKNOWLEDGMENTS

We are grateful to many colleagues and other researchers who have made discoveries and provided perspectives on the engineering of fatty acid compositions in oilseeds.

REFERENCES

Allakhverdiev, S. I., Los, D. A., and Murata, N. (2009). "Regulatory roles in photosynthesis of unsaturated fatty acids in membrane lipids," in *Advances in Photosynthesis and Respiration. Lipids in Photosynthesis: Essential and Regulatory Functions*. eds. H. Wada and N. Murata (New York: Springer), 373–388.

Amico, A., Wootan, M. G., Jacobson, M. F., Leung, C., and Willett, W. C. (2021). The demise of artificial trans fat: a history of a public health achievement. *Milbank Q.* 99, 746–770. doi: 10.1111/1468-0009.12515

Ardisson Korat, A. V., Willett, W. C., and Hu, F. B. (2014). Diet, lifestyle, and genetic risk factors for type 2 diabetes: a review from the nurses' health study, nurses' health study 2, and health professionals' follow-up study. *Curr. Nutr. Rep.* 3, 345–354. doi: 10.1007/s13668-014-0103-5

Arondel, V., Lemieux, B., Hwang, I., Gibson, S., Goodman, H. M., and Somerville, C. R. (1992). Map-based cloning of a gene controlling omega-3 fatty acid desaturation in Arabidopsis. *Science* 258, 1353–1355. doi: 10.1126/science.1455229

Ascherio, A., Katan, M. B., Zock, P. L., Stampfer, M. J., and Willett, W. C. (1999). Trans fatty acids and coronary heart disease. *N. Engl. J. Med.* 340, 1994–1998. doi: 10.1056/NEJM199906243402511

Bai, S., Wallis, J. G., Denolf, P., and Browse, J. (2016). Directed evolution increases desaturation of a cyanobacterial fatty acid desaturase in eukaryotic expression systems. *Biotechnol. Bioeng.* 113, 1522–1530. doi: 10.1002/bit.25922

Bai, S., Engelen, S., Denolf, P., Wallis, J. G., Lynch, K., Bengtsson, J., et al. (2019). Identification, characterization and field testing of brassica napus mutants producing high-oleic oils. *Plant J.* 98, 33–41. doi: 10.1111/tpj.14195

Ballweg, S., and Ernst, R. (2017). Control of membrane fluidity: the OLE pathway in focus. *Biol. Chem.* 398, 215–228. doi: 10.1515/hsz-2016-0277

Bates, P. D., and Browse, J. (2012). The significance of different Diacylgycerol synthesis pathways on plant oil composition and bioengineering. *Front. Plant Sci.* 3:147. doi: 10.3389/fpls.2012.00147

Bates, P. D., Fatihi, A., Snapp, A. R., Carlsson, A. S., Browse, J., and Lu, C. (2012). Acyl editing and headgroup exchange are the major mechanisms that direct polyunsaturated fatty acid flux into triacylglycerols. *Plant Physiol.* 160, 1530–1539. doi: 10.1104/pp.112.204438

Bates, P. D., Stymne, S., and Ohlrogge, J. (2013). Biochemical pathways in seed oil synthesis. *Curr. Opin. Plant Biol.* 16, 358–364. doi: 10.1016/j.pbi.2013.02.015

Baud, S., and Lepiniec, L. (2010). Physiological and developmental regulation of seed oil production. *Prog. Lipid Res.* 49, 235–249. doi: 10.1016/j.plipres.2010.01.001

Bhandari, S., and Bates, P. D. (2021). Triacylglycerol remodeling in *Physaria fendleri* indicates oil accumulation is dynamic and not a metabolic endpoint. *Plant Physiol.* 187, 799–815. doi: 10.1093/plphys/kiab294

Bonaventure, G., Salas, J. J., Pollard, M. R., and Ohlrogge, J. B. (2003). Disruption of the FATB gene in Arabidopsis demonstrates an essential role of saturated fatty acids in plant growth. *Plant Cell* 15, 1020–1033. doi: 10.1105/tpc.008946

Bondaruk, M., Johnson, S., Degafu, A., Boora, P., Bilodeau, P., Morris, J., et al. (2007). Expression of a cDNA encoding palmitoyl-acyl carrier protein desaturase from cat's claw (*Doxantha unguis-cati* L.) in *Arabidopsis thaliana* and *Brassica napus* leads to accumulation of unusual unsaturated fatty acids and increased stearic acid content in the seed oil. *Plant Breed.* 126, 186–194. doi: 10.1111/j.1439-0523.2007.01316.x

Browse, J., McConn, M., James, D., and Miquel, M. (1993). Mutants of *Arabidopsis* deficient in the synthesis of a-linolenate. Biochemical and genetic characterization of the endoplasmic reticulum linoleoyl desaturase. *J. Biol. Chem.* 268, 16345–16351. doi: 10.1016/S0021-9258(19)85427-3

Browse, J. (2009). Jasmonate passes muster: a receptor and targets for the defense hormone. *Annu. Rev. Plant Biol.* 60, 183–205. doi: 10.1146/annurev.arplant.043008.092007

Browse, J., and Wallis, J. G. (2019). Arabidopsis flowers unlocked the mechanism of jasmonate signaling. *Plan. Theory* 8:285. doi: 10.3390/plants8080285

Browse, J., Kunst, L., Anderson, S., Hugly, S., and Somerville, C. (1989). A mutant of Arabidopsis deficient in the chloroplast 16:1/18:1 desaturase. *Plant Physiol.* 90, 522–529.

Cahoon, E. B., and Shanklin, J. (2000). Substrate-dependent mutant complementation to select fatty acid desaturase variants for metabolic engineering of plant seed oils. *Proc. Natl. Acad. Sci.* 97, 12350–12355. doi: 10.1073/pnas.210276297

Cahoon, E. B., Shah, S., Shanklin, J., and Browse, J. (1998). A determinant of substrate specificity predicted from the acyl-acyl carrier protein desaturase of developing cat's claw seed. *Plant Physiol.* 117, 593–598. doi: 10.1104/pp.117.2.593

CDC (US Centers for Disease Control) (2021). *Dietary Intake for Adults Aged 20 and Over.* Atlanta: CDC.

Chen, H., and Lin, Y. (2013). Promise and issues of genetically modified crops. *Curr. Opin. Plant Biol.* 16, 255–260. doi: 10.1016/j.pbi.2013.03.007

Chen, Y., Zhou, X.-R., Zhang, Z.-J., Dribnenki, P., Singh, S., and Green, A. (2015). Development of high oleic oil crop platform in flax through RNAi-mediated multiple FAD2 gene silencing. *Plant Cell Rep.* 34, 643–653. doi: 10.1007/s00299-015-1737-5

Chung, H. S., Niu, Y., Browse, J., and Howe, G. A. (2009). Top hits in contemporary JAZ: an update on jasmonate signaling. *Phytochemistry* 70, 1547–1559. doi: 10.1016/j.phytochem.2009.08.022

Craig-Schmidt, M. C. (2006). World-wide consumption of *trans* fatty acids. *Atheroscler. Suppl.* 7, 1–4. doi: 10.1016/j.atherosclerosissup.2006.04.001

Dahlqvist, A., Stahl, U., Lenman, M., Banas, A., Lee, M., Sandager, L., et al. (2000). Phospholipid:diacylglycerol acyltransferase: an enzyme that catalyzes the acyl-CoA-independent formation of triacylglycerol in yeast and plants. *Proc. Natl. Acad. Sci. U. S. A.* 97, 6487–6492. doi: 10.1073/pnas.120067297

Dar, A. A., Choudhury, A. R., Kancharla, P. K., and Arumugam, N. (2017). The *FAD2* gene in plants: occurrence, regulation, and role. *Front. Plant Sci.* 8:1789. doi: 10.3389/fpls.2017.01789

Das, K., and Roychoudhury, A. (2014). Reactive oxygen species (ROS) and response of antioxidants as ROS-scavengers during environmental stress in plants. *Front. Environ. Sci.* 2:53. doi: 10.3389/fenvs.2014.00053

Dawczynski, C., and Lorkowski, S. (2016). Trans-fatty acids and cardiovascular risk: does origin matter? *Expert Rev. Cardiovasc. Ther.* 14, 1001–1005. doi: 10.1080/14779072.2016.1199956

De Souza, R. J., Mente, A., Maroleanu, A., Cozma, A. I., Ha, V., Kishibe, T., et al. (2015). Intake of saturated and *trans* unsaturated fatty acids and risk of all-cause mortality, cardiovascular disease, and type 2 diabetes: systematic review and meta-analysis of observational studies. *BMJ* 351:h3978. doi: 10.1136/bmj.h3978

Demorest, Z. L., Coffman, A., Baltes, N. J., Stoddard, T. J., Clasen, B. M., Luo, S., et al. (2016). Direct stacking of sequence-specific nuclease-induced mutations to produce high oleic and low linolenic soybean oil. *BMC Plant Biol.* 16, 1–8. doi: 10.1186/s12870-016-0906-1

Doherty, G. J., and McMahon, H. T. (2009). Mechanisms of endocytosis. *Ann. Rev. Biochemist* 78, 857–902. doi: 10.1146/annurev.biochem.78.081307.110540

Downs, S. M., Bloem, M. Z., Zheng, M., Catterall, E., Thomas, B., Veerman, L., et al. (2017). The impact of policies to reduce trans fat consumption: a systematic review of the evidence. *Curr. Dev. Nutr.* 1, 1–10. doi: 10.3945/cdn.117.000778

Dratz, E. A., and Deese, A. J. (1986). "The role of docosahexaenoic acid (22: 6Sω3) in biological membranes: examples from photoreceptors and model membrane bilayers," in *Health Effects of Polyunsaturated Fatty Acids in Seafoods*. eds. A. P. Simopoulos, R. R. Kifer and R. E. Martin (New York: Elsevier), 319–351.

Elinder, F., and Liin, S. I. (2017). Actions and mechanisms of polyunsaturated fatty acids on voltage-gated ion channels. *Front. Physiol.* 8:43. doi: 10.3389/fphys.2017.00043

Fahy, D., Scheer, B., Wallis, J. G., and Browse, J. (2013). Reducing saturated fatty acids in Arabidopsis seeds by expression of a *Caenorhabditis elegans* 16:0–specific desaturase. *Plant Biotechol. J.* 11, 480–489. doi: 10.1111/pbi.12034

Falcone, D. L., Ogas, J. P., and Somerville, C. R. (2004). Regulation of membrane fatty acid composition by temperature in mutants of Arabidopsis with alterations in membrane lipid composition. *BMC Plant Biol.* 4, 17–15. doi: 10.1186/1471-2229-4-17

Foyer, C. H., and Shigeoka, S. (2011). Understanding oxidative stress and antioxidant functions to enhance photosynthesis. *Plant Physiol.* 155, 93–100. doi: 10.1104/pp.110.166181

Gilabert-Escrivá, M. V., Gonçalves, L. G., Silva, C. R. S., and Figueira, A. (2002). Fatty acid and triacylglycerol composition and thermal behaviour of fats from seeds of Brazilian Amazonian Theobroma species. *J. Sci. Food Agric.* 82, 1425–1431. doi: 10.1002/jsfa.1107

Gill, S. S., and Tuteja, N. (2010). Reactive oxygen species and antioxidant machinery in abiotic stress tolerance in crop plants. *Plant Physiol. Biochem.* 48, 909–930. doi: 10.1016/j.plaphy.2010.08.016

Gillingham, L. G., Harris-Janz, S., and Jones, P. J. (2011). Dietary monounsaturated fatty acids are protective against metabolic syndrome and cardiovascular disease risk factors. *Lipids* 46, 209–228. doi: 10.1007/s11745-010-3524-y

Goddard, T. D., Huang, C. C., Meng, E. C., Pettersen, E. F., Couch, G. S., Morris, J. H., et al. (2018). UCSF ChimeraX: meeting modern challenges in visualization and analysis. *Protein Sci.* 27, 14–25. doi: 10.1002/pro.3235

Goldsmith, P. D. (2008). "Economics of soybean production, marketing, and utilization" in *Soybeans*. eds. L. A. Johnson, P. J. White and R. Galloway (New York: Elsevier), 117–150.

Graham, I. A. (2008). Seed storage oil mobilization. *Annu. Rev. Plant Biol.* 59, 115–142. doi: 10.1146/annurev.arplant.59.032607.092938

Gunstone, F. (1998). Movements towards tailor-made fats. *Prog. Lipid Res.* 37, 277–305. doi: 10.1016/S0163-7827(98)00012-5

Gurr, M. I. (1992). *Role of Fats in Food and Nutrition*. New York: Elsevier Applied Science.

Gutla, P. V. K., Boccaccio, A., De Angeli, A., Gambale, F., and Carpaneto, A. (2012). Modulation of plant TPC channels by polyunsaturated fatty acids. *J. Exp. Bot.* 63, 6187–6197. doi: 10.1093/jxb/ers272

Han, L., Usher, S., Sandgrind, S., Hassall, K., Sayanova, O., Michaelson, L. V., et al. (2020). High level accumulation of EPA and DHA in field-grown transgenic Camelina–a multi-territory evaluation of TAG accumulation and heterogeneity. *Plant Biotechnol. J.* 18, 2280–2291. doi: 10.1111/pbi.13385

Harris, W. S., Poston, W. C., and Haddock, C. K. (2007). Tissue n-3 and n-6 fatty acids and risk for coronary heart disease events. *Atherosclerosis* 193, 1–10. doi: 10.1016/j.atherosclerosis.2007.03.018

Haun, W., Coffman, A., Clasen, B. M., Demorest, Z. L., Lowy, A., Ray, E., et al. (2014). Improved soybean oil quality by targeted mutagenesis of the fatty acid desaturase 2 gene family. *Plant Biotechnol. J.* 12, 934–940. doi: 10.1111/pbi.12201

Heppard, E. P., Kinney, A. J., Stecca, K. L., and Miao, G. H. (1996). Developmental and growth temperature regulation of two different microsomal omega-6 desaturase genes in soybeans. *Plant Physiol.* 110, 311–319. doi: 10.1104/pp.110.1.311

Hilditch, T. P., and Williams, P. N. (1964). *The Chemical Constitution of Natural Fats. The Chemical Constitution of Natural Fats. 4th Edn.* Chapman Hall, London.

Hooper, L., Martin, N., Jimoh, O. F., Kirk, C., Foster, E., and Abdelhamid, A. S. (2020). Reduction in saturated fat intake for cardiovascular disease. *Cochrane Database Syst. Rev.* 5:CD011737. doi: 10.1002/14651858.CD011737

Hou, Q., Ufer, G., and Bartels, D. (2016). Lipid signalling in plant responses to abiotic stress. *Plant Cell Environ.* 39, 1029–1048. doi: 10.1111/pce.12666

Ishizaki-Nishizawa, O., Fujii, T., Azuma, M., Sekiguchi, K., Murata, N., Ohtani, T., et al. (1996). Low-temperature resistance of higher plants is significantly enhanced by a nonspecific cyanobacterial desaturase. *Nat. Biotechnol.* 14, 1003–1006. doi: 10.1038/nbt0896-1003

Johnson, M., Pace, R. D., and Mcelhenney, W. H. (2018). Green leafy vegetables in diets with a 25: 1 omega-6/omega-3 fatty acid ratio modify the erythrocyte fatty acid profile of spontaneously hypertensive rats. *Lipids Health Dis.* 17, 1–7. doi: 10.1186/s12944-018-0723-7

Jones, A., Davies, H. M., and Voelker, T. A. (1995). Palmitoyl-acyl carrier protein (ACP) thioesterase and the evolutionary origin of plant acyl-ACP thioesterases. *Plant Cell* 7, 359–371. PMID: 7734968

Jumper, J., Evans, R., Pritzel, A., Green, T., Figurnov, M., Ronneberger, O., et al. (2021). Highly accurate protein structure prediction with AlphaFold. *Nature* 596, 583–589. doi: 10.1038/s41586-021-03819-2

Kamble, A., and Roshan, D. (2022). Oilseeds Market by Oilseed Type, Product, Breeding Type and Biotech Trait: Global Opportunity Analysis and Industry Forecast, 2022-2031. Available at: https://www.alliedmarketresearch.com/oilseeds-market (Accessed April 2022).

Katan, M. B. (2006). Regulation of trans fats: the gap, the polder, and McDonald's French fries. *Atheroscler. Suppl.* 7, 63–66. doi: 10.1016/j.atherosclerosissup.2006.04.013

Kaur, N., Chugh, V., and Gupta, A. K. (2014). Essential fatty acids as functional components of foods—a review. *J. Food Sci. Technol.* 51, 2289–2303. doi: 10.1007/s13197-012-0677-0

Keereetaweep, J., Liu, H., Zhai, Z., and Shanklin, J. (2018). Biotin attachment domain-containing proteins irreversibly inhibit acetyl CoA carboxylase. *Plant Physiol.* 177, 208–215. doi: 10.1104/pp.18.00216

Kiage, J. N., Merrill, P. D., Robinson, C. J., Cao, Y., Malik, T. A., Hundley, B. C., et al. (2013). Intake of *trans* fat and all-cause mortality in the reasons for geographical and racial differences in stroke (REGARDS) cohort. *Am. J. Clin. Nutr.* 97, 1121–1128. doi: 10.3945/ajcn.112.049064

Kim, H. U., Li, Y., and Huang, A. H. (2005). Ubiquitous and endoplasmic reticulum–located lysophosphatidyl acyltransferase, LPAT2, is essential for female but not male gametophyte development in Arabidopsis. *Plant Cell* 17, 1073–1089. doi: 10.1105/tpc.104.030403

Kinney, A. J. (1996). Development of genetically engineered soybean oils for food applications. *J. Food Lipids* 3, 273–292. doi: 10.1111/j.1745-4522.1996.tb00074.x

König, S., Ischebeck, T., Lerche, J., Stenzel, I., and Heilmann, I. (2008). Salt-stress-induced association of phosphatidylinositol 4,5-bisphosphate with clathrin-coated vesicles in plants. *Biochem. J.* 415, 387–399. doi: 10.1042/BJ20081306

Konishi, T., and Sasaki, Y. (1994). Compartmentalization of two forms of acetyl-CoA carboxylase in plants and the origin of their tolerance toward herbicides. *Proc. Natl. Acad. Sci.* 91, 3598–3601. doi: 10.1073/pnas.91.9.3598

Korver, O., and Katan, M. B. (2006). The elimination of *trans* fats from spreads: how science helped to turn an industry around. *Nutr. Rev.* 64, 275–279. doi: 10.1301/nr.2006.jun.275-279

Kučerka, N., Heberle, F. A., Pan, J., and Katsaras, J. (2015). Structural significance of lipid diversity as studied by small angle neutron and X-ray scattering. *Membranes* 5, 454–472. doi: 10.3390/membranes5030454

Kuhnt, K., Degen, C., Jaudszus, A., and Jahreis, G. (2012). Searching for health beneficial n-3 and n-6 fatty acids in plant seeds. *Eur. J. Lipid Sci. Technol.* 114, 153–160. doi: 10.1002/ejlt.201100008

Kummerow, F. A., Mahfouz, M., Zhou, Q., and Masterjohn, C. (2013). Effects of *trans* fats on prostacyclin production. *Scand. Cardiovasc. J.* 47, 377–382. doi: 10.3109/14017431.2013.856462

Kwon, Y. (2016). Effect of trans–fatty acids on lipid metabolism: mechanisms for their adverse health effects. *Food Rev. Int.* 32, 323–339. doi: 10.1080/87559129.2015.1075214

L'abbé, M. R., Stender, S., Skeaff, C., and Tavella, M. (2009). Approaches to removing trans fats from the food supply in industrialized and developing countries. *Eur. J. Clin. Nutr.* 63, S50–S67. doi: 10.1038/ejcn.2009.14

Lager, I., Glab, B., Eriksson, L., Chen, G., Banas, A., and Stymne, S. (2015). Novel reactions in acyl editing of phosphatidylcholine by lysophosphatidylcholine transacylase (LPCT) and acyl-CoA: glycerophosphocholine acyltransferase (GPCAT) activities in microsomal preparations of plant tissues. *Planta* 241, 347–358. doi: 10.1007/s00425-014-2184-1

Lee, K.-R., Kim, E.-H., Roh, K. H., Kim, J.-B., Kang, H.-C., Go, Y. S., et al. (2016). High-oleic oilseed rapes developed with seed-specific suppression of FAD2 gene expression. *Applied Biol. Chem.* 59, 669–676. doi: 10.1007/s13765-016-0208-1

Lemieux, B., Miquel, M., Somerville, C., and Browse, J. (1990). Mutants of Arabidopsis with alterations in seed lipid fatty acid composition. *Theor. Appl. Genet.* 80, 234–240. doi: 10.1007/BF00224392

Lessire, R., and Stumpe, P. K. (1983). Nature of the fatty acid synthetase systems in parenchymal and epidermal cells of *Allium porrum* L. leaves. *Plant Physiol.* 73, 614–618. doi: 10.1104/pp.73.3.614

Leth, T., Jensen, H. G., Mikkelsen, A. A., and Bysted, A. (2006). The effect of the regulation on trans fatty acid content in Danish food. *Atheroscler. Suppl.* 7, 53–56. doi: 10.1016/j.atherosclerosissup.2006.04.019

Lin, L., Ding, Y., Wang, Y., Wang, Z., Yin, X., Yan, G., et al. (2017). Functional lipidomics: palmitic acid impairs hepatocellular carcinoma development by modulating membrane fluidity and glucose metabolism. *Hepatology* 66, 432–448. doi: 10.1002/hep.29033

Lindqvist, Y., Huang, W., Schneider, G., and Shanklin, J. (1996). Crystal structure of delta9 stearoyl-acyl carrier protein desaturase from castor seed and its relationship to other di-iron proteins. *EMBO J.* 15, 4081–4092. doi: 10.1002/j.1460-2075.1996.tb00783.x

Lipp, M., Simoneau, C., Ulberth, F., Anklam, E., Crews, C., Brereton, P., et al. (2001). Composition of genuine cocoa butter and cocoa butter equivalents. *J. Food Compos. Anal.* 14, 399–408. doi: 10.1006/jfca.2000.0984

List, G. (2014). "Trans fats replacement Solutions in North America" in *Trans Fats Replacement Solutions*. ed. D. Kodali (New York: AOCS Press/ Elsevier), 275–285. doi: 10.1016/B978-0-9830791-5-6.50017-4

Liu, Q., Singh, S. P., and Green, A. G. (2002). High-stearic and high-oleic cottonseed oils produced by hairpin RNA-mediated post-transcriptional gene silencing. *Plant Physiol.* 129, 1732–1743.

Liu, X., Teng, Y., Li, B., and Meng, Q. (2013). Enhancement of low-temperature tolerance in transgenic tomato plants overexpressing Lefad7 through regulation of trienoic fatty acids. *Photosynthetica* 51, 238–244. doi: 10.1007/s11099-013-0014-5

Liu, Y., Wang, G., and Wang, X. (2015). Role of aminoalcoholphosphotransferases 1 and 2 in phospholipid homeostasis in Arabidopsis. *Plant Cell* 27, 1512–1528. doi: 10.1105/tpc.15.00180

Los, D. A., Mironov, K. S., and Allakhverdiev, S. I. (2013). Regulatory role of membrane fluidity in gene expression and physiological functions. *Photosynth. Res.* 116, 489–509. doi: 10.1007/s11120-013-9823-4

Lu, C., Xin, Z., Ren, Z., Miquel, M., and Browse, J. (2009). An enzyme regulating triacylglycerol composition is encoded by the ROD1 gene of Arabidopsis. *Proc. Natl. Acad. Sci.* 106, 18837–18842. doi: 10.1073/pnas.0908848106

Lu, C., Napier, J. A., Clemente, T. E., and Cahoon, E. B. (2011). New frontiers in oilseed biotechnology: meeting the global demand for vegetable oils for food, feed, biofuel, and industrial applications. *Curr. Opin. Plant Biotechnol.* 22, 252–259. doi: 10.1016/j.copbio.2010.11.006

McConn, M., and Browse, J. (1998). Polyunsaturated membranes are required for photosynthetic competence in a mutant of Arabidopsis. *Plant J.* 15, 521–530. doi: 10.1046/j.1365-313X.1998.00229.x

Mensink, R. P., and Katan, M. B. (1990). Effect of dietary *trans* fatty acids on high-density and low-density lipoprotein cholesterol levels in healthy subjects. *N. Engl. J. Med.* 323, 439–445. doi: 10.1056/NEJM199008163230703

Mhaske, V., Beldjilali, K., Ohlrogge, J., and Pollard, M. (2005). Isolation and characterization of an Arabidopsis thaliana knockout line for phospholipid: diacylglycerol transacylase gene (At5g13640). *Plant Physiol. Biochem.* 43, 413–417. doi: 10.1016/j.plaphy.2005.01.013

Micha, R., and Mozaffarian, D. (2008). *Trans* fatty acids: effects on cardiometabolic health and implications for policy. *Prostaglandins Leukot. Essent. Fatty Acids* 79, 147–152. doi: 10.1016/j.plefa.2008.09.008

Micha, R., and Mozaffarian, D. (2009). Trans fatty acids: effects on metabolic syndrome, heart disease and diabetes. *Nat. Rev. Endocrinol.* 5, 335–344. doi: 10.1038/nrendo.2009.79

Micha, R., Khatibzadeh, S., Shi, P., Fahimi, S., Lim, S., Andrews, K. G., et al. (2014). Global, regional, and national consumption levels of dietary fats and oils in 1990 and 2010: a systematic analysis including 266 country-specific nutrition surveys. *Br. Med. J.* 348:g2272. doi: 10.1136/bmj.g2272

Miquel, M., and Browse, J. (1992). Arabidopsis mutants deficient in polyunsaturated fatty acid synthesis. Biochemical and genetic characterization of a plant oleoyl-phosphatidylcholine desaturase. *J. Biol. Chem.* 267, 1502–1509. doi: 10.1016/S0021-9258(18)45974-1

Miquel, M. F., and Browse, J. A. (1994). High-oleate oilseeds fail to develop at low temperature. *Plant Physiol.* 106, 421–427. doi: 10.1104/pp.106.2.421

Miquel, M., James, D., Dooner, H., and Browse, J. (1993). Arabidopsis requires polyunsaturated lipids for low-temperature survival. *Proc. Natl. Acad. Sci.* 90, 6208–6212.

Mishra, S. K., Belur, P. D., and Iyyaswami, R. (2021). Use of antioxidants for enhancing oxidative stability of bulk edible oils: a review. *Int. J. Food Sci. Technol.* 56, 1–12. doi: 10.1111/ijfs.14716

Moon, H., Hazebroek, J., and Hildebrand, D. F. (2000). Changes in fatty acid composition in plant tissues expressing a mammalian Δ9 desaturase. *Lipids* 35, 471–479. doi: 10.1007/s11745-000-546-6

Mori, T. A. (2014). Dietary n-3 PUFA and CVD: a review of the evidence. *Proc. Nutr. Soc.* 73, 57–64. doi: 10.1017/S0029665113003583

Mozaffarian, D., Katan, M. B., Ascherio, A., Stampfer, M. J., and Willett, W. C. (2006). *Trans* fatty acids and cardiovascular disease. *N. Engl. Med.* 354, 1601–1613. doi: 10.1056/NEJMra054035

Msanne, J., Kim, H., and Cahoon, E. B. (2020). Biotechnology tools and applications for development of oilseed crops with healthy vegetable oils. *Biochimie* 178, 4–14. doi: 10.1016/j.biochi.2020.09.020

Mukherjee, S., and Mitra, A. (2009). Health effects of palm oil. *J. Human Ecol.* 26, 197–203. doi: 10.1080/09709274.2009.11906182

Murphy, A. S., Bandyopadhyay, A., Holstein, S. E., and Peer, W. A. (2005). Endocytotic cycling of PM proteins. *Annu. Rev. Plant Biol.* 56, 221–251. doi: 10.1146/annurev.arplant.56.032604.144150

Napier, J. A., and Graham, I. A. (2010). Tailoring plant lipid composition: designer oilseeds come of age. *Curr. Opin. Plant Biol.* 13, 329–336. doi: 10.1016/j.pbi.2010.01.008

Napier, J. A., Olsen, R. E., and Tocher, D. R. (2019). Update on GM canola crops as novel sources of omega-3 fish oils. *Plant Biotechnol. J.* 17:703.

Natto, Z. S., Yaghmoor, W., Alshaeri, H. K., and Van Dyke, T. E. (2019). Omega-3 fatty acids effects on inflammatory biomarkers and lipid profiles among diabetic and cardiovascular disease patients: a systematic review and meta-analysis. *Sci. Rep.* 9:18867. doi: 10.1038/s41598-019-54535-x

Nguyen, H. T., Mishra, G., Whittle, E., Pidkowich, M. S., Bevan, S. A., Merlo, A. O., et al. (2010). Metabolic engineering of seeds can achieve levels of omega-7 fatty acids comparable with the highest levels found in natural plant sources. *Plant Physiol.* 154, 1897–1904. doi: 10.1104/pp.110.165340

Nguyen, H. T., Silva, J. E., Podicheti, R., Macrander, J., Yang, W., Nazarenus, T. J., et al. (2013). Camelina seed transcriptome: a tool for meal and oil improvement and translational research. *Plant Biotechnol. J.* 11, 759–769. doi: 10.1111/pbi.12068

NIDA (National Institute on Drug Abuse) (2020). Trends and Statistics: Overdose Death Rates. Available at: https://nida.nih.gov/drug-topics/trends-statistics/overdose-death-rates (Accessed February 26, 2022).

Niebylski, C. D., and Jr Salem, N. (1994). A calorimetric investigation of a series of mixed-chain polyunsaturated phosphatidylcholines: effect of sn-2 chain length and degree of unsaturation. *Biophys. J.* 67, 2387–2393. doi: 10.1016/S0006-3495(94)80725-8

Oh, K., Hu, F. B., Manson, J. E., Stampfer, M. J., and Willett, W. C. (2005). Dietary fat intake and risk of coronary heart disease in women: 20 years of follow-up of the nurses' health study. *Am. J. Epidemiol.* 161, 672–679. doi: 10.1093/aje/kwi085

Ohlrogge, J., and Browse, J. (1995). Lipid biosynthesis. *Plant Cell* 7, 957–970.

Ohlrogge, J., Thrower, N., Mhaske, V., Stymne, S., Baxter, M., Yang, W., et al. (2018). Plant FA db: a resource for exploring hundreds of plant fatty acid structures synthesized by thousands of plants and their phylogenetic relationships. *Plant J.* 96, 1299–1308. doi: 10.1111/tpj.14102

Okuley, J., Lightner, J., Feldmann, K., Yadav, N., Lark, E., and Browse, J. (1994). Arabidopsis FAD2 gene encodes the enzyme that is essential for polyunsaturated lipid synthesis. *Plant Cell* 6, 147–158.

Ozseyhan, M. E., Li, P., Na, G., Li, Z., Wang, C., and Lu, C. (2018). Improved fatty acid profiles in seeds of camelina sativa by artificial microRNA mediated FATB gene suppression. *Biochem. Biophys. Res. Commun.* 503, 621–624. doi: 10.1016/j.bbrc.2018.06.051

Peng, Q., Hu, Y., Wei, R., Zhang, Y., Guan, C., Ruan, Y., et al. (2010). Simultaneous silencing of FAD2 and FAE1 genes affects both oleic acid and erucic acid contents in *Brassica napus* seeds. *Plant Cell Rep.* 29, 317–325. doi: 10.1007/s00299-010-0823-y

Pettersen, E. F., Goddard, T. D., Huang, C. C., Meng, E. C., Couch, G. S., Croll, T. I., et al. (2021). UCSF ChimeraX: structure visualization for researchers, educators, and developers. *Protein Sci.* 30, 70–82. doi: 10.1002/pro.3943

Pham, A.-T., Lee, J.-D., Shannon, J. G., and Bilyeu, K. D. (2010). Mutant alleles of FAD2-1A and FAD2-1B combine to produce soybeans with the high oleic acid seed oil trait. *BMC Plant Biol.* 10, 1–13. doi: 10.1186/1471-2229-10-195

Pham, A.-T., Lee, J.-D., Shannon, J. G., and Bilyeu, K. D. (2011). A novel FAD2-1 A allele in a soybean plant introduction offers an alternate means to produce soybean seed oil with 85% oleic acid content. *Theor. Appl. Genet.* 123, 793–802. doi: 10.1007/s00122-011-1627-3

Pilch, P. F., Thompson, P. A., and Czech, M. P. (1980). Coordinate modulation of D-glucose transport activity and bilayer fluidity in plasma membranes derived from control and insulin-treated adipocytes. *Proc. Natl. Acad. Sci.* 77, 915–918. doi: 10.1073/pnas.77.2.915

Restrepo, B. J., and Rieger, M. (2016). Denmark's policy on artificial *trans* fat and cardiovascular disease. *Am. J. Prev. Med.* 50, 69–76. doi: 10.1016/j.amepre.2015.06.018

Roberts, L. J., and Milne, G. L. (2009). Isoprostanes. *J. Lipid Res.* 50, S219–S223. doi: 10.1194/jlr.R800037-JLR200

Ryckebosch, E., Bruneel, C., Muylaert, K., and Foubert, I. (2012). Microalgae as an alternative source of omega-3 long chain polyunsaturated fatty acids. *Lipid Technol.* 24, 128–130. doi: 10.1002/lite.201200197

Saini, R. K., and Keum, Y.-S. (2018). Omega-3 and omega-6 polyunsaturated fatty acids: dietary sources, metabolism, and significance: a review. *Life Sci.* 203, 255–267. doi: 10.1016/j.lfs.2018.04.049

Salie, M. J., Zhang, N., Lancikova, V., Xu, D., and Thelen, J. J. (2016). A family of negative regulators targets the committed step of de novo fatty acid biosynthesis. *Plant Cell* 28, 2312–2325. doi: 10.1105/tpc.16.00317

Satchithanandam, S., Oles, C. J., Spease, C. J., Brandt, M. M., Yurawecz, M. P., and Rader, J. I. (2004). *Trans*, saturated, and unsaturated fat in foods in the United States prior to mandatory trans-fat labeling. *Lipids* 39, 11–18.

Schneider, C. (2009). An update on products and mechanisms of lipid peroxidation. *Mol. Nutr. Food Res* 53, 315–321. doi: 10.1002/mnfr.200800131

Schnurr, J. A., Shockey, J. M., De Boer, G.-J., and Browse, J. A. (2002). Fatty acid export from the chloroplast. Molecular characterization of a major plastidial acyl-coenzyme A synthetase from Arabidopsis. *Plant Physiol.* 129, 1700–1709. doi: 10.1104/pp.003251

Schuppert, G. F., Tang, S., Slabaugh, M. B., and Knapp, S. J. (2006). The sunflower high-oleic mutant Ol carries variable tandem repeats of FAD2-1, a seed-specific oleoyl-phosphatidyl choline desaturase. *Mol. Breeding* 17, 241–256.

Serhan, C. N., and Savill, J. (2005). Resolution of inflammation: the beginning programs the end. *Nat. Immunol.* 6, 1191–1197. doi: 10.1038/ni1276

Shi, Z., Bachleda, N., Pham, A. T., Bilyeu, K., Shannon, G., Nguyen, H., et al. (2015). High-throughput and functional SNP detection assays for oleic and linolenic acids in soybean. *Mol. Breeding* 35, 1–10. doi: 10.1007/s11032-015-0368-4

Shockey, J. M., Fulda, M. S., and Browse, J. A. (2002). Arabidopsis contains nine long-chain acyl-coenzyme A synthetase genes that participate in fatty acid and glycerolipid metabolism. *Plant Physiol.* 129, 1710–1722. doi: 10.1104/pp.003269

Shockey, J., Regmi, A., Cotton, K., Adhikari, N., Browse, J., and Bates, P. D. (2016). Identification of Arabidopsis GPAT9 (At5g60620) as an essential gene involved in triacylglycerol biosynthesis. *Plant Physiol.* 170, 163–179. doi: 10.1104/pp.15.01563

Simopoulos, A. (2003). The importance of the ratio of omega-6/omega-3 essential fatty acids. *Altern. Med. Rev.* 8, 83–84.

Singer, S. D., Chen, G., Mietkiewska, E., Tomasi, P., Jayawardhane, K., Dyer, J. M., et al. (2016). Arabidopsis GPAT9 contributes to synthesis of intracellular glycerolipids but not surface lipids. *J. Exp. Bot.* 67, 4627–4638. doi: 10.1093/jxb/erw242

Sivakanthan, S., and Madhujith, T. (2020). Current trends in applications of enzymatic interesterification of fats and oils: a review. *LWT Food Sci. Technol.* 132:109880. doi: 10.1016/j.lwt.2020.109880

Smirnoff, N., and Arnaud, D. (2019). Hydrogen peroxide metabolism and functions in plants. *New Phytol.* 221, 1197–1214. doi: 10.1111/nph.15488

Soyeurt, H., Dardenne, P., Dehareng, F., Lognay, G., Veselko, D., Marlier, M., et al. (2006). Estimating fatty acid content in cow milk using mid-infrared spectrometry. *J. Dairy Sci.* 89, 3690–3695. doi: 10.3168/jds.S0022-0302(06)72409-2

Ståhl, U., Carlsson, A. S., Lenman, M., Dahlqvist, A., Huang, B., Banas, W., et al. (2004). Cloning and functional characterization of a phospholipid: diacylglycerol acyltransferase from Arabidopsis. *Plant Physiol.* 135, 1324–1335. doi: 10.1104/pp.104.044354

Ståhl, U., Stålberg, K., Stymne, S., and Ronne, H. (2008). A family of eukaryotic lysophospholipid acyltransferases with broad specificity. *FEBS Lett.* 582, 305–309.

Stillwell, W., and Wassall, S. R. (2003). Docosahexaenoic acid: membrane properties of a unique fatty acid. *Chem. Phys. Lipids* 126, 1–27. doi: 10.1016/S0009-3084(03)00101-4

Stymne, S., and Appelqvist, L. Å. (1978). The biosynthesis of linoleate from oleoyl-CoA via oleoyl-phosphatidylcholine in microsomes of developing safflower seeds. *Eur. J. Biochem.* 90, 223–229. doi: 10.1111/j.1432-1033.1978.tb12594.x

Tarrago-Trani, M. T., Phillips, K. M., Lemar, L. E., and Holden, J. M. (2006). New and existing oils and fats used in products with reduced trans-fatty acid content. *J. Am. Diet. Assoc.* 106, 867–880. doi: 10.1016/j.jada.2006.03.010

Troisi, R., Willett, W. C., and Weiss, S. T. (1992). Trans-fatty acid intake in relation to serum lipid concentrations in adult men. *Am. J. Clin. Nutr.* 56, 1019–1024. doi: 10.1093/ajcn/56.6.1019

United Soybean Board (2012). Industry Partnership Seeks Significant High-Oleic Expansion. Available at: www.unitedsoybean.org (Accessed January 17, 2022).

United Soybean Board (2013). FY 2013 Action Plan (Draft 2012), 49–56. Available at: www.unitedsoybean.org (Accessed January 17, 2022).

Upchurch, R. G. (2008). Fatty acid unsaturation, mobilization, and regulation in the response of plants to stress. *Biotechnol. Lett.* 30, 967–977. doi: 10.1007/s10529-008-9639-z

USDA FAS (2022). *Oilseeds: World Markets and Trade B*. ed. George (Washington DC: USDA FAS).

Varadi, M., Anyango, S., Deshpande, M., Nair, S., Natassia, C., Yordanova, G., et al. (2021). AlphaFold protein structure database: massively expanding the structural coverage of protein-sequence space with high-accuracy models. *Nucleic Acids Res.* 50, D439–D444. doi: 10.1093/nar/gkab1061

Voelker, T., and Kinney, A. J. (2001). Variations in the biosynthesis of seed-storage lipids. *Annu. Rev. Plant Biol.* 52, 335–361. doi: 10.1146/annurev.arplant.52.1.335

Vrenna, M., Peruccio, P. P., Liu, X., Zhong, F., and Sun, Y. (2021). Microalgae as future superfoods: fostering adoption through practice-based design research. *Sustainability* 13:2848. doi: 10.3390/su13052848

Wallis, J. G., and Browse, J. (2010). Lipid biochemists salute the genome. *Plant J.* 61, 1092–1106. doi: 10.1111/j.1365-313X.2010.04125.x

Wallis, J. G., Watts, J. L., and Browse, J. (2002). Polyunsaturated fatty acid synthesis: what will they think of next? *Trends Biochem. Sci.* 27, 467–473. doi: 10.1016/s0968-0004(02)02168-0

Wanders, A. J., Zock, P. L., and Brouwer, I. A. (2017). *Trans* fat intake and its dietary sources in general populations worldwide: a systematic review. *Nutrients* 9:840. doi: 10.3390/nu9080840

Wang, L., Shen, W., Kazachkov, M., Chen, G., Chen, Q., Carlsson, A. S., et al. (2012). Metabolic interactions between the lands cycle and the Kennedy pathway of glycerolipid synthesis in Arabidopsis developing seeds. *Plant Cell* 24, 4652–4669. doi: 10.1105/tpc.112.104604

Wang, D. D., Li, Y., Chiuve, S. E., Stampfer, M. J., Manson, J. E., Rimm, E. B., et al. (2016a). Association of specific dietary fats with total and cause-specific mortality. *JAMA Internal Med.* 176, 1134–1145. doi: 10.1001/jamainternmed.2016.2417

Wang, F. C., Gravelle, A. J., Blake, A. I., and Marangoni, A. G. (2016b). Novel *trans* fat replacement strategies. *Curr. Opin. Food Sci.* 7, 27–34. doi: 10.1016/j.cofs.2015.08.006

Wang, Q., Afshin, A., Yakoob, M. Y., Singh, G. M., Rehm, C. D., Khatibzadeh, S., et al. (2016c). Impact of nonoptimal intakes of saturated, polyunsaturated, and trans fat on global burdens of coronary heart disease. *J. Am. Heart Assoc.* 5:e002891. doi: 10.1161/JAHA.115.002891

Watts, J. L., and Browse, J. (2000). A Palmitoyl-CoA-specific Δ9 fatty acid Desaturase from *Caenorhabditis elegans*. *Biochem. Biophys. Res. Commun.* 272, 263–269. doi: 10.1006/bbrc.2000.2772

Weiss, T. J. (1983). *Food Oils and Their Uses. 2nd Edn*. AVI Publishing, Westport, CT.

Whittle, E., and Shanklin, J. (2001). Engineering delta 9-16:0-acyl carrier protein (ACP) desaturase specificity based on combinatorial saturation mutagenesis and logical redesign of the castor delta 9-18:0-ACP desaturase. *J. Biol. Chem.* 276, 21500–21505. doi: 10.1074/jbc.M102129200

WHO (World Health Organization) (2019). *REPLACE Trans Fat: An Action Package to Eliminate Industrially Produced Trans-Fatty Acids: Module 2: Promote: How-to Guide for Determining the Best Replacement Oils and Interventions to Promote Their Use*. Geneva: WHO.

Willett, W. C., and Ascherio, A. (1994). Trans fatty acids: are the effects only marginal. *Am. J. Public Health* 84, 722–724.

Willett, W. C., Stampfer, M. J., Manson, J., Colditz, G. A., Speizer, F. E., Rosner, B. A., et al. (1993). Intake of *trans* fatty acids and risk of coronary heart disease among women. *Lancet* 341, 581–585. doi: 10.1016/0140-6736(93)90350-P

Wilson, R. F. (2012). The role of genomics and biotechnology in achieving global food security for high-oleic vegetable oil. *J. Oleo Sci.* 61, 357–367. doi: 10.5650/jos.61.357

Wood, C. C., Okada, S., Taylor, M. C., Menon, A., Mathew, A., Cullerne, D., et al. (2018). Seed-specific RNAi in safflower generates a superhigh oleic oil with extended oxidative stability. *Plant Biotechnol. J.* 16, 1788–1796. doi: 10.1111/pbi.12915

Zandalinas, S. I., Fritschi, F. B., and Mittler, R. (2020). Signal transduction networks during stress combination. *J. Exp. Bot.* 71, 1734–1741. doi: 10.1093/jxb/erz486

Conflict of Interest: The authors declare that the research was conducted in the absence of any commercial or financial relationships that could be construed as a potential conflict of interest.

Publisher's Note: All claims expressed in this article are solely those of the authors and do not necessarily represent those of their affiliated organizations, or those of the publisher, the editors and the reviewers. Any product that may be evaluated in this article, or claim that may be made by its manufacturer, is not guaranteed or endorsed by the publisher.

frontiers | Frontiers in Plant Science

ORIGINAL RESEARCH
published: 03 June 2022
doi: 10.3389/fpls.2022.931310

Suppression of *Physaria fendleri* SDP1 Increased Seed Oil and Hydroxy Fatty Acid Content While Maintaining Oil Biosynthesis Through Triacylglycerol Remodeling

*Abdul Azeez, Prasad Parchuri and Philip D. Bates**

Institute of Biological Chemistry, Washington State University, Pullman, WA, United States

Physaria fendleri is a burgeoning oilseed crop that accumulates the hydroxy fatty acid (HFA), lesquerolic acid, and can be a non-toxic alternative crop to castor for production of industrially valuable HFA. Recently, *P. fendleri* was proposed to utilize a unique seed oil biosynthetic pathway coined "triacylglycerol (TAG) remodeling" that utilizes a TAG lipase to remove common fatty acids from TAG allowing the subsequent incorporation of HFA after initial TAG synthesis, yet the lipase involved is unknown. SUGAR DEPENDENT 1 (SDP1) has been characterized as the dominant TAG lipase involved in TAG turnover during oilseed maturation and germination. Here, we characterized the role of a putative PfeSDP1 in both TAG turnover and TAG remodeling. *In vitro* assays confirmed that PfeSDP1 is a TAG lipase and demonstrated a preference for HFA-containing TAG species. Seed-specific RNAi knockdown of *PfeSDP1* resulted in a 12%–16% increase in seed weight and 14%–19% increase in total seed oil content with no major effect on seedling establishment. The increase in total oil content was primarily due to ~4.7% to ~14.8% increase in TAG molecular species containing two HFA (2HFA-TAG), and when combined with a smaller decrease in 1HFA-TAG content the proportion of total HFA in seed lipids increased 4%–6%. The results are consistent with PfeSDP1 involved in TAG turnover but not TAG remodeling to produce 2HFA-TAG. Interestingly, the concomitant reduction of 1HFA-TAG in PfeSDP1 knockdown lines suggests PfeSDP1 may have a role in reverse TAG remodeling during seed maturation that produces 1HFA-TAG from 2HFA-TAG. Overall, our results provide a novel strategy to enhance the total amount of industrially valuable lesquerolic acid in *P. fendleri* seeds.

Keywords: ***Lesquerella fendleri*** **L., lipase, hydroxy fatty acid, oilseed crop, Brassicaceae, SUGAR DEPENDENT 1, castor (*Ricinus communis* L.), triacylglycerol remodeling**

OPEN ACCESS

Edited by:
Hyun Uk Kim,
Sejong University, South Korea

Reviewed by:
Kyeong-Ryeol Lee,
Rural Development Administration, South Korea
Shaoping Lu,
Huazhong Agricultural University, China

***Correspondence:**
Philip D. Bates
phil_bates@wsu.edu

Specialty section:
This article was submitted to Crop and Product Physiology, a section of the journal Frontiers in Plant Science

Received: *28 April 2022*
Accepted: *16 May 2022*
Published: *03 June 2022*

Citation:
Azeez A, Parchuri P and Bates PD (2022) Suppression of Physaria fendleri SDP1 Increased Seed Oil and Hydroxy Fatty Acid Content While Maintaining Oil Biosynthesis Through Triacylglycerol Remodeling. Front. Plant Sci. 13:931310. doi: 10.3389/fpls.2022.931310

INTRODUCTION

Physaria fendleri, previously known as *L. fendleri*, belongs to the mustard family (*Brassicaceae*) and is an emerging industrial oilseed crop native to the southwestern United States and northern Mexico (Al-Shehbaz and O'kane, 2002; Dierig et al., 2011; Von Mark and Dierig, 2015). *Physaria fendleri* seeds contain oil with a fatty acid composition comprised of approximately

60% of the unusual hydroxylated fatty acid, lesquerolic acid (20:1-OH; (11Z,14R)-14-hydroxyeicos-11-enoic acid; Cocuron et al., 2014). Hydroxy fatty acids (HFAs) are unusual fatty acids that accumulate in the seeds of various plant species (Ohlrogge et al., 2018) and are used as feedstocks in several industries such as pharmaceuticals, cosmetics, plastics, biodegradable polyesters, and biofuels (Mutlu and Meier, 2010; Patel et al., 2016; Chen, 2017). The primary source of HFA for the industry is castor (*Ricinus communis*) seed oil, which contains 85%–90% of the HFA ricinoleic acid (18:1-OH; [9Z,12R]-12-hydroxyoctadec-9-enoic acid; Mckeon, 2016). Unfortunately, castor seeds also produce the toxic protein ricin (Chen et al., 2005), of which has greatly limited its production in the USA and several other countries. The continued development of *P. fendleri* as an oilseed crop with enhanced oil and HFA content can provide a non-toxic alternative to castor and a valuable alternative oilseed crop containing fatty acids suitable for multiple industries.

The underlying molecular mechanisms of HFA-containing oil biosynthesis have been investigated in *P. fendleri* with the ultimate goal to enhance crop development through increasing seed oil amount and HFA content. Similar to castor, *P. fendleri* synthesizes HFA by hydroxylation of oleic acid esterified to the membrane lipid phosphatidylcholine (PC) producing ricinoleic acid (18:1-OH; Bafor et al., 1991; Vandeloo et al., 1995; Reed et al., 1997; Broun et al., 1998). In castor, PC acyl editing produces ricinoleoyl-CoA which is utilized by *de novo* glycerolipid biosynthesis (e.g., Kennedy pathway; Weiss et al., 1960) to sequentially acylate glycerol-3-phosphate producing first *de novo sn*-1/2-diacylglycerol (DAG) containing two 18:1-OH, and subsequently triacylglycerol (TAG) molecular species containing three 18:1-OH (e.g., 3HFA-TAG; Bafor et al., 1991; Lager et al., 2013; Bates, 2016, 2022). However, *P. fendleri* predominantly accumulates TAG species containing only two lesquerolic acids (2HFA-TAG), with each HFA strictly localized to the *sn*-1 and *sn*-3 positions of TAG (Hayes et al., 1995; Hayes and Kleiman, 1996). In *P. fendleri*, the 18:1-OH produced on PC is also incorporated into the acyl-CoA pool through acyl editing, but it is further elongated to 20:1-OH prior to incorporation into TAG (Reed et al., 1997; Moon et al., 2001). Until recently, the pathway of 20:1-OH incorporation into TAG was previously unclear. A Kennedy pathway similar to castor would make logical sense to limit unusual fatty acids in membrane lipids, which adversely affect membrane structure–function (Millar et al., 2000). However, transcriptomic studies on developing *P. fendleri* seeds indicated high expression of phosphatidylcholine:diacylglycerol cholinephosphotransferase (PDCT; Kim and Chen, 2015; Horn et al., 2016), which is a hallmark of TAG biosynthesis from PC-derived DAG (rather than *de novo* DAG of the Kennedy pathway) in Brassica species (Lu et al., 2009; Bates and Browse, 2011, 2012; Yang et al., 2017; Bai et al., 2020). To synthesize 2HFA-TAG by a PC-derived DAG pathway utilizing PDCT, *de novo* DAG containing *sn*-1 20:1-OH would need to move through the membrane lipid PC pool to produce a PC-derived DAG containing *sn*-1 20:1-OH. Subsequent *sn*-3 acylation with 20:1-OH would generate the 2HFA-TAG molecular species. However, analysis of lipid fluxes in HFA-producing Arabidopsis and characterization of *Camelina sativa* PDCT properties suggested that PDCT enzymes discriminate against HFA-containing substrates for PC synthesis (Bates and Browse, 2011; Lager et al., 2020). In addition, lesquerolic acid had not been found in *P. fendleri* seed PC (Chen et al., 2011), thus making it unclear if a PDCT promoted PC-derived DAG pathway of TAG biosynthesis exists in *P. fendleri.*

Recently we utilized *in vivo* isotopic labeling of lipid metabolism in developing *P. fendleri* embryos to trace the pathway of newly synthesized fatty acids and glycerol backbones through the lipid metabolic network into different TAG molecular species (Bhandari and Bates, 2021). This lipid flux analysis demonstrated a novel TAG biosynthetic pathway in *P. fendleri* that combined PC-derived DAG production with TAG remodeling as the major mechanism to accumulate 2HFA-TAG while limiting HFAs in membrane lipids (**Supplementary Figure S1**). *Physaria fendleri* TAG biosynthesis elucidated by the isotopic tracing starts with the use of PC-derived DAG that does not contain HFA for the *sn*-3 acylation with 20:1-OH, producing initially a TAG molecular species containing only one HFA (1HFA-TAG). The isotopic tracing further indicated the glycerol backbone and HFA of 1HFA-TAG are converted into 2HFA-TAG over time. The proposed mechanism is that 1HFA-TAG is remodeled into 2HFA-TAG involving a TAG lipase that removes the *sn*-1 non-HFA from 1HFA-TAG transiently producing *sn*-2-acyl-*sn*-3-HFA-DAG. Subsequent acylation with 20:1-OH at the *sn*-1 position generates the final 2HFA-TAG (**Supplementary Figure S1**; Bhandari and Bates, 2021). Thus, the isotopic tracing revealed how *P. fendleri* can utilize PDCT activity for a PC-derived DAG pathway of TAG biosynthesis, without the need to move lesquerolic acid through the PC membrane lipid pool.

While the *P. fendleri* lipid metabolic tracing indicated the major pathway of carbon flux into TAG, the identity of the enzymes involved are unclear. Especially, the TAG lipase at the center of the TAG remodeling pathway. TAG lipases in plants have multiple roles, including TAG turnover during: oilseed germination to provide energy and carbon for seedling establishment; pollen tube growth to provide fatty acids for membrane lipid production; and senescence or various stresses that produce transient TAG pools from membrane lipid turnover (Theodoulou and Eastmond, 2012; Troncoso-Ponce et al., 2013; Kelly and Feussner, 2016; Pyc et al., 2017; Shimada et al., 2017; Wang et al., 2019; Ischebeck et al., 2020). Developing *P. fendleri* seeds express 12 genes annotated as TAG lipases (Horn et al., 2016), including a homolog of the *SUGAR DEPENDENT 1* (SDP1) TAG lipase. SDP1 was first characterized as the dominant TAG lipase involved in TAG turnover during seed germination in *Arabidopsis thaliana* (Eastmond, 2006; Kelly et al., 2011). Yet, *SDP1* expression increases during seed development in preparation for germination, which leads to a reduction in total seed TAG during seed maturation. The suppression of *SDP1* during seed development has led to increased levels of seed oil in Arabidopsis (Van Erp et al., 2014), *Brassica napus* (Kelly et al., 2013), jatropha (Kim et al., 2014), and soybean (Kanai et al., 2019; Aznar-Moreno et al., 2022).

The proposed TAG remodeling pathway of oil biosynthesis in *P. fendleri* involves a TAG lipase (Bhandari and Bates, 2021); therefore, we considered the possibility that PfeSDP1 may be involved in TAG remodeling during seed development, and/or SDP1 may be involved in TAG turnover during seed germination as previously characterized in other species through three hypotheses (**Supplementary Figure S1**). In hypothesis 1, if PfeSDP1 was involved in TAG remodeling then there would be two key features of PfeSDP1: (1) the enzymatic selectivity for TAG molecular species would either favor non-HFA, or be non-selective to TAG molecular species so as to not preferentially turnover the major 2HFA-TAG molecular species produced during seed development and (2) that the suppression of *PfeSDP1* during seed development would lead to increased accumulation of 1HFA-TAG at the expense of 2HFA-TAG reducing the total HFA content of the seed oil. In hypothesis 2, if the role of PfeSDP1 is similar to that of SDP1 in other species being primarily for TAG turnover during germination, then the enzymatic activity may favor turnover of 2HFA-TAG, and that suppression of *PfeSDP1* during seed development would increase total seed TAG without affecting fatty acid composition. In hypothesis 3, if PfeSDP1 was involved in both TAG biosynthesis and TAG turnover during seed maturation, then the enzymatic activity would be non-selective to TAG molecular species, and suppression of PfeSDP1 during seed development would both increase the proportion of 1HFA-TAG and total seed oil. Therefore, to further understand the potential roles of PfeSDP1 in *P. fendleri* lipid metabolism in the context of these three hypotheses we pursued both *in vitro* and *in vivo* studies through enzymatic investigations of heterologously expressed *PfeSDP1*, analysis of SDP1 expression at different developmental stages, and produced seed-specific *PfeSDP1*_RNAi knockdown lines of *P. fendleri*.

MATERIALS AND METHODS

RNA Isolation and Quantitative Real-Time PCR Analysis

Physaria fendleri seed pods of 24, 30, and 42 (mature seed) days after pollination (DAP) were harvested to collect developing seeds and immediately frozen in liquid nitrogen and stored at −80°C till used for RNA extraction. Three replicates of 10 seeds per time point including 1 day germinated seeds were used for RNA extraction. Total RNA was extracted using a Spectrum plant total RNA kit (Sigma). Total RNA (10 μg) was treated with RNase-Free DNase (Qiagen) and cleaned using a RNeasy® Mini Kit (Qiagen). One microgram of the RNA was used to generate cDNA using an iScript cDNA synthesis kit (Bio-Rad). Quantitative real-time PCR (qRT-PCR) analyses were carried out with CFX96 Real-Time System (Bio-rad), using Maxima SYBR Green qPCR Master Mix (Thermo Fisher Scientific Co.), and relative expression values were calculated using the Δ-Ct-method. A complete list of the primers used for RT-PCR is presented in **Supplementary Table S1**.

Over Expression and Purification of PfeSDP1 Protein

The full-length coding sequence of *PfeSDP1* was ordered from Integrated DNA Technologies (IDT) based on prior developing *P. fendleri* RNAseq results (Horn et al., 2016) and amplified using the gene-specific primers (**Supplementary Table S1**), PfeSDP1-FW (added *Kpn*I) and PfeSDP1-RV (added *Not*I). The amplified product was excised with *Kpn*I and *Not*I and cloned into the yeast expression vector, pYES2/NT-C (Invitrogen), under the control of galactose-inducible promoter, GAL1 and with a His-Tag at the N-terminus. The recombinant plasmid, pYES2/NT-C + *PfeSDP1* and empty vector (pYES2/NT-C) was transformed into *Saccharomyces cerevisiae* expression strain, INVScI by using lithium acetate method as described in the Invitrogen user manual. The yeast transformants were grown overnight in yeast synthetic media without uracil (SM-URA) + 2% glucose, and the transgene was induced by adding 0.4 A_{600} overnight culture to 500 ml of induction media (SM-URA + 2% galactose +1% raffinose). After 36 h of shaking at 220 rpm at 28°C, the cells were harvested by centrifugation and resuspended in the lysis buffer [50 mM sodium phosphate buffer pH 8.0; 250 mM NaCl; 5% glycerol; 2 mM sodium taurodeoxycholate, 1 mM phenylmethylsulfonyl fluoride (PMSF) and 1x ProteaseArrest™ for yeast/fungal; G-biosciences, United States]. The cells were lysed with 0.5 mm Zirconia/Silica beads using a bead beater (BioSpec Products, United States), and the resulting cell lysate was subjected to centrifugation at 20,000 rpm for 20 min to remove cell debris and glass beads. Recombinant SDP1 protein was purified under native conditions using ProBond™ purification system (Invitrogen, United States). Briefly, the supernatant from cell lysate was loaded on to Ni-NTA column and the protein was eluted using 250 mM imidazole according to the manufacturer's instructions. Two millimolar sodium taurodeoxycholate was included in all the buffers. The eluted protein fractions were pooled after SDS-PAGE (10%) analysis and subjected to concentration and buffer exchange (50 mM sodium phosphate pH 8.0, 2 mM sodium taurodeoxycholate, and 10% glycerol) using Amicon Ultra-15 centrifugal unit (Millipore Sigma, United States; Cat. no: UFC903008). Recombinant purified protein was confirmed by immunoblotting using anti 6X-His Tag monoclonal antibody (HIS.H8; Invitrogen, United States) produced in mouse at a dilution of 1:3000(v/v) and rabbit anti-mouse IgG secondary antibody tagged with HRP (Invitrogen, United States) at a dilution of 1:5,000 (v/v). Blots were developed with Clarity™ western ECL substrate (BIO-RAD, United States). Protein content was determined using Pierce BCA protein assay kit (Thermo Scientific, United States) using BSA as standard.

In vivo Metabolic Labeling and Neutral Lipid Profiling of Yeast Expressing PfeSDP1

Yeast transformants harboring pYES2/NT-C + *PfeSDP1* and empty vector (pYES2/NT-C) were pre-cultured overnight in SM-URA + 2% glucose. For *in vivo* labeling, cells at an A_{600} of 0.4 were inoculated into an induction medium (SM-URA + 2% galactose +1% raffinose) containing 0.2 μCi/ml [^{14}C]acetate

(American Radiolabeled Chemicals, Inc., United States) and grown at 28°C up to stationary phase. Total Lipid extraction with chloroform:methanol:2% phosphoric acid (2:1:1, v/v/v) was performed on yeast cells, pellet from a volume of culture in ml x A_{600} = 40. Neutral lipids were separated on sillica TLC plates (Analtech Silica gel HL; 20 cm × 20 cm; 250 µm thickness; 15 µm particle size) using petroleum ether:diethyl ether:acetic acid (70:30:1, v/v/v) as a solvent system. The labeled neutral lipids were measured on a Typhoon FLA 7000 phosphor imager and the relative amount of radioactivity in TAG, free fatty acid (FFA), and DAG were using quantified ImageQuant TL 7.0 (GE healthcare, United States).

Preparation of 1HFA- and 2HFA-TAG Substrates

[^{14}C]1HFA- and [^{14}C]2HFA-TAG substrates for *in vitro* lipase assay were purified using thin layer chromatrography (TLC) from total lipids extracts of *P. fendleri* developing embryos which are cultured in the presence of [^{14}C]acetate as described in Bhandari and Bates (2021). Unlabeled [^{12}C]2HFA-TAG was purified using TLC from Physaria seed oil as per previously defined (Bhandari and Bates, 2021). The purified substrates are quantified by GC-FID as described below.

In vitro Lipase Activity Assays

Lipase activity of PfeSDP1 was measured by monitoring the release of [^{14}C]fatty acid from [^{14}C]TAG. The assay was carried out in a reaction volume of 250 µl consisting of 50 mM Tris-(HCl) pH 8.0, 2 mM DTT, 2 mM sodium taurodeoxycholate, and 2 mM $CaCl_2$. A total of 0.02 µCi of [^{14}C]triolein (0.363 nmol; American Radiolabeled Chemicals, Inc., United States) or [^{14}C]1HFA-TAG (1 nmol) or [^{14}C]2HFA-TAG (1 nmol) dissolved in ethanol was added to the reaction buffer and sonicated using water bath sonicator to disperse the lipid. For competitive lipase assay, equimolar ratio (1:1) of [^{14}C]triolein:[^{12}C]triolein or [^{14}C]triolein:[^{12}C]2HFA-TAG was dissolved in ethanol and added to reaction buffer. The reaction was started by the addition of 50 µg recombinant protein and incubated at 30°C for 45 min with shaking (1,000 rpm). The assay was stopped by adding chloroform:methanol:acetic acid (2:1:0.1, v/v/v). After vortex and centrifugation, chloroform phase was transferred into a new tube and dried using nitrogen evaporator. Dried lipids were solubilized in 40 µl chloroform and separated and neutral lipids separated by TLC and quantified by phosphor imaging as above.

RNAi Constructs Preparation

PfeSDP1 RNAi target gene fragments of 240 bp were PCR amplified using synthesized SDP1 DNA (IDT) as a template with Phusion Taq (New England Biolabs). The primers used for the PCR reaction were: PfeSDP1-RNAiF (added *Sac*II and *Not*I) and PfeSDP1-RNAiR (added *Pst*I and *Xma*I restriction sites). The forward arm was cloned at *Not*I/*Xma*I, whereas the reverse arm was cloned at *Pst*I/*Sac*II sites of the J2 vector under seed-specific 2S albumin promoter (Shockey et al., 2015). This clone was sequence-verified, and the promoter:gene:terminator cassette was released by digestion with *Asc*I and cloned into binary vector pB9 (Shockey et al., 2015). A complete list of the primers used for RT-PCR is presented in **Supplementary Table S1**.

Tissue Culture and Transformation

Plant transformation was performed using the Agrobacterium GV3101 strain carrying the *P. fendleri* SDP1-RNAi construct in binary vector pB9 (Shockey et al., 2015). The *in vitro P. fendleri* grown plant's mature leaves were used for the transformation. Tissue culture and transformation protocol followed as described previously (Chen, 2011) with some modifications, using Basta 1.2 mg/L for transgenic selection. The leaves were harvested from the *in vitro* grown plants in sterile conditions and cut into four pieces. The agrobacterium solution in half strength Murashige and Skoog (MS) harbored SDP1-RNAi construct for 5 min with gentle shaking. Following inoculation, the excess Agrobacterium solution was removed by soaking on sterilized filter paper. Leaf segments were transferred to the callus and shoot induction media (CSI) composed of basal media (BM; 1/2 strength MS with 3% sucrose, 0.6% agar, pH 5.7), supplemented with 0.1% 6-BA (6-benzylaminopurine) and 0.01% NAA (naphthaleneacetic acid). Co-cultivated in the dark for 2 days (to increase transformation efficiency) and then 2 days in the light. After 2 days of incubation under light, leaves were again cut into 5 mm sizes and transferred on CSI media containing 0.6 mg/L Basta for transgenic selection and 100 mg/L timentin to repress agrobacterium growth. After 6–8 weeks, Basta resistant yellowish-green calli come from the leaf segments were cut into small pieces (each calli from the leaf segment were marked as an independent line) and transferred on CSI media containing 1.2 mg/L Basta for strong selection. After four rounds of successive selection to get rid of chimeric tissues, shoots were subculture on BM supplemented with 1 mg/L 6-BA, 1 mg/L indole-3-butyric acid (IBA), and 1.2 mg/L Basta for the shoot induction. After 3–4 weeks, shoots of 10–15 mm were transferred to BM supplemented with 1 mg/L IBA and 1.2 mg/L Basta for rooting. After 3–5 weeks, shoots with 3–5 roots were carefully removed from the media and dipped into an antifungal solution of Terbinafine hydrochloride (1 µM) and then transferred to the soil pot (2" × 2"). After root establishment, the plants were transferred to larger pots (4" × 4") in growth room set at 16/8 h light/dark cycle with a light intensity of approximately 250 µmol m^{-2} s^{-1}, 23°C–24°C temperature, and 50% humidity. Seeds from T1 selfed plants (T2 seed) were obtained after forced pollination using the pollen of different flowers from the same plant.

Germination Assay

Around 20–25 seeds for each genotype were surface sterilized with ethanol for 1 min, washed with sterilized water three times, transferred to wet blotting papers in half-strength MS, and kept in the dark for 2 days to germinate. After germination, the plates were transferred under the light. The seedling establishment percentage was calculated after 4 days in light (16 h light/8 h dark), defined by the development of the green cotyledonary leaves.

Quantification of Different TAG Species by HPLC and GC-FID

Total lipids were extracted from ~30–40 mg mature seeds using hexane-isopropanol method (Hara and Radin, 1978) with some modification as described in Shockey et al. (2019). Extracted lipids were dried using N_2 gas and dissolved in hexane:isopropanol (60:40) for separation of different TAG species (0, 1, and 2HFA-TAGs) by high performance liquid chromatography (HPLC) on an Agilent 1260 Infinity II LC with YMC Pack PVA-SIL (250 mm × 4.6 mm, 5 µm particle size) column. The HPLC instrumentation setup, gradient, and fraction collection methods for different TAG species are reported previously (Kotapati and Bates, 2020). The collected fractions were dried under nitrogen gas after adding 25 µg of internal standard, Tri-17:0 TAG (Nucheck Prep, United States) and converted to fatty acid methyl esters (FAMEs) using 2.5% H_2SO_4 in methanol at 85°C for 1 h. FAMES were extracted into hexane after phase separation with 0.88% potassium chloride and quantified with Agilent 7,890 Gas Chromatograph with Flame Ionization Detection (GC-FID) on a DB-HeavyWAX column (30 m, 0.25 mm internal diameter, and 0.25 µm film thickness). The GC-FID conditions are as follows: split mode injection (1:20), 5 µl injection volume, injector at 250°C and FID at 270°C, with oven temperature programmed at 140°C for 0 min, ramped at the rate of 20°C per min to 200°C, then increasing at 6°C per min to 270°C and holding at 270°C for 5 min. Three replicates of five seeds for each SDP1_RNAi line and control were used for lipid extraction and analysis.

RESULTS

Physaria fendleri SDP1 Is Evolutionary Conserved and Highly Expressed During Late Seed Development and Germination

A full-length putative *SDP1* gene sequence from *P. fendleri* was identified from the developing seed transcriptome based on homology to *AtSDP1* (Horn et al., 2016). Phylogenetic analysis revealed that *P. fendleri* SDP1 is highly conserved among the Brassicaceae family, showing 89% and 90% amino acid sequence identity with *Camelina* and *Arabidopsis* SDP1 homologs, respectively (**Figure 1A**; **Supplementary Table S2**). Protein sequence alignment contains a conserved patatin-like domain with its close relative Arabidopsis and Camelina containing lipase motifs GXGXXG and GXSXG (**Figure 1B**). Arabidopsis *SDP1* is expressed during late seed development and germination (Eastmond, 2006), and prior transcriptomics of *P. fendleri* only reported on developing seeds, of which *SDP1* was expressed but low relative to other putative TAG lipases (Horn et al., 2016). Therefore, we quantified the relative *SDP1* expression during *P. fendleri* seed development and germination by qRT-PCR. *SDP1* expression increased from 24 to 30 DAP and was almost four-fold higher in mature seeds than at 24 DAP (**Figure 1C**). The *SDP1* expression further increased 8-fold compared to 24 DAP 1 day after seed germination (**Figure 1C**).

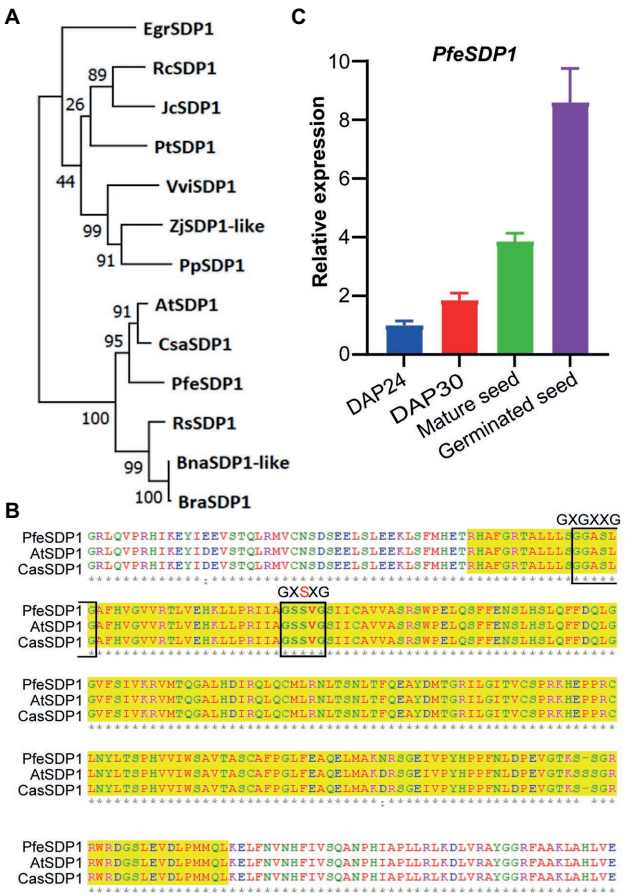

FIGURE 1 | Homology of *Physaria fendleri* SDP1 and expression in seed tissue. **(A)** Phylogenetic analysis of *P. fendleri* and other SDP1 proteins. The phylogenetic tree was constructed using MEGA11. Numbers at the tree branches indicate percent bootstrap support of 1,000 iterations. Species abbreviations and accession numbers of each protein given in **Supplementary Table S2**. **(B)** An amino acid alignment of patatin domain of *P. fendleri* with *Arabidopsis* and *Camelina* SDP1. Lipase motifs GXGXXG and GXSXG are highlighted with a black box. Protein aliment was performed using ClustalW. **(C)** Relative expression of the *PfeSDP1* gene during seed development and germinated seeds, the expression quantified by qRT-PCR and normalized to the reference *18S* gene. DAP24; DPA30; indicates 24 and 30 days after pollination, respectively. Expression values are the average of three biological replicates ± SE.

Characterization of Triacylglycerol Lipase Activity of PfeSDP1

To confirm the TAG lipase activity and evaluate possible fatty acid selectivity of the putative SDP1 gene from *P. fendleri*, we overexpressed PfeSDP1 protein in yeast strain, INVSc1 under GAL1 induction promoter and examined its lipolytic activities in *in vivo* by metabolic labeling using [^{14}C]acetate. Analysis of neutral lipids from whole-cell total extracts indicated the level of TAG decreased significantly in the cells expressing PfeSDP1 compared to the cells harboring empty vector. Concurrently, the levels of DAG and FFA were increased in PfeSDP1 overexpressed cells compared to vector control (**Figure 2A**), consistent with TAG lipolytic activity of PfeSDP1 in

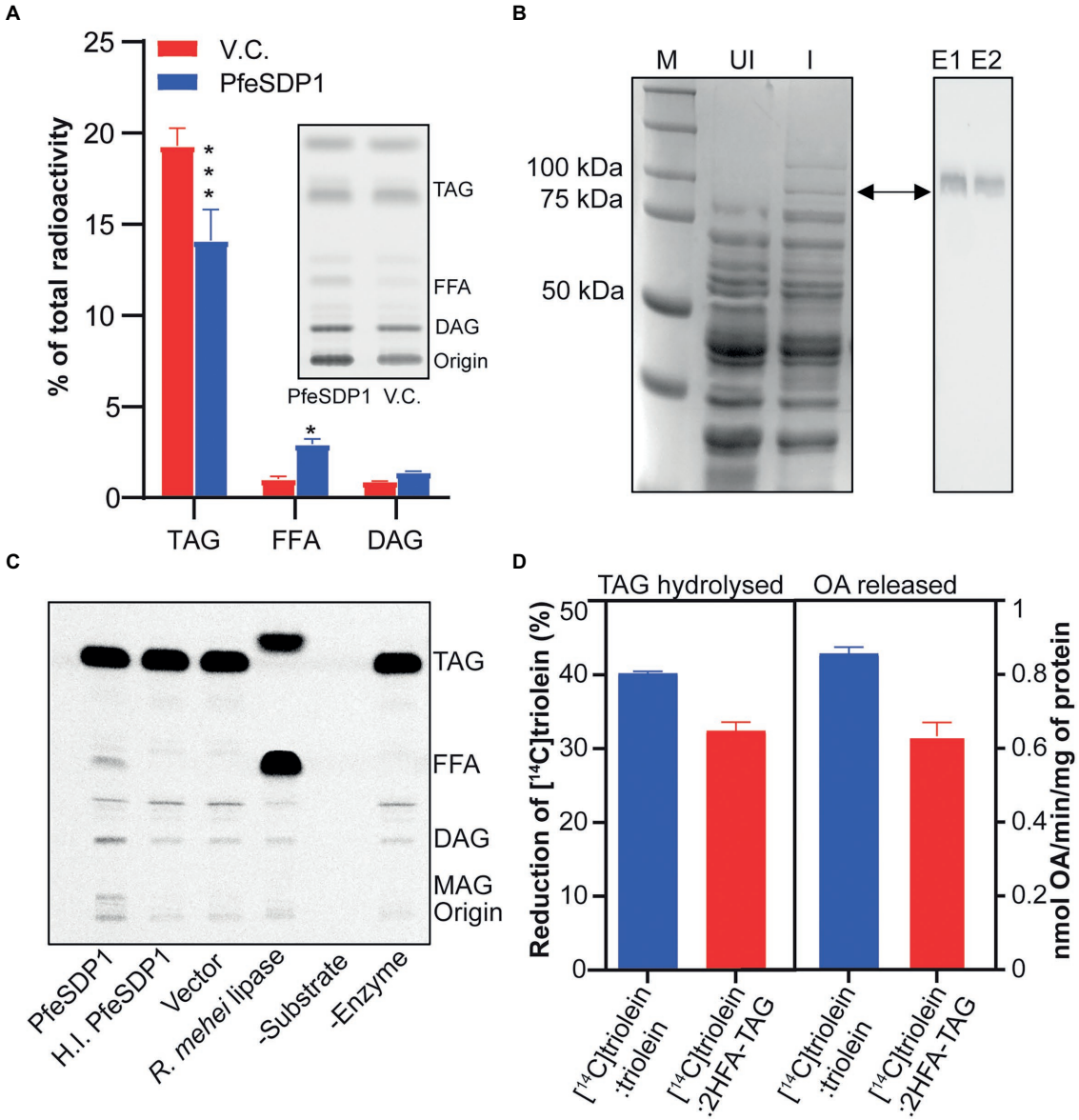

FIGURE 2 | Characterization of PfeSDP1 triacylglycerol lipase activity. **(A)** PfeSDP1 overexpressed in *S. cerevisiae* and *in vivo* metabolic labeling with [^{14}C]acetate to label fatty acid synthesis. The relative amount of radioactivity in TAG, FFA, and DAG neutral lipids quantified by thin-layer chromatography (TLC) separation and phosphor imaging (inset). **(B)** Purification of a His-tagged PfeSDP1 (96 KDa) expressed in *S. cerevisiae*. Left, SDS-PAGE of total protein from uninduced (UI) cells and induced (I) cells. M, protein marker. Right, Western blot with anti-(His)6 antibody from E1 and E2, elution fractions of purified protein from Ni-NTA column. **(C)** TAG lipase activity of purified PfeSDP1 protein. Phosphor image TLC of *in vitro* lipase assay reactions with [^{14}C]triolein as substrate. Lipase from *Rhizopus mehei* was used as positive control. Elution fraction from vector control (VC), heat inactivated (HI.) PfeSDP1 and no enzyme addition was used as negative controls. **(D)** Competitive lipase assay of PfeSDP1 protein with equimolar amounts (1:1) of [^{14}C]triolein:[^{12}C]triolein, or [^{14}C]triolein:[^{12}C]2HFA-TAG as substrates. Lipase activity was represented as amount (%) of [^{14}C]triolein degraded (left) and release of [^{14}C]oleic acid (right) as measured by phosphor imaging. TAG, triacylglycerol; FFA, free fatty acids; DAG, diacylglycerol; ST, sterol; MAG, monoacylglycerol; PL, phospholipids; OA, oleic acid. All the values are represented as Mean ± SD of three independent experiments and significant difference between wild-type control and PfeSDP1 knock-down lines was determined using two-way ANOVA (***$p \leq 0.001$ and *$p \leq 0.33$).

in vivo. We also tested the *in vitro* TAG lipase activity of PfeSDP1 by using a His-tagged recombinant protein overexpressed in INVSc1 and purified on Nickel-NTA agarose beads (**Figure 2B**). SDS-PAGE analysis of the purified fusion protein indicated a protein band of expected size (~96 kDa), which was further confirmed by western blotting (**Figure 2B**, right panel). The His-tagged fusion protein was directly used for enzymatic characterization using [^{14}C]triolein as a substrate. Isolated PfeSDP1 could hydrolyze [^{14}C]triolein to FFA and DAG similar to *Rhizopus mehei* lipase (positive control; **Figure 2C**). This validated the reduction of TAG and accumulation of FFA, and DAG phenotype observed in the

in vivo metabolic labeling study. No activity was detected in the vector and heat-inactivated protein controls. As *P. fendleri* seed oil is composed of more HFA-containing TAG molecular species compared to TAG only containing common fatty acids, we also tested its activity against HFA-containing TAG substrates and found that PfeSDP1 can hydrolyze [^{14}C]TAG with both 1 and 2 HFA (**Supplementary Figure S2**). To further characterize the common vs. HFA-TAG substrate preference of PfeSDP1, we carried out a competitive *in vitro* lipase assay using the equimolar ratio (1:1) of [^{14}C]triolein:[^{12}C]triolein or [^{14}C] triolein:[^{12}C]2HFA-TAG. The substrate specificity was determined by measuring the rate of [^{14}C]triolein degradation and the amount of [^{14}C]oleic acid released. In the assay, if PfeSDP1 has a higher selectivity for 2HFA-TAG the rate of [^{14}C]triolein degradation should decrease relative to the [^{14}C]triolein:[^{12}C] triolein control. However, if PfeSDP1 prefers triolein over 2HFA-TAG, we would expect the rate of [^{14}C]triolein degradation to increase. When the PfeSDP1 activities in the presence of equimolar mixtures of substrates were compared, the rate of [^{14}C]triolein degradation and the amount of oleic acid released was decreased by ~20% and ~26%, respectively, in the presence of HFA-containing TAG compared to common fatty acid-containing TAG (**Figure 2D**). Together, these results confirm that PfeSDP1 is a TAG lipase and can utilize TAG molecular species containing both common fatty acids and HFAs, but with a preference for HFA-TAG containing molecular species.

SDP1 Knockdown Increased Seed Weight With Limited Effect on Post-germination Seedling Establishment

To investigate the *in-planta* function of PfeSDP1, we designed an RNAi knockdown construct expressed under the strong seed-specific promoter 2S albumin (Guerche et al., 1990; Shockey et al., 2015) to repress the *SDP1* expression only in developing *P. fendleri* seeds to avoid any possible pleiotropic effects at other developmental stages. The PfeSDP1_RNAi transgenic plants were produced by Agrobacterium transformation of leaf tissue and plant regeneration through tissue culture. Out of 12 regenerated plants, nine transgenic PfeSDP1_RNAi plants were confirmed by PCR using vector and gene-specific primers (**Supplementary Figure S3A**). Seeds harvested from T1 generation plants (T2 seeds) were utilized to determine the effect of *PfeSDP1* knockdown on seed weight, lipid content, germination, and seedling establishment. Based on increased seed weight the top four transgenic lines were selected (PfeSDPi_3, 4, 9, and 13; **Supplementary Figure S3B**), and the knockdown of *PfeSDP1* expression in these lines was confirmed by qRT-PCR of RNA extracted from the germinating T2 seeds (**Supplementary Figure S4**). These four selected transgenic lines were used for further analysis in this study. The PfeSDP1_RNAi knockdown lines had a significant increase in seed weight ranging from 0.74–0.77 mg (12%–16%) in line 13 and line 3, respectively, compared to the wild-type average seed weight of 0.66 mg (**Figure 3A**). No considerable difference in seed germination was measured, and there was a limited effect on post-germination seedling establishment in the PfeSDP1_RNAi plants compared to control plants (94% seedling establishment), except for line 9 which had 74% seedling establishment (**Figure 3B**).

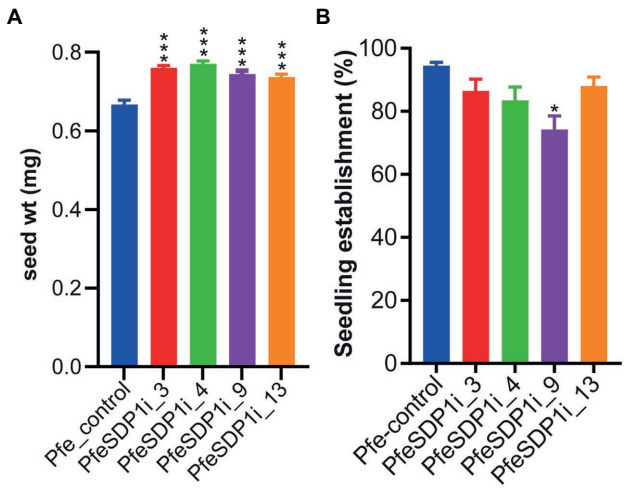

FIGURE 3 | Seed-specific *PfeSDP1_RNAi* increases seed weight and has a limited effect on seed establishment. **(A)** The seed weight of PfeSDP1_RNAi T1 generation plant seeds (T2 seeds) represent the average seed weight ($n = 10$). **(B)** Percentage of seedling establishment after 4 days in light (16 h light/8 h dark), defined by the development of the green cotyledonary leaves. Asterisks (*) and (***) indicate significant differences at $p \leq 0.05$ and $p \leq 0.0005$ to the control by two-tailed paired *t*-tests.

SDP1 Suppression Increased Both Total Oil Content and Hydroxy Fatty Acid Content

The total seed fatty acid content and fatty acid composition was quantified by gas chromatography in seeds (T2) produced from the top selected T1 SDP1_RNAi lines. All four of the top SDP1_RNAi lines had a significant increase in total seed fatty acid content, with total fatty acid content increasing 14%–19% to 261–271 µg per mg seed in line 3 and line 9, respectively, compared to the control seeds containing an average of 228 µg per mg seed (**Figure 4A**; **Supplementary Table S3**). The increase in total fatty acid content was attributed primarily to the HFAs 20:1-OH and 20:2-OH, which increased significantly in the transgenic lines to 144.8–155 and 8.9–10.8 µg per mg seed, whereas control seeds contained only 122.2 and 7 µg per mg seed, respectively (**Figure 4B**; **Supplementary Table S4**). In addition, *SDP1* knockdown lines had a slight but significant increase in the 18 carbon fatty acids 18:1, 18:2, and 18:3, which increased to 41.6–44.3, 18.2–19.8, and 31.6–35.9 µg per mg seed, whereas control seeds had 38.3, 18.1, and 30.4 µg per mg seed, respectively (**Figure 4B**; **Supplementary Table S4**). When the seed fatty acid composition is considered as a weight percentage of total fatty acids, there was a significant increase in total HFA (4%–6%). In contrast, there was no substantial proportional change in individual non-HFAs compared to the control (**Figures 5A,B**).

Previous research has indicated that *P. fendleri* accumulates TAG molecular species groups of 0HFA-, 1HFA-, or 2HFA-TAG,

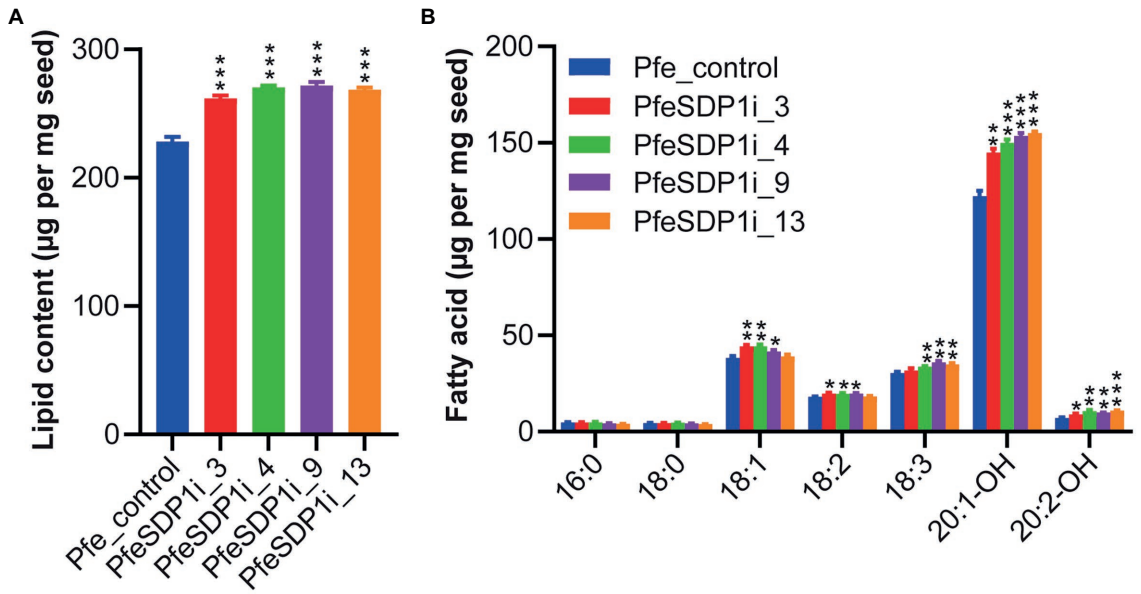

FIGURE 4 | Total fatty acid amount increased in *Physaria fendleri* SDP1_RNAi seeds. **(A)** Total fatty acid content of PfeSDP1_RNAi lines, data represents mean ± SEM ($n = 3$–10) per line. **(B)** Individual fatty acid content of lines in **(A)**. Additional minor fatty acids (18:1-OH, 18:2-OH, 20:0, 20:1) each representing less than 1% of total fatty acids are included in **Supplementary Table S2**. Asterisks (*), (**), and (***) indicate significant differences at $p < 0.05$, $p \leq 0.002$, and $p \leq 0.0006$ compared to their respective control by two-tailed paired *t*-tests.

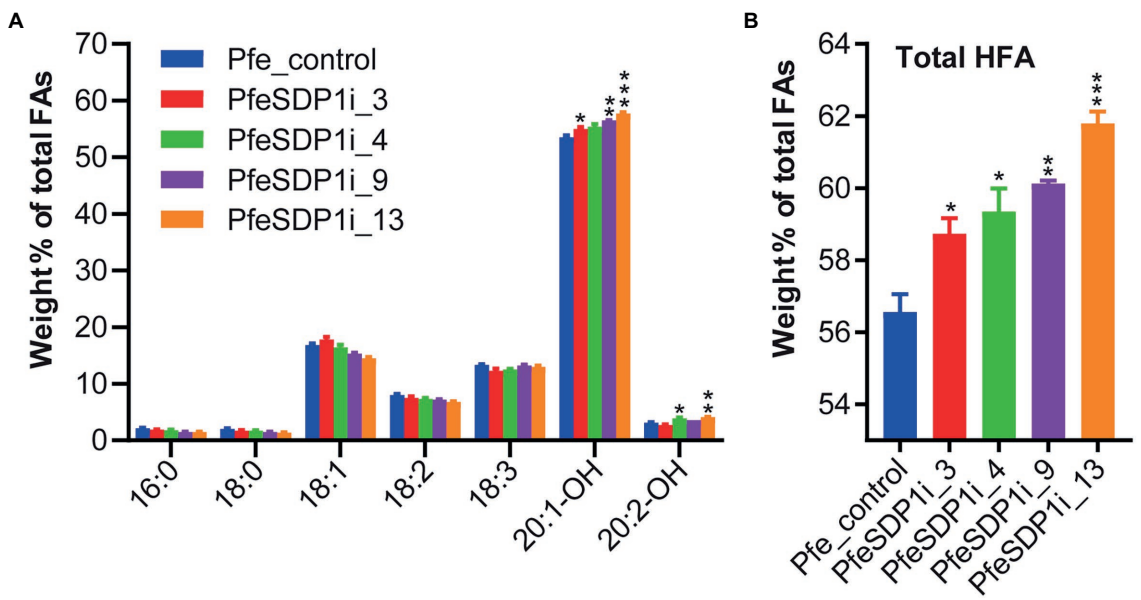

FIGURE 5 | Increased proportion of hydroxy fatty acids in PfeSDP1_RNAi seeds. **(A)** Weight percent of total fatty acids (FA) of PfeSDP1_RNAi lines 3, 4, 9, and 13. **(B)** Total HFAs combined (18:1-OH, 18:2-OH, 20:1-OH, and 20:2-OH). Data represents mean ± SEM ($n = 3$–10) per line. Additional minor fatty acids (18:1-OH, 18:2-OH, 20:0, 20:1) each representing less than 1% of total fatty acids are included in **Supplementary Table S3**. Asterisks (*), (**), and (***) indicate significant differences at $p \leq 0.05$, ≤ 0.002, and ≤ 0.0006 compared to their respective control by two-tailed paired *t*-tests.

and that 1HFA-TAG is a metabolic precursor to 2HFA-TAG through TAG remodeling (**Supplementary Figure S1**). Therefore, to determine if the changes in seed fatty acid content and composition are due to differential accumulation of various TAG molecular species, total lipids were extracted from three independent plants of SDP1 RNAi lines, PfeSDP1i_3, PfeSDP1i_4, and PfeSDP1i_9 and the non-hydroxy-, 1HFA-, and 2HFA-TAG molecular species were separated and collected by HPLC and quantified by GC. No significant changes in the levels of non-hydroxy-TAG were observed between control plants and

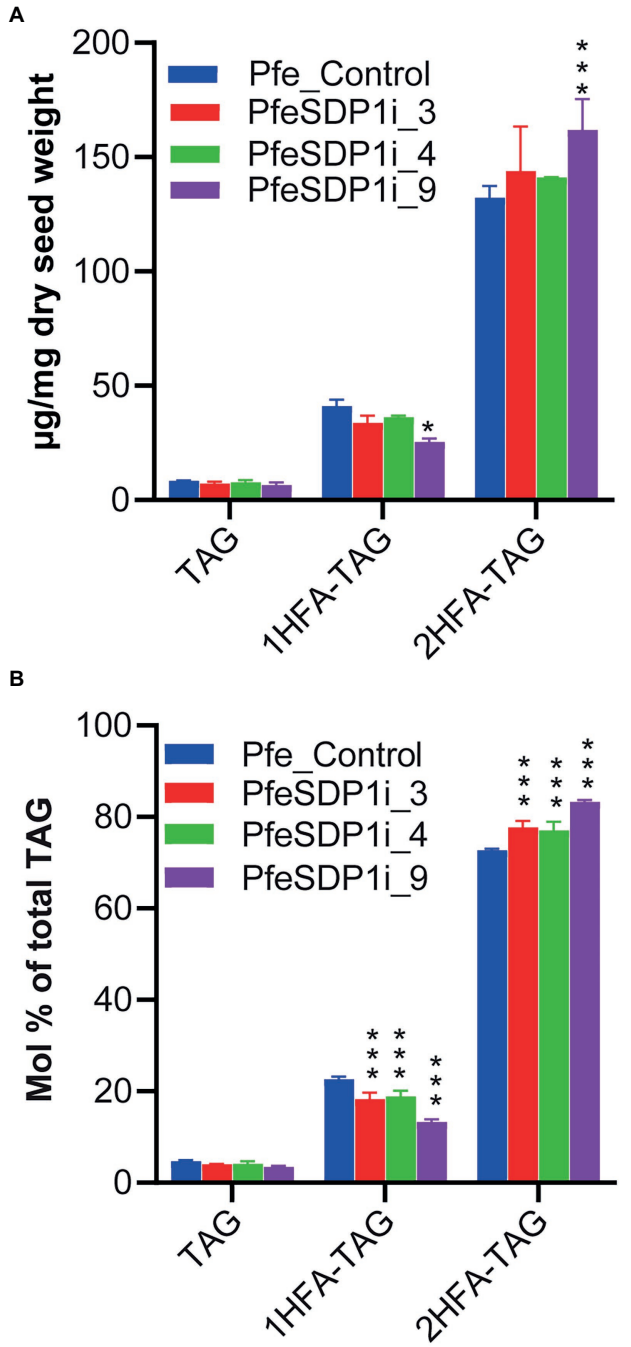

FIGURE 6 | Analysis of different TAG species in the seeds of SDP1 RNAi lines. The levels of different TAG molecular species were expressed as µg/mg dry seed weight **(A)** and relative percent (mol%) of total TAG **(B)**. 1HFA-TAG and 2HFA-TAG represents TAG with one and two hydroxy fatty acids, respectively. Significant difference between wild-type control and PfeSDP1 knock-down lines was determined using two-way ANOVA (***$p \leq 0.001$ and *$p \leq 0.33$).

PfeSDP1 RNAi plants. The amount of 1HFA-TAG in all the PfeSDP1 RNAi lines was significantly reduced compared to the control by 1.2–1.6-fold (**Figure 6A**), representing a ~12.7% to ~40.7% decrease in the relative proportion of total TAG species (**Figure 6B**). The amount of 2HFA-TAG was significantly increased by 1–1.2-fold compared to control plants, representing an ~4.7% to ~14.8% increase in the relative proportion of total TAG species (**Figure 6**). Other than the amount of TAG molecular species, there were small changes in TAG molecular species fatty acid compositions (**Supplementary Figure S5**). The largest changes were in 1HFA-TAG, where the levels of 18:1 decreased significantly by ~7.5 to 14.1% in all the SDP1 RNAi lines compared to wild-type and were compensated by mostly increases in 18:0 (**Supplementary Figure S5**). Overall, reduced seed expression of *PfeSDP1* increased total seed fatty acids and the proportion of HFAs in the seed oil predominantly by the enhanced accumulation of 2HFA-TAG.

DISCUSSION

Physaria fendleri is a burgeoning oilseed crop that has gained considerable interest in basic oilseed research because of the natural presence of the industrially important HFA, lesquerolic acid in its seeds. Our previous attempt to understand the channeling of newly synthesized common and HFA to seed storage lipids using *in vivo* isotopic labeling has demonstrated a novel TAG remodeling pathway in *P. fendleri* with a proposed TAG lipase as a central player (Bhandari and Bates, 2021). Various TAG lipases were previously reported to be expressed in *P. fendleri* during seed development (Horn et al., 2016). Among these, SDP1 is known to be involved in mobilizing TAG during maturation and desiccation stages of seed development, besides its major TAG turnover role during seed germination (Kelly et al., 2013; Kim et al., 2014; Kanai et al., 2019). Therefore, we hypothesized three possible roles of *P. fendleri* SDP1 during seed development. Firstly, if PfeSDP1 is involved in the proposed pathway of TAG remodeling to produce 2HFA-TAG, its knockdown might block 1HFA-TAG remodeling, thereby reducing the accumulation of 2HFA-TAG in its seeds. Secondly, if the role is similar to other oilseeds for TAG mobilization during the desiccation stage of seed development, its suppression might decrease TAG catabolism, specifically 2HFA-TAG and increase total oil and 2HFA-TAG content. Third, PfeSDP1 may be involved in both TAG remodeling and TAG turnover of which the suppression should lead to increased oil with more 1HFA-TAG, and less 2HFA-TAG. To test the above hypotheses, we isolated the *P. fendleri* SDP1 homolog, demonstrated its lipolytic activity and fatty acid substrate selectivity by heterologous expression in yeast and generated seed-specific SDP1_RNAi knockdown lines of *P. fendleri* to understand the effect of its suppression on total oil content and fatty acid composition. Together our results are most consistent with hypothesis 2 (**Figure 7**).

PfeSDP1 Is a HFA Selective Lipase Involved in 2HFA-TAG Turnover

Overexpression of PfeSDP1 in yeast confirmed the lipolytic activity of the protein to hydrolyze triacylglycerols. A similar activity

specifically for TAG substrates has been reported for SDP1 proteins from Arabidopsis and soybean (Eastmond, 2006; Kanai et al., 2019). Previously soybean SDP1 preferentially cleaved triolein than trilinolein (Kanai et al., 2019), indicating that substrate selectivity of SDP1 may have a role in the mobilization of certain TAG molecular species over others. Similarly, it is evident from our *in vitro* competitive lipase assay that PfeSDP1 preferentially uses HFA-containing TAG as a substrate over common fatty acid-containing TAG (triolein). Although, SDP1 suppression studies in Brassica and Jatropha (Kelly et al., 2013; Kim et al., 2014) increased seed oil content but without any major changes to the fatty acid composition. However, we observed both a significant increase in seed oil accumulation and an increase in the HFA content of the oil. The increase in HFA content in the PfeSDP1_RNAi lines came from enhanced accumulation of 2HFA-TAG, which is the major TAG species. Therefore, this clearly demonstrates the importance of both TAG anabolic and catabolic pathways during *P. fendleri* seed development for the control of both oil amount and oil quality. Based on our initial stated hypothesis 2, the increase in total seed oil and specifically the final 2HFA-TAG molecular species (rather than the TAG remodeling intermediate, 1HFA-TAG) support the role of PfeSDP1 for predominantly mobilization of the major TAG molecular species during seed germination and late seed maturation. Therefore, PfeSDP1 is likely not the lipase involved in remodeling 1HFA-TAG to 2HFA-TAG, which when suppressed would have led to increased 1HFA-TAG (**Figure 7A**). However, we have demonstrated that the inhibition of TAG degradation, specifically 2HFA-TAG turnover, by suppression (or mutation) of *PfeSDP1*, would be an excellent strategy to enhance the total amount of industrially valuable lesquerolic acid in *P. fendleri* seeds (**Figure 7C**).

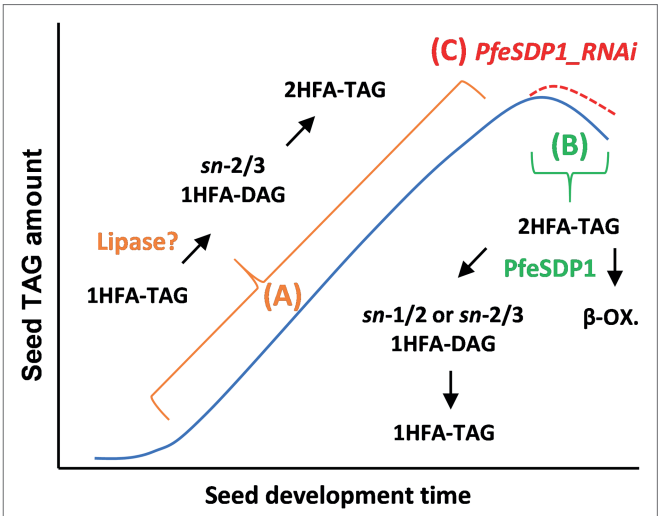

FIGURE 7 | Model of lipase action in *P. fendleri* oil accumulation. In many oilseeds TAG accumulates over seed development, then TAG levels drop ~10%–20% during seed maturation (blue line). **(A)** In *P. fendleri* recent results suggest an uncharacterized lipase is involved in remodeling 1HFA-TAG to 2HFA-TAG during TAG biosynthesis. **(B)** In wild-type *P. fendleri* PfeSDP1 action during late seed development and/or seed maturation leads to TAG turnover and the β-oxidation (β-ox.) of fatty acids reducing total oil amount. Some of the products of 2HFA-TAG turnover are remodeled into 1HFA-TAG. **(C)** The *PfeSDP1_RNAi* lines reduce TAG turnover and remodeling of 2HFA-TAG to 1HFA-TAG, thus increasing total oil amount (red dashed line) and HFA amount. Because *PfeSDP1_RNAi* lines only decreased expression of *PfeSDP1* up to 50%, this result suggests a knockout mutation of *PfeSDP1* may further increase seed oil.

Connection of SDP1 to TAG Remodeling in *Physaria fendleri* Seeds

According to the pathway of *P. fendleri* 2HFA-TAG production through TAG remodeling elucidated by isotopic labeling in developing seeds (**Figure 7A**; Bhandari and Bates, 2021), 1HFA-TAG is synthesized from PC-derived DAG, and subsequently, the *sn*-1 common fatty acid is removed by a lipase to generate *sn*-2-acyl-*sn*-3-HFA-DAG that is finally acylated at the *sn*-1 position with a HFA to make 2HFA-TAG. As hypothesized, if *PfeSDP1* is part of TAG remodeling, then the knockdown of SDP1 activity will produce less 2HFA-TAG and more 1HFA-TAG. The SDP1_RNAi lines accumulate more 2HFA-TAG, and thus we have concluded that PfeSDP1 is likely not involved in the dominant TAG remodeling pathway that produces 2HFA-TAG (thus rejection of initial hypotheses 1 and 3). However, surprisingly the SDP1_RNAi lines also had a significant decrease in total 1HFA-TAG (**Figure 6A**). This result suggests that some of the 1HFA-TAG that accumulates in mature seeds is due to the action of PfeSDP1 and may involve reverse TAG remodeling of 2HFA-TAG that generates at least part of the substrates utilized for 1HFA-TAG biosynthesis (**Figure 7B**). Reverse TAG remodeling of 2HFA-TAG likely involves PfeSDP1 cleavage of 2HFA-TAG producing 1HFA-DAG and free HFA. Subsequent 1HFA-TAG production may occur either by acylation of the 1HFA-DAG with a common fatty acid or utilization of the HFA for acylation of a non-HFA-containing DAG molecule. Considering total oil is reduced by PfeSDP1 action in wild-type, the degradation of the free HFA and acylation of some of the 1HFA-DAG by a common fatty acid may be the more likely mechanism. Additionally, the formation of 1HFA-TAG (rather than 2HFA-TAG resynthesis) may be favored by reduced *de novo* lesquerolic acid synthesis during late seed maturation. Interestingly, the remaining 1HFA-TAG in the *PfeSPD1*_RNAi lines had decreases in oleic acid (18:1) content (**Supplementary Figure S5B**). Oleic acid is the substrate for hydroxylation, thus this result is consistent with a reverse TAG remodeling mechanism in wild-type where PfeSDP1 produced 1HFA-DAG is acylated with 18:1 (from *de novo* fatty acid synthesis) during seed maturation, rather than 20:1-OH that is abundantly produced during the seed filling stage (Bhandari and Bates, 2021; **Figure 7B**). To further elucidate the mechanisms of TAG remodeling in *P. fendleri*, future studies should target lipases other than PfeSDP1 by RNAi to identify the lipase involved in the dominant TAG remodeling mechanism that produces 2HFA-TAG. Further clarification of PfeSDP1 induced reverse TAG remodeling of 2HFA-TAG to 1HFA-TAG may be elucidated by isotopic labeling studies during the late seed maturation phase and/or measurements of PfeFAH12 activity during this stage of development, of which reduced PfeFAH12 activity would favor the acylation of 1HFA-DAG with oleic acid to produce 1HFA-TAG, rather than resynthesis of 2HFA-TAG.

PfeSDP1 Suppression as a Tool to Enhance Seed Oil and HFA Content

The expression pattern of *PfeSDP1* in *P. fendleri*, the preferred activity of PfeSDP1 for 2HFA-TAG, and the increased oil content of PfeSDP1_RNAi lines are consistent with Arabidopsis, Jatropha, and soybean *SDP1* (Eastmond, 2006; Kelly et al., 2013; Kim et al., 2014; Aznar-Moreno et al., 2022), where SPD1 activity is involved in TAG turnover during germination to provide free fatty acids for ß-oxidation, thus producing carbon skeletons and energy for post-germination seedling establishment (Eastmond and Rawsthorne, 2000; Eastmond, 2006). The *PfeSDP1* suppression lines do not indicate any major defect in seed germination or post-germination seedling establishment. In this study, RNAi lines with only up to 50% decrease in *SDP1* transcript were produced (**Supplementary Figure S4**). The limited effect on seedling establishment may suggest that this reduced *PfeSDP1* expression level still provides enough lipase activity for TAG turnover at this stage. Additionally, previous reports indicate that SDP1 activity greatly enhances germination but is not essential for germination due to low activity of other lipases (Kelly et al., 2011). Transcriptomics of developing *P. fendleri* seeds indicated 12 genes annotated as TAG lipases were also expressed, thus it is likely additional lipases also contribute to *P. fendleri* seed germination and seedling establishment. The ability of other lipases to allow sufficient germination and seedling establishment will require analysis of a *PfeSDP1* null mutant. Additionally, based on our results with only up to 50% knockdown, a CRISPR based mutation of PfeSDP1 may be a valuable approach to further increase total seed oil and HFA levels (**Figure 7C**). If significant germination issues arise in a *PfeSDP1* mutant, combining *PfeSDP1* knockout with a PfeSDP1 construct under control of a germination-specific promoter may be an ideal bioengineering approach to improving seed oil amount and HFA content without any germination defect.

CONCLUSION

The seed-specific knockdown of the HFA-selective TAG lipase *PfeSDP1* demonstrated a significant increase in seed weight and increased seed oil content, and more importantly, increased amount of industrially valuable HFA. In addition, we demonstrate that PfeSDP1 is not directly involved in the *P. fendleri* TAG remodeling pathway that is utilized to synthesize the dominant TAG molecular species 2HFA-TAG; instead, it may have a minor role in reverse TAG remodeling during seed maturation that produces 1HFA-TAG molecular species from 2HFA-TAG. Thus, the elimination of both the 2HFA-TAG turnover during seed maturation and the minor reverse TAG remodeling role together enhances the total HFA content of *P. fendleri* seeds.

DATA AVAILABILITY STATEMENT

The original contributions presented in the study are included in the article/**Supplementary Material**, further inquiries can be directed to the corresponding author.

AUTHOR CONTRIBUTIONS

PB conceived the project, procured the funding, agrees to serve as the author responsible for contact, and ensures communication. AA, PP, and PB designed experiments, analyzed the data, and wrote the article. AA and PP performed the experiments. All authors contributed to the article and approved the submitted version.

FUNDING

This work is supported by the United States Department of Agriculture National Institute of Food and Agriculture #2020-67013-30899, the Hatch Umbrella Project #1015621, the Multi-State Project #NC1203, and the National Science Foundation #PGRP-IOS-1829365.

ACKNOWLEDGMENTS

We would like to thank Grace Chen (USDA, Albany, CA) for kindly providing *P. fendleri* (fen32) seeds and for tips on the tissue culture and transformation protocol, Jay Shockey (USDA, New Orleans, LA) for providing the RNAi pB9 vector, and Patrick Horn (UNT, Denton, TX) for providing the full-length PfeSDP1 sequence assembled from developing *P. fendleri* seed transcriptome analysis (Horn et al., 2016).

SUPPLEMENTARY MATERIAL

The Supplementary Material for this article can be found online at: https://www.frontiersin.org/articles/10.3389/fpls.2022.931310/full#supplementary-material

REFERENCES

Al-Shehbaz, I. A., and O'kane, S. L. Jr. (2002). Lesquerella is united with Physaria (Brassicaceae). *Novon* 12, 319–329. doi: 10.2307/3393073

Aznar-Moreno, J. A., Mukherjee, T., Morley, S. A., Duressa, D., Kambhampati, S., Chu, K. L., et al. (2022). Suppression of SDP1 improves soybean seed composition by increasing oil and reducing undigestible oligosaccharides. *Front. Plant Sci.* 13:863254. doi: 10.3389/fpls.2022.863254

Bafor, M., Smith, M. A., Jonsson, L., Stobart, K., and Stymne, S. (1991). Ricinoleic acid biosynthesis and triacylglycerol assembly in microsomal preparations from developing castor-bean (*Ricinus communis*) endosperm. *Biochem. J.* 280, 507–514. doi: 10.1042/bj2800507

Bai, S., Wallis, J. G., Denolf, P., Engelen, S., Bengtsson, J. D., Van Thournout, M., et al. (2020). The biochemistry of headgroup exchange during triacylglycerol synthesis in canola. *Plant J.* 103, 83–94. doi: 10.1111/tpj.14709

Bates, P. D. (2016). Understanding the control of acyl flux through the lipid metabolic network of plant oil biosynthesis. *Biochim. Biophys. Acta* 1861, 1214–1225. doi: 10.1016/j.bbalip.2016.03.021

Bates, P. D. (2022). "Chapter 6: The plant lipid metabolic network for assembly of diverse triacylglycerol molecular species," in *Advances in Botanical Research*. eds. F. Rébeillé and E. Maréchal (Academic Press), 225–252.

Bates, P. D., and Browse, J. (2011). The pathway of triacylglycerol synthesis through phosphatidylcholine in Arabidopsis produces a bottleneck for the accumulation of unusual fatty acids in transgenic seeds. *Plant J.* 68, 387–399. doi: 10.1111/j.1365-313X.2011.04693.x

Bates, P. D., and Browse, J. (2012). The significance of different diacylgycerol synthesis pathways on plant oil composition and bioengineering. *Front. Plant Sci.* 3:147. doi: 10.3389/fpls.2012.00147

Bhandari, S., and Bates, P. D. (2021). Triacylglycerol remodeling in *Physaria fendleri* indicates oil accumulation is dynamic and not a metabolic endpoint. *Plant Physiol.* 187, 799–815. doi: 10.1093/plphys/kiab294

Broun, P., Boddupalli, S., and Somerville, C. (1998). A bifunctional oleate 12-hydroxylase: desaturase from *Lesquerella fendleri*. *Plant J.* 13, 201–210. doi: 10.1046/j.1365-313X.1998.00023.x

Chen, G. Q. (2011). Effective reduction of chimeric tissue in Transgenics for the stable genetic transformation of *Lesquerella fendleri*. *HortScience* 46, 86–90. doi: 10.21273/HORTSCI.46.1.86

Chen, G. Q. (2017). *Castor and Lesquerella Oils: Production, Composition and Uses*. Nova Science Publishers, Inc.

Chen, G. Q., He, X., and Mckeon, T. A. (2005). A simple and sensitive assay for distinguishing the expression of ricin and *Ricinus communis* agglutinin genes in developing castor seed (*R. communis* L.). *J. Agric. Food Chem.* 53, 2358–2361. doi: 10.1021/jf040405t

Chen, G. Q., Lin, J.-T., and Lu, C. (2011). Hydroxy fatty acid synthesis and lipid gene expression during seed development in *Lesquerella fendleri*. *Ind. Crop. Prod.* 34, 1286–1292. doi: 10.1016/j.indcrop.2010.08.003

Cocuron, J.-C., Anderson, B., Boyd, A., and Alonso, A. P. (2014). Targeted metabolomics of *Physaria fendleri*, an industrial crop producing hydroxy fatty acids. *Plant Cell Physiol.* 55, 620–633. doi: 10.1093/pcp/pcu011

Dierig, D. A., Wang, G., Mccloskey, W. B., Thorp, K. R., Isbell, T. A., Ray, D. T., et al. (2011). Lesquerella: new crop development and commercialization in the US. *Ind. Crop. Prod.* 34, 1381–1385. doi: 10.1016/j.indcrop.2010.12.023

Eastmond, P. J. (2006). SUGAR-DEPENDENT1 encodes a patatin domain triacylglycerol lipase that initiates storage oil breakdown in germinating Arabidopsis seeds. *Plant Cell* 18, 665–675. doi: 10.1105/tpc.105.040543

Eastmond, P. J., and Rawsthorne, S. (2000). Coordinate changes in carbon partitioning and plastidial metabolism during the development of oilseed rape embryos. *Plant Physiol.* 122, 767–774. doi: 10.1104/pp.122.3.767

Guerche, P., Tire, C., De Sa, F. G., De Clercq, A., Van Montagu, M., and Krebbers, E. (1990). Differential expression of the Arabidopsis 2S albumin genes and the effect of increasing gene family size. *Plant Cell* 2, 469–478. doi: 10.2307/3869096

Hara, A., and Radin, N. S. (1978). Lipid extraction of tissues with a low-toxicity solvent. *Anal. Biochem.* 90, 420–426. doi: 10.1016/0003-2697(78)90046-5

Hayes, D. G., and Kleiman, R. (1996). A detailed triglyceride analysis of *Lesquerella fendleri* oil: column chromatographic fractionation followed by supercritical fluid chromatography. *J. Am. Oil Chem. Soc.* 73, 267–269.

Hayes, D., Kleiman, R., and Phillips, B. (1995). The triglyceride composition, structure, and presence of estolides in the oils of *Lesquerella* and related species. *J. Am. Oil Chem. Soc.* 72, 559–569. doi: 10.1007/BF02638857

Horn, P. J., Liu, J., Cocuron, J. C., Mcglew, K., Thrower, N. A., Larson, M., et al. (2016). Identification of multiple lipid genes with modifications in expression and sequence associated with the evolution of hydroxy fatty acid accumulation in *Physaria fendleri*. *Plant J.* 86, 322–348. doi: 10.1111/tpj.13163

Ischebeck, T., Krawczyk, H. E., Mullen, R. T., Dyer, J. M., and Chapman, K. D. (2020). Lipid droplets in plants and algae: distribution, formation, turnover and function. *Semin. Cell Dev. Biol.* 108, 82–93. doi: 10.1016/j.semcdb.2020.02.014

Kanai, M., Yamada, T., Hayashi, M., Mano, S., and Nishimura, M. (2019). Soybean (*Glycine max* L.) triacylglycerol lipase GmSDP1 regulates the quality and quantity of seed oil. *Sci. Rep.* 9:8924. doi: 10.1038/s41598-019-45331-8

Kelly, A. A., and Feussner, I. (2016). Oil is on the agenda: lipid turnover in higher plants. *Biochim. Biophys. Acta* 1861, 1253–1268. doi: 10.1016/j.bbalip.2016.04.021

Kelly, A. A., Quettier, A.-L., Shaw, E., and Eastmond, P. J. (2011). Seed storage oil mobilization is important But not essential for germination or seedling establishment in Arabidopsis. *Plant Physiol.* 157, 866–875. doi: 10.1104/pp.111.181784

Kelly, A. A., Shaw, E., Powers, S. J., Kurup, S., and Eastmond, P. J. (2013). Suppression of the SUGAR-DEPENDENT1 triacylglycerol lipase family during seed development enhances oil yield in oilseed rape (*Brassica napus* L.). *Plant Biotechnol. J.* 11, 355–361. doi: 10.1111/pbi.12021

Kim, H. U., and Chen, G. Q. (2015). Identification of hydroxy fatty acid and triacylglycerol metabolism-related genes in lesquerella through seed transcriptome analysis. *BMC Genomics* 16:230. doi: 10.1186/s12864-015-1413-8

Kim, M. J., Yang, S. W., Mao, H. Z., Veena, S. P., Yin, J. L., and Chua, N. H. (2014). Gene silencing of Sugar-dependent 1 (JcSDP1), encoding a patatin-domain triacylglycerol lipase, enhances seed oil accumulation in *Jatropha curcas*. *Biotechnol. Biofuels* 7:36. doi: 10.1186/1754-6834-7-36

Kotapati, H. K., and Bates, P. D. (2020). Normal phase HPLC method for combined separation of both polar and neutral lipid classes with application to lipid metabolic flux. *J. Chromatogr. B Analyt. Technol. Biomed. Life Sci.* 1145:122099. doi: 10.1016/j.jchromb.2020.122099

Lager, I., Jeppson, S., Gippert, A.-L., Feussner, I., Stymne, S., and Marmon, S. (2020). Acyltransferases regulate oil quality in *Camelina sativa* through both acyl donor and acyl acceptor specificities. *Front. Plant Sci.* 11:1144. doi: 10.3389/fpls.2020.01144

Lager, I., Yilmaz, J. L., Zhou, X.-R., Jasieniecka, K., Kazachkov, M., Wang, P., et al. (2013). Plant acyl-CoA:Lysophosphatidylcholine Acyltransferases (LPCATs) have different specificities in their forward and reverse reactions. *J. Biol. Chem.* 288, 36902–36914. doi: 10.1074/jbc.M113.521815

Lu, C., Xin, Z., Ren, Z., Miquel, M., and Browse, J. (2009). An enzyme regulating triacylglycerol composition is encoded by the ROD1 gene of Arabidopsis. *Proc. Natl. Acad. Sci.* 106, 18837–18842. doi: 10.1073/pnas.0908848106

Mckeon, T. A. (2016). "Chapter 4: Castor (*Ricinus communis* L.)," in *Industrial Oil Crops*. eds. T. A. Mckeon, D. G. Hayes, D. F. Hildebrand and R. J. Weselake (AOCS Press), 75–112.

Millar, A. A., Smith, M. A., and Kunst, L. (2000). All fatty acids are not equal: discrimination in plant membrane lipids. *Trends Plant Sci.* 5, 95–101. doi: 10.1016/S1360-1385(00)01566-1

Moon, H., Smith, M. A., and Kunst, L. (2001). A condensing enzyme from the seeds of *Lesquerella fendleri* that specifically elongates hydroxy fatty acids. *Plant Physiol.* 127, 1635–1643. doi: 10.1104/pp.010544

Mutlu, H., and Meier, M. A. R. (2010). Castor oil as a renewable resource for the chemical industry. *Eur. J. Lipid Sci. Technol.* 112, 10–30. doi: 10.1002/ejlt.200900138

Ohlrogge, J., Thrower, N., Mhaske, V., Stymne, S., Baxter, M., Yang, W., et al. (2018). PlantFAdb: a resource for exploring hundreds of plant fatty acid structures synthesized by thousands of plants and their phylogenetic relationships. *Plant J.* 96, 1299–1308. doi: 10.1111/tpj.14102

Patel, V. R., Dumancas, G. G., Kasi Viswanath, L. C., Maples, R., and Subong, B. J. J. (2016). Castor oil: properties, uses, and optimization of processing parameters in commercial production. *Lipid Insights* 9, 1–12. doi: 10.4137/LPI.S40233

Pyc, M., Cai, Y., Greer, M. S., Yurchenko, O., Chapman, K. D., Dyer, J. M., et al. (2017). Turning Over a new leaf in lipid droplet biology. *Trends Plant Sci.* 22, 596–609. doi: 10.1016/j.tplants.2017.03.012

Reed, D. W., Taylor, D. C., and Covello, P. S. (1997). Metabolism of hydroxy fatty acids in developing seeds in the genera *Lesquerella* (Brassicaceae) and *Linum* (Linaceae). *Plant Physiol.* 114, 63–68. doi: 10.1104/pp.114.1.63

Shimada, T. L., Hayashi, M., and Hara-Nishimura, I. (2017). Membrane dynamics and multiple functions of oil bodies in seeds and leaves. *Plant Physiol.* 176, 199–207. doi: 10.1104/pp.17.01522

Shockey, J., Lager, I., Stymne, S., Kotapati, H. K., Sheffield, J., Mason, C. et al. (2019). Specialized lysophosphatidic acid acyltransferases contribute to unusual fatty acid accumulation in exotic Euphorbiaceae seed oils. *Planta* 249, 1285–1299. doi: 10.1007/s00425-018-03086-y

Shockey, J., Mason, C., Gilbert, M., Cao, H., Li, X., Cahoon, E., et al. (2015). Development and analysis of a highly flexible multi-gene expression system for metabolic engineering in Arabidopsis seeds and other plant tissues. *Plant Mol. Biol.* 89, 113–126. doi: 10.1007/s11103-015-0355-5

Theodoulou, F. L., and Eastmond, P. J. (2012). Seed storage oil catabolism: a story of give and take. *Curr. Opin. Plant Biol.* 15, 322–328. doi: 10.1016/j.pbi.2012.03.017

Troncoso-Ponce, M. A., Cao, X., Yang, Z., and Ohlrogge, J. B. (2013). Lipid turnover during senescence. *Plant Sci.* 205-206, 13–19. doi: 10.1016/j.plantsci.2013.01.004

Vandeloo, F. J., Broun, P., Turner, S., and Somerville, C. (1995). An oleate 12-hydroxylase from *Ricinus communis* L. is a fatty acyl desaturase homolog. *Proc. Natl. Acad. Sci. U. S. A.* 92, 6743–6747. doi: 10.1073/pnas.92.15.6743

Van Erp, H., Kelly, A. A., Menard, G., and Eastmond, P. J. (2014). Multigene engineering of triacylglycerol metabolism boosts seed oil content in Arabidopsis. *Plant Physiol.* 165, 30–36. doi: 10.1104/pp.114.236430

Von Mark, V. C., and Dierig, D. A. (2015). "Germplasm improvement to develop commercially viable lines of the new oilseed crop Lesquerella," in *Industrial Crops* (Springer), 315–334.

Wang, K., Durrett, T. P., and Benning, C. (2019). Functional diversity of glycerolipid acylhydrolases in plant metabolism and physiology. *Prog. Lipid Res.* 75:100987. doi: 10.1016/j.plipres.2019.100987

Weiss, S. B., Kennedy, E. P., and Kiyasu, J. Y. (1960). Enzymatic synthesis of triglycerides. *J. Biol. Chem.* 235, 40–44. doi: 10.1016/S0021-9258(18)69581-X

Yang, W., Wang, G., Li, J., Bates, P. D., Wang, X., and Allen, D. K. (2017). Phospholipase Dzeta enhances Diacylglycerol flux into triacylglycerol. *Plant Physiol.* 174, 110–123. doi: 10.1104/pp.17.00026

Conflict of Interest: The authors declare that the research was conducted in the absence of any commercial or financial relationships that could be construed as a potential conflict of interest.

Publisher's Note: All claims expressed in this article are solely those of the authors and do not necessarily represent those of their affiliated organizations, or those of the publisher, the editors and the reviewers. Any product that may be evaluated in this article, or claim that may be made by its manufacturer, is not guaranteed or endorsed by the publisher.

frontiers | Frontiers in Plant Science

ORIGINAL RESEARCH
published: 20 June 2022
doi: 10.3389/fpls.2022.909759

Comparative *de novo* Transcriptome Analysis of Two Cultivars With Contrasting Content of Oil and Fatty Acids During Kernel Development in *Torreya grandis*

Chi Zhang[1,2,3†], Haokai Liu[4†], Hui Zhang[5], Wanyu Dang[1], Caihong Zhou[1] and Min Zhang[1]*

[1] State Key Laboratory of Subtropical Silviculture, Zhejiang A & F University, Hangzhou, China, [2] Collaborative Innovation Center for Efficient and Green Production of Agriculture in Mountainous Areas of Zhejiang Province, College of Horticulture Science, Zhejiang A & F University, Hangzhou, China, [3] Key Laboratory of Quality and Safety Control for Subtropical Fruit and Vegetable, Ministry of Agriculture and Rural Affairs, College of Horticulture Science, Zhejiang A & F University, Hangzhou, China, [4] Jingning Natural Resources and Planning Bureau, Lishui, China, [5] Jingning Ecological Forestry Development Center, Lishui, China

OPEN ACCESS

Edited by:
Dongdong Li,
Hainan University, China

Reviewed by:
Qingqin Cao,
Beijing University of Agriculture, China
Xiaoming Pang,
Beijing Forestry University, China

***Correspondence:**
Min Zhang
mzhang@zafu.edu.cn

[†] These authors have contributed equally to this work

Specialty section:
This article was submitted to Crop and Product Physiology, a section of the journal Frontiers in Plant Science

Received: *31 March 2022*
Accepted: *26 April 2022*
Published: *20 June 2022*

Citation:
Zhang C, Liu H, Zhang H, Dang W, Zhou C and Zhang M (2022) Comparative de novo Transcriptome Analysis of Two Cultivars With Contrasting Content of Oil and Fatty Acids During Kernel Development in Torreya grandis. Front. Plant Sci. 13:909759. doi: 10.3389/fpls.2022.909759

Vegetable oil is an indispensable nutritional resource for human health and mainly characterized by the composition and content of fatty acids (FAs). As a commercial species of gymnosperm, *Torreya grandis* produces oil-rich nuts with high unsaturated fatty acids content in the mature kernels. In this study, two cultivars, *T. grandis* 'Xifei' and *T. grandis* 'Dielsii,' with distinct oil content were employed to compare the profiles of FAs accumulation during kernel development. The accumulation rate of oil content was significantly different between 'Xifei' and 'Dielsii.' Besides, the final oil content of 'Xifei' (52.87%) was significantly higher than that of 'Dielsii' (41.62%) at maturity. The significant differences in main FAs were observed at almost each kernel development stages between the two cultivars. $C_{16:0}$, $C_{18:1}$, and $C_{20:3}$ FA exhibited different accumulation patterns between cultivars. The content and the initiation of accumulation of $C_{20:3}$ FA were different between the two cultivars. To explore the molecular mechanism associated with different content of oil and FAs between two cultivars, *de novo* transcriptome of kernels was compared between 'Xifei' (high oil) and 'Dielsii' (low oil) at three stages of oil accumulation, respectively. Totally 142,213 unigenes were assembled and 16,379 unigenes with a length of over 1,000 nt were successfully annotated, including 139 unigenes related to FA biosynthesis, elongation, and metabolism. Compared with 'Dielsii,' totally 1,476, 2,140, and 1,145 differentially expressed genes (DEGs) were upregulated in 'Xifei' at the stage of the initiative, the rapid rise, and the stationary oil accumulation, respectively; the number of downregulated DEGs reached 913, 1,245, and 904, respectively. Relative expressions of 11 DEGs involved in FAs biosynthesis and metabolism were confirmed by RT-qPCR. Abundant differentially expressed transcription factors and pathway DEGs were correlated to oil and FAs according to Pearson's correlation analysis between transcriptome and metabolites (oil and FAs), suggesting their contributions to the differential oil and FAs between the two cultivars during kernel development of *T. grandis*. To conclude, our

findings can provide novel insights into the developmental differences in metabolites and *de novo* transcriptome correlated to lipid accumulation and FA synthesis of kernels between cultivars with contrasting oil deposits and demystify the regulatory mechanism of high oil accumulation in *T. grandis*.

Keywords: *Torreya grandis*, comparative *de novo* transcriptome, fatty acid (composition), correlation analysis, oil content, kernel development, cultivars

INTRODUCTION

Vegetable oil is indispensable and consumed in the human diet that requires high-quality edible lipids mainly characterized by the composition and proportion of saturated fatty acids (SFAs) and unsaturated fatty acids (UFAs). In most cases, fatty acids (FAs) have evolved during the *de novo* synthesis, elongation, and desaturation process. Most nature oil from plants frequently contains polyunsaturated fatty acids (PUFAs), which contain a long chain of at least 18 carbon atoms and 1 methylene (Lisa et al., 2007) or polymethylene interrupted double bonds (UPIFAs). Sciadonic acid (SA) is a *cis*5, 11, 14-eicosatrienoic acid (Δ5-UPIFAs) with the first unsaturation site at the fifth carbon atom that differs from the structure of other PUFAs (Endo et al., 2009; Xie et al., 2016). Due to the beneficial function for health such as regulating the blood pressure (Sugano et al., 1994; Asset et al., 1999; Endo et al., 2006), anti-inflammatory (Chuang et al., 2009; Chen et al., 2015), and prophylactic impacts on angiosclerosis and obesity (Meng et al., 2020), the plant oils with a certain amount of Δ5-UPIFAs such as SA are essential for dietary modification of human to stem some chronic illnesses.

Torreya grandis is a gymnosperm species of six members in *Torreya* genus belonging to the Taxaceae family with wide distribution in South China (Shi et al., 2018). *T. grandis* produces nut-seeds with approximately 50% of dry weight (DW) high-quality oils. Due to dioecious flowers, *T. grandis* possesses abundant variation of seedlings, from which a considerable number of landraces and cultivars were developed and identified with distinct SSR fingerprints (Chen et al., 2020a,b; Meng et al., 2020; Zhang et al., 2021). The commercial value of the rare conifer tree derives mainly from the oil-rich nuts with high UFA content in the mature kernels (Ni et al., 2015; Chen and Jin, 2019a). Great variation in seeds phenotype and qualities of mature nuts exist extensively between cultivars in *T. grandis* (Ni and Shi, 2014; Chen and Jin, 2019b). The oil content of *T. grandis* kernels was reported to range from 51.52 to 55.64% depending on the certain cultivar applied in the test (Ni and Shi, 2014). The content of FAs in mature kernels was significantly different between landraces or cultivars in *T. grandis* (Shi et al., 2018). Oleic ($C_{18:1}$) and linoleic acids ($C_{18:2}$) were dominant FAs in mature kernels based on 10 landraces of *T. grandis*, ranging from 17.62 to 35.11% and 39.77 to 46.06% of total FAs, respectively. The beneficial SA ranged from 9.18 to 18.15% of the total FAs in tested *T. grandis* oil. The difference in the oil content and FA composition influences the flavor of nuts in *T. grandis*.

Underlying the final difference of oil deposition is a complex transcriptional network. Genes that encode enzymes related to *de novo* lipid synthesis pathways, including acetyl-CoA carboxylase, ketoacyl-ACP synthases (KAS), stearoyl-ACP desaturase, acyl-ACP thioesterases (FATA and FATB), and acyl-CoA synthesis (LACS) are characterized and cloned in oil crops such as *Arabidopsis*, *Brassica napus*, and *Zea mays*. In addition, acyltransferases like glycerol-3-phosphate acyltransferase (GPAT), lysophosphatidic acid acyltransferase (LPAT), diacylglycerol acyltransferase (DGAT), or phospholipid: diacylglycerol acyltransferase are responsible for assembly of triacylglycerol (TAG). The oil content could be raised in LPAT overexpression transgenic *Arabidopsis* and *B. napus* (Rao and Hildebrand, 2009). Research showed that DGAT was dominantly responsible for TAG accumulation (Shiu-Cheung and Weselake, 2006; Meng et al., 2009), oil, and oleic acid content (Zheng et al., 2008). Although these pathway genes contributed directly to the distinct biosynthesis of lipids between species and cultivars, little was known about the profiles of regulation of their expression.

The further identification of the transcription factors (TFs) such as *LEAFY COTYLEDON1* (*LEC1*), *WRINKLED1* (*WRI*1), *FUSCA3* (*FUS3*), APETALA2 (AP2)/ETHYLENE RESPONSE FACTOR family, and *ABSCISIC ACID3* (*ABI3*) promote a deeper understanding of oil synthesis during seed development. These TFs were well known in seed storage reserve of nutrients such as lipids, protein, and starch, exhibiting distinct timing patterns, and differentiation of responsibilities that trigger the oil pathway genes (Ruuska et al., 2002). *WRI1* was reported to activate oil accumulation by facilitating the carbon flux by glycolysis (Focks and Benning, 1998; Cernac and Benning, 2004). A homeobox TF GLABRA2 was discovered to prevent the accumulation of seed oil in *Arabidopsis* (Shen et al., 2006). *ABI3*, *AtbZIP10*, and *AtbZIP25* were found for the activation of transcription of storage protein (Lara et al., 2003). In an attempt at developmental control of storage product accumulation, *LEC1* and *LEC2* were found expressed early in transgenic Arabidopsis and subsequently induced *FUS3*, *ABI3,* and *ABI5* expression (Wang et al., 2007), indicating an upstream role of regulation on *FUS3* in oil deposition aided by related increase of FUS3 transcripts and transcripts of enzyme genes involved in oil syntheses during seed development.

Recently, a few studies reported differences in FA composition between landraces and amounts of differentially expressed genes (DEGs) between fruits and vegetable samples (leaf, root, and stem; Wu et al., 2018; Ding et al., 2020), indicating a final profile that coordinates oil deposition at mature kernels in *T. grandis*. Although profiles of oil and FAs are clear at mature kernels, little information is available on dynamic patterns and molecular mechanisms leading to a final difference of oil and FAs with kernel development between cultivars in *T. grandis*.

Torreya grandis 'Xifei' is a representative cultivar with high oil content and is applied extensively in main producing areas for long periods (He et al., 2016), while *T. grandis* 'Dielsii' is well known for rootstock in the propagation of *T. grandis*. A significant difference in oil accumulation was observed in mature kernels between the two cultivars in practice. Due to the large and high heterozygous genome of gymnosperm, a complete genome sequence of *T. grandis* has not been reported up to now. In this study, integrative strategies of lipid measurement and *de novo* transcriptome were employed to compare and understand the dynamic variation of oil and FA biosynthesis and underlying molecular mechanism during kernel development between *T. grandis* 'Xifei' and *T. grandis* 'Dielsii.'

MATERIALS AND METHODS

Samples Collection

Nut seeds with different developmental stages were collected from three individual adult trees of 'Xifei' and 'Dielsii,' respectively. Sampling was performed on the 408, 426, 438, 448, 458, 468, 475, 485, 498, 510, and 521 day after pollination (DAP). Nut seeds were harvested and immediately preserved at −80°C before RNA preparation, and the corresponding samples for lipid extraction were stored at −20°C in darkness until needed.

Lipid Extraction and Determine

Frozen-dried powders were individually incubated in petroleum ether at 50°C for 8 h to extract the lipids of kernels harvested with development of the two cultivars. The oil content was shown as a percent of sample DW. The fatty acid composition of the lipid sample was measured by gas chromatography (Waters H-class UPLC, Agilent Technologies, United States) as described in Wolff et al. (1999a) based on a 37-kinds of fatty acid methyl ester standard mixture. The relative content of FA composition was individually determined by the retention time of the FA-methyl ester standard.

Transcriptome Assembly and Functional Annotation

High-quality RNAs derived from different developmental kernels was prepared and then sequenced on the Illumina HiSeq2500 platform to generate raw reads with reads length of PE125. Following the removal of reads with the adaptor, reads with more than 10% poly-N, and low-quality reads [>50% with Phred quality score (Q) _5 bases] from the raw sequencing data according to in-house Perl scripts (Biomarker Biological Information Technology Co., Ltd., Beijing, China), high-quality clean data were acquired and assembled by Trinity software, in which min_kmer_cov was set 2 and the other parameters are set to default (Grabherr et al., 2011). Briefly, clean reads were assembled into contigs by the de Bruijn graph using k-mer 25 after trials in varying k-mer sizes. Then, mapping of the reads to contigs containing paired-end reads was made to examine contigs of the same transcript and calculate the distance of these contigs. Eventually, the contigs were connected to obtain assembled transcripts unable to be extended on both end. The longest transcripts were considered the unigenes of gene functional annotation.

Gene function annotation was made on the basis of public protein databases: Nr (NCBI non-redundant protein sequences); Nt (NCBI non-redundant nucleotide sequences); KOG (clusters of orthologous groups of proteins); and Swiss-Prot (a protein sequence database with manual annotation and review) with NCBI blast 2.2.28 + with *e*-value 1.0e-5; Pfam (Protein family) *via* HMMER 3.0 package using *e*-value 0.01as well as KO (KEGG Ortholog database) with KEGG Automatic Annotation Server using *e*-value 1.0e-10. According to the annotation for Nr and Pfam databases, the assignment of unigenes was made in Gene Ontology (GO) with Blast2GO 2.5 (Conesa and Gotz, 2008) using *e*-value 1.0e-6. GO classification was distributed with the Web Gene Ontology Annotation Plot, which included biological process, molecular function, and cellular component.

The calculation method of the fragments per kilobase per million fragments (FPKM) was employed to determine the transcript abundance of each gene (Mortazavi et al., 2008). The DEGs between compared groups were evaluated with the threshold of FC (fold change) >2 and FDR (false discovery rate) <0.01 (Benjamini et al., 2001).

Reverse Transcript Quantitative PCR

Total RNA was individually extracted from kernels of two cultivars sampled at 408, 438, 458, 475, 510, and 521 DAP with a modified method of RNAiso Plus (Takara Bio Inc, Japan), respectively. The cDNA template of each sample for reverse transcription quantitative PCR (qRT-PCR) was prepared by EasyScript One-Step gDNA removal and cDNA synthesis supermix (TRANSGEN). Pathway genes and TFs involved in FA metabolism were chosen for validation using qRT-PCR. Specific primers of qRT-PCR were obtained with Primer Quest[1] based on the assembly sequences in the transcriptome. The *Actin* gene was used as reference gene, and the primer sequences were described in the **Supplementary Table 9**. SYBR Premix Ex Taq^{TM}II (Takara) was employed in qRT-PCR with 20 μl volumes on the Roche Light Cycler480 system (Roche Diagnostics, CA, United States). All samples were tested in triplicate. Each reaction was conducted as below: 95°C for 30 s, followed by 40 cycles at 95°C for 5 s, and 60°C for 34 s.

Statistical Analysis

The determinations of metabolites were performed thrice and error bars in presented figures stand for SD. Statistical analysis was performed with SPSS 20.0. Data comparison was made with one-way analysis of variance (ANOVA), and differences among tested metabolites of two cultivars were evaluated with Duncan's multiple-range tests at $p < 0.05$. Pearson correlation coefficient (r) was calculated for correlation analysis on DEGs and metabolites.

[1]https://www.genscript.com/ssl-bin/app/primer

RESULTS

Dynamic Changes in the Oil Content and Fatty Acids Composition Between *T. grandis* 'Xifei' and *T. grandis* 'Dielsii' During Kernel Development

Concerning 17 months for ripening duration in kernels, nut-fruits derived from *T. grandis* 'Xifei' and *T. grandis* 'Dielsii', respectively, were sampled from 408 to 521 DAP (**Figure 1A**) to characterize the temporal variation of the oil content and FA composition during kernel development. Generally, the oil content was raised gradually with kernel development (**Figure 1B** and **Supplementary Table 1**). During the initiation phase, no difference in the oil content was observed and the curve line of the oil content almost overlapped from 408 to 438 DAP between the two cultivars. A wider gap occurred in the subsequent 10 days, and a significant difference in the oil content was observed at 448 DAP. Then, the oil content in 'Xifei' raised more rapidly and exceeded that in 'Dielsii.'

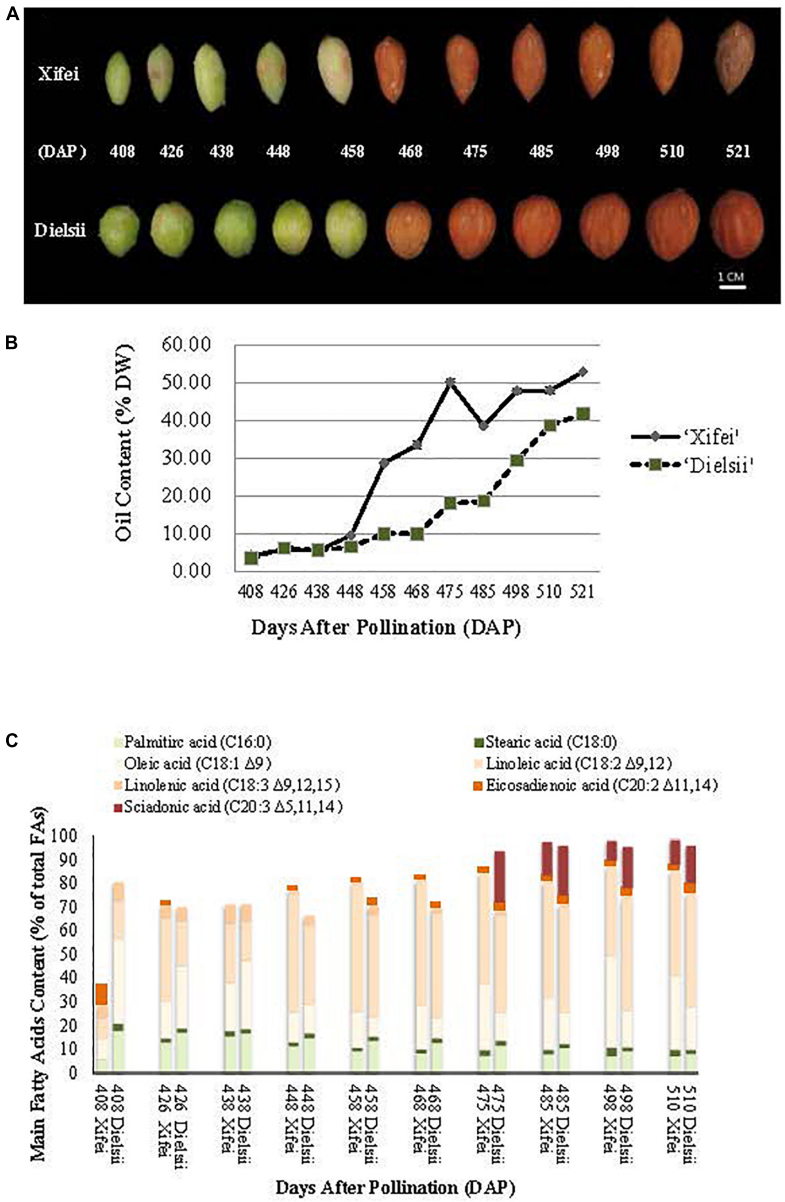

FIGURE 1 | Developing nut-seeds, the content of oil, and FAs in *Torreya grandis* 'Xifei' and *T. grandis* 'Dielsii,' respectively. DAP, day after pollination. **(A)** Developing nut-seeds of two cultivars at each sampling time. **(B)** Oil content of 'Xifei' (black dots) and 'Dielsii' (white dots) at each sampling time, respectively. Values of oil content were expressed as the percentage of dry weight (%DW) of kernels. **(C)** The content of FA composition in 'Xifei' and 'Dielsii' at each sampling time was presented as a percentage of total FAs (%), respectively.

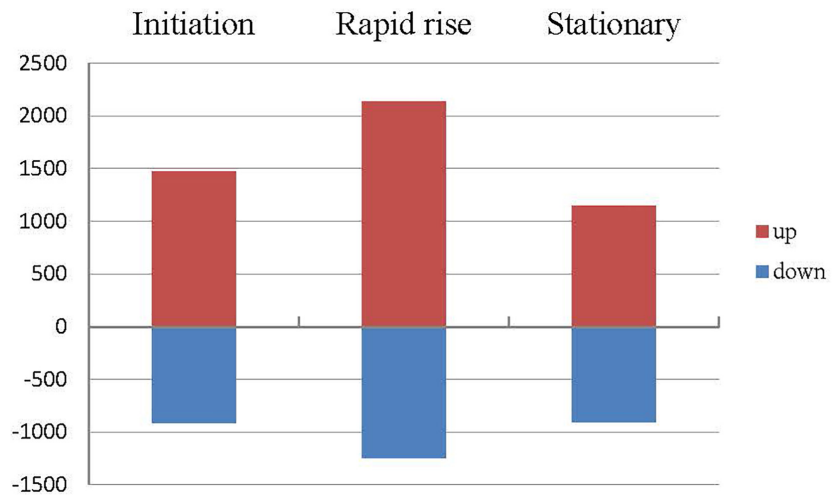

FIGURE 2 | Differentially expressed genes (DEGs) related to fatty acids metabolism between 'Xifei' and 'Dielsii' at initiation, rapid rise and stationary stage of kernel development, respectively.

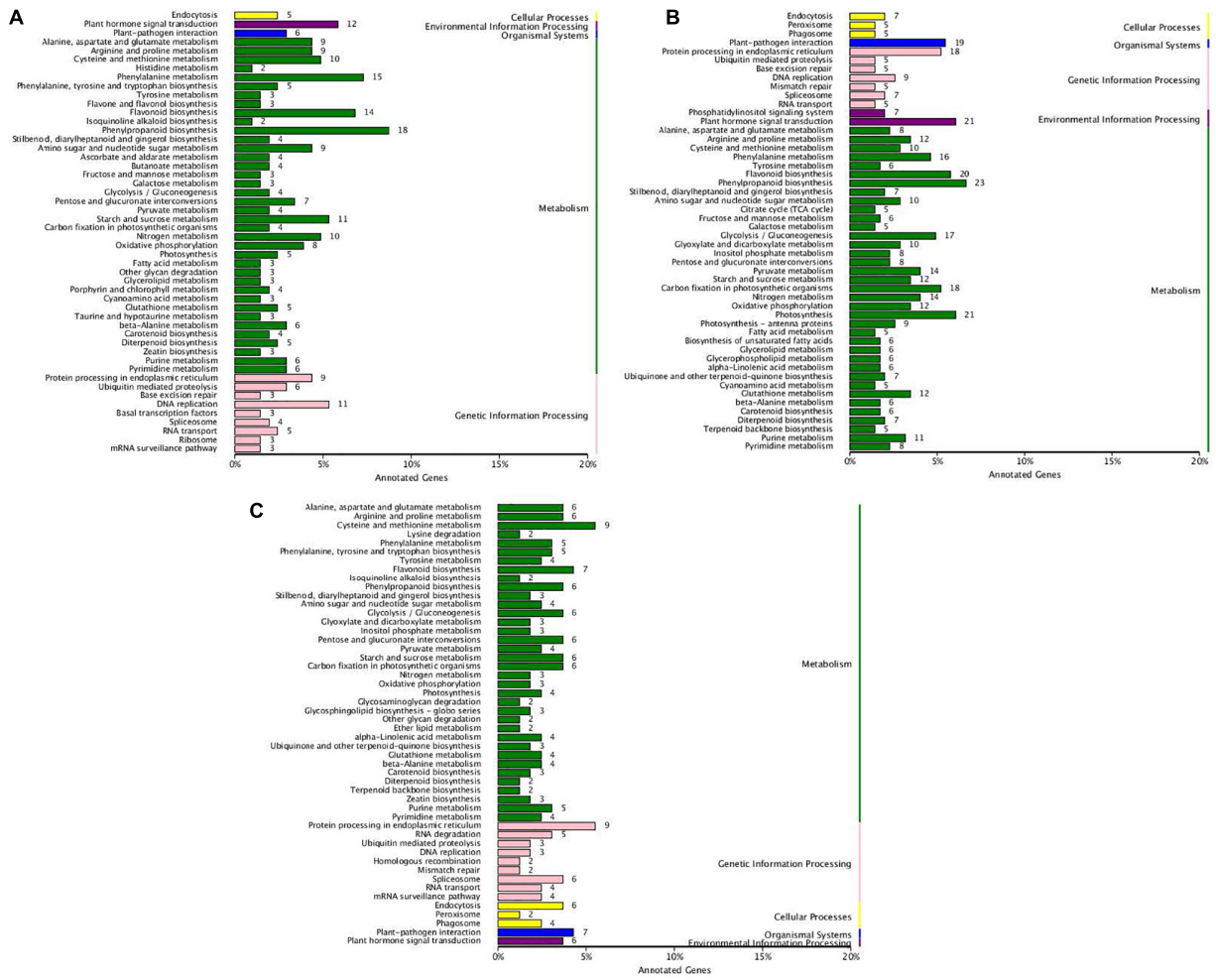

FIGURE 3 | KEGG enrichment of DEGs between *T. grandis* 'Xifei' and *T. grandis* 'Dielsii' at the development of the initiative **(A)**, rapid rise **(B)**, and stationary **(C)** oil accumulation.

TABLE 1 | DEGs involved in pathways related to fatty acid biosynthesis and metabolism between *T. grandis* 'Xifei' and *T. grandis* 'Dielsii'.

KEGG pathway	Swissprot_ annotation	Initial stage			Rapid rise			Stationary		
		FDR	log2FC	Regulated	FDR	log2FC	Regulated	FDR	log2FC	Regulated
Biosynthesis of unsaturated fatty acids (6)										
c99245.graph_c0	Protein ODORANT1 (ODO1)	0.002124202	–1.71072342	Down	–	–	–	–	–	–
c90340.graph_c0	Transcription factor RAX2	3.76E-08	–1.1885191	Down	–	–	–	–	–	–
c92934.graph_c0	Transcription factor MYB86	4.36E-08	–2.40718869	Down	–	–	–	–	–	–
c94730.graph_c1	Nuclear transcription factor Y subunit C-1	0.006910842	–1.21805909	Down	–	–	–	–	–	–
c85671.graph_c0	–	0.000918138	1.44437094	Up	0.003367907	1.853099391	Up	1.86E-05	2.28933565	Up
c98417.graph_c0	NADPH–cytochrome P450 reductase	–	–	–	0.002346744	5.974724421	Up	–	–	–
Fatty acid biosynthesis (2)										
c98678.graph_c0	–	–	–	–	–	–	–	3.49E-05	–1.20285232	Down
c99245.graph_c0	GRAS family transcription factor	–	–	–	0.000103453	3.378469799	Up	–	–	–
Fatty acid metabolism (8)										
c43899.graph_c0	–	1.98E-06	–2.89845052	Down	–	–	–	–	–	–
c101043.graph_c0	26S protease regulatory subunit 6B homolog	–	–	–	2.44E-13	2.426790509	Up	–	–	–
c91980.graph_c0	–	–	–	–	–	–	–	0.005208433	–1.21416289	Down
c94509.graph_c0	–	–	–	–	2.48E-05	1.337339018	Up	–	–	–
c89303.graph_c0	F-box/kelch-repeat protein At5g43190	–	–	–	9.65E-20	–1.97495432	Down	–	–	–
c90340.graph_c0	MAR-binding filament-like protein 1 (MFP1)	–	–	–	1.52E-11	–1.31606418	Down	–	–	–
c99307.graph_c0	Probable WRKY transcription factor 11 (WRKY11)	0.00384533	1.57568211	Up	–	–	–	–	–	–
c81605.graph_c0	(R,S)-reticuline 7-O-methyltransferase (PSOMT1)	0.001091065	2.283869688	Up	2.61E-13	4.464544002	Up	–	–	–
Glycerolipid metabolism (7)										
c69013.graph_c0	Diacylglycerol O-acyltransferase 1-like	–	–	–	0.000733551	–1.89319743	Down	–	–	–
c101495.graph_c0	UDP-sulfoquinovose synthase, chloroplastic	5.55E-07	–2.71208322	Down	–	–	–	–	–	–
c72149.graph_c0	Alpha-galactosidase	–	–	–	1.15E-12	1.452865054	Up	6.99E-05	1.075970917	Up
c80383.graph_c0	–	–	–	–	0.001237479	1.285968585	Up	–	–	–
c89559.graph_c0	Hypothetical protein AMTR	–	–	–	1.95E-06	–1.08251029	Down	–	–	–
c81605.graph_c0	Aldehyde dehydrogenase family 3 member F1	0.001091065	2.283869688	Up	2.61E-13	4.464544002	Up	–	–	–
c92777.graph_c0	–	3.24E-05	1.342914101	Up	4.48E-15	1.610510221	Up	–	–	–
Glycerophospholipid metabolism (7)										
c102929.graph_c0	Hypothetical protein AMTR	–	–	–	1.03E-08	Inf	Up	–	–	–
c89559.graph_c0	Hypothetical protein AMTR	–	–	–	1.95E-06	–1.08251029	Down	–	–	–
c86728.graph_c0	Non-specific phospholipase C2	–	–	–	–	–	–	6.54E-06	1.724029337	Up
c92777.graph_c0	–	3.24E-05	1.342914101	Up	4.48E-15	1.610510221	Up	–	–	–
c101355.graph_c0	–	–	–	–	2.95E-14	1.46223635	Up	5.36E-08	1.695178981	Up
c91802.graph_c0	Non-specific phospholipase C6	–	–	–	2.30E-11	–1.4210226	Down	–	–	–
c91903.graph_c0	Phospholipase D	–	–	–	0.00147208	1.307370985	Up	–	–	–

When the fruits get mature at 521 DAP, the oil content is distinct between 'Xifei' and 'Dielsii,' reaching 52.87 ± 0.19% and 41.62 ± 0.23%, respectively. To summarize, the oil content of 'Xifei' was raised more rapidly and higher than that of 'Dielsii' during kernel development, suggesting a differentially regulatory mechanism underlying the phenotype of oil between two cultivars of *T. grandis*.

Meanwhile, FA composition and content of 'Xifei' and 'Dielsii' were measured and compared during the whole development of kernels (**Figure 1C** and **Supplementary Table 2**). Generally, palmitic acid ($C_{16:0}$) was the dominant SFA in both 'Xifei' and 'Dielsii.' $C_{16:0}$ FA of 'Xifei' fell down after a transitory rise before 438 DAP, while $C_{16:0}$ FA of 'Dielsii' kept plummeting during the whole development of kernels. $C_{16:0}$ FA of 'Xifei' was significantly less than that of 'Dielsii' at each stage of kernel development. $C_{18:0}$ FA of two cultivars was less than 4% during the whole development. UFAs recognized and studied by the current research included oleic acid ($C_{18:1}$), linoleic acid ($C_{18:2\Delta9,12}$ and $C_{18:3\Delta9,12,15}$), eicosadienoic acid ($C_{20:2\Delta11,14}$), and SA ($C_{20:3\Delta5,11,14}$). In general, dominant UFA was $C_{18:2\Delta9,12}$, $C_{18:1}$, and $C_{20:3\Delta5,11,14}$ in both cultivars, and total main UFAs were raised with kernel growing. Besides, the content of UFAs in 'Xifei' surpassed that in 'Dielsii' at almost all stages of kernel development and reached 88.27% significantly higher than that in 'Dielsii' (85.88%) at maturation. Among three main UFAs, $C_{18:2}$ accounted for the majority of UFA in both cultivars, and the significant differences in $C_{18:2}$ content were observed between cultivars at each developmental phase, which ranged from 16.69 ± 2.65% to 47.69 ± 0.7% and 9.10 ± 0.02% to 43.91 ± 0.15% in 'Dielsii' and 'Xifei' during kernel development, respectively. $C_{18:1}$ is the secondary UFA. The content of $C_{18:1}$ in 'Dielsii' was significantly exceeded that in 'Xifei' during the initiation phase. However, $C_{18:1}$ FA of 'Xifei' surpassed that of 'Dielsii' in the subsequent development of kernels. UFAs with 20 carbon atoms mainly include $C_{20:2\Delta11,14}$ and $C_{20:3\Delta5,11,14}$ in this study. $C_{20:2\Delta11,14}$ FA contributed approximately 2% in 'Xifei' and 2–4% in 'Dielsii' to total FAs during the maturation of kernels. $C_{20:3\Delta5,11,14}$ FA accounted for 8–14.16% and 2.17–21.76% of total FAs in 'Xifei' and 'Dielsii.' $C_{20:2\ \Delta11,14}$ had been accumulated almost from the initiation phase, whereas $C_{20:3\Delta5,11,14}$ was not detected until 475 and 485 DAP in 'Dielsii' and 'Xifei,' respectively. When the kernels developed into maturation, the content of $C_{20:3\Delta5,11,14}$ FA reached 15.76 ± 0.28% in 'Dielsii' and 10.56 ± 0.08% in 'Xifei.' In conclusion, a significant difference was obtained in $C_{16:0}$, $C_{18:1}$, and $C_{20:3\Delta5,11,14}$ FA between two cultivars during kernel development.

De novo Assembly Sequencing and Annotations

To decipher the molecular mechanism responsible for the difference of oil and FAs between 'Xifei' and 'Dielsii' during kernel development, comparative transcriptome analysis was further performed between two cultivars at 438 DAP (initiation), 475 DAP (rapid rise), and 510 DAP (stationary) in accordance with distinct oil content in lipid measurement, respectively. Over 6.0 Gb of clean data were obtained and Q30 is more than 90% in each sample (**Supplementary Table 3**). The *de novo* transcriptome assembly was conducted to obtain 142,213 non-redundant unigenes and 22,976 unigenes with over 1 kb in length (**Supplementary Figure 1**). Annotation of unigenes was carried out based on the best-matched known sequences. The

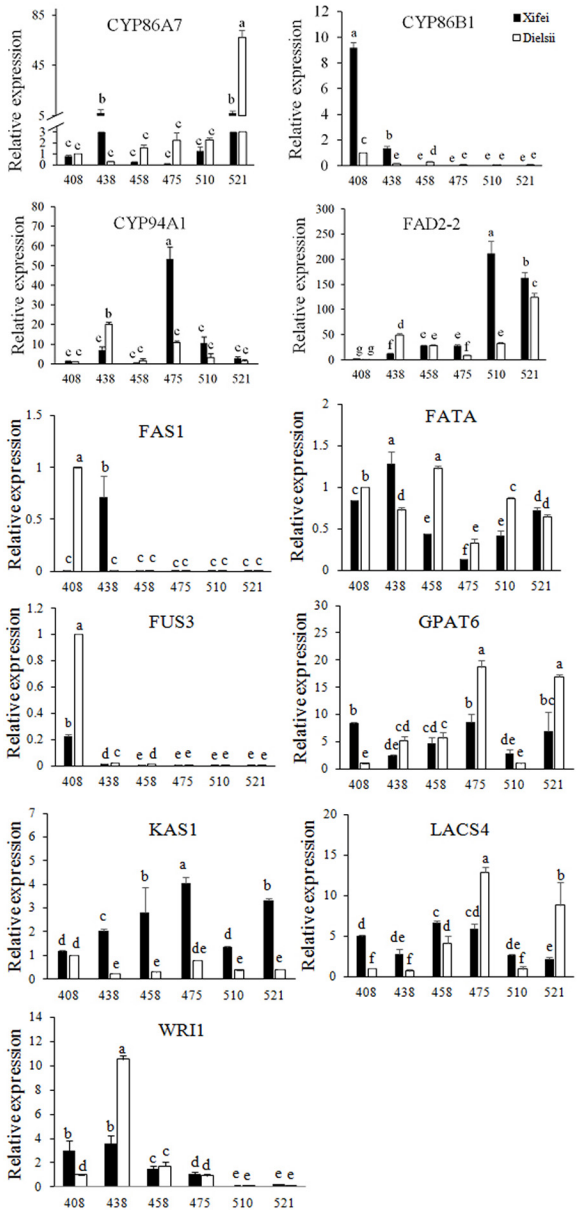

FIGURE 4 | RT-qPCR of 11 DEGs related to fatty acid biosynthesis and metabolism measured during development. Relative expression of DEGs was shown with means of triplicates. Samples were collected at 408, 438, 458, 475, 510, and 521 days after pollination (DAP). The dark square represents *T. grandis* 'Xifei.' White square represents *T. grandis* 'Dielsii.' The significant difference of the DEG expression between development stages were labelled with a to g according to Duncan's multiple comparison test ($P < 0.05$).

TABLE 2 | Differentially expressed transcription factors (DETFs) between cultivars and their correlation to metabolites.

Cultivar	Gene ID	Annotation	Metabolites	Cor_r	*p*-value
T. grandis 'Xifei'	c99504.graph_c0	WRKY45	Oil content of kernels(%)	–0.99997	0.00482
	c99963.graph_c0	ERF017	Oil content of kernels(%)	–0.99996	0.00599
	c99588.graph_c0	ERFABR1	SFA	–0.99991	0.00841
	c99428.graph_c0	GATA22	Palmitirc acid (C16:0)	0.99990	0.00905
	c99573.graph_c0	ERF018	Palmitirc acid (C16:0)	0.99999	0.00255
	c99605.graph_c0	GATA2	Palmitirc acid (C16:0)	0.99995	0.00667
	c99682.graph_c0	PLATZ	Palmitirc acid (C16:0)	0.99997	0.00508
	c99972.graph_c0	MADS6	Palmitirc acid (C16:0)	0.99993	0.00760
	c99390.graph_c0	MYB (APL)	Stearic acid (C18:0)	0.99989	0.00937
	c99250.graph_c0	ARF31	UFA	–0.99988	0.00992
	c99458.graph_c0	bHLH66	UFA	0.99999	0.00291
	c99731.graph_c0	PLATZ	UFA	–0.99999	0.00321
	c99816.graph_c0	MYB (GTL1)	UFA	–0.99997	0.00525
	c99957.graph_c1	MYB23	UFA	–0.99998	0.00415
	c99494.graph_c0	ERF1A	Oleic acid (C18:1 Δ9)	0.99999	0.00263
	c99828.graph_c0	MYB (GTL1)	Oleic acid (C18:1 Δ9)	1.00000	0.00154
	c99904.graph_c0	ERF003	Oleic acid (C18:1 Δ9)	0.99991	0.00860
	c99241.graph_c0	WOX9	Linolenic acid (C18:3 Δ9,12,15)	0.99988	0.00993
	c99472.graph_c0	bHLH95	Linolenic acid (C18:3 Δ9,12,15)	0.99998	0.00450
	c99635.graph_c0	ICE1	Linolenic acid (C18:3 Δ9,12,15)	0.99999	0.00317
	c99772.graph_c0	UVR8	Linolenic acid (C18:3 Δ9,12,15)	0.99993	0.00754
	c99276.graph_c0	MYB	Sciadonic acid (C20:3 Δ5,11,14)	0.99991	0.00866
	c99348.graph_c0	MYB (GTL1)	Sciadonic acid (C20:3 Δ5,11,14)	0.99998	0.00413
	c99613.graph_c0	FUS3	Sciadonic acid (C20:3 Δ5,11,14)	–0.99993	0.00766
T. grandis 'Dielsii'	c99573.graph_c0	ERF018	Palmitirc acid (C16:0)	0.99994	0.00688
	c99891.graph_c0	ODORANT1	Palmitirc acid (C16:0)	–0.99989	0.00935
	c99372.graph_c0	bHLH49	Stearic acid (C18:0)	1.00000	0.00185
	c99580.graph_c2	bHLH118	Stearic acid (C18:0)	–1.00000	0.00152
	c99587.graph_c0	bHLH30	Stearic acid (C18:0)	0.99988	0.00997
	c99651.graph_c0	ERF3	Stearic acid (C18:0)	0.99991	0.00865
	c99731.graph_c0	PLATZ	Stearic acid (C18:0)	1.00000	0.00196
	c99427.graph_c0	FAMA	UFA	–0.99998	0.00439
	c99667.graph_c0	ERF RAP2-3	UFA	–0.99995	0.00645
	c99615.graph_c0	DIVARICATA	Linoleic acid (C18:2 Δ9,12)	–0.99988	0.00987
	c99676.graph_c0	ERF3	Linoleic acid (C18:2 Δ9,12)	–0.99989	0.00960
	c99682.graph_c0	PLATZ	Linoleic acid (C18:2 Δ9,12)	–0.99994	0.00669
	c99757.graph_c0	IIB	Linoleic acid (C18:2 Δ9,12)	0.99990	0.00907
	c99961.graph_c0	ILI6	Linolenic acid (C18:3 Δ9,12,15)	0.99999	0.00273
	c99412.graph_c0	bHLH110	Sciadonic acid (C20:3 Δ5,11,14)	–1.00000	0.00001
	c99452.graph_c0	GATA5	Sciadonic acid (C20:3 Δ5,11,14)	–1.00000	0.00013
	c99475.graph_c0	ERF RAP2-3	Sciadonic acid (C20:3 Δ5,11,14)	0.99988	0.009995
	c99584.graph_c0	bHLH74	Sciadonic acid (C20:3 Δ5,11,14)	–0.99990	0.00921
	c99602.graph_c0	bHLH93	Sciadonic acid (C20:3 Δ5,11,14)	–0.99994	0.00679
	c99746.graph_c2	BRX	Sciadonic acid (C20:3 Δ5,11,14)	–0.99995	0.00621
	c99982.graph_c0	HY5	Sciadonic acid (C20:3 Δ5,11,14)	–1.00000	0.00065

best-matched species of the unigenes in *T. grandis* successively included *Picea sitchensis* (22%), *Amborella trichopoda* (7%), *Nelumbo nucifera* (6%), *Vitis vinifera* (5%), and *Prunus persica* (3%; **Supplementary Figure 2A**).

Functional classification was carried out to better understand the unigenes on biological function and interaction in development. A total of 6,485 unigenes were allocated to 119 pathways, and 139 unigenes were related to fatty acid biosynthesis, elongation, and metabolism pathways. A total of 17,783 unigenes were annotated into 52 subgroups in accordance with GO function terms including biological process, cellular component, and molecular function subgroups (**Supplementary Table 4** and **Supplementary Figure 2B**). The dominating biological processes were metabolic, cellular, and

single-organism processes. The top molecular function was catalytic activity and binding.

Differentially Expressed Genes Involved in Fatty Acid Biosynthesis and Metabolism During Kernel Development Between Two Cultivars

A total of 5,683 DEGs were obtained in comparison between cultivars (**Supplementary Table 5**). Compared to 'Dielsii,' a total of 1,476, 2,140, and 1,145 DEGs were upregulated during the stage of initiation, rapid rise, and the stationary oil accumulation in 'Xifei,' respectively. DEGs with significantly decreased expression sum up to 913, 1,246, and 904 at three stages in 'Xifei,' respectively, (**Figure 2**). Interestingly, a total of 177 differentially expressed transcription factors (DETFs) were captured between cultivars, which contained 13 DETFs involved in three stages, 41 DETFs activated or suppressed at two stages, and 123 DETFs with functions only at one stage of kernel development.

By comparing development stages, DEGs associated with development were 5,933 and 5,406 in 'Xifei' (**Supplementary Table 6**) and 'Dielsii' (**Supplementary Table 7**), respectively. In 'Xifei,' DEGs of upregulation and downregulation were up to 1,236 and 1,769 when the oil content increased rapidly. A total of 714 and 873 DEGs were increased and decreased in expression when oil was steadily stored, respectively. Similarly, in 'Dielsii,' the up- and down-regulated DEGs reached 1,637 and 2,065 when oil accumulated rapidly, while 1,316 and 1,012 DEGs were up and down expressed during the stationary phase of oil accumulation. In addition, more DETFs were found in the comparison between stages of kernel development, which were captured by 213 DETFs in 'Xifei' and 206 DETFs in 'Dielsii.'

KEGG pathway of DEGs was analyzed and the comparison between cultivars was focused on (**Figure 3**). Abundant DEGs between cultivars were dominantly involved in metabolism pathways (**Supplementary Table 8**). DEGs involved in fatty acid metabolism were enriched at both initiation (**Figure 3A**) and rapid rise stage (**Figure 3B**). DEGs involved in the biosynthesis of UFAs were enriched only at the rapid rise stage. More DEGs were found in the rapid rise phase of oil production between cultivars (**Table 1**). Besides, up- or down-streamed pathways of fatty acid biosynthesis, such as glycolysis, pyruvate metabolism, glycerolipid metabolism, and glycerophospholipid metabolism, were specifically enriched in the rapid rise stage when compared between cultivars.

Differentially expressed genes expression related to fatty acid biosynthesis and the metabolism was verified in kernel development (**Figure 4** and **Supplementary Table 9**), which included 3 *CYP* family genes, *FAD2-2*, *FAS1*, *KAS1*, *GPAT6*, *LACS4*, *FUS3*, *WRI1*, and *FATA*. The expression patterns of DEGs were almost consistent with the transcriptome.

Integrative Analyses of Fatty Acid and Transcriptome

To further identify the related DEGs contributing to the oil and FAs differences, the analyses of the Pearson Correlation Coefficient (r) were carried out with the total available 5,683, 5,933, and 5,406 non-redundant DEGs identified from the comparison of cultivars and development in 'Xifei' and 'Dielsii,' respectively, (**Supplementary Tables 5–7**). A total of 922 and 574 DEGs ($p < 0.01$) derived from the comparison of the two cultivars (cultivar-DEGs) were closely associated with the synthesis and metabolism of oil and FAs in 'Xifei' and 'Dielsii,' respectively, (**Supplementary Tables 10,11**). The numbers of cultivar-DEGs correlated to different types of FA were extremely different between cultivars. Totally 24 and 21 correlated DETFs were identified in 'Xifei' and 'Dielsii,' respectively, (**Table 2**), and the expression profile of DETFs was individually correlated to different FAs according to the FPKM value of transcriptome (**Figure 5** and **Supplementary Table 12**). Concerning distinct oil content between cultivars, WRKY45 (c99504.graph.c0, $r = -0.99997$, and $p = 0.00482$) and ERF017 (c99963.graph_c0, $r = -0.99996$, and $p = 0.00599$) were involved in oil content of kernels with negative coefficient in 'Xifei,' exhibiting downregulated expression with kernel development in 'Xifei.' A total of 15 DETFs were correlated to syntheses of unsaturated FAs in 'Xifei,' containing 5 involved in UFA, 3 DETFs in $C_{18:1}$ FA, 4 DETFs in $C_{18:3}$ FA, and 3 in $C_{20:3}$ FA. Among three DETFs of MYB type termed as GTL1, two exhibited positive correlation to $C_{18:1}$ FA (c99828.graph_c0, $r = 1.00000$, and $p = 0.00154$) and $C_{20:3}$ FA (c99348.graph_c0, $r = 0.99998$, and $p = 0.00413$), and one was negatively correlated to UFA (c99816.graph_c0, $r = -0.99997$, and $p = 0.00525$). FUS3 (c99613.graph_c0) was involved in $C_{20:3}$ FA syntheses in 'Xifei' with negative coefficient ($r = -0.99993$, $p = 0.00766$). Given that $C_{20:3}$ FA in 'Dielsii' was significantly different from that in 'Xifei,' a total of 6 DETFs were concerned in $C_{20:3}$ FA syntheses with negative correlation, and only one DETF was positively correlated (ERF RAP2-3, $r = 0.99988$, and $p = 0.009995$) and significantly upregulated with the development of kernels in 'Dielsii.'

To better understand the difference in regulation on the pathway of FA syntheses, DEGs were identified based on references and paralleled with the pathway of FA biosynthesis. The pathway of FA syntheses was initiated from malony-CoA and subsequently catalyzed by enzymes of FA syntheses. The profiles of DEGs were shown in the form of a heatmap (**Figure 6** and **Supplementary Table 13**). Given that $C_{16:0}$ FA was differentially produced between two cultivars, the expression of FAS was upregulated at the initial development of kernels development and responsible for the nascent rise of $C_{16:0}$ FA in 'Xifei,' whereas the declined expression of FAS accounted for $C_{16:0}$ FA in 'Dielsii.' When $C_{18:0}$ FA was converted into $C_{18:1}$ FA, FATA (c100682.graph_c0) was upregulated by kernel development in 'Xifei' and 'Dielsii,' while FATA (c100688.graph_c0) was upregulated only at nascent syntheses of FA in 'Xifei,' indicating a different rule accounting for the more accumulation of C18:1 between two cultivars. Given that a total of 10 DETFs were significantly associated with $C_{20:3}$ FA syntheses, the expression of these DETFs was different between cultivars during kernel development. Eight DETFs were upregulation at the early stage of kernel development in 'Xifei.' Only one DETF (c99475.graph_c0) was specifically upregulated at kernel maturation in 'Dielsii,' whereas the expression of c99613.graph_c0 was upregulated at the early stage of 'Dielsii,' suggesting the differential regulation rules on the deposition of $C_{20:3}$ FA between 'Xifei' and 'Dielsii.'

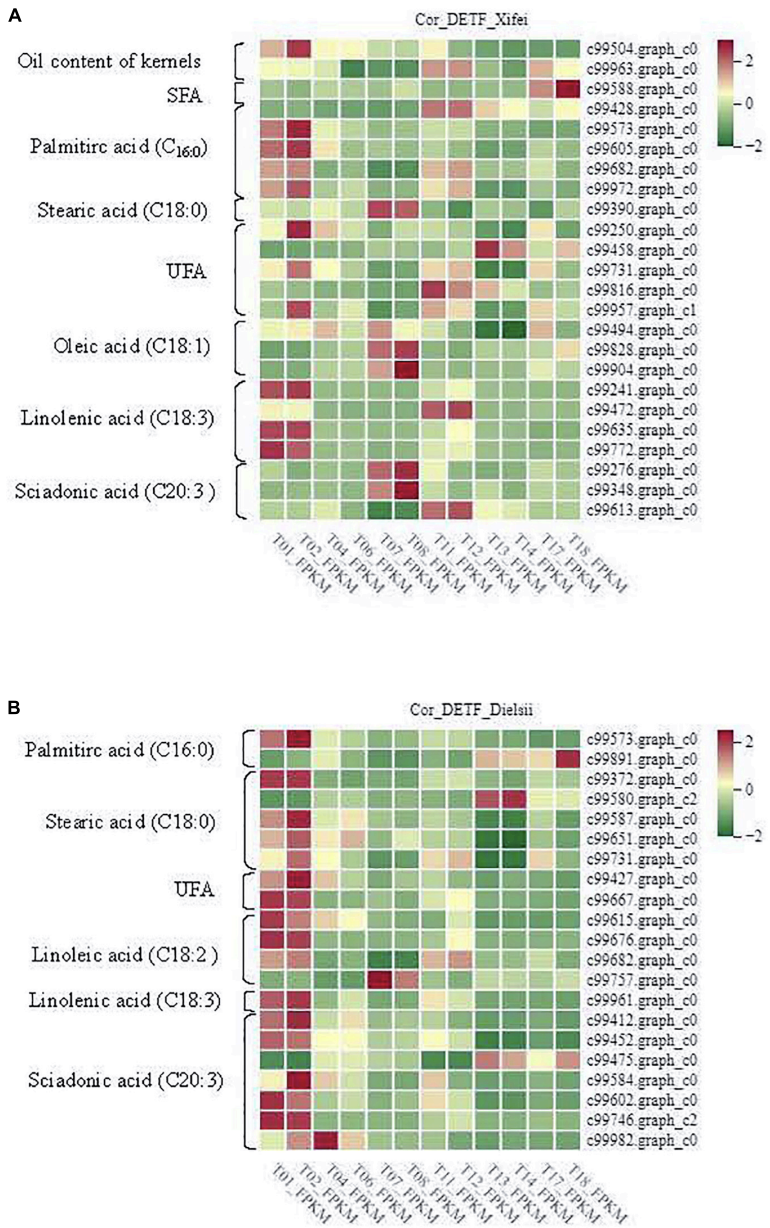

FIGURE 5 | Differentially expressed transcription factors (DETFs) were correlated to metabolites at different stages of kernel developments. **(A)** Samples termed as T01, T02, T04, T06, T07, and T08 represent the stage of the initiative, rapid and stationary oil accumulation in kernels of *T. grandis* 'Xifei,' respectively. **(B)** Samples termed as T011, T12, T13, T14, T17, and T18 represent the stage of the initiative, rapid and stationary oil accumulation in kernels of *T. grandis* 'Dielsii,' respectively. The correlated metabolite ($p < 0.01$) was listed in the left column.

DISCUSSION

Dynamic Characters and Difference of Oil and Fatty Acid Composition During Kernel Development in *T. grandis* 'Xifei' and *T. grandis* 'Dielsii'

Torreya grandis was one of the rare conifer trees in China, and was famous for the high content of oil in dry nuts. Although the final profiles of oil and FA have been reported in a few published reports (Niu et al., 2011; Ni and Shi, 2014; Shi et al., 2018), the rules of differential accumulation with kernel development remained unclear. In the current study, oil deposition was compared between two cultivars, 'Xifei' and 'Dielsii,' suggesting a dynamic profile of oil and FA biosyntheses during kernel development. The oil content of the two cultivars was within the variant scale in previous reports (Shi et al., 2018). The oil content of 'Xifei' rose more rapidly with kernel growth and was significantly higher than that of 'Dielsii' at mature, suggesting a more efficient mechanism of regulation and biosynthesis of lipids

in 'Xifei.' Interestingly, FA syntheses were significantly different between the two cultivars. The content of $C_{18:1}$ FA in 'Xifei' had been increased more rapidly than 'Dielsii' after 448 DAP responsible for the higher final deposition of $C_{18:1}$ FA in 'Xifei.'

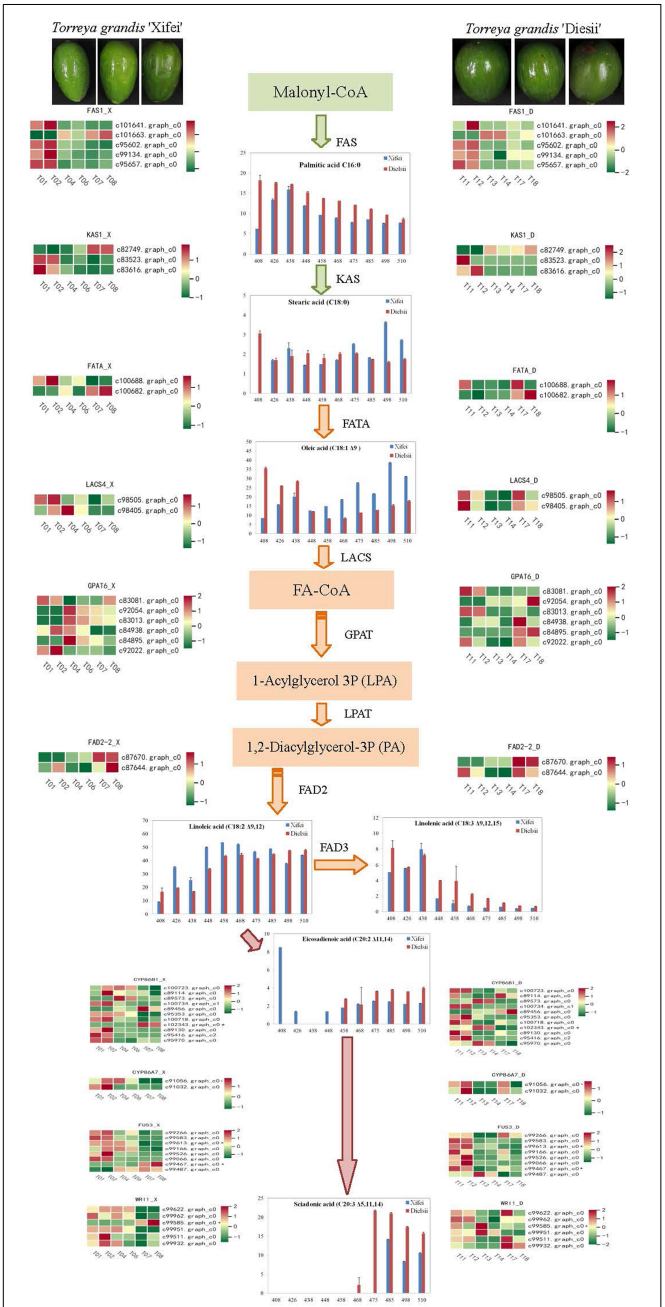

FIGURE 6 | Differential expression of unigenes associated with fatty acid biosynthesis with kernel development between *T. grandis* 'Xifei' (left) and *T. grandis* 'Dielsii' (right). Enzyme, unigene, and expression profiles are individually indicated at each primary step of biosyntheses. Colorful grids ranging from green to red in the row indicated the FPKM value of each unigene at the different development stages of kernels. Unigenes with significant correlation to $C_{20:3}$ FA were indicated with an asterisk (*) beside the sequence ID.

$C_{20:3}$ FA (especially refers to SA) was reported to exist in almost all coniferophyte families (Wolff et al., 2001). Besides, *T. grandis* was a rare species that contain high levels of $C_{20:3}$ FA (Niu et al., 2011). Although different final deposition of $C_{20:3}$ FA has been reported between landraces, the developmental changes of $C_{20:3}$ FA were poorly understood. In this study, accumulation of $C_{20:3}$ FA was initiated at 468 DAP in 'Dielsii' and 485 DAP in 'Xifei,' indicating a novel rule of biosyntheses different from other FAs and a delayed deposition in 'Xifei' accounting for the final lower content of $C_{20:3}$ FA. It was reported that the $C_{20:3}$ FA presence and its content varied between varieties (Ni and Shi, 2014; He et al., 2016; Wang et al., 2016; Shi et al., 2018), which are depending on certain cultivars of *T. grandis* and promising a potential correlation to the function of PUFA. As is well known for rootstock, 'Dielsii' has a lower content of oil and UFAs but higher content of $C_{20:3}$ FA, suggesting a smart strategy that enrichment of more beneficial polyUFAs such as C20:3 at the expanse of reduction in the oil content in non-edible cultivars of *T. grandis*.

Comprehensive Regulation of Differentially Expressed Genes Involved in Fatty Acid Biosynthesis

The supply of FAs is a factor restricting oil accumulation in embryo development (Bao and Ohlrogge, 1999). Based on the comparison of DEGs between two cultivars, the most enriched KEGG pathways were glycolysis and oxidative phosphorylation, implying a difference in supplies of substances of fatty acids biosynthesis or processing between 'Xifei' and 'Dielsii.'

Acyl carrier protein (ACP) is crucial for elongation of acyl chain in *de novo* FA synthesis in plants. Acyl-ACP thioesterases are required to catalyze acyl-ACP hydrolysis to discharge free FA (Dussert et al., 2013). FatA and FatB are two classes of Acyl-ACP thioesterases (Jones et al., 1995). FatA enzymes preferentially hydrolyzed18:1-ACP whereas FatB usually catalyzed saturated acyl-ACP (Dussert et al., 2013). Temperate oil crops, such as Arabidopsis, are typically accepted to accumulate low saturated FAs in accordance with the low level of FatB transcripts (Troncoso-Ponce et al., 2011). *T. grandis* is a precious conifer tree with high lipid-rich nut-fruits, the unsaturated FAs of *T. grandis* usually occupy over 85% approximately (Shi et al., 2018). In this study, two DEGs encoding FATA, c100688.graph_c0 in 'Xifei' and c100682.graph_c0 in 'Dielsii,' differentially expressed with kernel development. FATA (c100682.graph_c0) was upregulated during kernel development, which was in contrast to the lower accumulation of $C_{18:1}$ FA in 'Dielsii.' FATA (c100688.graph_c0) in 'Xifei' was upregulated at initiation and then declined with the kernel growing, associating with the nascent rise of $C_{18:1}$ FA content in 'Xifei.' Interestingly, the expression of three DETFs correlated to $C_{18:1}$ FA was consistent with the presence of $C_{18:1}$ FA in 'Xifei' and 'Dielsii' (**Figure 6**). In this study, two DEGs encoding FATA were expressed differentially during kernel development, revealing a novel regulation mechanism of $C_{18:1}$ FA syntheses in *T. grandis*.

$C_{20:3}$ FA (SA) was first found in *Taxus cuspidate* (Japanese yew; Itabashi and Takagi, 1982), mainly distributed in gymnosperm species with wide content variation between family, genus, or even the species (Aitzetmuller, 1995; Wolff et al., 1999a,b; Berger et al., 2002). Concerning the outstanding benefits to health, $C_{20:3}$ FA was widely studied in extraction, purification, characteristics, and pharmacodynamics (Tanaka et al., 2001; Berger et al., 2002). Subsequently, functional characterization of candidate genes encoding Δ5-desaturase in transgenic Arobidopsis was carried out (Sayanova et al., 2007). Recently, an attempt on the exploration of genes involved in the biosyntheses of $C_{20:3}$ FA was performed in *T. grandis* using mature seeds and vegetable organs (leaf, stem, and root; Wu et al., 2018). However, the regulation mechanism of $C_{20:3}$ FA biosyntheses during kernel development remains unclear. In this study, the DEGs between two cultivars with contrasting content of $C_{20:3}$ FA were explored by *de novo* transcriptome during the whole maturation of kernels. Combined with correlation analyses, abundant DEGs correlated to $C_{20:3}$ FA deposition were captured (**Supplementary Tables 10,11**), including particularly 10 DETFs with significantly different expressions between the two cultivars and responsible for different content of $C_{20:3}$ FA, promising a regulation mechanism in the process of $C_{20:3}$ FA biosyntheses.

ONE SENTENCE SUMMARY

Lipid synthesis and *de novo* transcriptome were compared between two cultivars during kernel development in *Torreya grandis*.

DATA AVAILABILITY STATEMENT

The datasets presented in this study can be found in online repositories. The names of the repository/repositories and accession number(s) can be found in the article/ **Supplementary Material**.

AUTHOR CONTRIBUTIONS

CZ, HL, and MZ wrote the manuscript. CZ and MZ analyzed the data. HZ, WD, and CHZ performed the experiments. All authors contributed to the article and approved the submitted version.

FUNDING

This work was financially supported by the Basic Public Welfare Project of Zhejiang Province (LGN19C160005); Economy, Commerce and Technology Bureau of Jingning (2021A18); and Science Technology Department of Zhejiang Province (2021C02066-11).

SUPPLEMENTARY MATERIAL

The Supplementary Material for this article can be found online at: https://www.frontiersin.org/articles/10.3389/fpls.2022.909759/full#supplementary-material

Supplementary Figure 1 | Length distribution of unigenes with over 1 kb in length.

Supplementary Figure 2 | The best-matched species of the unigenes **(A)** and the GO function classifications **(B)** in *T. grandis*.

Supplementary Table 1 | Changes of oil content with development of kernels in *T. grandis* 'Xifei' and *T. grandis* 'Dielsii.'

Supplementary Table 2 | Changes in content of FA composition with development of kernels in 'Xifei' and 'Dielsii.'

Supplementary Table 3 | Sequencing information of samples.

Supplementary Table 4 | GO, KEGG, and Swissprot annotation of unigenes in *T. grandis*.

Supplementary Table 5 | DEGs between *T. grandis* 'Xifei' and *T. grandis* 'Dielsii.'

Supplementary Table 6 | DEGs between developmental stages in *T. grandis* 'Xifei.'

Supplementary Table 7 | DEGs between developmental stages in *T. grandis* 'Dielsii.'

Supplementary Table 8 | The numbers of DEGs involved in pathways related to fatty acid biosynthesis and metabolism between *T. grandis* 'Xifei' and *T. grandis* 'Dielsii.'

Supplementary Table 9 | Primer sequences of DEGs used for RT-qPCR.

Supplementary Table 10 | A total of 922 DEGs with p-value < 0.01 correlated to oil and fatty acids variation in *T. grandis* 'Xifei.'

Supplementary Table 11 | A total of 574 DEGs with p-value<0.01 correlated to oil and fatty acids variation in *T. grandis* 'Dielsii.'

Supplementary Table 12 | DETFs correlated to metabolites in *T. grandis* 'Xifei' and *T. grandis* 'Dielsii', respectively.

Supplementary Table 13 | FPKM value of DEGs involved in pathway of FA syntheses used for heatmaps in *T. grandis* 'Xifei' and *T. grandis* 'Dielsii', respectively.

REFERENCES

Aitzetmuller, K. (1995). Fatty acid patterns of Ranunculaceae seed oils: phylogenetic relationships. *Plant Syst. Evol.* 9, 229–240. doi: 10.1007/BF02522621

Asset, G., Staels, B., Wolff, R. L., Baugé, E., Madj, Z., Fruchart, J. C., et al. (1999). Effects of Pinus pinaster and Pinus koraiensis seed oil supplementation on lipoprotein metabolism in the rat. *Lipids* 34, 39–44. doi: 10.1007/s11745-999-335-2

Benjamini, Y., Drai, D., Elmer, G., Kafkafi, N., and Golani, I. (2001). Controlling the false discovery rate in behavior genetics research. *Behav. Brain Res.* 125, 279–284. doi: 10.1016/s0166-4328(01)00297-2

Bao, X., and Ohlrogge, J. (1999). Supply of fatty acid is one limiting factor in the accumulation of triacylglycerol in developing embryos1. *Plant Physiol.* 120, 1057–1062. doi: 10.1104/pp.120.4.1057

Berger, A., Baur, M., Charbonnet, C., Safonova, I., and Jomard, A. (2002). Epidermal anti-inflammatory properties of 20:3Δ5,11,14: effects on mouse ear edema, PGE2 levels in cultured keratinocytes, and

PPAR activation. *Lipids Health Dis.* 1, 1–12. doi: 10.1186/1476-511x-1-5

Cernac, A., and Benning, C. (2004). WRINKLED1 encodes an AP2/EREB domain protein involved in the control of storage compound biosynthesis in *Arabidopsis*. *Plant J* 40, 575–585. doi: 10.1111/j.1365-313X.2004.02235.x

Chen, H. X., Li, G. R., Zhang, S. J., Ma, W. M., Yao, X. H., Zhang, C., et al. (2020a). Breeding report of a new Torreya grandis cultivar'Pan'an Changfei'. *J. Fruit. Sci.* 37, 297–300. doi: 10.13925/j.cnki.gsxb.20190386

Chen, H. X., Tang, H. Y., Zhang, S. J., Zhang, C., Yu, W. W., and Zhang, M. (2020b). Breeding report of a new Torreya grandis cultivar 'Yushanyufei'. *J Fruit Sci* 37, 779–782. doi: 10.13925/j.cnki.gsxb.20190593

Chen, S. J., Chuang, L. T., Liao, J. S., Huang, W. C., and Lin, H. H. (2015). Phospholipid incorporation of non-methylene-interrupted fatty acids (NMIFA) in murine microglial BV-2 cells reduces pro-Inflammatory mediator production. *Inflammation* 38, 2133–2145. doi: 10.1007/s10753-015-0196-z

Chen, X., and Jin, H. (2019a). Review of cultivation and development of Chinese Torreya in China. *Forest Trees Liveli.* 28, 68–78. doi: 10.1080/14728028.2018.1553690

Chen, X., and Jin, H. (2019b). A case study of enhancing sustainable intensification of Chinese Torreya forest in Zhuji of China. *Envir. Nat. Res. Res.* 9, 53–60. doi: 10.5539/enrr.v9n2p53

Chuang, L. T., Tsai, P. J., Lee, C. L., and Huang, Y. S. (2009). Uptake and incorporation of pinolenic acid reduces n-6 polyunsaturated fatty acid and downstream prostaglandin formation in murine macrophage. *Lipids* 44, 217–224. doi: 10.1007/s11745-008-3276-0

Conesa, A., and Gotz, S. (2008). Blast2GO: a comprehensive suite for functional analysis in plant genomics. *Int. J. Plant Genom.* 2008:619832. doi: 10.1155/2008/619832

Ding, M. Z., Lou, H. Q., Chen, W. C., Zhou, Y., Zhang, Z. H., and Xiao, M. H. (2020). Comparative transcriptome analysis of the genes involved in lipid biosynthesis pathway and regulation of oil body formation in *Torreya grandis* kernels. *Industrial Crops Products* 145:11205. doi: 10.1016/j.indcrop.2019.112051

Dussert, S., Guerin, C., Andersson, M., Joet, T., Tranbarger, T. J., Pizot, M., et al. (2013). Comparative transcriptome analysis of three oil palm fruit and seed tissues that differ in oil content and fatty acid composition. *Plant physiol.* 162, 1337–1358. doi: 10.1104/pp.113.220525

Endo, Y., Ph, D., Osad, Y., Kimur, F., and Fujimoto, K. (2006). Effects of Japanese torreya (*Torreya nucifera*) seed oil on lipid metabolism in rats. *Nutrition* 22, 553–558. doi: 10.1016/j.nut.2005.08.012

Endo, Y., Tsunokake, K., and Ikeda, I. (2009). Effects of non-methylene-interrupted polyunsaturated fatty acid, sciadonic (all-cis-5,11,14-eicosatrienoic acid) on lipid metabolism in rats. *J. Agric. Chem. Soc. Japan* 73, 577–581. doi: 10.1271/bbb.80646

Focks, N., and Benning, C. (1998). wrinkled1: a novel, low-seed-oil mutant of *Arabidopsis* with a deWciency in the seed-speciWc regulation of carbohydrate metabolism. *Plant Physiol.* 118, 91–101. doi: 10.1104/pp.118.1.91

Grabherr, M. G., Haas, B. J., Yassour, M., Levin, J. Z., Thompson, D. A., Amit, I., et al. (2011). Full length transcriptome assembly from RNA Seq data without a reference genome. *Nat. Biotechnol.* 29, 644–652. doi: 10.1038/nbt.1883

He, Z., Zhu, H., Li, W., Zeng, M., Wu, S., Chen, S., et al. (2016). Chemical components of cold pressed kernel oils from different *Torreya grandis* cultivars. *Food Chem.* 209, 196–202. doi: 10.1016/j.foodchem.2016.04.053

Itabashi, Y., and Takagi, T. (1982). Cis-5-olefinic nonmethylene-interrupted fatty acids in lipids of seeds, arils and leaves of Japanese Yew. *J. Jpn. Oil Chem. Soc.* 31, 574–579.

Jones, A., Davies, H. M., and Voelker, T. A. (1995). Palmitoyl-acyl carrier protein (ACP) thioesterase and the evolutionary origin of plant acyl-ACP thioesterases. *Plant Cell* 7, 359–371. doi: 10.1105/tpc.7.3.359

Lara, P., Onate-Sanchez, L., Abraham, Z., Ferrandiz, C., Diaz, I., Carbonero, P., et al. (2003). Synergistic activation of seed storage protein gene expression in *Arabidopsis* by ABI3 and two bZIPs related to OPAQUE2. *J. Biol. Chem* 278, 21003–21011. doi: 10.1074/jbc.M210538200

Lisa, M., Holcapek, M., Rezanka, T., and Kabatova, N. (2007). High-performance liquid chromatography–atmospheric pressure chemical ionization mass spectrometry and gas chromatography–flame ionization detection characterization of Δ5-polyenoic fatty acids in triacylglycerols from conifer seed oils. J. Chromatogr. A 1146, 67–77. doi: 10.1016/j.chroma.2007.01.122

Meng, X. H., Xiao, D., Ye, Q., Nie, X. H., Wu, J. S., and Song, L. L. (2020). Positional distribution of Δ5-olefinic acids in triacylglycerols from *Torreya grandis* seed oil: Isolation and purification of sciadonic acid. *Ind. Crops Prod.* 143:111917. doi: 10.1016/j.indcrop.2019.111917

Meng, Z., Jilian, F., Taylor, D. C., and Ohlrogge, J. B. (2009). DGAT1 and PDAT1 acyltransferases have overlapping functions in *Arabidopsis* triacylglycerol biosynthesis and are essential for normal pollen and seed development. *Plant Cell* 21, 3885–3901. doi: 10.1105/tpc.109.071795

Mortazavi, A., Williams, B. A., McCue, K., Schaeffer, L., and Wold, B. (2008). Mapping and quantifying mammalian transcriptomes by RNA-Seq. *Nat. Methods* 5, 621–628. doi: 10.1038/nmeth.1226

Ni, L., and Shi, W. Y. (2014). Composition and free radical scavenging activity of kernel oil from. Torreya grandis: carya cathayensis and Myrica rubra. *Iran. J. Pharm. Res.* 13, 221–226.

Ni, Q., Gao, Q., Yu, W., Liu, X., Xu, G., and Zhang, Y. (2015). Supercritical carbondioxide extraction of oils from two torreya grandis, cultivars seeds and their physicochemical and antioxidant properties. *LWT –Food Sci. Technol.* 60, 1226–1234. doi: 10.1016/j.lwt.2014.09.007

Niu, L. Y., Wu, X. Q., and Zhang, Y. (2011). Analysis on fatty acid and unsaponifiable matter in Torreya grandis var. Merriii seed oil. *J. Chin. Cereals Oils Assoc.* 26, 52–55.

Rao, S. S., and Hildebrand, D. (2009). Changes in oil content of transgenic soybeans expressing the yeast gene. *Lipids* 44, 945–951. doi: 10.1007/s11745-009-3337-z

Ruuska, S. A., Girke, T., Benning, C., and Ohlrogge, J. B. (2002). Contrapuntal networks of gene expression during *Arabidopsis* seed wlling. *Plant Cell* 14, 1191–1206. doi: 10.1105/tpc.000877

Sayanova, O., Haslam, R., Caleron, M. V., and Napier, J. A. (2007). Cloning and characterization of unusual fatty acid desaturases from anemone leveillei: identification of an acylcoenzyme A C20Δ5-desaturase responsible for the synthesis of sciadonic acid. *Plant Physiol.* 144, 455–467. doi: 10.1104/pp.107.098202

Shen, B., Sinkevicius, K. W., Selinger, D. A., and Tarczynski, M. C. (2006). The homeobox gene GLABRA2 aVects seed oil content in Arabidopsis. *Plant Mol. Biol.* 60, 338–377. doi: 10.1007/s11103-005-4110-1

Shi, L. K., Mao, J. H., Zheng, L., Zhao, C. W., Jin, Q. Z., and Wang, X. G. (2018). Chemical characterization and free radical scavenging capacity of oils obtained from *Torreya grandis* Fort. ex. lindl. and torreya grandis fort. var. merrillii: a comparative study using chemometrics. *Ind. Crops Prod.* 115, 250–260. doi: 10.1016/j.indcrop.2018.02.037

Shiu-Cheung, L., and Weselake, R. J. (2006). Diacylglycerol acyltransferase: a key mediator of plant triacylglycerol synthesis. *Lipids* 41, 1073. doi: 10.1007/s11745-006-5057-y

Sugano, M., Ikeda, I., Wakamatsu, K., and Oka, T. (1994). Influence of Korean pine (Pinus koraiensis)-seed oil containing cis-5, cis-9, cis-12-octadecatrienoic acid on polyunsaturated fatty acid metabolism, eicosanoid production and blood pressure of rats. *Br. J. Nutr* 72, 775. doi: 10.1079/bjn19940079

Tanaka, T., Morishige, J., Takimoto, T., Takai, Y., and Satouchi, K. (2001). Metabolic characterization of sciadonic acid (5c,11c,14c-eicosatrienoic acid) as an effective substitute for arachidonate of phosphatidylinositol. *Eur. J. Biochem.* 268, 4928–4939. doi: 10.1046/j.0014-2956.2001.02423.x

Troncoso-Ponce, M. A., Kilaru, A., Cao, X., Durrett, T. P., Fan, J., Jensen, J. K., et al. (2011). Comparative deep transcriptional profiling of four developing oilseeds. *Plant J.* 68, 1014–1027. doi: 10.1111/j.1365-313X.2011.04751.x

Wang, H., Guo, J., Lambert, K. N., and Lin, Y. (2007). Developmental control of Arabidopsis seed oil biosynthesis. *Planta* 226, 773–783. doi: 10.1007/s00425-007-0524-0

Wang, Y. B., Liu, B. T., Qin, Y. C., Wang, L. L., Tong, X. Q., Tong, P. Z., et al. (2016). Compositions of fatty acid and flavor compounds in different cultivars of Torrey grandis seed oil. *Chin. Oil Fat* 41, 101–105.

Wolff, R. L., Christie, W. W., Pedrono, F., Marpeau, A. M., Tsevegsuren, N., Aitzetmuller, K., et al. (1999a). Δ5-olefinic acids in the seed lipids from four *Ephedra* species and their distribution between the alpha and beta positions of triacylglycerols. characteristics common to coniferophytes and cycadophytes. *Lipids* 34, 855–864. doi: 10.1007/s11745-999-0433-1

Wolff, R. L., Lavialle, O., Pedrono, F., Pasquier, E., Deluc, L. G., Marpeau, A. M., et al. (2001). Fatty acid composition of Pinaceae as taxonomic markers. *Lipids* 36, 439–451. doi: 10.1007/s11745-001-0741-5

Wolff, R. L., Pédrono, F., Marpeau, A. M., and Gunstone, F. D. (1999b). The seed fatty acid composition and the distribution of Δ5-olefinic acids in the triacylglycerols of some Taxares (*Cephalotaxus* and *Podocarpus*). *J. Am. Oil Chem. Soc.* 76, 469–473.

Wu, J. S., Huang, J. D., Hong, Y. W., Zhang, H. Z., Ding, M. Z., Lou, H. Q., et al. (2018). De novo transcriptome sequencing of Torreya grandis reveals gene regulation in sciadonic acid biosynthesis pathway. *Ind. Crops Prod.* 120, 47–60.

Xie, K., Miles, E. A., and Calder, P. C. (2016). A review of the potential health benefits of pine nut oil and its characteristic fatty acid pinolenic acid. *J. Funct. Foods* 23, 464–473. doi: 10.1016/j.jff.2016.03.003

Zhang, C., Chen, H. X., Hu, W. C., Ye, X. L., Wang, X. X., and Zhang, M. (2021). Breeding report of a new *Torreya* grandis 'panyuefei'. *J. Fruit Sci.* 38, 155–159. doi: 10.13925/j.cnki.gsxb.20210386

Zheng, P., Allen, W. B., Roesler, K., Williams, M. E., Zhang, S., Li, J., et al. (2008). A phenylalanine in DGAT is a key determinant of oil content and composition in maize. *Nat. Genet* 40, 367–372. doi: 10.1038/ng.85

Conflict of Interest: The authors declare that the research was conducted in the absence of any commercial or financial relationships that could be construed as a potential conflict of interest.

Publisher's Note: All claims expressed in this article are solely those of the authors and do not necessarily represent those of their affiliated organizations, or those of the publisher, the editors and the reviewers. Any product that may be evaluated in this article, or claim that may be made by its manufacturer, is not guaranteed or endorsed by the publisher.

frontiers | Frontiers in Plant Science

ORIGINAL RESEARCH
published: 06 July 2022
doi: 10.3389/fpls.2022.942054

Genetic and Biochemical Investigation of Seed Fatty Acid Accumulation in Arabidopsis

*Chinedu Charles Nwafor[1,2], Delin Li[1], Ping Qin[1], Long Li[1], Wei Zhang[3], Yuanwei Zhou[4], Jingjing Xu[1], Yongtai Yin[5], Jianbo Cao[6], Limin He[6], Fu Xiang[7], Chao Liu[1], Liang Guo[1], Yongming Zhou[1], Edgar B. Cahoon[8] and Chunyu Zhang[1]**

[1]National Key Laboratory of Crop Genetic Improvement, College of Plant Science and Technology, Huazhong Agricultural University, Wuhan, China, [2]Department of Crop Science, Faculty of Agriculture, University of Benin, Benin City, Nigeria, [3]Department of Biology, College of Chemistry and Life Sciences, Zhejiang Normal University, Jinhua, China, [4]Yichang Academy of Agricultural Science, Yichang, China, [5]Department of Biotechnology, College of Life Science and Technology, Huazhong University of Science and Technology, Wuhan, China, [6]Public Laboratory of Electron Microscopy, Huazhong Agricultural University, Wuhan, China, [7]Collaborative Innovation Center for the Characteristic Resources Exploitation of Dabie Mountains and College of Biology and Agriculture Resource, Huanggang Normal University, Huanggang, China, [8]Center for Plant Science Innovation and Department of Biochemistry, University of Nebraska-Lincoln, Lincoln, NE, United States

OPEN ACCESS

Edited by:
Hyun Uk Kim,
Sejong University, South Korea

Reviewed by:
Antonio Javier Moreno-Perez,
Institute for Fats (CSIC), Spain
Agnieszka Mostowska,
University of Warsaw, Poland

***Correspondence:**
Chunyu Zhang
zhchy@mail.hzau.edu.cn

Specialty section:
This article was submitted to Crop and Product Physiology, a section of the journal Frontiers in Plant Science

Received: *18 May 2022*
Accepted: *13 June 2022*
Published: *06 July 2022*

Citation:
Nwafor CC, Li D, Qin P, Li L, Zhang W, Zhou Y, Xu J, Yin Y, Cao J, He L, Xiang F, Liu C, Guo L, Zhou Y, Cahoon EB and Zhang C (2022) Genetic and Biochemical Investigation of Seed Fatty Acid Accumulation in Arabidopsis. Front. Plant Sci. 13:942054. doi: 10.3389/fpls.2022.942054

As a vegetable oil, consisting principally of triacylglycerols, is the major storage form of photosynthetically-fixed carbon in oilseeds which are of significant agricultural and industrial value. Photosynthesis in chlorophyll-containing green seeds, along with photosynthesis in leaves and other green organs, generates ATP and reductant (NADPH and NADH) needed for seed fatty acid production. However, contribution of seed photosynthesis to fatty acid accumulation in seeds have not been well-defined. Here, we report the contribution of seed-photosynthesis to fatty acid production by probing segregating green (photosynthetically-competent) and non-green or yellow (photosynthetically-non-competent) seeds in siliques of an Arabidopsis chlorophyll synthase mutant. Using this mutant, we found that yellow seeds lacking photosynthetic capacity reached 80% of amounts of oil in green seeds at maturity. Combining this with studies using shaded siliques, we determined that seed-photosynthesis accounts for 20% and silique and leaf/stem photosynthesis each account for ~40% of the ATP and reductant for seed oil production. Transmission electron microscopy (TEM) and pyridine nucleotides and ATP analyses revealed that seed photosynthesis provides ATP and reductant for oil production mostly during early development, as evidenced by delayed oil accumulation in non-green seeds. Transcriptomic analyses suggests that the oxidative pentose phosphate pathway could be the source of carbon, energy and reductants required for fatty acid synthesis beyond the early stages of seed development.

Keywords: fatty acid biosynthesis, chlorophyll synthase, photosynthesis, oxidative pentose phosphate pathway, NADPH, oil bodies, Arabidopsis, seed development

INTRODUCTION

Seeds accumulate oil in the form triacylglycerol (TAG) as one of their primary storage reserves. TAG is a major energy source for germinating seeds and for human and animal diets. Seed oil content is a major target of breeding and biotechnological efforts to increase the value of oilseed crops such as soybean and canola for edible, industrial, and biofuel applications (Cahoon et al., 2007; Lu et al., 2011). Oil production in seeds starts with *de novo* fatty acid (FA) biosynthesis and elongation, followed by the use of these fatty acids for TAG biosynthesis (Baud and Lepiniec, 2009; Hua et al., 2014). Acetyl-CoA production and the generation of reducing power from NADPH and energy from ATP are essential for FA biosynthesis, elongation, and storage (Singh et al., 1998; Ruuska et al., 2004; Goffman et al., 2005; Zhang et al., 2016).

Chlorophyll is important for light-driven production of reductants and energy that supports growth and development and formation of seed storage components, including seed oil (Ruuska et al., 2004; Schwender et al., 2004; Goffman et al., 2005; Hua et al., 2014; Zhang et al., 2016). Developing seeds can be classified as either photoheterotrophic green seeds (e.g., soybean, rapeseed, and Arabidopsis) or heterotrophic non-green seeds (e.g., castor, sunflower, and safflower; Zhang et al., 2016). The biochemical pathways and their subcellular distribution for FA biosynthesis in seeds are well-understood (Ohlrogge and Browse, 1995; Eastmond et al., 1996; Cernac and Benning, 2004; Allen et al., 2009; Li-Beisson et al., 2010; Troncoso-Ponce et al., 2011; Bates et al., 2013; Shahid et al., 2019). Less clear are the major tissue and organ sources of reductant for fatty acid biosynthesis in green seeds. Does reductant derive primarily from photosynthesis in leaves and stems, seed pods and siliques, or seeds or from metabolism of imported carbon in these tissues? Previous studies that investigated the role of light and seed photosynthesis in rapeseed (Fuhrmann et al., 1994; Willms et al., 1999), Arabidopsis (Goffman et al., 2005), and soybean (Quebedeaux and Chollet, 1975; Ruuska et al., 2004; Allen et al., 2009; Tschiersch et al., 2011), have proposed several hypotheses on the sources of reducing power for oil biosynthesis and accumulation (Fuhrmann et al., 1994; Ruuska et al., 2004; Schwender et al., 2004; Goffman et al., 2005). So far, it is believed that fatty acid synthesis and oil accumulation in green seeds, such as soybean is strongly controlled by light which is necessary for grain filling (Allen et al., 2009), and light-dependent seed photosynthesis is the major source of reductive power supporting FA biosynthesis and elongation in green seeds (Fuhrmann et al., 1994; Goffman et al., 2005).

Multiple labeling experiments (Fuhrmann et al., 1994; Goffman et al., 2005; Rolletschek et al., 2005; Allen et al., 2009; Lonien and Schwender, 2009; Tschiersch et al., 2011; Carey et al., 2020), have described energy balances and biosynthetic flux in growing embryos *in vitro*, and have provided insights into photosynthetically-derived energy and carbon flux required for seed oil production. Because these studies were conducted with excised embryos exposed to light, the findings may not fully mimic *in situ* metabolic flux that can be obtained by assessment of metabolic flux in seeds attached to plants, because dissecting plant tissues is known to impair metabolism (Geigenberger et al., 1994; Ruuska et al., 2004).

A growing body of evidence has brought into question the contribution of seed photosynthesis to reducing power required for fatty acid and oil biosynthesis in seeds (Borisjuk et al., 2005; Borisjuk and Rolletschek, 2009). One report that argues against the role of seed photosynthesis, suggests that G6PDH plays a role in supplying NADPH for oil accumulation in developing seeds in which photosynthesis may be light limited (Wakao et al., 2008). The authors showed that (pds1) mutants seeds that are non-photosynthetic had 60% of oil in photosynthetic green seeds at maturity and concluded that loss of cytosolic G6PDH activity impacted metabolism of developing seeds by increasing carbon substrates for synthesis of storage compounds rather than by decreasing the NADPH supply specifically for fatty acid synthesis. Additionally, Eastmond et al. (1996) suggests that the low light penetrance through *Brassica napus* siliques is insufficient for photosynthetic reductant production in seeds and that reductant supply to the plastid may underpin storage product synthesis. Also, it has been shown that loss of photosynthetic capacity in the soybean embryo is accompanied by a steady accumulation of starch and lipids bodies (Borisjuk et al., 2005). Together these results points to perhaps limited metabolic contribution of seed photosynthesis to fatty acid production in seeds during development.

In this report, we aimed to provide genetic evidence on the contribution of seed-photosynthesis to fatty acid biosynthesis during seeds development. To which we exploited the Arabidopsis chlorophyll synthase knockout mutant and its complement that segregate green (photosynthetically-competent) and, non-green or yellow (photosynthetically-non-competent) seeds in the silique combined with electron microscopy, and chlorophyll and fatty acid measurements, RNA-seq based transcriptomics/gene expression analysis, and LC/MS/MS-based Pyridine nucleotides and ATP analysis. Our results showed that photosynthesis in seeds has only a small contribution to NADPH reductant needed for fatty acid synthesis and deposition. The LC–MS/MS and gene expression studies provided clues that supported a role for the oxidative pentose phosphate pathway (OPPP) as a major pathway for NADPH production for fatty acid synthesis in Arabidopsis seeds. Also, we highlighted the metabolic impact of lacking chlorophyl in developing seeds and the potential biotechnological implication of metabolic engineering of both photosynthetic and OPPP pathway genes for enhancing seed oil production through efficient NADPH supply in developing seeds.

MATERIALS AND METHODS

Plant Material and Growth Conditions

The *Arabidopsis thaliana* Wild-type Col-0 ecotype, chlorophyll synthase knockout mutant (chlsyn1-1) and complemented (chlsyn1-1/CHLSYN) lines used for this study was previously described by Zhang et al. (2015). All plants were grown in the glasshouse at 22°C with 50% relative humidity and 16 h light (120 μE m^{-2} s^{-1}/8 h dark).

Sampling of Plant Material

Developing silique were labeled throughout the flowering period (Lorenz et al., 2018). Siliques produced between the third and seventh flower on the main axis were used. For tagging of each stage of seed development, we classified green and yellow seed developing seeds into (6, 8, 10, 12, 14, 16, and 18 days after flowering (DAF), and dry seeds at 40 DAF), two or three experimental replicates were achieved. For the shading experiment of siliques from light penetration, aluminum foil was used to cover siliques for the whole life, and unshaded siliques were used as control. The foils were draped around the siliques and with vents at the tip to allow air circulation. For FAs analysis, at least 48 plants of each of the WT and mutant lines were used. For histological studies, seeds from the same silique were used (at least three siliques from each line). For RNA-seq and LC–MS/MS-based pyridine nucleotides and ATP analysis, seeds were collected from more than 96 plants for each replicate and developmental stage. All plants were grown side by side under identical conditions. The photosynthetic, green seeds were used as control.

Measurement of Chlorophyll Content

For estimation of the Total chlorophyll content was measured according to the method previously described (Zhang et al., 2015). Chlorophyll was extracted after freshly harvested seed were weighed and homogenized in liquid nitrogen, subsequently extracted in three volumes of 80% (v/v) acetone containing 1 μM KOH. After centrifugation for 2 min at 16,000 *g*, the supernatant was used for spectrophotometric analysis of chlorophyll concentrations.

Fatty Acid Analysis and Protein Analysis

Fatty acid methyl esters (FAMEs) were prepared from developing seeds and dry seeds, as described in Niewiadomski et al. (2005). FAs estimation was performed by gas chromatography with flame ionization detector (GC-FID) after direct transesterification was made by the addition of 2.5% sulfuric acid in methanol (v/v) and incubating at 90°C for 2 h as described in Niewiadomski et al. (2005) and Cahoon et al. (2006). Fatty acid amounts were determined by comparing detector response relative to an internal standard (C17:0) from triheptadecanoin added prior to sample transesterification. Fatty acid composition was calculated as percentage of seed weight.

Protein content estimation was performed by extracting total protein from dry seeds as described in Job et al. (2005). In brief, seeds were homogenized to a fine powder in liquid nitrogen and then transferred to a 1.5 ml Eppendorf tube. Next, 10% TCA/0.07% dithiothreitol (DTT) in acetone (v/v), was added to the samples and incubated at −20°C overnight, followed by centrifugation for 30 min at 20,000 g at 4°C. Afterward, the pellets were then washed three times with 1.5 ml of pre-cooled acetone containing 0.07% DTT at −20°C followed by centrifugation for 30 min at 20,000 g at 4°C. The sample pellets were then solubilized in the lysis buffer containing 7 mM urea, 2 mM thiourea, 4% CHAPS, 50 mM DTT, 0.5% Triton X-100, 1% protease inhibitor cocktail, and 2% IPG buffer (v/v). The solution was incubated at 25°C for 1 h with gentle mixing and then centrifuged at 12,000 g for 20 min. The supernatant was subjected to second clarifying centrifugation as above with the supernatants collected into fresh tubes and stored at −80°C in aliquots. The spectrophotometer was used to quantify the proteins. Bovine serum albumin was used as a standard.

Transmission Electron Microscopy

Transmission electron microscopy (TEM) was performed as described (Gan et al., 2013). For TEM, developing (8 and 12 DAF, and dry seeds 40 DAF), described in section Sampling of Plant Material were used. Developing and dry seeds from the same siliques were removed, cut into 1 mm × 1 mm blocks and fixed immediately in 2.5% (w/v) glutaraldehyde in 0.1 mol L–1 phosphate buffer solution (PBS) at 4oC overnight. The fixed samples were then rinsed with PBS three times for 30 min each at room temperature (20°C–25°C), and post-fixed in 1% OsO4 in phosphate buffer overnight at 4oC. Next, samples were washed with Milli-Qwater and dehydrated through an acetone series (20%, 50%, 70%, and 90%, and 3% × 100% v/v). The samples were cut into ultrathin sections (60–70 nm thick) using a diatome diamond knife on a UC6 Ultratome (Leica, Germany), stained with 2% uranyl acetate (v/v). The mages were viewed and collected with a Hitachi transmission electron microscope (TEM; H-7650; Hitachi, Japan) at 80 kv. Each sample had three biological replicates with each replicate having at least three ultrathin sections observed under the electron microscope. The imageJ software (Girish and Vijayalakshmi, 2004) was used to measure the area of oil bodies in embryos cotyledons from three sections of each of the three independent biological replicates of each sample.

Pyridine Nucleotides and ATP Analyses by LC-MS/MS

Measurement of pyridine nucleotides and ATP analysis *via* LC-MS/MS was conducted as described previously in Guo et al. (2014). About 100 mg of green and yellow seeds at 8 and 10 DAFs were used. After the seed was harvested on ice and immediately ground in liquid nitrogen, 3 ml of methanol/chloroform (7:3, v/v; −20°C) was added to each sample, then mixed by vortex. Next, 0.9 μg PIPES was added as the internal standard, and the mixture was stored in −20° C for 2 h with occasional mixing. Subsequently, polar metabolites were extracted by the addition of 1.6 ml water followed by vigorous vortexing and centrifugation at 8,000 rpm for 20 min. Followed by the transfer of the upper methanol–water phase to a new tube. This step was repeated twice. Afterward, the first and second upper methanol–water phases were pooled and dried by N_2 aspiration at room temperature. The dried extract was reconstituted with 100 μl water and filtered with 0.45 μM cellulose acetate centrifuge tube filter and then diluted by 10- or 100-fold for analyses by LC–MS/MS.

Absolute quantification of pyridine nucleotides and ATP metabolites (ATP, ADP, NAD, NADH, NADP, and NADPH), was achieved by the use of high purity external standards. For each metabolite, a calibration curve was made by preparing eight standard solutions with known concentrations in water. Each standard solution was analyzed three times and metabolites

were determined by plotting average peak areas against standard concentration using a linear regression model.

RNA-Seq Analysis

Total RNA from developing seeds was extracted with the TRIzol Reagent Kit (Ambion) according to the manufacturer's protocol. The RNA quality and quantity were determined using a Nanodrop 8000 (Thermo Scientific, Wilmington, DE) and a Bioanalyzer 2100 (Agilent, Santa Clara, CA). Before RNA extraction, green and yellow developing seed at 10 DAF were separated from silique and quickly grounded in liquid nitrogen. All samples were collected in three biological replicates. Afterward, samples from each biological replicate were pooled. In total, six samples were used to construct the cDNA library with Illumina® TruSeq™ RNA Sample Preparation Kit following the manufacturer's instructions. All samples were sequenced using an Illumina HiSeq 2000 sequencer at the Beijing Genome Institute, Shenzhen, China. Analysis of sequence data was according to the method described in Ramakers et al. (2003). RNA-seq sequence data can be found in the GEO database with ID no GSE152614.

Real-Time Polymerase Chain Reaction

For validation of RNA-Seq data and expression analysis of other genes, quantitative real-time PCR (qRT-PCR) was performed on RNA obtained from all the biological replicates belonging to green and yellow seeds used for RNA sequencing. For all RNA samples, the first-strand cDNA was synthesized using the Thermo Scientific RevertAid Kit according to the manufacturer's protocol. qRT-PCRs were completed with the SYBR Green Premix system (Newbio Industry) and gene-specific primers using the CFX Connect™ real-time PCR detection system (BIO-RAD, Hercules, CA). The expression profiles of all genes were analyzed, with Actin7 (AT5G09810) as the constitutive gene for normalization. PCR conditions were as follows 95°C for 1 min, for 44 cycles at 95°C, 12 s, 60°C, 30 s and 72°C, 30 s. After cycling, the melting curves of the reaction were run from 55°C to 95°C. Relative expression was calculated with the software LINREG, as described by Ling et al. (2017).

Statistical Analysis

Each experiment was performed in triplicate except otherwise stated. All data are expressed as the means ± SDs. A Student's *t*-test was used to interpret the differences among the data. Differences between groups were considered to be statistically significant at $p \leq 0.05$.

RESULTS AND DISCUSSION

Oil Concentrations Are Moderately Reduced in Mature Seeds Lacking Photosynthetic Capacity

In this study, we used the Arabidopsis chlorophyll synthase knockout mutant Atchlsyn1-1 complemented with the Arabidopsis chlorophyll synthase cDNA linked to a DsRed fluorescent protein marker (Zhang et al., 2015; **Supplementary Figures S1A,B**). This system allowed us to distinguish seeds in individual siliques segregating for lack of chlorophyll (non-photosynthetic) from those with chlorophyll (photosynthetic), which also fluoresced red from the DsRed marker. This system was advantageous for our studies because photosynthetic and non-photosynthetic seeds could be readily identified at the very earliest stages of seed development and dry seeds. For these experiments, we used two independent complemented lines of Atchlsyn1-1 designated "CHLSYN7" and "CHLSYN8" (**Supplementary Figures S1A–C**). To understand the effects of loss of photosynthetic capacity, we measured seed biomass, oil and protein contents, and fatty acid composition in non-photosynthetic and photosynthetic dry seeds (40 DAF). Seed weight was reduced by ~8% in non-photosynthetic (non-red) seeds compared to the complemented photosynthetic (red) seeds (**Figure 1A**). FA amount in seeds were significantly reduced by ~20% (**Figure 1B**) and protein amount in seeds were ~6% lower in non-photosynthetic seeds relative to photosynthetic seeds (**Figure 1C**). The only significant difference in fatty acid composition between these seeds was a reduction in linoleic acid content from 29% of total fatty acids in photosynthetic seeds to 25% in non-photosynthetic seeds (**Figure 1D**). We suspect the reduction in C18:2 could result from lack of photosynthesis which could limit the lengthening of fatty acid chain in the non-photosynthetic seeds during development. Overall, non-photosynthetic seeds accumulated ~80% of oil relative to photosynthetic seeds at maturity.

Non-photosynthetic Seeds Display Significantly Reduced Oil Content During Early Seed Development

In many photosynthetic organisms, previous studies have linked photosynthesis activity to chlorophyll concentrations (De La Harpe et al., 1979; Kura-Hotta et al., 1987; Gratani et al., 1998; Lodish et al., 2000; Baker and Oxborough, 2004; Govindjee, 2004; Raven et al., 2005), These studies indicated that chlorophyll is essential for photosynthesis because of the porphyrin ring of Chl-a and b that interacts directly in the light requiring reactions of photosynthesis. In the present study, we found that the non-photosynthetic seeds at early developmental stages had no residual chlorophyll pigment and chlorophyll levels were also not detectable in these seeds by our method (see **Supplementary Figure S1**; Zhang et al., 2015). We next explored the stages of seed development that are most affected in seed oil accumulation in the non-photosynthetic seeds. For these studies, we measured oil and chlorophyll content in seeds over a time course of 6 DAF to maturity (**Figure 2**). In wild-type seeds, oil content increased over seed development, while chlorophyll concentrations were highest at 8 DAF and declined gradually at 16 DAF to <5% of 8 DAF concentrations (**Figure 2A**). Of note, no significant differences in chlorophyll content were observed during development in seeds of complemented Atchlsyn1-1 plants compared to those of wild-type plants (**Supplementary Figure S2**). Seeds lacking chlorophyll had

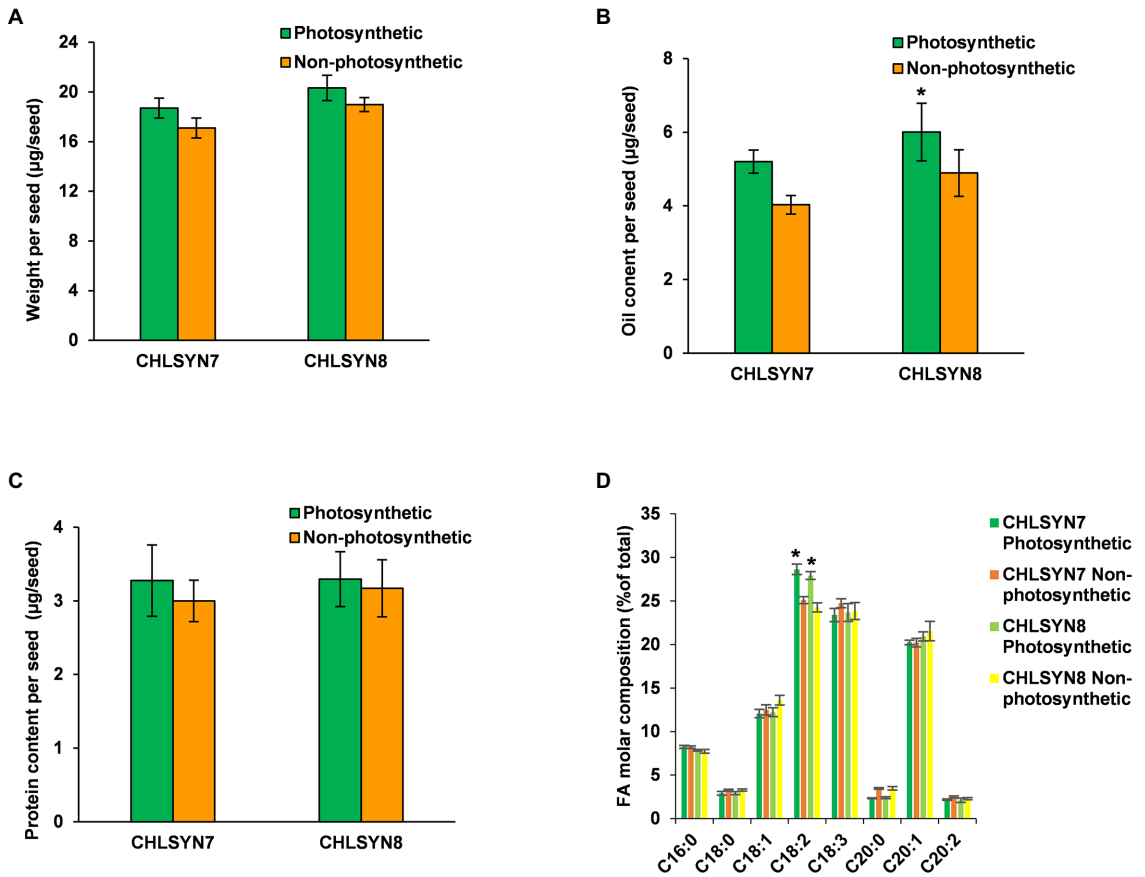

FIGURE 1 | Analyses of seed biomass, oil, and protein contents. **(A)** Comparison of seed weight in photosynthetic, green seeds (red) and non-photosynthetic, yellow seeds (non-red) from two (CHLSYN7 and CHLSYN8) independent Atchlsyn1-1/CHLSYN lines. **(B)** FAMEs analysis of seed oil content of red/green (photosynthetic) seeds and, non-red/yellow (non-photosynthetic) seeds from two independent mutant lines CHLSYN7 and CHLSYN8, respectively. **(C)** Comparison of red/green (photosynthetic) seeds and, non-red/yellow (non-photosynthetic) seeds protein content in two independent complemented lines, CHLSYN7 and CHLSYN8. The two independent lines are represented by orange and green bars, respectively. **(D)** Fatty acid composition of seed wildtype and mutant seeds. Orange and cyan bar indicates green (photosynthetic) and yellow (non-photosynthetic) seeds of CHLSYN7, yellow and light-green bar indicates green (photosynthetic) and yellow (non-photosynthetic) seeds from CHLSYN8, respectively. Values are means ± SD ($n = 3$ biological replicates). Statistical significance was analyzed using the two-sided Student's *t*-test. The asterisk indicates a significant difference (*$p < 0.05$).

significantly lower oil content than that of wild-type seeds at 8 DAF, but oil content increased to 80% of wild-type oil content by 40 DAF (**Figure 2B**).

To better understand how seed photosynthesis affects oil accumulation during development, we examined the ultrastructural characteristics of oil bodies of developing (8 and 12 DAF) and dry seeds (40 DAF) from non-photosynthetic, yellow/non-red and photosynthetic, and green/red seeds at different stages of development (**Figure 3**; **Supplementary Figure S3**). TEM analysis showed that the developing embryos cotyledons from non-photosynthetic yellow/non-red seeds had fewer and small oil bodies compared to the embryos cotyledons from the photosynthetic, green seeds at the early stages of 8 and 12 DAF (**Figures 3A–F**). Also, the percentage area covered by oil bodies was significantly lower ($p \leq 0.05$) in the non-photosynthetic, yellow sheds when compared to the photosynthetic, green seeds (**Figures 3C,F**). Remarkably, there were no observable differences in the oil bodies of embryos cotyledons from photosynthetic and non-photosynthetic dry seeds (**Figures 3G–I**), the percentage area of the oil-bodies (dark regions of g and h) observed in embryos in these seeds at maturity was not significantly different ($p > 0.05$; **Figure 3I**).

Overall, these findings indicate that lack of chlorophyll which inhibited seed-photosynthesis in these Arabidopsis seeds largely affects oil accumulation during early development, and another sources of reductant supply largely support these requirements for oil production during subsequent developmental stages both in yellow and green seeds.

Quantification of Photosynthetic Organs Contribution to Total Oil Production in Arabidopsis Seeds

In this study, we have shown that seed photosynthesis is important for oil deposition during early development as seen in the delay of oil accumulation (**Figure 2**) and in total accounts

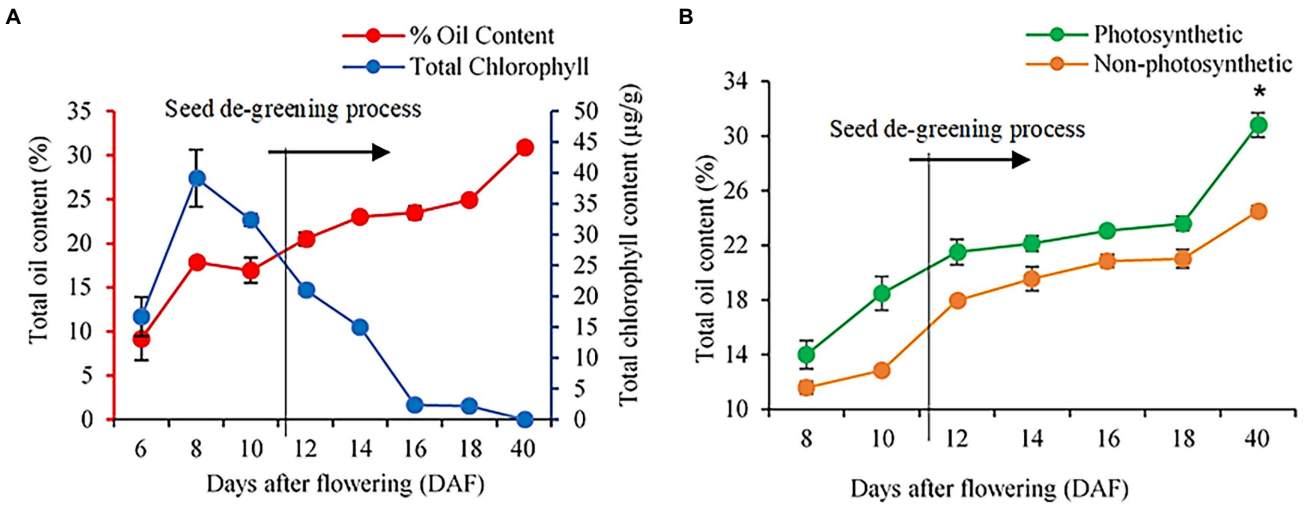

FIGURE 2 | Analysis of seed oil and chlorophyll content in WT and Atchlsyn1-1 mutant during development. **(A)** Biochemical estimation of total FAs and chlorophyll content in WT. Oil content is on the left or the primary Y-axis and chlorophyll content is on the right or secondary Y-axis. **(B)** The seed oil content of seeds from photosynthetic, green seeds (red), and non-photosynthetic, yellow (non-red) seeds. Blue lines indicate WT seed chlorophyll content. The Red line indicates WT seed oil content. The green line indicates photosynthetic, green/(red) seed oil content. The orange line indicates non-photosynthetic, yellow/(non-red) seed oil content. Values are means ±SD ($n = 3$ biological replicates). Statistical significance was analyzed using the two-sided Student's *t*-test. The asterisk indicates a significant difference ($*p < 0.05$).

for ~20% of total FA for Arabidopsis seeds (**Figure 1**). To examine the organ photosynthetic source for the remaining 80% of FA in Arabidopsis seeds, we shaded siliques of wild-type Arabidopsis over their entire development to completely block light penetration (**Supplementary Figure S4**). Dry seeds from shaded siliques had a ~40% reduction in weight relative to those from unshaded control siliques (**Figure 4A**). Seed oil content was reduced by ~59% (**Figure 4B**) and protein content was decreased by ~50% (**Figure 4C**) in seeds from shaded siliques compared to those from unshaded siliques. The most significant changes in fatty acid composition in seeds from shaded siliques versus unshaded siliques were an increase in oleic acid (18:1) and linoleic acid (18:2) balance by decrease in relative amounts of linolenic acid (18:3) and eicosenoic acid (20:1; **Figure 4D**). Here, it is likely that shading could lead to low oxygen levels in the silique which may contribute to the significant reduction observed in seed weight and oil content. Also, blocking photosynthesis through shading in developing seeds, could limit carbon, cofactors, and reductants supply required for *de novo* fatty acid biosynthesis and possibly inhibited elongation of fatty acid chains in the shaded seeds resulting in variation in the proportions of fatty acids in shaded compared to unshaded. Nevertheless, by combining these results with those from Atchlsyn1-1 plants, we derived that silique photosynthesis contributes to ~40% of the seed oil biosynthesis and storage versus ~20% from seed photosynthesis (**Figure 4E**). By inference, leaf and stem photosynthesis contribute to the remaining 40% of seed oil production and accumulation (**Figure 4F**). Considering that seeds are attached to siliques, we conclude that photosynthetic products coming from the silique seems to be the most important contributor to seed oil production.

Comparative Analysis of Pyridine Nucleotides and ATP Levels of Photosynthetic and Non-photosynthetic Seeds

Cellular energy and reductant supply play a significant role in the overall plant physiology, including the production of seed storage reserves (Agrawal and Calvin, 1971; Wakao et al., 2008; Chen and Shachar-Hill, 2012; Carey et al., 2020). Photosynthesis provides both carbon source and reducing power directly for FA synthesis, and we have shown that seed-photosynthetic reductant supply is critical for seed oil production particularly at the early stages of development (**Figures 2**, **4**). We next aimed to identify reducing power sources in seeds where photosynthetic capacity is absent and to clarify the metabolic consequence of lack of seed-photosynthesis-derived reducing power to seeds oil content during early stages of seed development. For these studies, we performed targeted LC–MS/MS-based quantification of the pool sizes of cofactors associated with fatty acid biosynthesis and storage and central metabolism in photosynthetic and non-photosynthetic seeds at 8 and 10 DAF (see Materials and Methods section, **Figure 5**; **Supplementary Table S1**). ATP, ADP, NADH, NAD, NADP, and NADPH levels were quantitatively determined, and their ratios estimated as a parameter for measuring seed cellular energy status (**Figure 5**).

We observed significant changes in ATP levels in photosynthetic, and non-photosynthetic, seeds at 8 DAF (**Figure 5A**). ADP concentrations in non-photosynthetic seeds were significantly lower compared to ADP levels in photosynthetic seeds (**Figure 5B**) but were 2-fold higher than ATP. At 10 DAF, ATP levels in non-photosynthetic, seeds change little from concentrations at previous time points, but ATP pool size

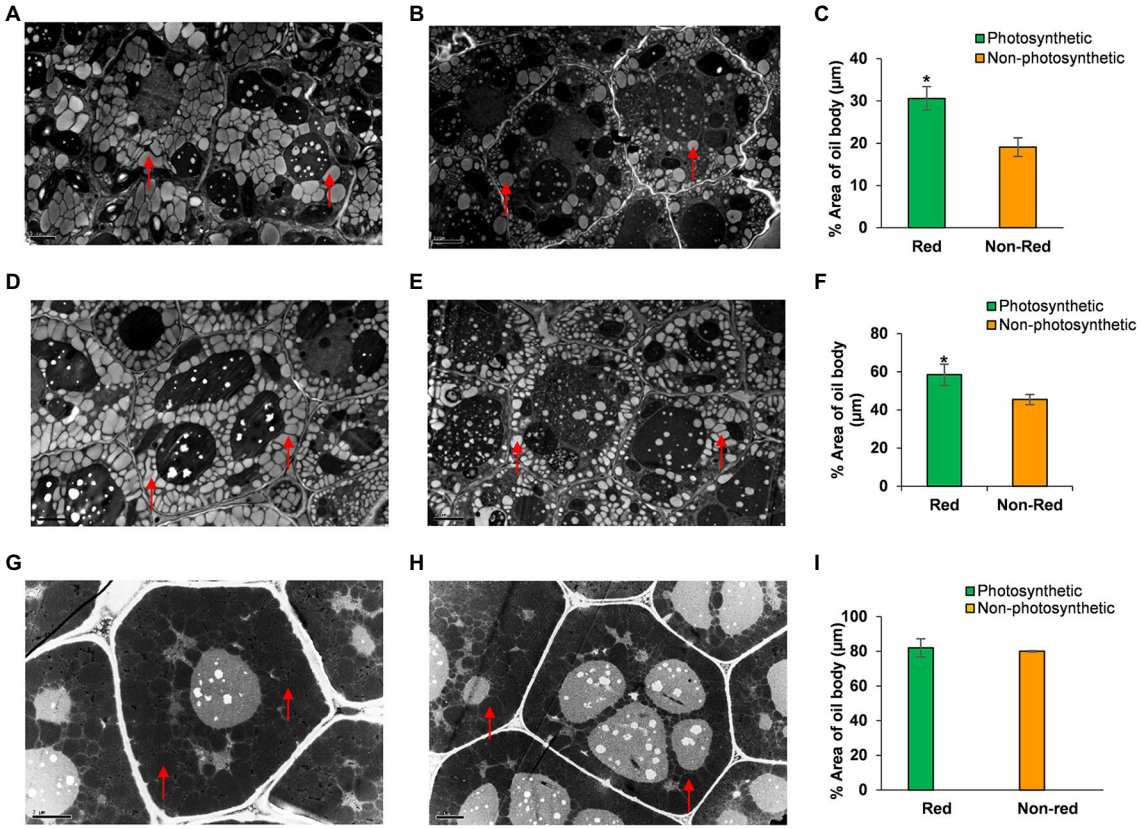

FIGURE 3 | TEM analysis of oil bodies of embryos cotyledons from the same silique of Arabidopsis chlorophyll synthase mutant line CHLSYN7. **(A)** Section of developing embryos from photosynthetic, green(red) seeds at 8 DAF. **(B)** Section of developing embryos from non-photosynthetic, yellow(non-red) seeds at 8 DAF. **(C)** Percentage area of oil bodies per cell of embryos from photosynthetic, green/(red) and non-photosynthetic yellow(non-red) seeds at 8 DAF. **(D)** Section of developing embryos from photosynthetic, green(red) at 12 DAF. **(E)** Section of developing embryos from non-photosynthetic, yellow(non-red) seeds at 12 DAF. **(F)** Percentage area of oil bodies per cell of embryos cotyledons from photosynthetic, green/(Red) and non-photosynthetic, yellow (Non-red) seeds at 12 DAF. **(G)** Section of embryos from dry seeds (Red). **(H)** Section of embryos from dry non-red seeds. **(I)** Percentage area of oil bodies per cell of embryos cotyledons from dry seeds (40 DAF) red and non-red. Red triangles indicate the oil body. Green and orange bars indicate red and non-red seeds of CHLSYN7 seeds. Scale bar = 2 µm. Values are means from 5 to 6 section obtained from three replicates. Statistical significance was analyzed using the two-sided Student *t*-test. The asterisk indicates a significant difference (*$p < 0.05$).

decreased significantly in photosynthetic seeds. At the same time, ADP concentrations in non-photosynthetic seeds were significantly lower compared to ADP concentrations in photosynthetic, green seeds which were 1.7-fold higher than ATP. The changes observed in ADP concentrations (**Figures 5B,C**) resulted in a higher ratio of ATP in non-photosynthetic seeds, when compared to control (**Figure 5C**). Here, the 2-fold increase in the ATP/ADP ratio in non-photosynthetic seeds indicates that these seeds utilized less energy than the photosynthetic green seed. This result seems consistent with the reduction in seed biomass and protein contents in non-photosynthetic seeds (**Figures 1**, **4**). Because ATP is an essential cofactor that drives various cellular biochemical processes in living organisms (Bonora et al., 2012), it seems that inhibition of photosynthesis in non-photosynthetic seeds probably abolishes ATP- and reductant-dependent cellular metabolism, which could have limited the ATP consumption by the cellular metabolism, resulting in accumulation of ATP or an increased ATP/ADP ratio.

Substrate level phosphorylation in the plastid or mitochondria could impact energy production (ATP) through NADH generation (Agrawal and Calvin, 1971; Alberts et al., 2002; Voon et al., 2018). In this study, the NADH levels at 8 DAF in photosynthetic and non-photosynthetic seeds were not significantly different but was slightly reduced in non-photosynthetic seeds (**Figure 5D**). At 10 DAF, NADH levels was significantly lower in non-photosynthetic seeds compared to photosynthetic seeds (**Figure 5D**). The NAD concentrations at 8 and 10 DAF in photosynthetic and non-photosynthetic seeds were not significantly different, but consistently reduced in non-photosynthetic, seeds, which resulted in a low NADH/NAD ratio in both seeds at the time points (**Figures 5E,F**). In photosynthetic seeds, the NADH/NAD ratio increased between 8 and 10 DAF. This increase may be supported by photosynthesis and is important for developing photosynthetically active embryos or transition from the globular to heart stage embryos, during which chloroplast development is enhanced and perhaps required for future accumulation of

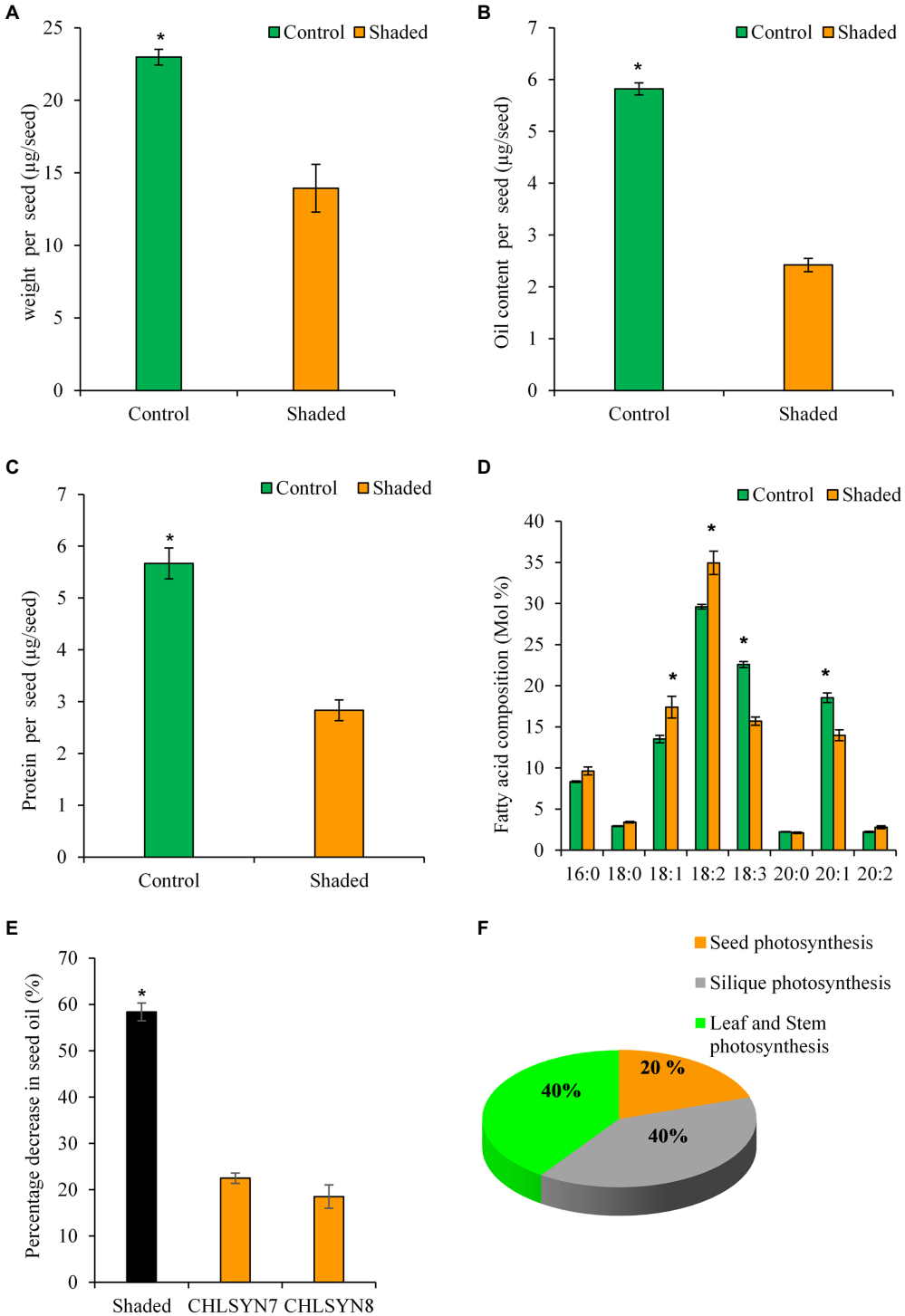

FIGURE 4 | Photosynthetic organ contribution to total oil production in seeds. **(A)** Analysis of the weight of dry shaded and control seeds (40 DAF). **(B)** The total oil content of dry shaded and control seeds. **(C)** The protein content of dry shaded and control seeds. **(D)** Fatty acid composition of shaded and control seeds. **(E)** The relative decrease in oil content per plant. **(F)** Contribution of different photosynthetic tissues to seed oil production (seed chlorophyll ± error = 1.53, silique chlorophyll ± error = 1.97). Values are means ± SD ($n = 3$ biological replicates). Green and orange bars indicate control and shaded. Statistical significance was analyzed using the two-sided Student's *t*-test. The asterisk indicates a significant difference (*$p < 0.05$).

lipids. On the other hand, in the non-photosynthetic seeds, the NADH/NAD ratio did not increase as seen in the photosynthetic seeds. Because of inhibition of seed photosynthesis in the chloroplasts in non-photosynthetic seeds, the cellular redox state could not be maintained as high as in photosynthetic seeds.

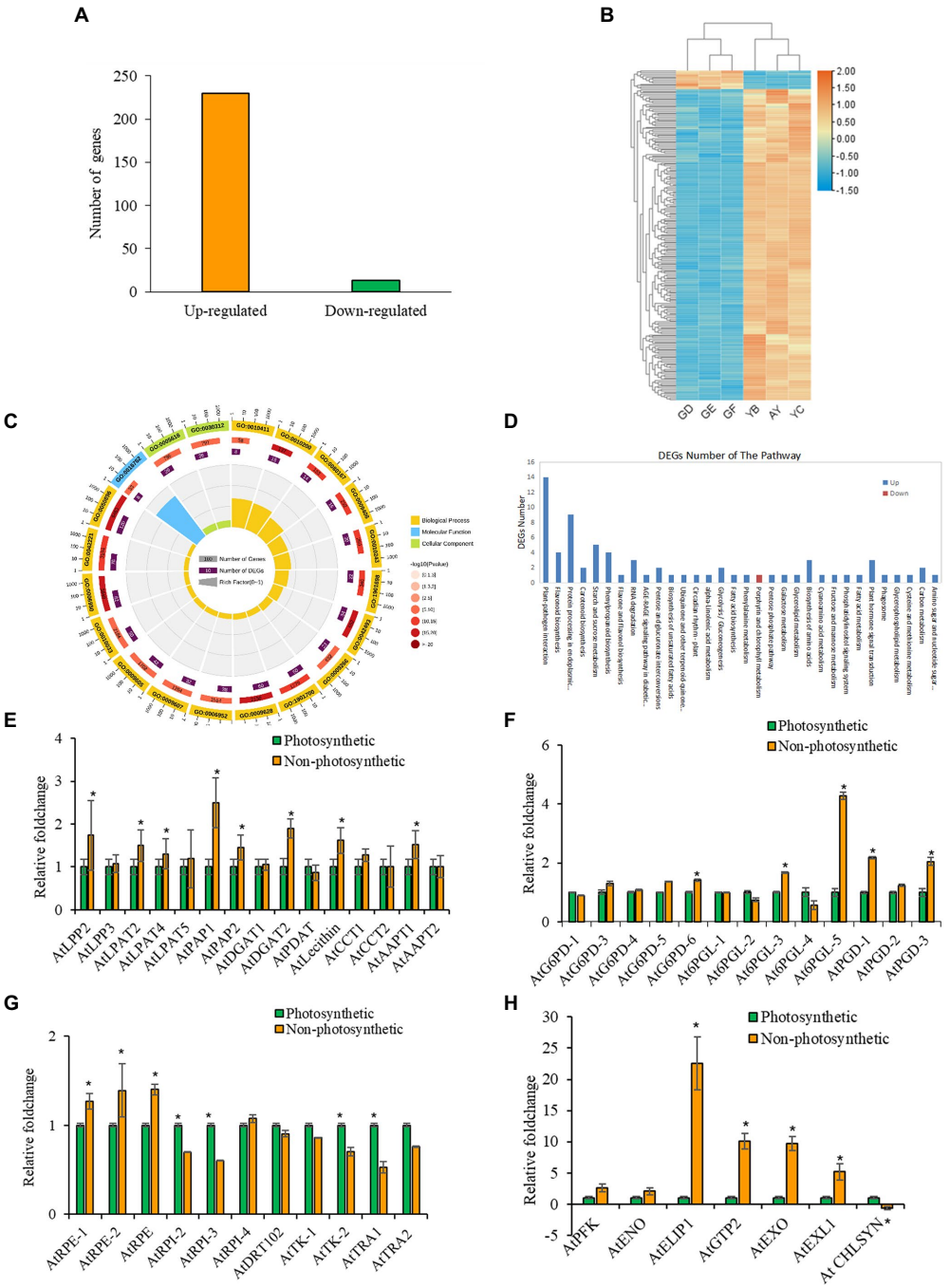

FIGURE 5 | Gene expression analysis of developing yellow and green seeds at 10 DAF. **(A)** Number of DEGs in the non-photosynthetic background. **(B)** Heat map showing expression profile of DEGs. **(C)** Showing the GO classification of DEGs in the non-photosynthetic background. **(D)** Differentially enrich pathways of DEGs in the non-photosynthetic background. **(E)** Real-time PCR analysis of TAG biosynthetic pathway genes. **(F)** Differentially expressed gene of the cytosolic and plastic branch of the oxidative pentose phosphate pathway. **(G)** Non-oxidative pentose phosphate pathway. **(H)** Sugar transport. Green and yellow bars indicate photosynthetic green seeds and non-photosynthetic seeds. Values are means ±SD ($n = 3$ biological replicates, i.e., GD, GE, GF are three replicated biological samples belonging to green seeds. While YB, YA, YC are three replicated biological samples of yellow seeds). Statistical significance was analyzed using the two-sided Student *t*-test. The asterisk indicates a significant difference (*$p < 0.05$).

Photosynthesis and the oxidative pentose phosphate pathway are the primary source of NADPH in the plastid, and NADPH supply and utilization are closely linked to FA biosynthesis (Agrawal and Calvin, 1971; Randhir, 1998; Alberts et al., 2002; Andriotis et al., 2010; Andriotis and Smitha, 2019; Carey et al., 2020). In this study, the NADPH levels in photosynthetic and non-photosynthetic seeds were comparable at 8 DAF (**Figure 5G**). The same levels of NADP concentration were also observed in

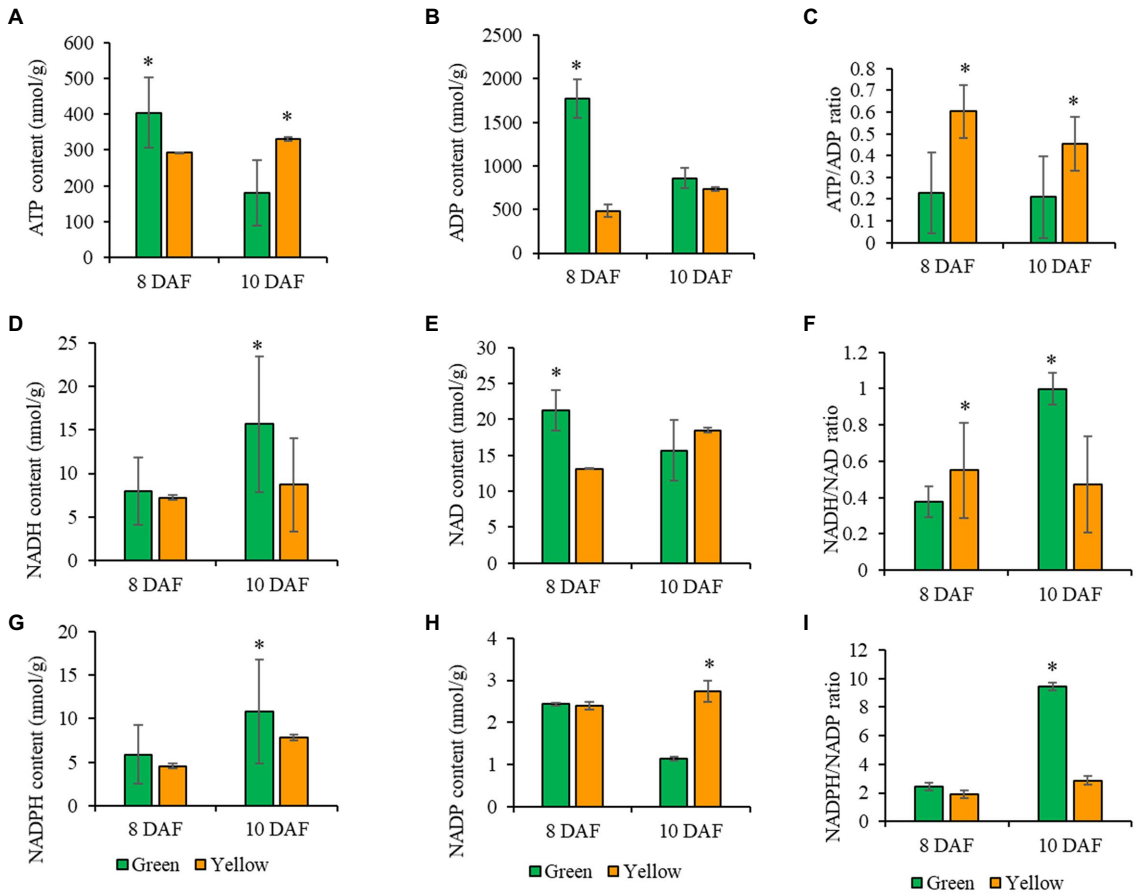

FIGURE 6 | Measurement of pyridine nucleotides and ATP analyses of photosynthetic and non-photosynthetic seeds at 8, and 10 DAF. **(A)** ATP content. **(B)** ADP content. **(C)** ATP/ADP ratio. **(D)** NADH content. **(E)** NAD content. **(F)** NADH/NAD ratio. **(G)** NADPH content. **(H)** NADP content. **(I)** NADPH/NADP ratio. Green bar represents photosynthetic seeds, and the orange bar represents non-photosynthetic seeds. Values are means ± SD ($n = 3$ biological replicates). Statistical significance was analyzed using a two-sided Student *t*-test. The asterisk indicates a significant difference ($*p < 0.05$).

photosynthetic and non-photosynthetic seeds at 8 DAF (**Figure 5H**). At 10 DAF, NADPH content decreased by almost 2-folds in non-photosynthetic seeds compared to photosynthetic, green seeds. Whereas NADP concentrations increased by over 2-folds opposite to photosynthetic green seeds (**Figure 5H**). In photosynthetic seeds, the NADPH/NADP ratio increased remarkably between 8 and 10 DAF. This increase is probably due to photosynthetic activity in photosynthetic seeds. Oppositely, in the non-photosynthetic seeds, such increase in NADPH/NADP ratio was totally abolished, indicating significant utilization of reductants for biosynthetic cellular activities (**Figures 5G–I**). In the present study, it is likely that the OPPP underpinned the NADPH/NADP ratio observed in non-photosynthetic seeds. To conclude, we hypothesize that the OPPP might play a dominant role in the supply of NADPH over seed photosynthesis in Arabidopsis seeds.

Gene Expression Studies Provide Clues to Other Pathways of Reductant Supply in Seeds

To gain insights into the transcriptional responses to lack of seed photosynthesis and the genes and pathways involved in the supply of carbon and reducing power (NADPH and ATP) at the early stage of seed development, mRNA-sequencing and qPCR-based genes expression studies were conducted with non-photosynthetic and photosynthetic seeds at 10 DAF (**Figure 6**; **Supplementary Figures S5–S8**; **Supplementary Tables S2–S7**; Supporting Results). The photosynthetic seeds were used as control. The results of RNA-Seq data preprocessing and read alignment are reported in (**Supplementary Tables S2–S6**; **Supplementary Figure S5**). Significant changes ($p < 0.01$, FDR = 0.05, log2FC > 1) in gene expression was detected among 230 genes between the non-photosynthetic and photosynthetic seeds (**Figures 6A,B**). About 94% of these genes were up-regulated and 6% were down-regulated in the pairwise comparison of yellow and green seeds transcripts (Y/G) as shown in **Figure 6A**. Gene ontology (GO) analysis showed that 177 genes were assigned to the biological process category, 171 genes were assigned to molecular functions and 193 genes were assigned to the cellular component organization (**Supplementary Figures S6, S7**; **Figure 6C**). The DEGs were broadly classified into cellular processes, environmental information processing, genetic information processing,

metabolism and organismal systems of KEGG pathways (**Supplementary Figure S7**; **Figure 6D**). The plant-pathogen interaction, flavonoid biosynthesis, protein processing in the endoplasmic reticulum, carotenoid biosynthesis and starch and sucrose metabolism pathways were significantly enriched ($p < 0.05$; **Figure 6D**; **Supplementary Figure S7**). The complete result of GO, clusters of orthologous groups (COG) function classification and KEGG Pathway enrichment analysis (FDR < 0.05, $p < 0.01$) are reported in **Supplementary Figures S6**, **S7**.

Further analysis of our RNA-seq data focused on the activity of gene transcripts encoding enzymes involved in expenditure and generation of reducing power. For gene functions related to the expenditure of NADPH, RNA-seq data in agreement with qPCR analysis showed that genes involved in TAG biosynthetic (LPP2, LPAT2, ATPAP1, PAP1, GDSL-motif esterase, FTM1, and PLIP1) and elongation (AT2G17845 and AT2G37540 coding for NAD(P)-binding Rossmann-fold superfamily protein, and KCR2) were significantly induced in the non-photosynthetic seeds (**Figure 6E**; **Supplementary Table S5**).

A similar trend was observed in the expression of genes coding for proteins involved in polysaccharide and protein synthesis and metabolism. For instance, we found 15 genes involved in xyloglucan biosynthesis significant up-regulation in non-photosynthetic seeds (**Supplementary Tables S5** and **S6**). Similarly, 33 genes involved in nitrogen compound metabolism were positively induced, in addition to several transcription factors (**Supplementary Tables S5** and **S6**). Together, the seed photosynthetic supply of reducing power is necessary for the normal expression of these genes, given their altered expression in the non-photosynthetic seeds. Moreover, biosynthesis of complex polysaccharides from glucose, and the polymerization of amino acids to form proteins comes at the cost of reducing power (Copper and Hausman, 2016; Heldt and Piechulla, 2016). Because these genes mentioned above are not directly related to the making of reducing power, we propose that they are seed photosynthesis responsive genes.

The glycolysis, oxidative pentose phosphate (OPPP) and tricarboxylic acid cycle (TCA) pathways are primarily associated with the generation of reducing power (Rolletschek et al., 2012; Stincone et al., 2015). Although the initial steps of glycolysis are ATP-dependent, the later reactions provide 2 ATP and 2 NADPH. The OPPP usually gives 2 NADPH per glucose unit, and TCA accounts for about 24 ATP and 4 NADH molecules (Mustroph et al., 2007; Kim et al., 2012; Rolletschek et al., 2012; Stincone et al., 2015). Exploring the transcriptional profile of genes functionally related to the glycolytic pathway in the non-photosynthetic seeds revealed phosphofructokinase 3 (PFK3) and Enolase 1 (ENO1; Mustroph et al., 2007; Prabhakar et al., 2010; Kim et al., 2012) were positively induced. We also observed a significant induction of 13 oxidoreductase genes, perhaps involved in either electron cycling, cellular homeostasis, or reduction of other compounds that may be related to the generation of reducing power. Equally, we detected a general increase in the expression level of several genes (G6PDs, 6-PGLs, PGDs, and RPE isoforms) belonging to the oxidative and non-oxidative branch of the Pentose phosphate pathway in the non-photosynthetic seeds compared to photosynthetic, green seeds which were confirmed by qPCR analysis (**Figures 6F,G**). Also, we confirmed the significant induction of the GTP2 gene (RNA-Seq FC = 3.2), a plastidic glucose-6-phosphate transmembrane transporter linked to the OPPP, was more than 3-folds higher in the non-photosynthetic than the photosynthetic, green seeds (**Figure 6F**). Furthermore, the analysis of the gene interaction network provided mechanistic clues that supported role of GTP2 (Niewiadomski et al., 2005; Athanasiou et al., 2010; Araújo et al., 2012) and the link to OPPP as major pathway for NADPH supply in non-photosynthetic seeds (Supporting Results; **Supplementary Figure S8**; **Supplementary Table S5**). In addition to other induced genes that may play role in the adjustment to carbon (C)- and energy-limiting growth conditions in the yellow seeds such as ELIP1, EXO EXL1 genes (**Figure 6H**; Hutin et al., 2003; Schroder et al., 2012). In this study, we confirmed that non-photosynthetic seeds were able to coordinate pathways capable of generating reducing power to support primary cellular function (**Figures 6D,E**). Here, we propose that OPPP might supply the reducing equivalent required to maintain FA biosynthesis in non-photosynthetic seeds, including the provision of ribose 5-phosphate for nucleotides synthesis (Kammerer et al., 1998; Niewiadomski et al., 2005; Copper and Hausman, 2016; Heldt and Piechulla, 2016). However, further studies are required to test these theories at the post-transcriptional and translational level of gene regulation.

CONCLUSION

For many decades, the potential contribution of photosynthesis-derived reductant for fatty acid biosynthesis in green seeds have remained unresolved. By using mutants impaired in chlorophyll synthesis and silique shading experiments; coupled with the measurement of seed oils and oil body ultrastructure, our estimates indicate that reductants derive primarily from photosynthesis in silique (40%) and leaf/stem (40%) compared to seed (20%) make the biggest contribution to FA biosynthesis in green seeds. Our interpretation of these findings is that photosynthetic products imported into the seed from the silique and/or leaf/stem are probably the most important source of carbon and reducing power for seed oil production. Our conclusions are in alignment with early studies that suggest that increase supply of carbon substrates may underpin the synthesis of storage compounds in seeds in which photosynthesis is limited (Wakao et al., 2008).

The role of light and seed photosynthesis in FA accumulation in rapeseed, Arabidopsis, and soybean were proposed based on previous measurements of biosynthetic flux and energy balances in growing embryos *in vitro* (Quebedeaux and Chollet, 1975; Fuhrmann et al., 1994; Ruuska et al., 2004; Goffman et al., 2005; Allen et al., 2009; Zhang et al., 2015). However, genetic evidence from the present work and other studies demonstrates that seed photosynthesis may not be the sole source of carbon and reducing power supporting FA biosynthesis

and accumulation in Arabidopsis seeds (Borisjuk et al., 2005; Rolletschek et al., 2005; Wakao et al., 2008; Borisjuk and Rolletschek, 2009) but makes a modest contribution which is important especially at the early stage of seed development (**Figures 2–4**). Here, we have confirmed an inverse relationship between seed photosynthesis and oil biosynthesis/accumulation (**Figure 2A**), and the pyridine nucleotides and ATP analyses show that without photosynthesis cellular NAD(P)H/NAD(P) levels cannot be maintained high enough to support FA and lipid synthesis at the early stage of seed development (**Figure 6I**). Nevertheless, we speculate that oxidative pentose phosphate pathway (OPPP) supplied reductant for *de novo* fatty acid biosynthesis in non-green mutant seeds used in this study (**Figures 1–3**, **6**) which is in agreement with preliminary observations from the characterization of PGL5 (cytoplasmic) and PGL3 (Chloroplastic) mutant seeds (Unpublished data).

Also, our transcriptomic studies implied increased carbon import into the non-photosynthetic seed plastid possibly from other photosynthetic tissues, as seen in the significant up-regulation of key genes of polysaccharide metabolism, and interactions with other pathways that could support the overall growth and development of non-photosynthetic embryo particularly genes involved in cellular homeostasis and adjustment to carbon and energy limiting condition, i.e., ELIP1, EXO and EXL1 (**Figure 5H**). Here, we uncovered another dimension in the transcriptional response to the general lack of chlorophyll in these seeds early in development, which involved coordinated action of several transcription factors, induction of many heat stress response genes, in addition to redox-stress responsive genes and carbohydrate catabolism, and sugar transport (**Figure 5**; Supporting Results; **Supplementary Figure S8**; **Supplementary Table S7**). For example, we observed the positive induction of GBSS1, APL4, DPE2 genes including GTP2 in the RNA-Seq data and qRT-PCR revealed the up-regulation of several OPPP enzymes in the non-photosynthetic seeds (see Supporting Results; **Supplementary Figure S8**; **Figure 5**). Therefore, it is likely that up-regulation of genes primarily involved in carbohydrate biosynthesis, metabolism and transport supported metabolism and translocation of carbon sources needed for *de novo* FA biosynthesis in the yellow seed. However, more experiment is needed to verify the enzyme activity of OPPP genes to further confirm their role in supply of reducing power in green developing seeds.

Nevertheless, taken all our results together, we propose a model for the supply of reducing power for FA biosynthesis in developing green seeds at the early stages of development (**Figure 7**). In this model, imported carbon could account for the reductant supply in non-green seeds that accumulated ~80% of wildtype oil (**Figure 1**). As shown in **Figure 3**, the few oil bodies observed in the non-photosynthetic seeds at the early developmental stage may be due to lack of seed photosynthesis, or that the lack of photosynthesis abolished the carbon fixation and, therefore, carbon supply from translocation could be the sole source of carbon and energy. Glycolysis and OPPP are important for the utilization of imported carbons for ATP and reductant generation, and in non-photosynthetic seeds, the production of reductants seems limited compared with photosynthetic seeds, it is likely therefore the available reductants were selectively utilized for the maintenance of basic metabolism supporting development. Thus, cellular reductants could be not efficiently used for FA biosynthesis, resulting in decreased lipid deposition in 8–10 DAF embryos.

Finally, by exploring the chlorophyll synthase gene in Arabidopsis, our study provides the first genetic framework

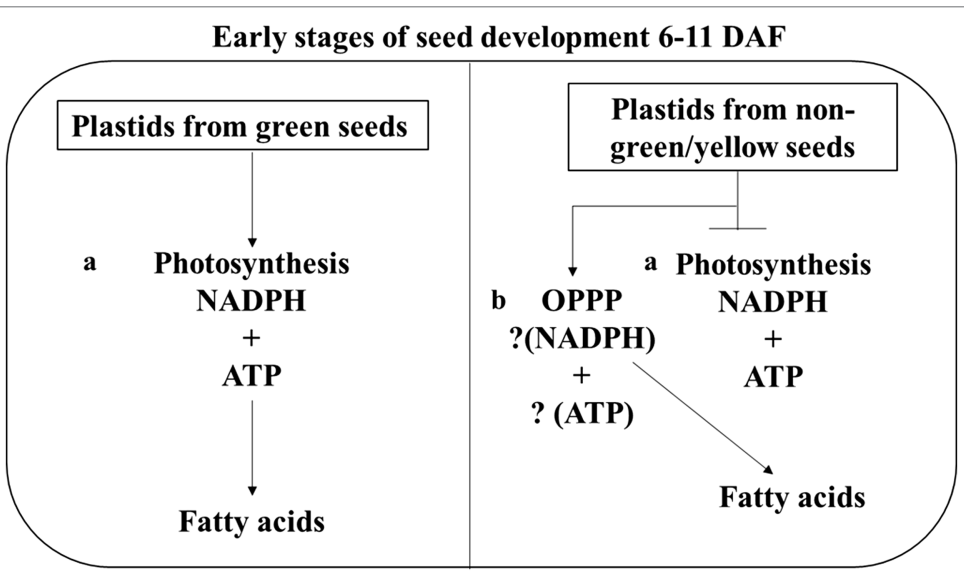

FIGURE 7 | Proposed model of reductant supply for FA biosynthesis seed. This model shows that green developing seeds have two pathways for generating NADPH for FA synthesis during seed development. i.e., **(A)** Photosynthesis **(B)** Oxidative pentose phosphate pathway (OPPP). Six to eleven days after flowering were chosen because seeds de-greening starts at 11 DAF.

for the genetic investigation of sources of reducing power required for *de novo* FA biosynthesis in agriculturally important crops. Similarly, our findings lay the foundation for further studies on the specific role of OPPP in different cellular compartments and how they contribute reducing power for seed oil production in green seeds throughout development. This knowledge can be useful in guiding future metabolic engineering opportunities for oilseed crops either through the overproduction of NADPH through Photosynthesis and OPPP dedicated to FA biosynthesis in seeds.

DATA AVAILABILITY STATEMENT

The original contributions presented in the study are publicly available. This data can be found here: Gene Expression Omnibus, GSE152614.

AUTHOR CONTRIBUTIONS

CN, DL, EC, and CZ designed the research. CN, DL, PQ, LL, WZ, YuZ, JX, YY, JC, LH, and FX performed the research. CN, LL, CL, and LG analyzed the data. LG, YoZ, EC, and CZ provided research resources and contributed to research conception. CN, EC, and CZ wrote the manuscript. All authors contributed to the article and approved the submitted version.

FUNDING

This project was supported by grants from the National Natural Science Foundation of China (grant no. 31671723) and the China Agriculture Research System (CARS-12) to CZ and National Key Research and Development Plan of China (2017YFE0104800) to YoZ. EC was supported by Hatch Multistate funding from the Nebraska Agricultural Experiment Station.

ACKNOWLEDGMENTS

The authors thank laboratory members and technicians for their contribution in growing the Arabidopsis plant.

SUPPLEMENTARY MATERIAL

The Supplementary Material for this article can be found online at: https://www.frontiersin.org/articles/10.3389/fpls.2022.942054/full#supplementary-material

REFERENCES

Agrawal, P. K., and Calvin, D. T. (1971). The pentose phosphate pathway in relation to fat synthesis in the developing castor oil seed. *Plant Physiol.* 47, 672–675. doi: 10.1104/pp.47.5.672

Alberts, B., Johnson, A., Lewis, J., Raff, M., Roberts, K., and Walter, P. (2002). *Chloroplasts and Photosynthesis. Molecular Biology of the Cell. 4th Edn*. New York: Garland Science.

Allen, D. K., Ohlrogge, J. B., and Shachar-Hill, Y. (2009). The role of light in soybean seed filling metabolism. *Plant J.* 58, 220–234. doi: 10.1111/j.1365-313X.2008.03771.x

Andriotis, V. M., Kruger, N. J., Pike, M. J., and Smith, A. M. (2010). Plastidial glycolysis in developing Arabidopsis embryos. *New Phytol.* 185, 649–662. doi: 10.1111/j.1469-8137.2009.03113.x

Andriotis, V. M. E., and Smith, A. M. (2019). The plastidial pentose phosphate pathway is essential for postglobular embryo development in Arabidopsis. *PNAS* 116, 15297–15306. doi: 10.1073/pnas.1908556116

Araújo, W. L., Nunes-Nesi, A., Nikoloski, Z., Sweetlove, L. J., and Fernie, A. R. (2012). Metabolic control and regulation of the tricarboxylic acid cycle in photosynthetic and heterotrophic plant tissues. *Plant Cell Environ.* 35, 1–21. doi: 10.1111/j.1365-3040.2011.02332.x

Athanasiou, K., Dyson, B. C., Webster, R. E., and Johnson, G. N. (2010). Dynamic acclimation of photosynthesis increases plant fitness in changing environments. *Plant Physiol.* 152, 366–373. doi: 10.1104/pp.109.149351

Baker, N. R., and Oxborough, K. (2004). "Chlorophyll fluorescence as a probe of photosynthetic productivity," in *Chlorophyll a Fluorescence, a Signature of Photosynthesis. Advances in Photosynthesis and Respiration*. ed. G. C. P. Govinjee, *Vol. 19* (Dordrecht: Springer), 65–82.

Bates, P. D., Stymne, S., and Ohlrogge, J. (2013). Biochemical pathways in seed oil synthesis. *Curr. Opin. Plant Biol.* 16, 358–364. doi: 10.1016/j.pbi.2013.02.015

Baud, S., and Lepiniec, L. (2009). Regulation of de novo fatty acid synthesis in maturing oilseeds of Arabidopsis. *Plant Physiol. Biochem.* 47, 448–455. doi: 10.1016/j.plaphy.2008.12.006

Bonora, M., Patergnani, S., Rimessi, A., De Marchi, E., Suski, J. M., Bononi, A., et al. (2012). ATP synthesis and storage. *Purinergic Signal* 8, 343–357. doi: 10.1007/s11302-012-9305-8

Borisjuk, L., Nguyen, T. H., Neuberger, T., Rutten, T., Tschiersch, H., Claus, B., et al. (2005). Gradients of lipid storage, photosynthesis, plastid differentiation in developing soybean seeds. *New Phytol.* 167, 761–776. doi: 10.1111/j.1469-8137.2005.01474.x

Borisjuk, L., and Rolletschek, H. (2009). The oxygen status of the developing seed. *New Phytol.* 182, 17–30. doi: 10.1111/j.1469-8137.2008.02752.x

Cahoon, E. B., Dietrich, C. R., Meyer, K., Damude, H. G., Dyer, J. M., and Kinney, A. J. (2006). Conjugated fatty acids accumulate to high levels in phospholipids of metabolically engineered soybean and Arabidopsis seeds. *Phytochemistry* 67, 1166–1176. doi: 10.1016/j.phytochem.2006.04.013

Cahoon, E. B., Shockey, J. M., Dietrich, C. R., Gidda, S. K., Mullen, R. T., and Dyer, J. M. (2007). Engineering oilseeds for sustainable production of industrial and nutritional feedstocks: solving bottlenecks in fatty acid flux. *Curr. Opin. Plant Biol.* 10, 236–244. doi: 10.1016/j.pbi.2007.04.005

Carey, L. M., Clark, T. J., Deshpande, R. R., Cocuron, J., Rustad, E. K., and Shachar-Hill, Y. (2020). High flux through the oxidative pentose phosphate pathway lowers efficiency in developing camelina seeds. *Plant Physiol.* 182, 493–506. doi: 10.1104/pp.19.00740

Cernac, A., and Benning, C. (2004). WRINKLED1 encodes a AP2/EREB domain protein involved in the control of storage compound biosynthesis in Arabidopsis. *Plant J.* 40, 575–585. doi: 10.1111/j.1365-313X.2004.02235.x

Chen, X., and Shachar-Hill, Y. (2012). Insights into metabolic efficiency from flux analysis. *J. Exp. Bot.* 63, 2343–2351. doi: 10.1093/jxb/ers057

Copper, G. M., and Hausman, R. E. (2016). *Bioenergetics and Metabolism—Mitochondria, Chloroplasts, and Peroxisomes: The Cell A Molecular Approach. 7th Edn.* Oxford University Press.

De La Harpe, A. C., Visser, J. H., and Grobbelaar, N. (1979). The chlorophyll concentration and photosynthetic activity of some parasitic flowering plants. *Z. Pflanzenphysiol.* 93, 83–87. doi: 10.1016/S0044-328X(79)80144-0

Eastmond, P., Kolacna, L., and Rawsthorne, S. (1996). Photosynthesis by developing embryos of oilseed rape (*Brassica napus* L.). *J. Exp. Bot.* 47, 1763–1769. doi: 10.1093/jxb/47.11.1763

Fuhrmann, J., Johnen, T., and Heise, K. P. (1994). Compartmentation of fatty acid metabolism in zygotic rape embryo. *J. Plant Physiol.* 143, 565–569. doi: 10.1016/S0176-1617(11)81825-0

Gan, L., Zhang, C. Y., Wang, X. D., Wang, H., Long, Y., Yin, Y. T., et al. (2013). Proteomic and comparative genomic analysis of two *Brassica napus* lines differing in oil content. *J. Proteome Res.* 12, 4965–4978. doi: 10.1021/pr4005635

Geigenberger, P., Merlo, L., Reimholz, R., and Stitt, M. (1994). When growing potato-tubers are detached from their mother plant there is a rapid inhibition of starch synthesis, involving inhibition of ADP-glucose pyrophosphorylase. *Planta* 193, 486–493. doi: 10.1007/BF02411552

Girish, V., and Vijayalakshmi, A. (2004). Affordable image analysis using NIH Image/Image J. *Indian J. Cancer* 41:47.

Goffman, F. D., Alonso, A. P., Schwender, J., Shachar-Hill, Y., and Ohlrogge, J. B. (2005). Light enables a very high efficiency of carbon storage in developing embryos of rapeseed. *Plant Physiol.* 138, 2269–2279. doi: 10.1104/pp.105.063628

Govindjee. (2004). "Chlorophyll a fluorescence: a bit of basics and history," in *Chlorophyll a Fluorescence, a Signature of Photosynthesis. Advances in Photosynthesis and Respiration*. ed. G. C. P. Govinjee, *Vol. 19* (Dordrecht: Springer), 1–42.

Gratani, L., Pesoli, P., and Crescente, M. (1998). Relationship between photosynthetic activity and chlorophyll content in an isolated *Quercus Ilex* L. Tree during the year. *Photosynthetica* 35, 445–451. doi: 10.1023/A:1006924621078

Guo, L., Ma, F., Wei, F., Fanella, B., Allen, D. K., and Wang, X. (2014). Cytosolic phosphorylating glyceraldehyde-3-phosphate dehydrogenases affect Arabidopsis cellular metabolism and promote seed oil accumulation. *Plant Cell* 26, 3023–3035. doi: 10.1105/tpc.114.126946

Heldt, H. W., and Piechulla, B. (2016). *Plant Biochemistry*. *4th Edn*. London, UK: Academic Press.

Hua, S., Chen, Z. H., Zhang, Y., Yu, H., Lin, B., and Zhang, D. (2014). Chlorophyll and carbohydrate metabolism in developing silique and seed are prerequisite to seed oil content of *Brassica napus* L. *Bot. Stud.* 55:34. doi: 10.1186/1999-3110-55-34

Hutin, C., Nussaume, L., Moise, N., Moya, I., Kloppstech, K., and Havaux, M. (2003). Early light-induced proteins protect Arabidopsis from photooxidative stress. *Proc. Natl. Acad. Sci. USA* 100, 4921–4926. doi: 10.1073/pnas.0736939100

Job, C., Rajjou, L., Lovigny, Y., Belghazi, M., and Job, D. (2005). Patterns of protein oxidation in Arabidopsis seeds and during germination. *Plant Physiol.* 138, 790–802. doi: 10.1104/pp.105.062778

Kammerer, B., Fischer, K., Hilpert, B., Schubert, S., Gutensohn, M., Weber, A., et al. (1998). Molecular characterization of a carbon transporter in plastids from heterotrophic tissues: the glucose 6-phosphate/phosphate antiporter. *Plant Cell* 10, 105–117. doi: 10.1105/tpc.10.1.105

Kim, Y., Kim, E. Y., Seo, Y. M., Yoon, T. K., Lee, W. S., and Lee, K. A. (2012). Function of the pentose phosphate pathway and its key enzyme, transketolase, in the regulation of the meiotic cell cycle in oocytes. *Clin. Exp. Reprod. Med.* 39, 58–67. doi: 10.5653/cerm.2012.39.2.58

Kura-Hotta, M., Satoh, K., and Katoh, S. (1987). Relationship between photosynthesis and chlorophyll content during leaf senescence of rice seedlings. *Plant Cell Physiol.* 28, 1321–1329.

Li-Beisson, Y., Shorrosh, B., Beisson, F., Andersson, M. X., Arondel, V., Bates, P. D., et al. (2010). Acyl lipid metabolism. *Arabidopsis Book* 8:e0133. doi: 10.1199/tab.0161

Ling, J., Li, R., Nwafor, C. C., Cheng, J., Li, M., Xu, Q., et al. (2017). Development of iFOX-hunting as a functional genomic tool and demonstration of its use to identify early senescence-related genes in the polyploid *Brassica napus*. *Plant Biotechnol. J.* 16, 591–602. doi: 10.1111/pbi.12799

Lodish, H., Berk, A., Zipursky, L., Matsudaira, P., Baltimore, D., Darnell, J., et al. (2000). *Molecular Cell Biology*. *4th Edn*. New York: W. H. Freeman.

Lonien, J., and Schwender, J. (2009). Analysis of metabolic flux phenotypes for two arabidopsis mutants with severe impairment in seed storage lipid synthesis. *Plant Physiol.* 151, 1617–1634. doi: 10.1104/pp.109.144121

Lorenz, C., Brandt, S., Borisjuk, L., Rolletschek, H., Heinzel, N., Tohge, T., et al. (2018). The role of persulfide metabolism during arabidopsis seed development under light and dark conditions. *Front. Plant Sci.* 9:1381. doi: 10.3389/fpls.2018.01381

Lu, C., Napier, J. A., Clemente, T. E., and Cahoon, E. B. (2011). New frontiers in oilseed biotechnology: meeting the global demand for vegetable oils for food, feed, biofuel, and industrial applications. *Curr. Opin. Biotech* 22, 252–259. doi: 10.1016/j.copbio.2010.11.006

Mustroph, A., Sonnewald, U., and Biemelt, S. (2007). Characterization of the ATP-dependent phosphofructokinase gene family from *Arabidopsis thaliana*. *FEBS Lett.* 581, 2401–2410. doi: 10.1016/j.febslet.2007.04.060

Niewiadomski, P., Knappe, S., Geimer, S., Fischer, K., Schulz, B., Unte, U. S., et al. (2005). The Arabidopsis plastidic glucose 6-phosphate/phosphate translocator GPT1 is essential for pollen maturation and embryo sac development. *Plant Cell* 17, 760–775. doi: 10.1105/tpc.104.029124

Ohlrogge, J. B., and Browse, J. (1995). Lipid biosynthesis. *Plant Cell* 7, 957–970.

Prabhakar, V., Löttgert, T., Geimer, S., Dörmann, P., Krüger, S., Vijayakumar, V., et al. (2010). Phosphoenolpyruvate provision to plastids is essential for gametophyte and sporophyte development in *Arabidopsis thaliana*. *Plant Cell* 22, 2594–2617. doi: 10.1105/tpc.109.073171

Quebedeaux, B., and Chollet, R. (1975). Growth and development of soybean (*Glycine max* [L.] Merr.) pods. *Plant Physiol.* 55, 745–748. doi: 10.1104/pp.55.4.745

Ramakers, C., Ruijter, J. M., Deprez, R. H. L., and Moorman, A. F. M. (2003). Assumption-free analysis of quantitative real-time polymerase chain reaction (PCR) data. *Neurosci. Lett.* 339, 62–66. doi: 10.1016/S0304-3940(02)01423-4

Randhir, S. (1998). Carbon and energy sources for fatty acid biosynthesis in non-photosynthetic plastids of higher plants. *Fatty Acid Biosynthesis.* SA B64, 335–354.

Raven, P. H., Evert, R. F., and Eichhorn, S. E. (2005). *Photosynthesis, Light, and Life. Biology of Plants*. *7th Edn.* San Francisco: W. H. Freeman, 119–127.

Rolletschek, H., Radchuk, R., Klukas, C., Schreiber, F., Wobus, U., and Borisjuk, L. (2005). Evidence of a key role for photosynthetic oxygen release in oil storage in developing soybean seeds. *New Phytol.* 67, 777–786. doi: 10.1111/j.1469-8137.2005.01473.x

Rolletschek, H., Weschke, W., Weber, H., Wobus, U., and Borisjuk, L. (2012). Energy state and its control on seed development: starch accumulation is associated with high ATP and steep oxygen gradients within barley grains. *Journal of Experimental Botany* 55, 1351–1359. doi: 10.1093/jxb/erh130

Ruuska, S. A., Schwender, J., and Ohlrogge, J. B. (2004). The capacity of green oilseeds to utilize photosynthesis to drive biosynthetic processes. *Plant Physiol.* 136, 2700–2709. doi: 10.1104/pp.104.047977

Schroder, F., Lisso, J., and Müssig, C. (2012). Expression pattern and putative function of EXL1 and homologous genes in Arabidopsis. *Plant Signal. Behav.* 7, 22–27. doi: 10.4161/psb.7.1.18369

Schwender, J., Goffman, F., Ohlrogge, J. B., and Shachar-Hill, Y. (2004). Rubisco without the Calvin cycle improves the carbon efficiency of developing green seeds. *Nature* 432, 779–782. doi: 10.1038/nature03145

Shahid, M., Cai, G., Zu, F., Zhao, Q., Qasim, M. U., Hong, Y., et al. (2019). Comparative Transcriptome analysis of developing seeds and Silique Wall reveals dynamic transcription networks for effective oil production in *Brassica napus* L. *Int. J. Mol. Sci.* 20:1982. doi: 10.3390/ijms20081982

Singh, N., Cairns, P., Morris, V. J., and Smith, A. C. (1998). Physical properties of extruded wheat starch-additive mixtures. *Cereal Chem.* 75, 325–330. doi: 10.1094/CCHEM.1998.75.3.325

Stincone, A., Prigione, A., Cramer, T., Wamelink, M. M., Campbell, K., Cheung, E., et al. (2015). The return of metabolism: biochemistry and physiology of the pentose phosphate pathway. *Biol. Rev. Camb. Philos. Soc.* 90, 927–963. doi: 10.1111/brv.12140

Troncoso-Ponce, M. A., Kilaru, A., Cao, X., Durrett, T. P., Fan, J., Jensen, J. K., et al. (2011). Comparative deep transcriptional profiling of four developing oilseeds. *Plant J.* 68, 1014–1027. doi: 10.1111/j.1365-313X.2011.04751.x

Tschiersch, H., Borisjuk, L., Rutten, T., and Rolletschek, H. (2011). Gradients of seed photosynthesis and its role for oxygen balancing. *Biosystems* 103, 302–308. doi: 10.1016/j.biosystems.2010.08.007

Voon, C. P., Guan, X., Sun, Y., Sahu, A., Chan, M. N., Gardeström, P., et al. (2018). ATP compartmentation in plastids and cytosol of *Arabidopsis thaliana* revealed by fluorescent protein sensing. *Proc. Natl. Acad. Sci. U. S. A.* 115, E10778–E10787. doi: 10.1073/pnas.1711497115

Wakao, S., Andre, C., and Benning, C. (2008). Functional analyses of cytosolic Glucose-6-phosphate dehydrogenases and their contribution to seed oil accumulation in Arabidopsis. *Plant Physiol.* 146, 277–288. doi: 10.1104/pp.107.108423

Willms, J. R., Salon, C., and Layzell, D. B. (1999). Evidence for light-stimulated fatty acid synthesis in soybean fruit. *Plant Physiol.* 120, 1117–1128. doi: 10.1104/pp.120.4.1117

Zhang, Y., Mulpuri, S., and Liu, A. (2016). High light exposure on seed coat increases lipid accumulation in seeds of castor bean (*Ricinus communis* L.), a nongreen oilseed crop. *Photosynth. Res.* 128, 125–140. doi: 10.1007/s11120-015-0206-x

Zhang, C., Zhang, W., Ren, G., Li, D., Cahoon, R. E., Chen, M., et al. (2015). Chlorophyll synthase under epigenetic surveillance is critical for vitamin E synthesis, and altered expression affects tocopherol levels in Arabidopsis. *Plant Physiol.* 168, 1503–1511. doi: 10.1104/pp.15.00594

Conflict of Interest: The authors declare that the research was conducted in the absence of any commercial or financial relationships that could be construed as a potential conflict of interest.

Publisher's Note: All claims expressed in this article are solely those of the authors and do not necessarily represent those of their affiliated organizations, or those of the publisher, the editors and the reviewers. Any product that may be evaluated in this article, or claim that may be made by its manufacturer, is not guaranteed or endorsed by the publisher.

frontiers | Frontiers in Plant Science

TYPE Review
PUBLISHED 31 August 2022
DOI 10.3389/fpls.2022.969844

OPEN ACCESS

EDITED BY
Anca Macovei,
University of Pavia,
Italy

REVIEWED BY
Rupam Kumar Bhunia,
National Agri-Food Biotechnology Institute, India
Nikolaos Tsakirpaloglou,
Texas A&M University, United States

*CORRESPONDENCE
Hyun Uk Kim
hukim64@sejong.ac.kr

SPECIALTY SECTION
This article was submitted to Crop and Product Physiology, a section of the journal Frontiers in Plant Science

RECEIVED 15 June 2022
ACCEPTED 08 August 2022
PUBLISHED 31 August 2022

CITATION
Park M-E and Kim HU (2022) Applications and prospects of genome editing in plant fatty acid and triacylglycerol biosynthesis. *Front. Plant Sci.* 13:969844. doi: 10.3389/fpls.2022.969844

Applications and prospects of genome editing in plant fatty acid and triacylglycerol biosynthesis

Mid-Eum Park[1] and Hyun Uk Kim[1,2]*

[1]Department of Molecular Biology, Sejong University, Seoul, South Korea, [2]Department of Bioindustry and Bioresource Engineering, Plant Engineering Research Institute, Sejong University, Seoul, South Korea

Triacylglycerol (TAG), which is a neutral lipid, has a structure in which three molecules of fatty acid (FA) are ester-bonded to one molecule of glycerol. TAG is important energy source for seed germination and seedling development in plants. Depending on the FA composition of the TAG, it is used as an edible oil or industrial material for cosmetics, soap, and lubricant. As the demand for plant oil is rising worldwide, either the type of FA must be changed or the total oil content of various plants must be increased. In this review, we discuss the regulation of FA metabolism by Clustered regularly interspaced short palindromic repeats (CRISPR)/Cas9, a recent genome-editing technology applicable to various plants. The development of plants with higher levels of oleic acid or lower levels of very long-chain fatty acids (VLCFAs) in seeds are discussed. In addition, the current status of research on acyltransferases, phospholipases, TAG lipases, and TAG synthesis in vegetative tissues is described. Finally, strategies for the application of CRISPR/Cas9 in lipid metabolism studies are mentioned.

KEYWORDS

acyltransferase, CRISPR/Cas9, *FAD2*, *FAE1*, *FATB*, *KASI*, lipase, TAG

Introduction

Fatty acids (FAs) are synthesized by the addition of two carbons by fatty acid synthase (FAS) in the plastid (Rawsthorne, 2002). FA biosynthesis is initiated by acetyl-CoA carboxylase, which converts acetyl-CoA to malonyl-CoA (Sasaki and Nagano, 2004). Malonyl-CoA is converted to malonyl-ACP by malonyl-CoA: acyl carrier protein (ACP) transacylase (Lessire and Stumpe, 1983). Malonyl-ACP is combined with acetyl-CoA by β-ketoacyl-acyl carrier protein synthase III (KAS III) to synthesize 4:0-ACP (Clough et al., 1992). KAS I is involved in the elongation from 4:0-ACP to 16:0-ACP and is synthesized as 18:0-ACP by KAS II (Shimakata and Stumpf, 1982). The 18:0-ACP is desaturated to 18:1-ACP by fatty acid biosynthesis 2 (FAB2; Lightner et al., 1994). Free FAs are removed from ACP by fatty acyl-ACP thioesterase A (FATA) and fatty acyl-ACP thioesterase B (FATB) and exit the plastid to form an acyl-CoA pool in the cytoplasm (Jones et al., 1995;

Salas and Ohlrogge, 2002). Subsequently, acyl-CoAs are sequentially transferred to glycerol-3-phosphate (G3P) by acyltransferase enzymes in the endoplasmic reticulum (ER) to form triacylglycerol (TAG; Li-Beisson et al., 2013). To synthesize TAG, lysophosphatidic acid (LPA) is formed by attaching acyl-CoA at the *sn-1* position of the G3P backbone by glycerol-3-phosphate acyltransferase (GPAT; Shockey et al., 2016). Lysophosphatidic acid acyltransferase (LPAT) then transfers acyl-CoA to the *sn-2* position of LPA to form phosphatidic acid (PA). Phosphate at the *sn-3* position of PA is cleaved by phosphatidate phosphatase (PAP) to form diacylglycerol (DAG; Carman and Han, 2006). Finally, TAG is produced by attaching acyl-CoA to the *sn-3* position of DAG using diacylglycerol acyltransferase (DGAT; Cases et al., 1998; Zou et al., 1999; Figure 1).

Polyunsaturated fatty acids (PUFAs) present in TAG are synthesized in phosphatidylcholine (PC), a membrane lipid (He et al., 2020). First, the oleic acid (18:1) of *sn-2* in PC is converted to linoleic acid (18:2) by fatty acid desaturase 2 (FAD2), and then, linoleic acid (18:2) is converted to linolenic acid (18:3) by FAD3 (Lemieux et al., 1990; Browse et al., 1993; Dar et al., 2017). PUFAs are released from PC to form an acyl-CoA pool by reverse reaction of LPCAT (Lager et al., 2013). These acyl-CoAs are transferred into TAG through the acyl-CoA-dependent pathway by ER acyltransferases, as discussed above (Zou et al., 1999; Kim et al., 2005; Shockey et al., 2016). In addition, an acyl-CoA-independent pathway can directly synthesize TAG by transferring PUFAs in PC to DAG by phospholipid:diacylglycerol acyltransferase (PDAT; Dahlqvist et al., 2000; Figure 1A).

The discovery and functional studies of genes related to FA and TAG synthesis were carried out by forward genetics using mutants induced by ethyl methanesulfonate (EMS), and reverse genetics using T-DNA insertion mutants in *Arabidopsis thaliana*, a model plant (Lemieux et al., 1990; Browse et al., 1993; Lightner et al., 1994; Mcconn et al., 1994; Wu et al., 1994). Genetic studies on lipid metabolism in various crops have been conducted based on the insights from studies on *Arabidopsis* (Li-Beisson et al., 2013).

In most crops, FA composition consists of five common FAs: 16:0, 18:0, 18:1, 18:2, and 18:3 (Buchanan et al., 2015). However, some wild plants have unusual FAs (e.g., ω-hydroxy, 9,10-epoxy, caprylic acid, and ricinoleic acid) with specific functional groups on the FA carbon chain (Cahoon and Li-Beisson, 2020). Unusual FAs present in wild plants are industrially useful because they serve as raw materials for various polymers produced by chemical processes (Cahoon and Li-Beisson, 2020). Common FAs present in crops can also be useful in the food industry if the proportion of single types of FAs increases. For instance, vegetable oil with increased oleic acid content is suitable for frying and cooking oils (Przybylski and Aladedunye, 2012). In plant lipid metabolism engineering, strategies have mainly been used to control the FA pathway by overexpressing or mutating a specific gene to eliminate its function (Napier et al., 2014; Haslam et al., 2016). Clustered regularly interspaced short palindromic repeats (CRISPR) and CRISPR-associated protein 9 (CRISPR/Cas9), a recently emerged gene-editing tool, can easily and quickly edit the genome by precisely targeting a gene. Compared with traditional breeding process which requires removal of unfavored traits through repeated backcrossing and selection (Chen et al., 2019), CRISPR/Cas9 technology allows rapid development of a new cultivar with desirable traits. Besides, the conventional EMS mutagenesis is being replaced by CRISPR/Cas9 method because of its precision and completeness of mutation. In this review, we summarize the studies of CRISPR/Cas9-based knockout of mutants involved in lipid metabolism and discuss future directions in implementing this technology for the development of new oilseed crops.

CRISPR/Cas9 and lipid metabolic engineering

Transcription activator-like effector nucleases (TALENs), zinc-finger nucleases (ZFNs), and CRISPR/Cas9 enable researchers to edit the genome in plants (Durai et al., 2005; Jinek et al., 2012; Joung and Sander, 2013). In TALENs, the Tal effector recognizes the DNA sequence and the FokI endonuclease cuts the DNA (Joung and Sander, 2013). In ZFNs, the Fok I endonuclease cuts DNA, however, unlike for TALEN, the zinc finger domain recognizes the DNA sequence (Durai et al., 2005). Both systems are widely used for genome editing; however, they are difficult to handle and require a long time for application to organisms compared to CRISPR/Cas9 (Chandrasegaran and Carroll, 2016). In contrast, CRISPR/Cas9 is less expensive and easy to use for any organism (Jinek et al., 2012; Chandrasegaran and Carroll, 2016).

CRISPR/Cas9 was first identified in the bacterial immune system (Brouns et al., 2008). The CRISPR/Cas9 system consists of two parts: a guide RNA (gRNA) and Cas9 protein. The gRNA has two parts: crispr RNA (crRNA) is a complementary sequence to the target gene, and trans-activating crispr RNA (tracrRNA) serves as a scaffold for linking with the Cas9 protein (Jinek et al., 2012). crRNA and tracrRNA are collectively called gRNA (Jinek et al., 2012; Ran et al., 2013). The Cas9 protein cuts double-stranded DNA, causing a double-strand break (DSB; Ran et al., 2013). The most used Cas9 protein is *Streptococcus pyogenes* Cas9 (SpCas9), which cuts the 3 bp position in front of the protospacer adjacent motif (PAM) corresponding to the NGG sequence in the DNA (Ran et al., 2013). Depending on the type of Cas9, Cas9 recognizes a PAM sequence that is different from NGG (Leenay and Beisel, 2017). Since the introduction of CRISPR/Cas9 technology, genome editing research has been conducted in various organisms, such as plants, humans, and microalgae (Jeon et al., 2017; Jaganathan et al., 2018; Subedi et al., 2020; Li et al., 2020b).

The mechanism of CRISPR/Cas9 involves the formation of DSB by Cas9, which leads to two DNA repair mechanisms: non-homologous end-joining (NHEJ) and homology-directed repair (HDR; Cong et al., 2013; Ran et al., 2013; Sander and Joung, 2014; Figure 2A). As the NHEJ process directly repairs through

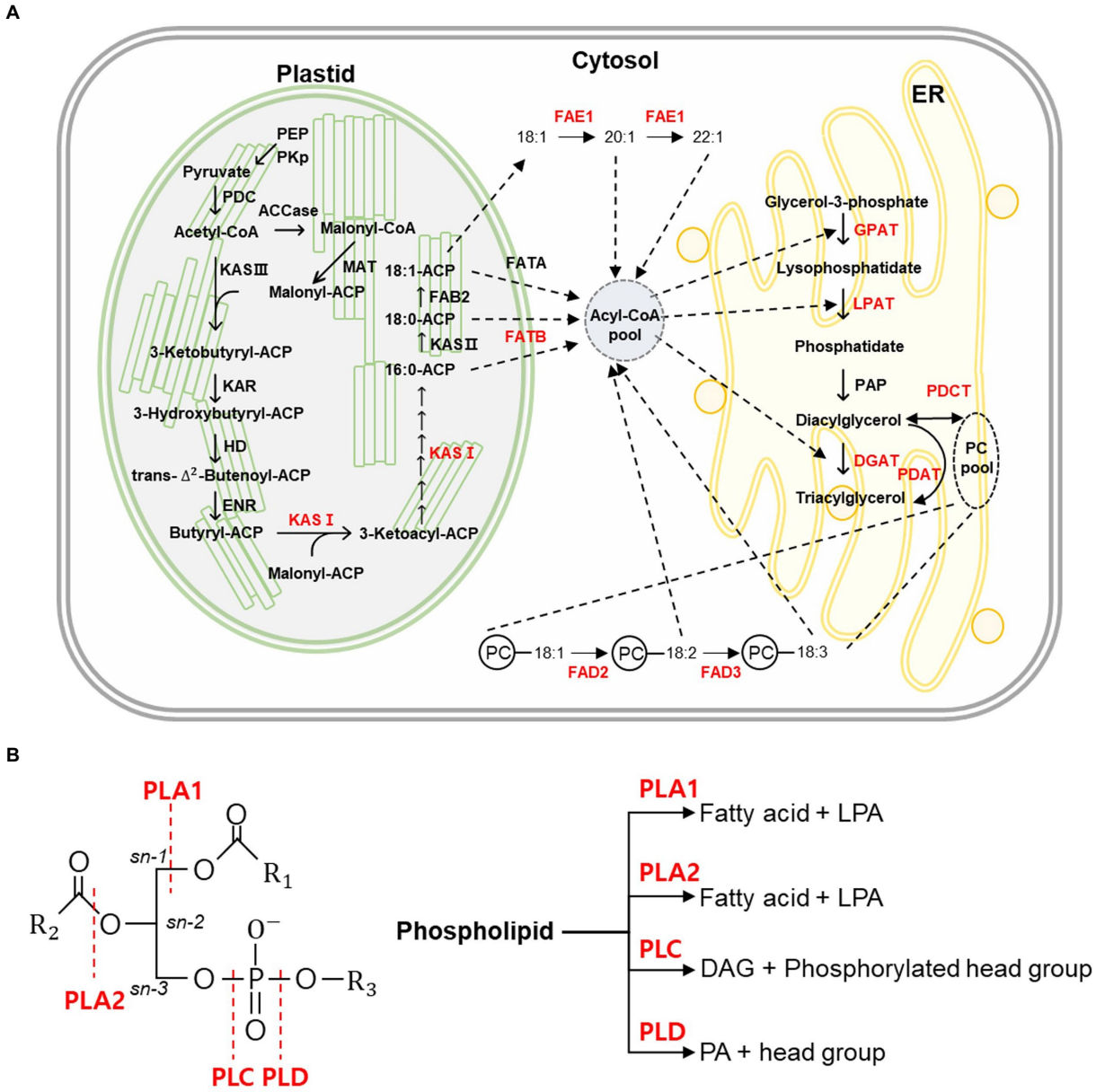

FIGURE 1
Fatty acid, triacylglycerol synthesis pathway, and function of phospholipase. **(A)** A schematic diagram of fatty acid and triacylglycerol synthesis pathway in plants. The figure illustrates the acyl-CoA synthesis pathway in the plastid and triacylglycerol (TAG) synthesis pathway by acyltransferase in endoplasmic reticulum (ER). Polyunsaturated fatty acids are synthesized in phosphatidylcholine (PC) by desaturase enzymes such as fatty acid desaturase 2 (FAD2) and FAD3. The FAE1 enzyme elongates the 18:1 fatty acid to 20:1 or 22:1, which are very long-chain fatty acids. Red-colored letters indicate the enzyme that was studied using Clustered regularly interspaced short palindromic repeats (CRISPR) and CRISPR-associated protein 9 (CRISPR/Cas9). The dotted lines represent the flow of the fatty acids in fatty acid and triacylglycerol synthesis. ACCase, acetyl-CoA carboxylase; ACP, acyl carrier protein; CoA, coenzyme A; DGAT, diacylglycerol acyltransferases; ENR, enoyl-ACP reductase; ER, endoplasmic reticulum; FAB2, fatty acid biosynthesis 2; FAD2, fatty acid desaturase 2; FAD3, fatty acid desaturase 3; FAE1, fatty acid elongase 1; FATA, fatty acyl-ACP thioesterase A; FATB, fatty acyl-ACP thioesterase B; GPAT, glycerol-3-phosphate acyltransferase; HD, 3-hydroxy acyl-ACP dehydratase; KAR, 3-ketoacyl-ACP reductase; KAS, β-ketoacyl-acyl carrier protein synthase; LPAT, lysophosphatidic acid acyltransferase; MAT, malonyl-CoA/ACP transacylase; PAP, phosphatidate phosphatase; PC, phosphatidylcholine; PDAT, phospholipid:diacylglycerol acyltransferase; PDC, pyruvate dehydrogenase complex; PDCT, phosphatidylcholine:diacylglycerol cholinephosphotransferase; PEP, phosphoenolpyruvate; and PKp, Plastidial pyruvate kinase. **(B)** The reaction of phospholipase in plants. Plants have four different forms of phospholipases (PLA1, PLA2, PLC, and PLD). Phospholipase is the enzyme that hydrolyzes phospholipids. The cleavage site of phospholipase is shown on the left figure and indicated by the red dotted lines. The right figure shows the product produced by phospholipase. DAG, diacylglycerol; LPA, lysophosphatidate; PA, phosphatidate; PLA1, phospholipase A1; PLA2, phospholipase A2; PLC, phospholipase C; and PLD, phospholipase D.

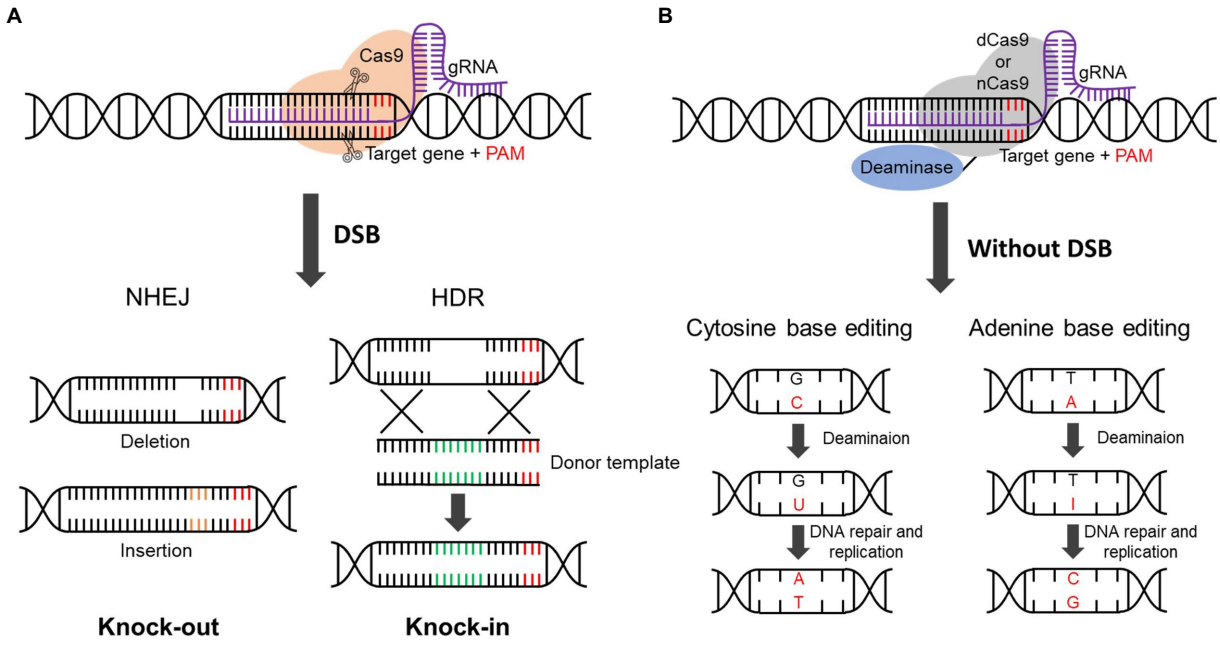

FIGURE 2
CRISPR/Cas9 and base editing mechanism. **(A)** Repair mechanism of CRISPR/Cas9. CRISPR/Cas9 is composed of Cas9 protein and gRNA. Cas9 recognizes the PAM sequence and cleaves 3bp upstream of PAM to cause the DSB. When a DSB occurs, the cellular repair mechanism, including NHEJ and HDR processes, is initiated. NHEJ causes deletion or insertion, resulting in gene knockout due to a frameshift change. The donor template is inserted by HDR, and knockin occurs. DSB, Double-strand break; NHEJ, non-homologous end joining; HDR, homology-directed repair; PAM, protospacer adjacent motif. **(B)** Mechanism of base editing. The cytosine base editor or adenine base editor is made up of dead Cas9 (dCas9) or nickase Cas9 (nCas9) fused with cytosine deaminase or adenine deaminase. Cytosine deaminase removes the amine group from cytosine, resulting in a U-G mismatch. The U-G pair is converted to T-A by DNA repair and DNA replication. Adenine deaminase converts adenine to inosine by removing the amine group, resulting in an I-T mismatch. The I-T pair is converted to G-C by DNA repair and DNA replication.

insertion or deletion, gene knockout follows where DSB has occurred (Jiang and Doudna, 2017). Compared to NHEJ, HDR leads to knock-in, in which a DNA fragment is inserted into the DSB region (Jiang and Doudna, 2017).

CRISPR/Cas9-based technology for editing specific nucleotide sequence has also emerged recently. Dead Cas9 (dCas9) or nickase Cas9 (nCas9) fused with cytosine deaminase or adenine deaminase can convert specific nucleotides (C–T or A–G) without any DNA cleavage, it is referred to as the cytosine base editor or adenine base editor (Figure 2B; Komor et al., 2016; Nishida et al., 2016; Gaudelli et al., 2017). If one amino acid needs to be changed rather than knocked out, the base editor can be a powerful tool. For example, rice (*Oryza sativa*) has been modified to be herbicide resistant plant through base editing in the *acetyl CoA carboxylase* (*ACCase*) gene (Liu et al., 2020). A strategy for base editing technology in oil palm is also being introduced (Yarra et al., 2020). In addition to Cas9 and deaminase types, an online tool to design gRNA, and analysis methods to confirm mutation pattern are discussed (Yarra et al., 2020). As CRISPR/Cas9 technology develops rapidly, it has become easier and faster to knock out genes. One or two gRNA are generally used to generate single-gene mutants (Cong et al., 2013; Wang et al., 2015). More than two guide RNAs can be designed using cellular tRNA processing to target multiple genes (Xie et al., 2015). In plants, to avoid issues related to GMOs, the gene is mutated by directly injecting Cas9 protein and gRNA into the plant protoplast rather than introducing the *Agrobacterium* plasmid vector (Woo et al., 2015). The transient expression of Cas9 is also good strategy to develop transgene-free mutants because Cas9 DNA or RNA is degraded (Zhang et al., 2016). Currently, plant lipid metabolic engineering using CRISPR/Cas9 involves reduction of PUFAs that cause rancidity in oil, while increasing monounsaturated fatty acids (MUFAs) and inhibiting the synthesis of unhealthy saturated fatty acids (SFAs) and very long-chain fatty acids (VLCFAs).

Mutation in *FAD2*

Polyunsaturated fatty acids (18:2 and 18:3) were synthesized from PC in the ER (Ohlrogge and Browse, 1995). In PUFA synthesis, FAD2 desaturases 18:1 at the *sn-2* position of PC into 18:2, and FAD3 desaturates from 18:2 to 18:3 (Lemieux et al., 1990; Browse et al., 1993; Dar et al., 2017; Figure 1A). As PUFAs are essential nutrients in humans, they can be beneficial to human health (Lee et al., 2016). However, it is easily oxidized at room temperature, and trans-fats are formed during deep-fat frying at high temperatures, they are unsuitable for salad dressings or cooking oils (Przybylski and Aladedunye, 2012; Saini and Keum,

2018). Therefore, making oil crops high in oleic acid is important in the food industry. Among oil crops, grape seed, sunflower, cotton, corn, soybean, camelina, perilla, and linseed have a high proportion of PUFAs in the oils (Dubois et al., 2007).

The function of FAD2 was first identified in the EMS and T-DNA mutants of *Arabidopsis* (Lemieux et al., 1990; Okuley et al., 1994). When FAD2 loses its activity, the PUFA content of the seed oil decreases, and the oleic acid content increases; however, it is sensitive to salt stress during seed germination and seedling growth (Zhang et al., 2012). Recently, various *fad2* alleles have been reported to weaken the function of FAD2 through base editing, increase oleic acid content, and confer resistance to salt stress (Park et al., 2021).

Studies have reported the elimination of the FAD2 function using CRISPR/Cas9 in various crops (Table 1). In tobacco (*Nicotiana tabacum* L.), two homozygous *ntfad2-2* mutants were found and their FA composition was checked. Consequently, the oleic acid content increased from 12 to 79% in mutants (Tian et al., 2020a). In rapeseed (*Brassica napus*), the *FAD2* gene was knocked out using CRISPR/Cas9 in two cultivars (Okuzaki et al., 2018; Huang et al., 2020). First, compared with the wild type, which produces 74% oleic acid, *BnFAD2_Aa* of the cultivar Westar was knocked out to increase the oleic acid content to 80% (Okuzaki et al., 2018). Second, oleic acid of each knockout mutant of *BnFAD2_A5* and *BnaFAD2_C5* in cultivar J9707 was enhanced to 73–82%, whereas oleic acid was 66% in the wild type (Huang et al., 2020). *FAD2* gene knockout studies of soybean (*Glycine max*) have been performed by several groups. In the cultivar Jinong38 (JN38), oleic acid content was 45–65% when *GmFAD2-2* was knocked out (Al Amin et al., 2019). Oleic acid content increased to 34.47 and 40.45% in *GmFAD2-1A* and *GmFAD2-2A* mutants, respectively, and double mutants of *GmFAD2-1A* and *GmFAD2-2A* induced a high oleic acid content of up to 72% (Wu et al., 2020). In another group, they targeted both *GmFAD2-1A* and *GmFAD2-1B* in order to create double knockout mutants in the cultivar Maverick, and the oleic acid content was dramatically increased to 80% (Do et al., 2019).

In *Camelina sativa*, which is a hexaploid oil crop, when all three *CsFAD2* were knocked out, oleic acid content increased up to 54–60% but showed a phenotype that did not grow properly in some studies (Jiang et al., 2017; Morineau et al., 2017; Lee et al., 2021). Four *OsFAD2* copies have been identified in rice, and among them, *OsFAD2-1* is most expressed in rice grains (Zaplin et al., 2013). Knockout of *OsFAD2-1* from Japonica with CRISPR/Cas9 did not result in FA analysis (Bahariah et al., 2021), whereas oleic acid levels increased up to 80% in Nipponbare (Abe et al., 2018). *FAD2* of peanut (*Arachis hypogaea*) was also mutated, but the seeds were not harvested; therefore, no FA analysis could be performed (Yuan et al., 2019). In cotton (*Gossypium hirsutum*), it was confirmed that among the eight *FAD2* homologs, *GhFAD2-1A* and *GhFAD2-1D* are mostly expressed in the ovule. Therefore, *GhFAD2-1A* and *GhFAD2-1D* are simultaneously targeted by CRISPR/Cas9. Consequently, the oleic acid content was 75–77% (Chen et al., 2021). In addition, knockout of the *FAD2* gene of pennycress (*Thlaspi arvense*) enhanced oleic acid from 12 to 35% in mutants but delayed the flowering and decreased the germination rate and seed weight (Jarvis et al., 2021).

Mutation in *FATB* and *KASI*

It is important to reduce the content of SFAs in the food industry because high SFA intake can cause arteriosclerosis in humans (Siri-Tarino et al., 2010). The 16:0-ACP, 18:0-ACP, and 18:1-ACP synthesized from plastids are converted to their free-acyl forms by FATB and FATA which are then released into the cytoplasm and converted into acyl-CoA (Jones et al., 1995; Salas and Ohlrogge, 2002). Knockout of the *FATB* gene through CRISPR/Cas9 has been performed in soybean and peanut (Table 2; Ma et al., 2021; Tang et al., 2022). Soybeans have four GmFATB proteins, all of which have at least 78% homology with *Arabidopsis* FATB at the protein level. *GmFATB2a* and *GmFATB2b* are mainly expressed in flowers, and *GmFATB1a* and *GmFATB1b* are expressed in leaves and seeds. As a result of the simultaneous knockout of *GmFATB1a* and *GmFATB1b* expressed in seeds, the line in which both genes were disrupted showed male sterility. The SFA (palmitic acid and stearic acid) levels of the lines that lost only one of these two genes were 16–21%, but 32.2% in the wild type (Ma et al., 2021). In peanuts, gRNA was designed to target both *AhFATB10a* and *AhFATB10b*, but only a mutation in *AhFATB10a* occurred, which decreased palmitic acid content by approximately 1%, which was slightly lower than that of the wild type (13.3%; Tang et al., 2022).

Among the fatty acid synthases *KASI, II*, and *III* genes, CRISPR/Cas9 was mainly used for *KASI* knockout (Table 2). The in-frame deletion (−54 bp) of *Arabidopsis KASI* causes a semi-dwarf phenotype (Xie et al., 2019). In the *KASI* homozygous mutant of soybean, 18:2 level decreased by 8% and 18:3 level increased by 8.5% compared to the wild-type cultivar Bert. At the same time, the seeds of mutants were wrinkled and shriveled, and the sucrose content increased, while the oil content decreased (Virdi et al., 2020).

Mutation in *FAE1*

Fatty acids with 12–20 carbons are called long-chain fatty acids (LCFAs), and VLCFAs are longer than 22 carbons (Kihara, 2012). Eicosenoic acid (20:1) and erucic acid (22:1) are produced by the elongation of oleic acid by fatty acid elongase1 (FAE1; Millar and Kunst, 1997). The *Arabidopsis FAE1* gene is mainly expressed in seed embryos (Rossak et al., 2001). Erucic acid, a VLCFA, is associated with myocardial infarction (Imamura et al., 2013). Therefore, researchers have studied the reduction of VLCFA using CRISPR/Cas9 in several plant oils (Table 2).

Simultaneously knocking out three *FAE1* genes in Camelina (cultivar Suneson) decreased erucic acid content to less than 1% (Ozseyhan et al., 2018). In addition, seed weight, oil content, and seed shape were not significantly different from those of "Suneson" (Ozseyhan et al., 2018). In rapeseed, the erucic acid content of the

TABLE 1 Decrease in polyunsaturated fatty acid by CRISPR/Cas9.

Gene name	Technique	Promoter of Cas9	Method	Phenotype	Oleic acid WT (%)	Oleic acid Mutant (%)	Mutation type	References
AhFAD2A *AhFAD2B*	CRISPR/Cas9	CamV 35S	Hairy root transformation	-	36 ~ 67%	Not harvest the seeds	G448A (*ahFAD2A*), +1 bp, and G451T (*ahFAD2B*)	Yuan et al., 2019
NtFAD2-2	CRISPR/Cas9	CamV 35S	*Agrobacterium*-mediated transformation	No side effect	~12%	79%	-1 and −5 bp	Tian et al., 2020a
AtFAD2	Base editing	RPS5A (*Arabidopsis*)	Floral dipping	Resistance to salt stress	18.5%	57.9% 64.7% 30.6% 29.6%	A295G, D298E A295V, T296M A295V A295G	Park et al., 2021
	CRISPR/Cas9	CamV 35S	Floral dipping	-	16.2%	~59.8%	+1 bp	Jiang et al., 2017
BnFAD2	CRISPR/Cas9	Ubiquitin4-2 (*Petroselinum crispum*)	*Agrobacterium*-mediated transformation	No difference	cv. Westar (74.6%)	*BnFAD2_Aa* (80%)	-4 bp	Okuzaki et al., 2018
		Ubiquitin (rice)			cv. J9707 (66.7%)	*BnaFAD2.A5* (73.1–82.3%)	−1bp, −1bp and S1, −2bp, −13bp, −80bp, +1bp, +1bp and +1bp, +1bp and −2bp, +1bp and −7bp	Huang et al., 2020
						BnaFAD2.C5 (73–74%)	−3 and +1 bp	
CsFAD2	CRISPR/Cas9	Ubiquitin4-2 (*Petroselinum crispum*)	Floral dipping	All *CsFAD2* gene mutants → slow growth, twisted leaves, delayed bolting	cv. Celine (9.8%)	10–62%	21 different mutant alleles	Morineau et al., 2017
		CamV 35S		-	cv. Suneson (15.9%)	~54.7%	A lot of mutant alleles	Jiang et al., 2017
		EC1.2		All *CsFAD2* gene mutants → Stunted bushy phenotype, small, and bloomed late	cv. Suneson (9.8%)	~59.5%	A lot of mutant alleles	Lee et al., 2021
GhFAD2-1A *GhFAD2-1D*	CRISPR/Cas9	Ubiquitin (rice)	*Agrobacterium*-mediated transformation	No difference (Fibre quality/length/ strength, micronaire, and germination)	13.9%	75.3–77.7%	m1-1 (−41 and +1 bp) m1-2 (+1 and −1 bp) m1-3 (+1 and +1 bp) m20-2 (−1 and +1 bp) m27-3 (−374 bp)	Chen et al., 2021
TaFAD2	CRISPR/Cas9	Ubiquitin4-2 (*Petroselinum crispum*)	Floral dipping	Late flowering, shorter plant height, low seed weight per plant, and low germination	12%	~35%	*fad2-4* (−2 bp) *fad2-5* (+1 bp) *fad2-6* (−29 bp)	Jarvis et al., 2021
OsFAD2-1	CRISPR/Cas9	Ubiquitin1 (maize)	Biolistic transformation	-	*Oryza sativa Japonica* (No result)	No result	+1 bp -302 bp	Bahariah et al., 2021
		2x 35S	*Agrobacterium*-mediated transformation	No difference	*Oryza sativa cv. Nipponbare* (32%)	~80%	1–1 (+1 bp) 3–11 (+1 bp) 5–17 (−8 bp) 6–23 (−8 bp)	Abe et al., 2018

(Continued)

TABLE 1 Continued

Gene name	Technique	Promoter of Cas9	Method	Phenotype	Oleic acid WT (%)	Oleic acid Mutant (%)	Mutation type	References
GmFAD2	CRISPR/Cas9	e35S	*Agrobacterium*-mediated transformation	-	cv. JN38 (17.34%)	*GmFAD2-2* (45.08–65.9%)	Substitution, −2, −3, +1, and +2 bp	Al Amin et al., 2019
		tipA	*Agrobacterium*-mediated transformation	No difference in plant height and grain weight. The grain is smaller and deeper in color	cv. JN38 (19.15%)	g3 strain (34.47%) g6 strain (40.45%) g36 strain (72.02%)	*GmFAD2-1A* JN38g3–1 (+1 bp 66.7%) JN38g3–3 (−1 bp 16.6%) JN38g3–4 (−2 bp 16.7%) *GmFAD2-2A* JN38g6–2 (+1 bp 50%) JN38g6–3 (−1 bp 50%) Double JN38g36–3 (+1 and −1 bp 50%) JN38g36–5 (−2 and −7 bp 50%)	Wu et al., 2020
		2x 35S	Hairy root transformation	-	cv. Maverick (~20%)	*GmFAD2-1A*, *GmFAD2-1B* homozygous lines (~80%)	A lot of mutant alleles	Do et al., 2019

a08c03 homozygous mutant was reduced to less than 0.1%, and the oil content decreased slightly, but there were no significant differences in other agronomic traits (Liu et al., 2022). In the case of a *c03* single gene mutation, there was no decrease in oil content, and the content of erucic acid was 31–35% in the wild type but decreased by half in the mutant (Liu et al., 2022). In pennycress, the candidate gene of *FAE1* with the highest homology to *Arabidopsis FAE1* was mutated using CRISPR/Cas9. As a result, both 20:1 and 22:1 FAs decreased by less than 1% (Mcginn et al., 2019).

Mutation in acyltransferases

GPAT, LPAT, and DGAT are acyltransferase enzymes that synthesize TAG by transferring FA from the acyl-CoA pool to G3P (Chapman and Ohlrogge, 2012). In addition, PDAT transfers FA at the *sn-2* position of PC to the *sn-3* position of DAG to synthesize TAG (Dahlqvist et al., 2000). In *Arabidopsis*, there are 10 GPATs, five LPATs, and three DGATs (Zou et al., 1999; Kim and Huang, 2004; Yang et al., 2012; Zhou et al., 2013; Ayme et al., 2018). Among the acyltransferases, GPAT9, LPAT2, DGAT1, and PDAT1 are known to be involved in TAG synthesis (Zou et al., 1999; Banas et al., 2000; Kim et al., 2005; Shockey et al., 2016). Table 3 shows the results of acyltransferase gene editing by CRISPR/Cas9.

As a result of the deletion of *Arabidopsis GPAT1*, SFAs content decreased and MUFAs content increased (Bai et al., 2021). Plant height and cell length increased, but oil content decreased in *gpat1* mutants (Bai et al., 2021). In rapeseed, *Bnlpat2* and *Bnlpat5* single mutants increased the content of 18:0 and 20:0, and decreased the content of 18:1, 18:2, and 18:3 (Zhang et al., 2019b). In the *Bnlpat2 Bnlpat5* double mutant, 20:0 level was increased, while 18:2 and 18:3 levels were decreased. In all these mutants, seed weight decreased, while oil body size increased (Zhang et al., 2019b). In the camelina, *DGAT1* and *PDAT1* were knocked out using CRISPR/Cas9 (Aznar-Moreno and Durrett, 2017). In the *csdgat1* homozygous mutant, 18:2 content was increased and 18:3 content was decreased, and the *cspdat1* homozygous mutant showed an FA composition similar to that of the wild type (Aznar-Moreno and Durrett, 2017). Both mutants showed decreased oil content and the seeds were wrinkled and darkened (Aznar-Moreno and Durrett, 2017). There was no significant change in phenotype when the *REDUCED OLEATE DESATURATION1* (*ROD1*) gene, which interconverts DAG and PC, was mutated in pennycress (Jarvis et al., 2021). FA analysis of mutant seeds showed that 18:1 content was increased and 18:2 content was decreased compared to the wild type (Jarvis et al., 2021).

TABLE 2 Mutation of *FATB*, *KASI* and decrease in the very long chain fatty acid by CRISPR/Cas9.

Gene name	Technique	Promoter of Cas9	Method	Phenotype	Fatty acid WT (%)	Fatty acid Mutant (%)	Mutation type	References
GmFATB1a *GmFATB1b*	CRISPR/Cas9	2x 35S	*Agrobacterium*-mediated transformation	*fatb1a*, *fatb1b* (No difference) *fatb1a*:*1b* (Growth defects, male sterility)	SFA (%) (32.28%)	SFA (%) *fatb1a-1* (18.66%) *fatb1a-2* (21.72%) *fatb1b-1* (16.87%) *fatb1b-2* (16.56%) *fatb1a:1b* (Male sterility)	*fatb1a-1* (−1 bp) *fatb1a-2* (−1 bp) *fatb1b-1* (−1 bp) *fatb1b-2* (−2 bp) *fatb1a:1b* (−1 bp, −30 bp)	Ma et al., 2021
AtKASI	CRISPR/Cas9	Ubiquitin	Floral dipping	Smaller and shorter seedlings and semi-dwarf plants	–	–	-54 bp	Xie et al., 2019
GmKASI	CRISPR/Cas9	Ubiquitin (soybean)	Whole plant transformation	Homozygous knockout—wrinkled and shriveled seed, increase in sucrose, and decrease in oil content.	cv. Bert 18:2 (49.42–52.56%) 18:3 (7.51–8.55%)	Homozygous mutant 18:2 (30.57–44.56%) 18:3 (15.48–16.99%)	Edit (site1, 2) WPT677-3–35 (+10/+107,WT/WT) WPT677-3–43 (WT/−1,WT/−1) WPT677-3–44 (−1/+1,WT/+1) WPT677-3–48 (WT/−6,WT/+1)	Virdi et al., 2020
AhFatB10a	CRISPR/Cas9	Not mentioned	*Agrobacterium*-mediated transformation	No differences	Huayu23 16:0 (13.3%)	16:0 PT1-3 (12.13%) PT1-12 (12.25%) PT1-21 (11.31%) PT2-4 (12.11%) PT2-17 (11.99%)	PT1-3 (1 substitution) PT1-12 (1 substitution) PT1-21 (−2 bp) PT2-4 (1 substitution) PT2-17 (1 substitution)	Tang et al., 2022
CsFAE1	CRISPR/Cas9	EC1.1	Floral dipping	No differences compared to Suneson	cv. Suneson 20:1 (14.4%)	Less than 1% of 20:1	3–3–1 (−5, −1, and −5 bp) 3–3–3 (−2, −14, and −1 bp) 3–3–4 (−2/+2, −2, and −1 bp) 3–3–14 (−2, −13, and −2 bp)	Ozseyhan et al., 2018
BnaFAE1	CRISPR/Cas9	Not metioned	*Agrobacterium*-mediated hypocotyl transformation	Decrease in the seed oil content No differences in agronomic traits	22:1 WH3411 (34.9%) WH3417 (31.0%) GY284 (34.6%)	22:1 WH3411 *c03* (19.3%) *a08c03* (0.07%) WH3417 *c03* (18.8%) *a08c03* (0.03%) GY284 *a08c03* (0.02%)	WH3411 *c03* (−1 bp) *a08c03* (−7/−7 bp) WH3417 *c03* (−2, +1 bp) *a08c03* (−3 bp, 1 substitution/ −2 bp) GY284 *a08c03* (−12 and −2 bp)	Liu et al., 2022
TaFAE1	CRISPR/Cas9	Ubiquitin4-2 (*Petroselinum crispum*)	Floral dipping (requires vacuum infiltration)	-	20:1 (15.0%) 22:1 (35.3%)	20:1, 22:1 *fae1-3* (0.9, 0.2%) *fae1-4* (0.9, 0%) *fae1-5* (1.2, 0.1%)	*fae1-3* (−4 bp) *fae1-4* (+1 bp) *fae1-5* (+1 bp)	Mcginn et al., 2019

TABLE 3 Mutation of acyltransferase and phospholipase by CRISPR/Cas9.

Gene name	Technique	Promoter of Cas9	Method	Phenotype	Fatty acid WT (%)	Fatty acid Mutant (%)	Mutation type	References
CsDGAT1	CRISPR/Cas9	CaMV 35S	Floral dipping	Wrinkled and darker seeds, lower oil content	cv. Suneson 18:2, 18:3 (22.8, 28.0%)	18:2, 18:3 D4 (25.1, 27.6%) D5 (29.7, 25.8%)	D4,D5 –DGAT1 homozygous mutant	Aznar-Moreno and Durrett, 2017
CsPDAT1					Similar to wild type		P1,P3 – PDAT1 homozygous mutant	
AtGPAT1	CRISPR/Cas9	CaMV 35S	Floral dipping	Increased the plant height and decreased the seed oil contents Increased the cell length	-	Saturated fatty acids are reduced MUFAs increase	−26 bp	Bai et al., 2021
BnLPAT2 *BnLPAT5*	CRISPR/Cas9	2x 35S	*Agrobacterium*-mediated hypocotyl transformation	Seed weight decreases, seeds are wrinkled, oil bodies increase	-	Oil content decreases	A lot of mutant alleles	Zhang et al., 2019b
TaROD1	CRISPR/Cas9	Ubiquitin4-2 (*Petroselinum crispum*)	Floral dipping	No difference	18:1 (12%) 18:2 (18%)	18:1 (~23%) 18:2 (~9%)	*rod1-3* (−18 bp) *rod1-4* (+1 bp) *rod1-5* (+1 bp)	Jarvis et al., 2021
OsPLDα1	CRISPR/Cas9	Ubiquitin	*Agrobacterium*-mediated transformation	Phytic acid content Xidao#1 (9.1 mg/g) *osplda1-1* (8.2 mg/g) *osplda1-2*(8.14 mg/g)			*osplda1-1* (−2 bp) *osplda1-2* (−1 bp)	Khan et al., 2019
				Amylose content, pasting properties, and retrogradation properties differ compared to wild type				Khan et al., 2020
GmpPLA-IIε *GmpPLA-IIζ*	CRISPR/Cas9	Not mentioned	*Agrobacterium*-mediated transformation	Knockout mutant is tolerant to iron-deficient condition, droughts, and flooding.			*ppla-IIε/ppla-IIζ-1* (−1 bp, −26 bp) *ppla-IIε/ppla-IIζ-2* (+1 bp, −4 bp) *ppla-IIε/ppla-IIζ-3* (−139 bp, larger –bp and + bp) *ppla-IIε-1* (−14 bp) *ppla-IIε-2* (−4 bp) *ppla-IIζ-1* (−7 bp)	Xiao et al., 2021

Mutation in phospholipases

Phospholipids are plasma membrane lipids (Reszczynska and Hanaka, 2020). Phospholipase is one of the enzymes that hydrolyze phospholipids and is related to various cellular functions (Takac et al., 2019). Plant phospholipases can be categorized as phospholipases A, C, and D (Takac et al., 2019). There are two subtypes of phospholipase A: phospholipase A1 and phospholipase A2. Phospholipase A1 cleaves the acyl group at the *sn-1* position, and phospholipase A2 cleaves the acyl group at the *sn-2* position to release lysophospholipids (LPL; Ryu, 2004). Phospholipase C hydrolyzes phospholipids to release DAG and

other phosphorylated head groups (Wang et al., 2012). Phospholipase D cleaves phosphate, releasing its head group and PA (Wang et al., 2012; Figure 1B).

Several studies have been conducted on phospholipase knockout or knockdown through genome editing or RNAi (Table 3; Li et al., 2006; Yamaguchi et al., 2009; Zhao et al., 2011; Guo et al., 2015; Zhang et al., 2019a). In the case of phospholipase research using CRISPR/Cas9, studies have only been conducted on soybeans and rice. In japonica rice cultivar Xidao#1, two independent knockout mutants were generated using CRISPR/Cas9. Analysis of the phytic acid and total phosphorous content of the grain showed a decrease of approximately 9 and 10%, respectively, in the *osplda1* mutants compared to the wild type (Khan et al., 2019). Additional experiments were performed using the same mutant (Khan et al., 2020). As the LPL content may affect the eating quality of rice, the LPL content in the mutants was checked (Liu et al., 2013). Except for LPC (14:0), the contents of LPC (16:0), LPC (18:1), LPE (14:0), LPE (16:0), and LPE (18:1) were increased by 11–32% in the *osplda1* mutant compared to the wild type (Khan et al., 2020). These mutants showed a decrease in amylose content, and consequently, low retrograded starch enthalpy, and high gelatinization enthalpy. The pasting property, peak viscosity, hot paste viscosity, breakdown, and cold paste viscosity all increased compared to the wild type, and only the setback viscosity decreased compared with the wild type (Khan et al., 2020). In soybean, three *ppla-Iiε/ppla-Iiζ* homozygous mutants, two *ppla-Iiε* mutants, and one *ppla-Iiζ* mutant were generated and studied (Xiao et al., 2021). Under P-deficient conditions, the main root length was longer in all mutant lines than in the wild type. In the Fe-deficient condition, all mutants had higher chlorophyll content, although there was a slight difference between mutants. The most shoot and root fresh weights of mutants were the same or higher than those of the wild type (Xiao et al., 2021).

Mutation in TAG lipases

Triacylglycerol lipase catalyzes the hydrolysis of TAG to release G3P and FAs (Graham, 2008). TAGs are stored and mobilized in the form of lipid droplets (LDs), and oleosins play a role in maintaining the LD structure (Huang, 2018). In *Arabidopsis*, TAG is degraded by *SUGAR DEPENDENT 1* (*SDP1*) to release FAs (Eastmond, 2006). In the *sdp1* mutant, it was identified that SDP1-LIKE (SDP1L) has a function to hydrolyze the TAG (Kelly et al., 2011). In addition to SDP1, OIL BODY LIPASE 1 (OBL1) was discovered in castor (*Ricinus communis*) and it can hydrolyze the TAG (Eastmond, 2004). The *OBL1* gene was also identified in Arabidopsis and tobacco, both of which are located in lipid droplets (LDs) and play an important role in pollen tube growth (Muller and Ischebeck, 2018). AtOBL1 has a lipase activity to TAG, DAG, and 1-MAG (Muller and Ischebeck, 2018). After the lipase degrades the TAG, FAs enter the peroxisome through *PEROXISOMAL ABC-TRANSPORTER1* (*PXA1*), where the beta-oxidation process occurs, in which carbon is broken down by two to form acetyl-CoA (Poirier et al., 2006). Acetyl-CoA enters the TCA cycle to generate energy sources, such as ATP, NADH, and FADH2 (Martinez-Reyes and Chandel, 2020). Disruption of TAG lipase using CRISPR/Cas9 has not been attempted in various plants. However, it has been reported that *SDP1* is disrupted using RNAi technology (Table 4; Kelly et al., 2013; Kim et al., 2014; Kanai et al., 2019; Azeez et al., 2022; Aznar-Moreno et al., 2022). When the *SDP1* expression in *rapeseed* was decreased by RNAi, the oil yield (g/ m^2) was further increased by 8% without affecting fatty acid composition (Kelly et al., 2013). The germination, shoot growth, and root growth are unaffected although the germination rate of seeds harvested 2 years ago decreased slightly (Kelly et al., 2013). When the *SDP1* gene in *Jatropha curcas* was knockdown, the total lipid content of endosperm was increased compared to the control, but there was no significant difference in fatty acid composition (Kim et al., 2014). The knockdown of four *GmSDP1* increased the seed weight, seed yield, and oil yield (g/plant), and oleic acid content was increased whereas linoleic acid content was decreased (Kanai et al., 2019). *GmSDP1* was targeted by RNAi, which lead to enhance seed weight and overall lipid content but decreased the content of raffinose family oligosaccharides (Aznar-Moreno et al., 2022). Seed-specific silencing of the *SDP1* gene in *Physaria fendleri* by RNAi increased seed weight and lipid content with the normal seedling establishment except for one line (Azeez et al., 2022). Based on previous results, it is possible to increase the oil content by knocking out TAG lipase using CRISPR/Cas9. Lipase has also been related to oil rancidity (Bhunia et al., 2021; Kumar et al., 2021). Rice bran oil (RBO) is abundant in nutrients but rapidly becomes rancid (Raghuram and Rukmini, 1995; Bhunia et al., 2021). Pearl millet seeds also have a high nutrition quality but the flour goes rancid rapidly (Kumar et al., 2021). Even though TAG is broken down by lipase and used as an energy source for germination, many fatty acids are released, which adversely affects rancidity (Kumar et al., 2021). The putative lipases were identified in rice and pearl millet (Bhunia et al., 2021; Kumar et al., 2021). In pearl millet, *PgTAGLip1* and *PgTAGLip2* polymorphisms were identified to cause loss-of-function mutation in an inbred line that low rancidity (Aher et al., 2022). Therefore, the disruption of lipase by CRISPR/Cas9 in rice or pear millet may be a key point in avoiding rancidity (Bhunia et al., 2021; Kumar et al., 2021).

Increase the TAG in vegetative tissue

In addition to plant seeds, TAG content can be increased in vegetative tissues such as leaf and tuber (Xu et al., 2018). In tobacco, oil enhancement is mainly achieved by overexpression of DGAT1 or positive transcription factors such as LEAFY COTYLEDON2 (LEC2) and WRINKLED1 (WRI1) (Table 4; Andrianov et al., 2010; Nookaraju et al., 2014; Vanhercke et al., 2014, 2017; Gao et al., 2018). TAG content was enhanced 20-fold in tobacco leaves when

TABLE 4 TAG lipase and increasing of TAG in vegetative tissues.

Gene name	Technique	Method	Promoter	Phenotype in transgenic	Oil content (WT)	Oil content (Transgenic)	References
BnaSDP1 (GN078283)	RNAi	*Agrobacterium*-mediated transformation	USP (from *Vicia faba*)	No difference in FA composition Little adverse impact on seed vigour	cv. Kumily 42.36 ± 0.12%	43.84 ± 0.10 ~ 45.86 ± 0.13%	Kelly et al., 2013
JcSDP1	RNAi	Electroporation	*JcSDP1*	No difference in seed size	-	Increased the total lipid content in endosperm (% w/w)	Kim et al., 2014
GmSDP1-1 *GmSDP1-2* *GmSDP1-3* *GmSDP1-4*	RNAi	*Agrobacterium*-mediated transformation	Soybean 11S globulin	Rupture of seed coat Increased the seed weight (g/seed) Increased the 18:1 but no difference in 16:0, 18:0 and 18:3	Kariyutaka	Increased the seed yield (g/plant), oil yield (g/plant)	Kanai et al., 2019
GmSDP1-1 *GmSDP1-2* *GmSDP1-3* *GmSDP1-4*	RNAi	*Agrobacterium*-mediated transformation	Soybean glycinin	Seed weight of mutants are ranging from 208 to 226 mg/seed (WT-183 mg/seed) Increased the total lipid (mg/seed) Germination rate is slower than WT	Williams82 (23.3%)	Fatty acid content (24.3%) Fatty acid content (24.4%)	Aznar-Moreno et al., 2022
PfrSDP1	RNAi	*Agrobacterium*-mediated transformation	2S albumin	Seed weight of mutants are ranging from 0.74 to 0.77 mg (WT-0.66 mg)	Lipid content (228 μg per mg seed) 20:1-OH, 20:2-OH (122.2 and 7 μg per mg seed)	Lipid content (261–271 μg per mg seed) 20:1-OH, 20:2-OH (144.8–155 and 8.9–10.8 μg per mg seed)	Azeez et al., 2022
AtDGAT1 *AtLEC2*	Overexpression	Leaf-disc *Agrobacterium*-mediated technique	*rbcS* *Alc*	Decrease the amount of 18:3 and increase the amount of 18:1	Total FA content (2.8%) FA content (2.9% of dry weight)	Total FA content (~5.6%) FA content (6.8% of dry weight)	Andrianov et al., 2010
AtDGAT1 *AtLEC2*	Overexpression	Leaf-disc *Agrobacterium*-mediated technique	*PtdCesA8A*	Minor difference about number of branches and stem diameter Increased the amount of 18:1, 18:2, and 18:3 in stems	-	Increased the oil bodies in pith, xylem, and cortex tissues Increased the total FA and TAG content	Nookaraju et al., 2014
AtDGAT1 *AtWRI1* *SiOLEOSIN*	Overexpression	*Agrobacterium*-mediated transformation	CaMV 35S, RuBisCO small subunit	No negative phenotype of development Increased the amount of 18:1, 18:2 and decreased the amount of 18:3 in leaves	TAG content (% DW) (~0.2%)	TAG content (% DW) (~15.8%)	Vanhercke et al., 2014
NtSDP1 *AtLEC2*	RNAi Overexpression	*Agrobacterium*-mediated transformation in transgenic lines (Vanhercke et al., 2014)	enTCUP2 SAG12	Reduction of starch content	TAG content (% DW) (0.1%)	TAG content (% DW) (~29.8%) TAG content (% DW) (~33.3%)	Vanhercke et al., 2017

(Continued)

TABLE 4 Continued

Gene name	Technique	Method	Promoter	Phenotype in transgenic	Oil content (WT)	Oil content (Transgenic)	References
VgDGAT1a	Overexpression	Transient expression	CaMV 35S	No difference of plant morphology but change the tuber morphology, germination rate and leaf chlorophyll content Increased the 18:2 and decreased the 18:3	-	TAG content (% DW) (~9.2%)	Gao et al., 2018
NtAn1	CRISPR/Cas9	Leaf-disc Agrobacterium-mediated technique	2x 35S	Yellow seed coat and white flower Decreased the PAs content and stearic acid No difference of seed size, seed weight and seed number per fruit	Lipid content (38.77 μg/seed)	Lipid content (44.97-45.91 μg/seed)	Tian et al., 2020b
AtACC1	Overexpression	Leaf-disc Agrobacterium-mediated technique	CaMV 35S	Increased the amount of 18:2 and decreased the amount of 18:3	Relative amount of TAG (1.2 mol %) Total FA content (1.08 mg/g FW)	Relative amount of TAG (4.6 mol %) Total FA content (1.35–1.39 mg/g FW)	Klaus et al., 2004
AtWRI1	Overexpression	Agrobacterium-mediated transformation	GBSS	No difference of plant morphology but change the tuber morphology Increased the amount of 18:2 and decreased the amount of 18:3	-	Increase the TAG and polar lipid (nmol FA/mg DW)	Hofvander et al., 2016
AtDGAT1 *AtWRI1* *SiOLEOSIN*	Overexpression	Agrobacterium-mediated transformation	CaMV 35S, patatin class I promoter B33	Increased the soluble sugar content and decrease the starch content Decreased the SFA and 18:3 but increase the MUFA in tuber	TAG content (% DW) (0.03%)	TAG content (% DW) (~3.3%) Increase the polar lipid	Liu et al., 2017
StAGPase *StSDP1*	RNAi	Electroporation	CaMV 35S	Incraease the total sugar content and decrease the total starch content in mature potato tuber	Total FA content in mature potato tuber (0.3%)	Total FA content in mature potato tuber (~2.95%)	Xu et al., 2019

AtDGAT1 was expressed under the control of the ribulose-biphosphate carboxylase small subunit promoter (Andrianov et al., 2010). *AtLEC2* was expressed under the control of the inducible *Alc* promoter (Andrianov et al., 2010). As a result, the FA content increased from 2.9% up to 6.8% (per dry weight) when treated with 1% acetaldehyde (Andrianov et al., 2010). Arabidopsis *DGAT1* or *LEC2* expression driven by the xylem-specific promoter in tobacco increases the FA and TAG content in the stem (Nookaraju et al., 2014). *AtWRI1*, *AtDGAT1*, and *Sesamum indicum OLEOSIN* (*SiOLEOSIN*) genes were transformed simultaneously into tobacco, and 15.8% of TAG was found in tobacco leaves (Vanhercke et al., 2014). *AtLEC2* overexpression or silencing of *SDP1* in transgenic tobacco (Vanhercke et al., 2014) accumulated the TAG up to 29.8 and 33.3% in the leaves, respectively (Vanhercke et al., 2017). Overexpression *DGAT1a* from *Vernonia galamensis* L. in tobacco, the TAG content of the leaves was enhanced up to 9.2% (per dry weight) without any deleterious phenotype (Gao et al., 2018). Two transgenic lines were generated using CRISPR/Cas9 by knocking out the *NtAN1* gene, which regulates proanthocyanidins (PAs) and lipid accumulation in tobacco (Tian et al., 2020b). These mutants enhanced the lipid and protein content and also displayed yellow seed coat (Tian et al., 2020b).

Triacylglycerol enhancement research in the potato (*Solanum tuberosum*) tuber was also conducted (Table 4; Klaus et al., 2004;

Hofvander et al., 2016; Liu et al., 2017; Xu et al., 2019). Arabidopsis *ACCase* was expressed in potato, the FA increased by 30% relative to the wild type, and showed a 5-fold increase in TAG accumulation compared to that of the wild type (Klaus et al., 2004). *AtWRI1* was expressed under the control of the *GBSS* promoter. TAG increased 20-fold compared to that of wild type, and the polar lipid was also increased (Hofvander et al., 2016). Three genes were expressed simultaneously in the potato: *AtDGAT1*, *AtWRI1*, and *SiOLEOSIN* controlled by the 35S and B33 potato patatin promoters (Liu et al., 2017). As a result, TAG, which was 0.03% in the wild type, was enhanced up to 3.3% in the tuber (Liu et al., 2017). When potato *ADP-glucose pyrophosphorylase* (*AGPase*) and *SDP1* were simultaneously silenced using RNAi, TAG content in the mature tuber of potato was increased by 16-fold compared to that of the wild type (Xu et al., 2019). TAG enhancement in vegetative tissue was mainly caused by overexpression or knockdown in tobacco and potato. In the future, if CRISPR is applied to enhance the TAG through lipid gene editing of tobacco or potato, it will be regarded as an important biofuel platform.

Conclusion and future perspective

Fatty acids constitute TAG, an energy source as well as a component of cell membranes and chloroplast membranes that are essential for plant cells (Kim, 2020). Since TAG in plant oil is a major source of food and industrial raw materials, attention has been focused on changing the FA composition and increasing the TAG content (Xu and Shanklin, 2016). So far, research has focused on creating high-oleic acid plant varieties by removing the FAD2 function (Table 1). Lately, research is underway to develop high-oleic acid varieties using multiple gRNAs to target both *FAD2* and *FATB* genes in soybean (Kim et al., 2021). In rapeseed, researchers used CRISPR/Cas9 to target *FAE1* and diminish the levels of 20:1 and 22:1 (Table 2). To lower the 20:1 and 22:1 content while further increasing the 18:1 content, *FAD2* of pennycress was mutated in the *fae1* knockout background (Jarvis et al., 2021). Moreover, CRISPR/Cas9 is commonly used in crops to investigate the roles of acyltransferase, phospholipase, and FAS genes (Tables 2, 3).

For future applications of CRISPR/Cas9 to lipid metabolism research, we suggest four possible strategies. First, CRISPR/Cas9 can be used to abolish the function of multiple lipid metabolism genes. Crops with high oleic acid content can be developed by simultaneously knocking out the *FAE1* gene, which elongates the 18:1 to 20:1, 22:1, and the *FAD2* gene, which desaturases the 18:1 to 18:2. Alternatively, it seems possible to develop crops with high oleic acid if *FATB* gene is mutated in *fad2* or *fae1* mutants (Figure 3A). Using CRISPR in mutants in which a specific gene has already been disrupted by EMS or RNAi may be a good strategy. For example, if *fad2* is mutated using CRISPR/Cas9 in the *fae1* EMS mutant line (Ozseyhan et al., 2018), a Camelina with higher oleic acid levels can also be developed. However, if there has no mutant background in which the lipid metabolism gene was disrupted by EMS or RNAi, multiple gRNAs can be used to target each distinct gene at once to abolish numerous gene functions simultaneously. Second, expression of the target gene can be controlled by removing the whole promoter region or *cis*-regulatory elements (CREs) using CRISPR/Cas9 (Figure 3B). For example, *DGAT2 UPSTREAM GENE 1* (*DUG1*) which exists upstream of *DGAT2* has a higher expression in leaves than *DGAT2*. Therefore, they deleted the 5′UTR region of *DUG1* to the 5′UTR region of *DGAT2* in Arabidopsis *sdp1* mutant using CRISPR/Cas9 so that *DGAT2* was controlled by the *DUG1* promoter (Bhunia et al., 2022). As a result, total lipid content (% cell dry weight) in leaves increased 2-fold and TAG content (% CDW) increased 30-fold compared to *sdp1* mutant (Bhunia et al., 2022). This method can be used only if the promoter direction of the upstream gene is appropriate (Bhunia et al., 2022). We think that the function of the upstream gene is irrelevant to plants since it will be eliminated by CRISPR/Cas9. It is also important to investigate the promoter expression level or tissue-specific expression of the upstream gene in advance. Deletion of CREs using CRISPR/Cas9 may be an effective strategy for regulating the transcription level of lipid genes (Figure 3B). Knockout causes complete loss of gene function, whereas deletion of CREs allows to fine-tune desirable traits more than knockout (Wolter et al., 2019). In fact, research was performed on the development of plants with agriculturally good traits by eliminating CREs using CRISPR/Cas9 (Li et al., 2020a, 2022; Wu et al., 2021). Third, it may be necessary to eliminate negative transcription factors that regulate the expression of lipid metabolism genes using CRISPR/Cas9 (Figure 3C). WRI1 (Baud et al., 2009), LEC1 (Mu et al., 2008), LEC2 (Kim et al., 2015), MYB96 (Lee et al., 2018), BASIC LEUCINE ZIPPER TF 67 (bZIP67; Mendes et al., 2013; Kim et al., 2022), ABSCISIC ACID INSENSITIVE 3 (ABI3; Giraudat et al., 1992), FUSCA3 (FUS3; Luerssen et al., 1998) have been reported as positive regulators of TAG biosynthesis. MYB89 (Li et al., 2017), WRKY6 (Song et al., 2020), MYB76 (Duan et al., 2017), TRANSPARENT TESTA GLABRA1 (TTG1; Chen et al., 2015), TRANSPARENT TESTA2 (TT2; Chen et al., 2012), and TT8 (Chen et al., 2014) have been reported as negative regulators. Therefore, knockout of the negative regulator using CRISPR/Cas9 in various oil crops may enhance the oil content. It is important to choose a negative TF that only increases oil content without any detrimental growth phenotype when the negative TF is eliminated because transcription factors can regulate not only lipid-related genes but also other genes. Finally, CRISPR/Cas9-based methods can be applied in plants by using dCas9 as a carrier, which is an inactive Cas9 (Figure 3D). Recently, DNMT3A, which methylates DNA, was fused with dCas9 to methylate DNA at a specific site to decrease gene expression, or TET was fused with dCas9 to demethylate DNA to increase gene expression (Xie et al., 2018). These techniques will be a new approach in the epigenetic study of genes involved in lipid metabolism. In addition, the base editor can be a good strategy to change one amino acid or mutate randomly in the plant genome (Figure 3D). For example, with random mutation of the *FAD2* gene of *Arabidopsis* using base editing, the activity of FAD2 was weakened, and individuals with high oleic acid and resistance to salt stress were selected (Park et al., 2021).

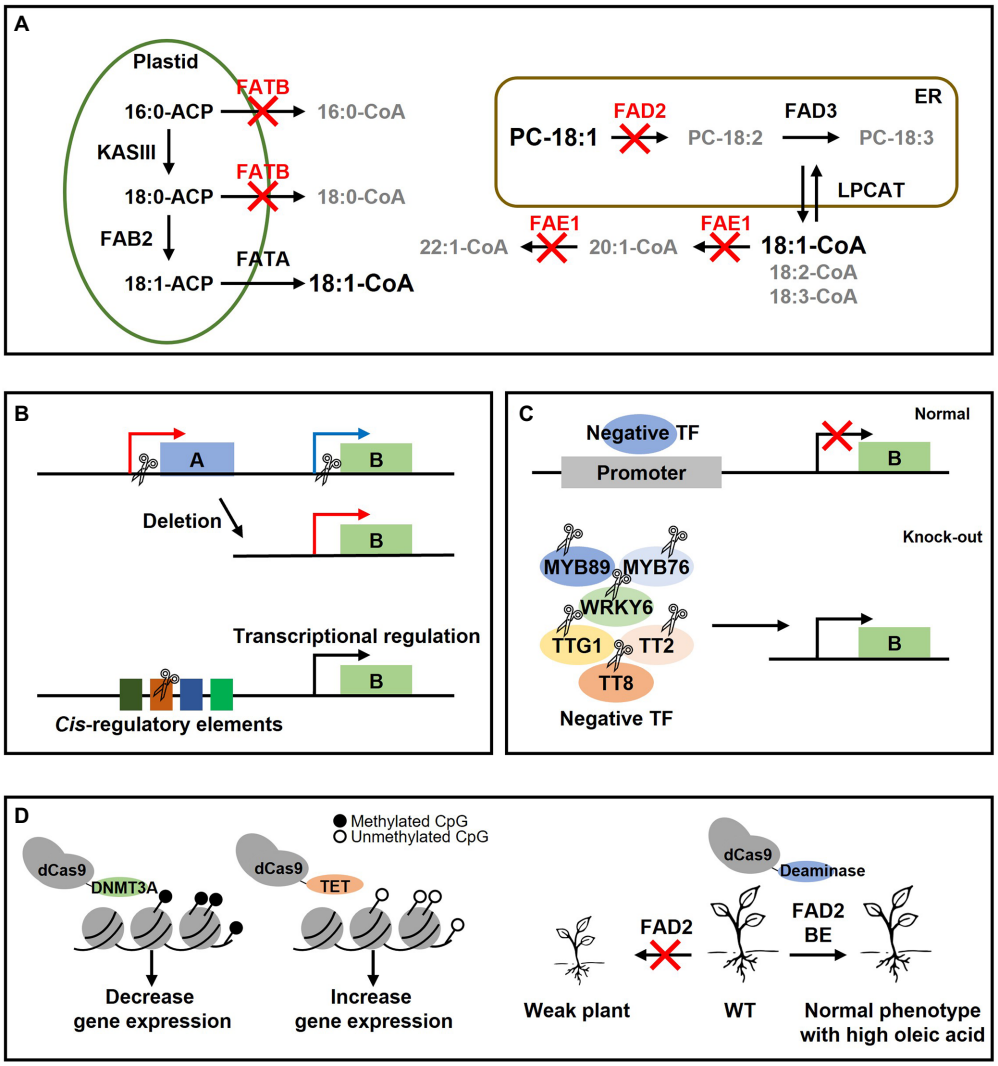

FIGURE 3
Future strategies of lipid metabolism research using CRISPR/Cas9 in this paper. **(A)** Schematic diagram of fatty acid synthesis for the development of plants with high oleic acid content in seeds. The flow of fatty acid synthesis is indicated by arrows. Red letters indicate three genes that may increase the oleic acid content if it is eliminated by CRISPR. Gray letters indicate fatty acids whose content is decreased when three genes (*FATB*, *FAE1*, and *FAD2*) are knocked out. It appears that plants with high oleic acid content may be created if three genes were deleted. **(B)** A study of promoter regulation using CRISPR/Cas9. B refers to the lipid gene and A is the upstream gene of the B gene. The scissor shape represents CRISPR/Cas9. By removing from the 5′UTR of the B gene to the 5′UTR of the A gene, the B gene can be controlled by the A promoter (Bhunia et al., 2022). In addition, the transcription level can be regulated by deleting the *cis*-regulatory elements of the B gene. **(C)** Knockout of the negative transcription factor in plant. The expression of lipid genes can be reduced in a normal plant by a variety of negative transcription factors. However, if the negative transcription factor is disrupted using CRISPR, the expression of the lipid gene can be increased. **(D)** CRISPR/Cas9-based technology. Epigenetic study of lipid gene seems possible if Cas9-based technique is used. For example, by methylation through dCas9-DNMT3A, lipid gene expression can be suppressed whereas demethylation *via* dCas9-TET can increase lipid gene expression. Alternatively, it is possible to develop a plant that slightly weakens the function of a specific protein by using base editing and has a normal phenotype than that of knockout mutants, but with a changed lipid composition.

There is a point to note when CRISPR/Cas9 is applied to mutate some genes. This is because mutations in lipid metabolism genes can alter lipid composition while also adversely affecting plant growth and development. For example, *Camelina* has three copies of the *FAD2* gene because it is allohexaploid (Kang et al., 2011). If all three copy *FAD2* genes are completely mutated, it adversely affects plant growth because this mutant is unable to synthesize polyunsaturated FAs, which are essential for maintaining the fluidity of cell membranes (Lee et al., 2021). To avoid such extreme phenotypes, it is necessary to specifically knockout only one or two *FAD2* genes in camelina (Lee et al., 2021). In addition, in plants with a single copy of *FAD2*, it may be preferable to create a weak allele using the base editor (Park et al., 2021). A potential problem is that Cas9 can bind to unintended sites causing accidental mutations, or off-target mutations. However, these off-target mutations can be overcome

in plants by backcrossing with wild type. In the future, oil crops that produce a large amount of useful FA for the industry should be developed by simultaneously controlling transcription factors and lipid metabolic genes using genome editing.

Author contributions

M-EP and HUK designed and structured the review, collected the information, organized the figures and tables, and wrote and revised the manuscript. All authors contributed to the article and approved the submitted version.

Funding

This work was supported by grants from the Mid-Career Researcher Program of the National Research Foundation of Korea (NRF-2020R1A2C2008175), the New Breeding Technologies Development Program (project no. PJ016533), and the Next Generation BioGreen21 associated program (project no. PJ015714), and the Rural Development Administration, Republic of Korea.

Conflict of interest

The authors declare that the research was conducted in the absence of any commercial or financial relationships that could be construed as a potential conflict of interest.

Publisher's note

References

Abe, K., Araki, E., Suzuki, Y., Toki, S., and Saika, H. (2018). Production of high oleic/low linoleic rice by genome editing. *Plant Physiol. Biochem.* 131, 58–62. doi: 10.1016/j.plaphy.2018.04.033

Aher, R. R., Reddy, P. S., Bhunia, R. K., Flyckt, K. S., Shankhapal, A. R., Ojha, R., et al. (2022). Loss-of-function mutations in novel triacylglycerol lipase genes are associated with low rancidity in pearl millet flour. *bioRxiv* [Preprint]. doi: 10.1101/2022.04.02.486827

Al Amin, N., Ahmad, N., Wu, N., Pu, X., Ma, T., Du, Y., et al. (2019). CRISPR-Cas9 mediated targeted disruption of *FAD2-2 microsomal omega-6 desaturase* in soybean (*Glycine max*.L). *BMC Biotechnol.* 19:9. doi: 10.1186/s12896-019-0501-2

Andrianov, V., Borisjuk, N., Pogrebnyak, N., Brinker, A., Dixon, J., Spitsin, S., et al. (2010). Tobacco as a production platform for biofuel: overexpression of *Arabidopsis DGAT* and *LEC2* genes increases accumulation and shifts the composition of lipids in green biomass. *Plant Biotechnol. J.* 8, 277–287. doi: 10.1111/j.1467-7652.2009.00458.x

Ayme, L., Arragain, S., Canonge, M., Baud, S., Touati, N., Bimai, O., et al. (2018). *Arabidopsis thaliana* DGAT3 is a [2Fe-2S] protein involved in TAG biosynthesis. *Sci. Rep.* 8:17254. doi: 10.1038/s41598-018-35545-7

Azeez, A., Parchuri, P., and Bates, P. D. (2022). Suppression of *Physaria fendleri* SDP1 increased seed oil and Hydroxy fatty acid content while maintaining oil biosynthesis through triacylglycerol remodeling. *Front. Plant Sci.* 13:931310. doi: 10.3389/fpls.2022.931310

Aznar-Moreno, J. A., and Durrett, T. P. (2017). Simultaneous targeting of multiple gene Homeologs to Alter seed oil production in *Camelina sativa*. *Plant Cell Physiol.* 58, 1260–1267. doi: 10.1093/pcp/pcx058

Aznar-Moreno, J. A., Mukherjee, T., Morley, S. A., Duressa, D., Kambhampati, S., Chu, K. L., et al. (2022). Suppression of *SDP1* improves soybean seed composition by increasing oil and reducing Undigestible oligosaccharides. *Front. Plant Sci.* 13:863254. doi: 10.3389/fpls.2022.863254

Bahariah, B., Masani, M. Y. A., Rasid, O. A., and Parveez, G. K. A. (2021). Multiplex CRISPR/Cas9-mediated genome editing of the *FAD2* gene in rice: a model genome editing system for oil palm. *J. Genet. Eng. Biotechnol.* 19:86. doi: 10.1186/s43141-021-00185-4

Bai, Y., Shen, Y., Zhang, Z., Jia, Q., Xu, M., Zhang, T., et al. (2021). A GPAT1 mutation in Arabidopsis enhances plant height but impairs seed oil biosynthesis. *Int. J. Mol. Sci.* 22, 1–18. doi: 10.3390/ijms22020785

Banas, A., Dahlqvist, A., Stahl, U., Lenman, M., and Stymne, S. (2000). The involvement of phospholipid:diacylglycerol acyltransferases in triacylglycerol production. *Biochem. Soc. Trans.* 28, 703–705. doi: 10.1042/bst0280703

Baud, S., Wuilleme, S., To, A., Rochat, C., and Lepiniec, L. (2009). Role of WRINKLED1 in the transcriptional regulation of glycolytic and fatty acid biosynthetic genes in Arabidopsis. *Plant J.* 60, 933–947. doi: 10.1111/j.1365-313X.2009.04011.x

Bhunia, R. K., Menard, G. N., and Eastmond, P. J. (2022). A native promoter-gene fusion created by CRISPR/Cas9-mediated genomic deletion offers a transgene-free method to drive oil accumulation in leaves. *FEBS Lett.* 596, 1865–1870. doi: 10.1002/1873-3468.14365

Bhunia, R. K., Sinha, K., Kaur, R., Kaur, S., and Chawla, K. (2021). A holistic view of the genetic factors involved in triggering hydrolytic and oxidative rancidity of rice bran lipids. *Food Rev. Int.*, 1–26. doi: 10.1080/87559129.2021.1915328

Brouns, S. J., Jore, M. M., Lundgren, M., Westra, E. R., Slijkhuis, R. J., Snijders, A. P., et al. (2008). Small CRISPR RNAs guide antiviral defense in prokaryotes. *Science* 321, 960–964. doi: 10.1126/science.1159689

Browse, J., Mcconn, M., James, D., and Miquel, M. (1993). Mutants of *Arabidopsis* deficient in the synthesis of alpha-linolenate. Biochemical and genetic characterization of the endoplasmic reticulum linoleoyl desaturase. *J. Biol. Chem.* 268, 16345–16351. doi: 10.1016/S0021-9258(19)85427-3

Buchanan, B. B., Gruissem, W., and Jones, R. L. (2015). *Biochemistry and Molecular Biology of Plants. (2nd Ed.).* Wiley: Hoboken, NJ, USA.

Cahoon, E. B., and Li-Beisson, Y. (2020). Plant unusual fatty acids: learning from the less common. *Curr. Opin. Plant Biol.* 55, 66–73. doi: 10.1016/j.pbi.2020.03.007

Carman, G. M., and Han, G. S. (2006). Roles of phosphatidate phosphatase enzymes in lipid metabolism. *Trends Biochem. Sci.* 31, 694–699. doi: 10.1016/j.tibs.2006.10.003

Cases, S., Smith, S. J., Zheng, Y. W., Myers, H. M., Lear, S. R., Sande, E., et al. (1998). Identification of a gene encoding an acyl CoA:diacylglycerol acyltransferase, a key enzyme in triacylglycerol synthesis. *Proc. Natl. Acad. Sci. U. S. A.* 95, 13018–13023. doi: 10.1073/pnas.95.22.13018

Chandrasegaran, S., and Carroll, D. (2016). Origins of programmable nucleases for genome engineering. *J. Mol. Biol.* 428, 963–989. doi: 10.1016/j.jmb.2015.10.014

Chapman, K. D., and Ohlrogge, J. B. (2012). Compartmentation of triacylglycerol accumulation in plants. *J. Biol. Chem.* 287, 2288–2294. doi: 10.1074/jbc.R111.290072

Chen, Y., Fu, M., Li, H., Wang, L., Liu, R., Liu, Z., et al. (2021). High-oleic acid content, nontransgenic allotetraploid cotton (*Gossypium hirsutum* L.) generated by knockout of GhFAD2 genes with CRISPR/Cas9 system. *Plant Biotechnol. J.* 19, 424–426. doi: 10.1111/pbi.13507

Chen, K., Wang, Y., Zhang, R., Zhang, H., and Gao, C. (2019). CRISPR/Cas genome editing and precision plant breeding in agriculture. *Annu. Rev. Plant Biol.* 70, 667–697. doi: 10.1146/annurev-arplant-050718-100049

Chen, M., Wang, Z., Zhu, Y., Li, Z., Hussain, N., Xuan, L., et al. (2012). The effect of *TRANSPARENT TESTA2* on seed fatty acid biosynthesis and tolerance to

environmental stresses during young seedling establishment in Arabidopsis. *Plant Physiol.* 160, 1023–1036. doi: 10.1104/pp.112.202945

Chen, M., Xuan, L., Wang, Z., Zhou, L., Li, Z., Du, X., et al. (2014). TRANSPARENT TESTA8 inhibits seed fatty acid accumulation by targeting several seed development regulators in Arabidopsis. *Plant Physiol.* 165, 905–916. doi: 10.1104/pp.114.235507

Chen, M., Zhang, B., Li, C., Kulaveerasingam, H., Chew, F. T., and Yu, H. (2015). TRANSPARENT TESTA GLABRA1 regulates the accumulation of seed storage reserves in Arabidopsis. *Plant Physiol.* 169, 391–402. doi: 10.1104/pp.15.00943

Clough, R. C., Matthis, A. L., Barnum, S. R., and Jaworski, J. G. (1992). Purification and characterization of 3-ketoacyl-acyl carrier protein synthase III from spinach. A condensing enzyme utilizing acetyl-coenzyme a to initiate fatty acid synthesis. *J. Biol. Chem.* 267, 20992–20998. doi: 10.1016/S0021-9258(19)36787-0

Cong, L., Ran, F. A., Cox, D., Lin, S., Barretto, R., Habib, N., et al. (2013). Multiplex genome engineering using CRISPR/Cas systems. *Science* 339, 819–823. doi: 10.1126/science.1231143

Dahlqvist, A., Stahl, U., Lenman, M., Banas, A., Lee, M., Sandager, L., et al. (2000). Phospholipid:diacylglycerol acyltransferase: an enzyme that catalyzes the acyl-CoA-independent formation of triacylglycerol in yeast and plants. *Proc. Natl. Acad. Sci. U. S. A.* 97, 6487–6492. doi: 10.1073/pnas.120067297

Dar, A. A., Choudhury, A. R., Kancharla, P. K., and Arumugam, N. (2017). The FAD2 gene in plants: occurrence, regulation, and role. *Front. Plant Sci.* 8:1789. doi: 10.3389/fpls.2017.01789

Do, P. T., Nguyen, C. X., Bui, H. T., Tran, L. T. N., Stacey, G., Gillman, J. D., et al. (2019). Demonstration of highly efficient dual gRNA CRISPR/Cas9 editing of the homeologous *GmFAD2-1A* and *GmFAD2-1B* genes to yield a high oleic, low linoleic and alpha-linolenic acid phenotype in soybean. *BMC Plant Biol.* 19:311. doi: 10.1186/s12870-019-1906-8

Duan, S., Jin, C., Li, D., Gao, C., Qi, S., Liu, K., et al. (2017). MYB76 inhibits seed fatty acid accumulation in Arabidopsis. *Front. Plant Sci.* 8:226. doi: 10.3389/fpls.2017.00226

Dubois, V., Breton, S., Linder, M., Fanni, J., and Parmentier, M. (2007). Fatty acid profiles of 80 vegetable oils with regard to their nutritional potential. *Eur. J. Lipid Sci. Technol.* 109, 710–732. doi: 10.1002/ejlt.200700040

Durai, S., Mani, M., Kandavelou, K., Wu, J., Porteus, M. H., and Chandrasegaran, S. (2005). Zinc finger nucleases: custom-designed molecular scissors for genome engineering of plant and mammalian cells. *Nucleic Acids Res.* 33, 5978–5990. doi: 10.1093/nar/gki912

Eastmond, P. J. (2004). Cloning and characterization of the acid lipase from castor beans. *J. Biol. Chem.* 279, 45540–45545. doi: 10.1074/jbc.M408686200

Eastmond, P. J. (2006). *SUGAR-DEPENDENT1* encodes a patatin domain triacylglycerol lipase that initiates storage oil breakdown in germinating *Arabidopsis* seeds. *Plant Cell* 18, 665–675. doi: 10.1105/tpc.105.040543

Gao, C.-Y., Mao, X., Shang, H.-Q., Li, F., and Li, R.-Z. (2018). Enhanced oil accumulation in tobacco (*Nicotiana tabacum* L.) leaves by ectopic overexpression of *VgDGAT1a* for renewable production of biofuels. *Curr. Sci.* 114, 1234–1240. doi: 10.18520/cs/v114/i06/1234-1240

Gaudelli, N. M., Komor, A. C., Rees, H. A., Packer, M. S., Badran, A. H., Bryson, D. I., et al. (2017). Programmable base editing of a*T to G*C in genomic DNA without DNA cleavage. *Nature* 551, 464–471. doi: 10.1038/nature24644

Giraudat, J., Hauge, B. M., Valon, C., Smalle, J., Parcy, F., and Goodman, H. M. (1992). Isolation of the Arabidopsis *ABI3* gene by positional cloning. *Plant Cell* 4, 1251–1261. doi: 10.1105/tpc.4.10.1251

Graham, I. A. (2008). Seed storage oil mobilization. *Annu. Rev. Plant Biol.* 59, 115–142. doi: 10.1146/annurev.arplant.59.032607.092938

Guo, Y., Abernathy, B., Zeng, Y., and Ozias-Akins, P. (2015). TILLING by sequencing to identify induced mutations in stress resistance genes of peanut (*Arachis hypogaea*). *BMC Genomics* 16:157. doi: 10.1186/s12864-015-1348-0

Haslam, R. P., Sayanova, O., Kim, H. J., Cahoon, E. B., and Napier, J. A. (2016). Synthetic redesign of plant lipid metabolism. *Plant J.* 87, 76–86. doi: 10.1111/tpj.13172

He, M., Qin, C. X., Wang, X., and Ding, N. Z. (2020). Plant unsaturated fatty acids: biosynthesis and regulation. *Front. Plant Sci.* 11:390. doi: 10.3389/fpls.2020.00390

Hofvander, P., Ischebeck, T., Turesson, H., Kushwaha, S. K., Feussner, I., Carlsson, A. S., et al. (2016). Potato tuber expression of Arabidopsis *WRINKLED1* increase triacylglycerol and membrane lipids while affecting central carbohydrate metabolism. *Plant Biotechnol. J.* 14, 1883–1898. doi: 10.1111/pbi.12550

Huang, A. H. C. (2018). Plant lipid droplets and their associated proteins: potential for rapid advances. *Plant Physiol.* 176, 1894–1918. doi: 10.1104/pp.17.01677

Huang, H., Cui, T., Zhang, L., Yang, Q., Yang, Y., Xie, K., et al. (2020). Modifications of fatty acid profile through targeted mutation at *BnaFAD2* gene with CRISPR/Cas9-mediated gene editing in *Brassica napus*. *Theor. Appl. Genet.* 133, 2401–2411. doi: 10.1007/s00122-020-03607-y

Imamura, F., Lemaitre, R. N., King, I. B., Song, X., Steffen, L. M., Folsom, A. R., et al. (2013). Long-chain monounsaturated fatty acids and incidence of congestive heart failure in 2 prospective cohorts. *Circulation* 127, 1512–1521. doi: 10.1161/CIRCULATIONAHA.112.001197

Jaganathan, D., Ramasamy, K., Sellamuthu, G., Jayabalan, S., and Venkataraman, G. (2018). CRISPR for crop improvement: an update review. *Front. Plant Sci.* 9:985. doi: 10.3389/fpls.2018.00985

Jarvis, B. A., Romsdahl, T. B., Mcginn, M. G., Nazarenus, T. J., Cahoon, E. B., Chapman, K. D., et al. (2021). CRISPR/Cas9-induced *fad2* and *rod1* mutations stacked with *fae1* confer high oleic acid seed oil in pennycress (*Thlaspi arvense* L.). *Front. Plant Sci.* 12:652319. doi: 10.3389/fpls.2021.652319

Jeon, S., Lim, J. M., Lee, H. G., Shin, S. E., Kang, N. K., Park, Y. I., et al. (2017). Current status and perspectives of genome editing technology for microalgae. *Biotechnol. Biofuels* 10:267. doi: 10.1186/s13068-017-0957-z

Jiang, F., and Doudna, J. A. (2017). CRISPR-Cas9 structures and mechanisms. *Annu. Rev. Biophys.* 46, 505–529. doi: 10.1146/annurev-biophys-062215-010822

Jiang, W. Z., Henry, I. M., Lynagh, P. G., Comai, L., Cahoon, E. B., and Weeks, D. P. (2017). Significant enhancement of fatty acid composition in seeds of the allohexaploid, *Camelina sativa*, using CRISPR/Cas9 gene editing. *Plant Biotechnol. J.* 15, 648–657. doi: 10.1111/pbi.12663

Jinek, M., Chylinski, K., Fonfara, I., Hauer, M., Doudna, J. A., and Charpentier, E. (2012). A programmable dual-RNA-guided DNA endonuclease in adaptive bacterial immunity. *Science* 337, 816–821. doi: 10.1126/science.1225829

Jones, A., Davies, H. M., and Voelker, T. A. (1995). Palmitoyl-acyl carrier protein (ACP) thioesterase and the evolutionary origin of plant acyl-ACP thioesterases. *Plant Cell* 7, 359–371. doi: 10.1105/tpc.7.3.359

Joung, J. K., and Sander, J. D. (2013). TALENs: a widely applicable technology for targeted genome editing. *Nat. Rev. Mol. Cell Biol.* 14, 49–55. doi: 10.1038/nrm3486

Kanai, M., Yamada, T., Hayashi, M., Mano, S., and Nishimura, M. (2019). Soybean (*Glycine max* L.) triacylglycerol lipase GmSDP1 regulates the quality and quantity of seed oil. *Sci. Rep.* 9:8924. doi: 10.1038/s41598-019-45331-8

Kang, J., Snapp, A. R., and Lu, C. (2011). Identification of three genes encoding microsomal oleate desaturases (FAD2) from the oilseed crop *Camelina sativa*. *Plant Physiol. Biochem.* 49, 223–229. doi: 10.1016/j.plaphy.2010.12.004

Kelly, A. A., Quettier, A. L., Shaw, E., and Eastmond, P. J. (2011). Seed storage oil mobilization is important but not essential for germination or seedling establishment in Arabidopsis. *Plant Physiol.* 157, 866–875. doi: 10.1104/pp.111.181784

Kelly, A. A., Shaw, E., Powers, S. J., Kurup, S., and Eastmond, P. J. (2013). Suppression of the *SUGAR-DEPENDENT1* triacylglycerol lipase family during seed development enhances oil yield in oilseed rape (*Brassica napus* L.). *Plant Biotechnol. J.* 11, 355–361. doi: 10.1111/pbi.12021

Khan, M. S. S., Basnet, R., Ahmed, S., Bao, J., and Shu, Q. (2020). Mutations of *OsPLDα1* increase Lysophospholipid content and enhance cooking and eating quality in rice. *Plants (Basel)* 9:390. doi: 10.3390/plants9030390

Khan, M. S. S., Basnet, R., Islam, S. A., and Shu, Q. (2019). Mutational analysis of *OsPLDα1* reveals its involvement in phytic acid biosynthesis in rice grains. *J. Agric. Food Chem.* 67, 11436–11443. doi: 10.1021/acs.jafc.9b05052

Kihara, A. (2012). Very long-chain fatty acids: elongation, physiology and related disorders. *J. Biochem.* 152, 387–395. doi: 10.1093/jb/mvs105

Kim, H. U. (2020). Lipid metabolism in plants. *Plants (Basel)* 9:871. doi: 10.3390/plants9070871

Kim, H. U., and Huang, A. H. (2004). Plastid lysophosphatidyl acyltransferase is essential for embryo development in Arabidopsis. *Plant Physiol.* 134, 1206–1216. doi: 10.1104/pp.103.035832

Kim, W. N., Kim, H. J., Chung, Y. S., and Kim, H. U. (2021). Construction of Multiple Guide RNAs in CRISPR/Cas9 Vector Using Stepwise or Simultaneous Golden Gate Cloning: Case Study for Targeting the FAD2 and FATB Multigene in Soybean. *Plants (Basel)* 10:2542. doi: 10.3390/plants10112542

Kim, H. U., Lee, K. R., Jung, S. J., Shin, H. A., Go, Y. S., Suh, M. C., et al. (2015). Senescence-inducible LEC2 enhances triacylglycerol accumulation in leaves without negatively affecting plant growth. *Plant Biotechnol. J.* 13, 1346–1359. doi: 10.1111/pbi.12354

Kim, I., Lee, K. R., Park, M. E., and Kim, H. U. (2022). The seed-specific transcription factor DPBF2 modulates the fatty acid composition in seeds. *Plant Direct* 6:e395. doi: 10.1002/pld3.395

Kim, H. U., Li, Y., and Huang, A. H. (2005). Ubiquitous and endoplasmic reticulum-located lysophosphatidyl acyltransferase, LPAT2, is essential for female but not male gametophyte development in Arabidopsis. *Plant Cell* 17, 1073–1089. doi: 10.1105/tpc.104.030403

Kim, M. J., Yang, S. W., Mao, H. Z., Veena, S. P., Yin, J. L., and Chua, N. H. (2014). Gene silencing of *sugar-dependent 1* (*JcSDP1*), encoding a patatin-domain triacylglycerol lipase, enhances seed oil accumulation in *Jatropha curcas*. *Biotechnol. Biofuels* 7:36. doi: 10.1186/1754-6834-7-36

Klaus, D., Ohlrogge, J. B., Neuhaus, H. E., and Dormann, P. (2004). Increased fatty acid production in potato by engineering of acetyl-CoA carboxylase. *Planta* 219, 389–396. doi: 10.1007/s00425-004-1236-3

Komor, A. C., Kim, Y. B., Packer, M. S., Zuris, J. A., and Liu, D. R. (2016). Programmable editing of a target base in genomic DNA without double-stranded DNA cleavage. *Nature* 533, 420–424. doi: 10.1038/nature17946

Kumar, R. R., Bhargava, D. V., Pandit, K., Goswami, S., Mukesh Shankar, S., Singh, S. P., et al. (2021). Lipase—the fascinating dynamics of enzyme in seed storage and germination—a real challenge to pearl millet. *Food Chem.* 361:130031. doi: 10.1016/j.foodchem.2021.130031

Lager, I., Yilmaz, J. L., Zhou, X. R., Jasieniecka, K., Kazachkov, M., Wang, P., et al. (2013). Plant acyl-CoA:lysophosphatidylcholine acyltransferases (LPCATs) have different specificities in their forward and reverse reactions. *J. Biol. Chem.* 288, 36902–36914. doi: 10.1074/jbc.M113.521815

Lee, K. R., Jeon, I., Yu, H., Kim, S. G., Kim, H. S., Ahn, S. J., et al. (2021). Increasing monounsaturated fatty acid contents in Hexaploid *Camelina sativa* seed oil by *FAD2* gene knockout using CRISPR-Cas9. *Front. Plant Sci.* 12:702930. doi: 10.3389/fpls.2021.702930

Lee, H. G., Kim, H., Suh, M. C., Kim, H. U., and Seo, P. J. (2018). The MYB96 transcription factor regulates triacylglycerol accumulation by activating *DGAT1* and *PDAT1* expression in Arabidopsis seeds. *Plant Cell Physiol.* 59, 1432–1442. doi: 10.1093/pcp/pcy073

Lee, J. M., Lee, H., Kang, S., and Park, W. J. (2016). Fatty acid desaturases, polyunsaturated fatty acid regulation, and biotechnological advances. *Nutrients* 8:23. doi: 10.3390/nu8010023

Leenay, R. T., and Beisel, C. L. (2017). Deciphering, communicating, and engineering the CRISPR PAM. *J. Mol. Biol.* 429, 177–191. doi: 10.1016/j.jmb.2016.11.024

Lemieux, B., Miquel, M., Somerville, C., and Browse, J. (1990). Mutants of *Arabidopsis* with alterations in seed lipid fatty acid composition. *Theor. Appl. Genet.* 80, 234–240. doi: 10.1007/BF00224392

Lessire, R., and Stumpe, P. K. (1983). Nature of the fatty acid Synthetase Systems in Parenchymal and Epidermal Cells of *Allium porrum* L. leaves. *Plant Physiol.* 73, 614–618. doi: 10.1104/pp.73.3.614

Li, Q., Feng, Q., Snouffer, A., Zhang, B., Rodriguez, G. R., and Van Der Knaap, E. (2022). Increasing fruit weight by editing a *Cis*-regulatory element in tomato *KLUH* promoter using CRISPR/Cas9. *Front. Plant Sci.* 13:879642. doi: 10.3389/fpls.2022.879642

Li, D., Jin, C., Duan, S., Zhu, Y., Qi, S., Liu, K., et al. (2017). MYB89 transcription factor represses seed oil accumulation. *Plant Physiol.* 173, 1211–1225. doi: 10.1104/pp.16.01634

Li, C., Li, W., Zhou, Z., Chen, H., Xie, C., and Lin, Y. (2020a). A new rice breeding method: CRISPR/Cas9 system editing of the *Xa13* promoter to cultivate transgene-free bacterial blight-resistant rice. *Plant Biotechnol. J.* 18, 313–315. doi: 10.1111/pbi.13217

Li, M., Qin, C., Welti, R., and Wang, X. (2006). Double knockouts of phospholipases Dζ1 and Dζ2 in Arabidopsis affect root elongation during phosphate-limited growth but do not affect root hair patterning. *Plant Physiol.* 140, 761–770. doi: 10.1104/pp.105.070995

Li, H., Yang, Y., Hong, W., Huang, M., Wu, M., and Zhao, X. (2020b). Applications of genome editing technology in the targeted therapy of human diseases: mechanisms, advances and prospects. *Signal Transduct. Target. Ther.* 5:1. doi: 10.1038/s41392-019-0089-y

Li-Beisson, Y., Shorrosh, B., Beisson, F., Andersson, M. X., Arondel, V., Bates, P. D., et al. (2013). Acyl-lipid metabolism. *Arabidopsis Book* 11:e0161. doi: 10.1199/tab.0161

Lightner, J., Wu, J., and Browse, J. (1994). A mutant of *Arabidopsis* with increased levels of stearic acid. *Plant Physiol.* 106, 1443–1451. doi: 10.1104/pp.106.4.1443

Liu, Y., Du, Z., Lin, S., Li, H., Lu, S., Guo, L., et al. (2022). CRISPR/Cas9-targeted mutagenesis of *BnaFAE1* genes confers low-erucic acid in *Brassica napus*. *Front. Plant Sci.* 13:848723. doi: 10.3389/fpls.2022.848723

Liu, Q., Guo, Q., Akbar, S., Zhi, Y., El Tahchy, A., Mitchell, M., et al. (2017). Genetic enhancement of oil content in potato tuber (*Solanum tuberosum* L.) through an integrated metabolic engineering strategy. *Plant Biotechnol. J.* 15, 56–67. doi: 10.1111/pbi.12590

Liu, X., Qin, R., Li, J., Liao, S., Shan, T., Xu, R., et al. (2020). A CRISPR-Cas9-mediated domain-specific base-editing screen enables functional assessment of ACCase variants in rice. *Plant Biotechnol. J.* 18, 1845–1847. doi: 10.1111/pbi.13348

Liu, L., Waters, D. L., Rose, T. J., Bao, J., and King, G. J. (2013). Phospholipids in rice: significance in grain quality and health benefits: a review. *Food Chem.* 139, 1133–1145. doi: 10.1016/j.foodchem.2012.12.046

Luerssen, H., Kirik, V., Herrmann, P., and Misera, S. (1998). *FUSCA3* encodes a protein with a conserved VP1/AB13-like B3 domain which is of functional importance for the regulation of seed maturation in *Arabidopsis thaliana*. *Plant J.* 15, 755–764. doi: 10.1046/j.1365-313X.1998.00259.x

Ma, J., Sun, S., Whelan, J., and Shou, H. (2021). CRISPR/Cas9-mediated knockout of *GmFATB1* significantly reduced the amount of saturated fatty acids in soybean seeds. *Int. J. Mol. Sci.* 22, 1–14. doi: 10.3390/ijms22083877

Martinez-Reyes, I., and Chandel, N. S. (2020). Mitochondrial TCA cycle metabolites control physiology and disease. *Nat. Commun.* 11:102. doi: 10.1038/s41467-019-13668-3

Mcconn, M., Hugly, S., Browse, J., and Somerville, C. (1994). A mutation at the *fad8* locus of *Arabidopsis* identifies a second chloroplast [omega]-3 desaturase. *Plant Physiol.* 106, 1609–1614. doi: 10.1104/pp.106.4.1609

Mcginn, M., Phippen, W. B., Chopra, R., Bansal, S., Jarvis, B. A., Phippen, M. E., et al. (2019). Molecular tools enabling pennycress (*Thlaspi arvense*) as a model plant and oilseed cash cover crop. *Plant Biotechnol. J.* 17, 776–788. doi: 10.1111/pbi.13014

Mendes, A., Kelly, A. A., Van Erp, H., Shaw, E., Powers, S. J., Kurup, S., et al. (2013). bZIP67 regulates the omega-3 fatty acid content of *Arabidopsis* seed oil by activating *FATTY ACID DESATURASE3*. *Plant Cell* 25, 3104–3116. doi: 10.1105/tpc.113.116343

Millar, A. A., and Kunst, L. (1997). Very-long-chain fatty acid biosynthesis is controlled through the expression and specificity of the condensing enzyme. *Plant J.* 12, 121–131. doi: 10.1046/j.1365-313X.1997.12010121.x

Morineau, C., Bellec, Y., Tellier, F., Gissot, L., Kelemen, Z., Nogue, F., et al. (2017). Selective gene dosage by CRISPR-Cas9 genome editing in hexaploid *Camelina sativa*. *Plant Biotechnol. J.* 15, 729–739. doi: 10.1111/pbi.12671

Mu, J., Tan, H., Zheng, Q., Fu, F., Liang, Y., Zhang, J., et al. (2008). *LEAFY COTYLEDON1* is a key regulator of fatty acid biosynthesis in Arabidopsis. *Plant Physiol.* 148, 1042–1054. doi: 10.1104/pp.108.126342

Muller, A. O., and Ischebeck, T. (2018). Characterization of the enzymatic activity and physiological function of the lipid droplet-associated triacylglycerol lipase AtOBL1. *New Phytol.* 217, 1062–1076. doi: 10.1111/nph.14902

Napier, J. A., Haslam, R. P., Beaudoin, F., and Cahoon, E. B. (2014). Understanding and manipulating plant lipid composition: metabolic engineering leads the way. *Curr. Opin. Plant Biol.* 19, 68–75. doi: 10.1016/j.pbi.2014.04.001

Nishida, K., Arazoe, T., Yachie, N., Banno, S., Kakimoto, M., Tabata, M., et al. (2016). Targeted nucleotide editing using hybrid prokaryotic and vertebrate adaptive immune systems. *Science* 353:aaf8729. doi: 10.1126/science.aaf8729

Nookaraju, A., Pandey, S. K., Fujino, T., Kim, J. Y., Suh, M. C., and Joshi, C. P. (2014). Enhanced accumulation of fatty acids and triacylglycerols in transgenic tobacco stems for enhanced bioenergy production. *Plant Cell Rep.* 33, 1041–1052. doi: 10.1007/s00299-014-1582-y

Ohlrogge, J., and Browse, J. (1995). Lipid biosynthesis. *Plant Cell* 7, 957–970. doi: 10.1105/tpc.7.7.957

Okuley, J., Lightner, J., Feldmann, K., Yadav, N., Lark, E., and Browse, J. (1994). Arabidopsis *FAD2* gene encodes the enzyme that is essential for polyunsaturated lipid synthesis. *Plant Cell* 6, 147–158. doi: 10.1105/tpc.6.1.147

Okuzaki, A., Ogawa, T., Koizuka, C., Kaneko, K., Inaba, M., Imamura, J., et al. (2018). CRISPR/Cas9-mediated genome editing of the fatty acid desaturase 2 gene in *Brassica napus*. *Plant Physiol. Biochem.* 131, 63–69. doi: 10.1016/j.plaphy.2018.04.025

Ozseyhan, M. E., Kang, J., Mu, X., and Lu, C. (2018). Mutagenesis of the *FAE1* genes significantly changes fatty acid composition in seeds of *Camelina sativa*. *Plant Physiol. Biochem.* 123, 1–7. doi: 10.1016/j.plaphy.2017.11.021

Park, M. E., Yun, J. Y., and Kim, H. U. (2021). C-to-G Base editing enhances oleic acid production by generating novel alleles of *FATTY ACID DESATURASE 2* in plants. *Front. Plant Sci.* 12:748529. doi: 10.3389/fpls.2021.748529

Poirier, Y., Antonenkov, V. D., Glumoff, T., and Hiltunen, J. K. (2006). Peroxisomal beta-oxidation—a metabolic pathway with multiple functions. *Biochim. Biophys. Acta* 1763, 1413–1426. doi: 10.1016/j.bbamcr.2006.08.034

Przybylski, O., and Aladedunye, F. A. (2012). Formation of trans fats during food preparation. *Can. J. Diet. Pract. Res.* 73, 98–101. doi: 10.3148/73.2.2012.98

Raghuram, T. C., and Rukmini, C. (1995). Nutritional significance of rice bran oil. *Indian J. Med. Res.* 102, 241–244.

Ran, F. A., Hsu, P. D., Wright, J., Agarwala, V., Scott, D. A., and Zhang, F. (2013). Genome engineering using the CRISPR-Cas9 system. *Nat. Protoc.* 8, 2281–2308. doi: 10.1038/nprot.2013.143

Rawsthorne, S. (2002). Carbon flux and fatty acid synthesis in plants. *Prog. Lipid Res.* 41, 182–196. doi: 10.1016/S0163-7827(01)00023-6

Reszczynska, E., and Hanaka, A. (2020). Lipids composition in plant membranes. *Cell Biochem. Biophys.* 78, 401–414. doi: 10.1007/s12013-020-00947-w

Rossak, M., Smith, M., and Kunst, L. (2001). Expression of the *FAE1* gene and *FAE1* promoter activity in developing seeds of *Arabidopsis thaliana*. *Plant Mol. Biol.* 46, 717–725. doi: 10.1023/A:1011603923889

Ryu, S. B. (2004). Phospholipid-derived signaling mediated by phospholipase A in plants. *Trends Plant Sci.* 9, 229–235. doi: 10.1016/j.tplants.2004.03.004

Saini, R. K., and Keum, Y. S. (2018). Omega-3 and omega-6 polyunsaturated fatty acids: dietary sources, metabolism, and significance: A review. *Life Sci.* 203, 255–267. doi: 10.1016/j.lfs.2018.04.049

Salas, J. J., and Ohlrogge, J. B. (2002). Characterization of substrate specificity of plant FatA and FatB acyl-ACP thioesterases. *Arch. Biochem. Biophys.* 403, 25–34. doi: 10.1016/S0003-9861(02)00017-6

Sander, J. D., and Joung, J. K. (2014). CRISPR-Cas systems for editing, regulating and targeting genomes. *Nat. Biotechnol.* 32, 347–355. doi: 10.1038/nbt.2842

Sasaki, Y., and Nagano, Y. (2004). Plant acetyl-CoA carboxylase: structure, biosynthesis, regulation, and gene manipulation for plant breeding. *Biosci. Biotechnol. Biochem.* 68, 1175–1184. doi: 10.1271/bbb.68.1175

Shimakata, T., and Stumpf, P. K. (1982). Isolation and function of spinach leaf beta-ketoacyl-[acyl-carrier-protein] synthases. *Proc. Natl. Acad. Sci. U. S. A.* 79, 5808–5812. doi: 10.1073/pnas.79.19.5808

Shockey, J., Regmi, A., Cotton, K., Adhikari, N., Browse, J., and Bates, P. D. (2016). Identification of Arabidopsis *GPAT9* (At5g60620) as an essential gene involved in triacylglycerol biosynthesis. *Plant Physiol.* 170, 163–179. doi: 10.1104/pp.15.01563

Siri-Tarino, P. W., Sun, Q., Hu, F. B., and Krauss, R. M. (2010). Saturated fatty acids and risk of coronary heart disease: modulation by replacement nutrients. *Curr. Atheroscler. Rep.* 12, 384–390. doi: 10.1007/s11883-010-0131-6

Song, G., Li, X., Munir, R., Khan, A. R., Azhar, W., Yasin, M. U., et al. (2020). The WRKY6 transcription factor affects seed oil accumulation and alters fatty acid compositions in *Arabidopsis thaliana*. *Physiol. Plant.* 169, 612–624. doi: 10.1111/ppl.13082

Subedi, U., Ozga, J. A., Chen, G., Foroud, N. A., and Singer, S. D. (2020). CRISPR/Cas-mediated genome editing for the improvement of oilseed crop productivity. *Crit. Rev. Plant Sci.* 39, 195–221. doi: 10.1080/07352689.2020.1782568

Takac, T., Novak, D., and Samaj, J. (2019). Recent advances in the cellular and developmental biology of phospholipases in plants. *Front. Plant Sci.* 10:362. doi: 10.3389/fpls.2019.00362

Tang, Y., Huang, J., Ji, H., Pan, L., Hu, C., Qiu, X., et al. (2022). Identification of AhFatB genes through genome-wide analysis and knockout of AhFatB reduces the content of saturated fatty acids in peanut (*Arichis hypogaea* L.). *Plant Sci.* 319:111247. doi: 10.1016/j.plantsci.2022.111247

Tian, Y., Chen, K., Li, X., Zheng, Y., and Chen, F. (2020a). Design of high-oleic tobacco (*Nicotiana tabacum* L.) seed oil by CRISPR-Cas9-mediated knockout of *NtFAD2-2*. *BMC Plant Biol.* 20:233. doi: 10.1186/s12870-020-02441-0

Tian, Y., Liu, X., Fan, C., Li, T., Qin, H., Li, X., et al. (2020b). Enhancement of tobacco (*Nicotiana tabacum* L.) seed lipid content for biodiesel production by CRISPR-Cas9-mediated knockout of *NtAn1*. *Front. Plant Sci.* 11:599474. doi: 10.3389/fpls.2020.599474

Vanhercke, T., Divi, U. K., El Tahchy, A., Liu, Q., Mitchell, M., Taylor, M. C., et al. (2017). Step changes in leaf oil accumulation via iterative metabolic engineering. *Metab. Eng.* 39, 237–246. doi: 10.1016/j.ymben.2016.12.007

Vanhercke, T., El Tahchy, A., Liu, Q., Zhou, X. R., Shrestha, P., Divi, U. K., et al. (2014). Metabolic engineering of biomass for high energy density: oilseed-like triacylglycerol yields from plant leaves. *Plant Biotechnol. J.* 12, 231–239. doi: 10.1111/pbi.12131

Virdi, K. S., Spencer, M., Stec, A. O., Xiong, Y., Merry, R., Muehlbauer, G. J., et al. (2020). Similar seed composition phenotypes are observed from CRISPR-generated in-frame and knockout alleles of a soybean *KASI* Ortholog. *Front. Plant Sci.* 11:1005. doi: 10.3389/fpls.2020.01005

Wang, G., Ryu, S., and Wang, X. (2012). Plant phospholipases: an overview. *Methods Mol. Biol.* 861, 123–137. doi: 10.1007/978-1-61779-600-5_8

Wang, Z. P., Xing, H. L., Dong, L., Zhang, H. Y., Han, C. Y., Wang, X. C., et al. (2015). Egg cell-specific promoter-controlled CRISPR/Cas9 efficiently generates homozygous mutants for multiple target genes in Arabidopsis in a single generation. *Genome Biol.* 16:144. doi: 10.1186/s13059-015-0715-0

Wolter, F., Schindele, P., and Puchta, H. (2019). Plant breeding at the speed of light: the power of CRISPR/Cas to generate directed genetic diversity at multiple sites. *BMC Plant Biol.* 19:176. doi: 10.1186/s12870-019-1775-1

Woo, J. W., Kim, J., Kwon, S. I., Corvalan, C., Cho, S. W., Kim, H., et al. (2015). DNA-free genome editing in plants with preassembled CRISPR-Cas9 ribonucleoproteins. *Nat. Biotechnol.* 33, 1162–1164. doi: 10.1038/nbt.3389

Wu, J., James, D. W., Dooner, H. K., and Browse, J. (1994). A mutant of Arabidopsis deficient in the elongation of palmitic acid. *Plant Physiol.* 106, 143–150. doi: 10.1104/pp.106.1.143

Wu, X., Liang, Y., Gao, H., Wang, J., Zhao, Y., Hua, L., et al. (2021). Enhancing rice grain production by manipulating the naturally evolved cis-regulatory element-containing inverted repeat sequence of *OsREM20*. *Mol. Plant* 14, 997–1011. doi: 10.1016/j.molp.2021.03.016

Wu, N., Lu, Q., Wang, P., Zhang, Q., Zhang, J., Qu, J., et al. (2020). Construction and analysis of *GmFAD2-1A* and *GmFAD2-2A* soybean fatty acid desaturase mutants based on CRISPR/Cas9 technology. *Int. J. Mol. Sci.* 21:1104. doi: 10.3390/ijms21031104

Xiao, Y., Karikari, B., Wang, L., Chang, F., and Zhao, T. (2021). Structure characterization and potential role of soybean phospholipases a multigene family in response to multiple abiotic stress uncovered by CRISPR/Cas9 technology. *Environ. Exp. Bot.* 188:104521. doi: 10.1016/j.envexpbot.2021.104521

Xie, X., Meesapyodsuk, D., and Qiu, X. (2019). Enhancing oil production in Arabidopsis through expression of a ketoacyl-ACP synthase domain of the PUFA synthase from Thraustochytrium. *Biotechnol. Biofuels* 12:172. doi: 10.1186/s13068-019-1514-8

Xie, K., Minkenberg, B., and Yang, Y. (2015). Boosting CRISPR/Cas9 multiplex editing capability with the endogenous tRNA-processing system. *Proc. Natl. Acad. Sci. U. S. A.* 112, 3570–3575. doi: 10.1073/pnas.1420294112

Xie, N., Zhou, Y., Sun, Q., and Tang, B. (2018). Novel epigenetic techniques provided by the CRISPR/Cas9 system. *Stem Cells Int.* 2018, 1–12. doi: 10.1155/2018/7834175

Xu, C., and Shanklin, J. (2016). Triacylglycerol metabolism, function, and accumulation in plant vegetative tissues. *Annu. Rev. Plant Biol.* 67, 179–206. doi: 10.1146/annurev-arplant-043015-111641

Xu, X., Vanhercke, T., Shrestha, P., Luo, J., Akbar, S., Konik-Rose, C., et al. (2019). Upregulated lipid biosynthesis at the expense of starch production in potato (*Solanum tuberosum*) vegetative tissues via simultaneous downregulation of *ADP-glucose Pyrophosphorylase* and *sugar Dependent1* expressions. *Front. Plant Sci.* 10:1444. doi: 10.3389/fpls.2019.01444

Xu, X.-Y., Yang, H.-K., Singh, S. P., Sharp, P. J., and Liu, Q. (2018). Genetic manipulation of non-classic oilseed plants for enhancement of their potential as a biofactory for triacylglycerol production. *Engineering* 4, 523–533. doi: 10.1016/j.eng.2018.07.002

Yamaguchi, T., Kuroda, M., Yamakawa, H., Ashizawa, T., Hirayae, K., Kurimoto, L., et al. (2009). Suppression of a phospholipase D gene, OsPLDβ1, activates defense responses and increases disease resistance in rice. *Plant Physiol.* 150, 308–319. doi: 10.1104/pp.108.131979

Yang, W., Simpson, J. P., Li-Beisson, Y., Beisson, F., Pollard, M., and Ohlrogge, J. B. (2012). A land-plant-specific glycerol-3-phosphate acyltransferase family in Arabidopsis: substrate specificity, sn-2 preference, and evolution. *Plant Physiol.* 160, 638–652. doi: 10.1104/pp.112.201996

Yarra, R., Cao, H., Jin, L., Mengdi, Y., and Zhou, L. (2020). CRISPR/Cas mediated base editing: a practical approach for genome editing in oil palm. 3. *Biotech* 10:306. doi: 10.1007/s13205-020-02302-5

Yuan, M., Zhu, J., Gong, L., He, L., Lee, C., Han, S., et al. (2019). Mutagenesis of FAD2 genes in peanut with CRISPR/Cas9 based gene editing. *BMC Biotechnol.* 19:24. doi: 10.1186/s12896-019-0516-8

Zaplin, E. S., Liu, Q., Li, Z., Butardo, V. M., Blanchard, C. L., and Rahman, S. (2013). Production of high oleic rice grains by suppressing the expression of the OsFAD2-1 gene. *Funct. Plant Biol.* 40, 996–1004. doi: 10.1071/FP12301

Zhang, G., Bahn, S. C., Wang, G., Zhang, Y., Chen, B., Zhang, Y., et al. (2019a). PLDα1-knockdown soybean seeds display higher unsaturated glycerolipid contents and seed vigor in high temperature and humidity environments. *Biotechnol. Biofuels* 12:9. doi: 10.1186/s13068-018-1340-4

Zhang, Y., Liang, Z., Zong, Y., Wang, Y., Liu, J., Chen, K., et al. (2016). Efficient and transgene-free genome editing in wheat through transient expression of CRISPR/Cas9 DNA or RNA. *Nat. Commun.* 7:12617. doi: 10.1038/ncomms12617

Zhang, J., Liu, H., Sun, J., Li, B., Zhu, Q., Chen, S., et al. (2012). Arabidopsis fatty acid desaturase FAD2 is required for salt tolerance during seed germination and early seedling growth. *PLoS One* 7:e30355. doi: 10.1371/journal.pone.0030355

Zhang, K., Nie, L., Cheng, Q., Yin, Y., Chen, K., Qi, F., et al. (2019b). Effective editing for lysophosphatidic acid acyltransferase 2/5 in allotetraploid rapeseed (*Brassica napus* L.) using CRISPR-Cas9 system. *Biotechnol. Biofuels* 12:225. doi: 10.1186/s13068-019-1567-8

Zhao, J., Wang, C., Bedair, M., Welti, R., Sumner, L. W., Baxter, I., et al. (2011). Suppression of phospholipase Dγs confers increased aluminum resistance in *Arabidopsis thaliana*. *PLoS One* 6:e28086. doi: 10.1371/journal.pone.0028086

Zhou, X. R., Shrestha, P., Yin, F., Petrie, J. R., and Singh, S. P. (2013). AtDGAT2 is a functional acyl-CoA:diacylglycerol acyltransferase and displays different acyl-CoA substrate preferences than AtDGAT1. *FEBS Lett.* 587, 2371–2376. doi: 10.1016/j.febslet.2013.06.003

Zou, J., Wei, Y., Jako, C., Kumar, A., Selvaraj, G., and Taylor, D. C. (1999). The *Arabidopsis thaliana TAG1* mutant has a mutation in a diacylglycerol acyltransferase gene. *Plant J.* 19, 645–653. doi: 10.1046/j.1365-313x.1999.00555.x

Advantages of publishing in Frontiers

OPEN ACCESS
Articles are free to read for greatest visibility and readership

FAST PUBLICATION
Around 90 days from submission to decision

HIGH QUALITY PEER-REVIEW
Rigorous, collaborative, and constructive peer-review

TRANSPARENT PEER-REVIEW
Editors and reviewers acknowledged by name on published articles

Frontiers
Avenue du Tribunal-Fédéral 34
1005 Lausanne | Switzerland

Visit us: www.frontiersin.org
Contact us: frontiersin.org/about/contact

REPRODUCIBILITY OF RESEARCH
Support open data and methods to enhance research reproducibility

DIGITAL PUBLISHING
Articles designed for optimal readership across devices

FOLLOW US
@frontiersin

IMPACT METRICS
Advanced article metrics track visibility across digital media

EXTENSIVE PROMOTION
Marketing and promotion of impactful research

LOOP RESEARCH NETWORK
Our network increases your article's readership